

AD A 095720

AFWAL-TR-80-4038

LEVEL II



METALLURGICAL CHARACTERIZATION OF SUPERPLASTIC FORMING

*T. L. MACKAY
S. M. L. SASTRY
C. F. YOLTON*

*DOUGLAS AIRCRAFT COMPANY ✓
McDONNELL DOUGLAS CORPORATION
LONG BEACH, CALIFORNIA 90846*

SEPTEMBER 1980

TECHNICAL REPORT AFWAL-TR-80-4038
Final Report for Period 17 September 1977 — 31 March 1980

Approved for public release; distribution unlimited.

DTIC
ELECTE
S MAR 3 1981 D

MATERIALS LABORATORY
AIR FORCE WRIGHT AERONAUTICAL LABORATORIES
AIR FORCE SYSTEMS COMMAND
WRIGHT-PATTERSON AIR FORCE BASE, OHIO 45433

DEC FILE COPY

81 2 27 02

NOTICE

When Government drawings, specifications, or other data are used for any purpose other than in connection with a definitely related Government procurement operation, the United States Government thereby incurs no responsibility nor any obligation whatsoever; and the fact that the government may have formulated, furnished, or in any way supplied the said drawings, specifications, or other data, is not to be regarded by implication or otherwise as in any manner licensing the holder or any other person or corporation, or conveying any rights or permission to manufacture, use, or sell any patented invention that may in any way be related thereto.

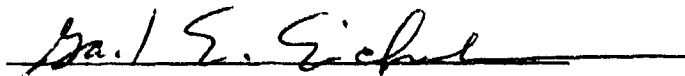
This report has been reviewed by the Office of Public Affairs (ASD/PA) and is releasable to the National Technical Information Service (NTIS). At NTIS, it will be available to the general public, including foreign nations.

This technical report has been reviewed and is approved for publication.



Mr. William R. Kerr
Project Engineer

FOR THE COMMANDER



Mr. Gail E. Eichelman, Chief
Structural Metals Branch
Metals and Ceramics Division

"If your address has changed, if you wish to be removed from our mailing list, or if the addressee is no longer employed by your organization please notify AFWAL/MLLS, W-PAFB, OH 45433 to help us maintain a current mailing list".

Copies of this report should not be returned unless return is required by security considerations, contractual obligations, or notice on a specific document.

Characterization

62102F

SECURITY CLASSIFICATION OF THIS PAGE (When Data Entered)

19 REPORT DOCUMENTATION PAGE		READ INSTRUCTIONS BEFORE COMPLETING FORM	
1. REPORT NUMBER AFML-TR-80-4038	2. GOVT ACCESSION NO. AD-A095 720	3. RECIPIENT'S CATALOG NUMBER	
4. TITLE (and Subtitle) METALLURGICAL CHARACTERISTICS OF SUPERPLASTIC FORMING		5. TYPE OF REPORT & PERIOD COVERED Final Technical Report - 17 Sep 77 - 31 Mar 80	
7. AUTHOR(s) T. L. Mackay & S. M. L. Sastry & C. F. Yelton		6. PERFORMING ORG. REPORT NUMBER	
9. PERFORMING ORGANIZATION NAME AND ADDRESS		8. CONTRACT OR GRANT NUMBER(s) F33615-77-C-5198	
11. CONTROLLING OFFICE NAME AND ADDRESS Materials Laboratory (AFWAL/MLLS) Air Force Wright Aeronautical Laboratories Wright-Patterson Air Force Base, Ohio, 45433		10. PROGRAM ELEMENT, PROJECT, TASK AREA & WORK UNIT NUMBERS 24181	
14. MONITORING AGENCY NAME & ADDRESS (if different from Controlling Office) 313		12. REPORT DATE September 1980	
		13. NUMBER OF PAGES 287	
		15. SECURITY CLASS. (of this report) UNCLASSIFIED	
		16a. DECLASSIFICATION/DOWNGRADING SCHEDULE	
16. DISTRIBUTION STATEMENT (of this Report) Approved for public release, distribution unlimited.			
17. DISTRIBUTION STATEMENT (of the abstract entered in Block 20, if different from Report)			
18. SUPPLEMENTARY NOTES			
19. KEY WORDS (Continue on reverse side if necessary and identify by block number) Forming, superplastic, titanium alloys, sheet metal, elevated temperature, inert gas pressure forming, strain-rate sensitivity, activation energy, grain growth, tensile properties, fatigue.			
20. ABSTRACT (Continue on reverse side if necessary and identify by block number) A systematic characterization of the superplasticity for regular-grade Ti-6Al-4V, ELI-grade Ti-6Al-4V, simulated coil-rolled Ti-6Al-4V, Ti-3Al-2.5V, Ti-6Al-2Sn-4Zr-2Mo, Ti-8Al-1Mo-1V, and Ti-15V-3Cr-3Sn-3Al sheets with several different microstructures and texture was performed. The effects of alloy chemistry, grain size, volume fraction of constituent phases, and anomalous microstructures on the superplastic parameters were determined by incremental strain-rate, constant stress, constant strain rate and biaxial constant stress			

DD FORM 1 JAN 73 1473

EDITION OF 1 NOV 65 IS OBSOLETE
S/N 0102-014-6601

Unclassified

SECURITY CLASSIFICATION OF THIS PAGE (When Data Entered)

116400

next page

cone-forming tests. The strain-rate time (or equivalently, strain) dependences of flow stress and strain-rate sensitivity were identified as the most important superplasticity parameters, with the continuous changes in alloy microstructures during superplastic deformation requiring proper consideration.

In the alpha-beta and near-alpha titanium alloys, the flow stress decreases and necking resistance increase with decreasing grain size at 850-950°F (1562 - 1742°F) with increasing strain and time the flow stress at constant strain-rate increases and the strain rate at constant applied stress decreases as a consequence of increasing grain size. Ti-6Al-4V alloys with elongated-alpha have significantly higher flow stress than equiaxed regular grade Ti-6Al-4V. Because of the extensive grain growth in the beta alloy, Ti-15V-3Cr-3Sn-3Al at high temperatures, the flow stress was considerably higher than in alpha-beta titanium alloys.

The flow stress at a constant strain rate of different alpha-beta alloys is uniquely related to grain size, beta transus temperature, and volume fractions of constituent phases at the test temperature. The effects of different compositions and microstructural modifications are implicit in the ratio of the forming temperature, T , to the beta-transus temperature, T_β , of a specific alloy. For a fixed T/T_β ratio, regardless of the alloy composition, the logarithm of flow stress is a function of the logarithm of the product of the strain-rate and the average grain size.

The biaxial cone-forming test was demonstrated to be a very viable tool for relating biaxial superplastic forming of titanium alloys to production inert gas forming methods.

Accession For	
NTIS GRA&I	<input checked="" type="checkbox"/>
DTIC TAB	<input type="checkbox"/>
Unannounced	<input type="checkbox"/>
Justification	
By	
Distribution/	
Availability Codes	
Dist	Avail and/or Special
A	

DTIC
ELECTE
MAR 3 1981
S D

PREFACE

This report presents the results of the work performed from 17 September 1977 to 31 March 1980 by the Douglas Aircraft Company under Air Force Contract F33615-77-C-5198 on Metallurgical Characterization of Superplastic Forming. The contract was administered by the Air Force Wright Aeronautical Laboratories, Wright-Patterson Air Force Base, Ohio, with Mr. W. R. Kerr as the program monitor.

The two-phase program was conducted in the Materials and Process Engineering Department of the Douglas Aircraft Company (DAC) of McDonnell Douglas Corporation with Dr. T. L. Mackay as the Program Manager. Phase I of the program on materials processing was conducted under a subcontract by DAC to Crucible Materials Research Center (CMRC), Colt Industries, Inc., and Mr. C. F. Yolton of CMRC directed this effort. For Phase II, superplastic testing was conducted by the McDonnell Douglas Research Laboratories under the direction of Dr. S. M. L. Sastry, and superplastic forming evaluation was performed by DAC under the direction of Dr. T. L. Mackay.

This program was undertaken to determine systematically the effects of micro-structural and process variables on the superplastic behavior of an alpha-beta titanium alloy, Ti-6Al-4V, and a beta-titanium alloy, Ti-15V-3Cr-3Sn-3Al. The scope of the program was subsequently expanded to include Ti-3Al-2.5V, Ti-6Al-2Sn-4Zr-2Mo, simulated coil-rolled Ti-6Al-4V, and Ti-8Al-1Mo-1V. The greater understanding of superplasticity in these titanium alloys gained from this program should lead to a more efficient utilization of superplastic forming/diffusion bonding (SPF/DB) of titanium alloy parts in advanced Air Force systems.

TABLE OF CONTENTS

	Page
Section I Introduction.....	1
Section II Technical Background and Program Plan.....	3
2.1 Superplasticity.....	3
2.2 Program Objectives.....	8
2.3 Program Plan.	9
Section III Alloy Processing and Characterization.....	18
3.1 Regular Grade Ti-6Al-4V (Normal Texture).....	18
3.2 Regular Grade Ti-6Al-4V (Textured).....	34
3.3 Regular-Grade Ti-6Al-4V with Microstructural Anomalies.....	41
3.4 ELI Grade Ti-6Al-4V.....	52
3.5 Simulated Coil Ti-6Al-4V.....	54
3.6 Ti-3Al-2.5V.....	60
3.7 Ti-6Al-2Sn-4Zr-2Mo.....	60
3.8 Ti-6Al-1Mo-1V.....	67
3.9 Ti-15V-3Cr-3Sn-3Al.....	67
Section IV Characterization of Superplasticity.....	74
4.1 Regular Grade Ti-6Al-4V.....	74
4.2 ELI Grade Ti-6Al-4V ($T_{\beta} = 968^{\circ}\text{C}$).....	112
4.3 Regular-Grade Ti-6Al-4V with Elongated Alpha, Blocky Alpha, Bonding, and Transverse-Basal Texture and Coil Rolled Ti-6Al-4V.....	123
4.4 Ti-6Al-2Sn-4Zr-2Mo ($T_{\beta} = 993^{\circ}\text{C}$).....	141
4.5 Ti-8Al-1Mo-1V ($T_{\beta} = 1032^{\circ}\text{C}$).....	141
4.6 Ti-3Al-2.5V ($T_{\beta} = 930^{\circ}\text{C}$).....	147
4.7 Ti-15V-3Cr-Sn-3Al ($T_{\beta} = 746^{\circ}\text{C}$).....	147
4.8 Comparison of Superplastic Behavior of Different Titanium Alloys.....	163

	Page
Section V Superplastic Forming Evaluation.....	170
5.1 Verification of Biaxial Conical Die Forming.....	170
5.2 Biaxial Conical-Die Forming Regular-Grade Ti-6Al-4V and ELI-Grade Ti-6Al-4V (normal texture).....	172
5.3 Grain-Growth During Superplastic Forming of Ti-6Al-4V.....	178
5.4 Effects of Diffusion Bonding Cycle on Superplastic Forming.....	180
5.5 Biaxial Cone-Forming of Basal-Textured and Transverse-Basal-Textured Ti-6Al-4V.....	184
5.6 Biaxial Conical-Die Forming of Ti-6Al-4V with Anomalous Micro-structure.....	190
5.7 Biaxial Conical-Die Forming of Simulated-Coil Ti-6Al-4V.....	193
5.8 Biaxial Conical Die Forming of Ti-3Al-2.5V.....	195
5.9 Biaxial Conical-Die Forming of Ti-8Al-1Mo-1V.....	198
5.10 Biaxial Conical-Die Forming of Ti-6Al-2Sn-4Zr-2Mo.....	201
5.11 Biaxial Conical-Die Forming of Ti-15V-3Cr-3Sn-3Al.....	204
5.12 Mechanical Properties of Superplastically Formed Panels.....	207
5.13 Effect of Superplastic Forming on Damage Tolerant Properties of Ti-6Al-4V.....	216
Section VI Constitutive Equation for Superplastic Forming.....	221
6.1 Time and Strain Dependence of Flow Stress-Strain Relationship...	221
6.2 Temperature Dependence of Strain Rates of Titanium Alloys.....	221
6.3 Constitutive Equations and Superplasticity Diagrams for Alpha-Beta Titanium Alloys.....	226
Section VII Summary and Conclusion.....	233
References.....	236
Appendices	
A. Conical Die for Superplastic Forming.....	239
B. Pole Figures for Ti-6Al-4V.....	247
C. Superplastic Conical-Die Forming of Titanium Alloys.....	252
D. Thickness Measurements of Superplastically Formed Pans.....	279

LIST OF ILLUSTRATIONS

FIGURE		PAGE
1	Typical strain-rate dependences of (a) flow stress and (b) strain-rate sensitivity, m , of flow stress for Ti-6Al-4V at superplastic-forming temperatures.....	4
2	Alloy compositions and microstructures evaluated in this study. Volume fraction of primary alpha is denoted by α , and grain size is denoted by d	10
3	Cross-section of conical die for superplastic-forming evaluation.	14
4	Multicone die configuration for superplastic-forming evaluation of titanium alloys.....	17
5	Microstructures of regular-grade Ti-6Al-4V (a) production rolled to 22-mm (0.87 inch) thickness and (b) laboratory hot-rolled at 941°C from 22-mm (0.87 inch) to 7.4-mm (0.291 inch) thicknesses....	23
6	Microstructures of Ti-6Al-4V laboratory pack-rolled at 843°C (1726°F) (1550°F) from 7.2mm (0.87 inch) to 1.7mm (0.067 inch) and (a) annealed at 705°C/(1301°F) for 1 h and (b) annealed at 760°C (1400°F) for 8 h.....	24
7	Microstructures of Ti-6Al-4V pack-rolled at 843°C from 7.2mm to 1.7mm and annealed at (a) 871°C (1600°F) for 1 h, (b) 927°C (1700°F) for 1 h, and (c) 982°C (1800°F) for 1 hr.....	25
8	Microstructures of production-processed 22mm (0.87 inch) regular-grade Ti-6Al-4V at (a) surface and (b) mid-thickness.....	27
9	Microstructure of production-processed 7mm (0.276 inch) regular-grade Ti-6Al-4V at quarter-thickness position.....	28
10	Growth of primary-alpha grain size with time at 982°C (1800°F) annealing temperature with furnace cooling to room temperature.....	29
11	Microstructures after furnace cooling to 25°C (77°F) of regular-grade Ti-6Al-4V annealed at (a) 927°C (1700°F) for 1 h, (b) 982°C (1800°F) for 8 h, and (c) 982°C (1800°F) for 24 h.....	30
12	Variation of volume fraction of primary alpha with annealing temperature for EL1-grade Ti-6Al-4V.....	31
13	Microstructures of regular-grade Ti-6Al-4V at a constant primary alpha grain size and (a) 90% primary alpha, (b) 65% primary alpha, and (c) 45% primary alpha.....	32
14	Microstructure of basal-textured Ti-6Al-4V annealed at 920°C (1688°F) for 1 h and furnace cooled to 25°C (77°F) at 56°C/h.....	38
15	Microstructures of transverse-basal-textured regular-grade Ti-6Al-4V sheet (Heat no. G52063) for (a) as-hot-rolled and (b) vacuum annealed at 927°C (1700°F) for 1 h and furnace cooled to 25°C (77°F) at 56°C/h.....	40

LIST OF ILLUSTRATIONS

FIGURE		PAGE
16	Microstructures of elongated alpha Ti-6Al-4V (Heat no. G52063) for (a) 2.3-mm thick sheet annealed at 1038°C (1900°C) for 15 min; air cooled to 25°C (77°F) + 995°C (1823°F) for 1 hr and air cooled to 25°C (77°F), (b) as-hot-rolled 1.8 mm (0.071 inch) thick sheet, and (c) 1.8 mm sheet vacuum (0.071 inch) annealed at 927°C (1900°F) for 1 hr and furnace cooled to 25°C (77°F).....	43
17	Microstructures of elongated alpha Ti-6Al-4V (heat no. G52063) for (a) 3.2 mm thick (.125 inch) sheet annealed at 1038°C (1900°F) for 15 min; air cooled to 25°C (77°F) + 995°C (1823°F) for 1 hr and air cooled at 1.8 mm (0.071 inch) sheet, vacuum annealed at 927°C (1700°F) for 1 hr; furnace cooled to 25°C (77°F).....	44
18	Banded microstructure of Ti-6Al-4V produced in the laboratory by thermal cascade-rolled 65% from 1045°C (1913°F) followed by annealing at 927°C (1700°F) for 1 hr and furnace cooled to 25°C (77°F).....	45
19	As-hot-rolled microstructure of Ti-6Al-4V plate thermal cascade-rolled 70% in a welded pack from 1024°C (1875°F).....	45
20	Microstructures of banded Ti-6Al-4V sheet (Heat no. G52070) for (a) initial microstructure, (b) hot-rolled at 843°C (1550°F) to 1.6mm (.065 inch) thickness (level I), and (c) hot-rolled at 885°C (1625°F) to 1.6mm (.065 inch) thickness (level II).....	46
21	Microstructures of banded Ti-6Al-4V sheet (level I) after vacuum annealing at 927°C (1700°F) for 1 hr and furnace cooled at 25°C (77°F).....	47
22	Microstructures of banded Ti-6Al-4V sheet (level II) after vacuum annealing at 927°C (1700°F) for 1 hr and furnace cooled at 25°C (77°F).....	48
23	Microstructures of blocky alpha (level I) Ti-6Al-4V sheet (Heat no. G52063) for (a) 3.7mm thick sheet annealed at 968°C (1775°F) for 4 h and air cooled to 25°C (77°F), (b) as-hot-rolled 1.8mm (0.071 inch) thick sheet, and (c) 1.8mm (0.071 inch) sheet vacuum annealed at 927°C (1700°F) for 1 hr and furnace cooled at 25°C (77°F).....	50
24	Microstructures of blocky alpha (level II) Ti-6Al-4V sheet (Heat no. G52063) for (a) 3.5mm (0.138 inch) sheet annealed at 954°C (1750°F) for 4 hr and air cooled to 25°C (77°F) (b) as-hot-rolled 1.9mm sheet vacuum annealed at 927°C (1700°F) for 1 hr and furnace cooled to 25°C (77°F).....	51
25	Microstructure of as-received Ti-6Al-4V hot band.....	55

LIST OF ILLUSTRATIONS

FIGURE		PAGE
26	Microstructure of Ti-6Al-4V sheet after four 15% cold-rolling cycles.....	56
27	Variation of primary-alpha level with temperature in the Ti-6Al-4V alloy. Bands represent 95% confidence limits.....	57
28	Microstructures of simulated coil-rolled Ti-6Al-4V (a) annealed at 954°C (1750°F) for 16 hr and furnace cooled to 25°C (77°F) (condition S1) and (b) annealed at 927°C (1700°F) for 1.5 hr, furnace cooled to 25°C (77°F) + 899°C (1650°F) for 10 min; air cooled to 25°C (77°F) (condition S2).....	58
29	Microstructures of simulated coil-rolled Ti-6Al-4V sheet (a) annealed at 954°C (1750°F) for 16 hr and furnace cooled to 25°C (77°F) (condition S2) and (b) annealed at 954°C (1750°F) for 24 hr furnace cooled to 25°C (77°F) + annealed at 899°C (1650°F) for 10 min, air cooled to 25°C (77°F) (condition S4).....	59
30	Microstructure of Ti-3Al-2.5V sheet after cold-rolling 38%.....	61
31	Grain growth in the Ti-3Al-2.5V alloy at 913°C (1675°F). Values determined after furnace cooling from the heat treatment temperature. Bands represent 95% confidence limits.....	62
32	Variation of primary-alpha level with temperature in the Ti-3Al-2.5V alloy. Bands represent 95% confidence limits.....	63
33	Microstructures of Ti-3Al-2.5V sheet (a) annealed at 871°C (1600°F) for 1 hr and furnace cooled to 25°C (77°F) (condition R1) and (b) annealed at 871°C (1600°F) for 1 hr; furnace cooled to 25°C (77°F) + 891°C (1636°F) for 10 min; air cooled to 25°C (77°F) (condition R2).....	64
34	Microstructures of Ti-3Al-2.5V sheet (a) annealed at 899°C (1650°F) for 20 hr; furnace cooled to 25°C (77°F) (condition R3) and (b) annealed at 899°C (1650°F) for 20 hr; furnace cooled to 25°C (77°F) + annealed at 891°C (1636°F) for 10 min and air cooled to 25°C (77°F) (condition R4).....	65
35	Grain growth in Ti-6Al-2Sn-4Zr-2Mo alloy at 968°C (1775°F). Values determined after furnace cooling from the heat treatment temperature. Bands represent 95% confidence limits.....	66
36	Variation of primary-alpha level with the temperature in the Ti-6Al-2Sn-4Zr-2Mo alloy. Bands represent 95% confidence limits....	68
37	Microstructures of the Ti-6Al-2Sn-4Zr-2Mo sheet (a) as-received and (b) annealed at 963°C for 10 min and air cooled to 25°C (77°F). 69	69

LIST OF ILLUSTRATIONS

FIGURE		PAGE
38	Microstructures of Ti-6Al-2Sn-4Zr-2Mo sheet (a) annealed at 960°C (1760°F) for 20 hr and furnace cooled to 25°C (77°F) and (b) annealed at 960°C (1760°F) for 20 hr, furnace cooled to 25°C (77°F) + annealed at 963°C (1765°F) for 10 min and air cooled to 25°C (77°F).....	70
39	Microstructures of as-received Ti-8Al-1Mo-1V sheet (a) 1.14-mm (.045 inch) thick and (b) 1.2-mm (0.050 inch) thick.....	71
40	Microstructures of Ti-15V-3Cr-3Al-3Sn alloy (Heat no. P3357) (a) as cold-rolled 57%, (b) annealed at 775°C (1427°F) for 5 min, (c) annealed at 775°C (1427°F) for 2.25 hr, and (d) annealed at 775°C (1427°F) for 5 min; air cooled to 25°C (77°F) + annealed at 482°C (900°F) for 8 h and air cooled to 25°C (77°F).....	73
41	Strain-rate dependence of (a) flow stress and (b) strain-rate sensitivity of regular-grade Ti-6Al-4V (volume % primary alpha = 88) at 850°C (1562°F).....	75
42	Strain-rate dependence of (a) flow stress and (b) strain-rate sensitivity of regular-grade Ti-6Al-4V (volume % primary alpha = 66) at 850°C (1562°F).....	76
43	Strain-rate dependence of (a) flow stress and (b) strain-rate sensitivity of regular-grade Ti-6Al-4V (volume % primary alpha = 45) at 850°C (1562°F).....	77
44	Strain-rate dependence of (a) flow stress and (b) strain-rate sensitivity of regular-grade Ti-6Al-4V (volume % primary alpha = 88) at 875°C (1607°F).....	78
45	Strain-rate dependence of (a) flow stress and (b) strain-rate sensitivity of regular-grade Ti-6Al-4V (volume % primary alpha = 66) at 875°C (1607°F).....	79
46	Strain-rate dependence of (a) flow stress and (b) strain-rate sensitivity of regular-grade Ti-6Al-4V (volume % primary alpha = 45) at 875°C (1607°F).....	80
47	Strain-rate dependence of (a) flow stress and (b) strain-rate sensitivity of regular-grade Ti-6Al-4V (volume % primary alpha = 88 at 907°C (1665°F).....	81
48	Strain-rate dependence of (a) flow stress and (b) strain-rate sensitivity of regular-grade Ti-6Al-4V (volume % primary alpha = 66) at 907°C (1665°F).....	82
49	Strain-rate dependence of (a) flow stress and (b) strain-rate sensitivity of regular-grade Ti-6Al-4V (volume % primary alpha = 45) at 907°C (1665°F).....	83

LIST OF ILLUSTRATIONS

FIGURE		PAGE
50	Flow stress at 850°C (1562°F) as a function of strain rate in recrystallization-annealed Ti-6Al-4V.....	86
51	Flow stress as a function of \ln (strain rate x grain size) at 850°C (1562°F) in regular-grade Ti-6Al-4V; (a) volume % primary alpha = 88, (b) volume % primary alpha = 66, and (c) volume % primary alpha = 45.....	89
52	Flow stress as a function of \ln (strain rate x grain size) at 875°C (1607°F) in regular-grade Ti-6Al-4V; (a) volume % primary alpha = 88, (b) volume % primary alpha = 66, and (c) volume % primary alpha = 45.....	90
53	Flow stress as a function of \ln (strain rate x grain size) at 907°C (1665°F) in regular-grade Ti-6Al-4V; (a) volume % primary alpha = 88, and (b) volume % primary alpha = 45.....	91
54	Grain-size dependence of strain rate at constant stress for regular-grade Ti-6Al-4V, volume % primary alpha = 45; (a) 850°C (1562°F), (b) 875°C (1607°F), and (c) 907°C (1665°F).....	93
55	Grain size dependence of flow stress at constant strain-rate for regular-grade Ti-6Al-4V at (a) 850°C (1562°F), and (b) 907°C (1665°F), and for EL1-grade Ti-6Al-4V at (c) 850°C (1562°F) and (d) 907°C (1665°F); volume % primary alpha = 46.	94
56	Effect of volume fraction of primary alpha on strain-rate dependence of (a) flow stress and (b) strain-rate sensitivity at 850°C (1562°F) of regular-grade Ti-6Al-4V.....	95
57	Effect of volume fraction of primary alpha on strain-rate dependence of (a) flow stress and (b) strain-rate sensitivity at 875°C (1607°F) of regular-grade Ti-6Al-4V.....	96
58	Effect of volume fraction primary alpha on strain-rate dependence of (a) flow stress and (b) strain-rate sensitivity at 907°C (1665°F) of regular-grade Ti-6Al-4V.....	97
59	Effect of temperature on strain-rate dependence of (a) flow stress and (b) strain-rate sensitivity of regular-grade Ti-6Al-4V. (Specimen I, volume % primary alpha = 45, grain size = 5.6 μm).....	99
60	Effects of alloy chemistry on the strain-rate dependences of (a) flow stress and (b) strain-rate sensitivity of flow stress of titanium alloys at 875°C. (1907°F).....	100
61	True-stress as a function of true-strain at 875°C (1907°F) of regular-grade Ti-6Al-4V (panel C, volume % primary alpha = 88, grain size = 17.6 μm) determined from constant strain-rate tests.....	101

FIGURE	LIST OF ILLUSTRATIONS	PAGE
62	True-stress as a function of true-strain at 875°C (1907°F) of regular-grade Ti-6Al-4V (panel E, volume % primary alpha = 45, grain size = 7.2 μm) determined from constant strain-rate tensile tests.....	101
63	Strain dependence of strain-rate sensitivity at 870°F (1598°F) of regular-grade Ti-6Al-4V and EL1-grade Ti-6Al-4V.....	102
64	True-stress as a function of true-strain at 875°C (1907°F) of regular-grade Ti-6Al-4V (panel F, volume % primary alpha = 45, grain size = 7.2 μm) determined from constant strain-rate tensile tests.....	102
65	True stress as a function of true-strain at 875°C (1907°F) of regular-grade Ti-6Al-4V determined from constant strain-rate tensile tests, constant crosshead speed tests, and flat-ring compression tests (Δ); (a) Specimen C, strain rate $\dot{\epsilon} = 10^{-4}\text{s}^{-1}$, (b) Specimen C, strain rate $\dot{\epsilon} = 10^{-3}\text{s}^{-1}$, and (c) Specimen F, strain rate $\dot{\epsilon} = 10^{-4}\text{s}^{-1}$	103
66	Variation of strain with time determined for constant stress tests for regular-grade Ti-6Al-4V at 907°C (Specimen K, volume % primary alpha = 66, grain size = 5.8 μm).....	106
67	Variation of \ln (strain rate x instantaneous grain-size) with time during constant stress testing of Ti-6Al-4V at 907°C. (1665°F).....	107
68	Variation of strain rate with time determined from constant stress tests for regular-grade Ti-6Al-4V at 907°C (1665°F); (a) stress = 4.1 MPa (.6 ksi) and (b) stress = 13.8 MPa (2 ksi)....	108
69	Variation of strain with time determined from constant stress tests for regular-grade Ti-6Al-4V at 907°C. (1665°F).....	109
70	Effect of grain size on strain rates of regular-grade Ti-6Al-4V determined from constant stress tests at 907°C. (1665°F).....	109
71	Effect of temperature on strain rate of Ti-6Al-4V determined from constant stress tests.....	110
72	Effect of soak time on strain rate of Ti-6Al-4V at 907°C (1665°F); (a) specimen L (volume % primary alpha = 88, grain size = 6 μm) and (b) specimen E (volume % primary alpha = 88, grain size = 12 μm).....	111
73	Strain-rate dependence of (a) flow stress and (b) strain-rate sensitivity for EL1-grade Ti-6Al-4V (volume % primary alpha = 88) at 850°C. (1562°F).....	113

LIST OF ILLUSTRATIONS

FIGURE		PAGE
74	Strain-rate dependence of (a) flow stress and (b) strain-rate sensitivity for EL1-grade Ti-6Al-4V (volume % primary alpha = 46) at 850°C (1562°F).....	114
75	Strain-rate dependence of (a) flow stress and (b) strain-rate sensitivity for EL1-grade Ti-6Al-4V (volume % primary alpha = 88) at 875°C (1607°F).....	115
76	Strain-rate dependence of (a) flow stress and (b) strain-rate sensitivity for EL1-grade Ti-6Al-4V (volume % primary alpha = 46) at 875°C (1607°F).....	116
77	Strain-rate dependence of (a) flow stress and (b) strain-rate sensitivity for EL1-grade Ti-6Al-4V (volume % primary alpha = 88) at 907°C (1665°F).....	117
78	Strain-rate dependence of (a) flow stress and (b) strain-rate sensitivity for EL1-grade Ti-6Al-4V (volume % primary alpha = 46) at 907°C (1665°F).....	118
79	Flow stress as a function of \ln (strain rate x grain size at 850°C (1562°F) in EL1-grade Ti-6Al-4V; (a) volume % primary alpha = 88, and (b) volume % primary alpha = 46.....	119
80	Flow stress as a function of \ln (strain rate x grain size at 875°C (1607°F) in EL1-grade Ti-6Al-4V; (a) volume % primary alpha = 88, and (b) volume % primary alpha = 46.....	120
81	Flow stress as a function of \ln (strain rate x grain size) at 907°C (1665°F) in EL1-grade Ti-6Al-4V; (a) volume % primary alpha = 88, and (b) volume % primary alpha = 46.....	121
82	Flow stress as a function of \ln (strain rate x grain size) at different fractions of beta-transus-temperature for regular-grade Ti-6Al-4V and EL1-grade Ti-6Al-4V.....	122
83	True-stress as a function of true-strain for EL1-grade Ti-6Al-4V at 875°C (1607°F) determined from constant strain-rate tensile tests.....	124
84	Variation of grain size with time in deformed and undeformed regions of EL1-grade Ti-6Al-4V during superplastic testing at 875°C (1607°F).....	124
85	True-stress as a function of true-strain for EL1-grade Ti-6Al-4V at 875°C (1607°F) determined from constant strain-stress tests and constant crosshead speed tests.....	125

LIST OF ILLUSTRATIONS

FIGURE		PAGE
86	Variation of (a) strain and (b) strain-rate with time determined from constant stress tests for ELI-grade Ti-6Al-4V (volume % primary alpha = 88, grain size = 5.5 μ m, sample X1) at 875°C. (1907°F).....	126
87	Effect of orientation on strain-rate dependence of flow stress in transverse-basal-textured Ti-6Al-4V (specimen T1); (a) stress direction parallel to rolling direction and (b) stress direction parallel to transverse direction.....	127
88	Effect of elongated alpha on strain-rate dependence of flow stress in Ti-6Al-4V; (a) specimen M and (b) specimen M1.....	128
89	Effect of blocky alpha on strain-rate dependence of flow stress in Ti-6Al-4V; (a) specimen N and (b) specimen N1.....	129
90	Effect of banding on strain-rate dependence of flow stress in Ti-6Al-4V; (a) specimen O and (b) specimen O1.....	130
91	Strain-rate dependence of (a) flow stress and (b) strain-rate sensitivity for coil-rolled Ti-6Al-4V sample S4 (volume % primary alpha = 63, grain size = 9.3 μ m).....	131
92	Strain-rate dependence of (a) flow stress and (b) strain-rate sensitivity for coil-rolled Ti-6Al-4V sample S3 (volume % primary alpha = 87, grain size = 4.4 μ m).....	132
93	Strain-rate dependence of (a) flow stress and (b) strain-rate sensitivity for coil-rolled Ti-6Al-4V sample S2 (volume % primary alpha = 63, grain size = 4.4 μ m).....	133
94	Strain-rate dependence of (a) flow stress and (b) strain-rate sensitivity for coil-rolled Ti-6Al-4V sample S1 (volume % primary alpha = 87, grain size = 5.1 μ m).....	134
95	Effects of microstructural anomalies on strain-rate dependence of (a) and (c) flow stress, and (b) and (d) strain-rate sensitivity of Ti-6Al-4V.....	138
96	Effects of microstructural anomalies on strain rate of Ti-6Al-4V at 907°C determined from constant-stress tests.....	140
97	Strain-rate dependence of (a) flow stress and (b) strain-rate sensitivity for Ti-6Al-2Sn-4Zr-2Mo sample Q1 (volume % primary alpha = 90, grain size = 3.5 μ m).....	142
98	Strain-rate dependence of (a) flow stress and (b) strain-rate sensitivity for Ti-6Al-2Sn-4Zr-2Mo sample Q2 (volume % primary alpha = 65, grain size = 3.4 μ m).....	143

LIST OF ILLUSTRATIONS

FIGURE		PAGE
99	Strain-rate dependence of (a) flow stress and (b) strain-rate sensitivity for Ti-6Al-2Sn-4Zr-2Mo sample Q3 (volume % primary alpha = 86, grain size = 8.2 μm).....	144
100	Strain-rate dependence of (a) flow stress and (b) strain-rate sensitivity for Ti-6Al-2Sn-4Zr-2Mo sample Q4 (volume % primary alpha = 55, grain size = 8.8 μm).....	145
101	Strain-rate dependence of (a) flow stress and (b) strain-rate sensitivity for Ti-8Al-1Mo-1V.....	146
102	Variation of (a) strain and (b) strain rate with time at 925°C (1697°F) determined from constant stress tests for Ti-8Al-1Mo-1V...	149
103	Variation of (a) strain and (b) strain rate with time at 950°C (1742°F) determined from constant stress tests for Ti-8Al-1Mo-1V...	150
104	Variation of (a) strain and (b) strain rate with time at 1010°C (1850°F) determined from constant stress tests for Ti-8Al-1Mo-1V...	151
105	Strain-rate dependence of (a) flow stress and (b) strain-rate sensitivity for Ti-3Al-2.5V sample R1 (volume % primary alpha = 87, grain size = 5.6 μm).....	152
106	Strain-rate dependence of (a) flow stress and (b) strain-rate sensitivity for Ti-3Al-2.5V sample R2 (volume % primary alpha = 57, grain size = 4.5 μm).....	153
107	Strain-rate dependence of (a) flow stress and (b) strain-rate sensitivity for Ti-3Al-2.5V sample R3 (volume % primary alpha = 87, grain size = 10.2 μm).....	154
108	Strain rate dependence of (a) flow stress and (b) strain-rate sensitivity for Ti-3Al-2.5V sample R4 (volume % primary alpha = 58, grain size = 8.6 μm).....	155
109	Strain-rate dependence of (a) flow stress and (b) strain-rate sensitivity for Ti-15V-3Al-3Sn-3Cr sample Z2.....	156
110	Strain-rate dependence of (a) flow stress and (b) strain-rate sensitivity for Ti-15V-Cr-Sn-3Al sample Z3.....	157
111	Strain-rate dependence of (a) flow stress and (b) strain-rate sensitivity for Ti-15V-Cr-Sn-3Al sample Z5.....	158
112	Strain-rate dependence of (a) flow stress and (b) strain-rate sensitivity for Ti-15V-Cr-Sn-3Al sample Z4.....	159
113	Strain-rate dependence of (a) flow stress and (b) strain-rate sensitivity for Ti-15V-Cr-Sn-3Al sample Z6.....	160

LIST OF ILLUSTRATIONS

FIGURE		PAGE
114	True-stress as a function of true-strain at 810°C (1490°F) for Ti-15V-3Cr-3Sn-3Ag sample Z1 determined from constant strain-rate tests.....	162
115	True-stress as a function of true-strain at 760°C (1400°F) for Ti-15V-3Cr-3Sn-3Ag sample Z1 determined from constant strain-rate tests.....	162
116	Effects of alloy chemistry on strain-rate dependence of (a) flow stress and (b) strain-rate sensitivity of titanium alloys.....	164
117	Effects of alloy chemistry on strain-rate dependence of (a) flow stress and (b) strain-rate sensitivity of titanium alloys.....	165
118	Effects of alloy chemistry on strain-rate dependence at 850°C (1562°F) of (a) flow stress and (b) strain-rate sensitivity of alpha-beta and near-alpha determined from incremental strain-rate tests.....	166
119	Effects of texture on strain-rate dependence of (a) flow stress and (b) strain-rate sensitivity of Ti-6Al-4V at 850°C (1562°F).....	167
120	Comparisons of variation of (a) strain and (b) strain-rate with time determined from constant stress tests for Ti-6Al-4V and Ti-8Al-1Mo-1V.....	168
121	Strain-rate dependence of flow stress for Ti-8Al-1Mo-1V, Ti-6Al-4V, and Ti-3Al-2.5V showing the unique dependence of flow stress at constant strain rate on T/T_g	169
122	Correlation of strain calculated from formed cone thickness with strain calculated from cone depth.....	171
123	Strain-rate dependence of flow stress at 907°C (1665°F) of normal-textured regular-grade Ti-6Al-4V determined from cone-forming tests (symbols) and strain-rate cycling tests (dashed curves).....	173
124	Strain-rate dependence of flow stress at 907°C (1665°F) of normal-textured regular-grade Ti-6Al-4V determined from cone-forming tests (symbols) and strain-rate cycling tests (dashed-curves).....	173
125	Strain-rate dependence of flow stress at 907°C (1665°F) of normal-textured regular-grade Ti-6Al-4V determined from cone-forming tests (symbols) and strain-rate cycling tests (dashed curves).....	174

LIST OF ILLUSTRATIONS

FIGURE		PAGE
126	Strain-rate dependence of flow stress at 907°C (1665°F) for normal-textured regular-grade Ti-6Al-4V determined from cone-forming tests (symbol) and strain-rate cycling tests (dashed curves); grain size = 6.0 μm , volume % primary alpha = 88.....	174
127	Strain-rate dependence of flow stress at 871°C (1600°F) for normal-textured regular-grade Ti-6Al-4V determined from cone-forming tests (symbol) and strain-rate cycling tests (dashed curves); grain size = 6.0 μm , volume % primary alpha = 88.....	175
128	Strain-rate dependence of flow stress at 907°C (1665°F) of EL1-grade Ti-6Al-4V determined from cone-forming tests (symbols) and strain-rate cycling tests (dashed curves).....	175
129	Strain-rate dependence of flow stress at 907°C (1665°F) for normal-textured EL1-grade Ti-6Al-4V determined from cone-forming tests (symbol) and strain-rate cycling tests (dashed curve); grain size = 5.5 μm , volume % primary alpha = 88.....	176
130	Strain-rate dependence of flow stress at 871°C (1600°F) of EL1-grade Ti-6Al-4V determined from cone-forming tests (symbols and strain-rate cycling tests (dashed curves).....	176
131	Strain-rate dependence of flow stress at 871°C (1600°F) for normal-textured EL1-grade Ti-6Al-4V determined from cone-forming tests (symbol) and strain-rate cycling tests (dashed curve; specimen X1, grain size = 5.5 μm , volume % primary alpha = 88.....	177
132	Strain-rate dependence of flow stress at 907°C (1665°F) for regular-grade Ti-6Al-4V determined from cone-forming tests (symbols) and strain-rate cycling tests (dashed curve); specimen J, grain size = 4.4 μm , volume % primary alpha = 47.....	182
133	Strain-rate dependence of flow stress at 907°C (1665°F) for regular-grade Ti-6Al-4V determined from cone-forming tests (symbols) and strain-rate cycling tests (dashed curve); specimen L, grain size = 6.0 μm , volume % primary alpha = 88.....	182
134	Strain-rate dependence of flow stress at 907°C (1665°F) for regular-grade Ti-6Al-4V determined from cone-forming tests (symbols) and strain-rate cycling tests (dashed curve); specimen E, grain size = 12.2 μm , volume % primary alpha = 88.....	183
135	Strain-rate dependence of flow stress at 907°C (1665°F) for EL1-grade Ti-6Al-4V determined from cone-forming tests (symbols) and strain-rate cycling tests (dashed curve); specimen X1, grain size = 5.5 μm , volume % primary alpha = 88.....	183

LIST OF ILLUSTRATIONS

FIGURE		PAGE
136	Photomicrographs of water-quenched specimens of superplastically-formed normal-textured regular-grade Ti-6Al-4V (initial grain size = $6.0\text{ }\mu\text{m}$ volume % primary alpha = 88) with a forming temperature of 907°C (1665°F) for (a) 1.0 h, strain = 0; (b) 1.0 h, strain = 0.9; (c) 4.25 h, strain = 0; and (d) 4.25 h, strain = 1.7.....	187
137	Photomicrographs of water-quenched specimens of superplastically-formed normal-textured EL1-grade Ti-6Al-4V (initial grain size = $5.5\text{ }\mu\text{m}$, volume % primary alpha = 88) with a forming temperature of 870°C (1598°F) for (a) 0.5 h, strain = 0; (b) 0.5 h, strain = 0.8; (c) 2.5 h, strain = 0; and (d) 2.5 h, strain = 2.1.....	188
138	Strain-rate dependence of flow stress at 907°C (1665°F) for basal texture Ti-6Al-4V determined from cone-forming tests (symbols) and strain-rate cycling tests (dashed curves).....	189
139	Strain-rate dependence of flow stress at 907°C (1665°F) of banded Ti-6Al-4V (panel O) determined from cone-forming and laboratory incremental strain-rate tests.....	191
140	Strain-rate dependence of flow stress at 907°C (1665°F) of blocky alpha Ti-6Al-4V (panels N and N1) determined from cone-forming and laboratory incremental strain-rate tests.....	191
141	Strain-rate dependence of flow stress at 907°C (1665°F) of simulated-coil Ti-6Al-4V determined from cone-forming tests (symbols) and strain-rate cycling tests (dashed curves).....	194
142	Strain-rate dependence of flow stress at 907°C (1665°F) for simulated-coil Ti-6Al-4V determined from cone-forming tests (symbols) and strain-rate cycling tests (dashed curves).....	194
143	Strain-rate dependence of flow stress at 870°C (1598°F) for simulated-coil Ti-6Al-4V determined from cone-forming tests (symbols) and strain-rate cycling tests (dashed curves).....	195
144	Strain-rate dependence of flow stress at 877°C (1611°F) for Ti-3Al-2.5V determined from cone-forming tests (symbols) and strain-rate cycling tests (dashed curves).....	196
145	Strain-rate dependence of flow stress at 877°C (1611°F) for Ti-3Al-2.5V determined from cone-forming tests (symbols) and strain-rate cycling tests (dashed curve).....	197
146	Strain-rate dependence of flow stress at 841°C (1544°F) for Ti-3Al-2.5V determined from cone-forming tests (symbols) and strain-rate cycling tests (dashed curves).....	197

LIST OF ILLUSTRATIONS

FIGURE		PAGE
147	Strain-rate dependence of flow stress at 949°C (1740°F) for regular-grade Ti-8Al-1Mo-1V determined from cone-forming tests (symbols) and strain-rate cycling tests (dashed curves).....	199
148	Strain-rate dependence of flow stress at 932°C (1710°F) for regular-grade Ti-8Al-1Mo-1V determined from cone-forming tests (symbols) and strain-rate cycling tests (dashed curve).....	200
149	Sandwich panels of Ti-8Al-1Mo-1V and Ti-6Al-4V fabricated by superplastic forming/diffusion bonding.....	202
150	X-ray photograph of cell arrangement of titanium alloy sandwich panels.....	202
151	Strain-rate dependence of flow stress at 907°C (1665°F) for Ti-6Al-2Sn-4Zr-2Mo determined from cone-forming tests (symbols) and strain-rate cycling tests (dashed curves).....	203
152	Strain-rate dependence of flow stress at 907°C (1665°F) for Ti-6Al-2Sn-4Zr-2Mo determined from cone-forming tests (symbols) and strain-rate cycling (dashed curve).....	203
153	Strain-rate dependence of flow stress at 871°C (1600°F) for Ti-6Al-2Sn-4Zr-2Mo determined from cone-forming tests (symbols) and strain-rate cycling tests (dashed curves).....	204
154	Superplastically-formed 254-mm (10 in.) diam Ti-6Al-4V pan.....	208
155	Superplastically-formed 254-mm (10 in.) diam Ti-6Al-4V pans sectioned for mechanical property evaluation.....	208
156	Photograph showing thickness variation of cross section of the bottom of superplastically-formed simulated-coil Ti-6Al-4V.....	214
157	Notch fatigue specimen.....	217
158	Fatigue crack propagation for normal-textured regular-grade Ti-6Al-4V sheet in as-fabricated and superplastically-formed condition.....	219
159	Fatigue-crack propagation for normal-textured EL1-grade Ti-6Al-4V in as-fabricated and superplastically-formed condition.....	220
160	Comparison of strain-rate dependence of flow stress of Ti-6Al-4V determined from cone-forming test, constant stress test, and strain-rate cycling tests; (a) specimen J, (b) specimen B, (c) specimen G, and (d) specimen F.....	222

LIST OF ILLUSTRATIONS

FIGURE		PAGE
161	Temperature dependence of strain rate in regular-grade Ti-6Al-4V; (a) $\sigma = 44.8$ MPa (6.5 ksi) and (b) $\sigma = 10.3$ MPa (1.5 ksi).....	223
162	Temperature dependence of strain rate in EL1-grade Ti-6Al-4V sample X1.....	224
163	Temperature dependence of strain rate in Ti-8Al-1Mo-1V.....	224
164	Temperature dependence of strain rate in Ti-3Al-2.5V sample R2.....	225
165	Temperature dependence of steady-state strain rate of regular-grade Ti-6Al-4V at a stress of 8.4 MPa (1.2 ksi).....	226
166	Variation of grain size with time and regular-grade Ti-6Al-4V annealed at 907°C (1665°F).....	229
167	Grain-size dependence of strain-rate sensitivity of regular-grade Ti-6Al-4V at 875°C (1607°F) at a strain rate of 10^{-4}s^{-1}	229
168	Three-dimensional representation of the constitutive equation for superplastic forming of alpha-beta titanium alloys. The surface shown is for $T/T_B = 0.905$; other forming temperatures generate different surfaces.....	230
169	Temperature and strain-rate dependence of strain-rate sensitivity for alpha-beta titanium alloys.....	231
170	Flow stress as a function of strain rate and grain size at different forming-temperature/beta-transus ratios for alpha-beta titanium alloys.....	231

LIST OF TABLES

TABLE		PAGE
1	Specifications and Chemical Compositions of Titanium Alloys.....	19
2	Effects of Rolling Temperature and Cross-Roll Factors on Tensile Properties of Pack-Rolled Ti-6Al-4V.....	20
3	Effects of Rolling Schedules on Recrystallized Grain sizes of Cross-Rolled Regular-Grade Ti-6Al-4V Annealed at 927°C (1700°F) for 1h and Furnace Cooled to 25°C (77°F).....	22
4	Effects of Heat Treatment on Microstructures of Normal-Textured Ti-6Al-4V Sheet.....	35
5	Tensile Properties of Normal-Textured Regular-Grade 1.7 mm (0.065 in.) Ti-6Al-4V Sheet.....	36
6	Tensile Properties of "Clock-Rolled" Ti-6Al-4V Alloy (Heat No. G52063A-1).....	37
7	Grain Size of Laboratory "Clock-Rolled" Regular-Grade Ti-6Al-4V Annealed at 927°C (1700°F) for 1h and Furnace Cooled to 25°C. (77°F).....	37
8	Tensile Properties of Transverse-Basal-Textured Ti-6Al-4V Sheet Annealed at 927°C (1700°F) for 1h; Furnace Cooled to 25°C (77°F) at 38°C/h.....	41
9	Heat Treatment Schedules and the Resulting Microstructural Parameters for 1.5 x 381 x 381 mm (0.060 x 15 x 15 in.) Eli-Grade Ti-6Al-4V Panels.....	53
10	Tensile Properties of 1.7 mm (0.065 in.) Eli-Grade Ti-6Al-4V.....	53
11	Heat Treatment and Microstructural Parameters of Simulated-Coil Ti-6Al-4V.....	57
12	Effects of Annealing Temperature and Time on Grain Sizes and Volume Fractions of Primary Alpha for Ti-3Al-2.5V.....	62
13	Effects of Heat Treatment on Grain Size and Volume Fractions of Primary Alpha of Ti-6Al-2Sn-4Zr-2Mo.....	68
14	Effects of Heat Treatments on Grain Sizes of Ti-15V-3Cr-3Sn-3Al..	72
15	Results of Strain-Rate-Cycling Tests on Regular-Grade Ti-6Al-4V and Eli-Grade Ti-6Al-4V at 850°C (1562°F).....	84
16	Results of Strain-Rate-Cycling Tests on Regular-Grade Ti-6Al-4V and Eli-Grade Ti-6Al-4V at 875°C (1607°F).....	84

LIST OF TABLES - Cont.

TABLE		PAGE
17	Results of Strain-Rate-Cycling Tests on Regular-Grade Ti-6Al-4V and Eli-Grade Ti-6Al-4V at 907°C. (1665°F).....	85
18	The Values of Slopes and Correlation Coefficients for Straight-Line Fit by the Method of Least-Squares Analysis to the Flow-Stress/Strain-Rate Data.....	87
19	Flow-Stress Data of Normal-Textured Ti-6Al-4V (From Flat-Ring Compression Tests).....	104
20	Effects of Stress and Time On Grain Growth During Superplastic Testing of Ti-6Al-4V at 907°C. (1665°F).....	110
21	Results of Strain-Rate-Cycling Tests on Ti-6Al-4V With Anomalous Microstructures and Texture Temperature = 850°C (1562°F).....	135
22	Results of Strain-Rate-Cycling Tests on Ti-6Al-4V With Anomalous Microstructures and Texture Temperature = 875°C (1607°F).....	136
23	Results of Strain-Rate-Cycling Tests on Ti-6Al-4V With Anomalous Microstructures and Texture Temperature = 907°C (1665°F).....	137
24	Microstructure Variables for the Study of the Superplasticity of Ti-15V-3Cr-3Sn-3Al.....	148
25	Grain Growth in Ti-15V-3Cr-3Sn-3Al During Strain-Rate-Cycling Tests.....	161
26	Comparison of Strain Dependence of Stress Calculated From Thickness Measurements with Predicted Values for Superplastic Cone-Forming at 907°C (1665°F) of 38°/Min (1.5 in.)/Diam Regular-Grade Ti-6Al-4V (Panel E; Grain Size = 12.2 μ m Volume % Primary Alpha = 87).....	170
27	Effect of Superplastic Strain on Grain Growth at 907°C (1665°F) in Regular-Grade Ti-6Al-4V (Initial Primary Alpha Volume Fraction = 88).....	179
28	Effects of Superplastic Strain on Grain Growth at 907°C (1665°F) in Regular-Grade Ti-6Al-4V (Initial Primary Alpha Volume Fraction = 66).....	179
29	Effects of Superplastic Strain on Grain Growth at 907°C (1665°F) in Regular-Grade Ti-6Al-4V (Initial Primary Alpha Volume Fraction = 46).....	180
30	Effects of Superplastic Strain on Grain Growth at 871°C (1600°F) in Regular-Grade Ti-6Al-4V (Initial Primary Alpha Volume Fraction = 88).....	181

LIST OF TABLES - Cont.

TABLE		PAGE
31	Effects of Superplastic Strain on Grain Growth in Eli-Grade Ti-6Al-4V.....	181
32	Effects of Forming Cycles at 907°C (1665°F) on Grain Growth in Normal-Textured Regular-Grade Ti-6Al-4V, Panel J (Grain Size = 4.4 μm, Volume % Primary Alpha = 47).....	185
33	Effects of Forming Cycle at 907°C (1665°F) on Grain Growth in Normal-Textured Regular-Grade Ti-6Al-4V, Panel K (Grain Size = 6.0 μm, Volume % Primary Alpha = 88).....	185
34	Effects of Forming Cycle at 907°C (1665°F) on Grain Growth in Normal-Textured Regular-Grade Ti-6Al-4V, Panel E (Grain Size = 12.2 μm, Volume % Primary Alpha = 88).....	186
35	Effects of Forming Cycle at 907°C (1665°F) on Grain Growth in Eli-Grade Ti-6Al-4V, Panel X1 (Grain Size = 5.5 μm, Volume % Primary Alpha = 88).....	186
36	Comparisons of Superplastic Strain Rates at 871°C (1600°F) Determined From Cone-Forming Tests and Laboratory Incremental Strain-Rate Tests.....	189
37	Comparisons of Superplastic Strain Rates at 871°C (1600°F) Determined From Cone-Forming Tests and Laboratory Incremental Strain-Rate Tests.....	192
38	Comparisons of Superplastic Strain Rates at 907°C (1665°F) Determined From Cone-Forming Tests and Laboratory Incremental Strain-Rate Tests.....	192
39	Effect of Superplastic Strain on Grain Growth of Commercial-Grade Ti-8Al-1Mo-1V Formed at 949°C (1740°F).....	199
40	Comparisons of Superplastic Strain Rates at 760°C (1400°F) of Ti-15V-3Cr-3Sn-3Al Determined From Cone-Forming Tests and Laboratory Incremental Strain-Rate Tests.....	205
41	Comparisons of Superplastic Strain Rates at 802°C (1475°F) of Ti-15V-3Cr-3Sn-3Al Determined From Cone-Forming Tests and Laboratory Incremental Strain-Rate Tests.....	206
42	Comparison of Mechanical Properties of Normal-Textured Regular-Grade Ti-6Al-4V and Eli-Grade Ti-6Al-4V in As-Fabricated and Superplastically-Formed Conditions With a Superplastic Forming Temperature of 907°C (1665°F).....	209
43	Properties of Normal-Textured Regular-Grade Ti-6Al-4V and Eli-Grade Ti-6Al-4V Superplastically Formed at 870°C (1600°F)....	211

LIST OF TABLES - Cont.

TABLE		PAGE
44	Comparison of Tensile Properties of Basal-Textured Ti-6Al-4V in As-Received and Superplastically Formed Conditions; Superplastic Forming Temperature = 907°C (1665°F).....	212
45	Comparison of Tensile Properties of Ti-3Al-2.5V Sheet in As-Fabricated and Superplastically Formed Conditions; Superplastic Forming Temperature = 877°C (1610°F).....	214
46	Comparison of Tensile Properties of Ti-6Al-2Sn-4Zr-2Mo Sheet in As-Received and Superplastically Formed Conditions; Superplastic Forming Temperature = 907°C (1665°F).....	215
47	Comparison of Mechanical Properties of 1.27 mm (0.05 in.) Ti-8Al-1Mo-1V Sheet in Mill-Annealed and Superplastically Formed Conditions; Forming Temperature = 949°C (1740°F).....	215
48	Fatigue Properties of Superplastically Formed Normal-Textured Regular-Grade Ti-6Al-4V and Eli-Grade Ti-6Al-4V.....	217
49	Apparent Activation Energies for High-Temperature Flow of Titanium Alloys.....	225

SUMMARY

The major objective of this program was to establish the effects of metallurgical variables on the superplastic behavior of alpha-beta and beta titanium alloys. The metallurgical variables that were studied included grain size, beta transus, primary alpha, texture and anomalous microstructures in alpha-beta titanium alloys. The alpha-beta titanium alloys selected for this program included Ti-6Al-4V, Ti-8Al-1Mo-1V, Ti-6Al-2Sn-4Zr-2Mo, Ti-3Al-2.5V. The beta alloy used in this study was Ti-15V-3Cr-3Sn-3Al.

The effects of alloy chemistry, grain size, volume fractions of constituent phases, and anomalous microstructures on the superplasticity parameters at 800-900°C (1472-1796°F) of alpha-beta titanium alloys near alpha alloys, and a beta alloy were determined by strain-rate cycling, flat-ring compression, constant-stress, and constant-strain-rate tests. The strain-rate and strain (or equivalently, time) dependences of flow stress and strain-rate sensitivity were identified as the most important superplasticity parameters, with the continuous changes in alloy microstructures during superplastic deformation requiring proper consideration.

In the alpha-beta and near-alpha titanium alloys, the flow stress decreases and the strain-rate-sensitivity and necking resistance increase with decreasing grain size at 350-950°C (1562-1742°F) for strain-rate of 10^{-5} , 10^{-3} s⁻¹. With increasing strain and time, the strain-rate-sensitivity, m , decreases, the flow stress at constant strain-rate increases, and the strain rate at constant applied stress decreases as a consequence of increasing grain size. The flow stress at a constant strain rate of different alpha-beta alloys is uniquely related to grain size, beta transus temperature, and volume fractions of constituent phases at the test temperature. ELI grade Ti-6Al-4V and Ti-3Al-2.5V have lower flow stresses than the other alpha-beta and near-alpha alloys tested. Ti-6Al-4V alloys with elongated-alpha have significantly higher flow stresses and lower strain-rate sensitivities than regular grade Ti-6Al-4V. The blocky-alpha texture and banding microstructures have only small effect on the superplastic characteristics of Ti-6Al-4V. Because of the extensive grain growth in the beta alloy at high temperatures, the flow stress is considerably higher and the strain-rate sensitivity is lower than in Ti-6Al-4V.

A conical die was designed to provide a constant stress during forming at a fixed pressure. The straining in cone was shown to be quite uniform for alpha-beta titanium alloys. Biaxial strain-rates in conical die agree quite well with uniaxial strain-rate cycling data at high strain rate and short forming times. The conical die forming provided a good measure of straining at the slower strain rates and longer forming times where strain-rate cycling data was very inadequate due to grain growth. Biaxial forming studies confirmed that the two basic properties for superplasticity in alpha-beta titanium alloys were fine equiaxed alpha grain size and the ratio of the forming temperature to the beta transus.

For all the alpha-beta titanium alloys studied a small drop in tensile properties was observed for superplastically formed sheet compared to the as-received material in full annealed high primary alpha condition. No appreciable degradation was observed in fatigue properties of superplastically formed alpha-beta titanium sheet.

A single constitutive equation was obtained for the grain size, time and temperature dependences of strain-rate and this equation accurately describes the superplastic behavior of all alpha-beta titanium alloys investigated. This constitutive equation can be used to construct various three-dimensional plots involving flow-stress, strain, strain rate, strain-rate sensitivity, grain size, and temperature, and these three-dimensional plots are useful for determining the conditions for superplastically forming a titanium alloy of known grain size and beta-transus temperature.

SECTION I

INTRODUCTION

Titanium alloys are attractive for use in aircraft structures because of their excellent corrosion resistance, high strength-to-weight ratio, and high fracture-toughness. The shortage of titanium sponge and escalating fabrication costs of titanium mandate that aircraft design and the utilization of titanium alloys be more efficient. To reduce structural weights and fabrication costs of titanium alloys, increasing attention is being given to near-net-shape processing techniques, which include powder metallurgy, isothermal forging, and superplastic forming. For the fabrication of thin-section sheet-metal parts, superplastic forming with concurrent diffusion bonding (SPF/DB) has emerged as a practical lower-cost and material-saving method of fabrication. SPF/DB offers design freedoms not possible with conventional forming processes (Reference 1).

The cost and success of superplastically forming titanium-alloy aircraft parts depend on the size of the parts, the microstructure of the alloy, and process variables (temperature, pressure and time). Because few systematic studies have been made of the effects of material and process variables on the superplasticity of titanium alloys, this investigation was conducted with the objectives of delineating the effects of metallurgical and process variables on SPF/DB processing and establishing guidelines for optimizing alloy/processing combinations.

Previous investigations have given inadequate attention to the strain and time dependences of the superplasticity indices (flow stress and strain-rate sensitivity of flow stress). No attempts were made in earlier studies to produce systematic variations in the starting microstructures, and the limited ranges of microstructural and process variables studied were not sufficient to completely determine the limits of superplastic formability of titanium alloys. Furthermore, no attempts were made to correlate laboratory test data with actual superplastic forming data. The alloys and processing schedules selected for this study provided wide variations in alloy compositions and microstructures, and the previously ignored time and strain dependences of the superplasticity indices were given special emphasis. The effects of microstructural modifications resulting from SPF/DB on the properties

of the formed parts were studied, and uniaxial laboratory tests as well as biaxial production tests were used to characterize superplastic formability. The results of the investigation advance the understanding of superplasticity of titanium alloys and indicate the potential for improving SPF/DB of titanium alloys.

SECTION II

TECHNICAL BACKGROUND AND PROGRAM PLAN

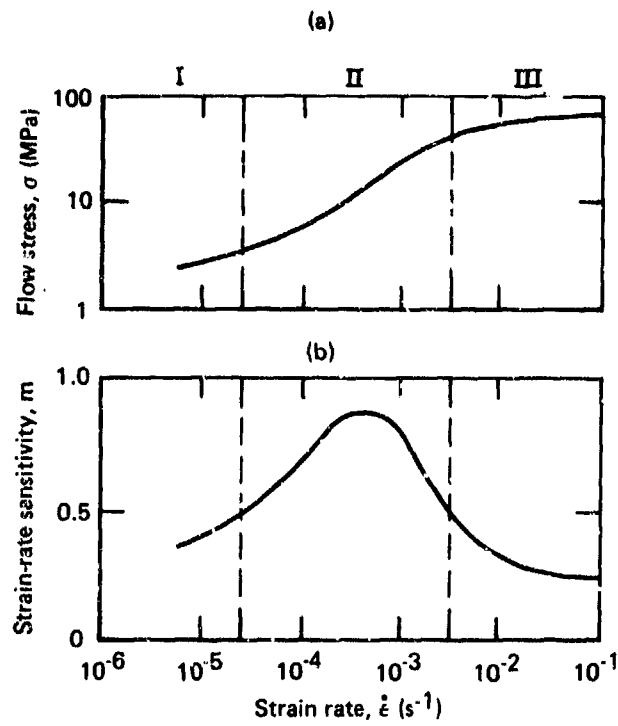
2.1 Superplasticity

2.1.1 The Superplasticity Phenomenon

Superplasticity, a necking-resistant flow which results from a high strain-rate sensitivity of flow stress, is generally associated with elongations of 100% or greater in tensile tests. The essential requirements for the occurrence of superplasticity are (1) a temperature greater than $0.5 T_m$, where T_m is the melting temperature, so that diffusional processes are dominant, (2) equiaxed grains, $<10 \mu m$ in size, so that flow stresses are low and the grain-boundary sliding contribution to strain is high, and (3) a two-phase microstructure to retard grain coarsening. Many studies have been devoted to the mechanisms of superplasticity, but comparable studies have not been conducted to provide guidelines for the practical utilization of superplasticity in manufacturing operations. Because of the capability of the process to produce, at low gas pressures of 0.3/-1MPa (50-150 psi), complex-contoured shapes of uniform thickness requiring greater than 300% deformation, superplastic forming has emerged as a practical advanced fabrication technique for large titanium alloy structural parts.

The superplastic formability of a material is related to the flow parameters (temperature, strain rate, flow stress, and strain), the initial microstructure, and the microstructural changes that occur during superplastic deformation. A sigmoidal relationship between the flow stress and strain rate and the corresponding variation of strain-rate sensitivity, m , with strain rate, as shown in Figure 1, have been proposed to be indicative of superplasticity. However, recent investigations (References 2 and 3) have established the inadequacy of plots such as those in Figure 1 for completely describing the superplastic characteristics of a material.

For superplastic behavior, the strain rate sensitivity of flow stress (defined by the relation $m = d \ln \sigma / d \ln \dot{\epsilon}$, where σ is the flow stress and $\dot{\epsilon}$ is the strain rate) is large ($m > 0.3$) compared with normal behavior ($m \approx 0.1-0.2$). The resistance of a material to the formation of an incipient neck during elongation increases as m increases because a developing neck increases the local strain rate and thus increases the strain required for necking to continue. If the applied stress is insufficient to propagate the neck, the remainder of the specimen continues to deform plastically.



QP03-0249-157

Figure 1. Typical strain-rate dependences of (a) flow stress and (b) strain-rate sensitivity, m , of flow stress for Ti-6Al-4V at superplastic-forming temperatures.

Empirically, m values of 0.3-0.5 are necessary for superplastic behavior, and most superplasticity at least have used only the m -value to characterize the superplasticity of a material. Soviet investigations (Reference 4) have not generally used the strain-rate-sensitivity index to describe the superplastic behavior. Instead, they characterize superplasticity by the simultaneous occurrence of anomalously large uniform elongation, absence of necking, and anomalous reduction of flow stress.

The mechanism of superplasticity involves grain-boundary sliding with accommodation at triple points by either atomic diffusion or dislocation motion (References 5-8). Diffusion-accommodated flow is less dominant as the strain-rate is increased above about 10^{-3} s^{-1} . At high strain-rates, dislocation interactions dominate and cause work-hardening; consequently, tensile elongations are not abnormally high. At high strain-rates, a finer grain-size nevertheless is advantageous because of lessened load requirements for high strain-rate forming.

2.1.2 Superplasticity of Titanium Alloys

Although phase-transformation superplasticity in titanium was reported in 1965, the first indication of structural superplasticity in titanium alloys under isothermal conditions was reported by Lytle, et.al. (Reference 9). The first detailed study of the superplasticity in titanium alloys was conducted by Lee and Backofen (Reference 10), who observed large tensile elongations up to 1000% and a high strain-rate sensitivity of flow stress ($m = 0.8$) at 900°C ($0.65 T_m$) in titanium alloy microstructures with grain sizes of 6-24 μm . A cursory study (Reference 11) of the superplasticity of six different heats of Ti-6Al-4V produced to MIL-T-9046 specifications reiterated the conclusions of Lee and Backofen, although the effects of microstructural and process variations on the degree of superplasticity were incomplete and inconclusive. The results of a recent study by Arieli and Rosen (Reference 12) invalidated the previously reported optimum superplasticity conditions, namely, peak m -value and a sigmoidal relationship between flow stress and strain rate.

2.1.3 Effects of Metallurgical Variables on the Superplasticity of Titanium Alloys

1. Alloy chemistry: The effects on superplasticity of alloy chemistry arise from (1) the solid-solution strengthening effect, (2) the effects of alloying elements on the beta-transus temperature and volume fractions of constituent phases, and (3) the effects of alloying elements on the diffusion rates. At the high temperatures and slow strain rates encountered in superplastic forming

of titanium alloys, the solid-solution strengthening contribution to the flow stress is not significant, although the alloying elements alter the strain-rate sensitivity of flow stress. Alloying additions such as aluminum, carbon, nitrogen, and oxygen are alpha stabilizers in titanium alloys and raise the beta-transus temperature, whereas vanadium, molybdenum, chromium, and iron stabilize the beta lattice and lower the beta-transus temperature. Thus, variations in concentrations of the alloying elements result in varying amounts of alpha and beta phases at high temperatures and affect the superplasticity indices. Depending on the relative sizes and crystal structures of the solute and solvent metals, the diffusion rates are either enhanced or lowered. Because superplastic deformation occurs predominantly by diffusion processes, enhanced diffusion rates are conducive to higher initial deformation rates, but because enhanced diffusion promotes faster grain growth, the deformation rate may decrease with increasing time.

2. Grain size: Grain size is the single material variable that has the most pronounced effect on superplasticity of titanium alloys. Superplastic behavior is generally observed for grain sizes $<10\text{ }\mu\text{m}$. For improved superplasticity, a smaller grain size is desired because with decreasing grain size, the flow stress decreases and the strain-rate sensitivity of flow stress increases. The reduction in flow stress with decreasing grain size is the opposite of the Hall-Petch grain-size dependence of flow stress observed at low temperatures, where deformation occurs by dislocation-glide processes. At any given applied stress in the superplastic region, a smaller grain size results in an increased strain rate because of the increased contribution to total strain from grain-boundary sliding.

3. Phase distributions: Early research on superplasticity indicated the requirement for superplasticity of a two-phase microstructure with approximately equal amounts of phases of similar deformation characteristics. A large number of interphase boundaries is beneficial for retarding grain growth. Recent investigations have shown that superplasticity can be conferred on fine-grained single-phase alloys by incorporating stable second-phase dispersoids to retard grain growth (References 13-15). Superplasticity is significantly affected by the nature of sliding boundaries. When grains of the same phase slide, local hardening in the heavily-strained boundary regions is relieved by grain boundary migration, which creates new strain-free material in which sliding can continue. Hardened regions created by sliding at interfaces between chemically dissimilar phases cannot be relieved by simple grain boundary migration without redistribution of the solute atoms.

The stability of a two-phase dispersion at temperature in the context of superplastic forming is discussed in detail by Edington (Reference 16). A large volume fraction and fine dispersion of one phase is desirable for good stability (low growth tendency) of the other phase. At relatively low temperatures in Ti-6Al-4V there will be a large volume fraction of alpha and a low volume fraction of beta. However, because the temperature is low, little grain growth of alpha will occur. At relatively high temperature, there will be a large volume fraction of beta and a low volume fraction of alpha. In this case the temperature is such that grain growth occurs. Little growth of alpha occurs because of the large volume of beta phase. However, rapid grain growth of the beta takes place since the small amount of alpha is insufficient to restrict beta grain boundary migration. At intermediate temperatures a combination of intermediate growth kinetics and relatively large volume fractions of the two phases (50%) exist.

4. Crystallographic texture: Crystallographic texture is an important structural parameter in assessing titanium alloys for service use. Texture influences the high-temperature flow behavior hexagonal close-packed alloys other than titanium alloys crystal structures. For example, with basal textured samples, high initial yield stress and flow-softening are observed when the stress axis is perpendicular to the sheet, whereas in samples that have fiber texture, normal stress-strain behavior is recorded (Reference 17). In titanium alloys, however, a systematic study of the influence of texture on high temperature flow behavior, particularly on superplastic deformation, is completely lacking. Because superplastic forming involves exposure of parts to high temperature for prolonged periods, an evaluation of the high temperature stability of texture is essential for predicting the properties of the formed components and for successful implementation of the fabrication processes.

5. Microstructural anomalies: The principal microstructural anomalies that may affect the superplasticity of titanium alloys are elongated-alpha, banding, and blocky-alpha. Elongated alpha results from insufficient working of Widmanstätten alpha needles and annealing at temperatures high in the alpha-beta field. Although Widmanstätten alpha has been shown to have a deleterious effect on titanium alloy superplasticity, the effect on superplasticity of coarse elongated-alpha has not been well established.

Banding is the term applied to alternate layers of heavily-worked alpha and lightly-worked Widmanstätten alpha. The reasons for the occurrence of banding are not clearly understood, but likely contributors to the phenomenon are inhomogeneities in chemical composition and the amount of deformation. The heterogeneous deformation is accentuated by further working, which strings the nonhomogeneous deformation regions into bands in the LT plane (along the L direction). Banding adversely affects SPF behavior because of the presence of undesirable Widmanstätten alpha.

Blocky-alpha is the term used for two different kinds of microstructural anomalies. Originally, the term was used to refer to "blocks" of oxygen-enriched alpha phase (basically rectangular on a polished surface) produced by holding the alloy for long times at temperatures just below the beta-transus temperature. This anomaly, once formed, is very difficult to remove. Blocky alpha has also been referred (Reference 11) to coarse distorted alpha formed in alloys that have been thermomechanically processed just below the beta-transus temperature and in the absence of further recrystallization, these grains appear blocky, particularly in the LT plane. These blocks of alpha are not enriched in oxygen and their influence on superplasticity depends on the matrix microstructure surrounding the alpha blocks. The amount of blocky alpha can be varied by varying the amount of deformation, processing temperature, and annealing.

2.2 Program Objectives

The objectives of this investigation were to:

- (1) Determine the effects of metallurgical variables (alloy composition, grain size, volume fractions of constituent phases, crystallographic texture, and temperature) on the strain and strain-rate dependences of flow stress for titanium alloys.
- (2) Identify superplasticity indices that characterize the superplastic formability of titanium alloys.
- (3) Develop a reliable, low-cost, biaxial production test method for evaluating the superplastic formability of titanium alloys under different parts-fabrication conditions and for validating laboratory measurements of superplasticity indices.
- (4) Determine the microstructural and mechanical properties modifications produced during superplastic forming.

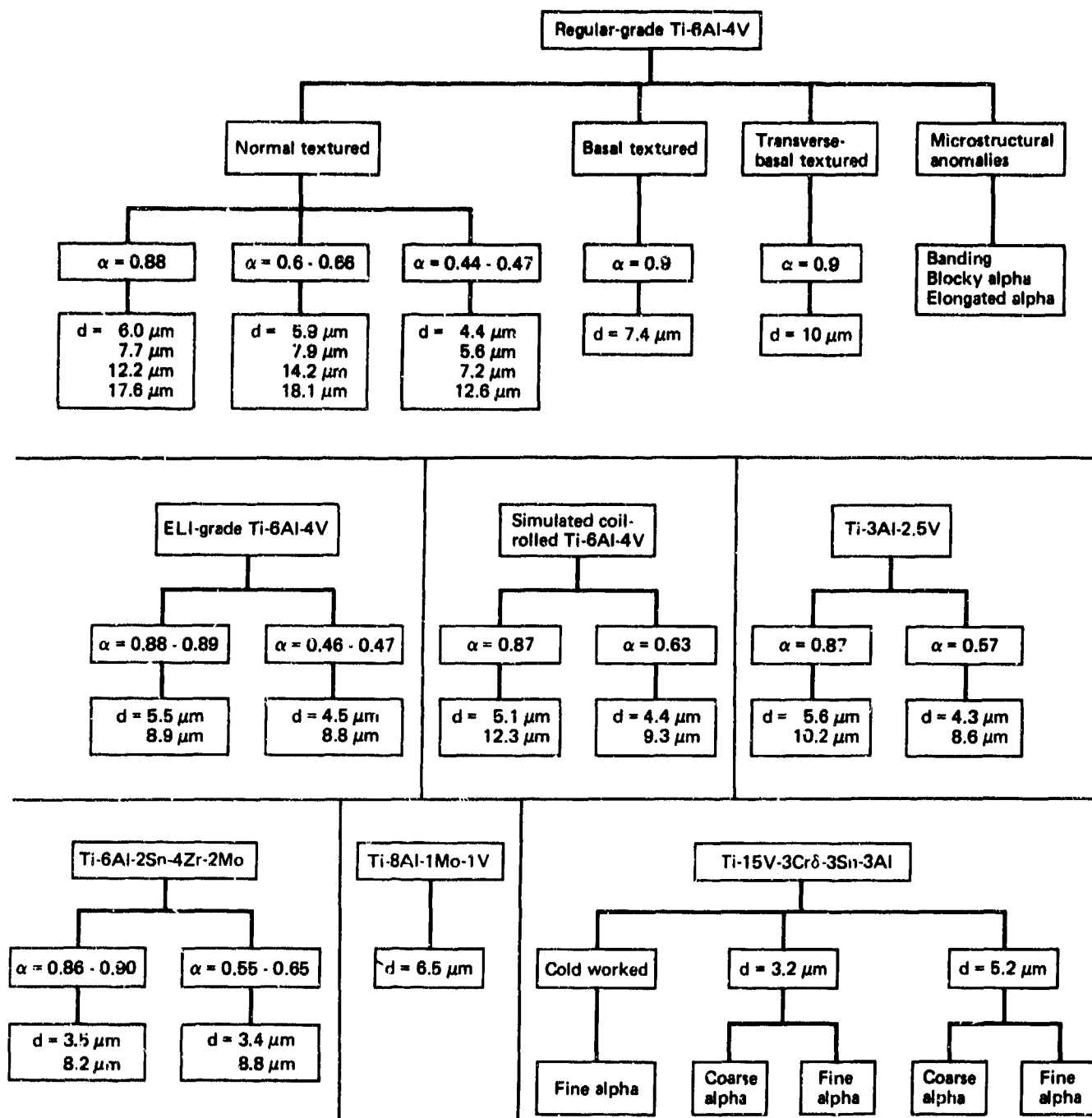
2.3 Program Plan

2.3.1 Alloy Selection and Processing

The alloys and microstructural variations selected for this investigation are summarized in Figure 2. This titanium alloy selection and microstructural variations were made by Douglas Aircraft Co. with Air Force Materials Lab concurrence. The selections were made to determine the effects of wide variations of alloy chemistry and microstructure on the superplasticity of titanium alloys and to determine the ranking of various alloys for superplastic forming of aircraft structural parts.

Ti-6Al-4V is the principal titanium alloy used in aircraft structures. Regular-grade, normal-textured Ti-6Al-4V was selected as the base alloy for developing a comprehensive metallurgical understanding of superplastic forming in alpha-beta titanium alloys. ELI grade Ti-6Al-4V was selected because of its lower beta-transus temperature, approximately 25°C (45°F) below the beta-transus temperature of regular-grade Ti-6Al-4V. Because of the lower processing cost, fine grain size, and potential for producing longer lengths that can be achieved by continuous coil rolling of Ti-6Al-4V, simulated coil-rolled Ti-6Al-4V was selected. The other alpha-beta alloy, Ti-3Al-2.5V, was selected because it has smaller concentrations of alloying elements and a much lower beta-transus temperature than Ti-6Al-4V, and it is used in aircraft secondary structures such as honeycomb and hydraulic tubing.

The near-alpha alloys selected for this investigation were Ti-6Al-2Sn-4Zr-2Mo and Ti-8Al-1Mo-1V. Ti-6Al-2Sn-4Zr-2Mo is a high-temperature creep-resistant alloy with potential for missile structure applications. The beta-transus temperature of Ti-6Al-2Sn-4Zr-2Mo is close to that of regular grade Ti-6Al-4V. Ti-8Al-1Mo-1V contains a large amount of the alpha stabilizer, aluminum, and small amounts of the beta stabilizers, molybdenum and vanadium. Ti-8Al-1Mo-1V has excellent elevated-temperature creep and short-time tensile strength. Because of the recent interest in Ti-8Al-1Mo-1V for missile applications, the conventionally-processed alloy was included in the investigation to determine the temperature and pressure ranges required for its superplastic forming and diffusion bonding. This alloy, which has a beta-transus temperature of 1030°C (1886°F), also increased the data base for determining the influence of beta-transus temperature on superplasticity. In the beta-alloy category, Ti-15V-3Cr-3Sn-3Al alloy was selected because its superplasticity



GP03-0248-150

Figure 2. Alloy compositions and microstructures evaluated in this study. Volume fraction of primary alpha is denoted by α and grain size is denoted by d .

was previously little studied. Ti-15V-3Cr-3Sn-3Al is a metastable beta alloy with excellent deep-hardenability and cold-formability, and it can be strengthened to high levels by aging to precipitate hexagonal alpha phase in the body-centered-cubic matrix.

The alloys were thermomechanically processed and heat-treated to produce the microstructural variations shown in Figure 2. The basic program was organized to provide a broad range of metallurgical variables for regular grade Ti-6Al-4V.

The above procuring, processing and characterization of the titanium alloys in this program was performed by Crucible Materials Research Center (CMRC), Colt Industries, Inc.

2.3.2 Superplasticity Characterization-Laboratory Tests

The method used by many investigators to determine the superplasticity indices consists of successively deforming a tensile specimen to fixed amounts of strain (usually 3-5%) at different strain rates and plotting the flow stress at a fixed strain as a function of strain rate. The method does not account for work hardening or softening because the flow stress is evaluated at small strains, and the effect on flow stress of the grain growth accompanying large deformations is ignored. In actual superplastic forming operations, the material is under load at high temperature for longer times. Thus, for the laboratory test-data to be useful for forming calculations, it is imperative to determine the flow stress as a function of both strain and holding time at the test temperature.

Since laboratory test methods must simulate manufacturing processes to yield practical information on the flow behavior of materials, incremental strain-rate tests, constant strain-rate tests, constant stress tests, and flat-ring compression tests were systematically evaluated and compared with the results of forming tests. These laboratory tests were made at McDonnell Douglas Research Laboratory (MDRL).

1. Incremental strain-rate test: For incremental strain-rate testing, a single specimen is strained at different strain rates, and the equilibrium load at each strain rate is determined. For this investigation, the true stress and true strain-rate were computed from load-displacement curves, and the strain-rate sensitivity or m-value was determined by the slope of the third-degree polynomial curve which best fit the flow-stress/strain-rate data. Previous investigations have used slightly different methods for computation of m-values (Reference 18). The time and strain dependences of microstructure and the variation of the steady-state strain with strain rate make attainment of a true equilibrium load impractical

Thus, the m -values obtained by short-time strain-rate-cycling tests are only approximate.

2. Constant strain-rate test: Constant-strain rate tensile tests in a dry argon atmosphere were performed on an MTS machine by changing the actuator speed at regular intervals in direct proportion to the increase in the specimen gauge length. The frequency of actuator speed changes was selected so that the instantaneous true-strain rate did not differ by more than 5% from the nominal value. Most existing data on superplasticity have been analyzed on the basis of constant-strain-rate testing although the experiments were conducted at constant cross-head speed. Because of the large strain-rate dependence and large elongations exhibited by superplastic materials, a correction must be applied to engineering-stress/engineering-strain curves to indicate the shape of the flow curves expected under constant strain-rate conditions, and these corrections significantly change the m values. To obtain comparisons between constant strain-rate and constant crosshead-speed (thus decreasing strain rate) conditions, constant-crosshead-speed tests were also conducted in a dry-argon atmosphere on a gear-driven Instron machine. The constant-strain-rate tests yield the best measures of the time and strain dependences of flow stress.

3. Constant stress test: For constant-stress testing, the elongation of a tensile specimen subjected to constant stress was monitored as a function of time, and the time dependences of strain and strain-rate were determined at different stress levels. This laboratory test simulates the actual forming operation because stress is the independent variable in both cases. The test provides an inexpensive and efficient means of determining quantitatively the effects of metallurgical variables and testing variables on superplastic behavior. As will be shown later, the data obtained from constant-stress tests agree well with cone-forming data.

4. Flat-ring compression test: The flat-ring compression test (References 19) incorporates the frictional effects at the tooling/work-piece interface and gives practical data on the flow properties of materials. The flat-ring specimen must satisfy certain geometrical requirements (namely, the ratios outer-diameter: inner-diameter: thickness must be in the range 6:3:2-6:3:0.5). The change in diameter produced by a given amount of compression in the thickness direction of the flat-ring specimen is related to the interfacial friction, M (defined as the ratio

of the shear stress of the die lubricant to the shear stress of the material undergoing deformation), between the specimen and the flat compression dies.

The interfacial friction factor and the strain dependence of flow stress can both be calculated from measurements of the loads required to deform the rings to different strains at a fixed strain rate. From tests on several rings at various strain rates, the compressive strain-rate-sensitivity of the material can be determined. The efficacy of different die lubricants can be quantitatively assessed from flat-ring compression tests.

The flat-ring compression tests of this study were performed on 19-mm (0.75 in.) O.D. x 9.5-mm (0.375 in.) I.D. x 1.5-mm (0.06 in.) thick ring specimens using 60-mm diameter 22-4-9 steel compression rams. The sample and the flat faces of the rams were coated with Delta Glaze 68 lubricant. The rams were heated to the desired temperature in a three-zone, resistance wound, split furnace. The ring specimen was placed on the flat face of the lower ram and maintained at temperature for 10 minutes before compression was begun. Compression tests were conducted in argon at 906°C for strain rates of 10^{-3} , 10^{-4} and $3 \times 10^{-5} \text{ s}^{-1}$. Some tests were conducted in a vacuum of 10^{-3} Pa to compare flow-stress/strain behavior in vacuum with that in argon.

The flat-ring compression tests provide accurate data for the variation of flow stress with strain because necking and the inhomogeneous deformation generally encountered in tensile tests do not occur in compression tests. The small initial thickness of the rings made accurate flow-stress data above $\approx 60\%$ strain difficult to obtain because the load measurements were not representative of the ring deformation loads.

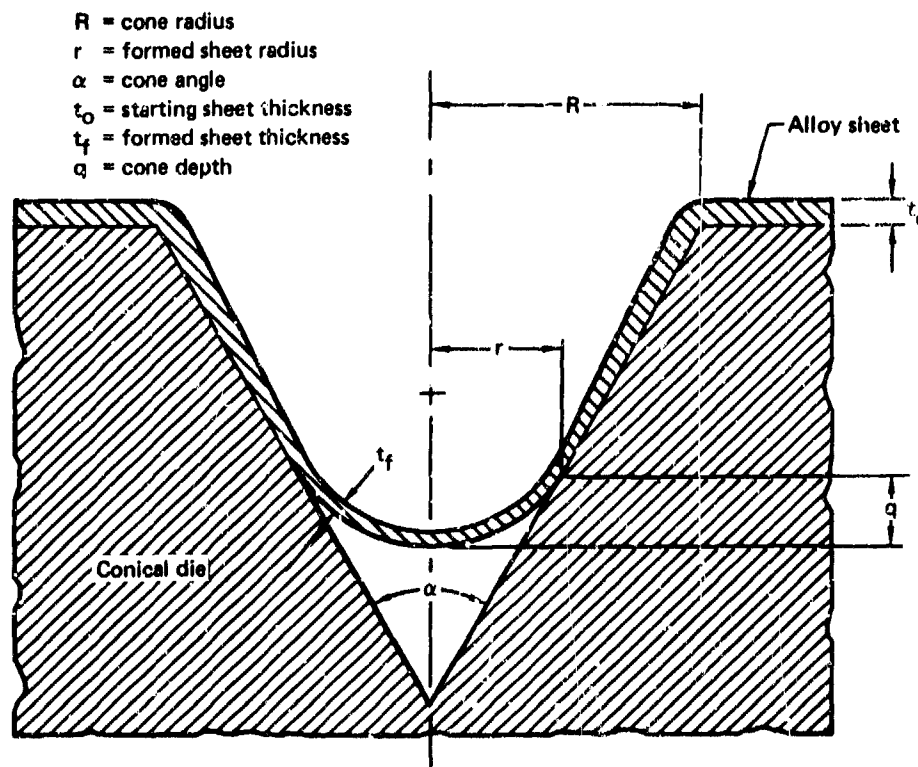
2.3.3 Superplastic-Forming Evaluation

Laboratory superplasticity tests performed on specimens under uniaxial tension provide quantitative information on the effects of metallurgical variables on the high temperature deformation of titanium alloys. However, the effects of superplastic-forming fabrication conditions and multiaxial stressing cannot be determined directly from laboratory tests, and the effects of gross material inhomogeneities on superplastic forming may go undetected in tests of small laboratory specimens. Hemispherical biaxial free forming of sheet material at constant strain rate, using

gas pressure requires a complex variable pressurization cycle. Therefore, a simplified, low-cost, test method was designed to evaluate the superplastic formability of titanium alloys under different fabrication conditions.

The superplastic forming evaluation was accomplished at Douglas Aircraft Company following the laboratory tests at MDRL.

A conical die was designed to provide a constant-stress condition at constant applied gas pressure during biaxial superplastic forming of titanium alloy sheet. A cross-section of the die is shown in Figure 3. Analytical expressions were derived for the stress and strain as functions of gas pressure, P , radius, R , cone angle, α , cone depth, q , and initial alloy-sheet thickness, t (see Appendix A). The results indicated that a cone angle of 57° provides a constant stress condition at a fixed gas pressure.



GP03-0230-137

Figure 3. Cross-section of conical die for superplastic forming evaluation.

The stress, σ , on the part being formed when the material first touches the die wall is given by (Reference 20).

$$\sigma = \frac{R}{4t_1} \frac{(1 + H^2)^2}{H} P, \quad (1)$$

where t_1 is the initial thickness, and $H = q/R \approx 0.595$ for a conical die angle of 57° . The stress on the forming part at any instant can also be determined from thickness measurements using the relation

$$\sigma = \frac{x}{2t} P, \quad (2)$$

where σ is the flow stress and x is the radius of membrane curvature.

The strain in the material undergoing superplastic forming is related to the cone depth by the relationship (see Appendix A),

$$\epsilon = \ln \frac{(q - q_2)}{(q - q_1)}, \quad (3)$$

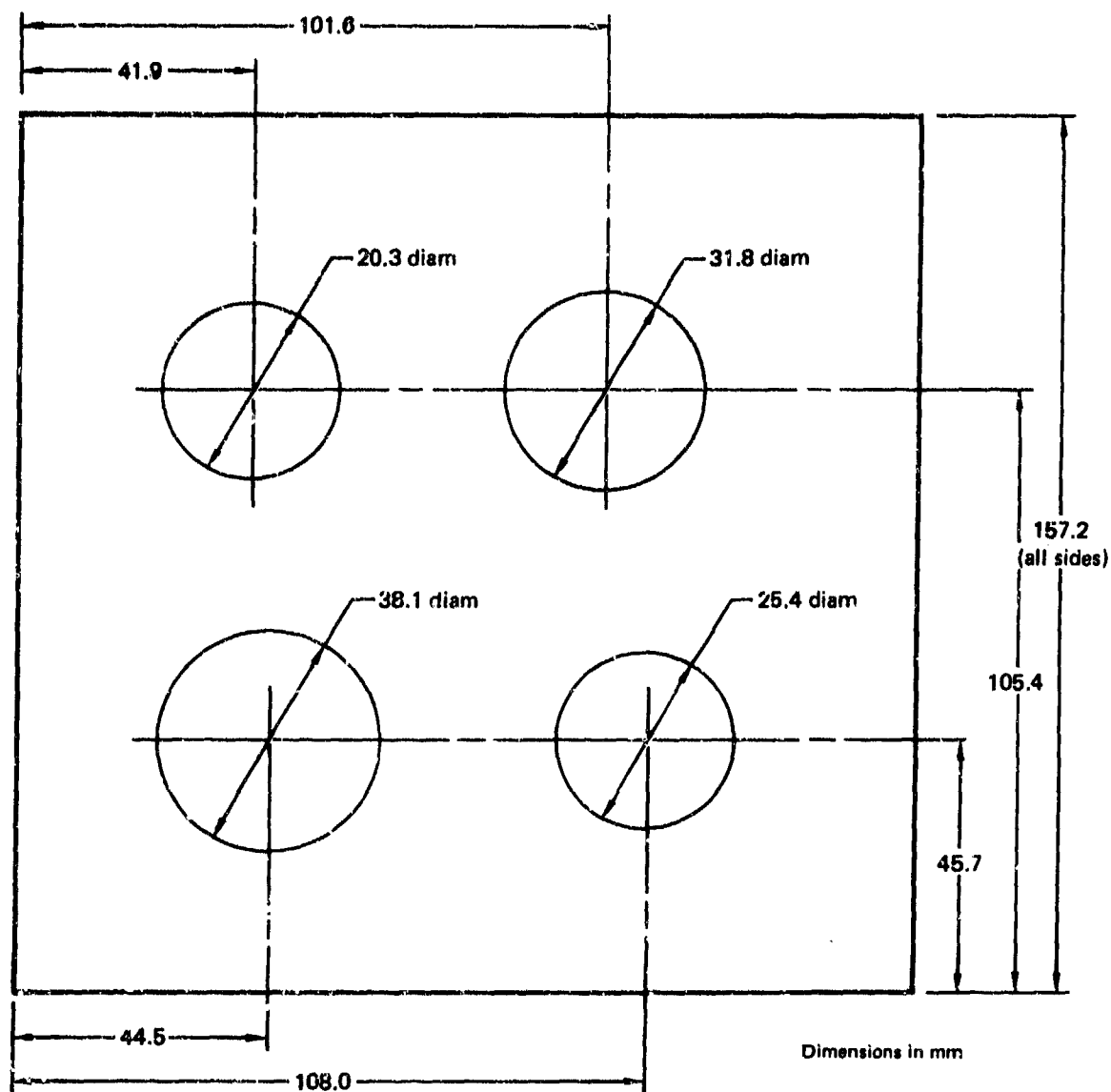
where q is the instantaneous depth of the cone, q_2 is the final depth of the formed cone, and q_1 is the depth of the cone when the material first touches the die wall.

Using a single die with several 57° cones having different cone radii, forming of a single panel can determine the strain-rate dependence of stress for an alloy from the applied gas pressure, the time of forming, and the final cone depths. Note that the strain rate determined by this method is the average strain rate. The sketch of the multiple-cone die with 57° cone angles that was used in this

program is shown in Figure 4. Type 430 steel was selected for the die based upon the compatibility of the thermal expansion of Type 430 steel with titanium alloys at elevated temperatures.

The experimental procedure used for biaxial forming consisted of the following steps:

- (1) Heat the conical dies and titanium alloy to the desired forming temperature in a flowing argon atmosphere.
- (2) Soak at temperature for 15 minutes.
- (3) Pressurize at a rate of 0.069 MPa (10 psi) per minute to the desired forming pressure.
- (4) Hold at constant pressure and temperature for the preselected forming time. The initial forming that occurs during the pressurization cycle was measured on titanium panels for each pressure and temperature cycle used in this program to evaluate the forming that occurs during the constant pressure period.



GP03-0249-149

Figure 4. Multicone die configuration for superplastic-forming evaluation of titanium alloys.

SECTION III

ALLOY PROCESSING AND CHARACTERIZATION

3.1 Regular Grade Ti-6Al-4V (Normal Texture)

Starting stock for the standard grade Ti-6Al-4V was purchased from the Stainless Steel Division, Colt Industries/Crucible Inc. Description of the materials and characterization data are given in Table 1 for the standard grade Ti-6Al-4V alloy. As is generally true for metallic systems, the grain size in Ti-6Al-4V can be changed by deforming (straining) the material sufficiently for subsequent elevated temperature annealing to result in recrystallization. Weakly textured material is produced by a standard hand sheet practice of cross rolling 3x to 5x final in the 816° - 927°C (1500°-1700°F). Temperature is maintained by the pack rolling technique, in which the material is enclosed in a pack which allows the temperature of the material to be maintained in the critical range during the rolling. The exact process sequence varies according to the structure/properties of the starting material and the converter's capabilities. Therefore, process verification trials were conducted before initiating production rolling.

The process verification trial covered two temperatures, 843° and 913°C (1550° and 1675°F) and three cross roll factors, 3x, 4x and 5x. The starting stock, 21 mm (0.840 inch) thick, was reduced to the penultimate gage by hot rolling from 941°C (1725°F). Reductions were 15-18 percent per pass with a reheat after every second pass. The sequence from the penultimate gage via pack rolling used a two sheet insert and 6.4 mm (0.25 inch) carbon steel cover plates. Again, reductions were 15-18 percent per pass with reheats after every second pass. Tensile test data for the mill annealed condition [1 hr - 705°C (1300°F), air cool] are given in Table 2. The data showed that either a 5x cross roll at 913°C (1675°C) or a 4x cross roll at 843°C (1550°F) gave the desired result of a nearly-isotropic 0.2 percent offset yield strength. The 843°C (1550°F) - 4 x cross roll process was selected because the microstructure appears to be more heavily worked and the recrystallized grain size is more uniform than the 913°C (1675°F) - 5x cross roll material.

TABLE 1. SPECIFICATIONS AND CHEMICAL COMPOSITIONS OF TITANIUM ALLOYS.

Alloy	Alloy supplier	Heat no.	Starting ingot description			Billet description						Chemical composition (wt%)										
			Mass Kg (lb)	Diam mm (in.)	Length mm (in.)	Mass Kg (lb)	Length mm (in.)	Width mm (in.)	Thickness mm (in.)	Beta transus °C (°F)	Al	V	Zr	Mo	Cr	Fe	O	N	C	H		
Standard-grade Ti-6Al-4V	Crucible	G52063	4311 (9405)	838 (33)	1722 (67.8)	445.5 (980)	5080 (200)	918 (36)	22 (0.850)	999 (1930)	6.4	4.0	-	-	-	0.16	1.175	0.021	0.03	0.0033		
ELI-grade Ti-6Al-4V	Crucible	RS1645	1845 (4060)	737 (29)	1008 (39.7)	90.9 (200)	508 (20)	508 (20)	76 (3)	968 (1775)	6.0	3.8	-	-	-	0.05	0.094	0.01	0.013	0.0044		
Ti-15V-3Cr-3Sn-3Al	Timet	P-3357	-	-	-	-	380 (15)	380 (15)	1.9 (0.075)	746 (1375)	3.1	15.2	2.9	-	2.7	0.14	0.11	0.017	0.018	0.014		
Ti-6Al-2Sn-4Zr-2Mo	RMI	802845	-	-	-	-	2489 (58)	914 (36)	1.4 (0.056)	993 (1920)	5.9	2.0	3.9	2.0	-	0.06	0.088	0.012	0.02	0.0101		
Coil-rolled Ti-3Al-2.5V	Crucible	PS2133	-	-	-	-	-	685 (27)	2.2 (0.086)	935 (1715)	3.1	2.6	-	-	-	0.08	0.08	0.01	0.025	0.0034		
Simulated-coil Ti-6Al-4V	Crucible	G50080	-	-	-	-	-	965 (38)	4.2 (0.166)	988 (1810)	6.2	4.2	-	-	-	0.10	0.137	0.013	0.052	0.002		
Ti-8Al-1Mo-1V	RMI	890597	-	-	-	-	2438 (56)	914 (36)	1.14 (0.045)	1032 (1890)	8.1	0.9	-	1.0	-	0.05	0.09	0.016	0.02	0.0079		
Ti-8Al-1Mo-1V	RMI	890597	-	-	-	-	2438 (56)	914 (35)	1.27 (0.050)	1032 (1890)	8.1	0.9	-	1.0	-	0.05	0.09	0.016	0.02	0.0079		

CP-55-504-146

TABLE 2. EFFECTS OF ROLLING TEMPERATURE AND CROSS-ROLL FACTORS ON TENSILE PROPERTIES OF PACK-ROLLED Ti-6Al-4V.

Furnace temperature °C (°F)	Cross-roll factor	Test direction	Ultimate tensile strength MPa (ksi)	0.2% offset yield stress MPa (ksi)	Total Elongation (%)	Young's modulus E x 10 ³ MPa (ksi)	Directionality, Δ(T-L)		
							UTS MPa (ksi)	YS MPa (ksi)	Modulus E x 10 ³ MPa (ksi)
913 (1675)	3X	L	1084 (157.2)	1024 (148.5)	18.0	127 (18.4)	-29.6 (-4.3)	-32.4 (-4.7)	±9.0 (±1.3)
		T	1054 (152.9)	992 (143.8)	13.0	136 (19.7)			
913 (1675)	4X	L	1082 (156.9)	995 (144.3)	19.0	130 (18.9)	-31.0 (-4.5)	-24.1 (-3.5)	±0.7 (±0.1)
		T	1051 (152.4)	971 (140.8)	17.0	131 (19.0)			
913 (1675)	5X	L	1076 (156.0)	1008 (146.2)	17.0	137 (19.9)	±6.9 (±1.0)	±5.5 (±0.8)	-0.7 (-0.1)
		T	1083 (157.0)	1014 (147.0)	12.0	137 (19.8)			
843 (1550)	3X	L	1103 (160.0)	1044 (151.4)	19.0	137 (19.9)	-26.9 (-3.9)	-29.0 (-4.2)	-1.4 (-0.2)
		T	1076 (156.1)	1015 (147.2)	18.0	136 (19.7)			
843 (1550)	4X	L	1087 (157.6)	1014 (147.0)	21.0	115 (16.7)	-4.1 (-0.6)	±6.2 (±0.9)	±23.4 (±3.4)
		T	1083 (157.0)	1020 (147.9)	15.0	139 (20.1)			
843 (1550)	5X	L	1078 (156.4)	1029 (149.3)	17.0	148 (21.5)	±54.5 (±7.9)	±18.6 (±2.7)	-18.6 (-2.7)
		T	1133 (164.3)	1048 (152.0)	19.0	130 (18.8)			

QP03-0249-107

Part of the process verification included characterization of the microstructure of the standard grade Ti-6Al-4V at each stage of the processing. Microstructures of the material processed to develop a normal of isotropic product are shown in Figures 5 and 6. The microstructure of the starting stock, 22 mm (0.850 inch) thick plate, is a well worked Widmanstätten structure which has undergone some recrystallization during rolling as shown in Figure 5a. Figure 5b illustrates the microstructure of the plate after laboratory rolling to 7.4 mm (0.29 inch) thickness. The microstructure of the 1.5 mm (0.06 inch) sheet pack rolled at 843°C (1550°F), 4x cross rolled and milled annealed at 704°C (1300°F) 1 hour is shown in Figure 6a and the microstructure after a subsequent anneal at 760°C (1400°F) for 8 hours in Figure 6b. Only a small amount of recrystallization occurred in the mill annealed material. The sheet annealed for 8 hours showed more complete recrystallization, but a substantial portion of the structure remained unrecrystallized.

Figure 7 illustrates the microstructures of material annealed for 1 hour at 871°C (1600°F), 927°C (1700°F), and 982°C (1800°F), and furnace cooled. A small amount of unrecrystallized material remained in the sheet given the lowest temperature anneal. The two high temperatures showed complete recrystallization.

Analysis of the heat treated samples included determinations of the phase proportions, alpha grain size, beta grain size, and the alpha plus beta grain size. Phase proportions were determined by point counting. The alpha plus beta grain size was obtained by the linear intercept method counting all phase boundaries. The separate alpha and beta grain sizes were determined by counting the number of alpha or beta grains per unit length of test line applied to the microstructure.

Alpha plus beta grain sizes for each of the six regular-grade and ELI-grade Ti-6Al-4V normal microstructures studied are listed in Table 3. The sheets were annealed for 1 hour at 927°C (1700°F) and furnace cooled to produce a uniform, equiaxed, recrystallized structure. This annealing temperature represents the maximum useful temperature for superplastic forming of regular-grade Ti-6Al-4V sheet. All alpha plus beta grain sizes were determined on the L-S plane by measuring the mean linear intercept of all phase boundaries with straight lines in the L direction and in the S direction. A minimum of five areas were counted for each sample. The results showed a somewhat finer grain size and a slightly lower mean grain aspect ratio for sheets rolled from 843°C (1550°F).

TABLE 3. EFFECTS OF ROLLING SCHEDULES ON RECRYSTALLIZED GRAIN SIZES OF CROSS-ROLLED REGULAR-GRADE Ti-6Al-4V ANNEALED AT 927°C (1700°F) FOR 1 h AND FURNACE COOLED TO 25°C.

Rolling conditions		Mean linear intercept L-S plane (μm)		Average linear intercept (μm)	Mean grain aspect ratio L/S
Furnace temperature °C (°F)	Cross- roll factor	L direction	S direction		
913 (1675)	3X	4.7	4.1	4.4	1.1
913 (1675)	4X	5.3	4.2	4.75	1.3
913 (1675)	5X	5.4	3.8	4.6	1.4
843 (1550)	3X	4.5	3.6	4.05	1.2
843 (1550)	4X	5.0	4.2	4.6	1.2
843 (1550)	5X	4.5	4.0	4.25	1.1

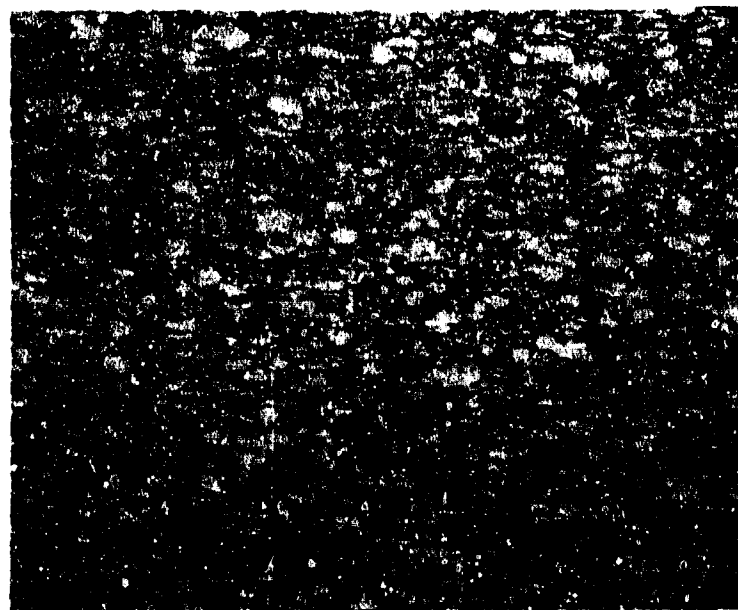
Mean linear intercept determined by counting intersections of all phase boundaries with a straight line. Each value represents an average of five areas counted.

GP03-0249-108

(a)



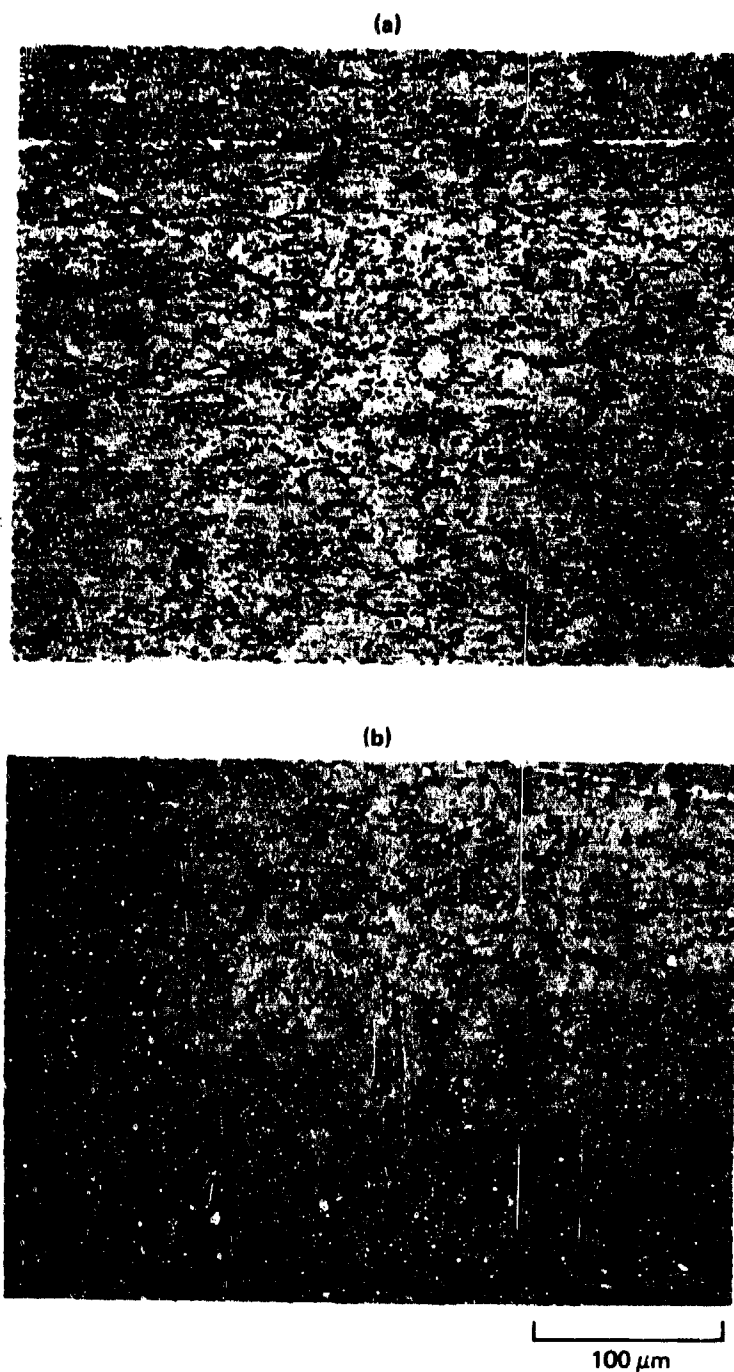
(b)



100 μm

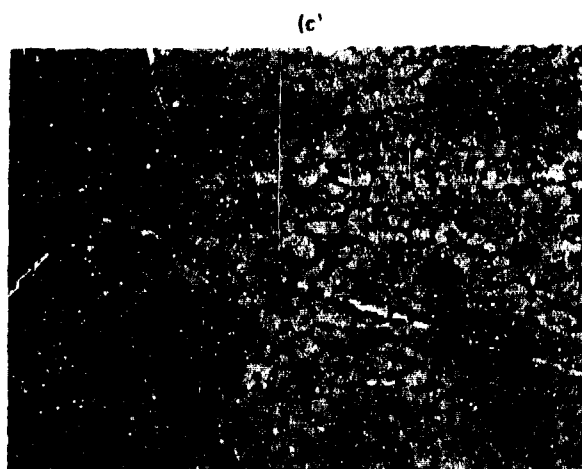
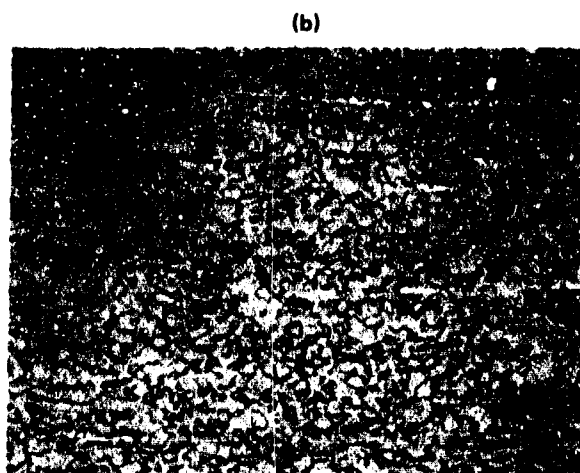
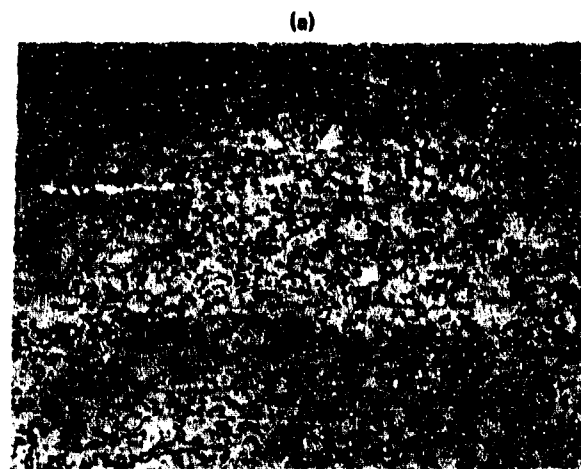
GP03-0245-187

Figure 5. Microstructures of regular-grade Ti-6Al-4V (a) production rolled to 22-mm thickness and (b) laboratory hot-rolled at 941°C (1725°F) from 22-mm to 7.4-mm thicknesses.



GP03-0248-188

Figure 6. Microstructures of Ti-6Al-4V laboratory pack-rolled at 843°C (1550°F) from 7.2-mm to 1.7-mm thickness and (a) annealed at 705°C (1300°F) for 1 h and (b) annealed at 760°C (1400°F) for 8 h.



100 μm

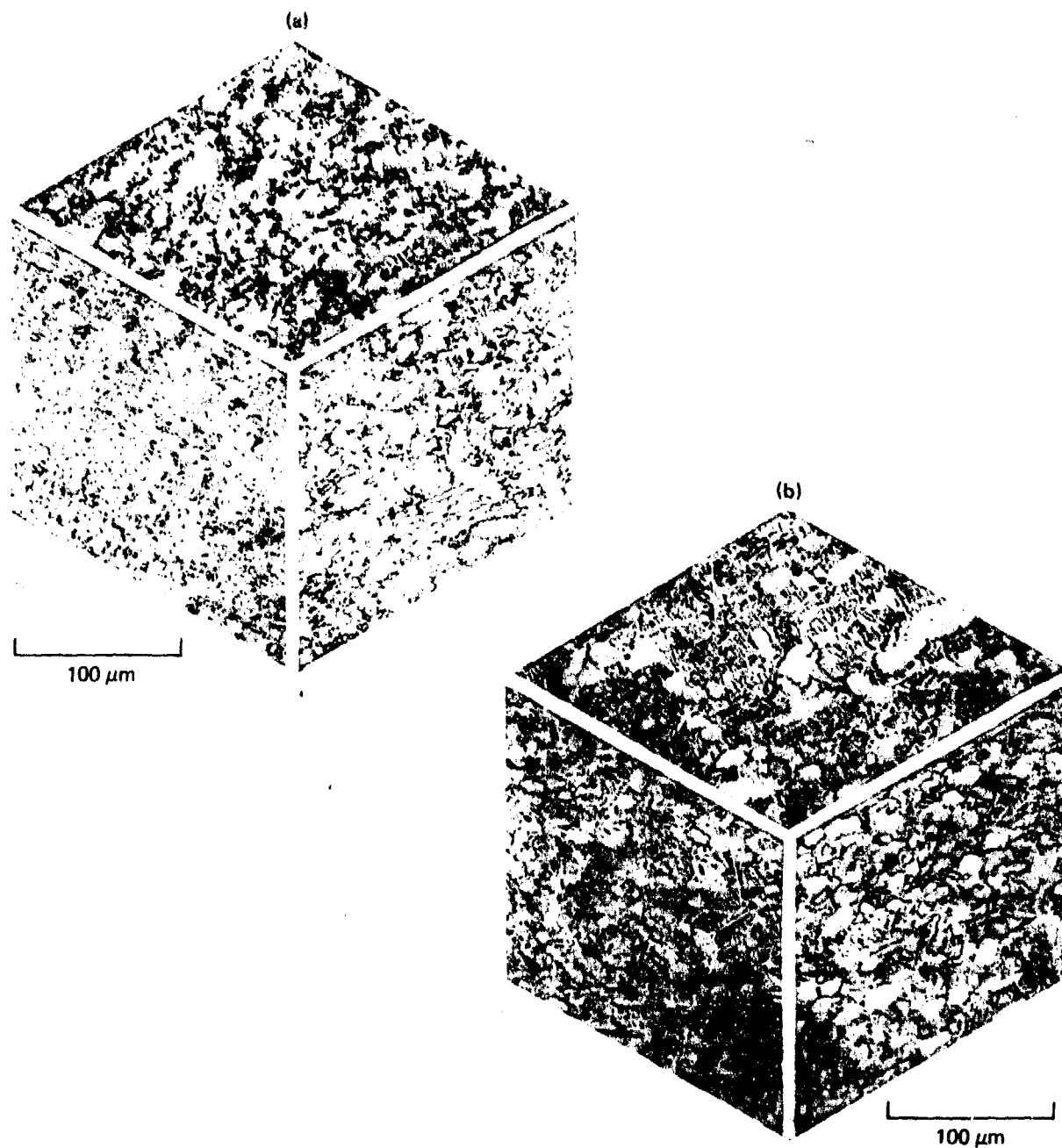
GP03-0249-189

Figure 7. Microstructures of Ti-6Al-4V pack-rolled at 843°C (1550°F) from 7.2-mm to 1.7-mm thickness and annealed at (a) 871°C (1600°F) for 1 h, (b) 927°C (1700°F) for 1 h, and (c) 982°C (1800°F) for 1 h.

Based on the results from these initial processing verification tests, full scale processing of regular grade Ti-6Al-4V material to develop the desired microstructures was made. The 21 mm/22 mm x 918 mm x 5080 mm (0.827 inch/0.850 inch x 36.125 inch x 200 inch) plate was conditioned and cut to yield eight lengths each approximately 610 mm (24 inch) long. Four of the lengths were heated to $941^{\circ} \pm 14^{\circ}\text{C}$ ($1725^{\circ} \pm 25^{\circ}\text{F}$) in a slightly oxidizing atmosphere and rolled to 13 mm/14 mm x 918 mm x 1016 mm (0.525 inch/0.540 inch x 36.125 in x 40 inch) plates in a single heating. All surfaces and edges looked good, and the four lengths were grit blasted and reinspected.

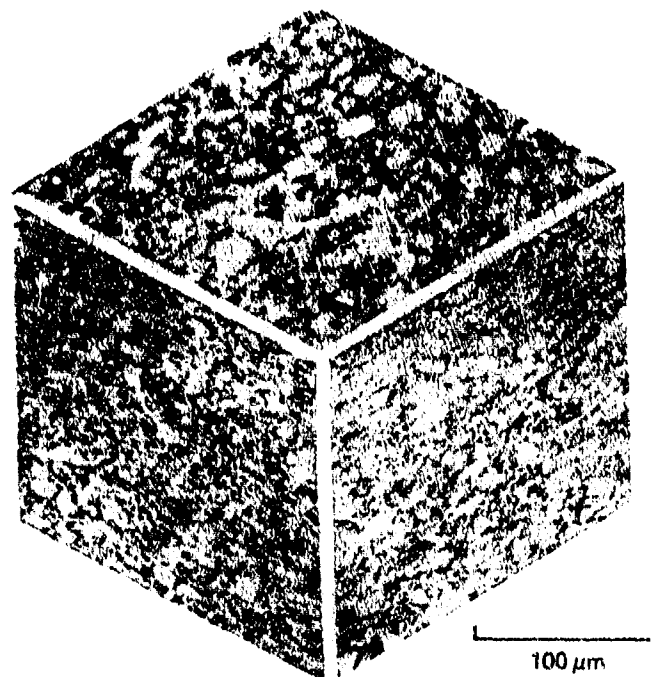
The plates were heated to $941^{\circ} \pm 14^{\circ}\text{C}$ ($1725^{\circ} \pm 25^{\circ}\text{F}$) in a slightly oxidizing atmosphere and rolled into 6 mm/7mm x 918 mm/921 mm x 1095 mm (0.270 inch/0.280 inch x 36.125 inch/36.25 inch x 75 inch) panels with one reheat. Three of the panels were cut in half, conditioned, heated to 843°C (1550°F), and finally cross rolled to 3.7 mm (0.145 inch) thickness. At this stage, the panels were again cut in half, grit blasted, and pickled. The twelve panels were annealed 1 hour at 704°C (1300°F) prior to final rolling. As-annealed panels were next paired and placed in carbon steel envelopes. Heating temperature for final rolling was 843°C (1550°F). Cross rolling was continued to a nominal finish thickness of 1.7 mm (0.066 inch). Because the as-rolled flatness was not acceptable the sheets were roller leveled after removing from the envelope to improve their flatness. The as-rolled sheets were then descaled and pickled prior to final heat treatment.

Microstructure of production rolled regular grade Ti-6Al-4V 22 mm (0.850 inch) thick plate prior to the initial rolling cycle is shown in Figure 8. Some residual Widmanstätten structure was present at the center of the plate. The surface which had been more heavily worked or worked at a lower temperature did not exhibit any Widmanstätten. Microstructure of the production processed plate at the intermediate 6.8 mm (0.270 inch) thick stage is shown in Figure 9. At this stage the plate microstructure was well worked and free of any coarse transformation product.



GP03-0240-100

Figure 8. Microstructures of production-processed 22-mm regular-grade Ti-6Al-4V at (a) surface and (b) mid-thickness.



GP03-0240-191

Figure 9. Microstructure of production-processed 7-mm regular-grade Ti-6Al-4V at quarter-thickness position.

Heat treatment studies were conducted on the as-rolled standard grade Ti-6Al-4V sheet to establish the time-temperature parameters for the desired grain sizes and primary alpha levels. The procedure used in this study was recrystallization-annealing the sheet material in vacuum at high temperatures, 927°C and 982°C (1700°F and 1800°F) and subsequently annealing in air at lower temperatures to obtain variations in alpha-beta volume fractions. The variation with time at temperature of the primary-alpha grain size of Ti-6Al-4V annealed at 982°C (1800°F) and furnace cooled to ambient temperature is shown in Figure 10. The grain size plotted in Figure 10 is that after furnace cooling from the annealing temperature and not the alpha grain size at temperature. Typical microstructures of specimens annealed at 927°C (1700°F) and 982°C (1800°F) covering a range of primary alpha grain sizes from 6-18 μm, are shown in Figure 11.

The primary alpha content can be varied by changing the annealing temperature. Then by cooling at an intermediate rate, the microstructure at room temperature will consist of equiaxed alpha surrounded by regions of transformed beta. As the annealing temperature is increased, the primary alpha content is decreased up to the beta transus, as illustrated for ELI-Grade Ti-6Al-4V in Figure 12 (Reference 21).

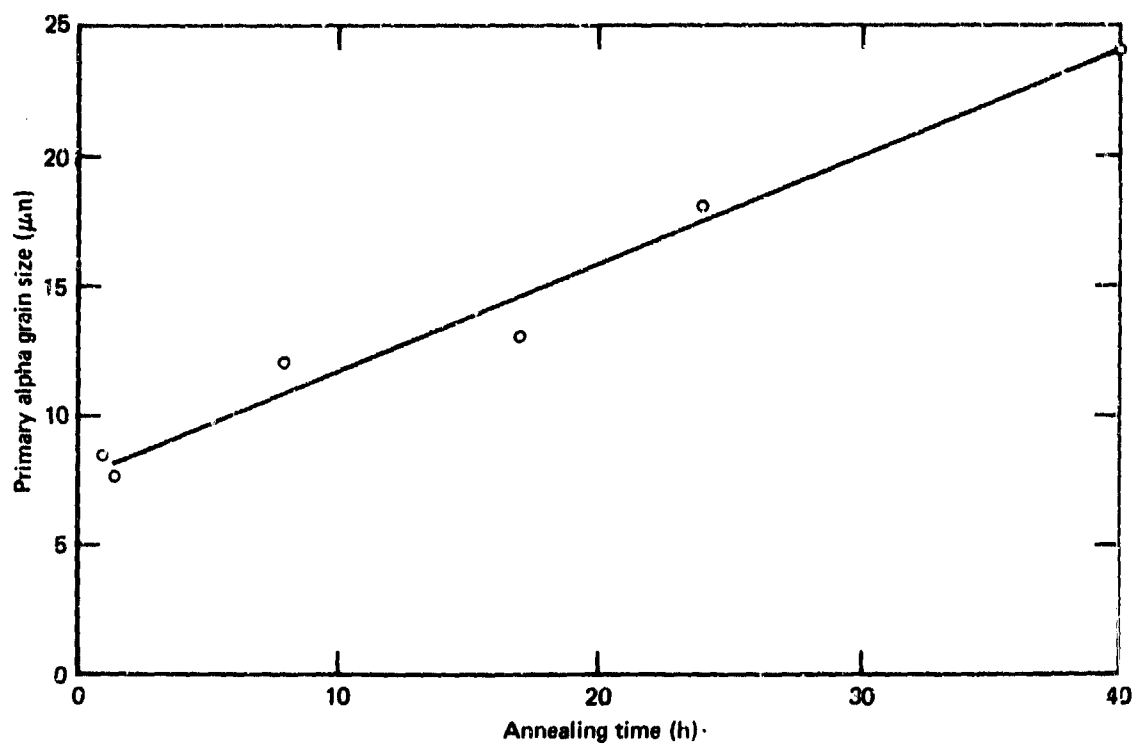
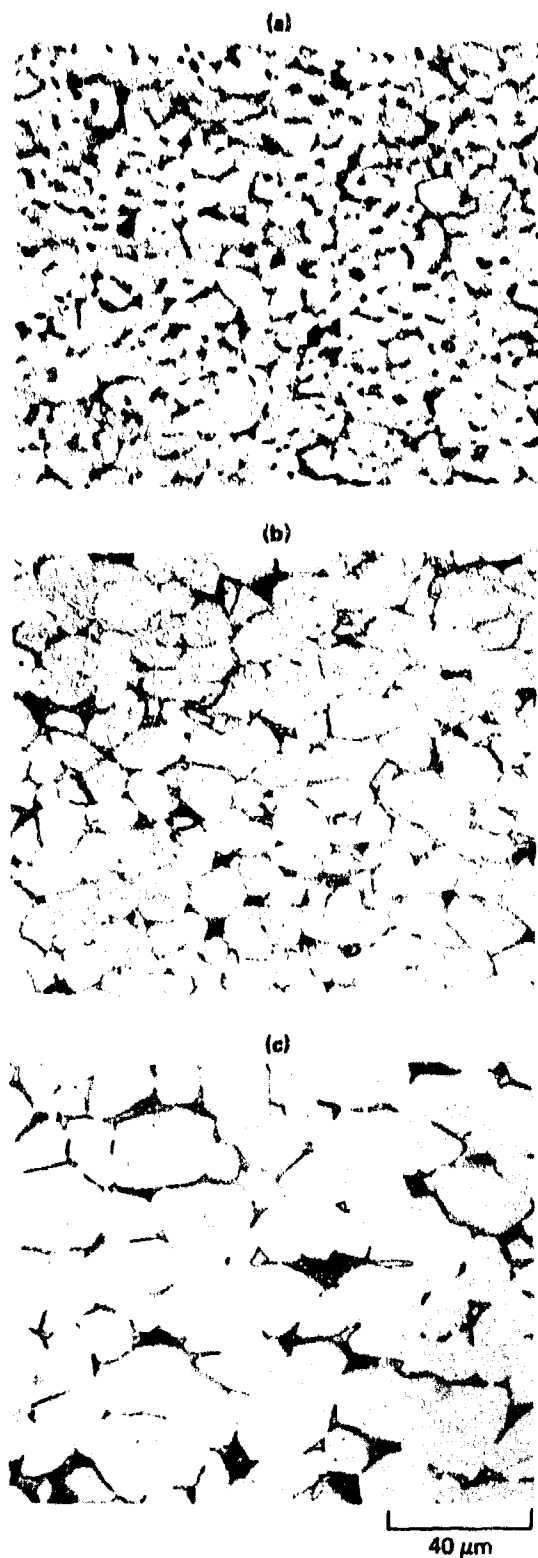
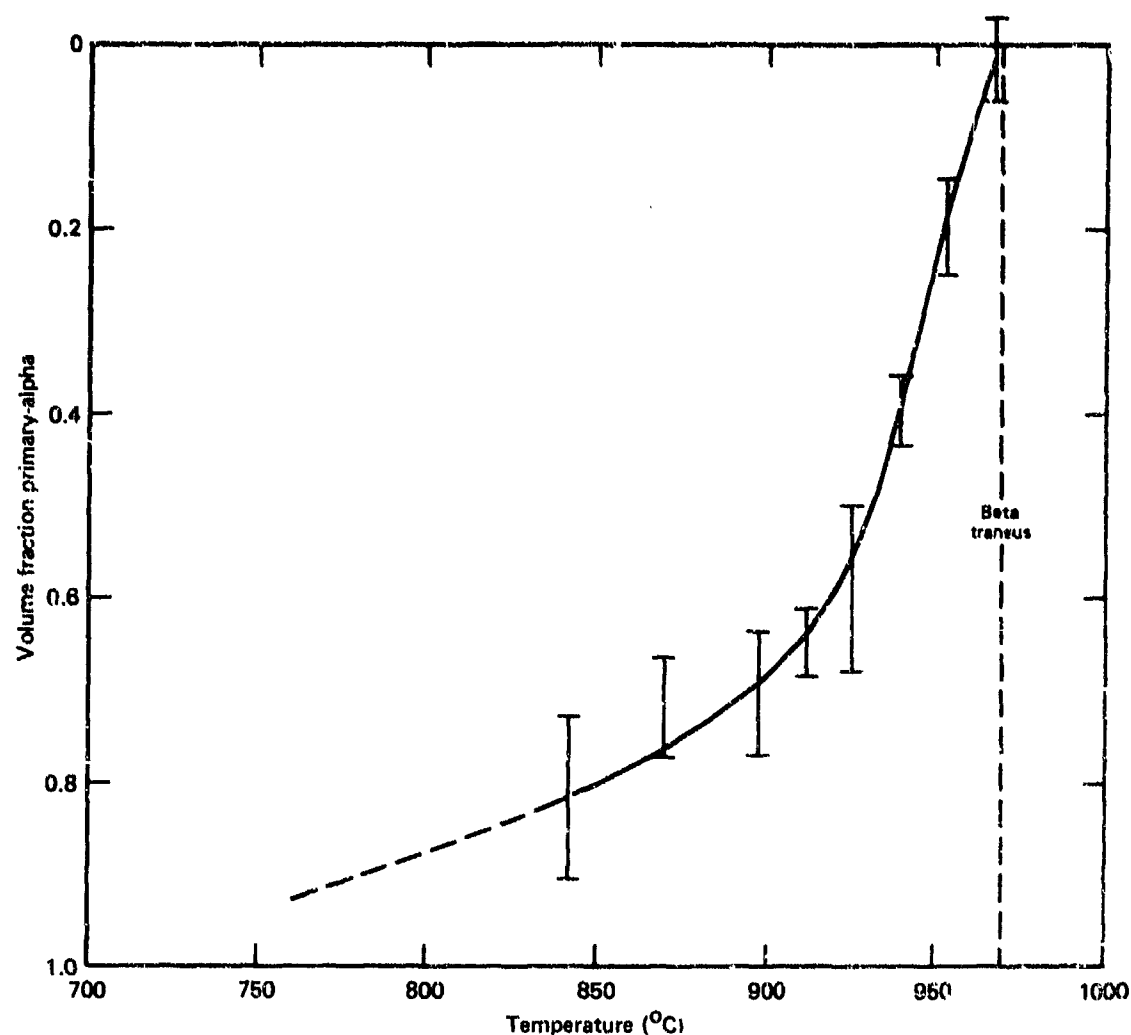


Figure 10. Growth of primary-alpha grain size with time in specimens annealed at 982°C (1800°F) and furnace cooled to room temperature.



GP03-0249-132

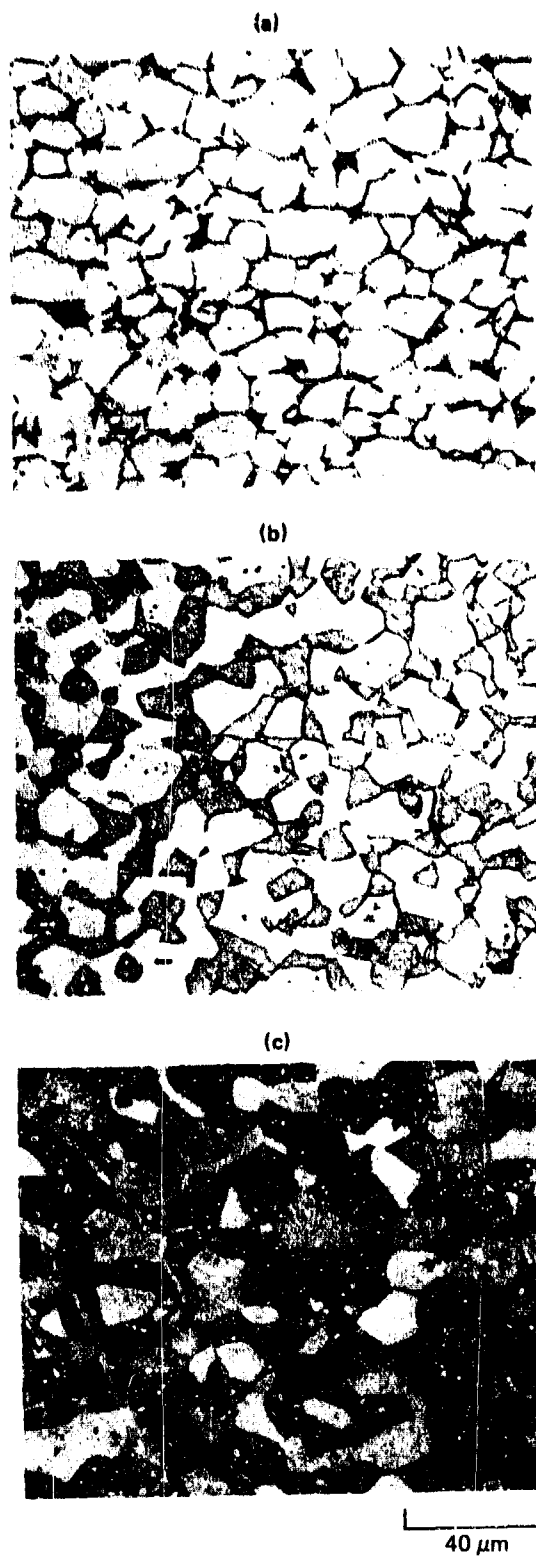
Figure 11. Microstructures after furnace cooling to 25°C (77°F) of regular-grade Ti-6Al-4V annealed at (a) 927°C (1700°F) for 1 h, (b) 982°C (1800°F) for 8 h, and (c) 982°C (1800°F) for 24 h.



GP03-0248-144

Figure 12. Variation of volume fraction of primary alpha with annealing temperature for ELI-grade Ti-6Al-4V.

The recrystallized samples were reheated for a short time at temperatures relatively high in the alpha-beta field, 840 - 925°C (1635-1700°F), and air cooled to determine the variation in volume fraction primary alpha with temperature. The microstructures in Figure 13 illustrates the variation in volume fraction primary alpha at a constant primary alpha grain size, obtained by the duplex heat treatment.



GP03-0249-193

Figure 13. Microstructures of regular-grade Ti-6Al-4V at a constant primary alpha grain size and (a) 90% primary alpha, (b) 65% primary alpha, and (c) 45% primary alpha.

The initial objectives for regular grade normal texture Ti-6Al-4V were to develop four grain sizes and three levels of primary alpha for each grain size. The heat treatment study showed the impracticality of obtaining such a matrix over the desired range of grain sizes. Since the alpha grain size decreases as the volume fraction decreases, a very large initial grain size would require a large primary alpha grain size at a low volume fraction primary alpha. Due to these constraints, the following grain-size/primary-alpha matrix was selected.

<u>Approximate</u> <u>Primary Alpha</u> <u>Grain Size</u>	<u>Volume Fraction Primary Alpha</u>		
	<u>0.9</u>	<u>0.65</u>	<u>0.45</u>
18 μm	X	X	-
12 μm	X	X	X
8 μm	X	X	X
6 μm	X	X	X
4.5 μm			X

The primary alpha grain size is considered to be the most important parameter in predicting superplastic behavior; therefore it has been used as the basic grain size throughout this program. The alpha grain sizes were determined using the method described by Underwood (Reference 22) from the relation

$$L_3 = \sigma - \lambda \quad (4)$$

Where L_3 is the mean intercept-length alpha grain size,

σ is the mean center-to-center distance between alpha-phase particles $\left(\sigma = \frac{1}{N_L \alpha} \right)$

and

λ is the mean distance between alpha phase particles $\left(\lambda = \frac{1 - V_V \alpha}{N_L \alpha} \right)$

Table 4 summarizes the heat treatments, primary alpha grain sizes and volume fractions of primary alpha for each of the twelve conditions produced in the normal texture material. Grain sizes were determined on each of the three orthogonal planes in both the major and minor directions. Six measurements were made on each plane. The results in Table 4 are the average of eighteen separate measurements per condition.

The crystallographic texture of the regular grade Ti-6Al-4V was obtained by determining the (0002) pole distributions. The (0002) pole figures of different panels are shown in Appendix B. It is seen that microstructures L (.64 α , 5.9 μ m) and K (.64 α , 5.9 μ m), have in addition to a strong near-basal texture component, basal pole distributions symmetrically oriented at angles of 20-45° from the rolling plane normal. The intensity of basal pole distributions decreases with increasing angle from the rolling plane normal. Deviations of 15-20° from basal texture were observed in the E (.88 α , 12.2 μ m), H (.88 α , 7.7 μ m) I (.47 α , 5.6 μ m) and J (.47 α , 4.4 μ m).

Table 5 gives room temperature tensile properties for normal-textured regular-grade Ti-6Al-4V sheet in several heat treated conditions. The trends in properties were as expected for the various conditions. The high-temperature recrystallization treatment [927°C (1700°F) 1 hr FC (furnace cooled) 56°C/hr (100°F/hr)] resulted in a substantial decrease in strength and improvement in transverse ductility over the mill-annealed (704°C (1300°F) 1 hr AC (air cooled) strength, but some loss of ductility was indicated for the largest grain size. The duplex-annealed condition showed an increase in strength and decrease in ductility over the base, furnace cooled, condition due to the transformation product in the structure.

3.2 Regular Grade Ti-6Al-4V (Textured)

3.2.1 Basal Normal Texture

When titanium alloys are cross rolled at 538°-816°C (1000°-1500°F) by changing the rolling direction after each reduction pass (clock rolling), the deformation occurs in such a way that the basal poles [(0002) directions] are forced into a direction parallel to the sheet normal thus producing a strong basal texture. Laboratory trials were conducted to verify the clock rolling process for the basal normal textured material. Sheet bar samples, 22 mm (0.840 inch) thick, were

**TABLE 4. EFFECTS OF HEAT TREATMENT ON MICROSTRUCTURES OF
NORMAL-TEXTURED Ti-6Al-4V SHEET.**

Panel code	Heat treatment	Primary alpha grain size (μm)	Primary alpha volume fraction
C	982°C (1800°F) for 24 h; furnace cool to 25°C at 38°C/h (100°F/h)	17.6	0.88
B	982°C (1800°F) for 40 h; furnace cool to 25°C at 38°C (100°F/h) + 910°C (1670°F) for 5 min; air cool to 25°C	18.1	0.66
E	982°C (1800°F) for 8 h; furnace cool to 25°C at 38°C/h (100°F/h)	12.2	0.87
D	982°C (1800°F) for 13 h; furnace cool to 25°C at 38°C/h (100°F/h) + 910°C (1670°F) for 5 min; air cool to 25°C	14.2	0.65
A	982°C (1800°F) for 40 h; furnace cool to 25°C at 38°C/h (100°F/h) + 949°C (1740°F) for 5 min; air cool to 25°C	12.6	0.46
H	982°C (1800°F) for 1.5 h; furnace cool to 25°C at 38°C/h (100°F/h)	7.7	0.89
G	982°C (1800°F) for 2.5 h; furnace cool to 25°C at 38°C/h (100°F/h) + 910°C (1670°F) for 5 min; air cool to 25°C	7.9	0.60
F	982°C (1800°F) for 8 h; furnace cool to 25°C at 38°C/h (100°F/h) + 949°C (1740°F) for 5 min; air cool to 25°C	7.2	0.44
L	927°C (1700°F) for 1 h; furnace cool to 25°C at 38°C/h (100°F/h)	6.0	0.88
K	927°C (1700°F) for 1 h; furnace cool to 25°C at 38°C/h (100°F/h) + 910°C (1670°F) 5 min; air cool to 25°C	5.9	0.64
I	982°C (1800°F) for 1.5 h; furnace cool to 25°C at 38°C/h (100°F/h) + 949°C (1740°F) for 5 min; air cool to 25°C	5.6	0.47
J	927°C (1700°F) for 1 h; furnace cool to 25°C at 38°C/h (100°F/h) + 949°C (1740°F) for 5 min; air cool to 25°C	4.4	0.47

GP03-C248-108

TABLE 5. TENSILE PROPERTIES OF NORMAL-TEXTURED REGULAR-GRADE 1.7-mm (0.065 IN.) Ti-6Al-4V SHEET.

Heat treatment	Panel	Volume fraction primary alpha	Grain size (μm)	Test direction	Ultimate tensile strength MPa (ksi)	0.2% offset yield stress MPa (ksi)	Total elongation (%)
704°C (1300°F) for 1 h; air cool to 25°C	—	—	—	L	972 (141.0)	932 (135.2)	17.0
				L	1006 (145.7)	936 (135.8)	15.5
				T	1021 (148.1)	959 (139.1)	12.5
				T	998 (144.8)	950 (137.8)	12.5
927°C (1700°F) for 1 h; furnace cool to 25°C at 38°C/h	L	0.88	6.0	L	879 (127.5)	845 (122.5)	15.0
				L	889 (129.0)	818 (118.7)	17.5
				T	872 (126.4)	847 (122.8)	18.0
				T	876 (127.0)	850 (123.3)	18.0
982°C (1800°F) for 1.5 h; furnace cool to 25°C at 38°C/h	H	0.89	7.7	L	879 (127.5)	825 (119.6)	17.5
				T	884 (128.2)	882 (119.2)	17.5
982°C (1800°F) for 1.5 h; furnace cool to 25°C at 38°C/h; + 910°C for 5 min; air cool to 25°C	G	0.60	7.9	L	1026 (148.8)	903 (130.9)	12.0
				L	1018 (147.6)	898 (130.2)	12.0
				T	1018 (147.6)	914 (132.5)	13.5
				T	1059 (153.6)	939 (135.2)	11.5
982°C (1800°F) for 1.5 h; furnace cool to 25°C at 38°C/h; + 949°C (1740°F) for t min; air cool to 25°C	I	0.47	5.6	L	1007 (146.1)	871 (126.3)	12.5
				L	1040 (150.9)	887 (128.7)	14.0
				T	1001 (145.2)	875 (126.9)	14.0
				T	1029 (149.3)	902 (130.8)	12.5
982°C (1800°F) for 24 h; furnace cool to 25°C at 38°C/h	C	0.88	17.6	L	909 (131.9)	851 (123.4)	16.0
				L	906 (131.4)	834 (120.9)	12.0
				T	975 (126.9)	794 (115.1)	5.0
				T	887 (128.7)	843 (122.3)	13.5

GP03-0249-110

cross rolled to 9.1 mm (0.360 inch) thickness from a 941°C (1725°F) furnace using 15-18 percent reductions per pass with two reheats. The 9.1 mm (0.360 inch) thick material was then reduced to 2.6 mm (0.102 inch) thick material by heating to 704°C (1300°F), with 10% reduction per pass and reheating after each pass to 704°C (1300°F). The plates were rotated 45° or 90° between passes. The tensile properties of the mill-annealed alloy rolled by the schedule just described are given in Table 6, and contrary to the expected near-isotropic behavior, the tensile properties have significant anisotropy. The anisotropy is corroborated by the pole figures in Appendix B, which show significant deviations ($\approx 20^\circ$) of the basal poles from the sheet normal. The grain sizes and aspect ratios of the laboratory clock-rolled Ti-6Al-4V annealed at 927°C (1700°F) for one hour are given in Table 7.

TABLE 6. TENSILE PROPERTIES OF "CLOCK-ROLLED" Ti-6Al-4V ALLOY (HEAT NO. G52083A-1).

Sample code	Angle of rotation between consecutive passes (deg)	Test direction	Ultimate tensile strength MPa (ksi)	0.2% offset yield stress MPa (ksi)	Total elongation (%)	Young's modulus $E \times 10^3$ MPa (ksi)	Directionality, $\Delta(T-L)$		
							UTS MPa (ksi)	YS MPa (ksi)	Modulus $E \times 10^3$ MPa (ksi)
D-1	90	L	1100 (159.6)	1056 (153.2)	20.0	137 (19.9)	-44.1 (-6.4)	-59.3 (-8.6)	-22.8 (-3.3)
		T	1056 (153.2)	997 (144.6)	22.0	114 (16.6)			
D-2	45	L	1147 (166.4)	1069 (155.0)	18.0	123 (17.9)	-29.0 (-4.2)	-51.0 (-7.4)	+28.3 (+4.1)
		T	1118 (162.2)	1018 (147.6)	22.0	152 (22.0)			

GP03-0249-111

TABLE 7. GRAIN SIZE OF LABORATORY "CLOCK-ROLLED" REGULAR-GRADE Ti-6Al-4V ANNEALED AT 927°C (1700°F) FOR 1 h AND FURNACE COOLED TO 25°C (77°F).

Rolling conditions		Mean linear intercept L-S plane (μm)		Average linear intercept (μm)	Mean grain aspect ratio L/S
Furnace temperature °C (°F)	Angle of rotation (deg)	L direction	S direction		
704 (1300)	90	4.4	3.6	4.0	1.2
704 (1300)	45	4.9	3.9	4.4	1.2

GP03-0249-112

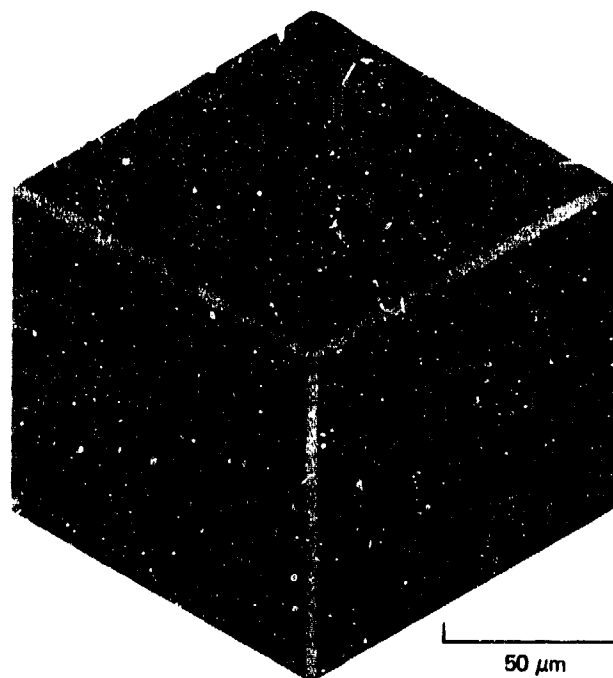
The clock rolling schedule with 90° rotation between consecutive passes, which results in lesser anisotropy in Young's modulus was selected for full scale processing.

Processing of basal normal texture panel Ti-6Al-4V to 7 mm (0.275 inch) thick followed the same sequence as the normal texture material. At this stage, continuous cross rolling at 704°C (1300°F) was initiated. The basic processing sequence was to heat to 704°C (1300°F), reduce 10-20 percent in two passes, reheat and

turn panel 90° prior to the next reduction. At 3.3 mm (0.130 inch) thickness, the panels were paired and the cross rolling reheat sequence was continued to final gage by open pair rolling. Considerable difficulty was encountered in this rolling campaign, particularly after pairing.

Because the panels were bowed, difficulty was experienced in getting the panels to enter the rolls properly which resulted in substantial temperature loss. Severe cracks were developed in one panel during an attempt to flatten the material by making a light reduction. Yield loss was greater than 50 percent, and only six full size 380 mm (15 inch) square panels could be obtained from this material. The balance of the panels were of smaller size sections. Two full size panels and one of the smaller sections contained pits on approximately one fourth of their surface areas. The pits appeared to be a result of scale which was embedded during the final rolling cycle.

The sheet was given a final treatment of 927°C (1700°F) 1 hour FC 56°C/hr (100°F/hr). Figure 14 shows the microstructure of the basal textured sheet after the final anneal. Grain size of clock-rolled microstructure was 7.4 mm which is slightly larger than the normal-textured Ti-6Al-4V microstructure L (.88 α , 6.0 μ m) similarly heat-treated.



GP03-0249-194

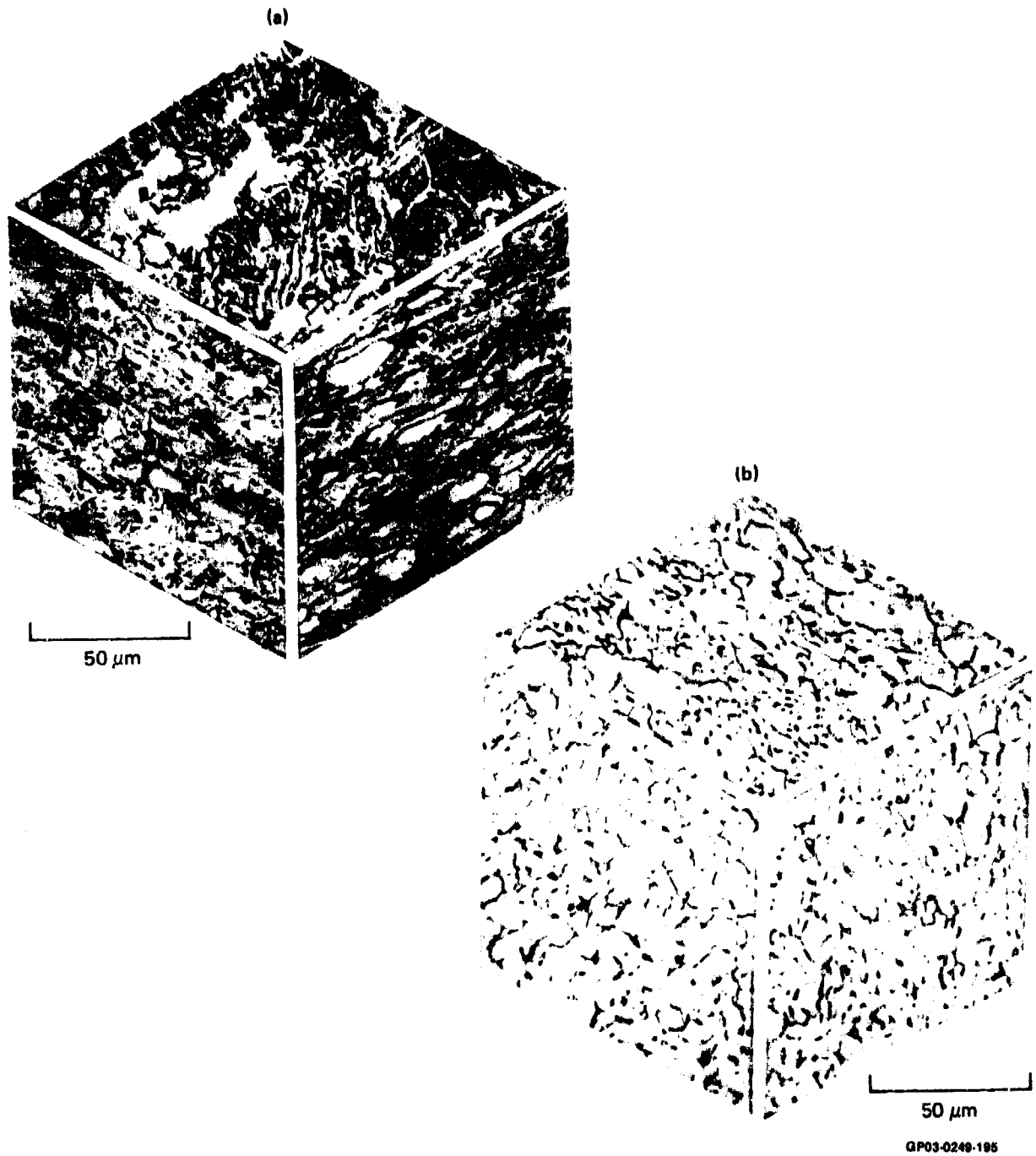
Figure 14. Microstructure of basal-textured Ti-6Al-4V annealed at 920°C (1688°F) for 1 h and furnace cooled to 25°C (77°F) at 56°C/h (100°F/h).

3.2.2 Regular Grade Ti-6Al-4V (Transverse Basal Texture)

The transverse basal texture was produced by unidirectional cascade rolling. In this practice, rolling is begun in the all-beta field and continued through the alpha-beta field to finish 260°C (470°F) below the beta transus, with total reduction in excess of 80 percent. Extensive unidirectional rolling in the 538°-816°C (1000°-1500°F) temperature range produces a texture where the [0002] directions are uniformly distributed along a great circle connecting the direction normal to the surface and the transverse directions of the rolled material. Four rolling trials were conducted in the laboratory to optimize the processing sequence to produce the transverse-basal texture. Unfortunately, the sequence which gives the strongest texture is the most difficult to duplicate on the production facility. Starting stock used for the present program was 21.5 mm (0.845 inch) thick plate. The plate was placed in a mild steel welded pack in preparation for rolling. Hot rolling of the material was accomplished from a single heating at 1049°C (1925°F). The pack was heated and held at temperature for 0.3 hour. A total reduction of 90 percent was obtained in twelve passes without reheating. Approximate finishing temperature for the pack was 816°C (1500°F). After rolling, the pack was warm sheared to 1219 mm (49 inch) lengths and the titanium sheet was removed from the pack. The cascade rolling caused the surface of the transverse-basal texture to be rougher than the normal texture material and a substantial amount of conditioning (grinding and pickling) was required to improve the surface.

The microstructure of the transverse basal textured sheet is shown in Figure 15. Some relatively large alpha grains were present in the as-hot rolled sheet. After annealing at 926°C (1700°F) 1 hr FC, the structure was more uniform although some vestiges of the worked Widmanstätten remained. The alpha grain size in this microstructure is 12.5 μm which is similar to microstructure in regular grade normal texture Ti-6Al-4V E (.87 α , 12.2 μm).

Tensile properties of the transverse basal textured sheet in the final annealed condition are given in Table 8. The high directionality of the tensile properties is in agreement with the strong transverse-basal texture of this microstructure (Figure B4).



GP03-0249-195

Figure 15. Microstructures of transverse-basal-textured regular-grade Ti-6Al-4V sheet (Heat no. G52083) for (a) as hot-rolled and (b) vacuum annealed at 927°C (1700°F) for 1 h and furnace cooled to 25°C (77°F) at 56°C/h (100°F/h).

TABLE 8. TENSILE PROPERTIES OF TRANSVERSE-BASAL-TEXTURED Ti-6Al-4V SHEET ANNEALED AT 927°C (1700°F) FOR 1 h; FURNACE COOLED TO 25°C AT 38°C/h (65°F/h).

Test direction	Ultimate tensile strength MPa (ksi)	0.2% offset yield stress MPa (ksi)	Total elongation (%)	Young's modulus $E \times 10^3$ MPa (ksi)
L	905 (131.3)	841 (122.1)	6.5	112 (16.3)
L	917 (133.1)	849 (123.2)	9.5	102 (14.8)
T	1076 (156.2)	993 (144.1)	10.0	137 (19.9)
T	1088 (157.9)	1013 (147.0)	11.5	132 (19.2)

QP03-0249-113

3.3 Regular-Grade Ti-6Al-4V With Microstructural Anomalies

3.3.1 Elongated Alpha

The elongated-alpha structures for this program were produced by beta annealing followed by two levels of hot work in the alpha-beta field. Conventionally processed 2.3 mm (0.090) and 3.2 mm (0.125 in) Ti-6Al-4V sheets were beta annealed at 1038°C (1925°F) for 0.25 hour and subsequently alpha-beta annealed at 954°C (1750°F) for one hour and air cooled. The purpose of the second anneal was to coarsen the Widmanstätten alpha needles and improve the hot workability of the sheet. After annealing, the sheets were grit blasted and pickled. Both sheets were hot rolled from an 885°C (1625°F) furnace to a final gage of 1.8 mm (0.070 inch) thick. The 2.3 mm (0.090 inch) thick material was rolled to final gage from one heating. The 3.2 mm (0.125 inch) thick sheet required one reheat at an intermediate gage. After rolling, the sheet was conditioned, vacuum annealed at 927°C (1700°F) for one hour, furnace cooled and pickled.

The two levels of elongated-alpha microstructures are shown in Figures 16 and 17. No significant microstructural changes occurred in the sheet material rolled from 2.3 mm to 1.8 mm (Level I), but the alpha platelets underwent some coarsening in the sheet material rolled from 3.2 mm to 1.8 mm (Level II). The post-rolling anneal resulted in partial recrystallization in the heavily-worked 3.2 mm (Level II) microstructure and had no significant effect on the lightly-worked 2.3 mm microstructure (Level I).

3.3.2 Banding

The banded microstructures in the laboratory scale heats were produced by cascade rolling 21.3-mm Ti-6Al-4V plate from 1024°C (1875°F) to 6.4-mm (0.25 in.) thickness. Although banded microstructures could be produced successfully in the laboratory, attempts to obtain the banded microstructures in the large scale heats were not successful. Figures 18 and 19 show the banded microstructure in laboratory-processed Ti-6Al-4V and the normal microstructure of production-processed Ti-6Al-4V.

To obtain the two levels of banded microstructure required for this study, a 3.8-mm (0.150 in.) thick Ti-6Al-4V sheet having banded microstructure was processed to the required thickness. The level of banding was varied by hot rolling at different temperatures. Material for the first level of banding was hot rolled at 843°C (1550°F) to a 1.6-mm (0.065 in.) final thickness in 14 passes with three intermediate reheats. The second level of banding was produced by rolling at 855°C (1625°F) in eleven passes with two intermediate reheats. Post-rolling heat treatment of the banded material was identical to that used for other anomalous microstructures.

The microstructure of the initial banded Ti-6Al-4V is shown in Figure 20a. The initial microstructure is heavily banded with alternating layers of heavily and lightly worked Widmanstätten alpha. The microstructures after rolling from 843°C (1550°F) and 885°C (1625°F) to final gage is shown also in Figure 20b and 20c. The microstructures after annealing at 927°C (1700°F) for one hour are shown in Figures 21 and 22, and they indicate the retention of banding.

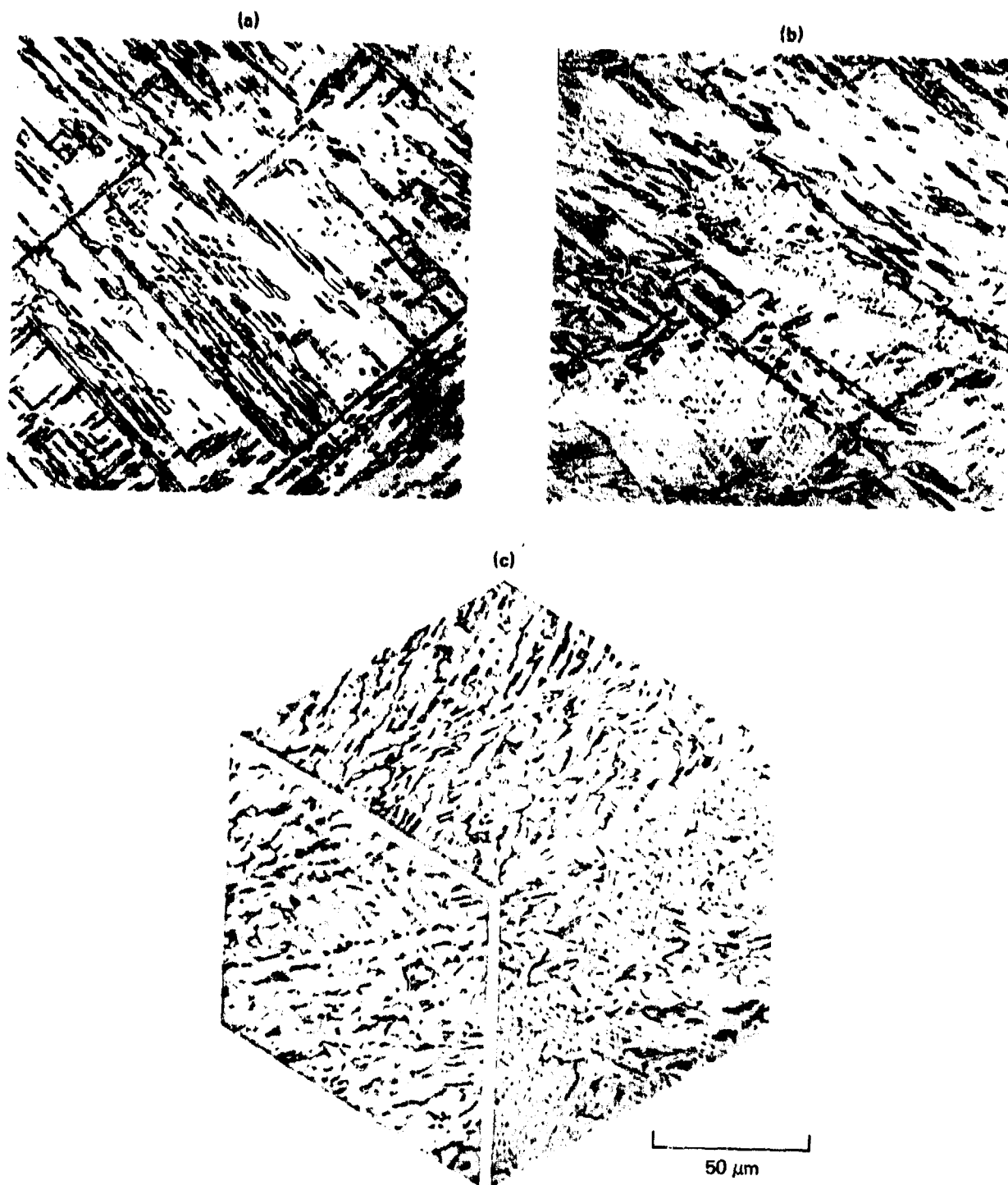
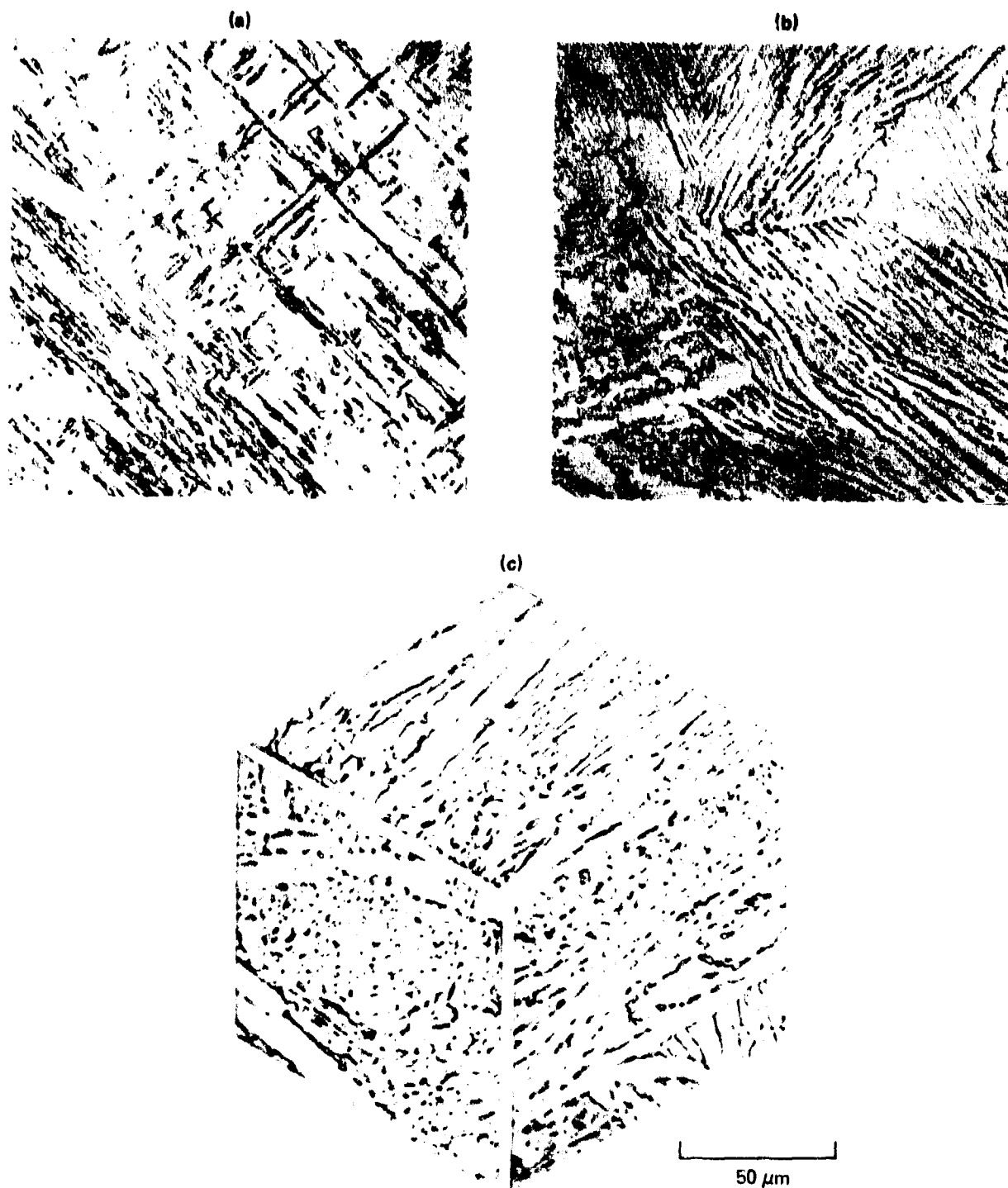


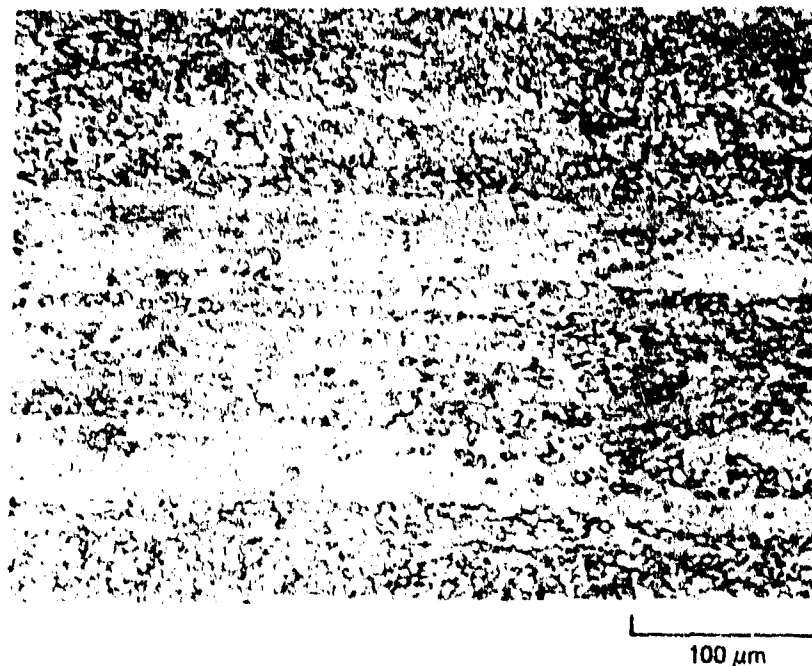
Figure 16. Microstructures of elongated alpha Ti-6Al-4V (Heat no. G52063) for (a) 2.3-mm thick sheet annealed at 1038°C (1900°F) for 15 min, air cooled to 25°C (77°F) + 995°C (1823°F) for 1 h, and air cooled to 25°C (77°F) (b) as-hot-rolled 1.8-mm thick sheet, and (c) 1.8-mm sheet vacuum annealed at 927°C (1700°F) for 1 h and furnace cooled to 25°C (77°F).

GP03-0249-196



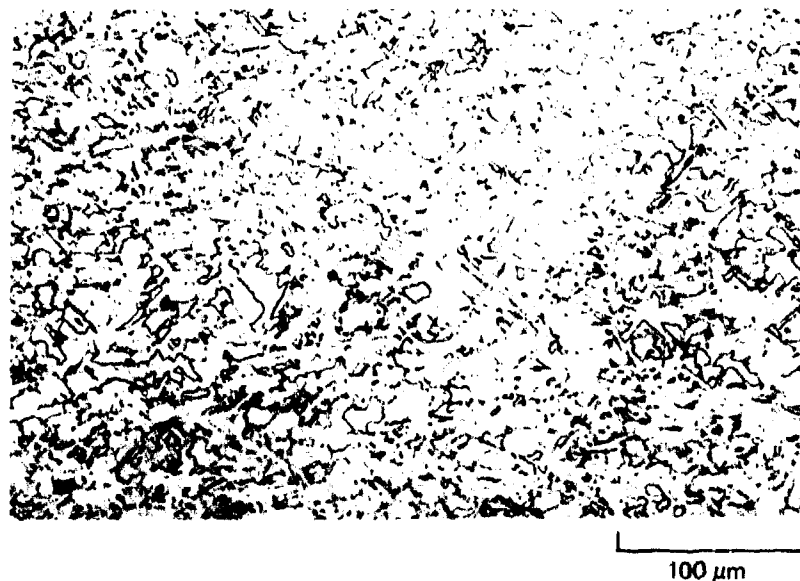
GP03-0248-187

Figure 17. Microstructures of elongated alpha Ti-6Al-4V (Heat No. G52063) for (a) 3.2-mm thick sheet annealed at 1038°C (1900°F) for 15 min, air cooled at 25°C (77°F) + 995°C (1823°F) for 1 h, and air cooled at 25°C (77°F) (b) as-hot-rolled 1.8-mm sheet, and (c) 1.8-mm sheet vacuum annealed at 927°C (1700°F) for 1 h furnace cooled to 25°C (77°F).



GP03-0249-199

Figure 18. Banded microstructure of Ti-6Al-4V produced in the laboratory by thermal cascade-rolling 65% from 1045°C (1913°F) followed by annealing at 927°C (1700°F) for 1 h and furnace cooled to 25°C (77°F).



GP03-0249-198

Figure 19. As-hot-rolled microstructure of Ti-6Al-4V plate thermal cascade-rolled 70% in a welded pack from 1024°C (1875°F).

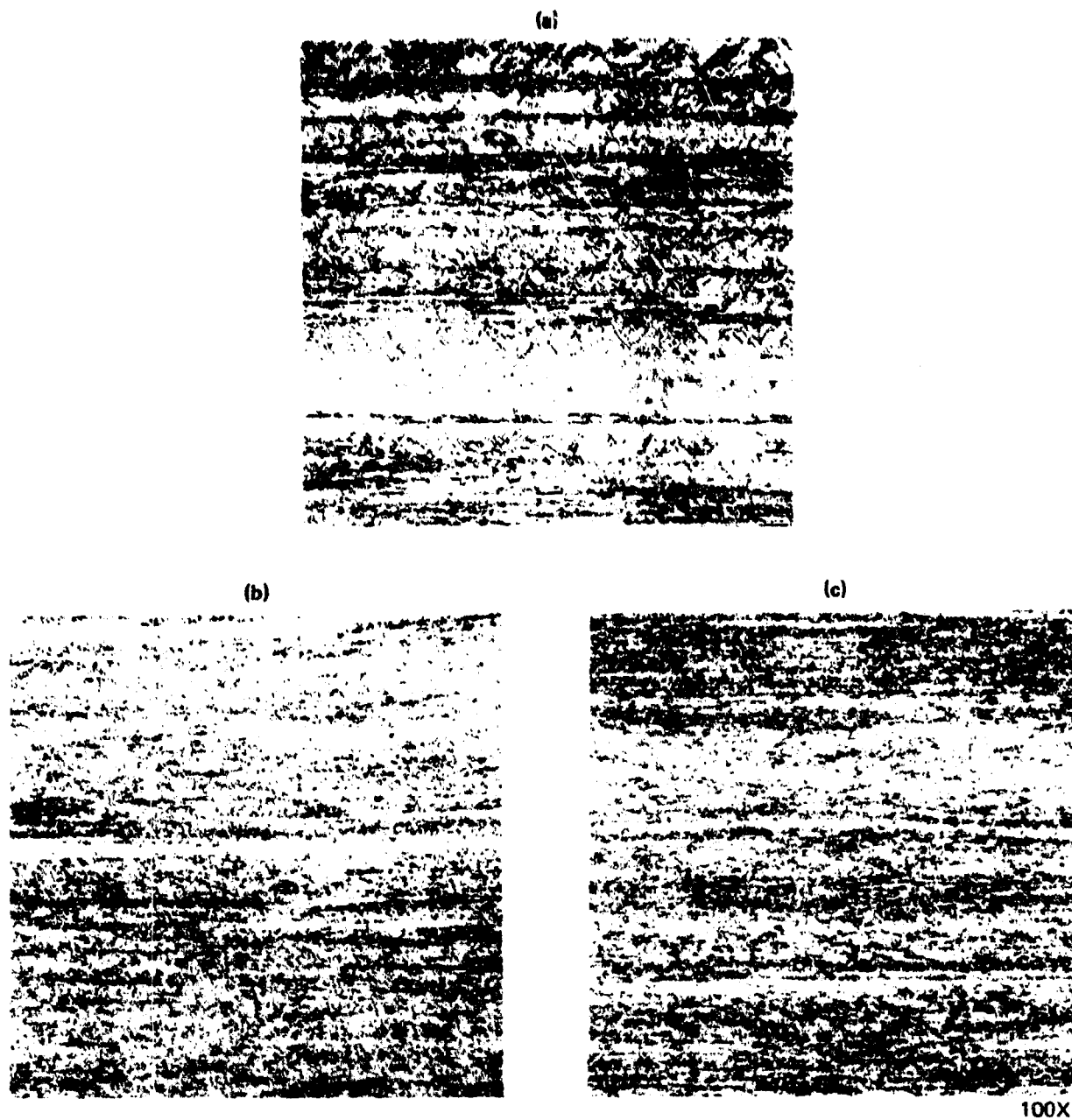
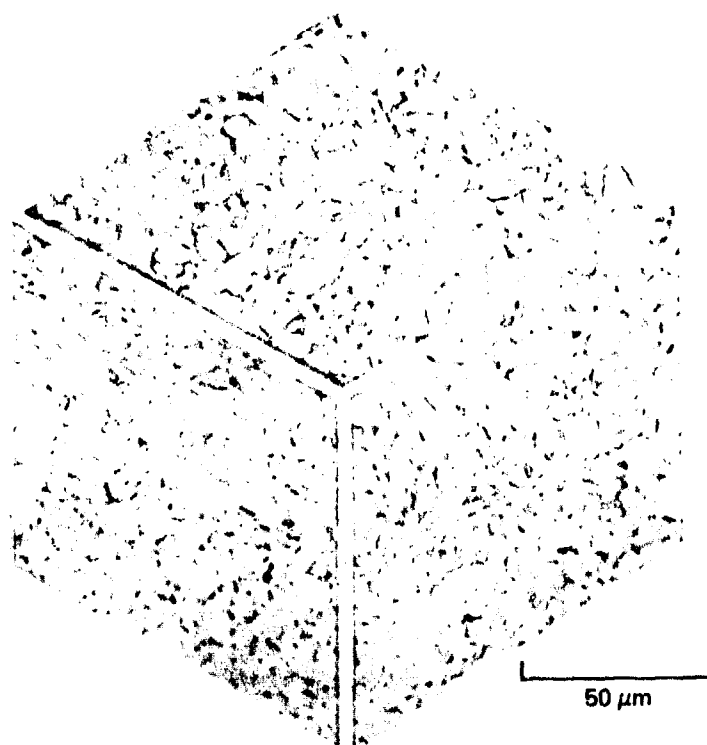


Figure 20. Microstructures of banded Ti-6Al-4V sheet (Heat no. G52070 for (a) initial microstructure, (b) hot-rolled at 843°C (1550°F) to 1.6-mm thickness (level I), and (c) hot-rolled at 885°C (1630°F) to 1.6-mm thickness (level II).

GP03-0249-200



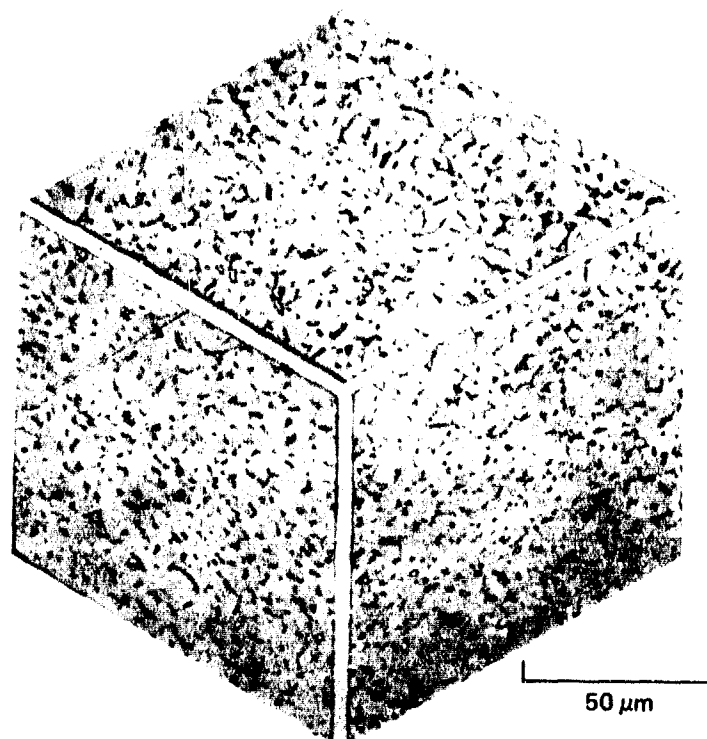
200 μm



50 μm

GP03-0249-201

Figure 21. Microstructures of banded Ti-6Al-4V sheet (level I) after vacuum annealing at 927°C (1700°F) for 1 h and furnace cooled to 25°C (77°F).



GP03-0249-202

Figure 22. Microstructures of banded Ti-6Al-4V sheet (level II) after vacuum annealing at 927°C (1700°F) for 1 h and furnace cooled to 25°C (77°F).

3.3.3 Blocky Alpha

The approach used to produce the blocky alpha structure was to hold material high in the alpha-beta field prior to rolling. This heat treatment has the effect of stabilizing the alpha phase present at temperature because of partitioning of the alpha stabilizers, oxygen, nitrogen, and aluminum. On subsequent rolling and annealing, the alpha-beta matrix is deformed and recrystallized, whereas the stabilized alpha remains relatively unchanged. The deformation temperature and amount of deformation must be carefully controlled because inadequate deformation does not produce recrystallization of the alpha-beta matrix, and excessive deformation results in fragmentation of the stabilized alpha particles and subsequent recrystallization of the entire structure.

Material used for the first level of blocky alpha was processed to 7-mm (0.275 in.) thickness as described for the normal-textured alloy. At this stage, the material was heat treated for 4 hour at 968°C (1775°F) and air cooled. After grit blasting and pickling, the material was hot rolled at 843°C (1550°F) to 3.7-mm (0.145 in.) thickness with only one reheat being required. The sheet was again heat treated for 4 hours at 968°C (1775°F), air cooled, grit blasted, and pickled. Hot rolling to a final thickness of 1.8 mm (0.070 in.) was conducted at 843°C (1550°F). Some problems were encountered in the final rolling because of cracking and tearing of the sheet edges. Following rolling, the sheet was conditioned, vacuum annealed at 927°C (1700°F) for one hour, furnace cooled, and pickled.

The second level of blocky alpha was processed conventionally to 3.5-mm (0.140 in.) thick sheet. At this stage, the sheet was annealed at 954°C (1750°F) for 4 hours and air cooled to 25°C (77°F). The sheet was grit blasted, pickled, and hot rolled at 843°C (1550°F) to a final thickness of 1.9-mm (0.075 in.). Rolling to final gage required five passes with one intermediate reheat.

Processing after rolling involved conditioning, vacuum annealing for 1 hour at 927°C (1700°F), furnace cooling, and pickling. Figures 23 and 24 illustrate the microstructures of the two levels of blocky alpha for sheets in the final condition and two intermediate stages of processing. In the vacuum annealed condition, Level I Ti-6Al-4V had blocky structures on all three major planes, but Level II alloy exhibited a blocky structure on only the L-T plane.

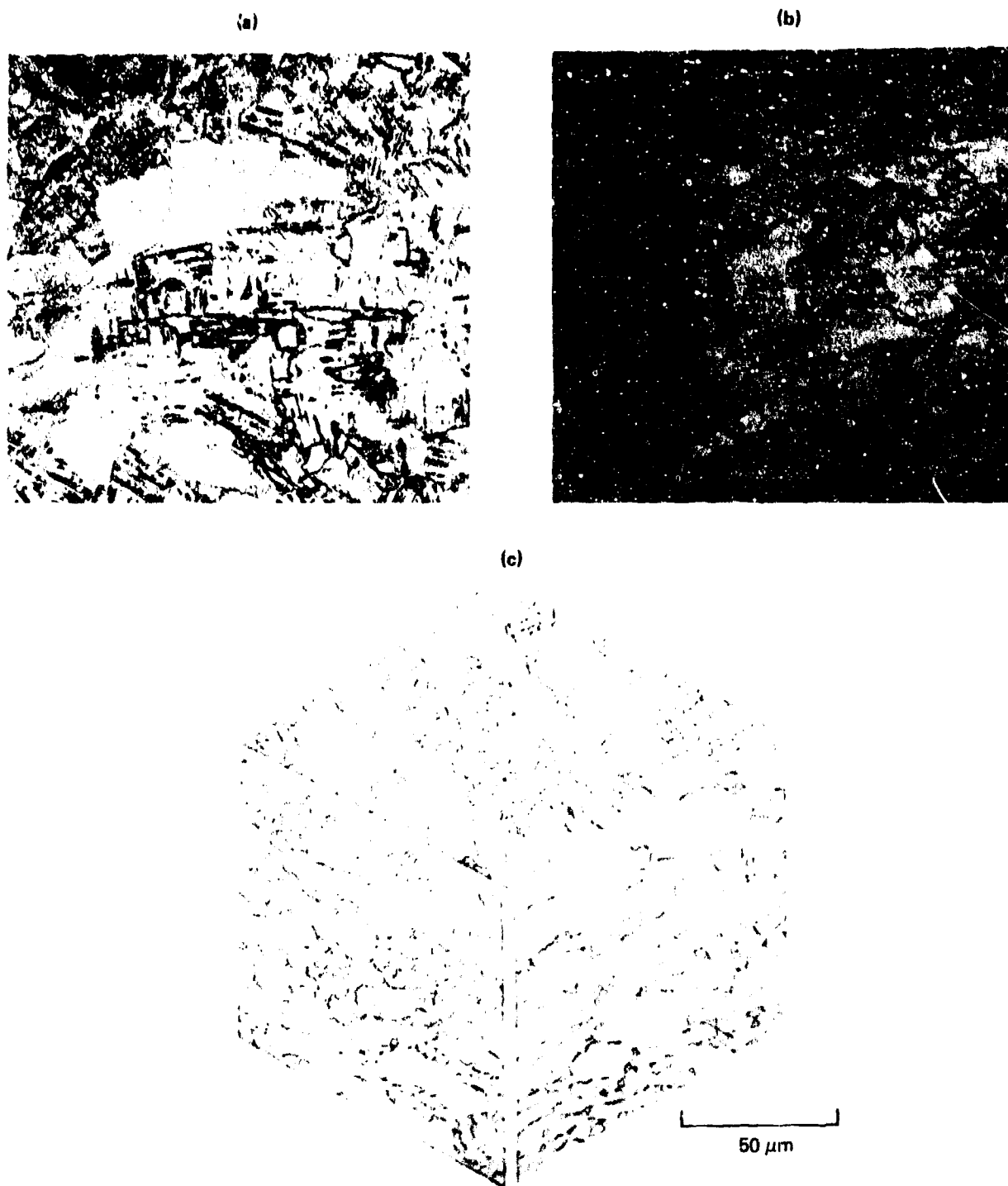
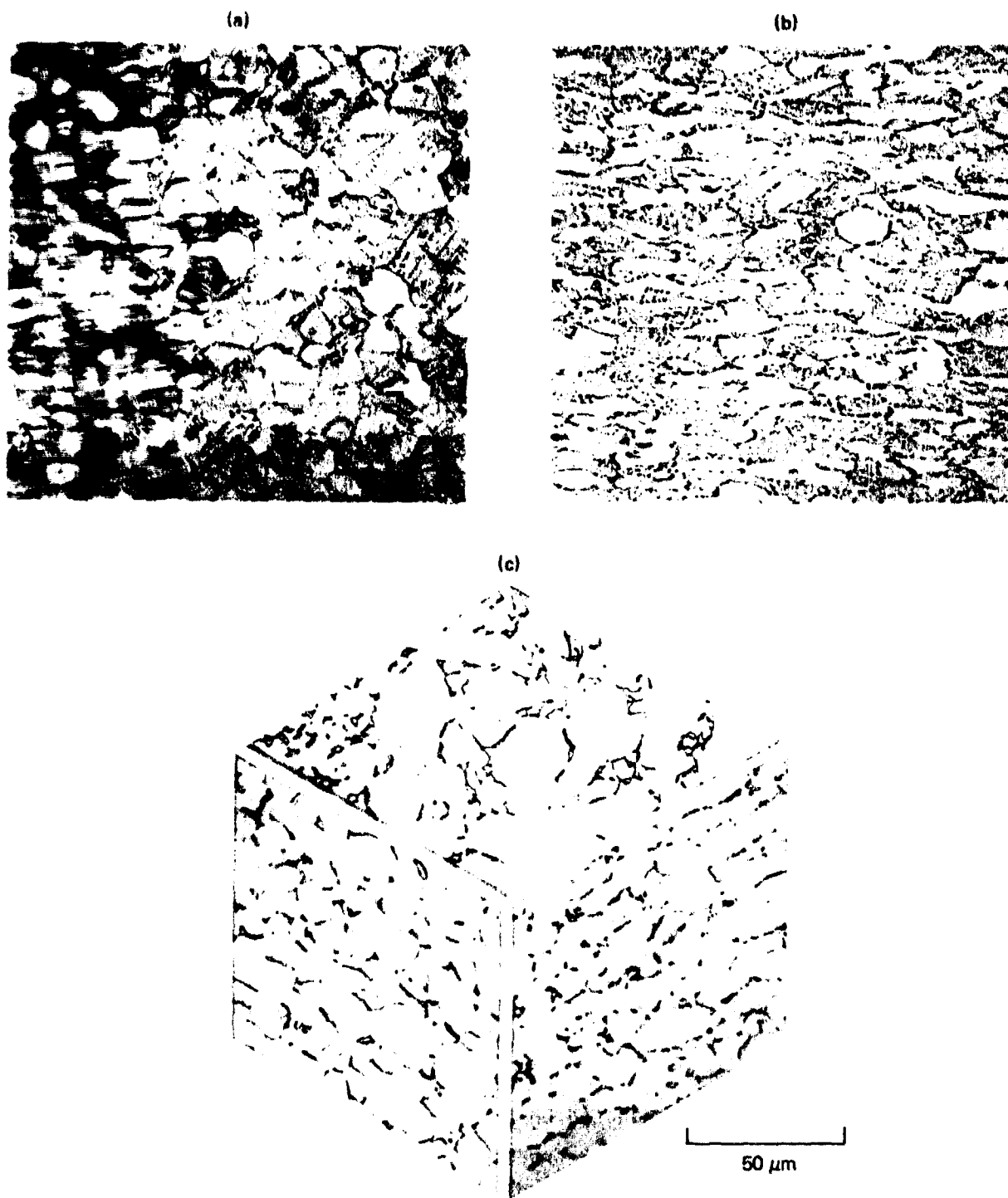


Figure 23. Microstructures of blocky alpha (level I) Ti-6Al-4V sheet (Heat no. G52063) for (a) 3.7-mm thick sheet annealed at 968°C (1774°F) for 4 h and air cooled to 25°C (77°F) (b) as-hot-rolled 1.8-mm thick sheet, and (c) 1.8-mm thick sheet vacuum annealed at 927°C (1700°F) for 1 h and furnace cooled to 25°C (77°F).

GP03-0240-203



GP03-0249-204

Figure 24. Microstructures of blocky alpha (level II) Ti-6Al-4V sheet (Heat no. G52063) for
 (a) 3.5-mm sheet annealed at 954°C (1750°F) for 4 h and air cooled to 25°C (77°F),
 (b) as-hot-rolled 1.9-mm sheet vacuum annealed at 927°C (1700°F) for 1 h and
 furnace cooled to 25°C (77°F).

3.4 ELI Grade Ti-6Al-4V

The description of starting stock of the ELI grade Ti-6Al-4V purchased from the Colt Industries/Crucible Inc., is given in Table 1. A normal texture was produced in this sheet with four variations in microstructure. Two grain sizes and two levels of primary alpha were produced. The microstructural variations were parallel to those produced in the regular grade Ti-6Al-4V.

Rolling of the ELI material generally followed the same schedule as the regular grade sheet. Heating temperatures for rolling were reduced 10°C (50°F) to adjust for the lower beta transus. The 75 mm (3 inch) thick plate was heated to 935°C (1715°F) max in a slightly oxidizing atmosphere and rolled to 14 mm (0.570 inch) thickness with one intermediate reheat. The plate was intentionally spread to 610 mm (24 inch) width during this rolling. Surface condition after rolling was good, therefore the plate was cut into two lengths in preparation for the next rolling cycle. The plates were then heated to 899°C (1650°F) and rolled to 7 mm (0.275 inch) thickness in five passes for the first plate and four passes for the second plate.

Following rolling, the plates were grit blasted, inspected and cut into two lengths once again. Cross-rolling was initiated at this stage. Panels were heated to 816°C (1500°F) and rolled to 3.7 mm (0.145 inch) thickness without reheating. Following this rolling, the panels were grit blasted and pickled prior to the final rolling cycle. Final rolling to 1.7 mm (0.066 inch) thickness was accomplished in open pairs rather than in carbon steel envelopes. Rolling temperature was again 816°C (1500°F). This procedure significantly improved the flatness of the finished sheet. The as-rolled sheets were descaled and pickled prior to final heat treatment.

Final heat treat studies were conducted on the as-hot rolled ELI sheet, as in the case of the regular grade material, to produce the required grain sizes and primary alpha levels. The panels were heat treated to produce grain sizes comparable to the smallest grain sizes in the regular grade sheet and an intermediate grain size. Table 9 summarizes the heat treat schedules, resulting grain sizes, and primary-alpha volume fractions for ELI-grade Ti-6Al-4V. The tensile properties are listed in Table 10.

TABLE 9. HEAT TREATMENT SCHEDULES AND THE RESULTING MICROSTRUCTURAL PARAMETERS FOR 1.5 x 381 x 381 mm (0.060 x 15 x 15 IN.) ELI-GRADE Ti-6Al-4V PANELS.

Panel code	Heat treatment	Primary alpha grain size (μm)	Volume fraction primary alpha
X1	899°C (1650°F) for 1.5 h; furnace cool to 25°C at 38°C/h (100°F/h)	5.5	0.88
X2	941°C (1725°F) for 3 h; furnace cool to 25°C at 38°C/h (100°F/h) + 935°C (1715°F) for 5 min; air cool to 25°C	4.5	0.47
X3	941°C (1725°F) for 4 h; furnace cool to 25°C at 38°C/h (100°F/h)	8.9	0.89
X4	941°C (1725°F) for 16 h; furnace cool to 25°C at 38°C/h (100°F/h) + 935°C (1715°F) for 5 min; air cool to 25°C	8.8	0.46

GP03-0249-114

TABLE 10. TENSILE PROPERTIES OF 1.7-mm (0.065 IN.) ELI-GRADE Ti-6Al-4V.

Heat treatment	Test direction	Ultimate tensile strength MPa (ksi)	0.2% offset yield stress MPa (ksi)	Elongation in 50.8 mm (2 in.) (%)
704°C (1300°F) for 1 h; air cool	L	830 (120.4)	794 (115.2)	15.5
	L	821 (119.1)	783 (113.5)	15.0
	T	838 (121.5)	818 (118.6)	11.0
	T	860 (124.8)	842 (122.1)	11.5

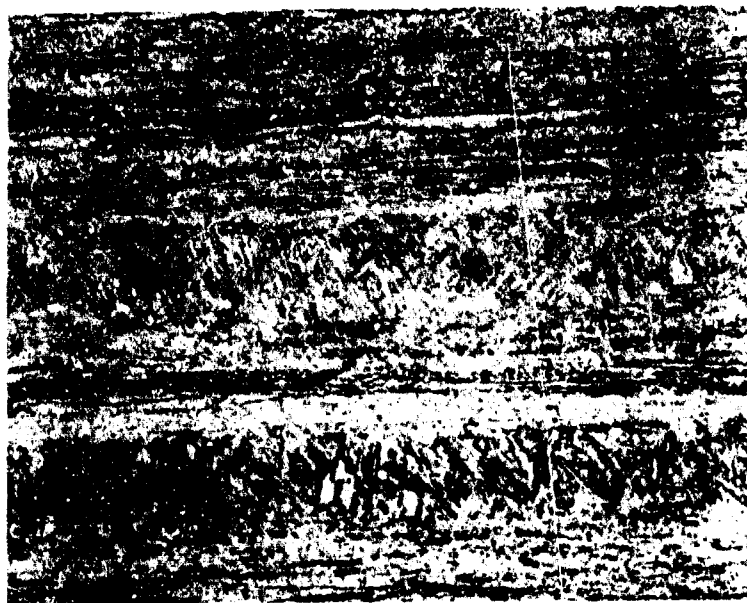
GP03-0249-115

3.5 Simulated Coil Ti-6Al-4V

Material used for production of the simulated coil Ti-6Al-4V was secured as mill processed hot band. This material is described in Table 1. The hot band was received in the as-hot rolled condition; therefore, heat treatment and conditioning were required prior to initiation of laboratory cold rolling. In order to obtain a highly ductile condition for cold rolling, the hot band was annealed at 927°C (1700°F) for 1 hour and furnace cooled. After annealing, the hot band was grit blasted, spot ground to remove surface defects and pickled.

The cold rollability of the Ti-6Al-4V alloy is limited. Reductions over about 25 percent generally result in excessive edge cracking. In order to avoid this cracking, the sheet was cold rolled a maximum of 15 percent between intermediate anneals. Following each cold rolling cycle, the sheet was annealed 5 minutes at 788°C (1450°F), air cooled, descaled and pickled prior to the next cold rolling cycle. Processing of the Ti-6Al-4V simulated coil involved four cycles of cold roll, anneal and pickle from hot band to the 1.7 mm (0.065 inch) final thickness. The processing went reasonably well although product yield was less than expected due to trimming required between rolling cycles. Following the final cold reduction, the sheet was sheared into panels for heat treatment.

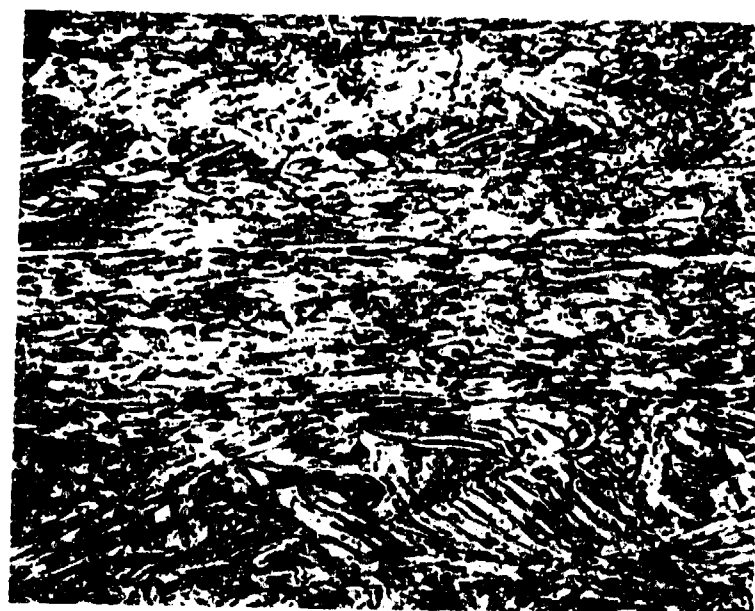
The Ti-6Al-4V hot band microstructure is shown in Figure 25. This material contained a considerable amount of banding from the hot rolling operation. Microstructure after the 927°C (1700°F) anneal produced a discernible coarsening of the alpha platelets. The as-rolled structure of the Ti-6Al-4V sheet after cold rolling cycles is shown in Figure 26. The other intermediate structures did not differ significantly from this microstructure. The variation of primary alpha with temperature for simulated coil Ti-6Al-4V is shown in Figure 27. The heat treatments, the primary grain sizes and the volume fractions for each of four conditions are shown in Table 11. The four final heat treated conditions are shown in Figures 28 and 29. The cold rolling and final recrystallization anneals essentially eliminated the banding from the starting material.



100 μm

GP03-0240-205

Figure 25. Microstructure of as-received Ti-6Al-4V hot band.



50 μm



100 μm

GP03-0248-208

Figure 26. Microstructures of Ti-6Al-4V sheet after four 15% cold-rolling cycles.

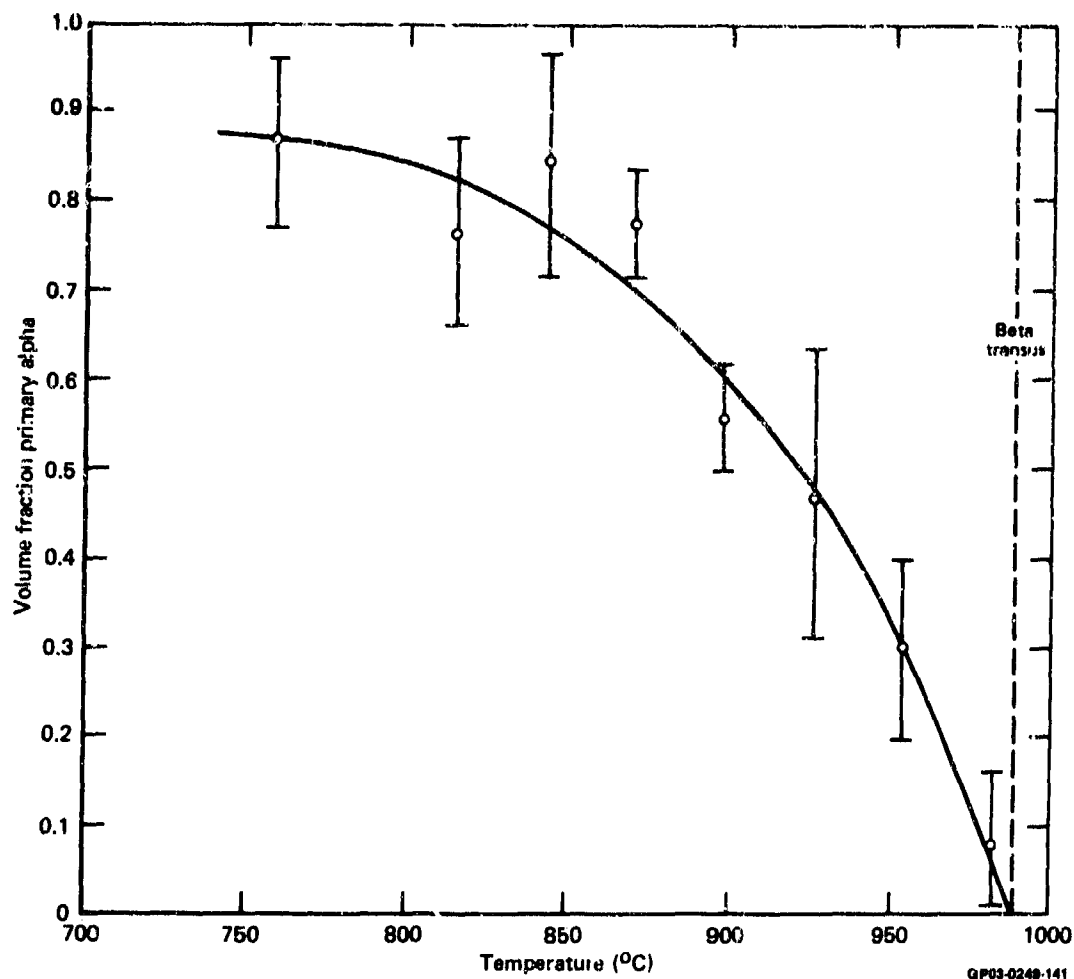
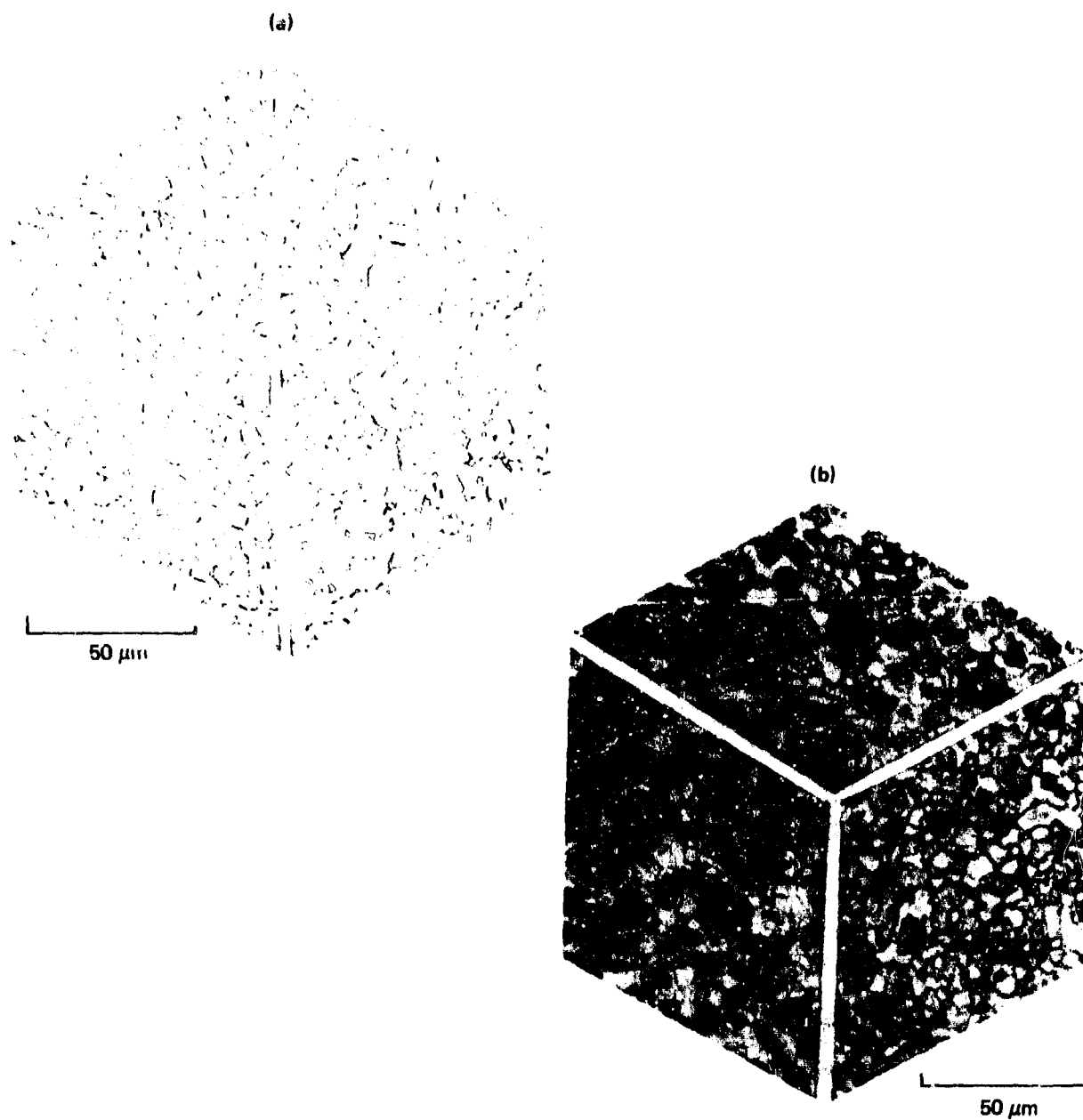


Figure 27. Variation of primary-alpha level with temperature in the Ti-6Al-4V alloy. Bands represent 95% confidence limits.

TABLE 11. HEAT TREATMENT AND MICROSTRUCTURAL PARAMETERS OF SIMULATED-COIL Ti-6Al-4V.

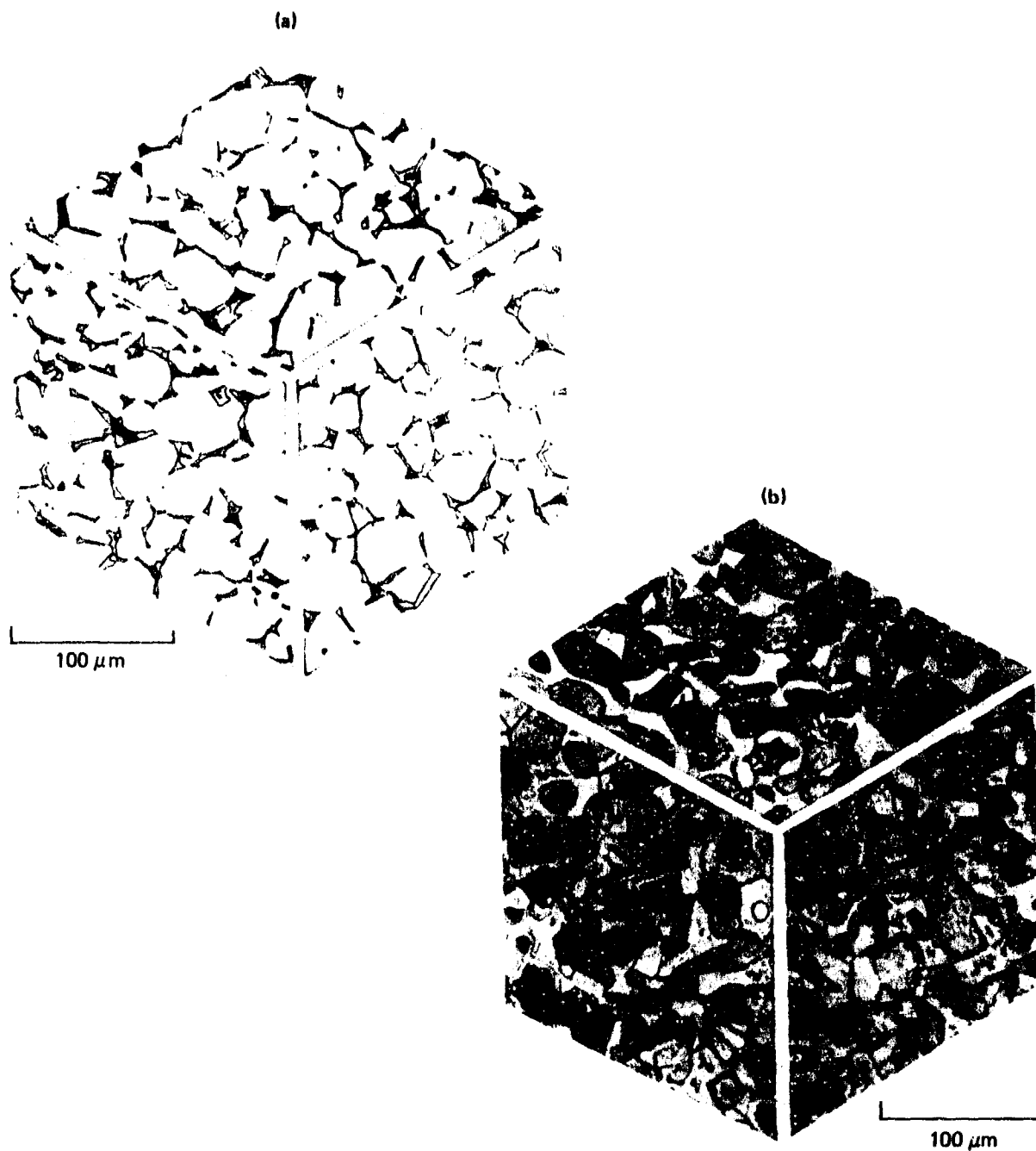
Panel code	Heat treatment	Primary alpha grain size (μm)	Standard deviation (μm)	Volume fraction primary alpha	Standard deviation (μm)
S1	927°C (1700°F)/1.5 h; furnace cool to 25°C	5.1	1.0	0.87	0.05
S2	927°C (1700°F)/1.5 h; furnace cool to 25°C + 899°C (1650°F)/10 min, air cool to 25°C	4.4	0.6	0.63	0.05
S3	995°C (1750°F)/16 h; furnace cool to 25°C	12.3	1.6	0.87	0.05
S4	899°C (1650°F)/10 min; air cool to 25°C	9.3	1.8	0.63	0.06

GP03-0240-116



9P03-0240-207

Figure 28. Microstructures of simulated coil-rolled Ti-6Al-4V (a) annealed at 954°C (1748°F) for 16 h and furnace cooled to 25°C (77°F) (condition S1) and (b) annealed at 927°C (1700°F) for 1.5 h, furnace cooled to 25°C (77°F) + 899°C (1650°F) for 10 min, and air cooled to 25°C (77°F) (condition S2).



GP03-0249-206

Figure 29. Microstructures of simulated coil-rolled Ti-6Al-4V sheet (a) annealed at 954°C (1749°F) for 16 h and furnace cooled to 25°C (77°F) (condition S3) and (b) annealed at 954°C (1749°F) for 24 h, furnace cooled to 25°C (77°F) + annealed at 899°C (1650°F) for 10 min, and air cooled to 25°C (77°F) (condition S4).

3.6 Ti-3Al-2.5V

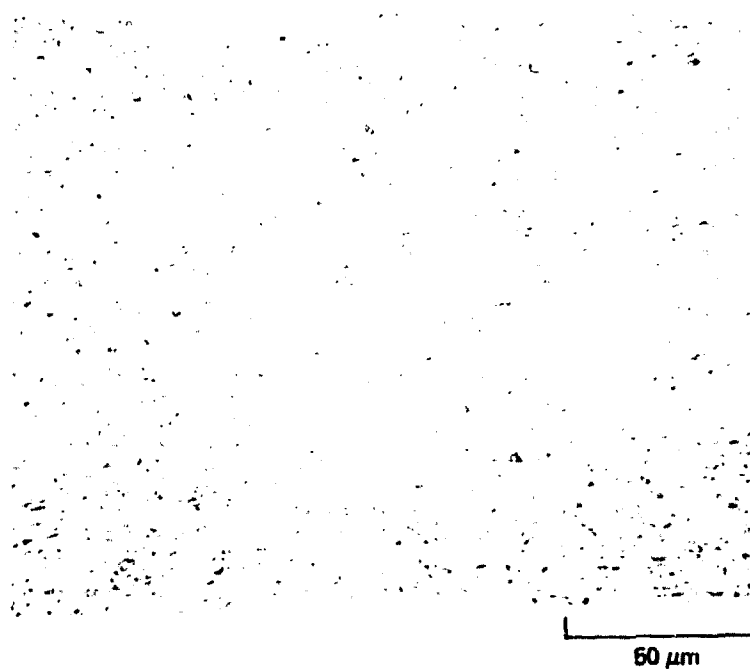
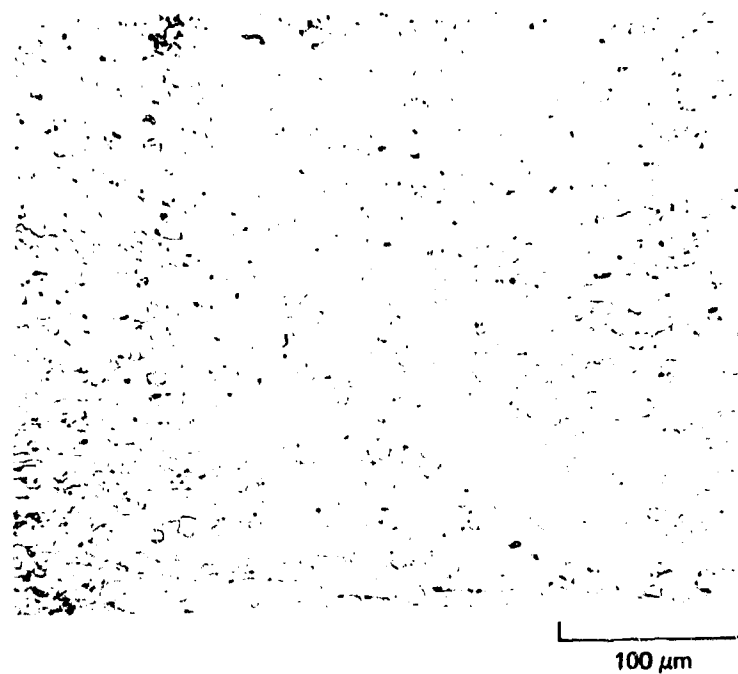
Starting stock for the Ti-3Al-2.5V, obtained in the form of 2.2 mm (0.086 in) thick mill-processed sheet, is described in Table 1. The basic mill processing steps were to hot roll a forged slab to 3.8 mm (0.150 inch) hot band, strand line anneal and pickle, cold roll 40 percent, final anneal, and pickle. As-received mill processed material was then sheared to convenient size sheets and laboratory cold rolled 39 percent to 1.3 mm (0.053 inch) thick sheet. Reductions per pass were 1-5 percent. Following cold rolling, the sheets were sheared to 381 mm (15 inch) square panels for heat treatment.

The microstructure of the 22-mm (0.086 inch) thick mill-processed Ti-3Al-2.5V sheet contains the partially recrystallized structure typical of a strand line annealed product. Figure 30 shows the microstructure of Ti-3Al-2.5V sheet after cold rolling 39 percent. Heat treatment studies were conducted to determine grain growth characteristics and variation of primary alpha with temperature. The variations with time and temperature of alpha grain size and volume-fraction of primary alpha are shown in Figures 31 and 32.

The primary-alpha grain sizes and volume fractions produced for this investigation are summarized in Table 12. The microstructures of the heat-treated panels shown in Figures 33 and 34 are similar to those observed in other alpha-beta titanium alloys. The finest grain size obtained in the alloy was comparable to that in panel L of regular grade Ti-6Al-4V (primary-alpha volume fraction = 0.88, grain size = 6.0 μm).

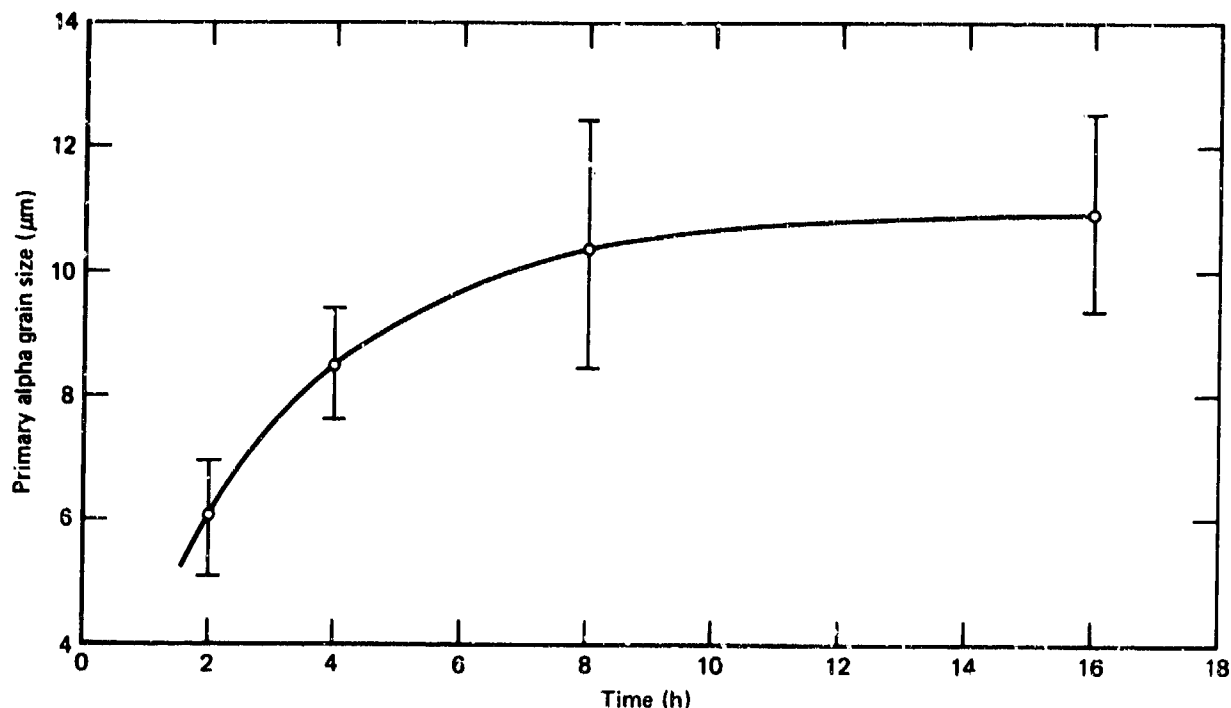
3.7 Ti-6Al-2Sn-4Zr-2Mo

Conventional mill processed Ti-6Al-2Sn-4Zr-2Mo sheet was obtained from RMI Company. A description of this material is given in Table 1. Variations in grain size and primary-alpha volume fractions were produced by annealing the sheets in the alpha-beta field. Results of grain growth determinations on the Ti-6Al-2Sn-4Zr-2Mo alloy are shown in Figure 35. Samples were vacuum annealed for the indicated time at temperature and then furnace cooled 56°C/hr (100°F/hr) to 760°C (1400°F).



GP03-0248-209

Figure 30. Microstructures of Ti-3Al-2.5V sheet after cold-rolling 38%.



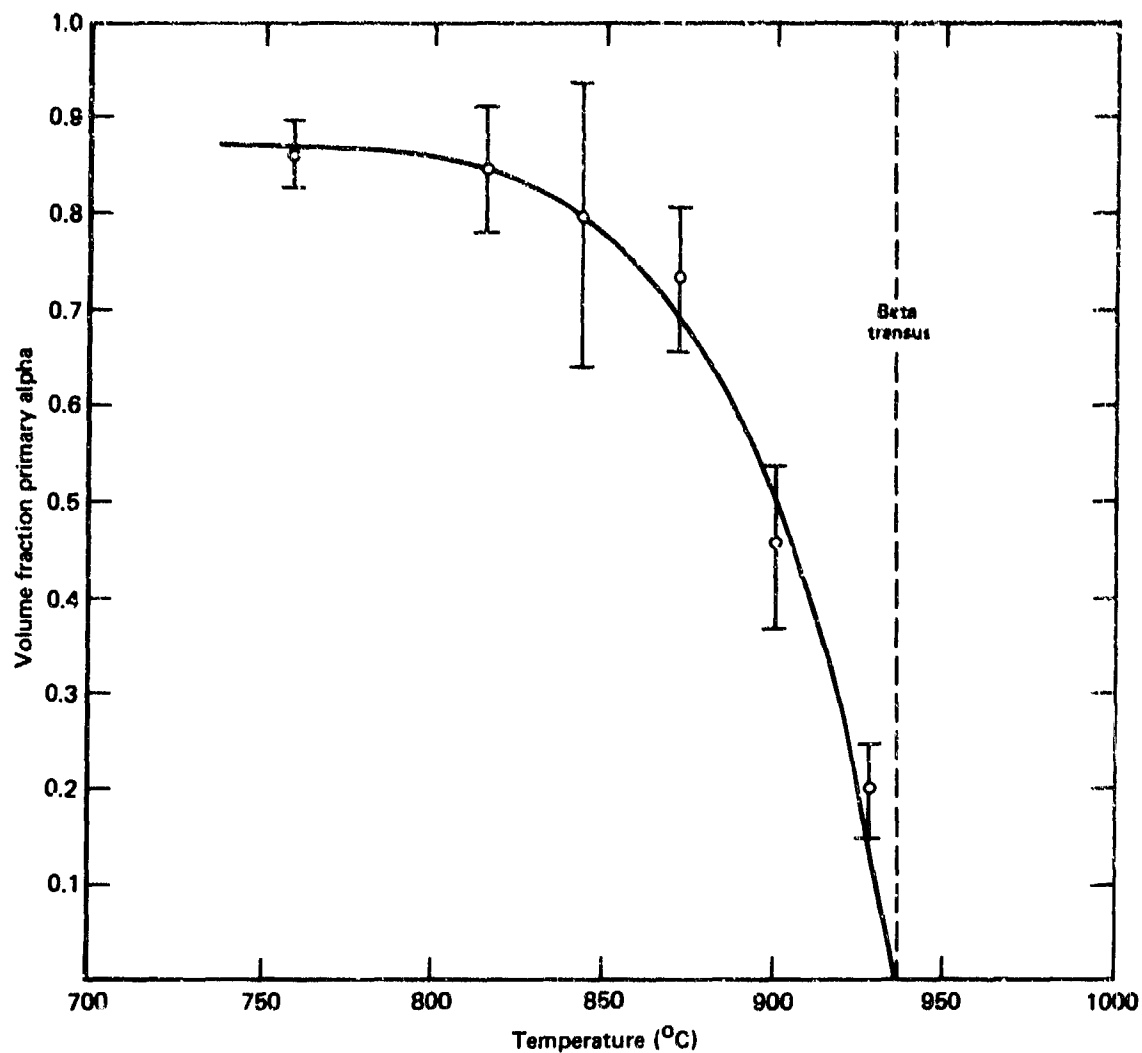
GP03-0249-139

Figure 31. Grain growth in the Ti-3Al-2.5V alloy at 913°C (1675°F). Values determined after furnace cooling from the heat treatment temperature. Bands represent 95% confidence limits.

TABLE 12. EFFECTS OF ANNEALING TEMPERATURE AND TIME ON GRAIN SIZES AND VOLUME FRACTIONS OF PRIMARY ALPHA FOR Ti-3Al-2.5V.

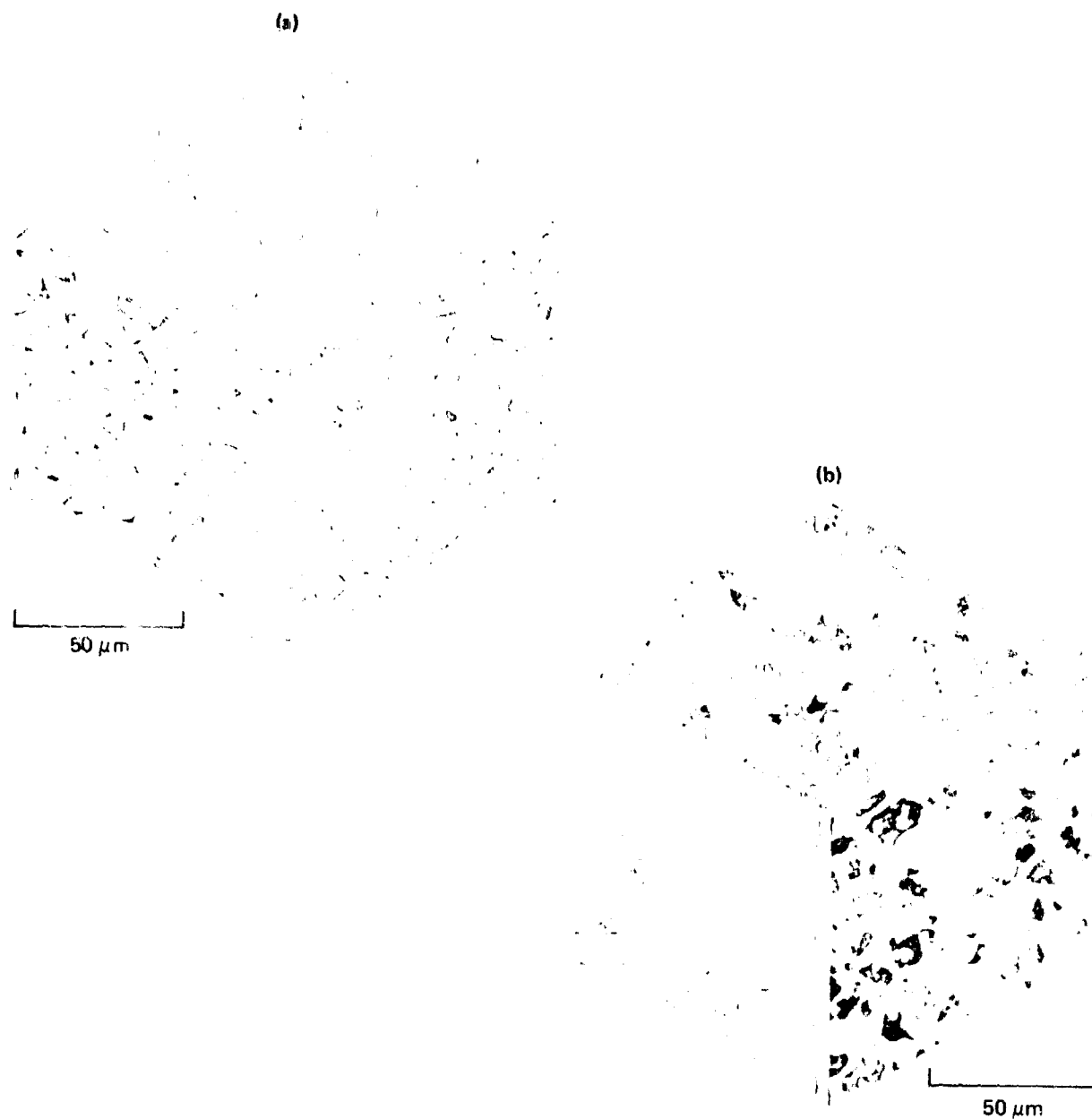
Panel code	Heat treatment	Primary alpha grain size (μm)	Standard deviation (μm)	Volume fraction primary alpha	Standard deviation (μm)
R1	Vacuum anneal at 871°C (1600°F) for 1 h; furnace cool to 25°C	5.6	0.7	0.87	—
R2	Vacuum anneal at 871°C (1600°F) for 1 h; furnace cool to 25°C + 891°C (1635°F) for 10 min; air cool to 25°C	4.3	0.5	0.57	0.06
R3	Vacuum anneal at 899°C (1650°F) for 20 h; furnace cool to 25°C	10.2	0.9	0.87	—
R4	Vacuum anneal to 899°C (1650°F) for 20 h; furnace cool to 25°C + 891°C (1635°F) for 10 min; air cool to 25°C	8.6	1.4	0.58	0.09

GP03-0249-117



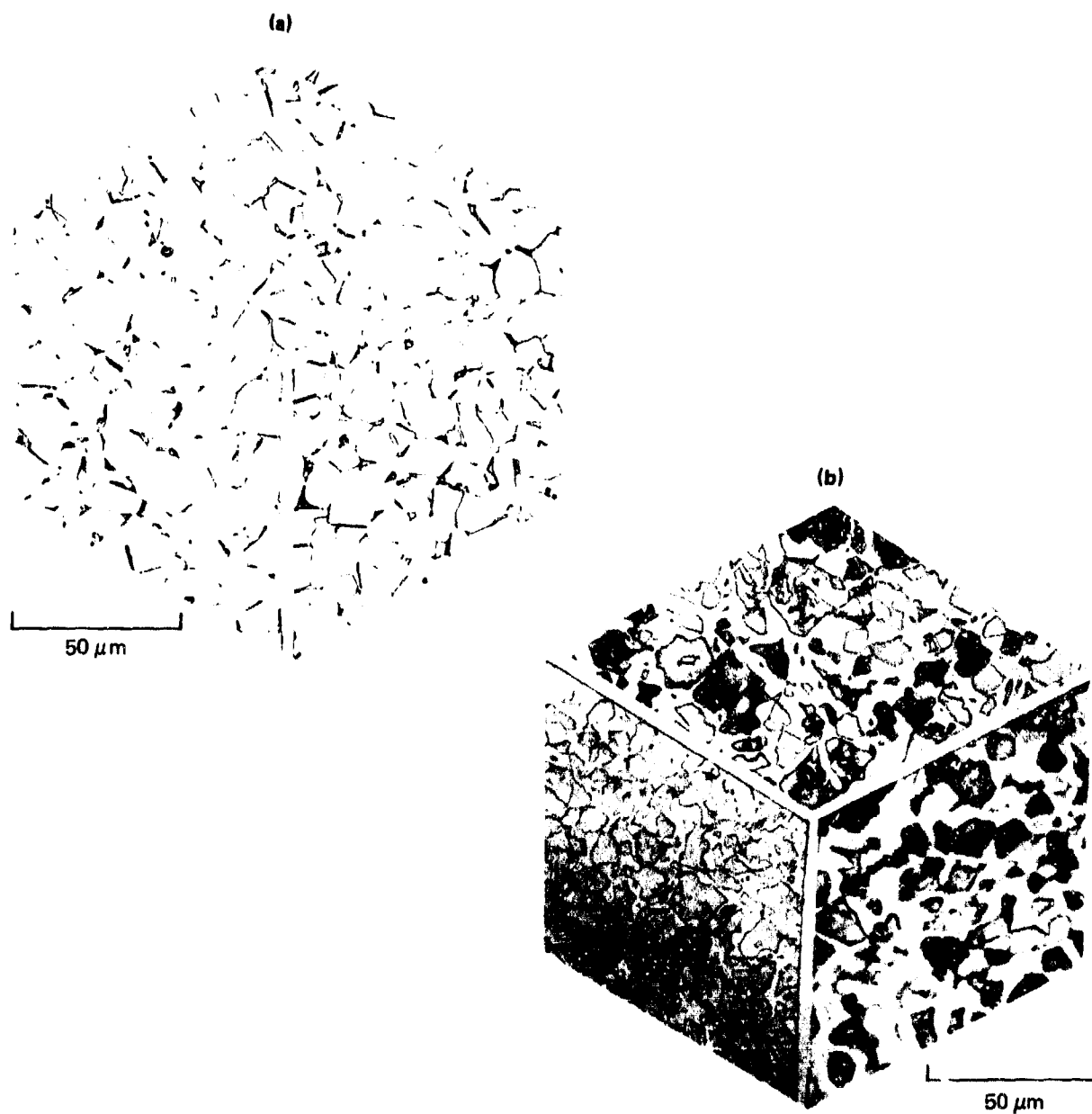
GP03-0248-143

Figure 32. Variation of primary-alpha level with temperature in the Ti-3Al-2.5V alloy. Bands represent 95% confidence limits.



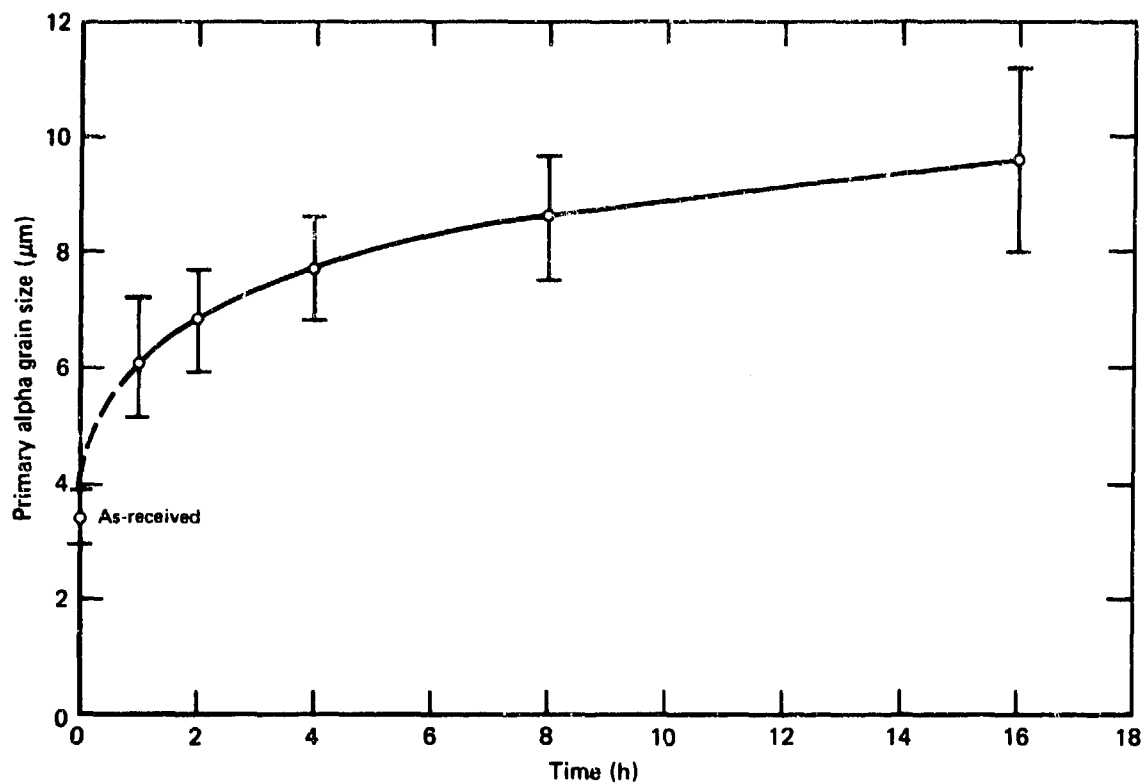
GP03-0249-211

Figure 33. Microstructures of Ti-3Al-2.5V sheet (a) annealed at 871°C (1600°F) for 1 h and furnace cooled to 25°C (77°F) (condition R1) and (b) annealed at 871°C (1600°F) for 1 h, furnace cooled to 25°C + 891°C (1636°F) for 10 min, and air cooled to 25°C (77°F) (condition R2).



GP03-0249-210

Figure 34. Microstructures of Ti-3Al-2.5V sheet (a) annealed at 899°C (1640°F) for 20 h, furnace cooled to 25°C (77°F) (condition R3) and (b) annealed at 899°C (1640°F) for 20 h, furnace cooled to 25°C (77°F) + annealed at 891°C (1636°F) for 10 min, and air cooled to 25°C (77°F) (condition R4).



GP03-0248-140

Figure 35. Grain growth in Ti-6Al-2Sn-4Zr-2Mo alloy at 968°C (1775°F). Values determined after furnace cooling from the heat treatment temperature. Bands represent 95% confidence limits.

Variation of primary-alpha volume fraction with temperature was determined by taking fully recrystallized samples and heating for 15 minutes at various temperatures and fast cooling. Figure 36 shows the variation of primary alpha with temperature.

Table 13 summarizes the heat treatments, the primary alpha grain sizes and volume fraction primary alpha for each of the four conditions produced in this alloy. The two grain sizes selected were the finest obtainable and an intermediate size.

The microstructure of the as-received Ti-6Al-2Sn-4Zr-2Mo sheet is shown in Figure 37a. This structure is fully recrystallized, and the grain size is very fine. Microstructure after heating to produce approximately 60 percent primary alpha is shown in Figure 37b. The structure of the larger grain size panels at the two levels of primary alpha are shown in Figure 38.

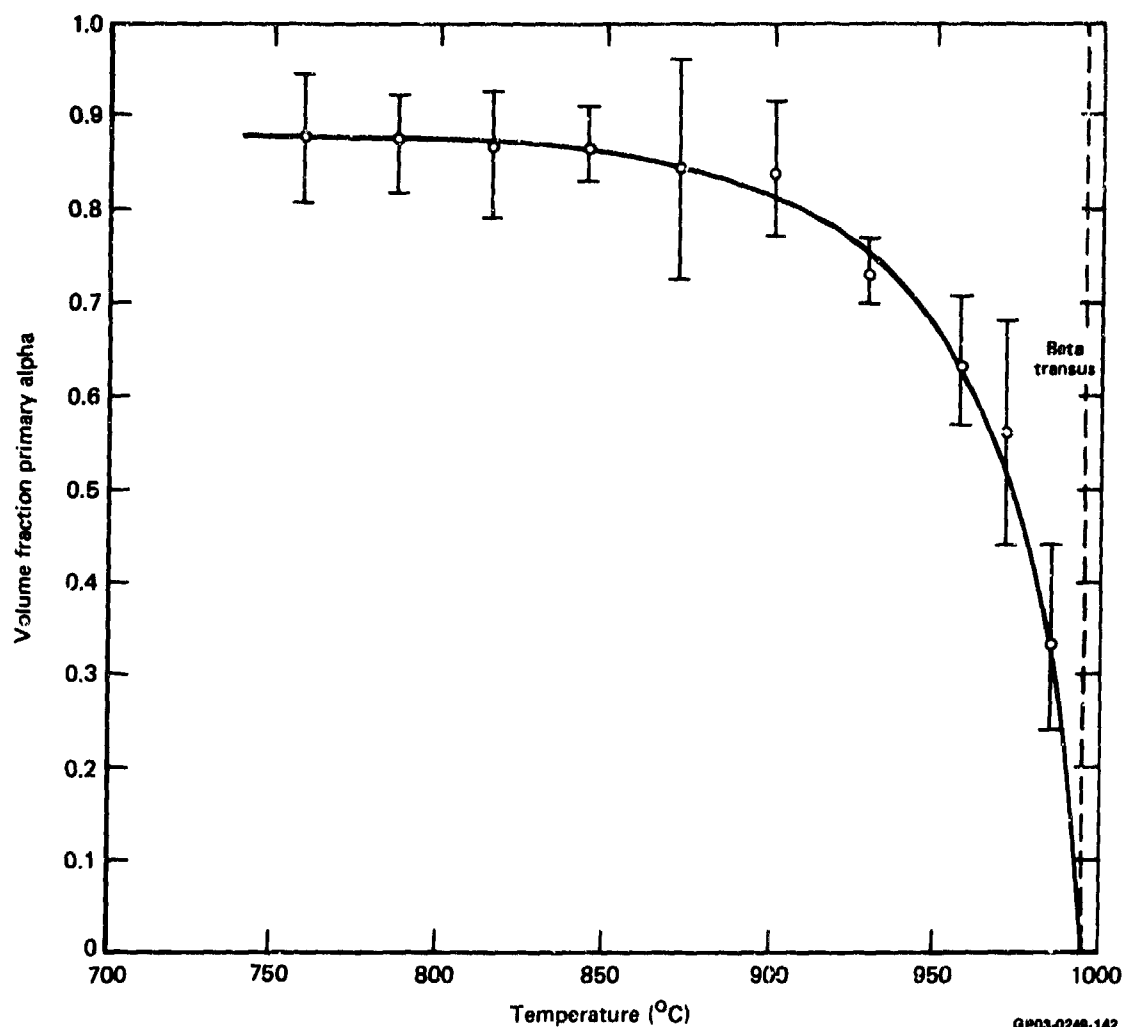
3.8 Ti-8Al-1Mo-1V

Conventionally mill-processed 1.1 mm (0.045 inch) and 1.3 mm (0.050 inch), Ti-8Al-1Mo-1V sheet were procured from RMI. Because the principal reason for including this alloy in the present investigation was to determine the superplastic formability of the alloy in the mill-processed condition, no additional heat treatments were performed on this alloy.

The microstructure of the as-received Ti-8Al-1Mo-1V is shown in Figure 39. The 1.1 mm (0.045 inch) thick sheet stock was fully recrystallized, and the grain size was very fine. The grain structure for the 1.27 mm (0.050 inch) thick sheet had some elongated alpha microstructure.

3.9 Ti-15V-3Cr-3Sn-3Al

The Ti-15V-3Cr-3Al-3Sn was purchased from Timet. A description of this material is given in Table 1. The Ti-15V-3Cr-3Sn-3Al alloy was received from Timet as 1.9 mm (0.075 inch) thick sheet in 57 percent cold rolled condition. Processing to this stage involved hot rolling to a 4.3 mm (0.170 inch) hot band, which was then conditioned, annealed at 788°C (1450°F), and cold rolled to finish gage. As-cold rolled material was ground 0.05 mm (0.002 inch) on each side and flash pickled.



GP03-0248-142

Figure 36. Variation of primary-alpha level with the temperature in the Ti-6Al-2Sn-4Zr-2Mo alloy. Bands represent 95% confidence limits.

TABLE 13. EFFECTS OF HEAT TREATMENT ON GRAIN SIZE AND VOLUME FRACTIONS OF PRIMARY ALPHA OF Ti-6Al-2Sn-4Zr-2Mo.

Panel code	Heat treatment	Primary alpha grain size (μm)	Standard deviation (μm)	Volume fraction primary alpha	Standard deviation (μm)
Q1	As-received	3.5	0.6	0.90	0.02
Q2	963°C (1765°F) for 10 min; air cool to 25°C	3.4	0.2	0.65	0.05
Q3	960°C (1760°F) for 20 h; air cool to 25°C	8.2	1.6	0.86	0.03
Q4	960°C (1760°F) for 24 h; furnace cool to 25°C +963°C (1765°F) for 10 min; air cool to 25°C	8.8	2.7	0.55	0.03

GP03-0248-118

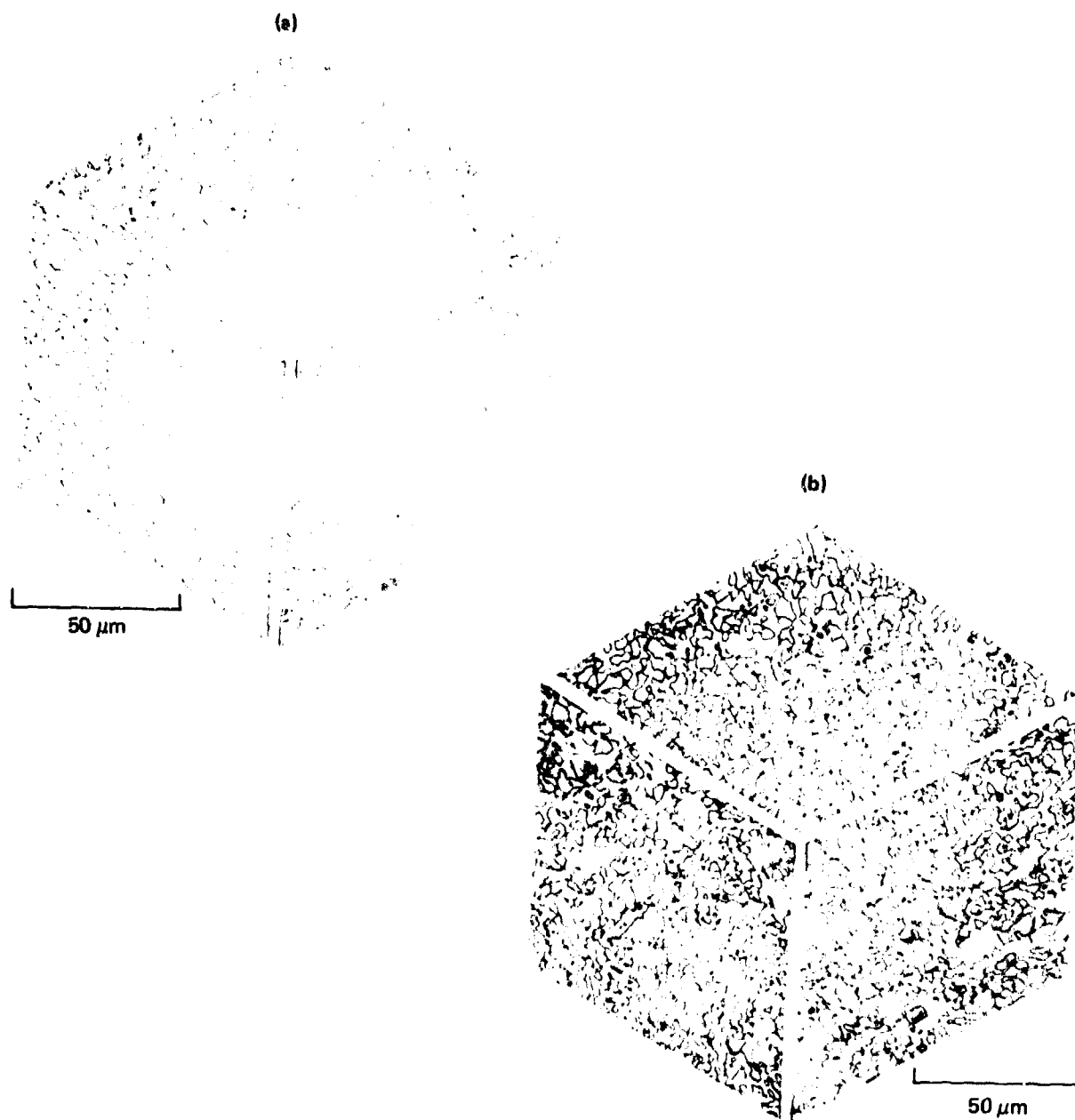
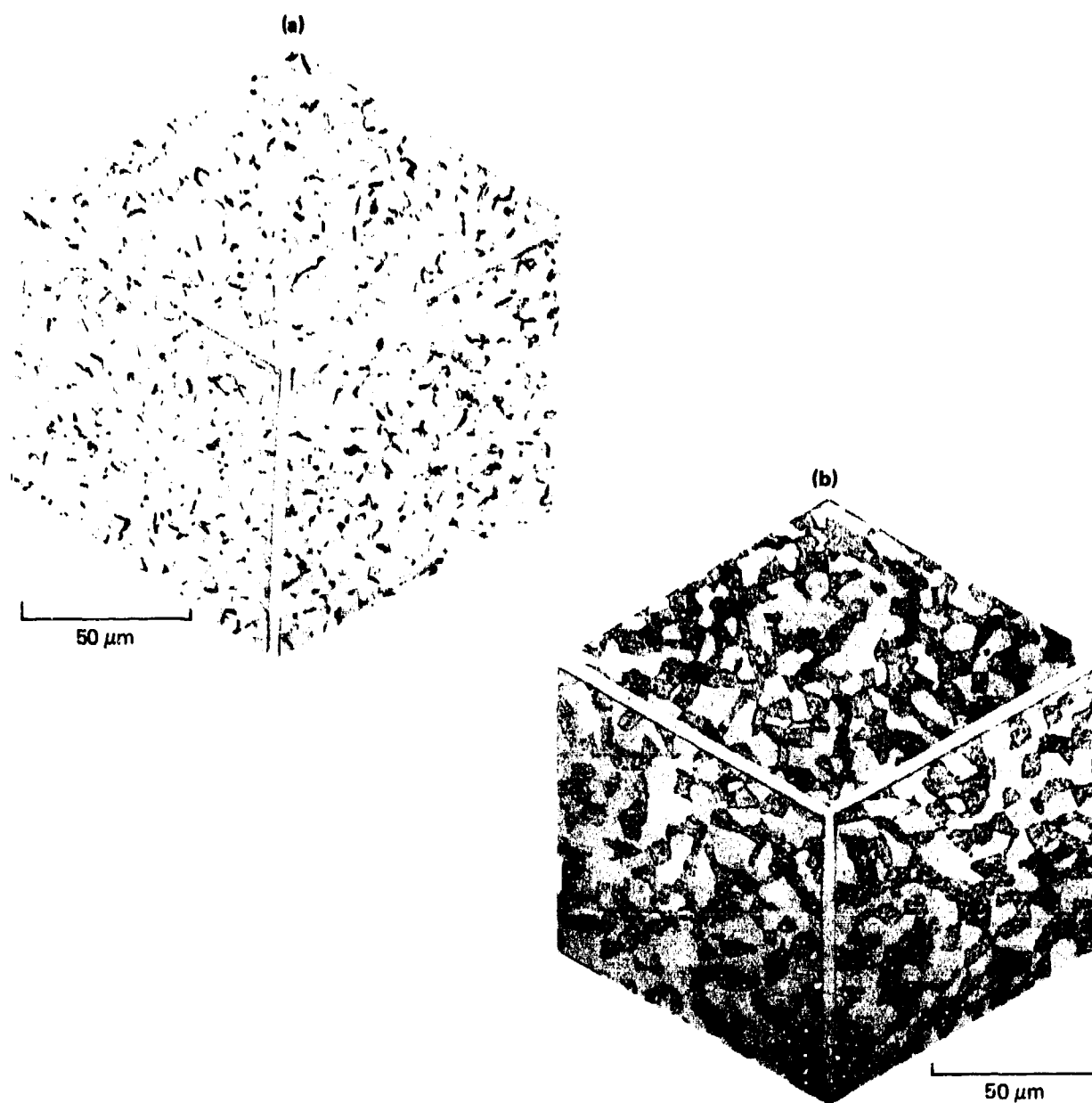


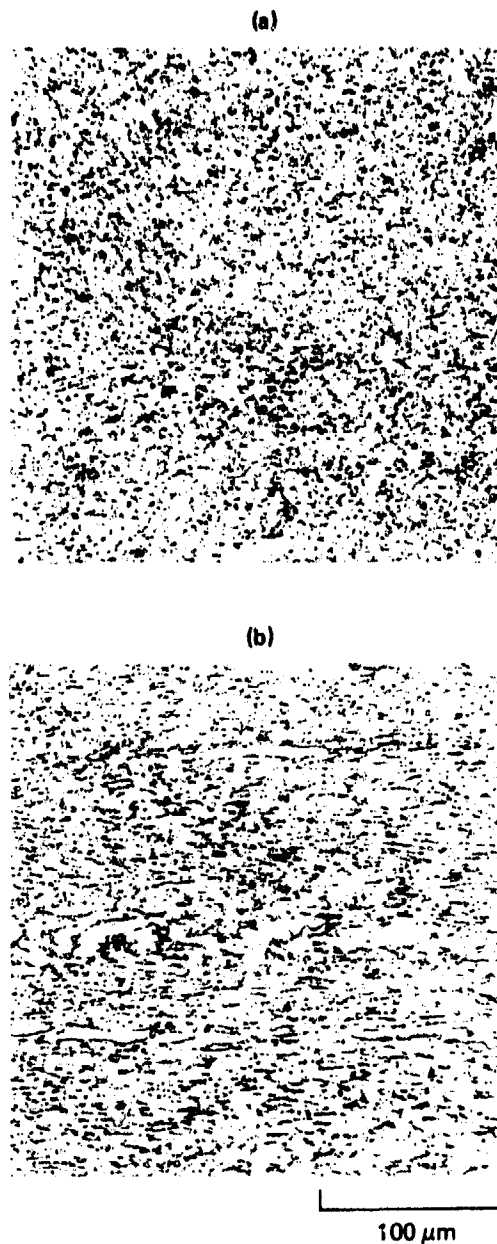
Figure 37. Microstructures of Ti-6Al-2Sn-4Zr-2Mo sheet (a) as-received and (b) annealed at 963°C (1765°F) for 10 min and air cooled to 25°C (77°F).

GP03-0249-212



GP03-0249-213

Figure 38. Microstructures of Ti-6Al-2Sn-4Zr-2Mo sheet (a) annealed at 960°C (1760°F) for 20 h and furnace cooled to 25°C (77°F) and (b) annealed at 960°C (1760°F) for 20 h, furnace cooled to 25°C (77°F) + annealed at 963°C (1765°F) for 10 min and air cooled to 25°C (77°F).



GP03-0249-214

Figure 39. Microstructures of as-received Ti-8Al-1Mo-1V sheet (a) 1.14-mm thick and (b) 1.2-mm thick.

This beta alloy was processed and heat treated to produce six variations in microstructure. Three grain sizes were produced, one of which was the as cold rolled condition. For each grain size, material was heat treated to an all beta condition and an aged condition to produce a fine dispersion of alpha phase in the beta matrix. Heat treatments to produce the required microstructures were conducted in air in all cases except one. The two hour anneal at 774°C (1425°F) was performed in vacuum to avoid excessive oxidation. All heat treatments were followed by an air cool or the equivalent. Following the heat treatment, all panels were descaled and pickled.

The microstructure of the as-cold rolled condition (Figure 40a) contains highly elongated beta. Recrystallization and grain growth characteristics were determined for this material at 774°C (1425°F) in the beta field. Recrystallization and grain growth occur rapidly (Figures 40b-40d). Because of this, grain sizes less than 30 μm could not be obtained in this alloy.

Table 14 gives the heat treatments and the resulting beta grain sizes for the Ti-15V-3Sn-3Al alloy. No beta grain size was shown for as-cold material since the beta grains are highly elongated and not equiaxed.

TABLE 14. EFFECTS OF HEAT TREATMENTS ON GRAIN SIZES OF Ti-15V-3Cr-3Sn-3Al.

Panel code	Heat treatment	Beta grain size (μm)
Z1	As cold-rolled 57%	—
Z2	Cold-rolled 57% + 482°C (900°F) 8 h, air cool	—
Z3	774°C (1425°F) for 5 min; air cool to 25°C	32
Z4	774°C (1425°F) for 5 min; air cool to 25°C + 482°C (900°F) for 8 h; air cool to 25°C	32
Z5	774°C (1425°F) for 5 min; air cool to 25°C + 566°C (1050°F) for 8 h; air cool to 25°C	32
Z6	774°C (1425°F) for 2.25 h; air cool to 25°C	52
Z7	774°C (1425°F) for 2.25 h; air cool to 25°C + 482°C (900°F) for 8 h; air cool to 25°C	52

GP03-0249-119

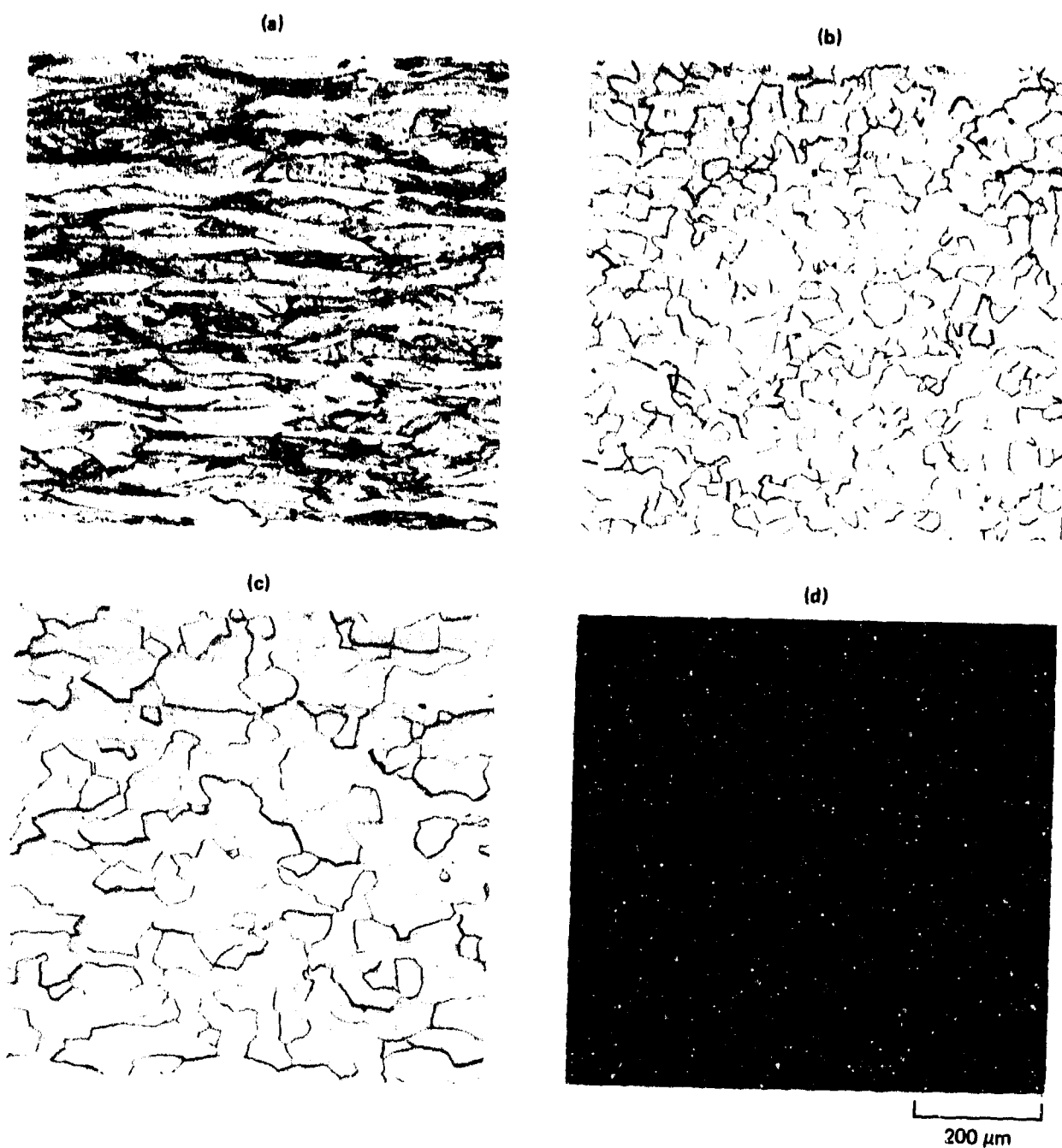


Figure 40. Microstructures of Ti-15V-3Cr-3Al-3Sn alloy (Heat no. P3357) (a) as-cold-rolled 57%, (b) annealed at 775°C (1425°F) for 5 min, (c) annealed at 775°C (1425°F) for 2.25 h, and (d) annealed at 775°C (1425°F) for 5 min, air-cooled at 25°C (77°F) + annealed at 482°C (900°F) for 8 h and air cooled to 25°C (77°F).

200 μm

GP03-0249-215

SECTION IV

CHARACTERIZATION OF SUPERPLASTICITY

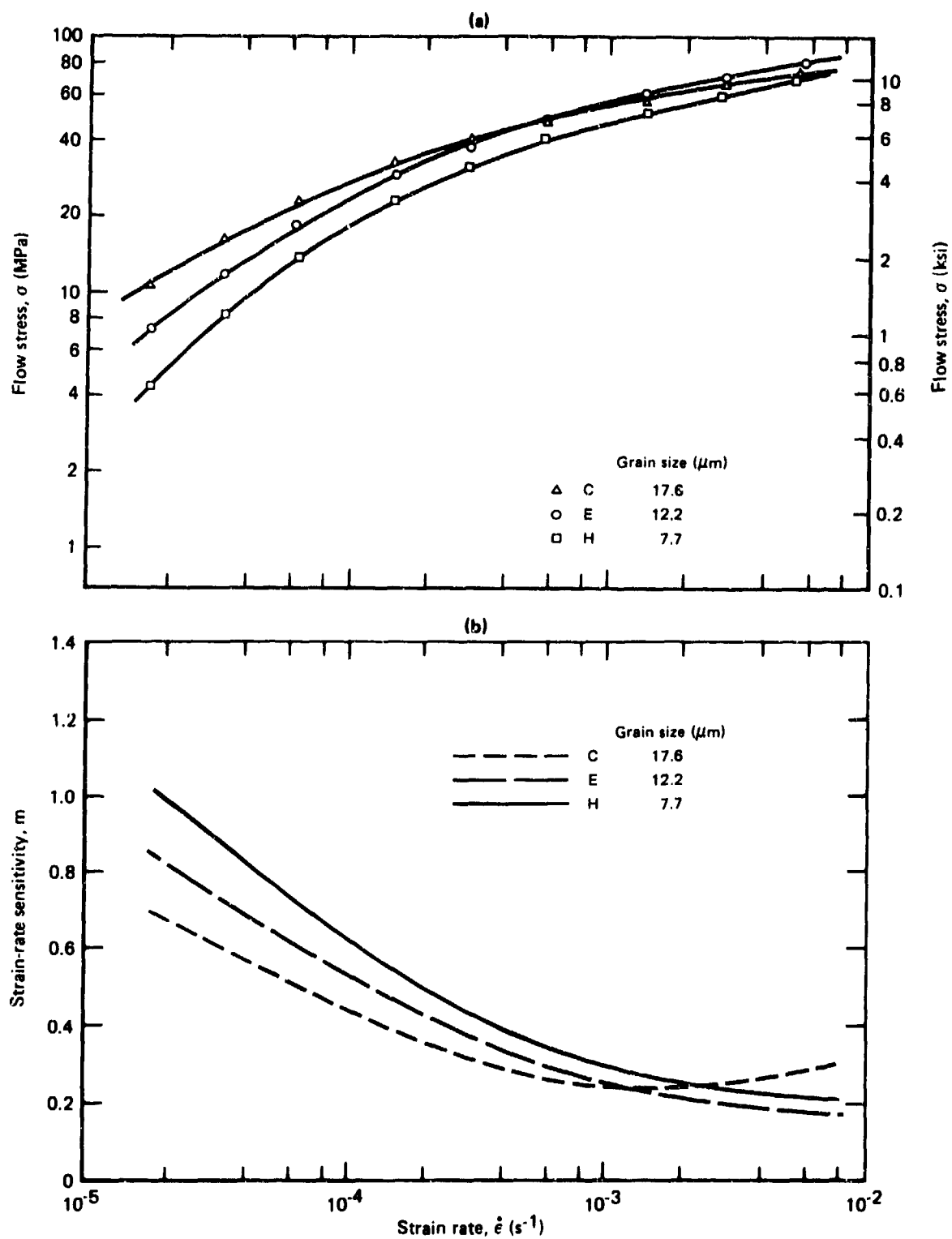
4.1 Regular Grade Ti-6Al-4V

4.1.1 Strain-rate dependences of flow stress and strain-rate-sensitivity

The strain-rate dependences of flow stress and strain-rate sensitivity at 850°C, (1562°F), 875°C (1607°F) and 906°C (1663°F) for different microstructural conditions of regular grade Ti-6Al-4V determined from incremental-strain-rate tests are shown in Figures 41 through 49, and the important superplasticity parameters are summarized in Tables 15-17. The stresses and strain rates shown in Figures 41 through 49 are the true stresses and true strain-rates computed from load-displacement curves, and the strain-rate sensitivity, m , was computed by fitting a third-degree polynomial to the flow-stress/strain-rate data and determining the values of the derivative of the polynomial at different values of strain rate.

With increasing grain size, the flow stress increases and the strain-rate sensitivity decreases at 850°C (1562°F), 875°C (1607°F), and 906°C (1663°F). The grain-size dependences of flow stress and strain-rate sensitivity, are less marked at 906°C (1663°F) than at 850°C (1562°F) and 875°C (1607°F) because of higher diffusion rates and rapid grain coarsening at the higher temperature.

The data in Tables 15-17 show that the incremental-strain-rate tests can be used as a screening test for evaluating the superplasticity of a given material. However, care must be exercised in using the maximum strain-rate sensitivity, m_{\max} , as the single superplasticity index of a material because the actual manifestation of the large deformation typical of superplasticity depends on the combination of grain size, temperature, and stress (or equivalently, strain-rate). The strain rate at which $m = 0.5$, denoted by $\dot{\epsilon}_{0.5}$, was found to be a useful superplasticity parameter because at strain-rates $> \dot{\epsilon}_{0.5}$, necking was observed in specimens deformed to large elongations at constant crosshead speed. The $\dot{\epsilon}_{0.5}$ value increases



GP03-0248-24

Figure 41. Strain-rate dependence of (a) flow stress and (b) strain-rate sensitivity of regular-grade Ti-6Al-4V (volume % primary α = 88) at 850°C (1562°F).

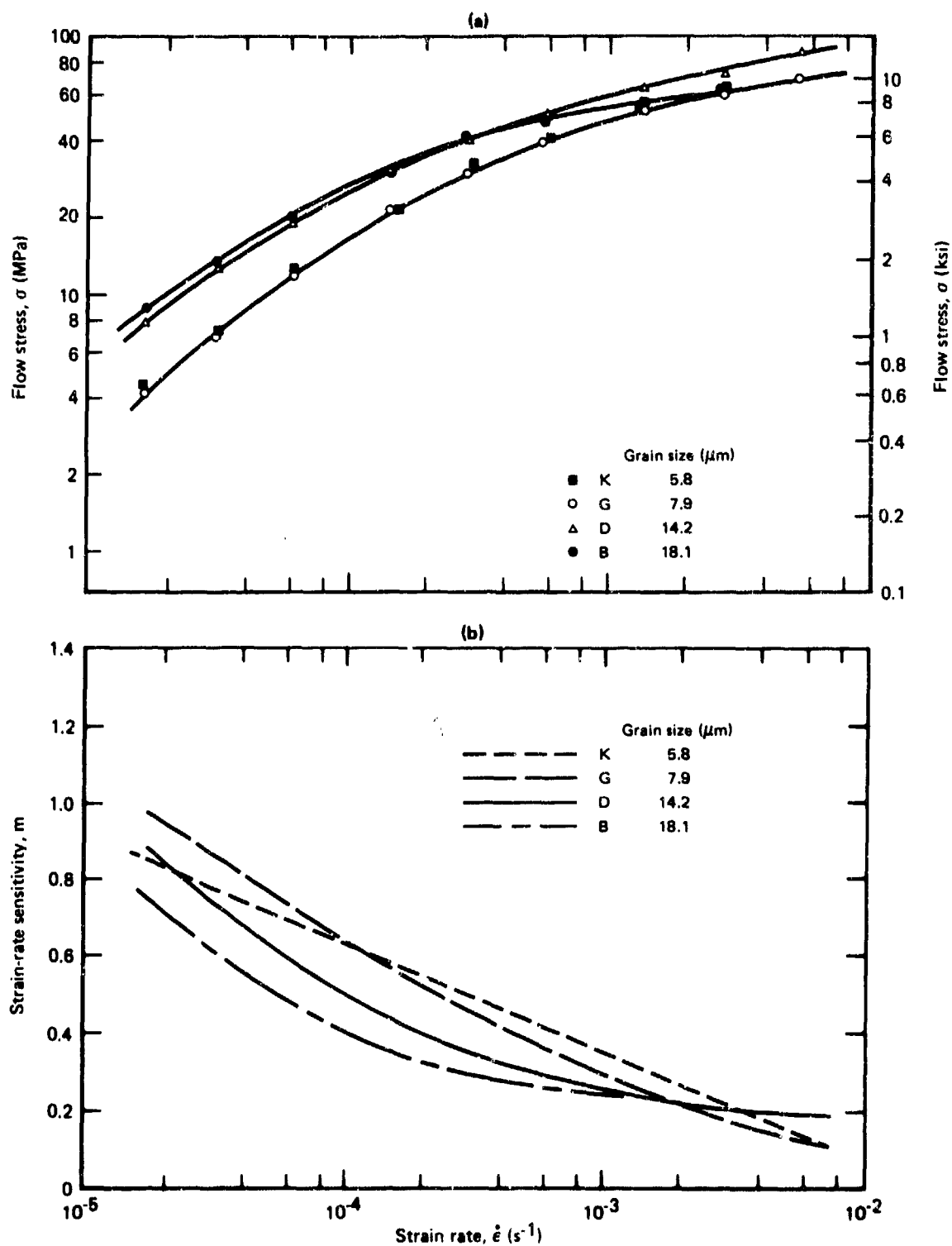
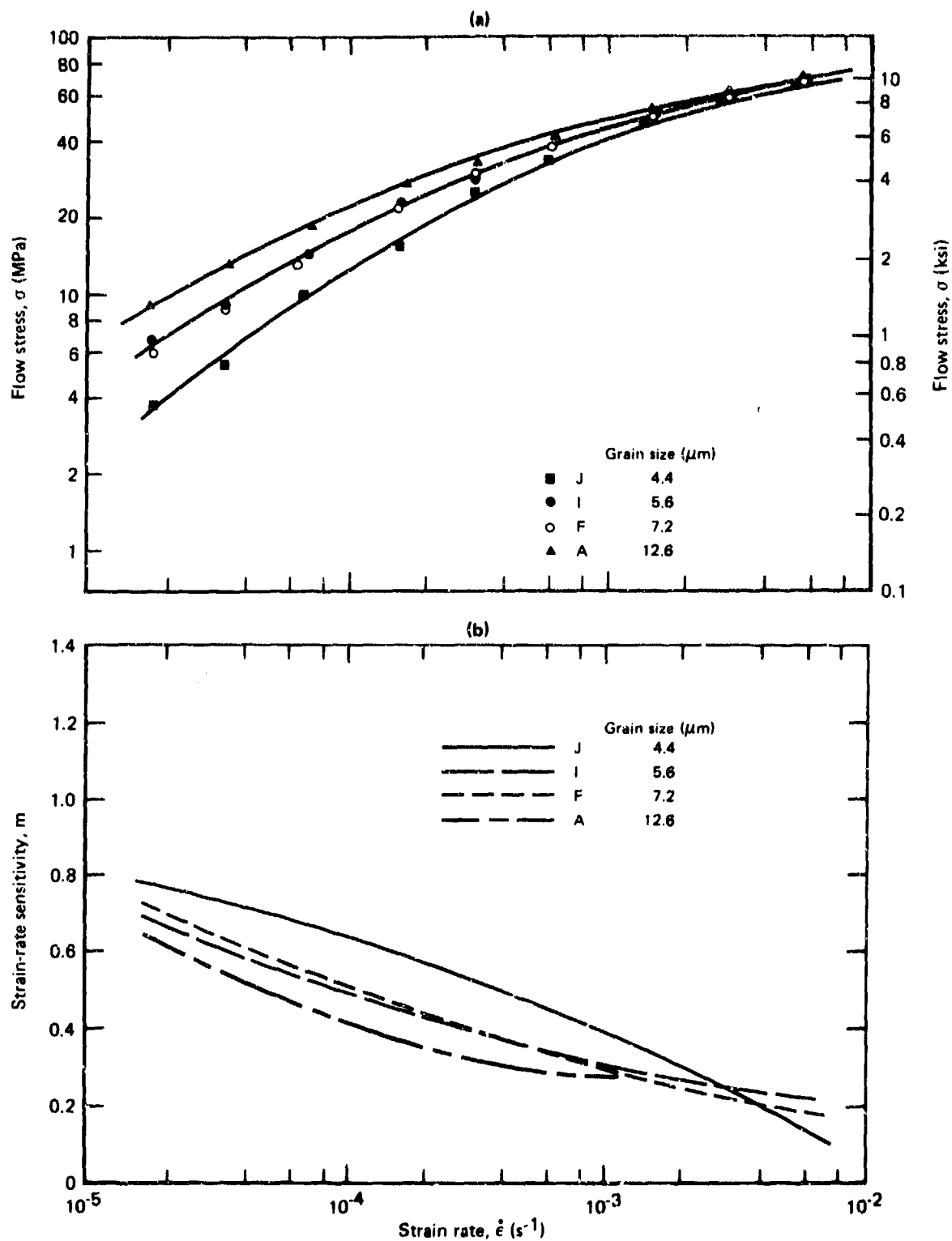


Figure 42. Strain-rate dependence of (a) flow stress and (b) strain-rate sensitivity of regular-grade Ti-6Al-4V (volume % primary α = 66) at 850°C (1562°F).



QP03-0249-26

Figure 43. Strain-rate dependence of (a) flow stress and (b) strain-rate sensitivity of regular-grade Ti-6Al-4V (volume % primary α = 45) at 850°C (1562°F).

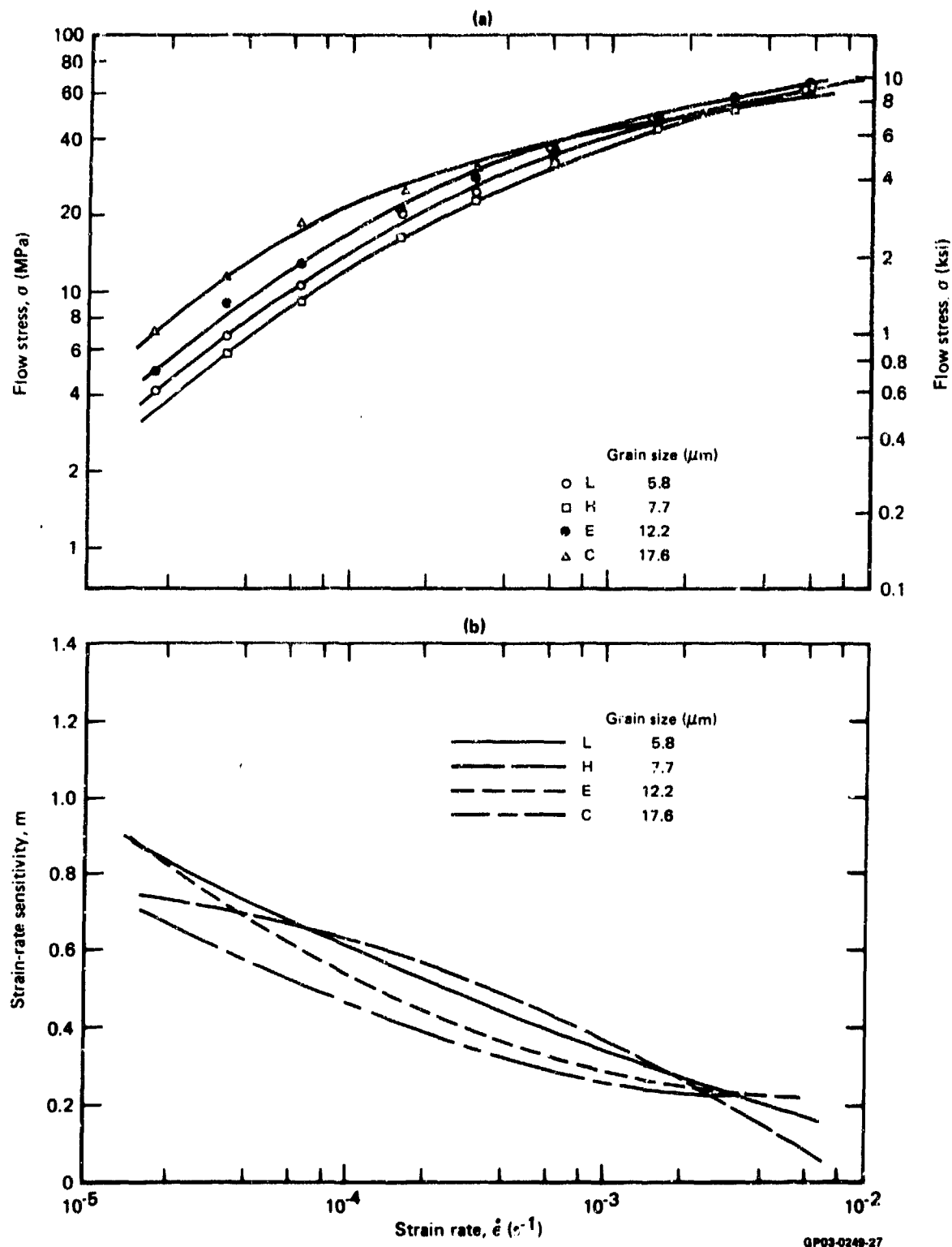
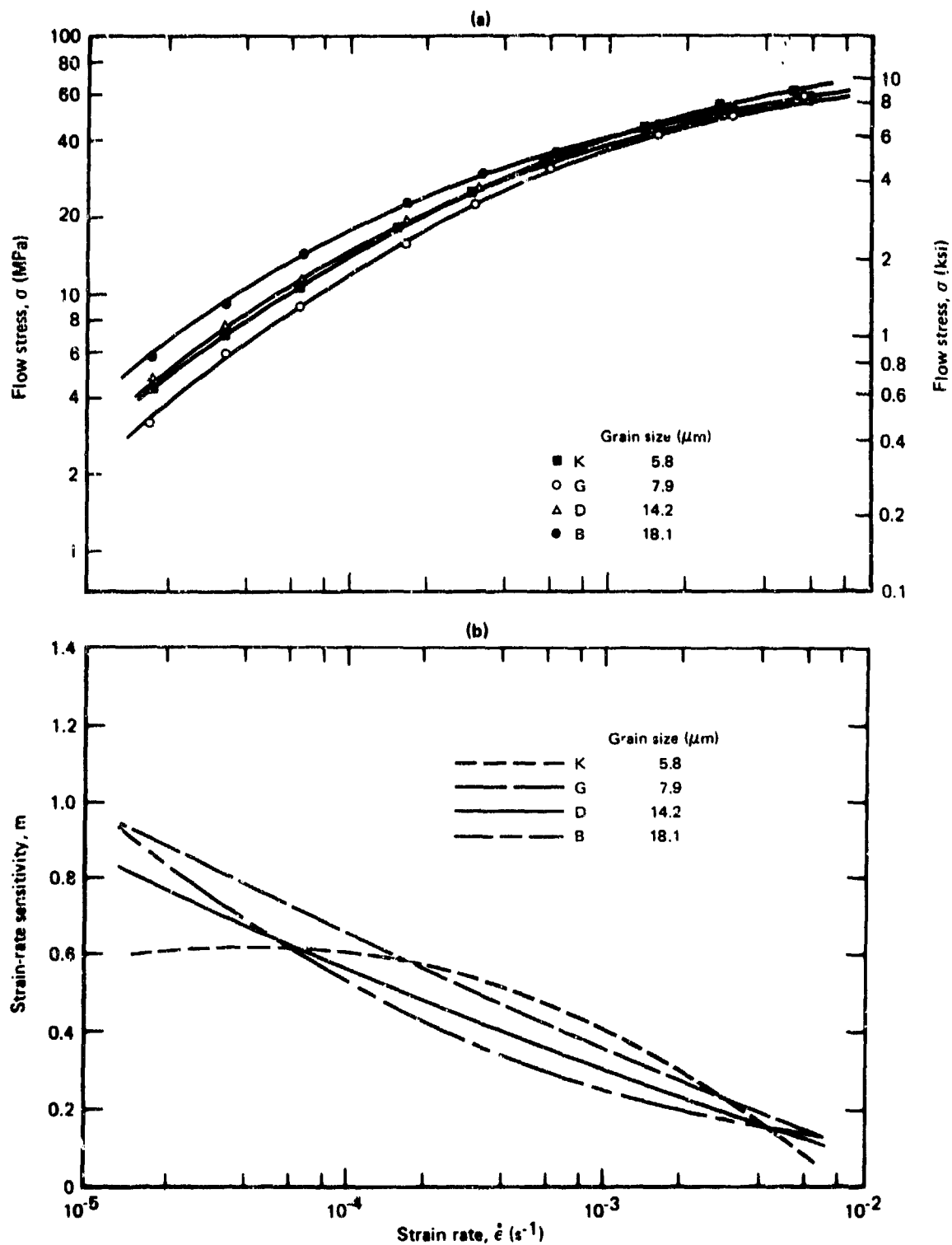


Figure 44. Strain-rate dependence of (a) flow stress and (b) strain-rate sensitivity of regular-grade Ti-6Al-4V (volume % primary alpha = 88) at 875°C (1662°F).



GP03-0249-28

Figure 45. Strain-rate dependence of (a) flow stress and (b) strain-rate sensitivity of regular-grade Ti-6Al-4V (volume % primary α = 66) at 875°C (1606°F).

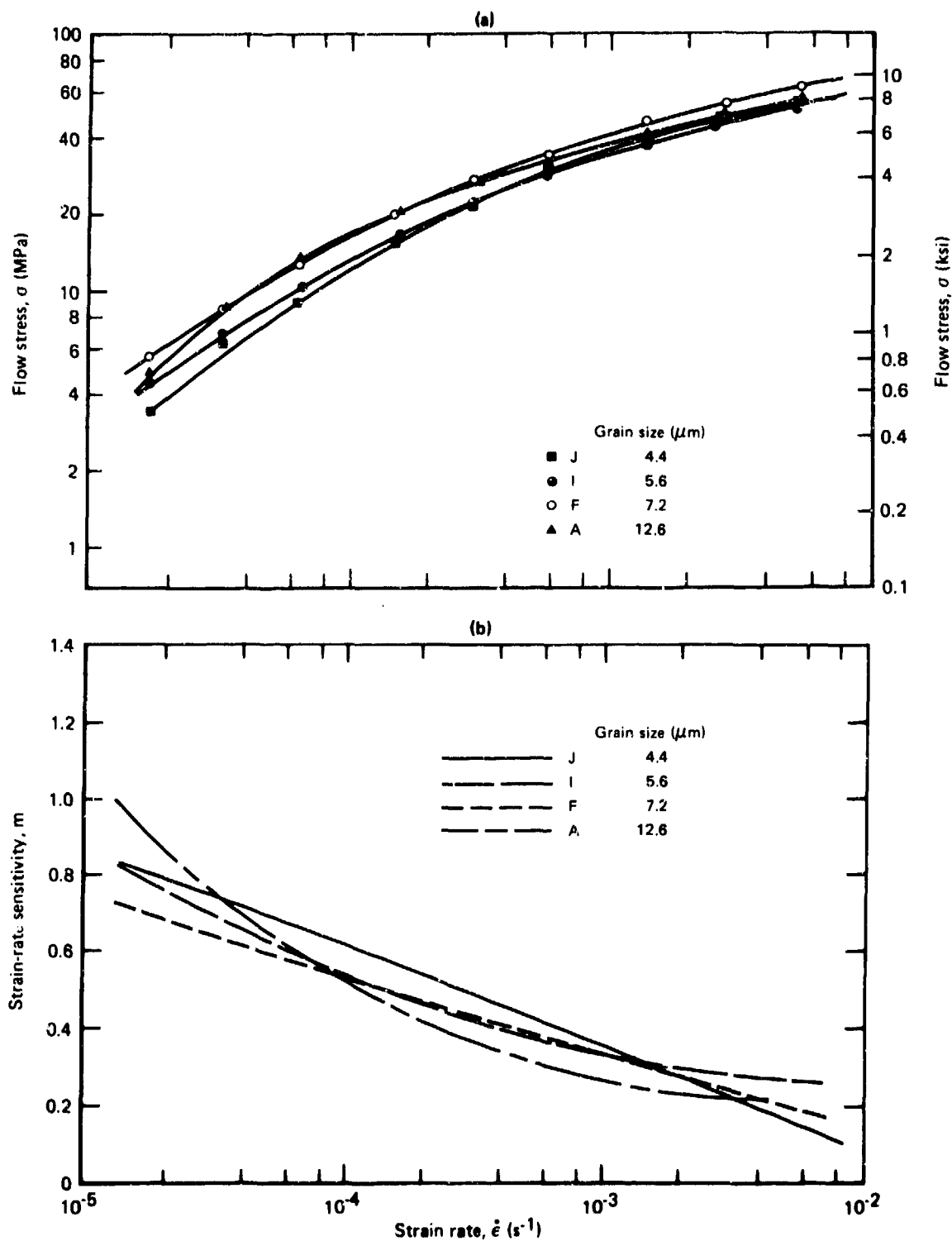
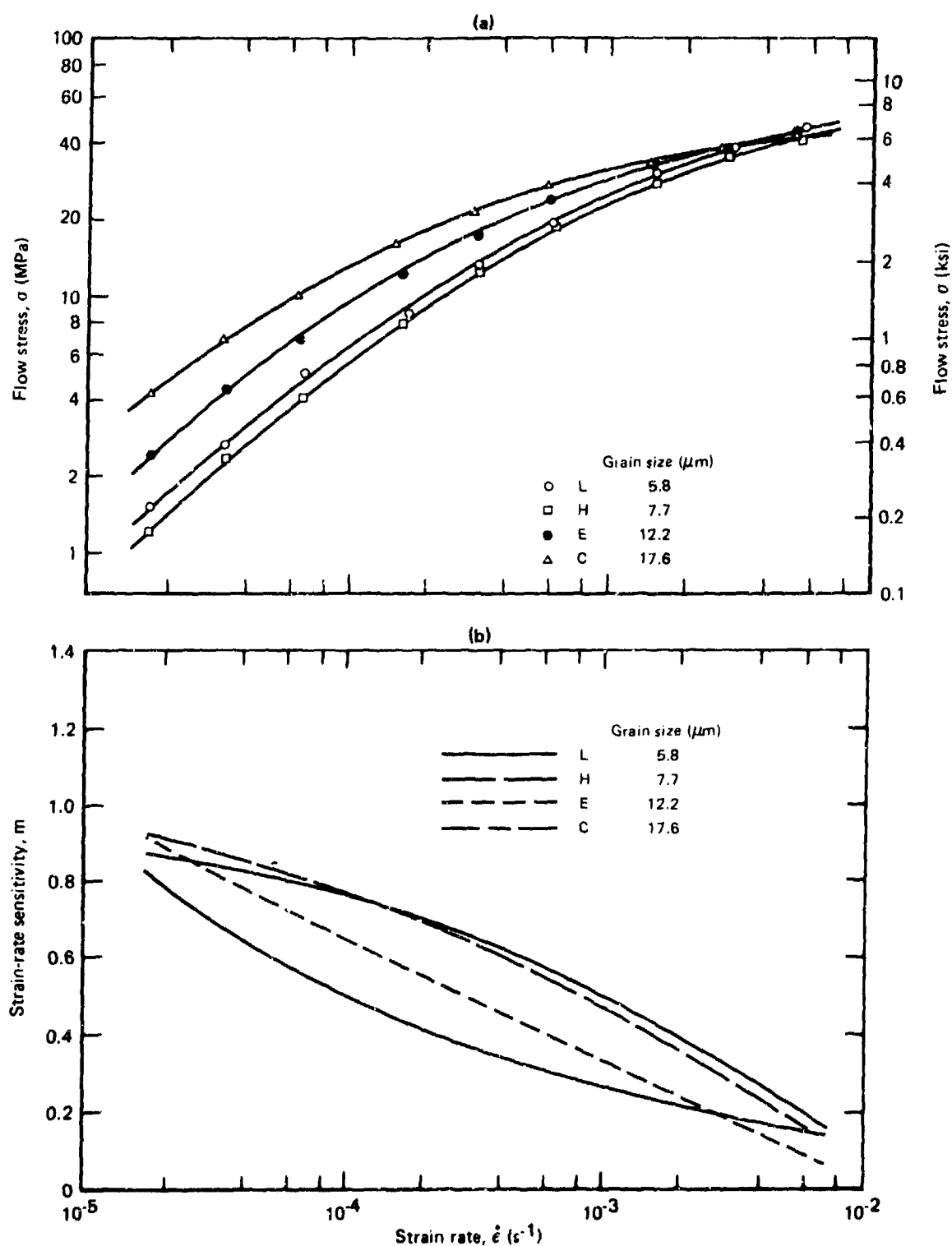
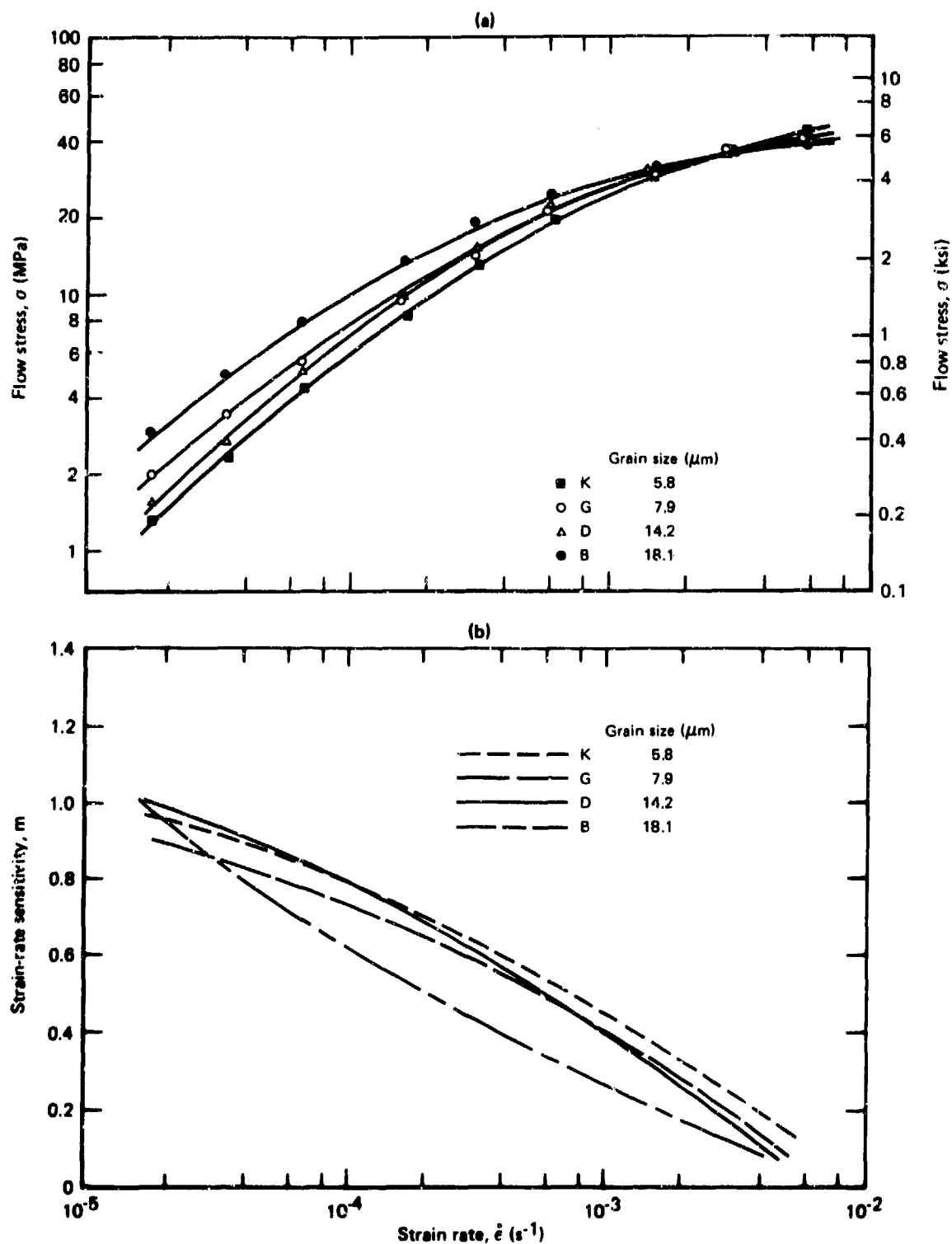


Figure 46. Strain-rate dependence of (a) flow stress and (b) strain-rate sensitivity of regular-grade Ti-6Al-4V (volume % primary α = 45) at 875°C (1606°F).



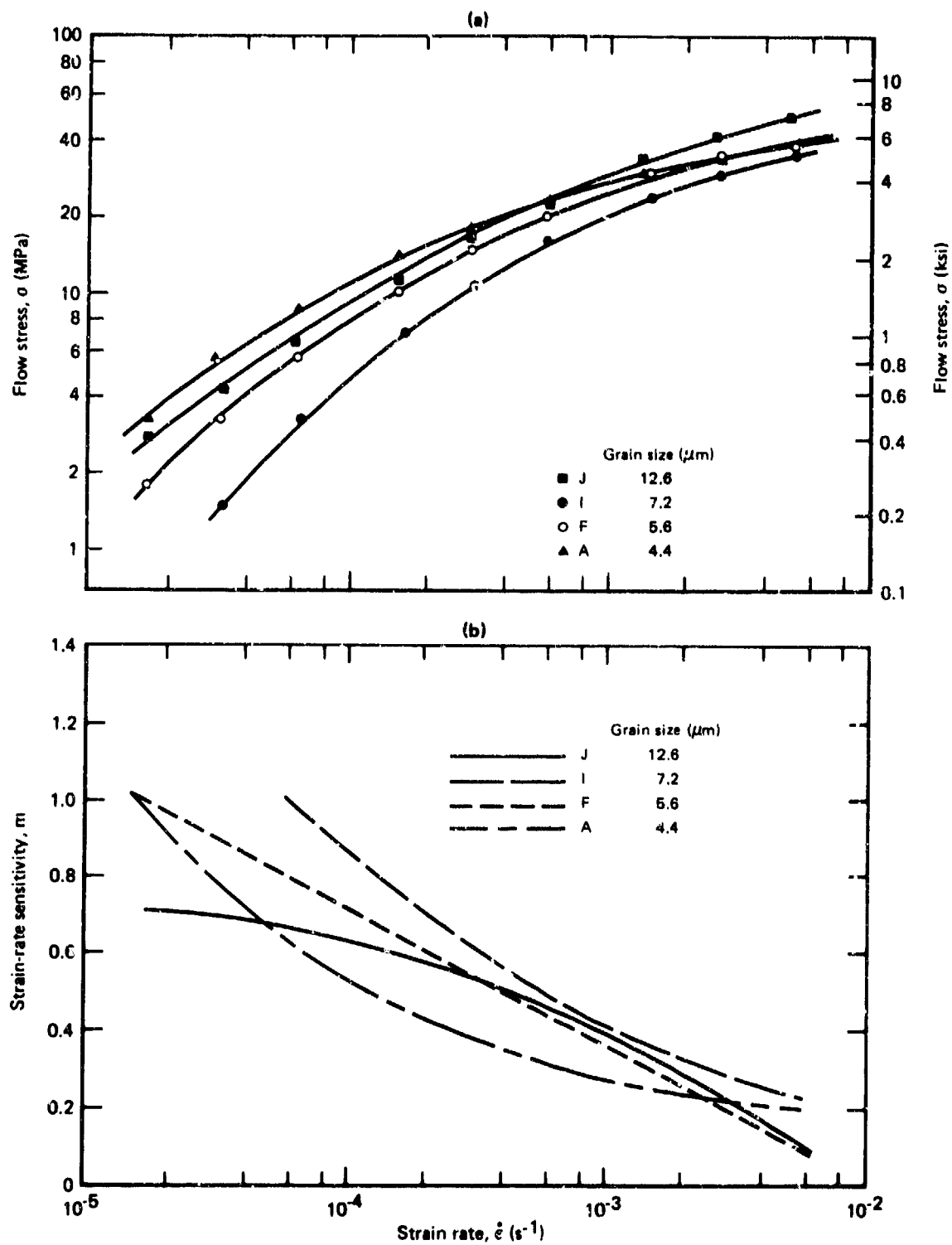
GP03-0248-31

Figure 47. Strain-rate dependence of (a) flow stress and (b) strain-rate sensitivity of regular-grade Ti-6Al-4V (volume % primary alpha = 88) at 907°C (1665°F).



GP03-0249-30

Figure 48. Strain-rate dependence of (a) flow stress and (b) strain-rate sensitivity of regular-grade Ti-6Al-4V (volume % primary α = 66) at 907°C (1665°F).



GP03-0240-32

Figure 49. Strain-rate dependence of (a) flow stress and (b) strain-rate sensitivity of regular-grade Ti-6Al-4V (volume % primary α = 45) at 907°C (1665°F).

TABLE 15. RESULTS OF STRAIN-RATE-CYCLING TESTS ON REGULAR-GRADE Ti-6Al-4V
AND ELI-GRADE Ti-6Al-4V AT 850°C (1562°F)

Sample	Volume % primary α (%)	Grain size (μm)	Maximum m (m)	Flow stress at maximum m [MPa (ksi)]	Flow stress at $m = 0.5$ [MPa (ksi)]	Flow stress at $\dot{\epsilon} = 10^{-4} \text{ s}^{-1}$ [MPa (ksi)]	Flow stress at $\dot{\epsilon} = 10^{-3} \text{ s}^{-1}$ [MPa (ksi)]	Strain rate at maximum m (10^{-5} s^{-1})	Strain rate at $m = 0.5$ (10^{-5} s^{-1})	Maximum elongation at $\dot{\epsilon} = 10^{-4} \text{ s}^{-1}$ (%)	*Extent of necking at $\dot{\epsilon} = 10^{-4} \text{ s}^{-1}$	Maximum elongation at $\dot{\epsilon} = 10^{-3} \text{ s}^{-1}$ (%)	*Extent of necking at $\dot{\epsilon} = 10^{-3} \text{ s}^{-1}$
L	88	5.6	—	—	—	13.8 (2.0)	48.3 (7.0)	1.5	1.5	—	—	—	—
H	88	7.5	1.00	4.1 (0.6)	22.8 (3.3)	24.1 (3.5)	55.2 (8.0)	1.5	1.5	—	—	—	—
E	88	12.0	0.87	6.9 (1.0)	26.5 (3.7)	28.3 (4.1)	55.2 (8.0)	1.5	1.5	—	—	—	—
C	89	17.5	0.72	10.3 (1.5)	20.7 (3.0)	—	—	1.5	5.0	>478	E	365	E
K	66	5.6	0.84	4.1 (0.6)	27.6 (4.0)	16.5 (2.4)	48.3 (7.0)	1.5	33.0	—	—	—	—
G	66	7.7	0.95	3.5 (0.5)	20.7 (3.0)	16.5 (2.4)	48.3 (7.0)	1.5	16.0	—	—	—	—
D	66	14.0	0.85	7.6 (1.1)	24.8 (3.6)	22.8 (3.3)	47.5 (8.1)	1.5	12.0	368	S	497	S
B	66	18.0	0.74	8.3 (1.2)	14.5 (2.1)	22.8 (3.3)	47.5 (8.1)	1.5	4.5	>470	N	365	E
J	45	4.3	0.81	3.5 (0.5)	29.6 (4.3)	11.0 (1.6)	41.4 (6.0)	1.5	43.0	—	—	—	—
I	45	5.5	0.70	5.5 (0.8)	19.3 (2.8)	17.2 (2.5)	44.8 (6.5)	1.5	12.0	—	—	—	—
F	45	7.0	0.76	5.5 (0.8)	21.4 (3.1)	17.2 (2.5)	44.8 (6.5)	1.5	15.0	>490	N	591	E
A	45	12.5	0.64	8.3 (1.2)	17.9 (2.6)	22.0 (3.2)	48.3 (7.0)	1.5	6.0	>530	N	390	E
X1	88	5.5	1.00	0.7 (0.1)	22.8 (3.3)	7.0 (1.0)	31.7 (4.6)	4.0	55.0	—	—	>460	N
X3	88	8.7	0.87	3.5 (0.5)	28.6 (4.3)	10.3 (1.5)	39.3 (5.7)	1.5	55.0	>527	N	>500	S
X2	46	4.5	0.77	2.1 (0.3)	27.6 (4.0)	10.3 (1.5)	37.9 (5.5)	1.6	55.0	>500	N	>440	S
X4	46	8.6	0.94	3.5 (0.5)	22.0 (3.2)	12.4 (1.8)	41.4 (6.0)	1.6	26.0	>500	N	>491	S

*E = Extensive necking
S = Slight necking
N = Negligible necking

TABLE 16. RESULTS OF STRAIN-RATE-CYCLING TESTS ON REGULAR-GRADE Ti-6Al-4V
AND ELI-GRADE Ti-6Al-4V AT 875°C (1606°F)

Sample	Volume % primary α (%)	Grain size (μm)	Maximum m (m)	Flow stress at maximum m [MPa (ksi)]	Flow stress at $m = 0.5$ [MPa (ksi)]	Flow stress at $\dot{\epsilon} = 10^{-4} \text{ s}^{-1}$ [MPa (ksi)]	Flow stress at $\dot{\epsilon} = 10^{-3} \text{ s}^{-1}$ [MPa (ksi)]	Strain rate at maximum m (10^{-5} s^{-1})	Strain rate at $m = 0.5$ (10^{-5} s^{-1})	Maximum elongation at $\dot{\epsilon} = 10^{-4} \text{ s}^{-1}$ (%)	*Extent of necking at $\dot{\epsilon} = 10^{-4} \text{ s}^{-1}$	Maximum elongation at $\dot{\epsilon} = 10^{-3} \text{ s}^{-1}$ (%)	*Extent of necking at $\dot{\epsilon} = 10^{-3} \text{ s}^{-1}$
L	88	5.6	0.96	3.4 (0.5)	18.6 (2.7)	11.0 (1.6)	37.9 (5.5)	1.5	22.0	—	—	—	—
H	88	7.5	0.77	3.4 (0.5)	27.6 (4.0)	13.8 (2.0)	41.4 (6.0)	1.5	33.0	—	—	—	—
E	88	12.0	0.89	4.1 (0.6)	18.6 (2.7)	17.2 (2.5)	41.4 (6.0)	1.5	12.0	—	—	—	—
C	88	17.5	0.83	6.9 (1.0)	19.3 (2.8)	21.4 (3.1)	43.4 (6.3)	1.5	8.1	478	E	320	E
K	66	5.6	0.60	1.6 (0.24)	29.6 (4.3)	12.4 (1.8)	39.3 (5.7)	1.2	45.0	—	—	—	—
G	66	7.7	0.89	2.8 (0.4)	27.6 (4.0)	14.5 (2.1)	42.1 (6.1)	1.5	30.0	>470	N	528	E
D	66	14.0	0.77	4.1 (0.6)	21.4 (3.1)	14.5 (2.1)	42.1 (6.1)	1.5	18.0	>300	N	277	E
B	66	18.0	0.84	5.5 (0.8)	20.7 (3.0)	17.9 (2.6)	43.4 (6.3)	1.5	12.0	472	S	277	E
J	45	4.3	0.81	3.4 (0.5)	20.7 (3.0)	12.4 (1.8)	35.2 (5.1)	1.5	25.0	—	—	—	—
I	45	5.5	0.78	4.1 (0.6)	15.2 (2.2)	13.8 (2.0)	35.2 (5.1)	1.5	13.0	—	—	—	—
F	45	7.0	0.69	5.5 (0.8)	18.6 (2.7)	17.2 (2.5)	39.3 (5.7)	1.5	13.0	>500	N	434	E
A	45	12.5	0.97	4.8 (0.7)	17.9 (2.6)	17.2 (2.5)	39.3 (5.7)	1.5	12.0	>490	S	353	E
X1	88	5.5	0.74	4.1 (0.6)	29.6 (4.3)	4.8 (0.7)	24.8 (3.6)	7.3	150.0	—	—	>490	S
X3	88	8.7	0.70	9.0 (1.3)	29.6 (4.3)	4.8 (0.7)	24.8 (3.6)	20.0	150.0	>440	N	>500	N
X2	46	4.5	0.79	1.4 (0.2)	24.8 (3.6)	5.5 (0.8)	25.5 (3.7)	1.5	91.0	>400	N	>500	S
X4	46	8.6	0.91	2.1 (0.3)	22.7 (3.3)	9.0 (1.3)	34.5 (5.0)	1.5	41.0	>400	N	>500	S

*E = Extensive necking
S = Slight necking
N = Negligible necking

TABLE 17. RESULTS OF STRAIN-RATE-CYCLING TESTS ON REGULAR-GRADE Ti-6Al-4V
AND ELI-GRADE Ti-6Al-4V AT 907°C (1665°F)

Sample	Volume % primary α (%)	Grain size (μm)	Maximum m (m)	Flow stress at maximum m [MPa (ksi)]	Flow stress at $m = 0.5$ [MPa (ksi)]	Flow stress at $\dot{\epsilon} = 10^{-4} \text{ s}^{-1}$ [MPa (ksi)]	Flow stress at $\dot{\epsilon} = 10^{-3} \text{ s}^{-1}$ [MPa (ksi)]	Strain rate at maximum m (10^{-5} s^{-1})	Strain rate at $m = 0.5$ (10^{-5} s^{-1})	Maximum elongation at $\dot{\epsilon} = 10^{-4} \text{ s}^{-1}$ (%)	*Extent of necking at $\dot{\epsilon} = 10^{-4} \text{ s}^{-1}$	Maximum elongation at $\dot{\epsilon} = 10^{-3} \text{ s}^{-1}$ (%)	*Extent of necking at $\dot{\epsilon} = 10^{-3} \text{ s}^{-1}$
L	88	5.7	0.81	1.4 (0.2)	24.1 (3.5)	6.2 (0.9)	24.1 (3.5)	1.5	91.0	—	—	—	—
H	88	7.6	0.92	0.7 (0.1)	24.1 (3.5)	4.8 (0.7)	24.1 (3.5)	1.5	91.0	—	—	—	—
E	88	12.1	0.89	2.1 (0.3)	17.9 (2.6)	9.0 (1.3)	29.6 (4.3)	1.5	33.0	—	—	—	—
C	88	17.5	0.82	4.1 (0.6)	13.8 (2.0)	13.8 (2.0)	33.1 (4.8)	1.5	10.0	> 470	N	—	—
K	66	5.7	0.89	0.7 (0.1)	22.8 (3.3)	5.5 (0.8)	24.1 (3.5)	1.5	91.0	—	—	—	—
G	66	7.8	0.83	1.4 (0.2)	21.4 (3.1)	6.9 (1.0)	27.6 (4.0)	1.5	61.0	> 400	N	—	—
D	66	14.1	0.94	1.4 (0.2)	21.4 (3.1)	6.9 (1.0)	27.6 (4.0)	1.5	61.0	> 400	N	—	—
B	66	18.0	0.93	2.1 (0.3)	15.2 (2.2)	10.3 (1.5)	28.3 (4.1)	1.5	20.0	> 400	N	—	—
J	45	4.3	—	—	—	—	—	—	—	—	—	—	—
I	45	5.5	1.90	1.4 (0.2)	16.5 (2.4)	4.1 (0.6)	20.7 (3.0)	1.5	61.0	—	—	—	—
F	45	7.1	0.95	1.4 (0.2)	17.2 (2.5)	6.9 (1.0)	24.8 (3.6)	1.5	40.0	> 440	N	—	—
A	45	12.5	0.33	2.8 (0.4)	12.4 (1.8)	11.0 (1.6)	26.2 (3.8)	1.5	12.0	> 440	N	—	—
X1	88	5.5	0.83	2.1 (0.3)	27.6 (4.0)	2.1 (0.3)	17.2 (2.5)	7.3	400.0	> 400	N	—	—
X3	88	8.8	0.85	1.4 (0.2)	28.3 (4.1)	3.4 (0.5)	17.9 (2.6)	3.5	150.0	> 453	N	—	—
X2	46	4.5	0.88	2.1 (0.3)	17.2 (2.5)	2.8 (0.4)	14.5 (2.1)	1.5	123.0	> 400	N	—	—
X4	46	8.7	0.74	2.1 (0.3)	18.6 (2.7)	4.8 (0.7)	19.6 (2.7)	7.3	91.0	> 460	N	—	—

*E = Extensive necking

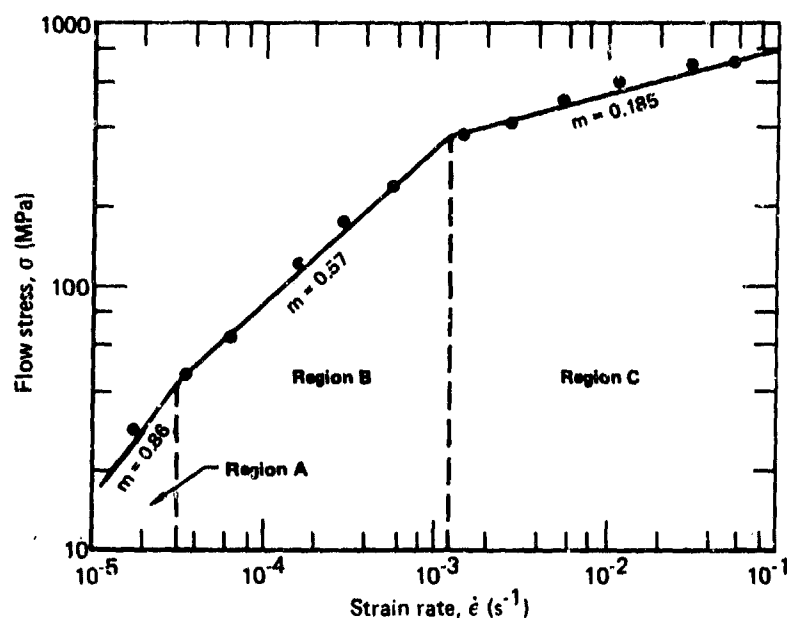
S = Slight necking

N = Negligible necking

GW-82-3

with decreasing grain size, and for a given microstructural condition, $\dot{\epsilon}_{0.5}$ decreases with increasing temperature. In specimens deformed at identical initial strain-rates, the resistance to necking was higher at 906°C (1663°F) than at 650°C (1562°F) and 875°C (1607°F), and necking resistance was higher in fine-grained specimens than in coarse-grained specimens.

Results of analyses of least-square linear fits to the experimental flow-stress/strain-rate data for the superplastic strain-rate range of $1.6 \times 10^{-5} \text{ s}^{-1}$ to $5.5 \times 10^{-3} \text{ s}^{-1}$, summarized in Table 18, indicate that the data cannot be adequately represented by a single straight line. However, as shown in Figure 50, the strain-rate dependence of flow stress of Ti-6Al-4V at strain-rates of $10^{-5} - 10^{-1} \text{ s}^{-1}$, encompassing the superplastic range and conventional high-temperature-forming strain rates, can be accurately represented by straight lines in each of three regions, A, B, and C, corresponding to strain-rate sensitivities of approximately 1, 0.5, and 0.2, respectively.



GPI/S-0240-130

Figure 50. Flow stress at 850°C (1562°F) as a function of strain rate in recrystallization-annealed Ti-6Al-4V.

TABLE 18. THE VALUES OF SLOPES AND CORRELATION COEFFICIENTS FOR STRAIGHT-LINE FIT BY THE METHOD OF LEAST-SQUARES ANALYSIS TO THE FLOW-STRESS/STRAIN-RATE DATA.

Sample	Slope of the straight line (m)			Correlation coefficient for straight-line fit		
	850°C	870°C	906°C	850°C	870°C	906°C
L	—	0.494	0.491	—	0.9798	0.9800
H	0.472	0.503	0.615	0.9865	—	—
E	0.411	0.423	0.498	0.9723	0.9730	0.9762
C	0.330	0.356	0.393	0.9788	0.0693	0.9718
K	0.495	0.489	0.619	0.9824	0.9797	0.9863
G	0.487	0.506	0.494	0.9731	0.9798	0.9798
D	0.402	0.437	0.578	0.9752	0.9791	0.9744
B	0.353	0.399	0.456	0.9817	0.9707	0.9650
J	0.518	0.487	0.514	0.9835	0.9822	0.9904
I	0.420	0.436	0.602	0.9863	0.9865	0.9735
F	0.427	0.418	0.539	0.9829	0.9853	0.9764
A	0.349	0.409	0.421	0.9869	0.9741	0.9716
X1	0.694	0.610	0.653	0.9775	—	0.9874
X3	0.615	0.570	0.621	0.9717	—	0.9832
X2	0.569	0.598	0.597	0.9889	—	0.9858
X4	0.492	0.540	0.558	0.9766	0.9813	0.9852

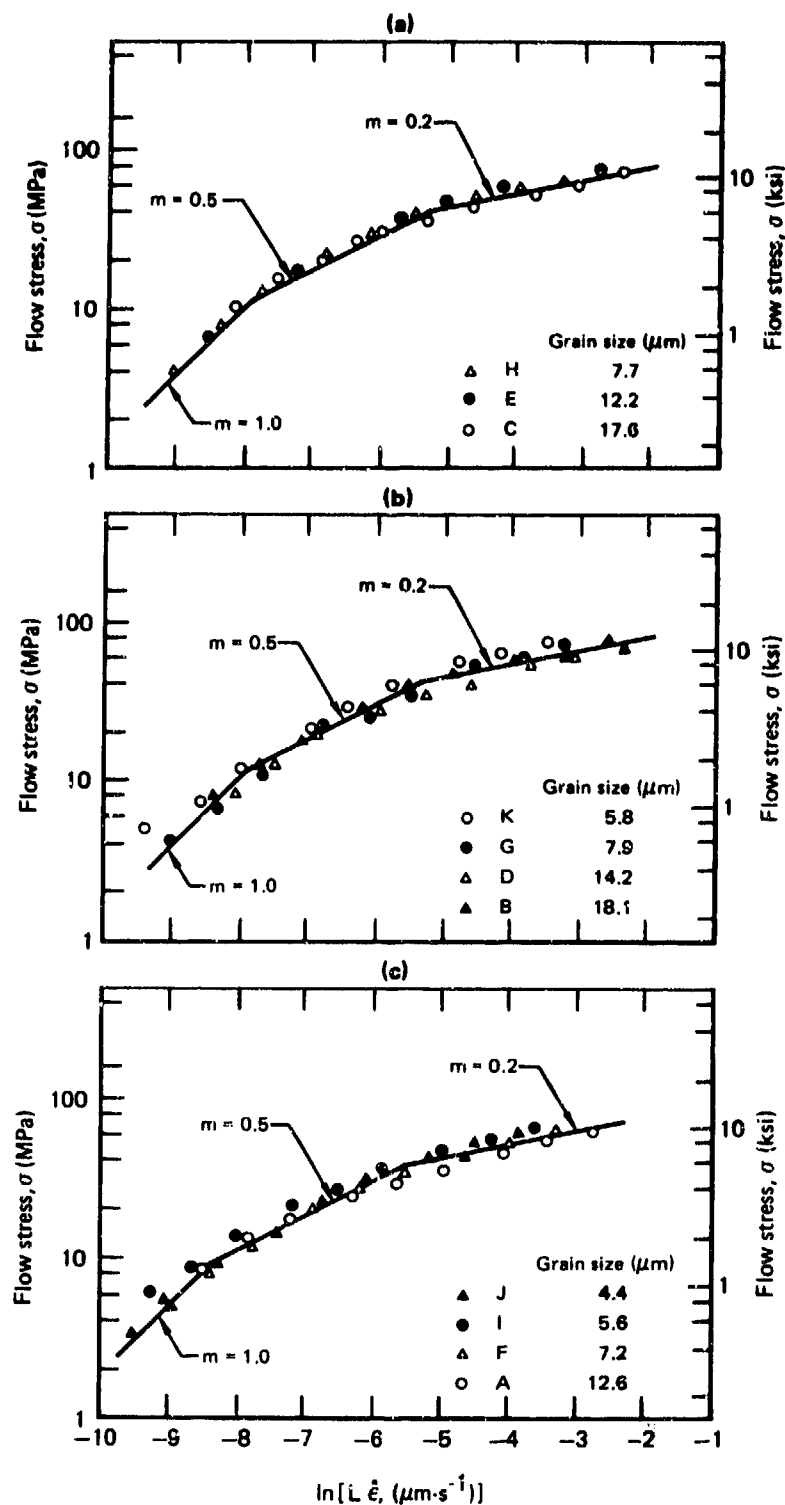
QP03-0246-4

The three different straight-line regions of the flow-stress/strain-rate indicate that the deformation mechanism changes from Nabarro-Herring creep (Reference 6) or diffusion-accommodated grain-boundary-sliding (Reference 5), both of which give $m = 1$, at low strain rates to an interface-reaction-controlled grain-boundary-sliding (Reference 7) or dislocation-motion-accommodated grain-boundary-sliding (Reference 12), for which $m = 0.5$, at intermediate strain-rates, to dislocation-climb-controlled deformation with $m = 0.2$ (or stress exponent of 5 in creep tests) at large strain-rates. Near the transitions from A to B and B to C, the deformation is governed by the superposition of the deformation mechanisms of two adjoining regions, and no discontinuity of slope of the flow-stress/strain-rate curve occurs.

The deformation substructures observed for the three strain-rate regions are consistent with the different deformation characteristics. Whereas extensive dislocation tangles and cell structures are produced at strain-rates $> 0.001 \text{ s}^{-1}$ (region C), alloys deformed in region A show no dislocation activity (Reference 23). Confirmatory evidence for the three regions of high-temperature deformation behavior of Ti-6Al-4V was obtained by texture measurements. The initial texture is retained in specimens deformed in region C because of the dominance of dislocation processes, but a reduction in texture sharpness and randomization of the texture occur in specimens deformed in region A because of extensive grain rotations arising from grain boundary sliding (Reference 24).

Figures 51 through 53 show plots of flow stress as a function of $\ln(\text{strain-rate} \times \text{grain-size})$ for different microstructural variations of Ti-6Al-4V. The good fit to the data by straight lines of slopes 1, 0.5, and 0.2 confirm the validity of a linear dependence of flow stress on the reciprocal of the grain size. To a first approximation, the strain-rate and grain size dependences of the flow stress, σ , at strain-rates of $10^{-5} - 10^{-2} \text{ s}^{-1}$ can be represented by a relation of the form

$$d\dot{\epsilon} \propto \sigma^{1/m}, \quad (5)$$



GP03-0240-33

Figure 51. Flow stress as a function of \ln (strain rate \times grain size) at 850°C (1562°F) in regular-grade Ti-6Al-4V; (a) volume % primary alpha = 88, (b) volume % primary alpha = 66, and (c) volume % primary alpha = 45.

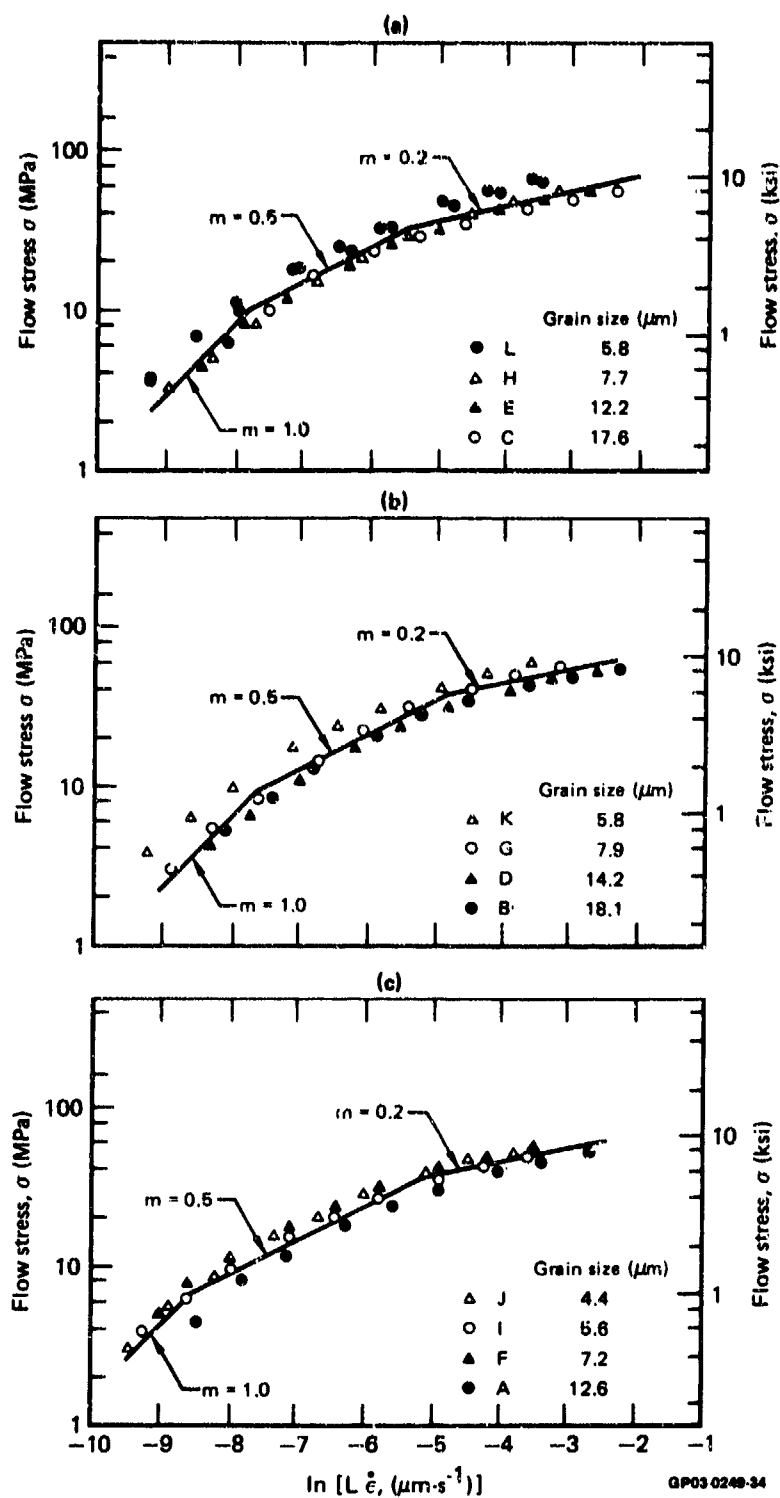
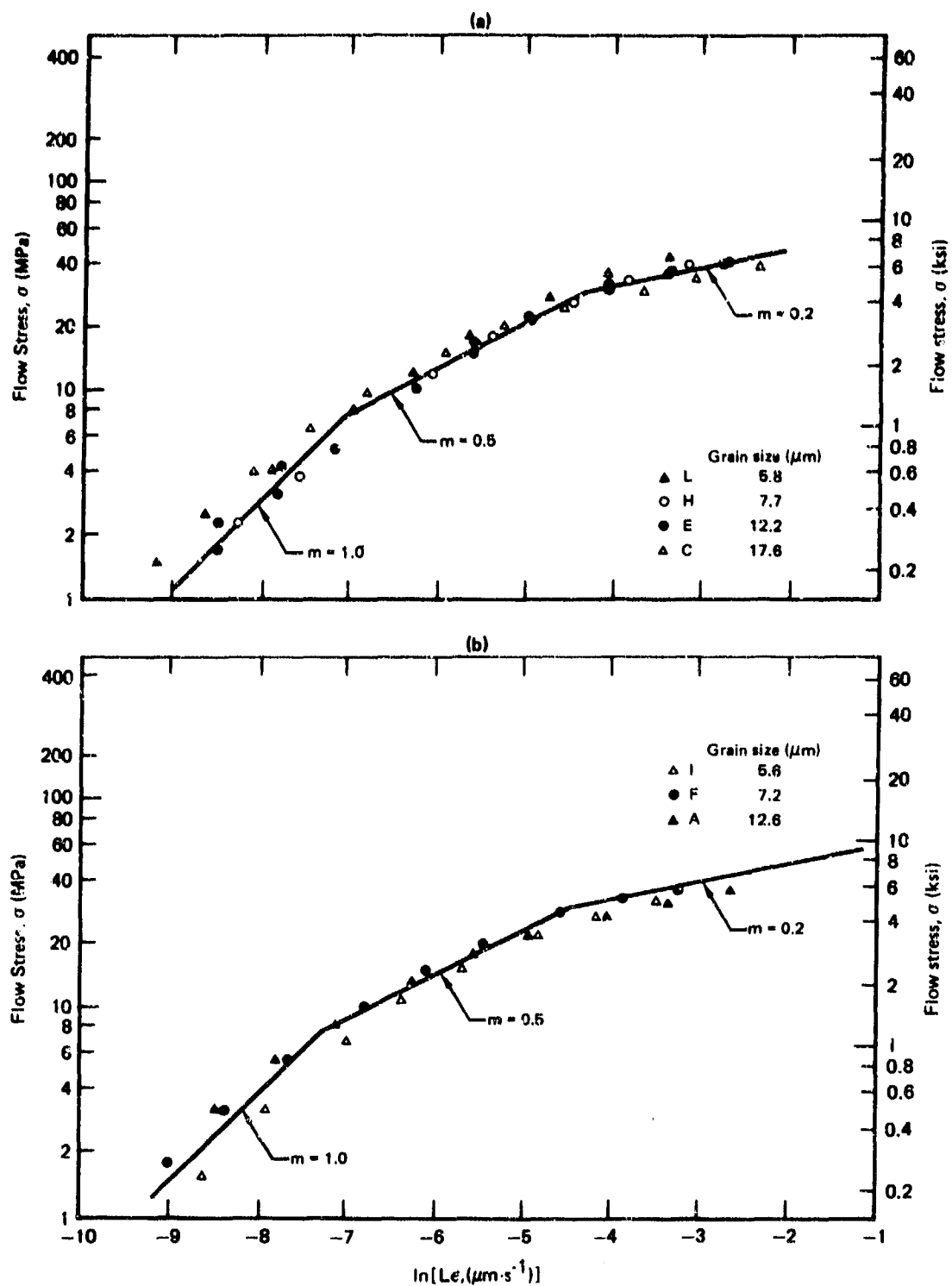


Figure 52. Flow stress as a function of \ln (strain rate \times grain size) at 875°C (1607°F) in regular-grade Ti-6Al-4V; (a) volume % primary $\alpha = 88$, (b) volume % primary $\alpha = 66$, and (c) volume % primary $\alpha = 45$.



GP03-0249-36

Figure 53. Flow stress as a function of \ln (strain rate \times grain size) at 907°C (1665°F) in regular-grade Ti-6Al-4V; (a) volume % primary alpha = 88, and (b) volume % primary alpha = 45.

with m ranging from 0.2 at high strain-rates to 1.0 at low strain-rates. The plots of grain-size dependence of flow stress and strain-rate shown for selected alloys in Figures 54 and 55 indicate relationships of the form

$$\text{flow stress} \propto (\text{grain size})^b \text{ for constant } \dot{\epsilon} \quad (6)$$

and

$$\text{strain-rate} \propto (\text{grain size})^{-a} \text{ for constant } \sigma, \quad (7)$$

with values of a ranging from 0.5 to 1.2 and b values ranging from 0.5 to 1.5. The values of a close to unity at low and intermediate strain rates strongly support the inverse linear dependence of strain rate on grain size in the superplastic region. The reduction of flow stress with decreasing grain size is as expected from the extensive grain-boundary sliding occurring at high temperatures and low strain-rates.

The normalized plots of grain-size and strain-rate dependences of flow stress shown in Figures 51 through 53 are useful in differentiating different mechanisms. Such plots additionally provide useful information for selecting suitable parameters for the superplastic forming of a structural part.

The effects of initial volume-fractions of alpha and beta phases on the strain-rate dependence of flow stress and strain-rate sensitivity are shown in Figures 56 through 58. The flow stress and m value do not depend significantly on the amounts of the phases at 850°C (1562°F) and 875°C (1607°F), but the volume fractions of the two phases have an effect at 906°C (1663°F) because of the effect on grain-growth retardation of changes in the volume fractions of the constituent phases.

The grain-size dependence of flow stress at different strain-rates shown in Figures 41 through 49 suggest that the the flow stress or, equivalently, the strain-rate is suitably normalized with respect to grain size, a single curve or straight line can represent the variations of flow stress with strain-rate for different grain-size specimens. The different theories of high-temperature deformation are at variance with respect to the grain-size dependence of strain-rate at any given stress (Reference 6). Earlier theories predict an inverse third-power dependence of strain-rate on grain size, d , at low stresses, but recent theories predict the strain-rate to be proportional to either $1/d^2$ or $1/d$.

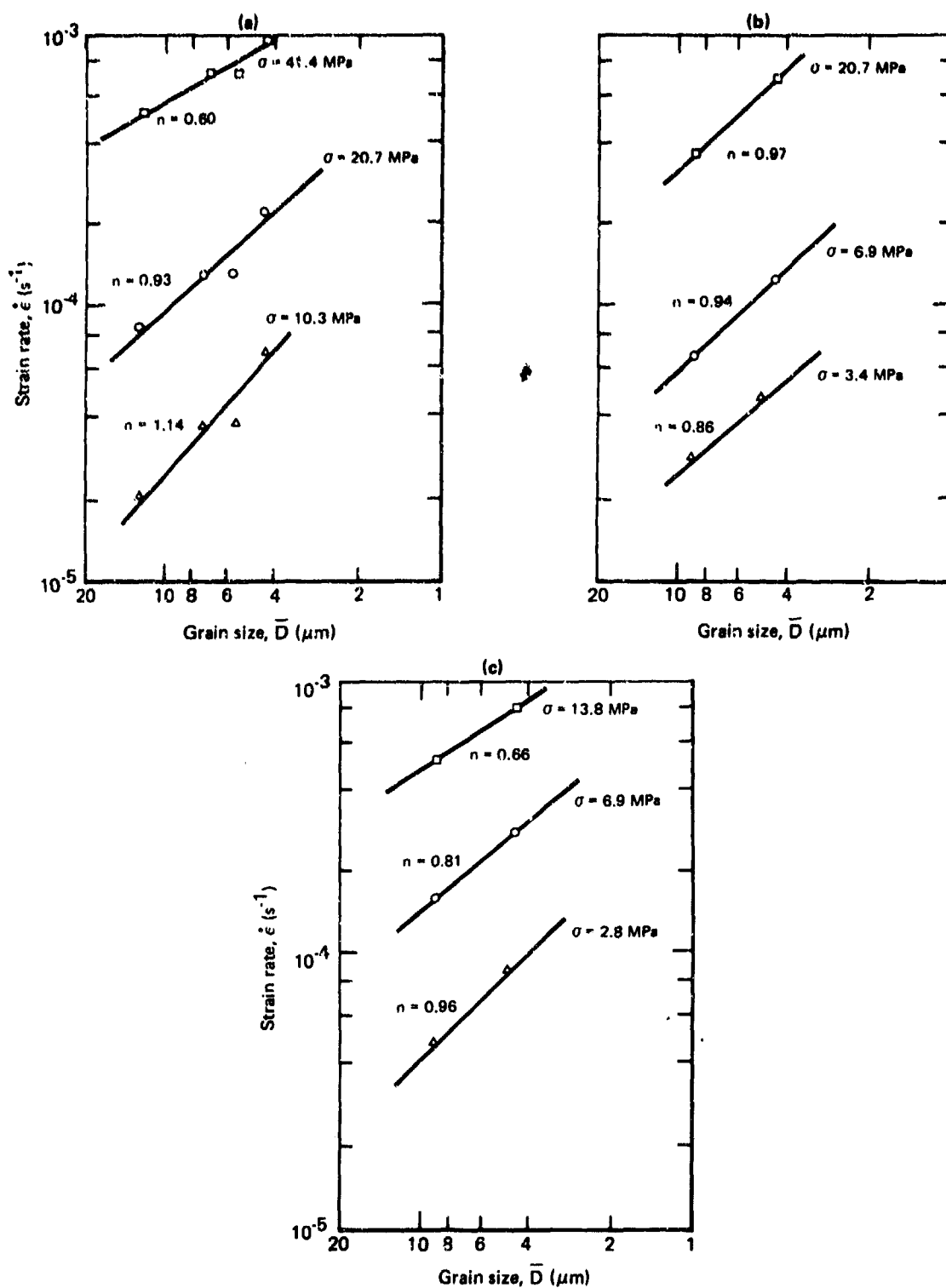
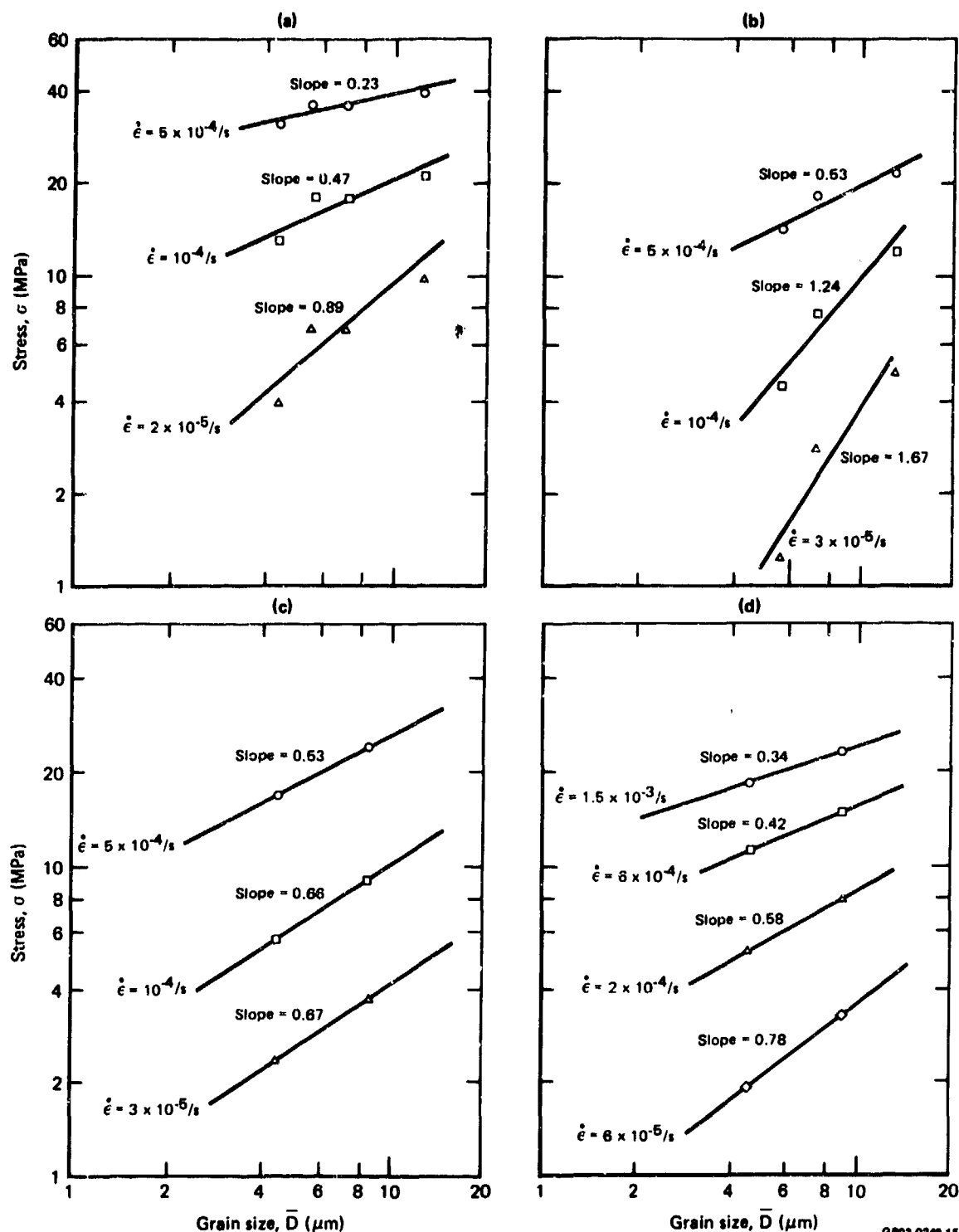


Figure 54. Grain-size dependence of strain rate at constant stress for regular-grade Ti-6Al-4V, volume % primary $\alpha = 45$; (a) 850°C, (1562°F); (b) 875°C, (1606°F); and (c) 907°C (1665°F)

GP03-0246-14



GP03-0246-15

Figure 55. Grain size dependence of flow stress at constant strain-rate for regular-grade Ti-6Al-4V at (a) 850°C (1562°F), and (b) 907°C (1665°F), and for ELI-grade Ti-6Al-4V at (c) 850°C (1562°F), and (d) 907°C (1665°F); volume % primary α = 46.

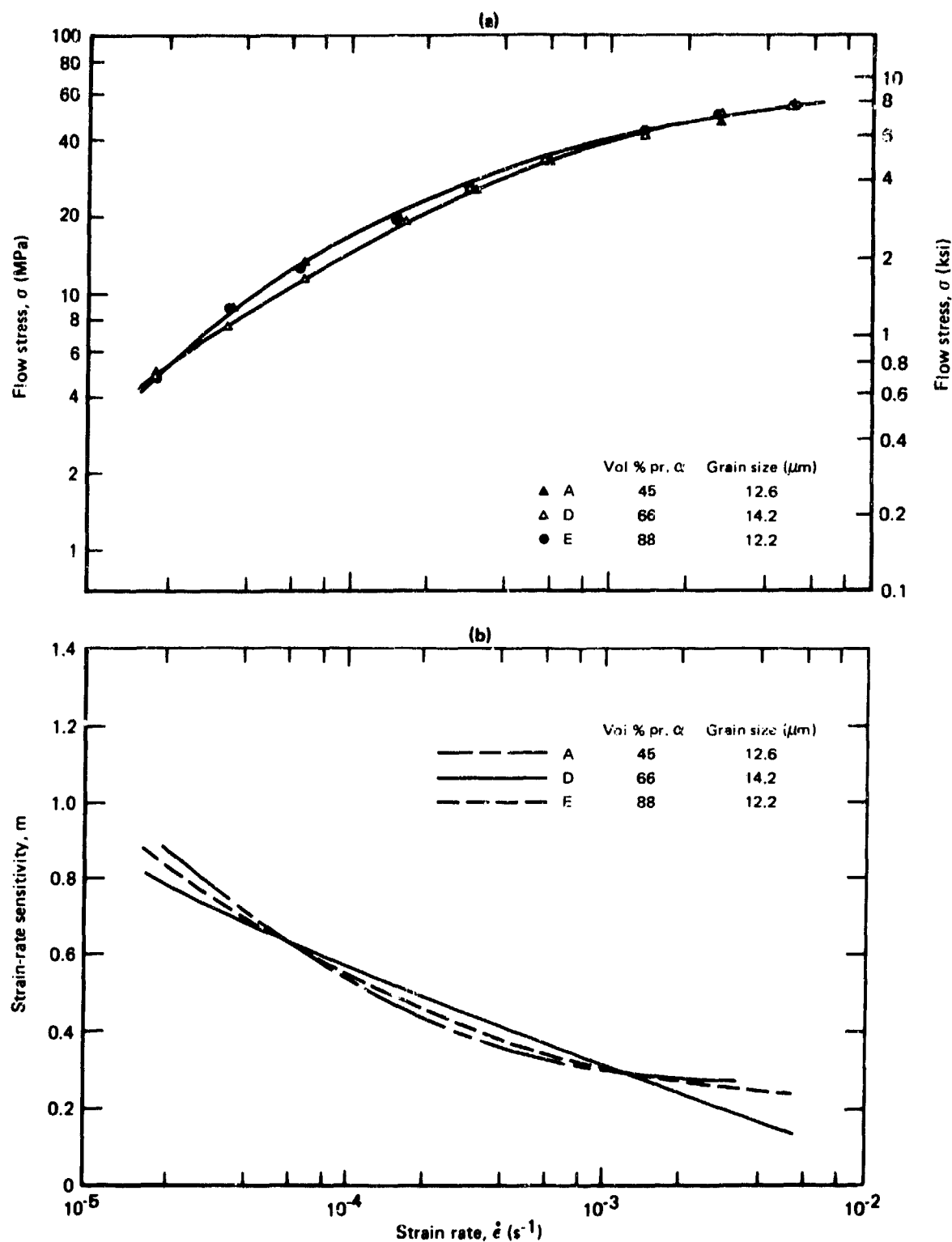
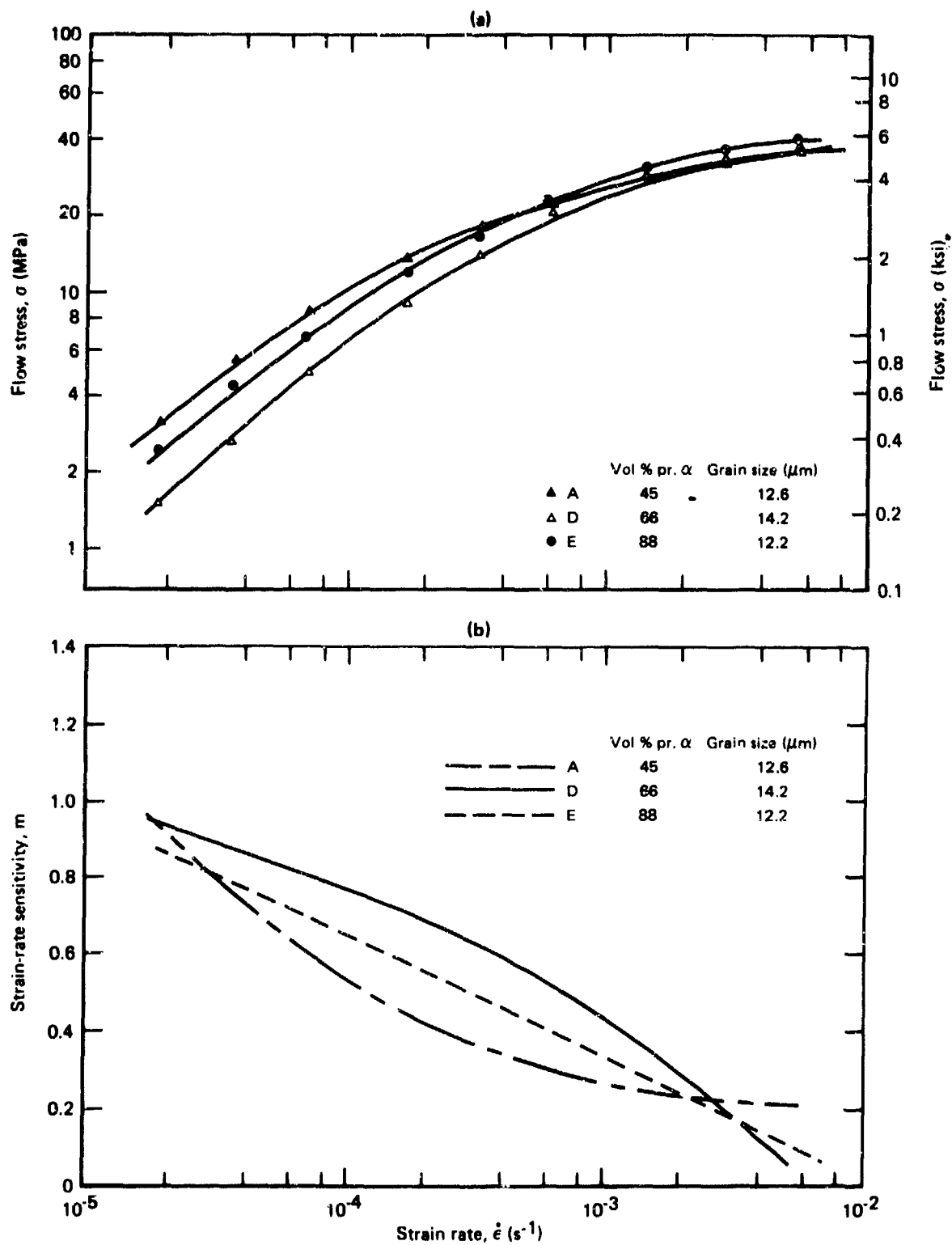
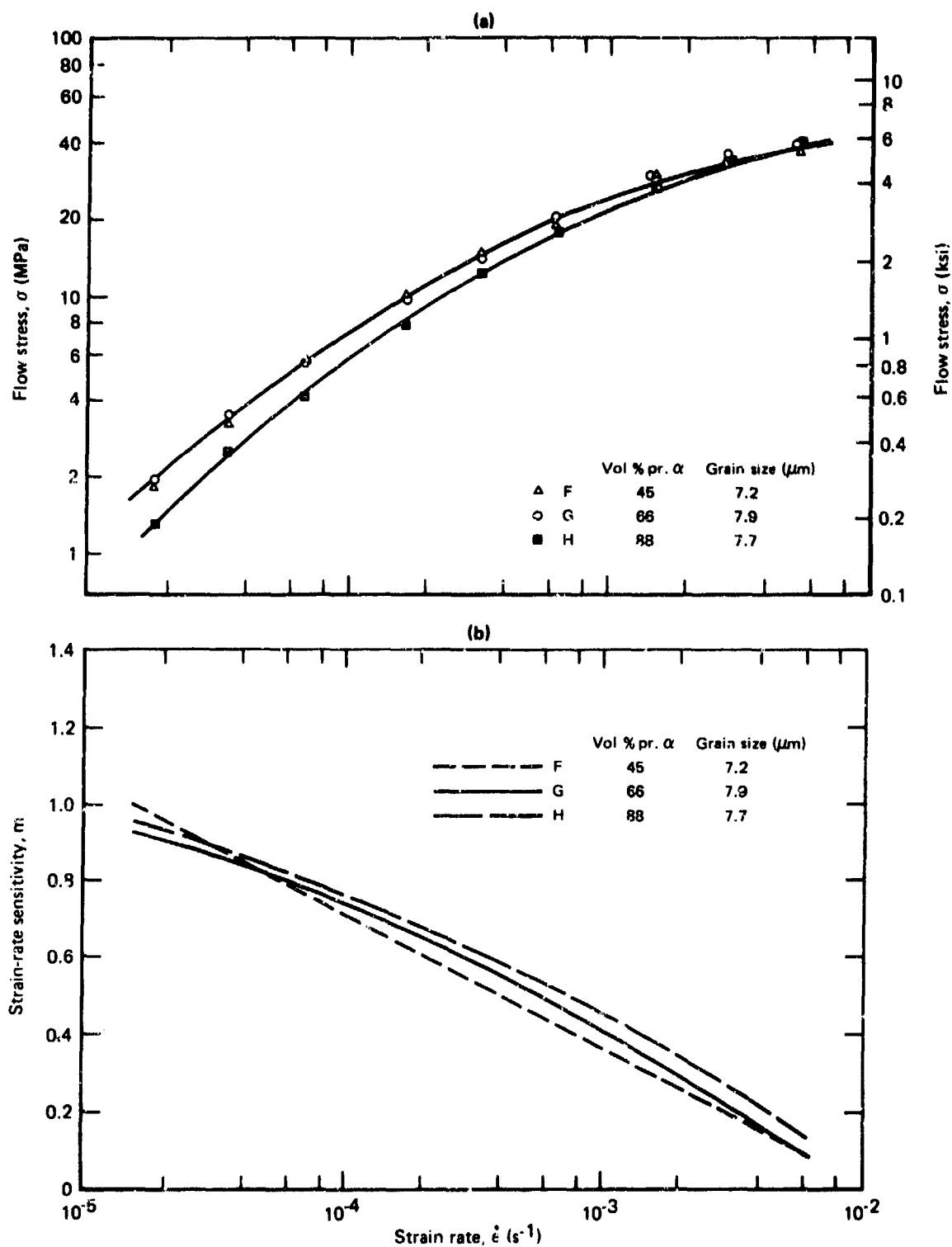


Figure 56. Effect of volume fraction of primary α on strain-rate dependence of (a) flow stress and (b) strain-rate sensitivity at 850°C (1562°F) of regular-grade Ti-6Al-4V.



GP03-0248-38

Figure 57. Effect of volume fraction of primary alpha on strain-rate dependence of (a) flow stress and (b) strain-rate sensitivity at 875°C (1607°F) of regular-grade Ti-6Al-4V.



GP03-0243-39

Figure 58. Effect of volume fraction of primary α on strain-rate dependence of (a) flow stress and (b) strain-rate sensitivity at 907°C (1665°F) of regular-grade Ti-6Al-4V.

The strain-rate dependences of flow stress and strain-rate-sensitivity at 815-975°C (1499-1787°F) shown in Figures 59a and 59b indicate that the best combinations of low flow-stresses and high-m values, both of which are conducive to superplasticity, are obtained in regular grade Ti-6Al-4V at 906°C (1663°F). The dependence of superplasticity parameters on temperature and equilibrium volume fraction of primary alpha shown in Figure 60 indicate that the best combinations of flow stress and m-values are obtained for an equilibrium-alpha volume fraction ≈ 0.6 . The increase in flow stress above 906°C is due to an increase in the equilibrium volume-fraction of the lesser-deforming beta phase and to rapid grain growth.

4.1.2 Strain Dependences of Flow Stress and Strain-Rate-Sensitivity

Since incremental-strain-rate test applies only to initial SPF behavior, the strain dependences of flow stress and strain-rate sensitivity of regular-grade Ti-6Al-4V were determined from constant-strain-rate tensile tests, constant-crosshead-speed tensile tests, and flat-ring compression tests.

Typical true-stress/true-strain plots determined from constant strain-rate tensile tests at different strain rates shown in Figures 61 and 62 for regular-grade Ti-6Al-4V and ELI-grade Ti-6Al-4V indicate significant increases in flow stress with strain, which clearly demonstrates the inadequacy of short-term incremental-strain-rate tests for determining the strain-rate dependence of flow stress. The variations of strain-rate sensitivity with strain determined from Figure 61 and 62 are shown in Figure 63. The value of m decreases with strain because of increasing grain size and, possibly, the formation of a substructure that alters the deformation mechanism. From a practical standpoint, this variation of m with strain has an important bearing on superplastic forming process-design calculations because provision must be made to compensate for decreasing strain-rate sensitivity with increasing strain.

Figures 64 and 65 are the stress/strain plots determined by constant-strain-rate tensile tests, constant-crosshead-speed tensile tests, and flat-ring compression tests at 875°C (1607°F) for strain rates of 10^{-4} and 10^{-3} s^{-1} . The tensile flow stress increases with increasing strain, the increase being more pronounced at 10^{-3} s^{-1} than at the lower strain rate. The strain dependence of compressive flow stress, listed in Table 19, follows a trend similar to that of the tensile

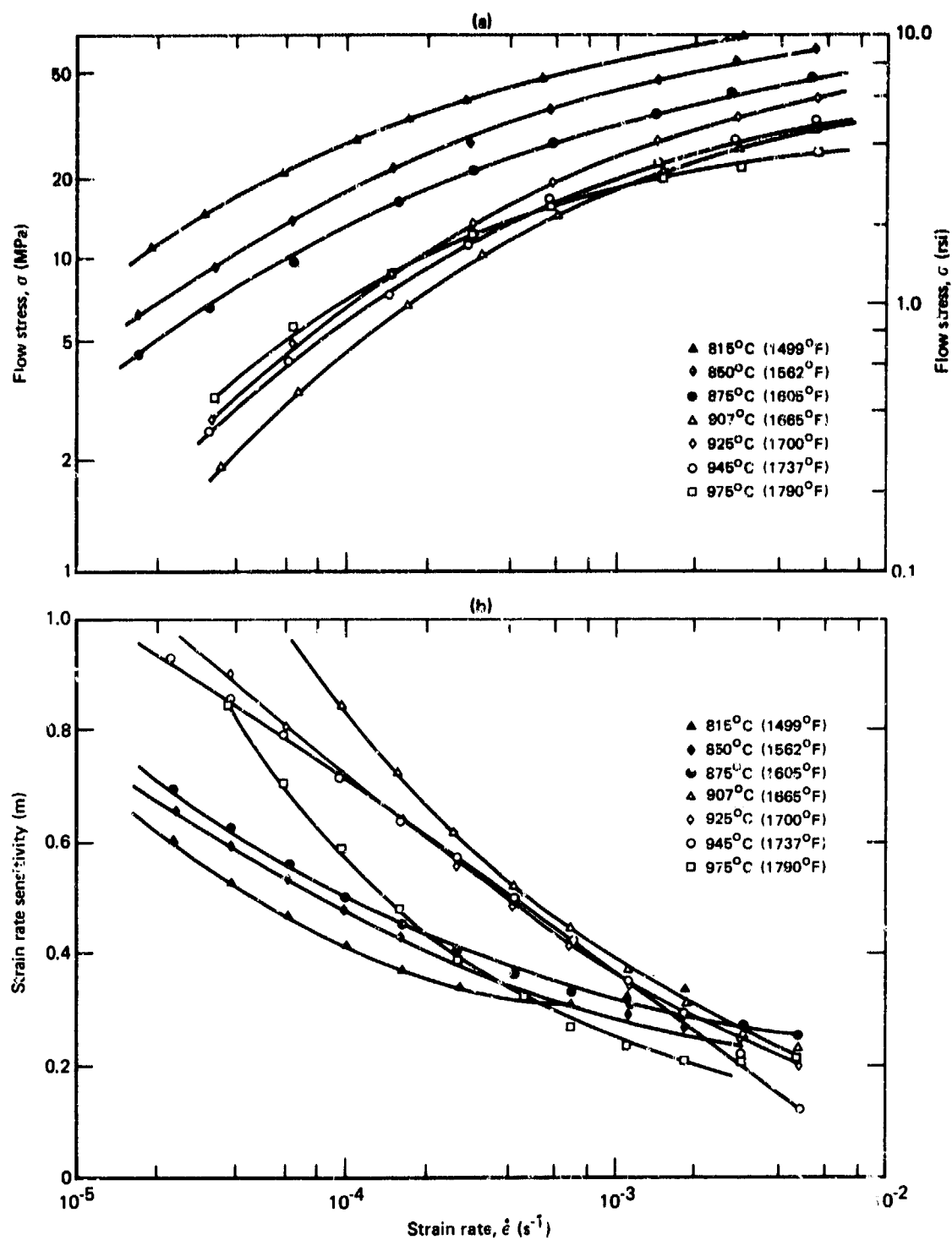
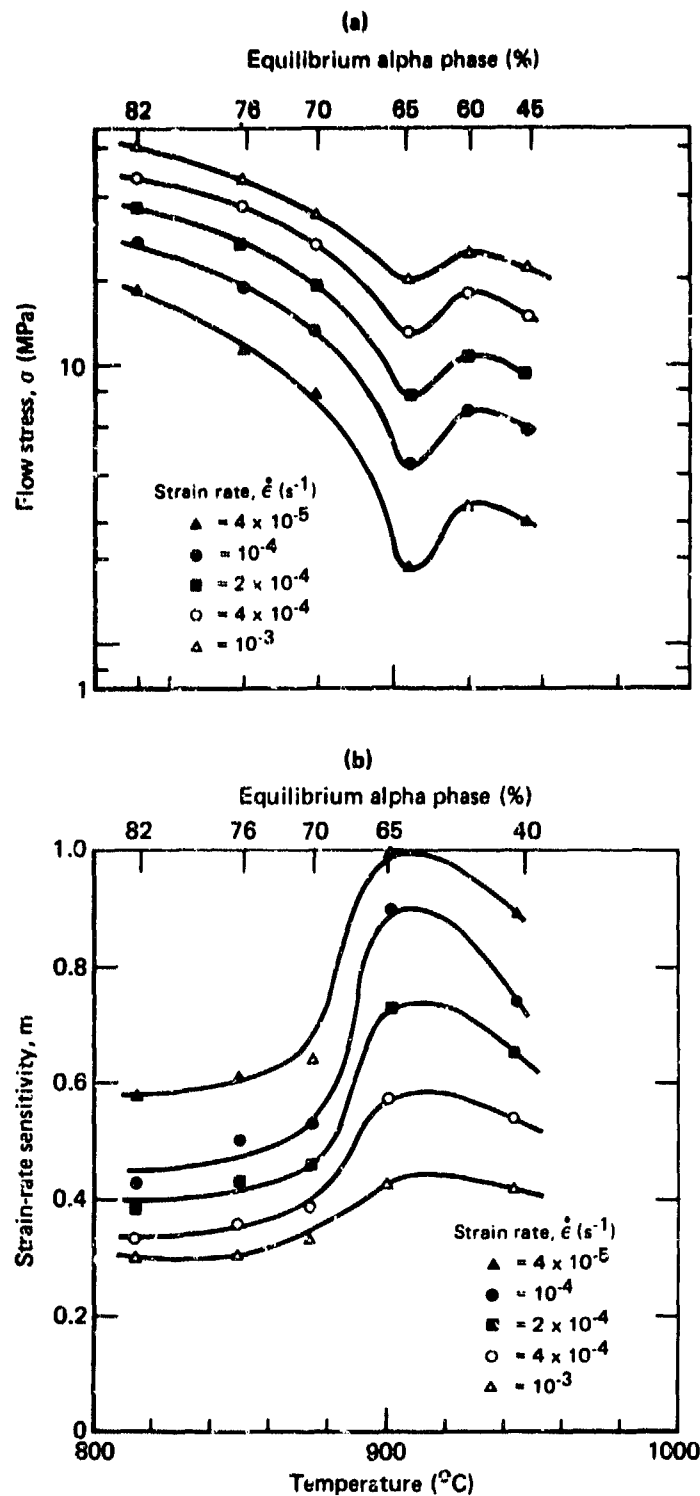


Figure 59. Effect of temperature on strain-rate dependence of (a) flow stress and (b) strain-rate sensitivity of regular-grade Ti-8Al-4V. (Specimen I, volume % primary alpha = 45, grain size = 5.6 μm).



GP03-0240-135

Figure 60. Effects of temperature and volume fraction of alpha phase on (a) flow stress and (b) strain-rate sensitivity of flow stress of Ti-6Al-4V.

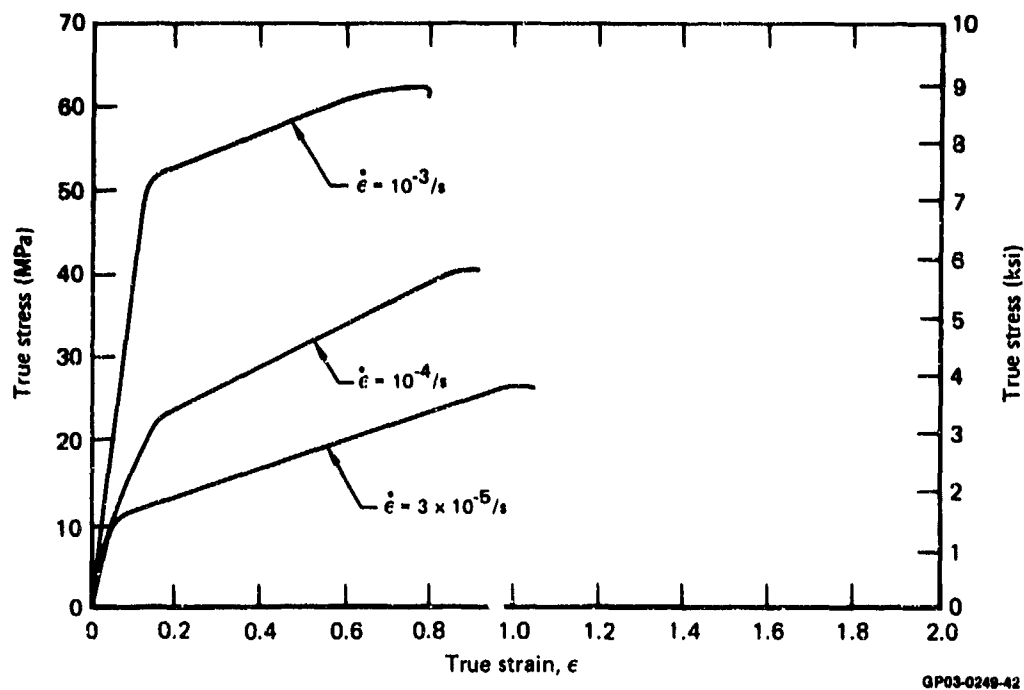


Figure 61. True-stress as a function of true-strain at 875°C (1606°F) of regular-grade Ti-6Al-4V (panel C, volume % primary alpha = 88, grain size = 17.6 μm) determined from constant strain-rate tensile tests.

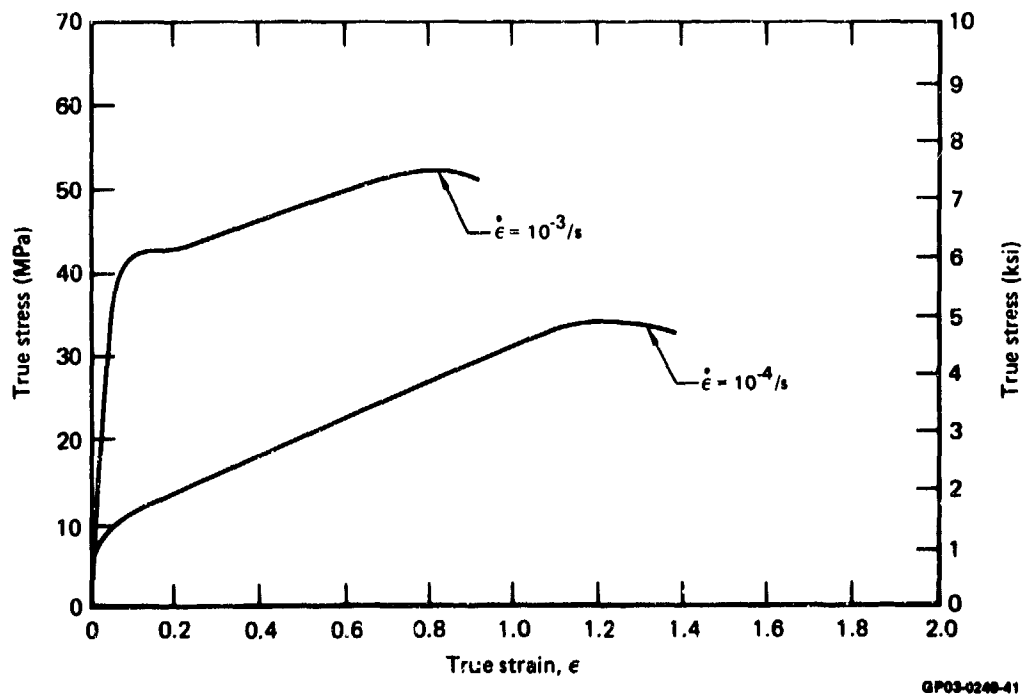


Figure 62. True-stress as a function of true-strain at 875°C (1607°F) of regular-grade Ti-6Al-4V (panel E, volume % primary alpha = 45, grain size = 7.2 μm) determined from constant strain-rate tensile tests.

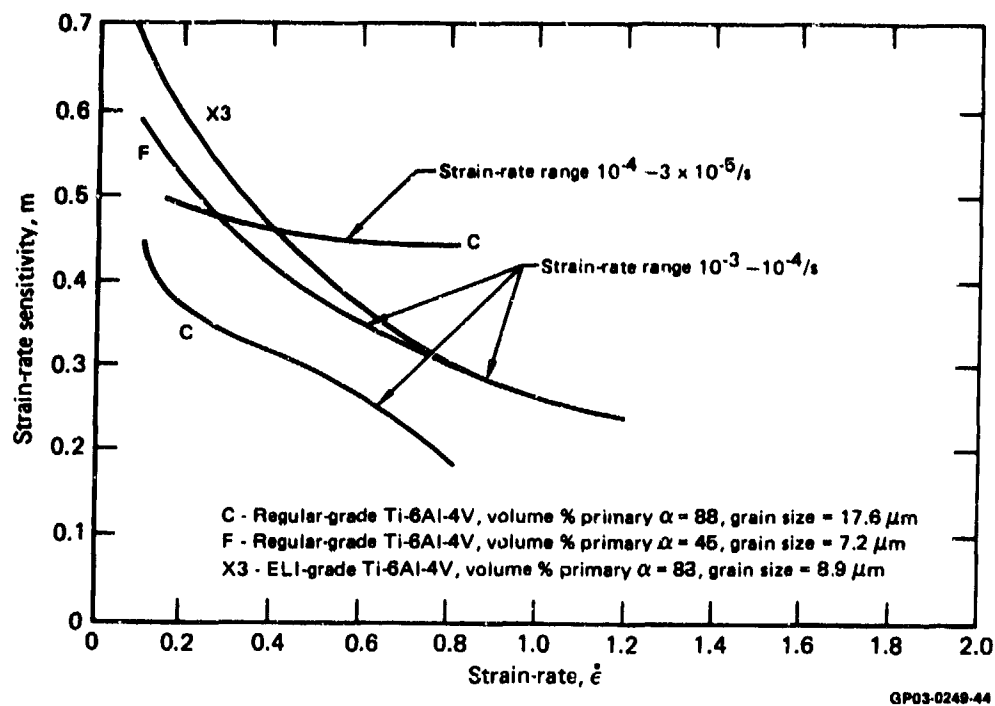


Figure 63. Strain dependence of strain-rate sensitivity at $875^{\circ}C$ ($1606^{\circ}F$) of regular-grade Ti-6Al-4V and ELI-grade Ti-6Al-4V.

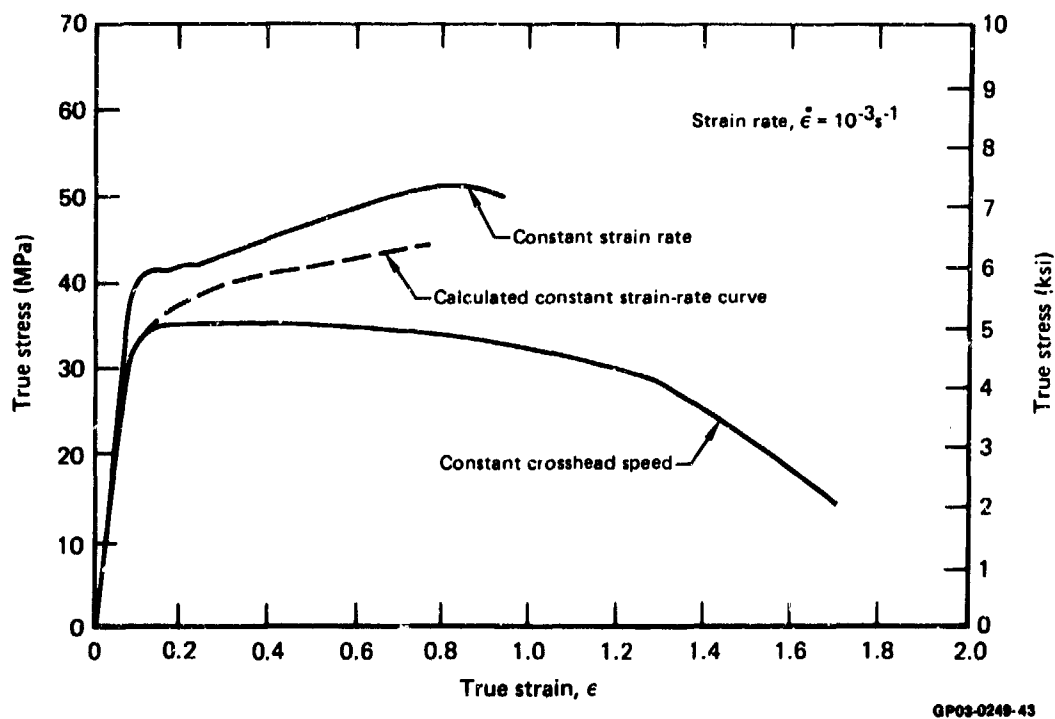
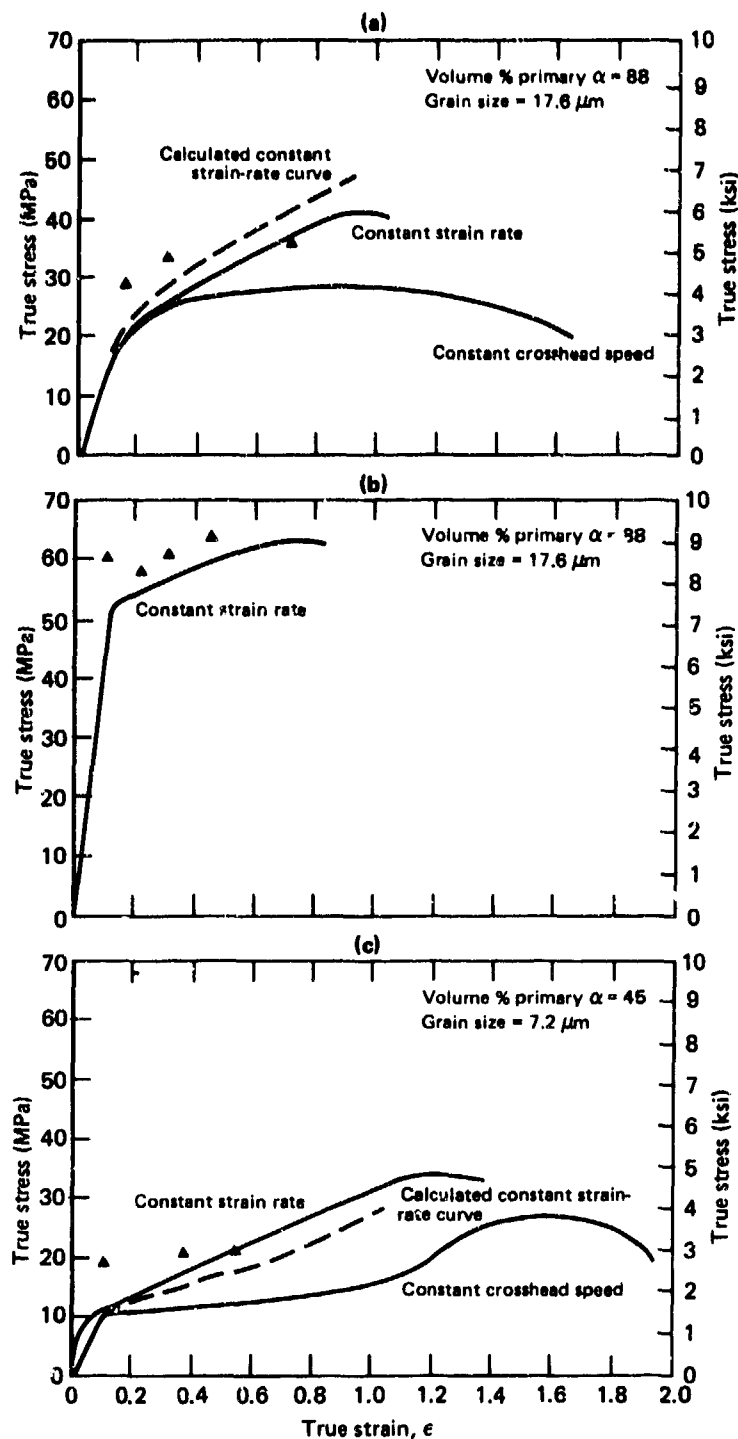


Figure 64. True-stress as a function of true-strain at $875^{\circ}C$ ($1606^{\circ}F$) of regular-grade Ti-6Al-4V (panel F, volume % primary $\alpha = 45$, grain size = $7.2 \mu m$) determined from constant strain-rate tensile tests.



GP03-0249-45

Figure 65. True-stress as a function of true-strain at 875°C (1606°F) of regular-grade Ti-6Al-4V determined from constant strain-rate tensile tests, constant crosshead speed tests, and flat-ring compression tests (Δ); (a) Specimen C, strain rate $\dot{\epsilon} = 10^{-4} \text{ s}^{-1}$, (b) Specimen C, strain rate $\dot{\epsilon} = 10^{-3} \text{ s}^{-1}$, and (c) Specimen F, strain rate $\dot{\epsilon} = 10^{-4} \text{ s}^{-1}$.

TABLE 19. FLOW-STRESS DATA OF NORMAL-TEXTURED Ti-6Al-4V
(FROM FLAT-RING COMPRESSION TESTS).

T = 907°C (1665°F) Lubricant: Boron nitride

Sample	Vol % α	Grain size (μm)	$\dot{\epsilon} = 0.00014 \text{ s}^{-1}$			$\dot{\epsilon} = 0.001 \text{ s}^{-1}$		
			Strain, ϵ	Flow stress (σ) [MPa (psi)]	Interfacial friction factor (M)	Strain ϵ	Flow stress (σ) [MPa (psi)]	Interfacial friction factor (M)
L	88	5.8	0.11	21(3037)	0.30	0.17	27(3879)	0.37
			0.26	22(3200)	0.30	0.28	30(4402)	0.43
			0.36	27(3930)	0.27	0.35	28(4119)	0.38
K	64	5.8	0.10	—	—	0.27	27(3940)	0.35
			0.27	—	—	0.31	29(4152)	0.35
			0.34	—	—	0.36	19(2768)	0.78
I	47	5.6	0.18	19(2752)	0.28	0.17	28(4107)	0.35
			0.31	16(2345)	0.54	0.29	31(4544)	0.26
			0.34	17(2512)	0.61	0.35	34(4955)	0.21
			0.16	18(2553)	0.16	0.27	27(3900)	0.25
J	4.4	4.4	0.30	22(3138)	0.18	0.33	27(3955)	0.26
			0.34	29(4154)	0.17	0.38	26(3755)	0.26
E	88	12.2	0.15	20(2888)	0.30	—	—	—
			0.27	24(3463)	0.24	—	—	—
			0.35	26(3814)	0.23	—	—	—
H	88	7.7	0.23	17(2393)	0.27	—	—	—
			0.33	18(2541)	0.40	—	—	—
			0.37	18(2636)	0.48	—	—	—

GP03-0249-6

flow stress, but the compressive flow stresses are slightly higher than the tensile flow stresses. Because the constant-crosshead-speed test yields a stress-strain characteristic under the condition of continuously decreasing strain-rate, the constant-crosshead-speed data were adjusted by the conventional method to obtain the calculated constant-strain-rate curves shown in Figures 64 and 65. The transformation of constant-crosshead-speed stress-strain curves into constant-strain-rate curves is clearly not satisfactory because it is based upon the stress/strain-rate relationship for small strains and does not incorporate the strain dependence of this relationship.

The elongations and necking-resistance observed for different specimens are listed in Tables 15-17. In specimens deformed at identical initial strain rates, the resistance to necking was higher at 906°C (1663°F) than at 850°C (1562°F) and 870°C (1607°F), and the necking resistance was higher in fine-grained specimens than in coarse-grained specimens.

4.1.3 Time dependence of strain rate at constant stress

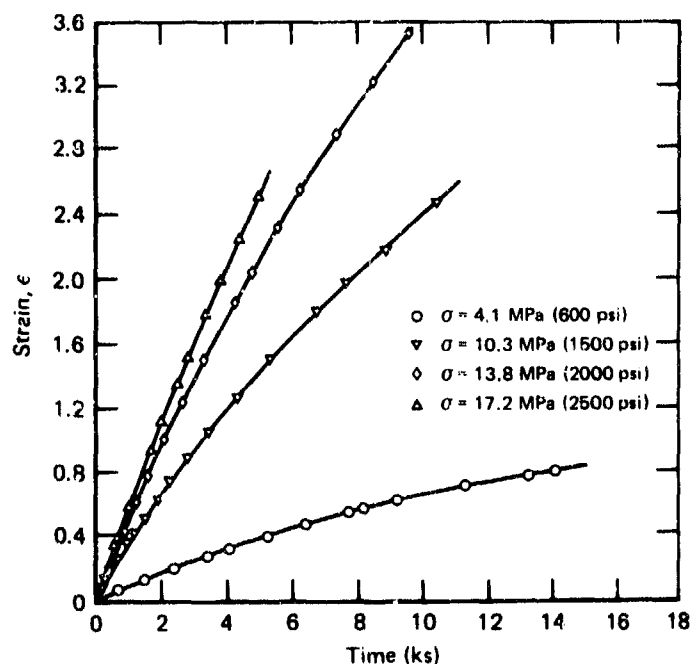
Constant-stress tests at 906°C (1663°F) were conducted on regular grade Ti-6Al-4V to determine the strain rate as a function of time and to evaluate the relationship between laboratory-test flow-stress/strain-rate data and cone-forming test data. Figure 66 shows plots of strain as a function of time for regular grade Ti-6Al-4V at stresses of 4.1 - 17.2 MPa. The continuously decreasing strain-rate with time is consistent with the hardening observed in constant-strain-rate tests and indicates that Ti-6Al-4V is metallurgically unstable during slow strain-rate high-temperature deformation. The metallurgical instabilities include grain growth, changes in volume-fractions and compositions of the alpha and beta phases, and deformation sub-structures. The stress dependence of strain rate follows a trend similar to that observed in constant-strain-rate tests and incremental-strain-rate tests. The variation of strain rate with time can be partially explained by the increasing grain size during superplastic forming. If the grain growth during superplastic forming is assumed to follow a parabolic law of the form

$$d - d_0 = Kt^{n_1}, \quad (8)$$

where d_0 is the initial grain size, t is the time, and n_1 is the grain growth exponent, and if the apparent hardening observed in Figure 66 is due solely to grain growth, then a plot of $\ln(\text{strain rate})$ as a function of $\ln(\text{time})$ should yield a straight line of slope equal to the negative of the grain-growth exponent, n_1 . The plots shown in Figure 67 exhibit a linear variation of $\ln(\text{strain rate})$ with $\ln(\text{time})$ with a slope ≈ -0.15 , in good agreement with the grain-growth exponents of 0.1-0.2 observed for Ti-6Al-4V at 800-900°C.

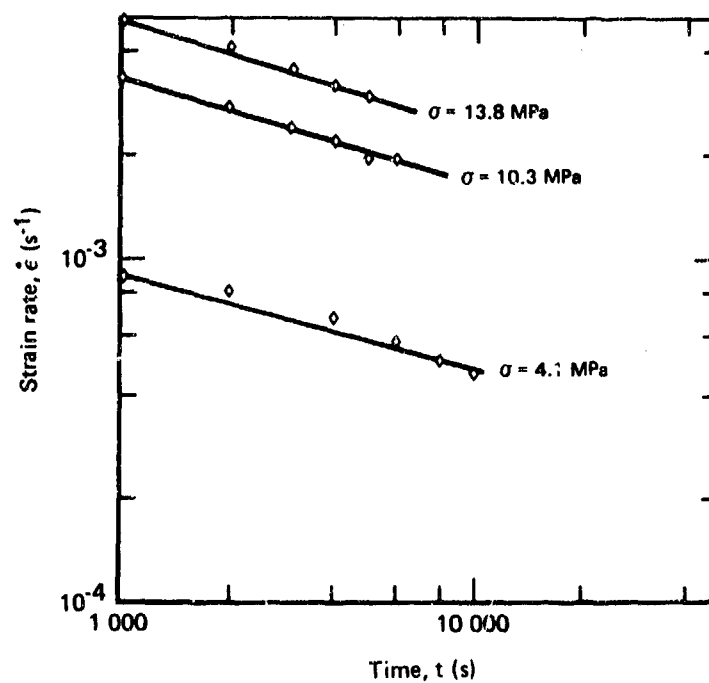
The effects of applied stress and initial grain sizes on the variation of strain rate and strain with time during constant-stress tests are shown in Figures 68 through 70. The strain rates are higher in fine-grained specimens than in coarse-grained specimens, in agreement with the results of incremental-strain-rate tests.

The effect of temperature on strain rates obtained during constant-stress tests is shown in Figure 71. The higher strain rates observed at higher temperatures are due to specimen necking and do not necessarily reflect continuously increasing superplasticity with increasing temperature.



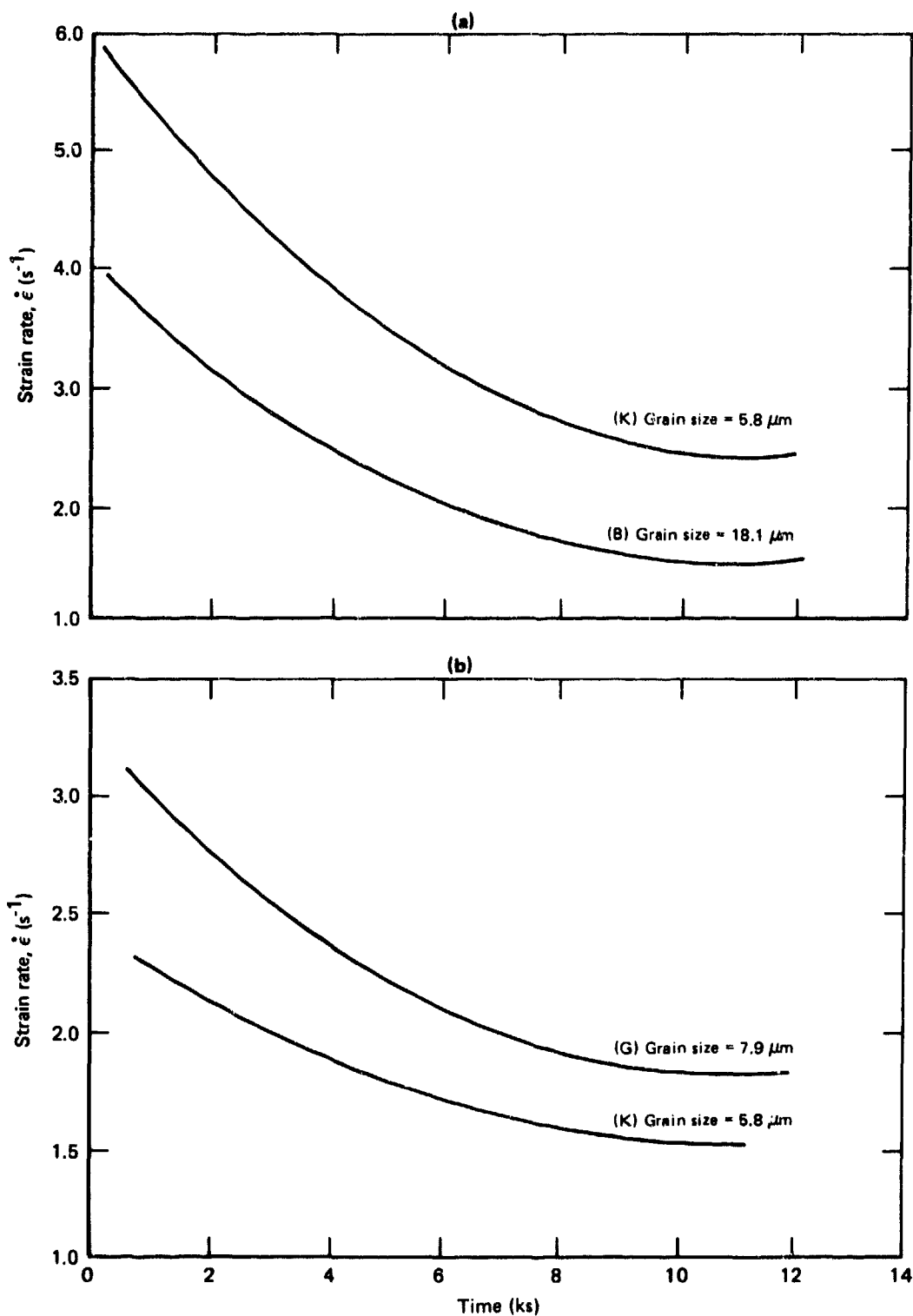
GP03-0249-46

Figure 66. Variation of strain with time determined for constant stress tests for regular-grade Ti-6Al-4V at 907°C (1665°F) (Specimen K, volume % primary alpha = 66, grain size = 5.8 μm).



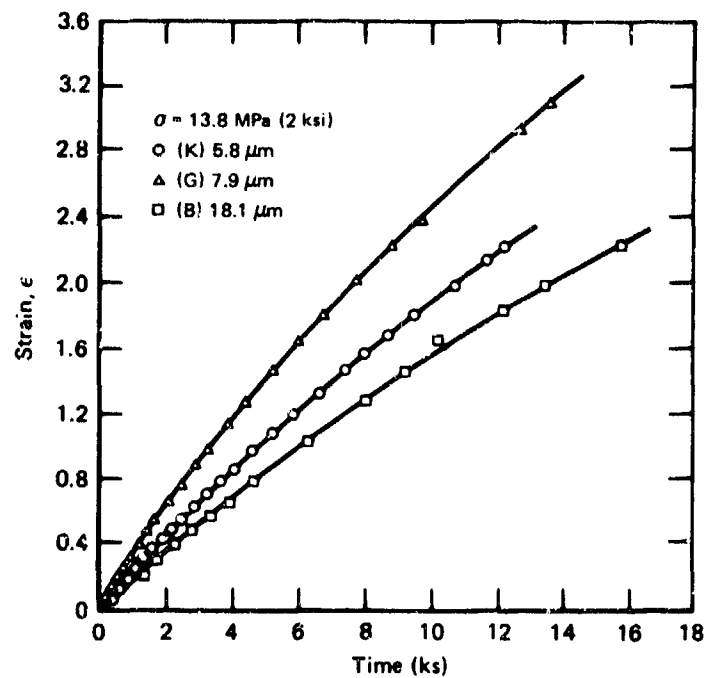
GP03-0248-18

Figure 67. Variation of \ln (strain rate \times instantaneous grain-size) with time during constant stress testing of Ti-6Al-4V at 907°C (1665°F).



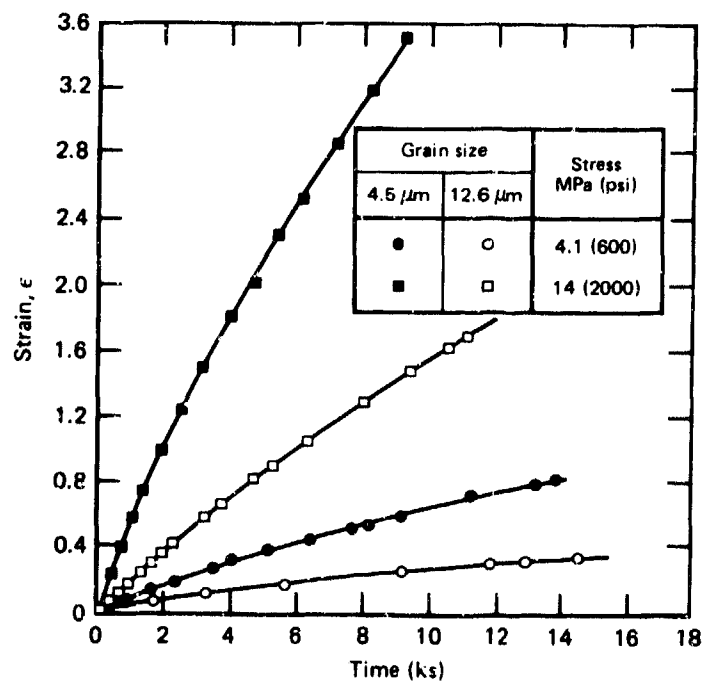
QP03-0248-48

Figure 68. Variation of strain rate with time determined from constant stress tests for regular-grade Ti-6Al-4V at 907°C (1665°F); (a) stress = 4.1 MPa (0.6 ksi) and (b) stress = 13.8 MPa (2 ksi).



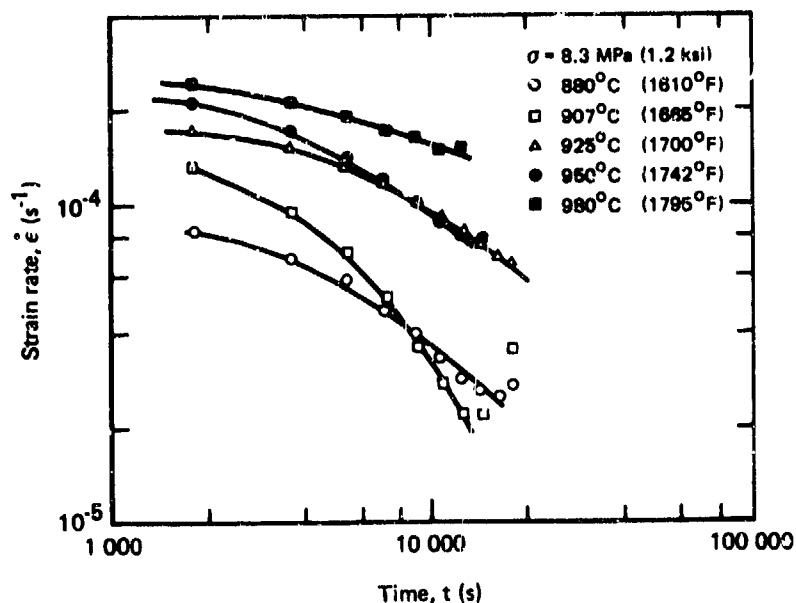
GP03-0249-105

Figure 69. Variation of strain with time determined from constant stress tests for regular-grade Ti-6Al-4V at 907°C (1665°F).



GP03-0249-47

Figure 70. Effect of grain size on strain rates of regular-grade Ti-6Al-4V determined from constant stress tests at 907°C (1665°F).



GP03-0246-48

Figure 71. Effect of temperature on strain rate of Ti-6Al-4V determined from constant stress tests.

To simulate a diffusion bonding cycle prior to superplastic forming, strain rates were measured on specimens soaked at temperature for 2 and 4 hours prior to testing. The effects of soak time on strain rates of regular-grade Ti-6Al-4V with a 6- μm grain size are shown in Figure 72 and the grain sizes of the specimen at different times are listed in Table 20. The initial soak results in a decrease in strain rate because of the increased grain size.

TABLE 20. EFFECTS OF STRESS AND TIME ON GRAIN GROWTH DURING SUPERPLASTIC TESTING OF Ti-6Al-4V AT 907°C(1665°F)

Specimen	Soak time (min)	Test duration (min)	Alpha grain size (μm)	
			Undeformed region	Deformed region
L	10	30	8	9
	10	60	10	13
	10	120	12	15
	10	190	22	24
	250	190	24	25

GP03-0246-8

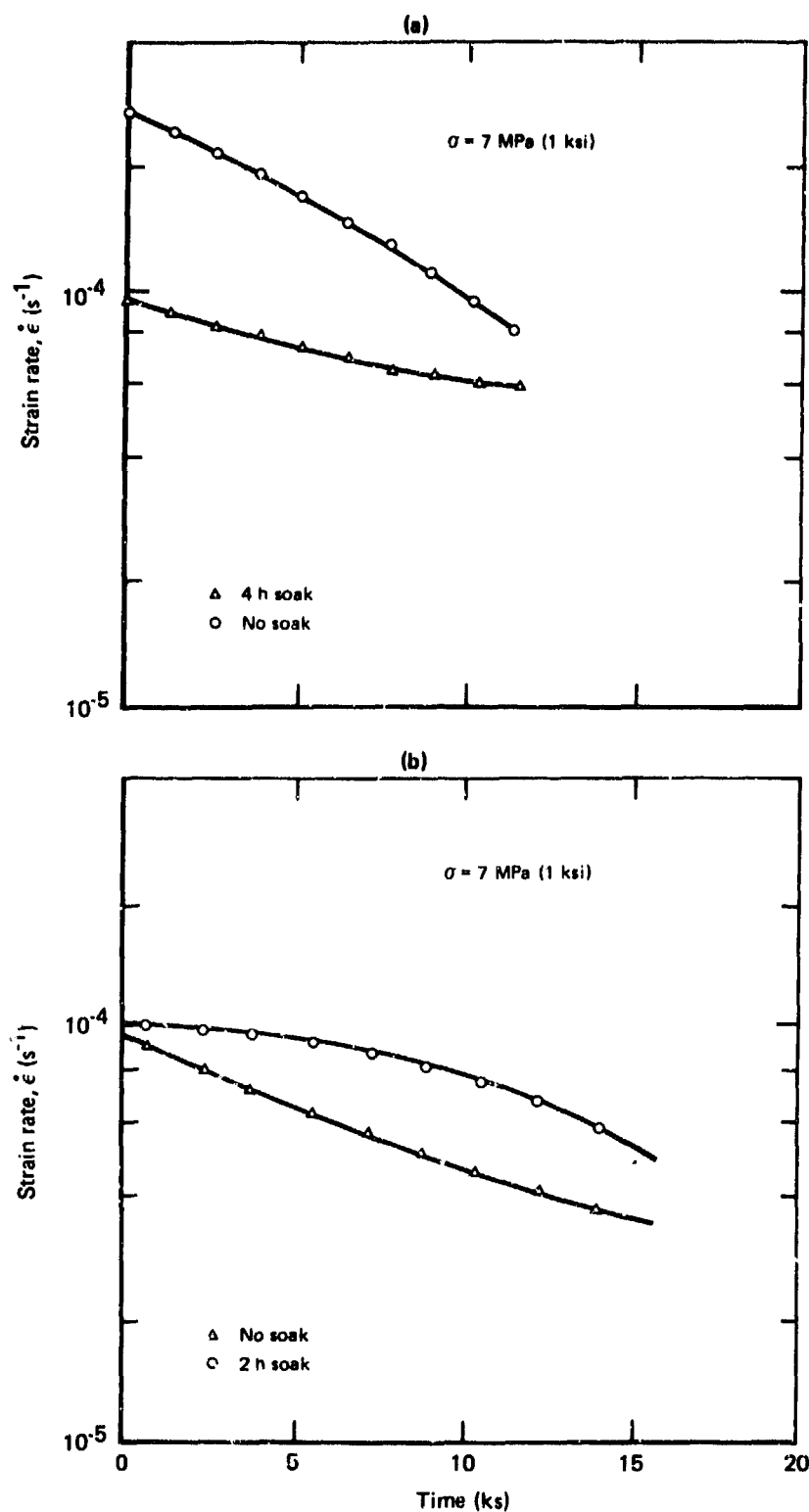


Figure 72. Effect of soak time on strain rate of Ti-6Al-4V at 907°C (1665°F); (a) specimen L (volume % primary alpha = 88, grain size = 6 μm) and (b) specimen E (volume % primary alpha = 88, grain size = 12 μm).

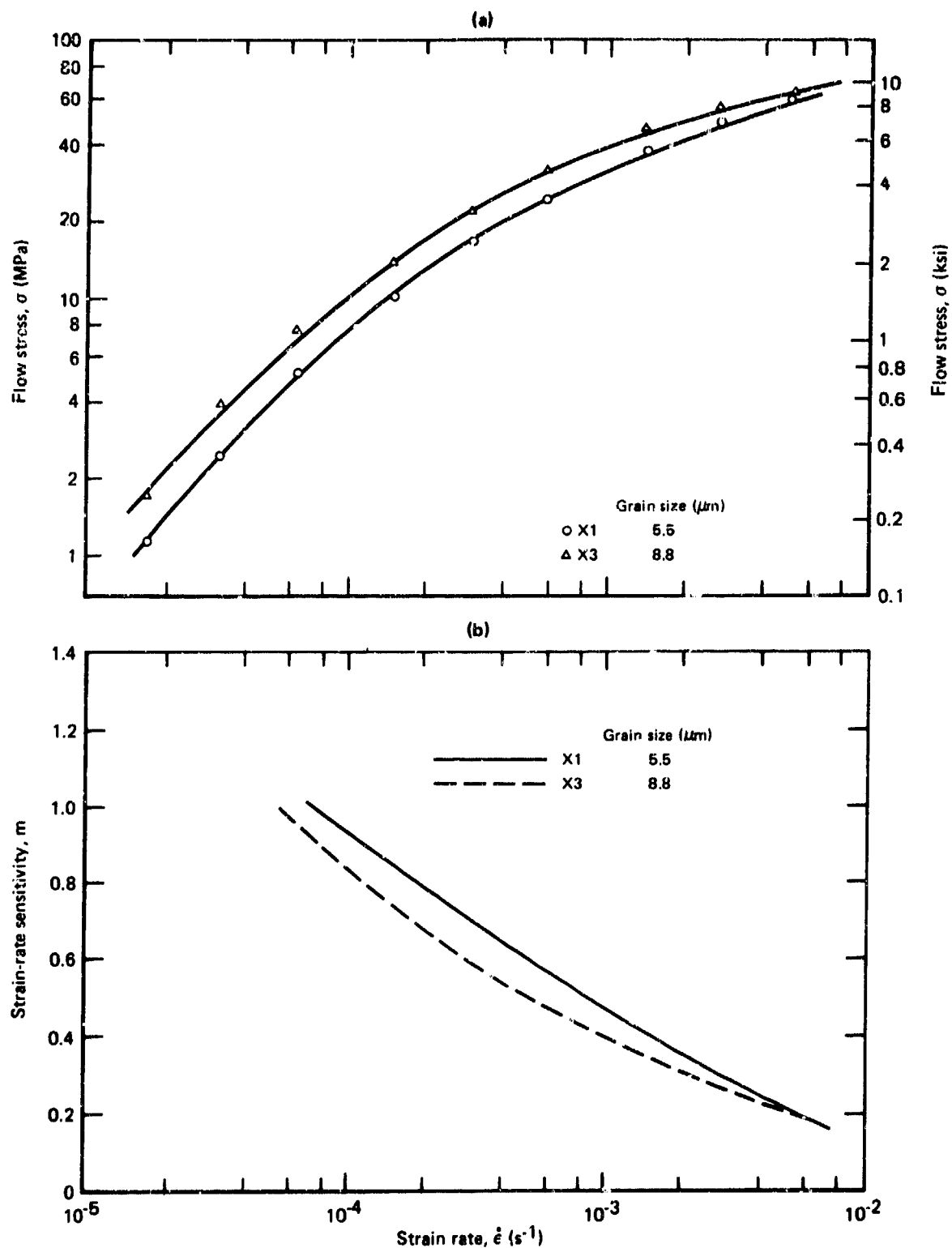
4.1.4 Flat-Ring Compression-Test Evaluation of Lubricants

The flat-ring compression test, in addition to measuring the strain dependence of compressive flow stresses, can be used to quantitatively assess metal-forming lubricants. The ability of a lubricant to transfer an applied load to the deforming material is related to the interfacial friction factor, M . In the present investigation, the characteristics of several commercial lubricants (Delta Glaze 347M, boron nitride, Formkote 750, Graphite AA, and Graphite AE) were studied by flat-ring compression tests at 850-950°C (1560-1740°F). Whereas Delta Glaze and boron nitride gave M values of 0.1 and 0.3, respectively, the other lubricants exhibited interfacial friction factors greater than 0.4, rendering them less efficient for high-temperature Ti-6Al-4V forming operations.

4.2 ELI-Grade Ti-6Al-4V ($T_\beta = 968^\circ\text{C}$)

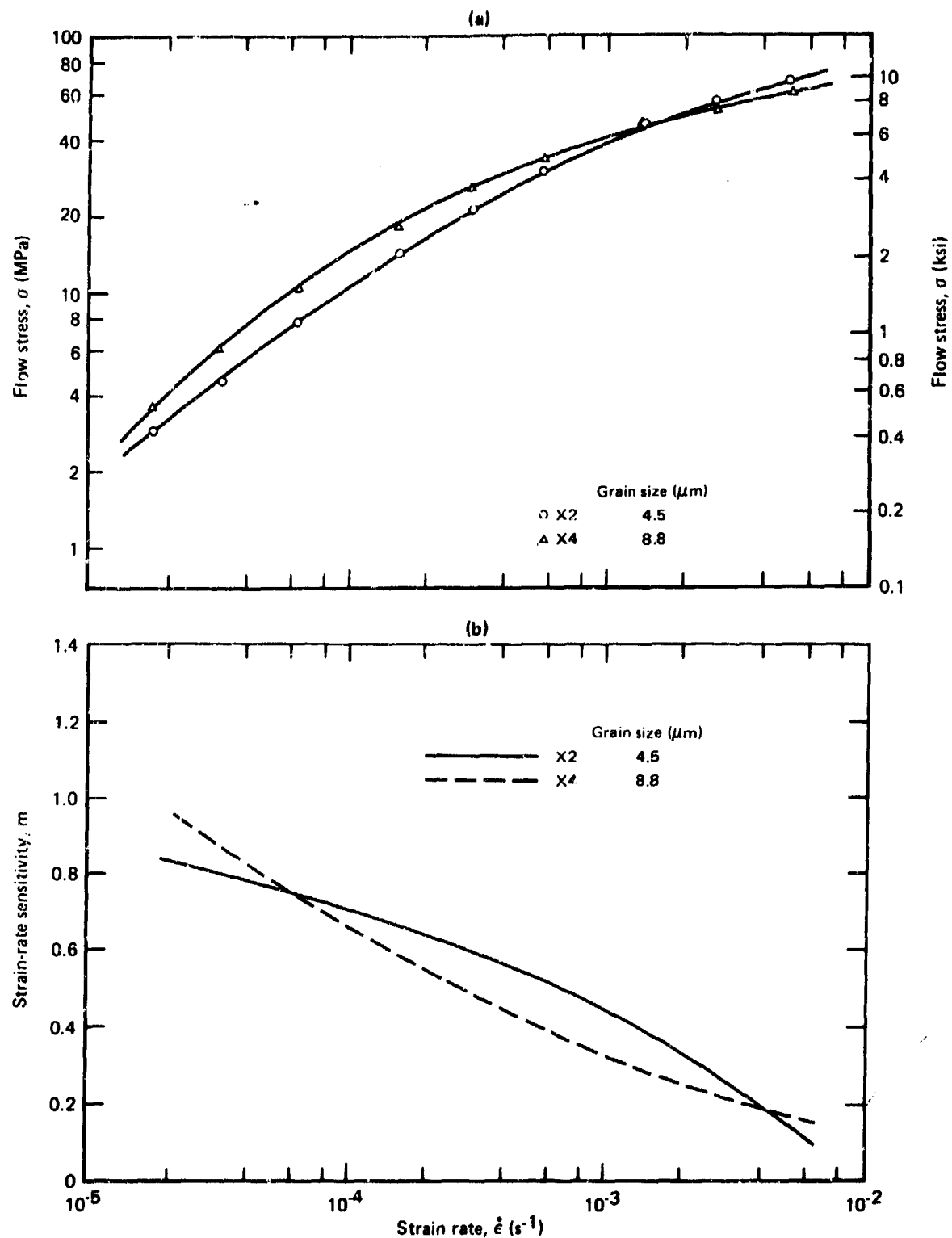
The strain-rate dependences of flow stress and strain-rate-sensitivity for ELI grade Ti-6Al-4V at 850°C (1562°F), 875°C (1607°F) and 906°C (1663°F) are shown in Figures 73 through 78 and the normalized plots of flow stress as a function of $\ln(\text{strain-rate} \times \text{grain-size})$ are shown in Figures 79 through 81. At constant temperature, the ELI grade Ti-6Al-4V has lower flow stress and higher strain-rate sensitivity than regular-grade Ti-6Al-4V.

Figure 82 shows the plots of $\ln(\sigma)$ as a function of $\ln(\text{strain-rate} \times \text{grain-size})$ for different microstructural conditions of the regular-grade and ELI-grade Ti-6Al-4V at different temperatures. The ratio of the test temperature, T , to the beta-transus temperature, T_β , is indicated for each alloy. As T/T_β decreases, the flow stress increases and the strain-rate region over which $m > 0.5$ shifts to lower strain rates. The differences in flow-stress/strain-rate behavior between ELI-grade and regular-grade Ti-6Al-4V can be described solely in terms of the lower beta-transus temperature and hence the higher amount of equilibrium alpha in ELI-grade Ti-6Al-4V. Any other effects of interstitial oxygen concentration on the flow-



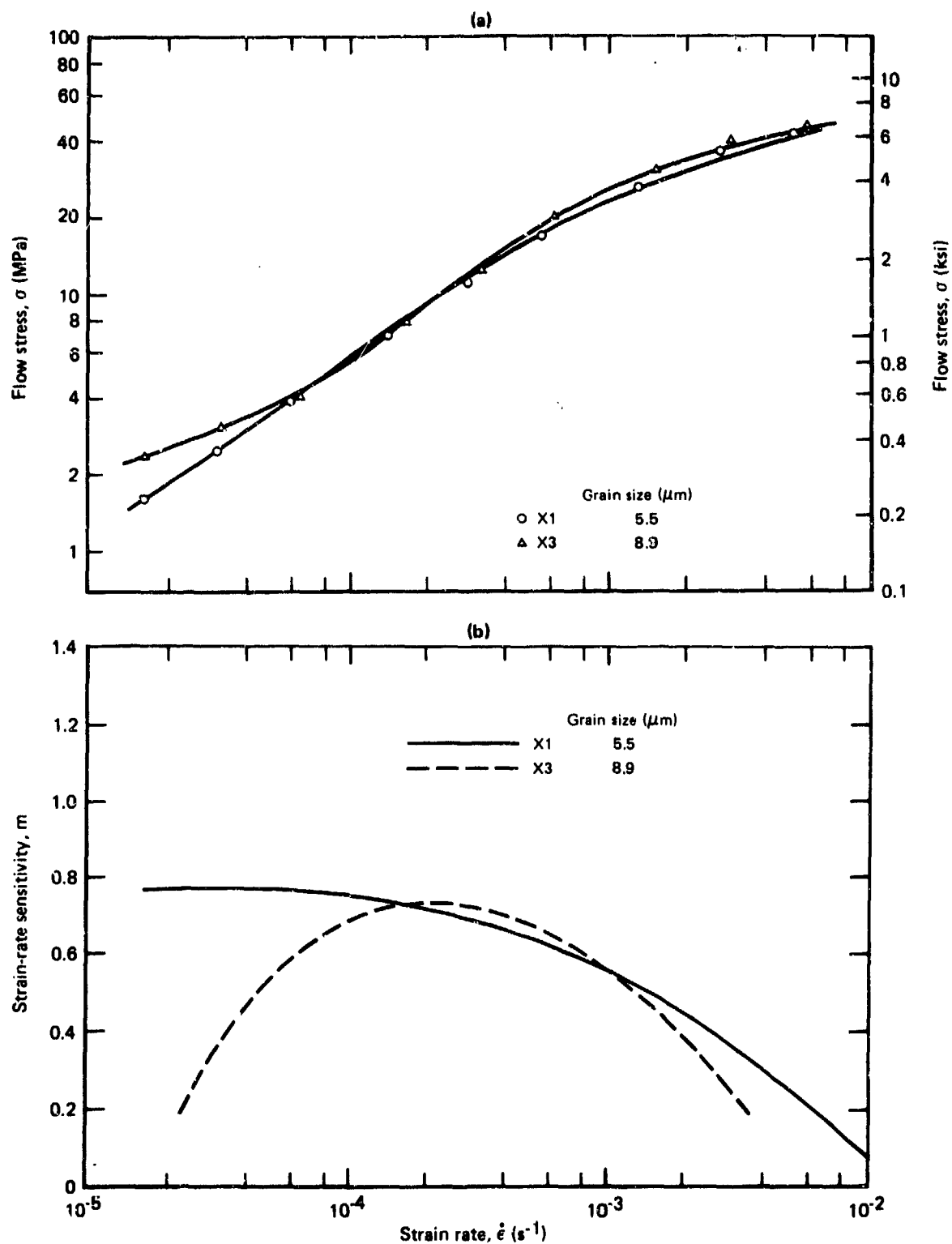
GP03-0240-51

Figure 73. Strain-rate dependence of (a) flow stress and (b) strain-rate sensitivity for ELI-grade Ti-6Al-4V (volume % primary α = 86) at 850°C (1562°F).



GP03-0240-52

Figure 74. Strain-rate dependence of (a) flow stress and (b) strain-rate sensitivity for ELI-grade Ti-6Al-4V (volume % primary α = 46) at 850°C (1562°F).



GP03-0248-53

Figure 75. Strain-rate dependence of (a) flow stress and (b) strain-rate sensitivity for ELI-grade Ti-6Al-4V (volume % primary α = 88) at 875°C (1607°F).

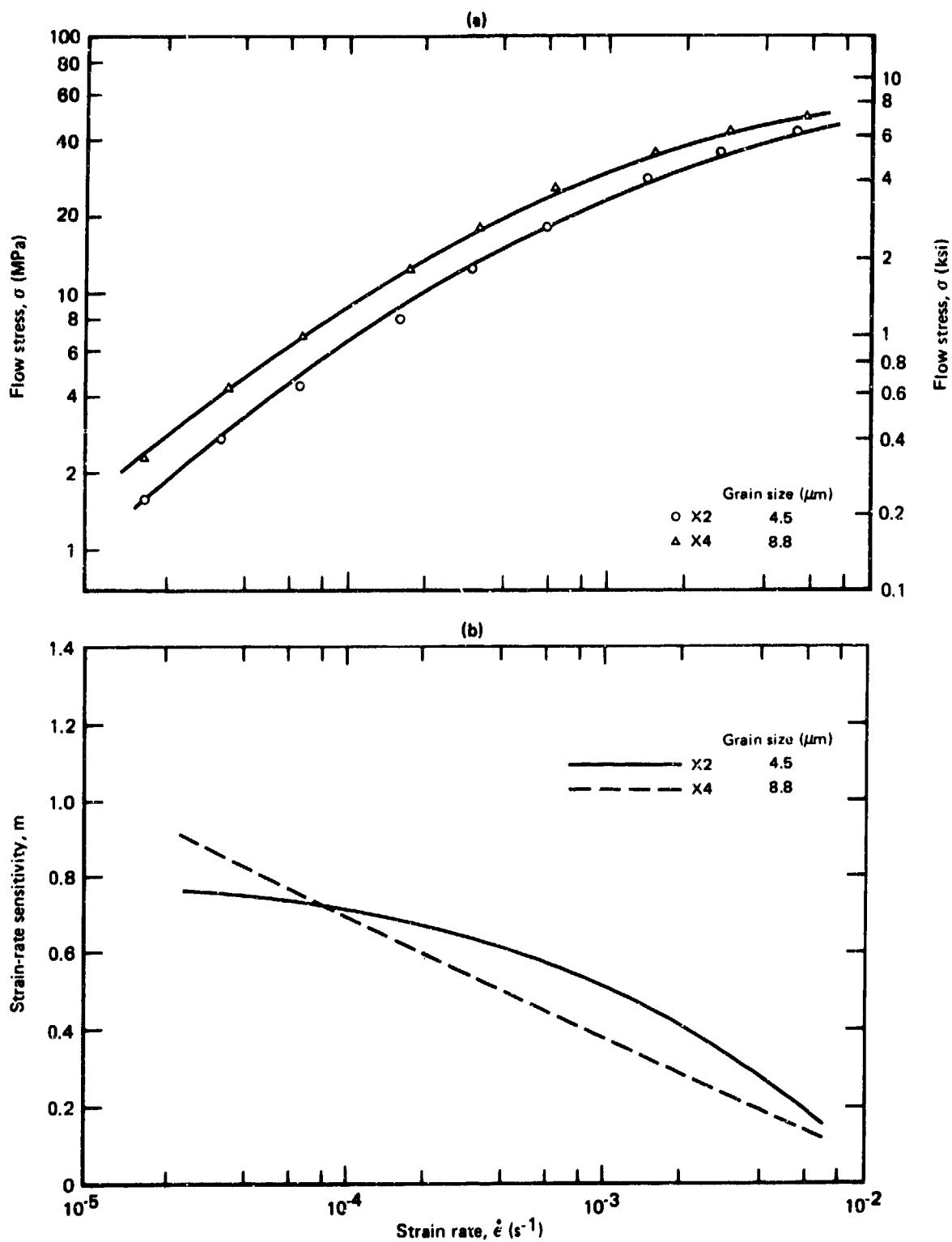


Figure 76. Strain-rate dependence of (a) flow stress and (b) strain-rate sensitivity for ELI-grade Ti-6Al-4V (volume % primary α = 46) at 875°C (1607°F).

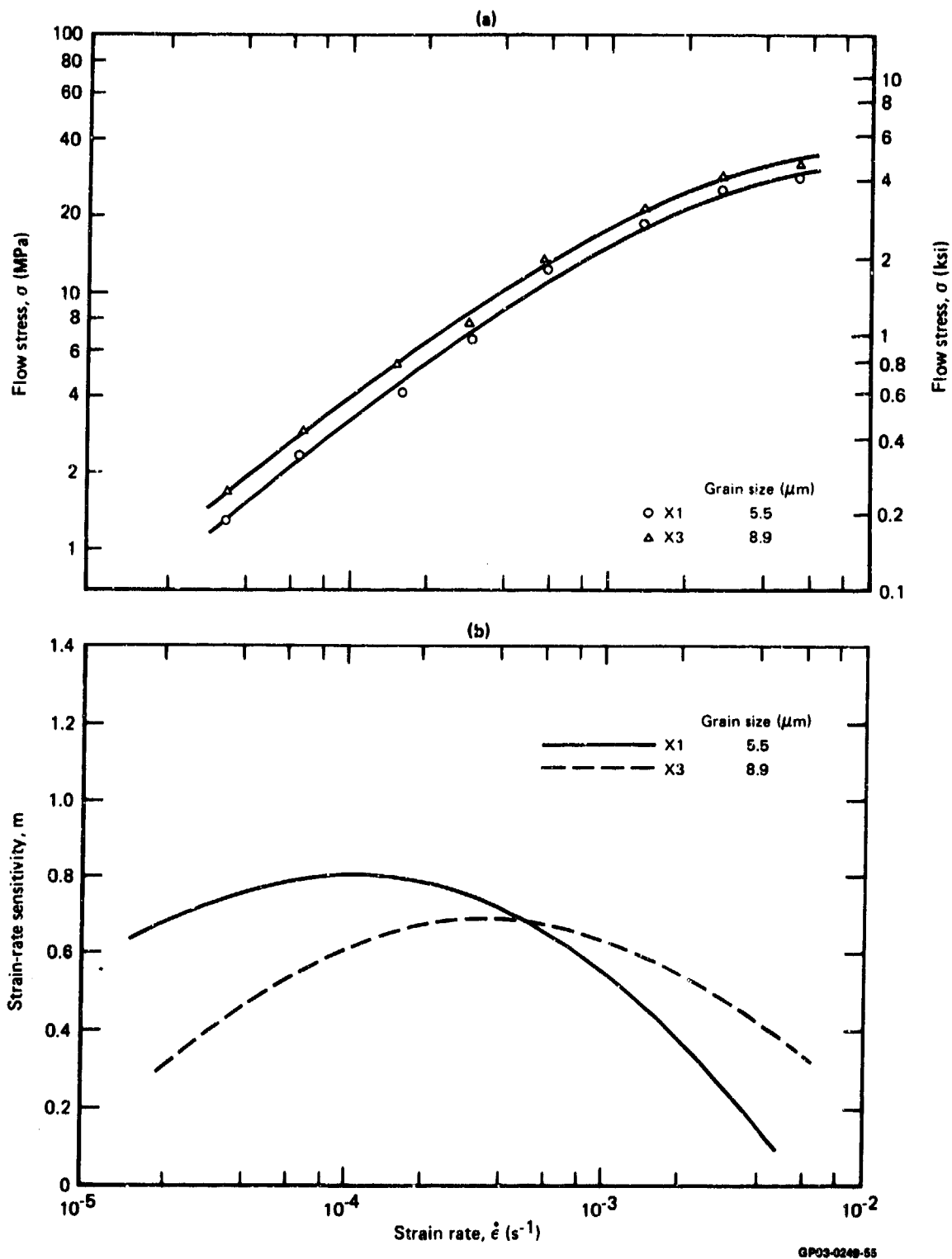


Figure 77. Strain-rate dependence of (a) flow stress and (b) strain-rate sensitivity for ELI-grade Ti-6Al-4V (volume % primary α = 88) at 907°C (1665°F).

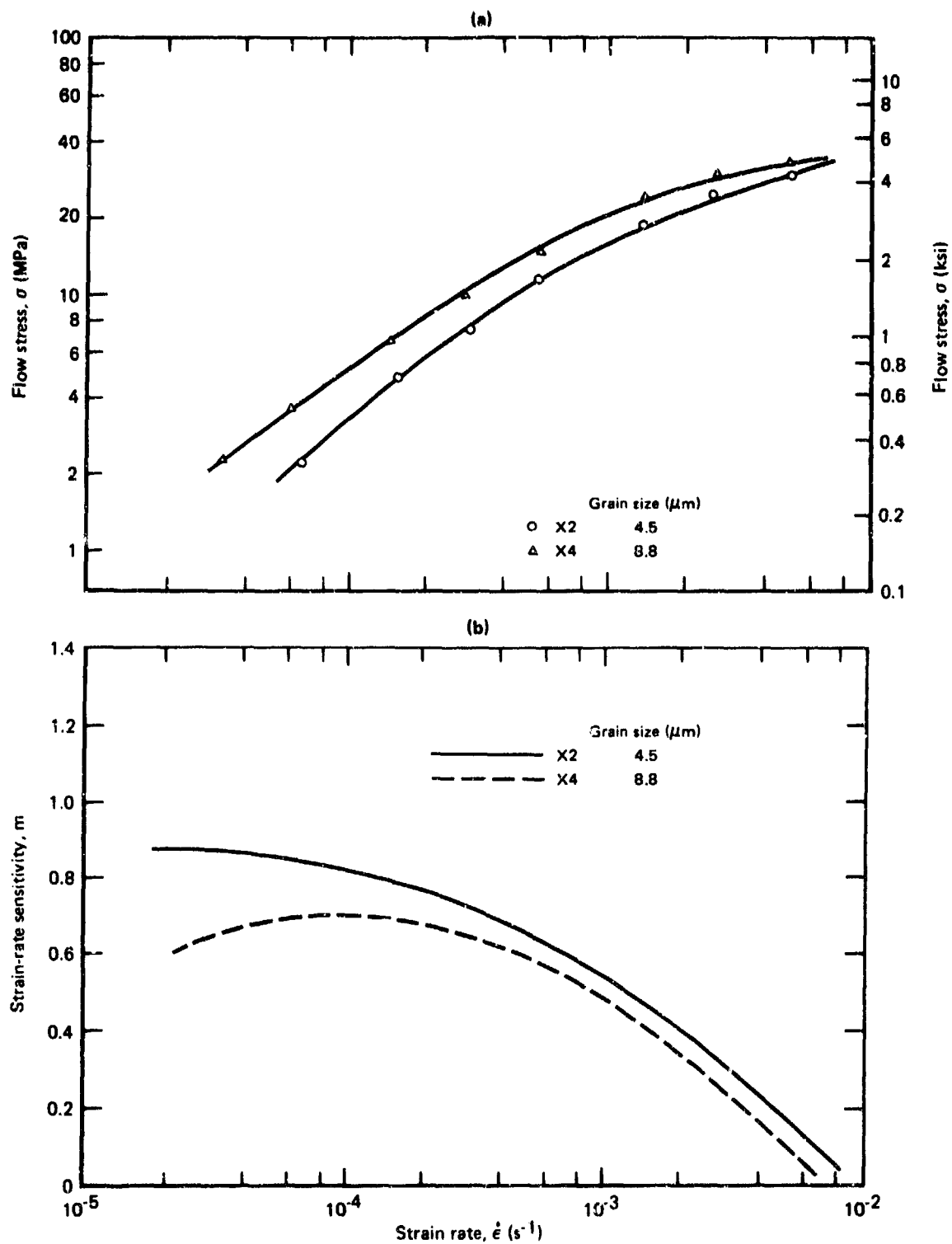


Figure 78. Strain-rate dependence of (a) flow stress and (b) strain-rate sensitivity for ELI-grade Ti-6Al-4V (volume % primary α = 40) at 907°C (1665°F).

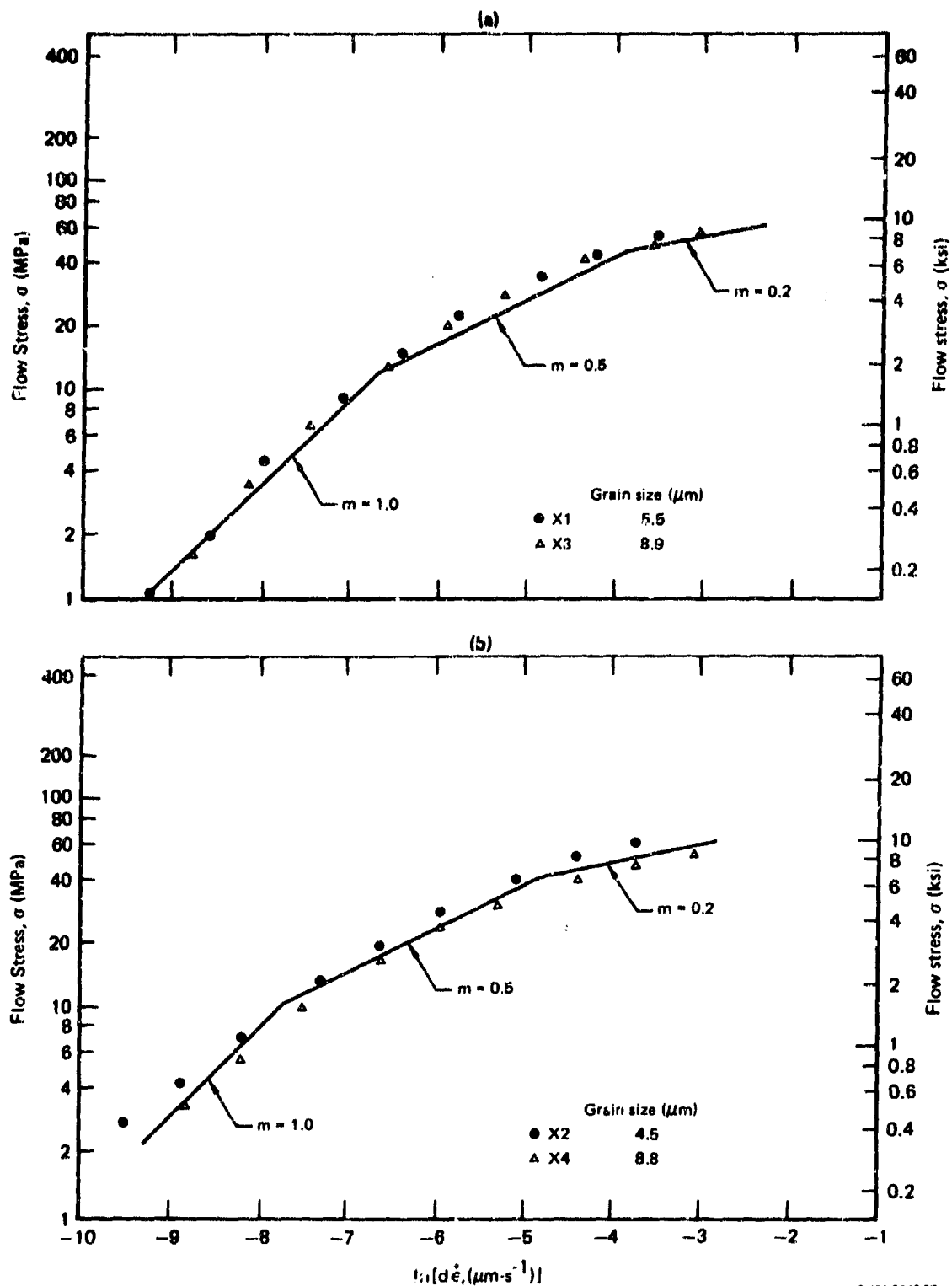
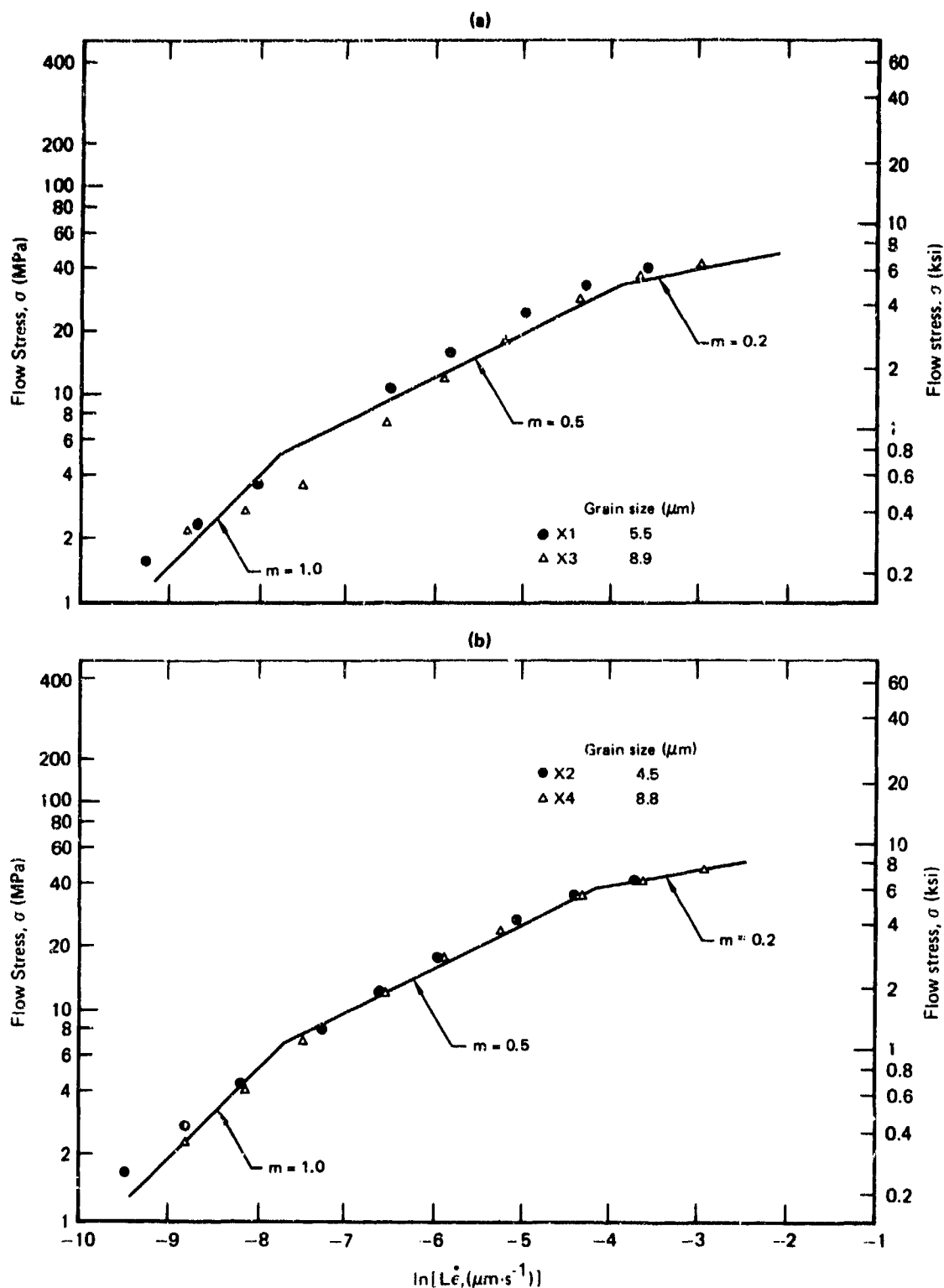
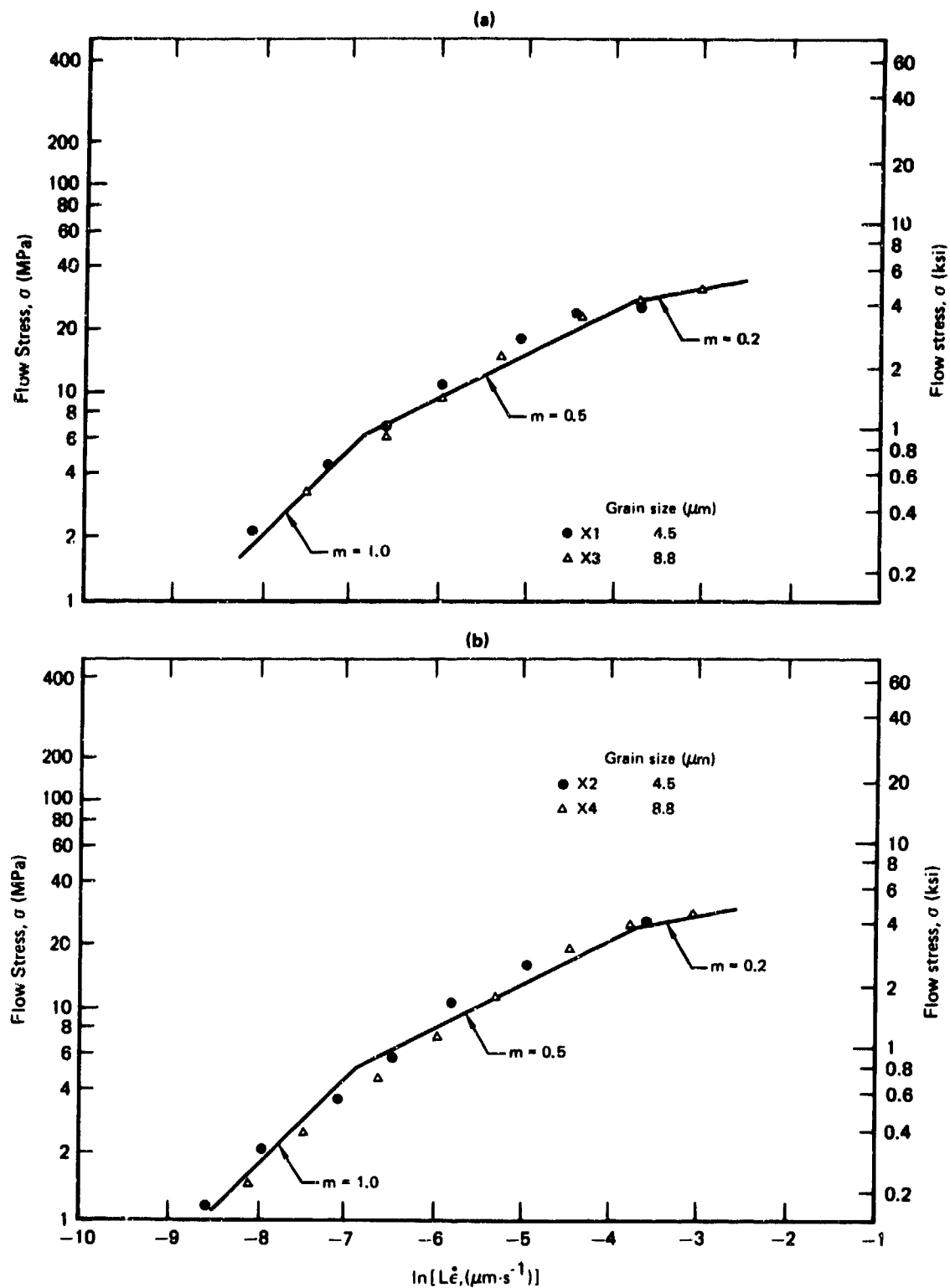


Figure 79. Flow stress as a function of \ln (strain rate \times grain size) at 850°C (1560°F) in ELI-grade Ti-6Al-4V; (a) volume % primary alpha = 88 and (b) volume % primary alpha = 48.



GP03-0249-58

Figure 80. Flow stress as a function of \ln (strain rate x grain size) at 875°C (1605°F) in ELI-grade Ti-6Al-4V; (a) volume % primary alpha = 88 and (b) volume % primary alpha = 46.



GP03-0248-50

Figure 81. Flow stress as a function of $\ln (\dot{\epsilon} \times \text{grain size})$ at 907°C (1665°F) in ELI-grade Ti-6Al-4V; (a) volume % primary $\alpha = 88$ and (b) volume % primary $\alpha = 48$.

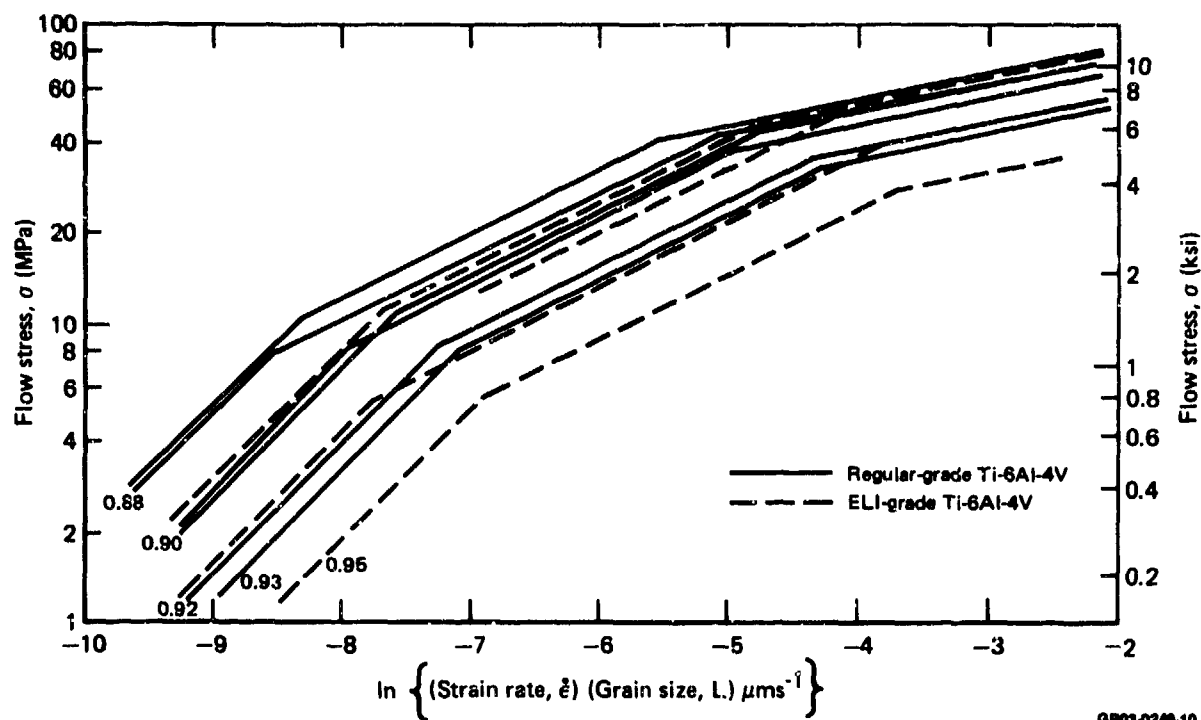


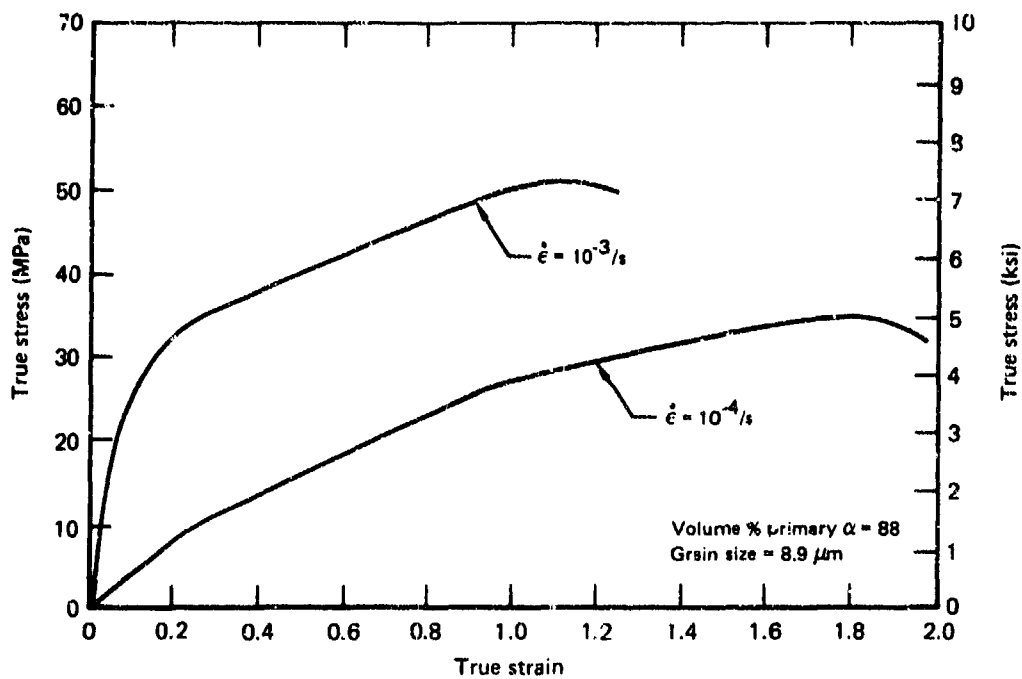
Figure 82. Flow stress as a function of \ln (strain rate \times grain size) at different fractions of beta-transus-temperature for regular-grade Ti-6Al-4V and ELI-grade Ti-6Al-4V.

Ti-6Al-4V. Any other effects of interstitial oxygen concentration on the flow-stress/strain-rate behavior at superplastic-forming temperatures are negligible. Since the plots shown in Figure 82 are normalized with respect to grain size and temperature, they can be used to obtain superplasticity parameters for a given alloy at any desired temperature.

To determine the influence of grain growth on flow stress during testing, the strain dependence of flow stress and the grain size variation with time in the deformed and grip sections of ELI-grade Ti-6Al-4V (Specimen X3) were measured at 875°C (1607°F). The stress-strain behavior determined from constant-strain-rate tests is shown in Figure 83, and the average of the alpha and beta grain sizes as a function of time is shown in Figure 84. Assuming a linear dependence of flow stress on grain size at a given strain rate, Figure 85 shows the flow-stress/strain behavior of Specimen X3 corrected for grain growth during testing. The variation of grain-growth-compensated flow-stress, σ/L , with strain, where L is the instantaneous grain size, indicates that there is an apparent strain hardening beyond that caused by grain growth at superplastic temperatures which should be taken into account when using laboratory flow-stress data in superplastic-forming calculations. The variations of strain and strain-rate with time determined from constant-stress tests for ELI-grade Ti-6Al-4V at 875°C (1590°F) are shown in Figure 86.

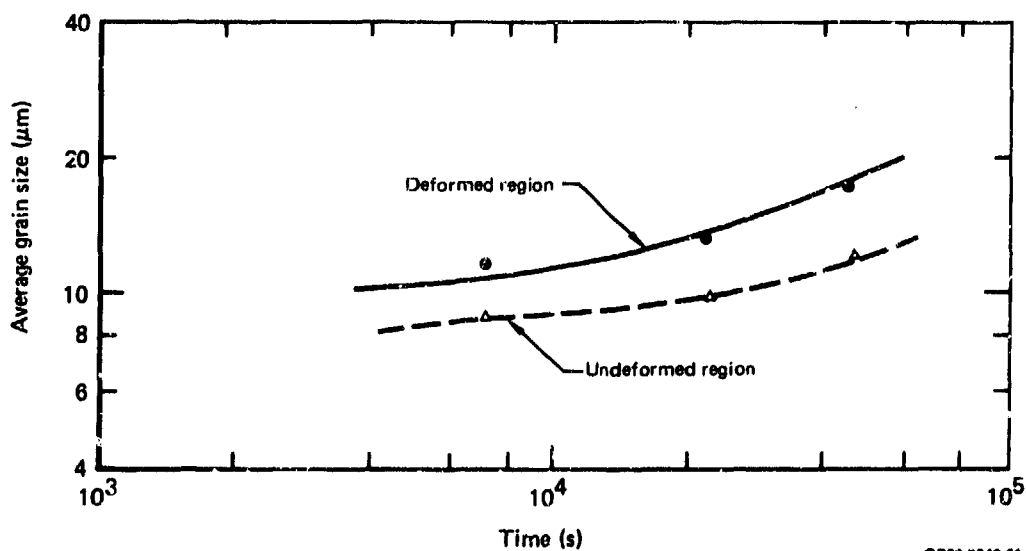
4.3 Regular-Grade Ti-6Al-4V with Elongated Alpha, Blocky Alpha, Banding, and Transverse-Basal Texture and Coil Rolled Ti-6Al-4V

Special processing schedules involved in the production of different grades of Ti-6Al-4V result in microstructures significantly different from that of regular-grade Ti-6Al-4V. The effects of such process variations on the strain-rate dependence of flow stress are shown in Figures 87 through 94 and the important superplastic parameters are listed in Tables 21-23. The superplastic characteristics of specially processed Ti-6Al-4V are compared with that of regular grade Ti-6Al-4V in Figure 95. The superplastic parameters of blocky-alpha and banded microstructures are similar to those of regular-grade Ti-6Al-4V, but the coil-rolled Ti-6Al-4V, elongated-alpha Ti-6Al-4V, and transverse-basal-textured Ti-6Al-4V have significantly higher



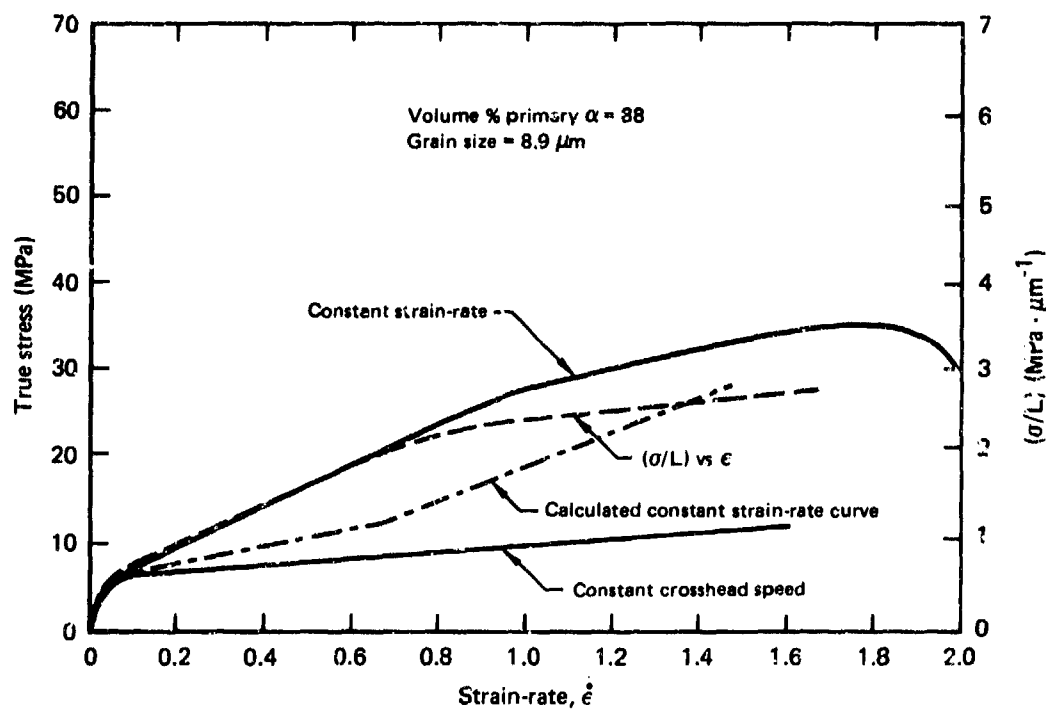
GP03-0240-00

Figure 83. True-stress as a function of true-strain for ELI-grade Ti-6Al-4V at 875°C (1605°F) determined from constant strain-rate tensile tests.



GP03-0240-01

Figure 84. Variation of grain size with time in deformed and undeformed regions of ELI-grade Ti-6Al-4V during superplastic testing at 875°C (1605°F).



GP03-0248-82

Figure 85. True-stress as a function of true-strain for ELI-grade Ti-6Al-4V at 875°C (1605°F) determined from constant strain-rate tests and constant crosshead speed tests.

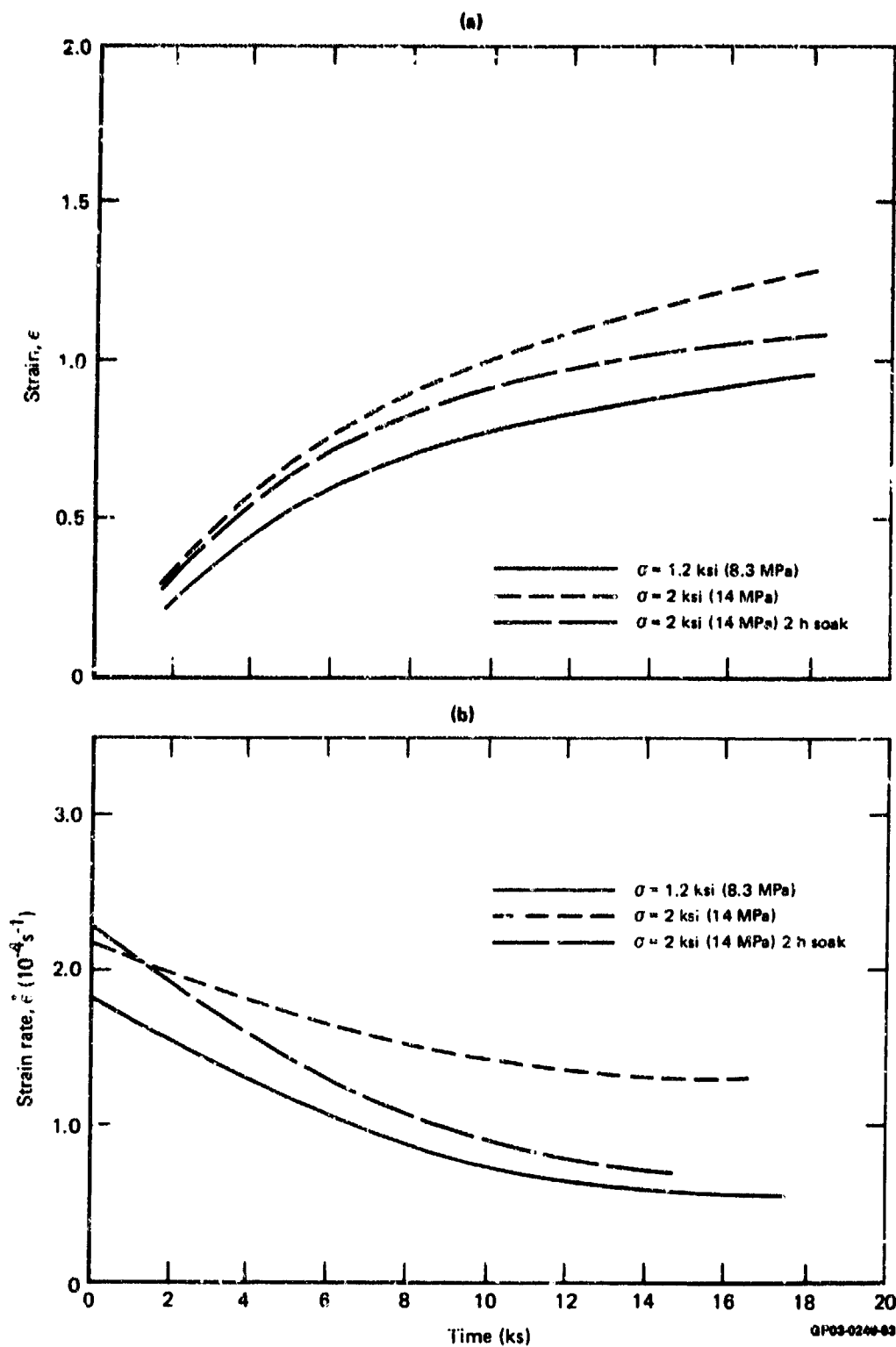
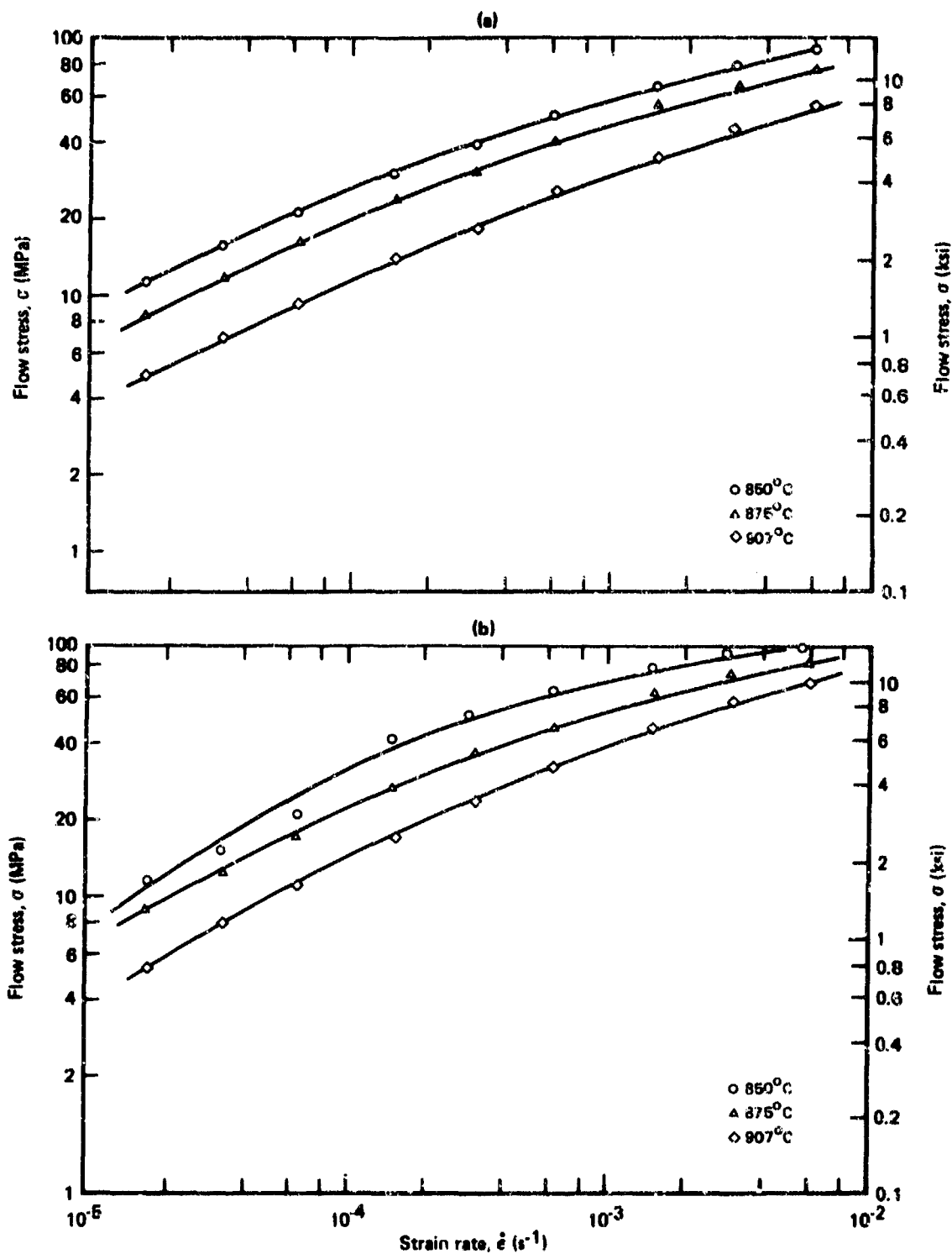


Figure 88. Variation of (a) strain and (b) strain rate with time determined from constant-stress tests for ELI-grade Ti-6Al-4V (volume % primary α = 88, grain size = $5.5 \mu\text{m}$, sample X1) at 875°C (1605°F).



OP03-0210-71

Figure 87. Effect of orientation on strain-rate dependence of flow stress in transverse-basal-textured Ti-6Al-4V (specimen T1); (a) stress direction parallel to rolling direction and (b) stress direction parallel to transverse direction.

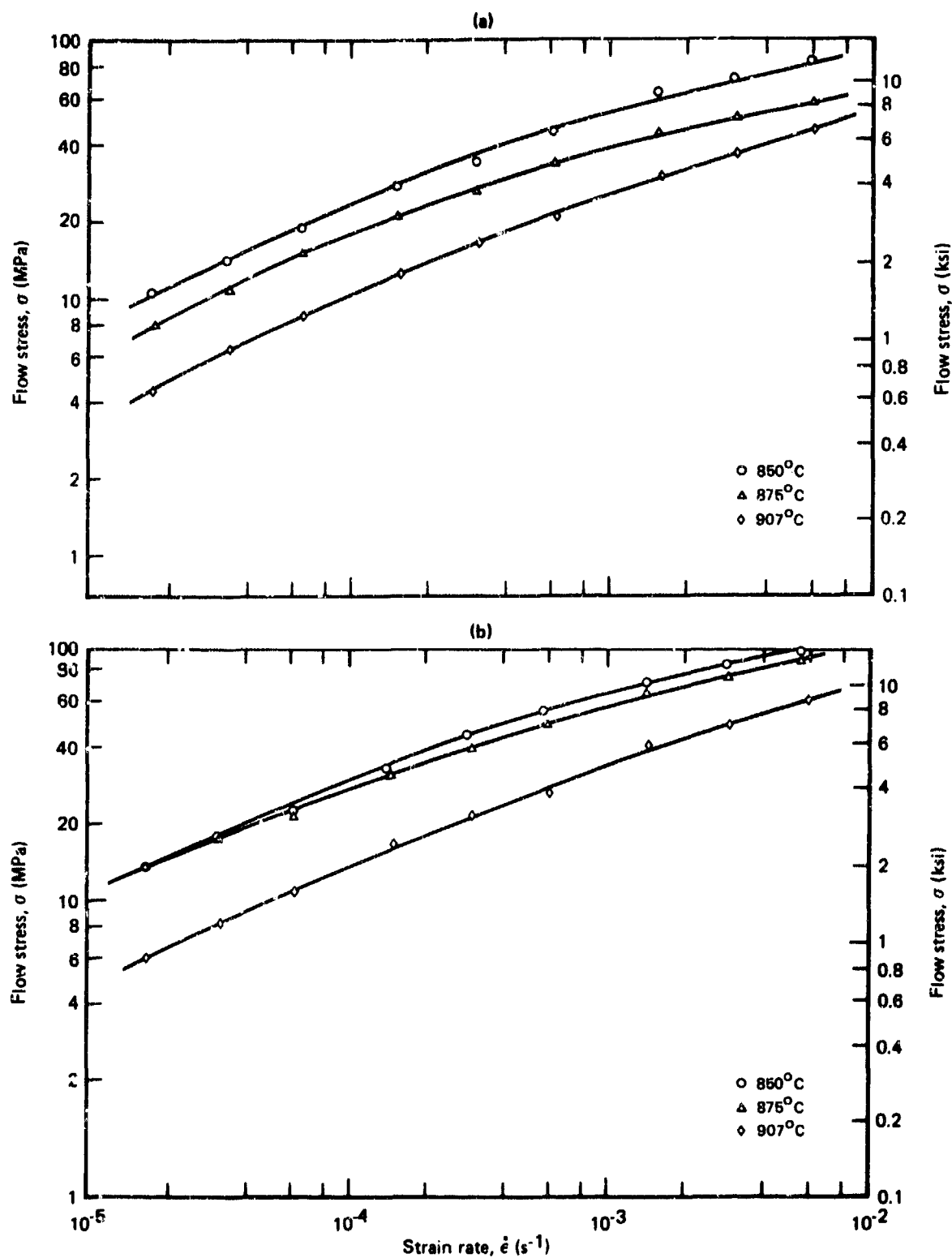


Figure 88. Effect of elongated alpha on strain-rate dependence of flow stress in Ti-6Al-4V; (a) specimen M and (b) specimen M1.

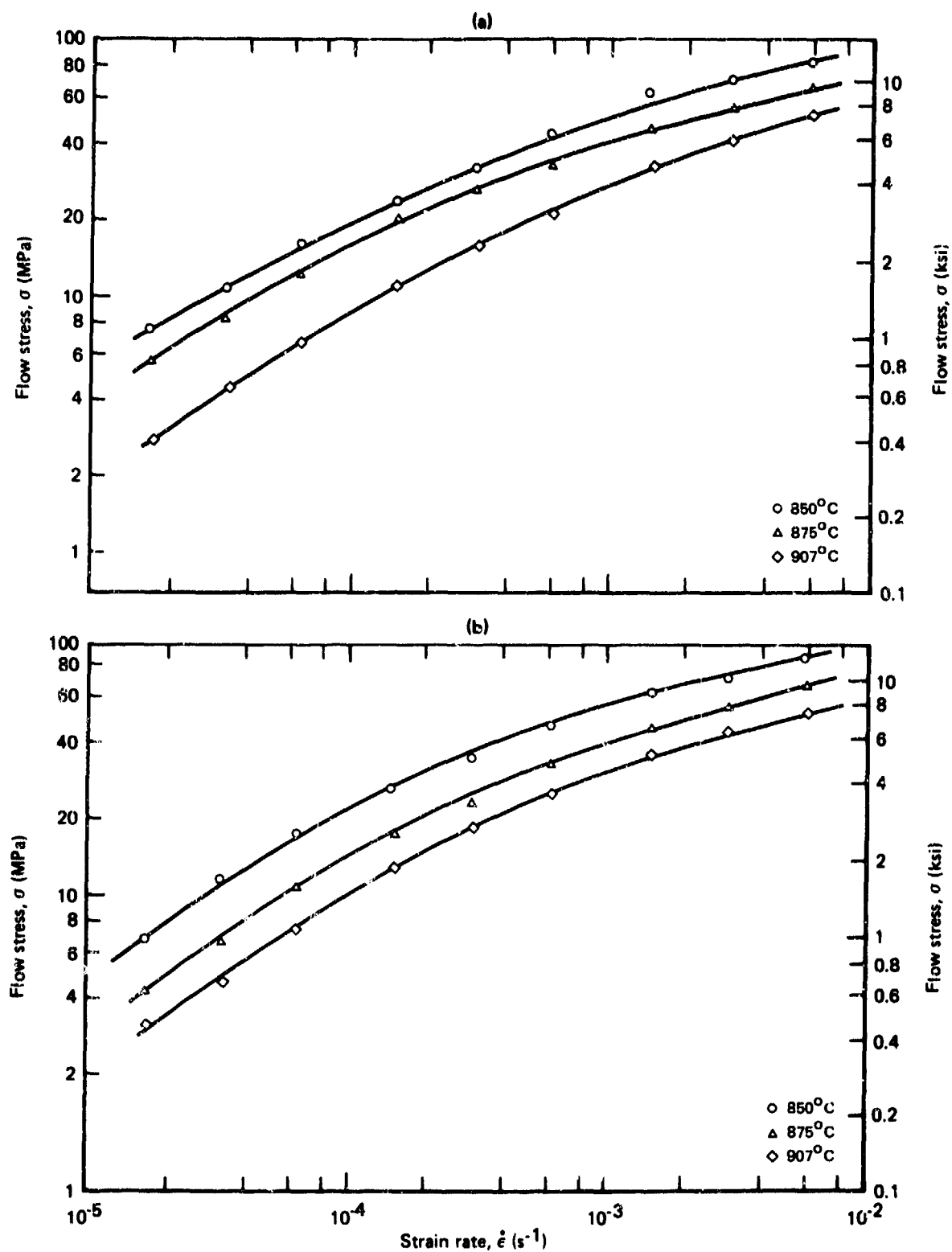
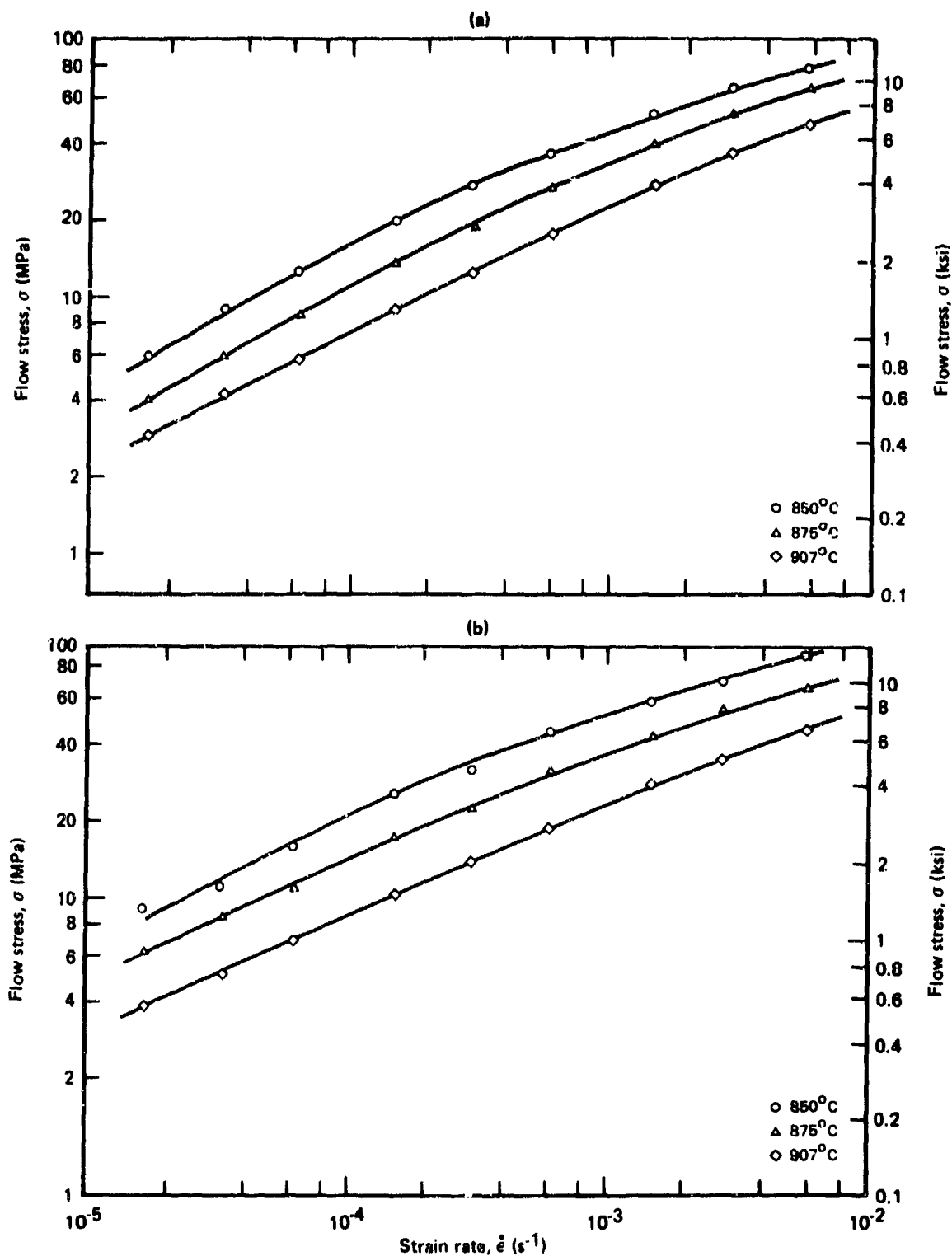


Figure 89. Effect of blocky alpha on strain-rate dependence of flow stress in Ti-6Al-4V; (a) specimen N and (b) specimen N1.



GP03-0248-00

Figure 90. Effect of banding on strain-rate dependence of flow stress in Ti-6Al-4V;
(a) specimen O and (b) specimen O1.

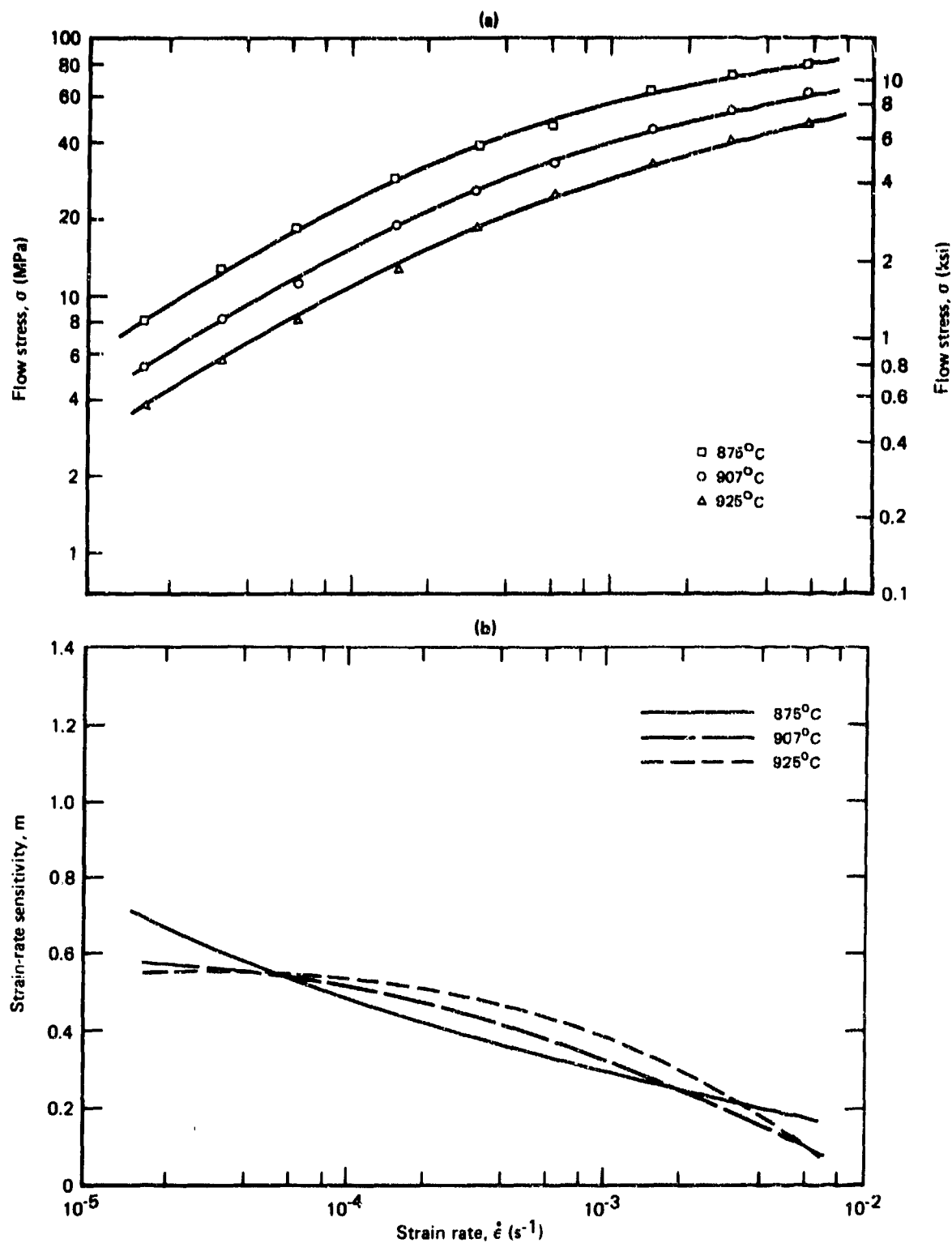
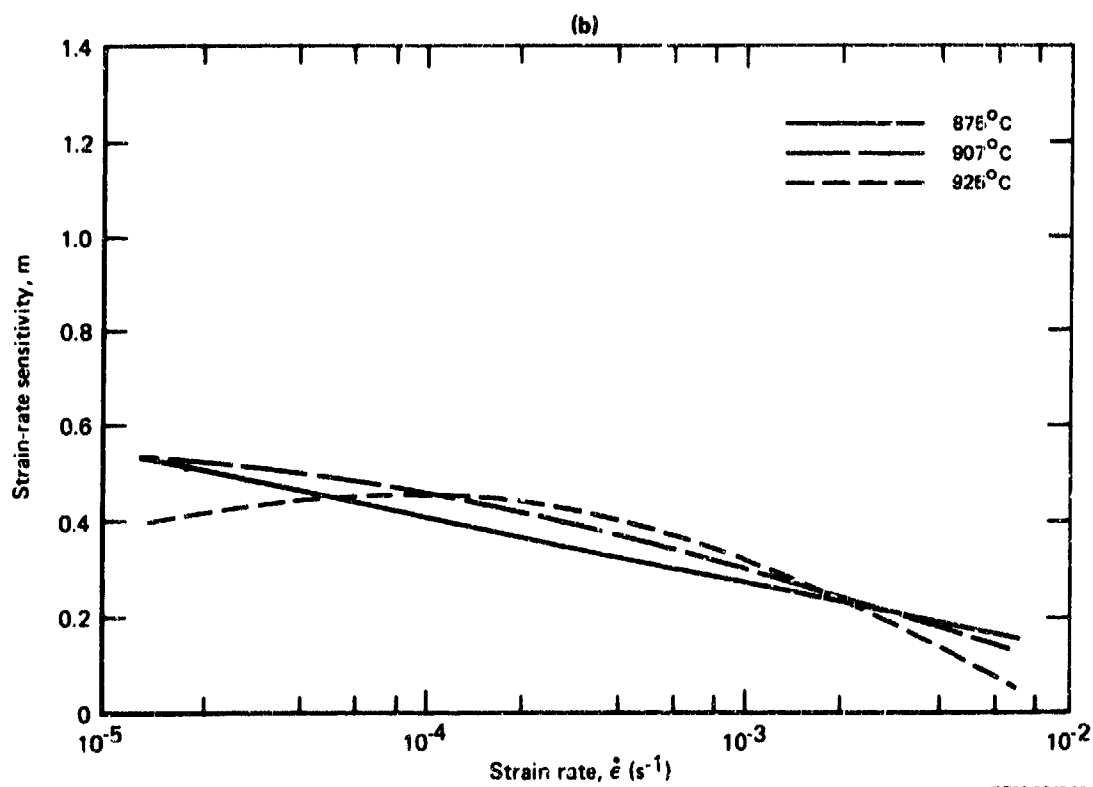
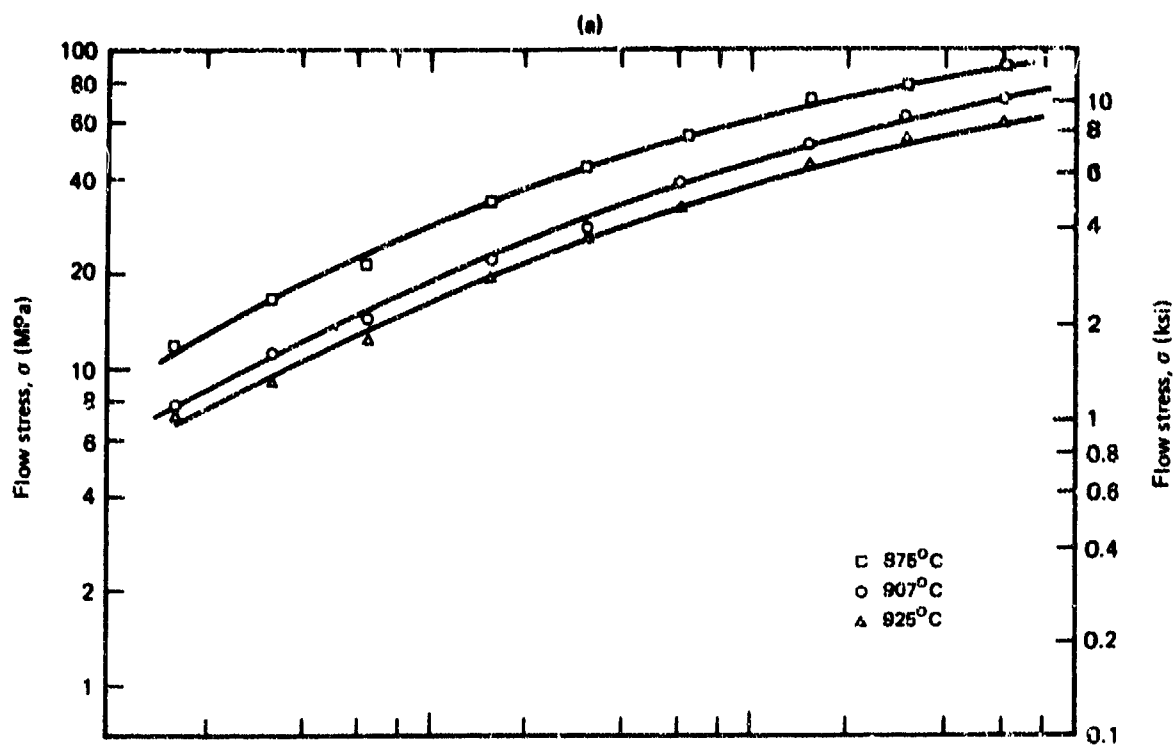


Figure 91. Strain-rate dependence of (a) flow stress and (b) strain-rate sensitivity for coil-rolled Ti-6Al-4V sample S4 (volume % primary α = 63, grain size = 9.3 μm).



GP03-0240-06

Figure 92. Strain-rate dependence of (a) flow stress and (b) strain-rate sensitivity for coil-rolled Ti-6Al-4V sample S3 (volume % primary α = 87, grain size = 4.4 μm).

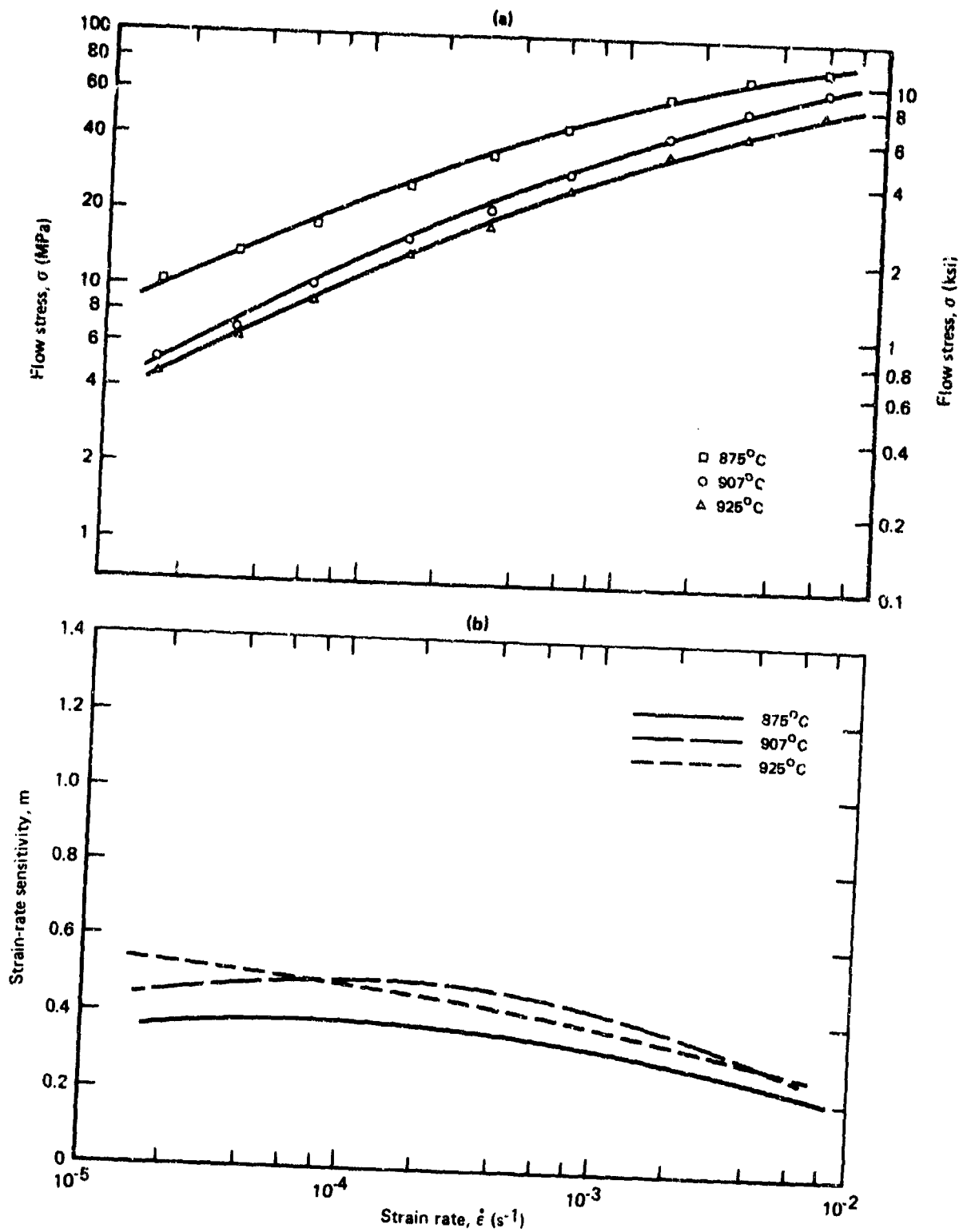


Figure 93. Strain-rate dependence of (a) flow stress and (b) strain-rate sensitivity for coil-rolled Ti-6Al-4V sample S2 (volume % primary alpha = 63, grain size = 4.4 μm).

GP03-0249-85

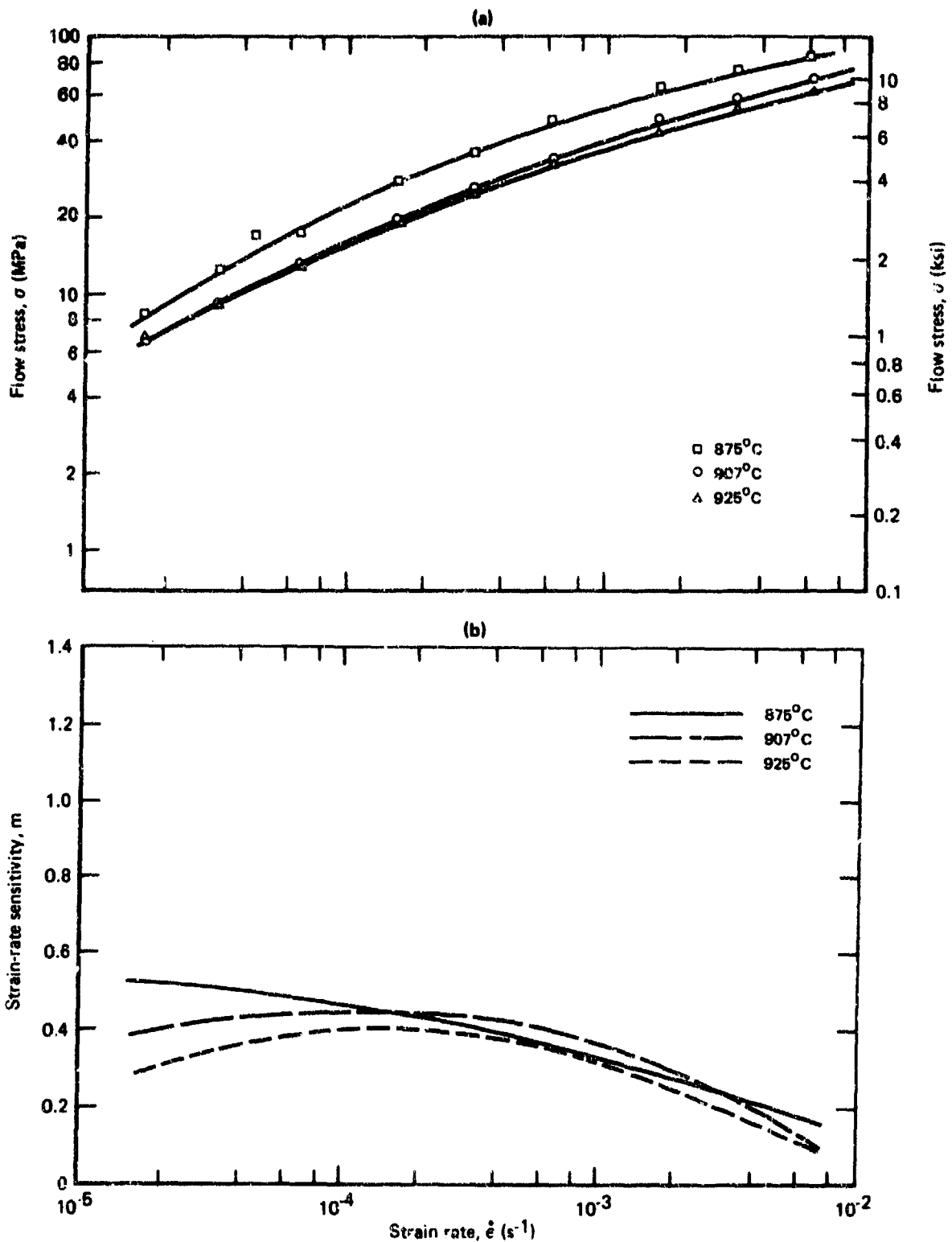


Figure 94. Strain-rate dependence of (a) flow stress and (b) strain-rate sensitivity for coil-rolled Ti-6Al-4V sample S1 (volume % primary α = 87, grain size = 5.1 μm).

TABLE 21. RESULTS OF STRAIN-RATE-CYCLING TESTS ON Ti-6Al-4V WITH ANOMALOUS MICROSTRUCTURES AND TEXTURE TEMPERATURE = 850°C (1562°F).

Sample	Microstructure anomaly	Maximum m (m)	Flow stress at maximum m (MPa (ksi))	Flow stress at $\dot{\epsilon} = 10^{-4} s^{-1}$ (MPa (ksi))	Flow stress at $\dot{\epsilon} = 10^{-3} s^{-1}$ (MPa (ksi))	Strain rate at maximum m ($10^{-5} s^{-1}$)	Strain rate at $m = 0.5$ ($10^{-5} s^{-1}$)
O	Banding	0.57	5.9 (0.86)	17.9 (2.6)	46.9 (6.8)	1.64	12.3
G1	Banding	0.46	9.3 (1.35)	—	56.6 (8.2)	1.64	—
N	Blocky α	0.61	7.6 (1.1)	20.7 (3.0)	57.9 (8.4)	1.64	9.6
N1	Blocky α	0.66	8.3 (1.2)	23.5 (3.4)	60.7 (8.8)	1.74	9.6
M	Elongated α	0.49	11.04 (1.6)	—	56.6 (8.2)	1.64	—
M1	Elongated α	0.46	13.8 (2.0)	—	69.0 (10.0)	1.64	—
T1L	Transverse-basal texture, longitudinal direction	0.49	11.0 (1.6)	—	63.5 (9.2)	1.64	—
T1T	Transverse-basal texture, transverse direction	0.54	11.7 (1.7)	16.6 (2.4)	82.8 (12.0)	1.60	3.5

GP00-0208-7

TABLE 22. RESULTS OF STRAIN-RATE-CYCLING TESTS ON Ti-6Al-4V WITH ANOMALOUS MICROSTRUCTURES AND TEXTURE TEMPERATURE = 875°C (1607°F).

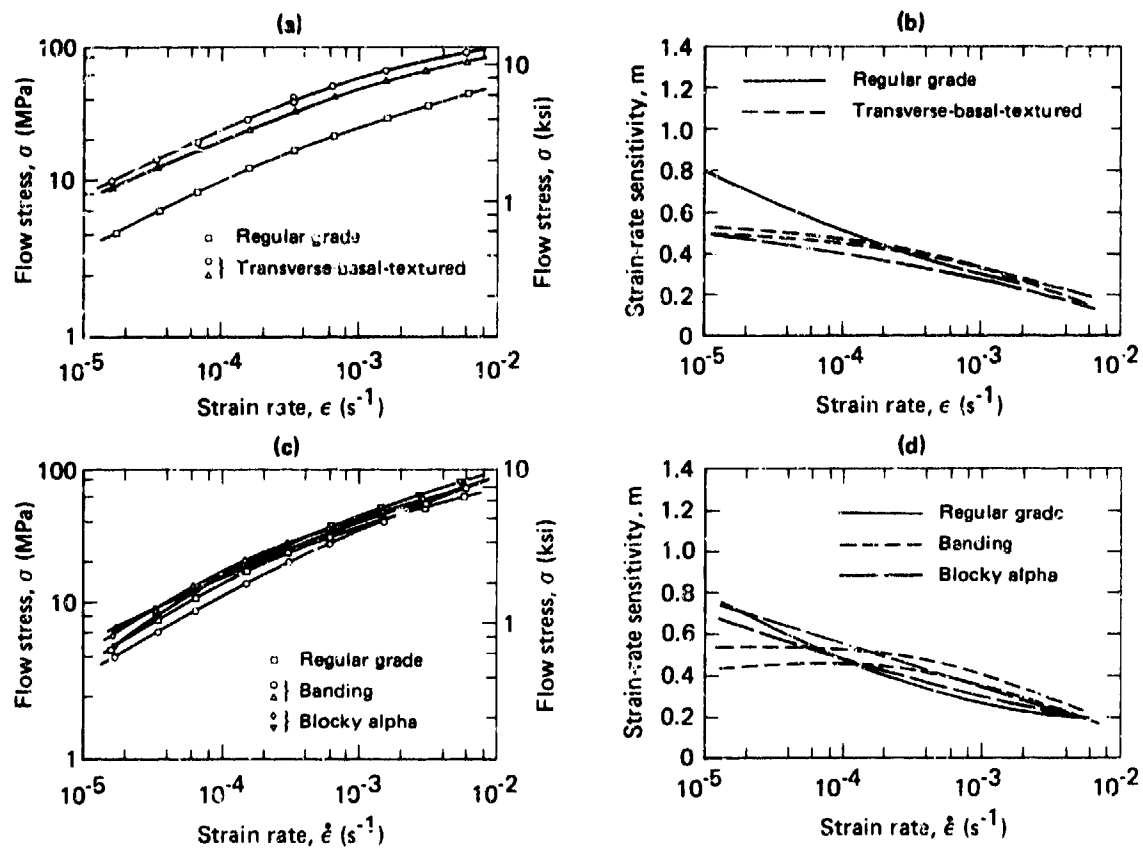
Sample	Microstructure anomaly	Maximum m (m)	Flow stress at maximum m [MPa (ksi)]	Flow stress at $\dot{\epsilon} = 10^{-5} s^{-1}$ [MPa (ksi)]	Flow stress at $\dot{\epsilon} = 10^{-4} s^{-1}$ [MPa (ksi)]	Flow stress at $\dot{\epsilon} = 10^{-3} s^{-1}$ [MPa (ksi)]	Strain rate at maximum m ($10^{-5} s^{-1}$)	Strain rate at $m = 0.5$ ($10^{-5} s^{-1}$)
O	Banding	0.54	4.1 (0.6)	22.1 (3.2)	10.7 (1.55)	33.12 (4.8)	1.7	43.0
O1	Banding	0.47	6.5 (0.94)	—	14.5 (2.1)	40.0 (5.8)	12.3	—
N	Blocky α	0.64	5.6 (0.82)	16.2 (2.35)	16.6 (2.4)	42.8 (6.2)	1.6	9.6
N1	Blocky α	0.73	4.4 (0.64)	22.1 (3.2)	16.6 (2.4)	44.2 (6.4)	1.6	20.3
M	Elongated α	0.48	8.3 (1.2)	—	19.3 (2.8)	42.8 (6.2)	1.6	—
M1	Elongated α	0.39	13.8 (2.0)	—	26.9 (3.9)	56.6 (8.2)	1.6	—
T1L	Transverse-basal texture, longitudinal direction	0.47	8.3 (1.2)	—	20.01 (2.9)	51.1 (7.4)	1.6	—
T1T	Transverse-basal texture, transverse direction	0.51	6.9 (1.3)	14.5 (2.1)	22.1 (3.2)	58.7 (8.5)	1.64	4.5

0000-0000-0

TABLE 23. RESULTS OF STRAIN-RATE-CYCLING TESTS ON Ti-6Al-4V WITH ANOMALOUS MICROSTRUCTURES AND TEXTURE TEMPERATURE = 907°C (1665°F).

Sample	Microstructure anomaly	Maximum m (m)	Flow stress at maximum m [MPa (ksi)]	Flow stress at $\dot{\epsilon} = 0.5$ [MPa (ksi)]	Flow stress at $\dot{\epsilon} = 10^{-4} s^{-1}$ [MPa (ksi)]	Flow stress at $\dot{\epsilon} = 10^{-3} s^{-1}$ [MPa (ksi)]	Strain rate at maximum m ($10^{-5} s^{-1}$)	Strain rate at $m = 0.5$ ($10^{-5} s^{-1}$)
O	Banding	0.52	6.2 (0.9)	18.0 (2.6)	7.2 (1.05)	24.1 (3.5)	12.3	33.0
O1	Randing	0.49	4.1 (0.6)	—	9.7 (1.4)	24.1 (3.5)	1.7	—
N	Blocky α	0.67	2.8 (0.40)	19.3 (2.8)	8.3 (1.2)	29.0 (4.2)	1.7	43.0
N1	Blocky α	0.70	3.3 (0.48)	21.4 (3.1)	11.0 (1.6)	33.1 (4.8)	1.7	33.0
M	Elongated α	0.48	4.6 (0.67)	—	11.0 (1.6)	28.3 (4.1)	1.7	—
M1	Elongated α	0.52	5.8 (0.85)	7.6 (1.1)	13.8 (2.0)	35.9 (5.2)	1.7	2.7
T1L	Transverse-basal texture, longitudinal direction	0.49	5.0 (0.73)	—	12.4 (1.8)	33.8 (4.9)	1.6	—
T1T	Transverse-basal texture, transverse direction	0.55	5.5 (0.79)	20.7 (3.0)	14.5 (2.1)	41.4 (6.0)	1.5	12.0

GP03-0246-9



GP03-0249-72

Figure 95. Effects of microstructural anomalies on strain-rate dependence of (a) and (c) flow stress, and (b) and (d) strain-rate sensitivity of Ti-6Al-4V at 850°C (1562°F).

flow stresses and lower strain-rate sensitivities than regular-grade Ti-6Al-4V. Although the blocky-alpha Ti-6Al-4V consists of a high volume-fraction of coarse alpha grains, the low flow-stress values and high m -values of this alloy apparently result from a fine-grain microstructure present between coarse alpha grains.

Banding in Ti-6Al-4V should adversely affect superplastic characteristics because of the presence of lightly-worked Widmanstätten alpha. The absence of any such effect in the alloys investigated in this study is probably due to the low levels of Widmanstätten alpha in these alloys.

Although the coil-rolled Ti-6Al-4V has an equiaxed microstructure with the average alpha and beta grain sizes similar to those in regular-grade Ti-6Al-4V, the large disparity between the grain sizes of the individual phases lead to higher flow stresses and lower strain-rate-sensitivity values.

The inferior superplastic characteristics of elongated-alpha Ti-6Al-4V are as expected from the long Widmanstätten alpha-beta plates, which render grain boundary sliding extremely difficult because of the long diffusion distances involved in flow accommodation processes.

The higher flow stress and lower strain-rate sensitivity of transverse-basal-textured Ti-6Al-4V are probably due to the undesirable microstructures resulting from the processing rather than a direct effect of the texture.

The effects of various microstructural anomalies on the strain rate at 906°C (1663°F) at a stress of 8.4 MPa (1.2 ksi) are shown in Figure 96. The strain rate for banding and blocky-alpha microstructures is comparable to that of regular-grade Ti-6Al-4V, but the strain rates of transverse-basal-textured and elongated-alpha microstructures are as much as an order of magnitude lower than that of regular-grade Ti-6Al-4V.

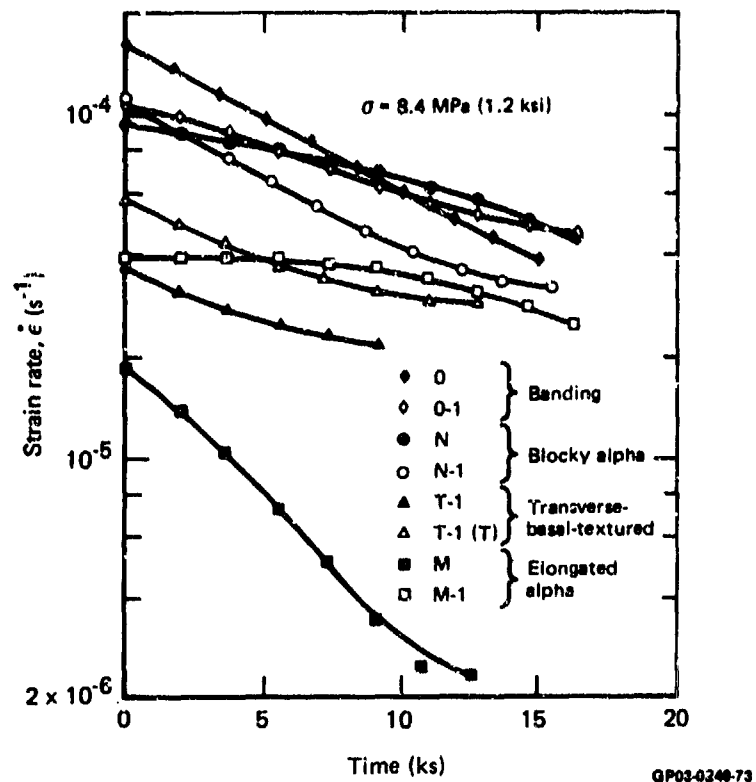


Figure 96. Effects of microstructural anomalies on strain rate of Ti-6Al-4V at 907°C (1665°F) determined from constant-stress tests.

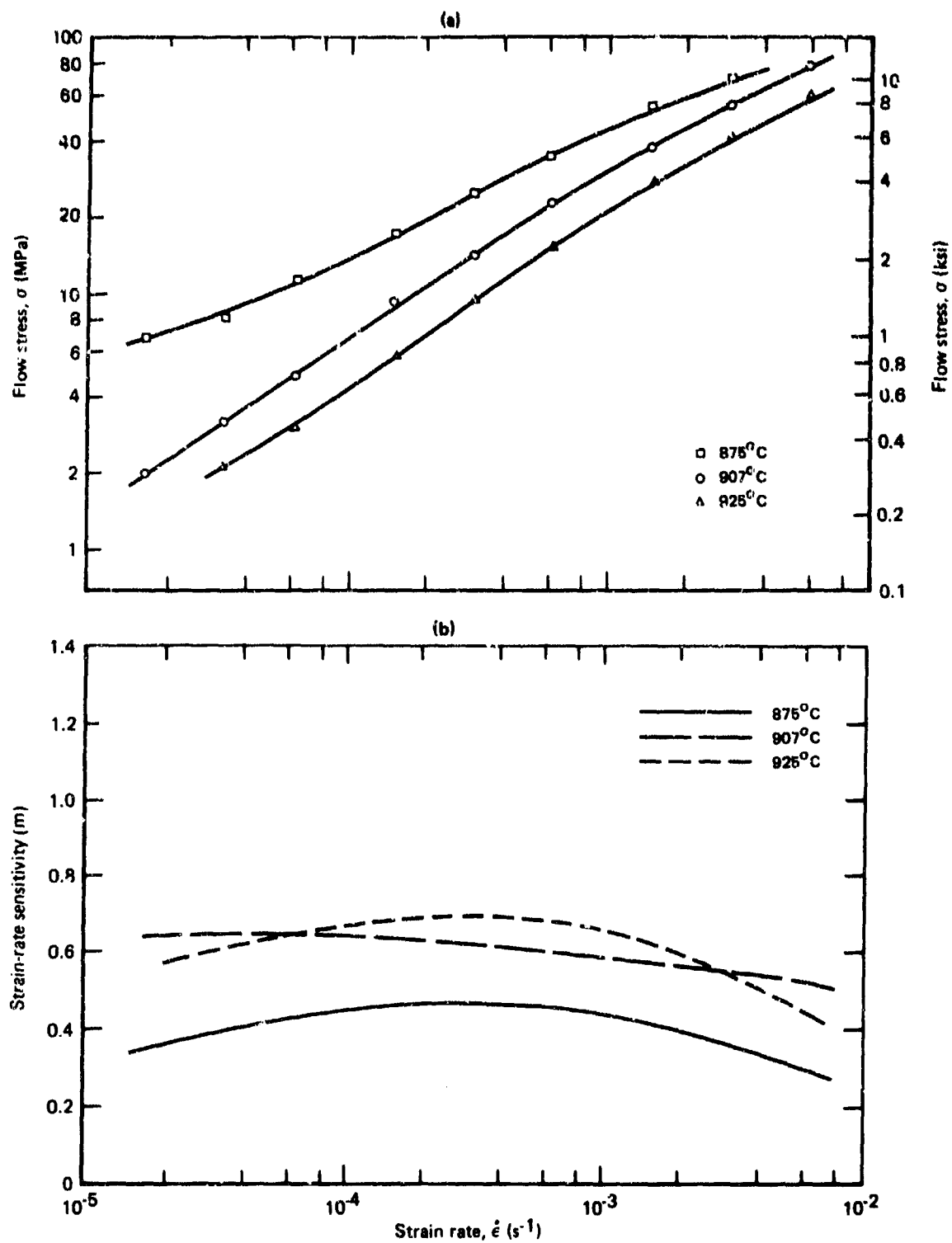
Thus, among the common microstructural anomalies encountered in Ti-6Al-4V, elongated alpha adversely affects the superplastic formability whereas blocky alpha and banding have no significant effect on superplasticity.

4.4 Ti-6Al-2Sn-4Zr-2Mo ($T_{\beta} = 993^{\circ}\text{C}$)

The strain-rate dependences at 875°C (1607°F), 906°C (1663°F), and 925°C (1697°F) of flow stress and strain-rate sensitivity of different microstructural variations of the super-alpha alloy, Ti-6Al-2Sn-4Zr-2Mo, are shown in Figures 97 through 100. Flow stresses are slightly higher and strain-rate sensitivities are lower than for regular-grade Ti-6Al-4V. In contrast with the weak dependence of flow stress on volume fraction of primary alpha in Ti-6Al-4V, the flow stress of Ti-6Al-2Sn-4Zr-2Mo alloy increases with increasing volume fraction of primary alpha. The higher flow stress in the alpha-rich alloy arises from the solid-solution effect of Al, Sn, and Zr, and the dependence on volume fraction of primary alpha arises from narrower alpha + beta region in the Ti-6Al-2Sn-4Zr-2Mo alloy. Whereas in regular grade Ti-6Al-4V, because of the faster diffusion of V, the equilibrium volume fractions are attained at relatively short times and hence the effect of initial volume-fraction of alpha on high-temperature flow stress is negligible, the slower diffusivity of Mo in the super-alpha alloy leads to longer times for equilibration and, consequently, dominance of the effect of initial primary-alpha content on flow stress. At any temperature, the equilibrium volume-fraction of primary alpha is higher in Ti-6Al-2Sn-4Zr-2Mo than in Ti-6Al-4V. The alpha alloy, although it does not have as high a strain-rate sensitivity of flow stress as Ti-6Al-4V, has m values greater than 0.5 over a wider range of strain rates. Nevertheless, at 875°C (1607°F) the superplasticity of the super-alpha alloy is only marginal, whereas fine grained Ti-6Al-4V exhibits excellent superplasticity. For realizing superplasticity comparable to that of Ti-6Al-4V for equivalent grain sizes in Ti-6Al-2Sn-4Zr-2Mo, the temperature must be approximately 25°C (45°F) higher for the super alpha alloy.

4.5 Ti-8Al-1Mo-1V ($T_{\beta} = 1032^{\circ}\text{C}$)

Incremental-strain-rate tests at 870 - 980°C (1600 - 1800°F), for T/T_{β} ratios of 0.84 - 0.95 , were conducted on two heats of Ti-8Al-1Mo-1V with gage thicknesses of 1.14 - 1.27 mm. All tests were with the tensile axis parallel to the rolling direction of the sheets. The strain-rate dependences of flow stress and strain-rate-sensitivity are shown in Figure 101. For a given strain rate, the flow stress is considerably higher for Ti-8Al-1Mo-1V than for Ti-6Al-4V at the same temperature. However, at constant T/T_{β} , where T is the test temperature and T_{β} is the beta-transus temperature, the variation of flow stress with strain rate is identical for the two alloys. Above 870°C (1600°F), the strain-rate dependence of the



QP03-0249-74

Figure 97. Strain-rate dependence of (a) flow stress and (b) strain-rate sensitivity for Ti-6Al-2Sn-4Zr-2Mo sample Q1 (volume % primary α = 90, grain size = 3.5 μm).

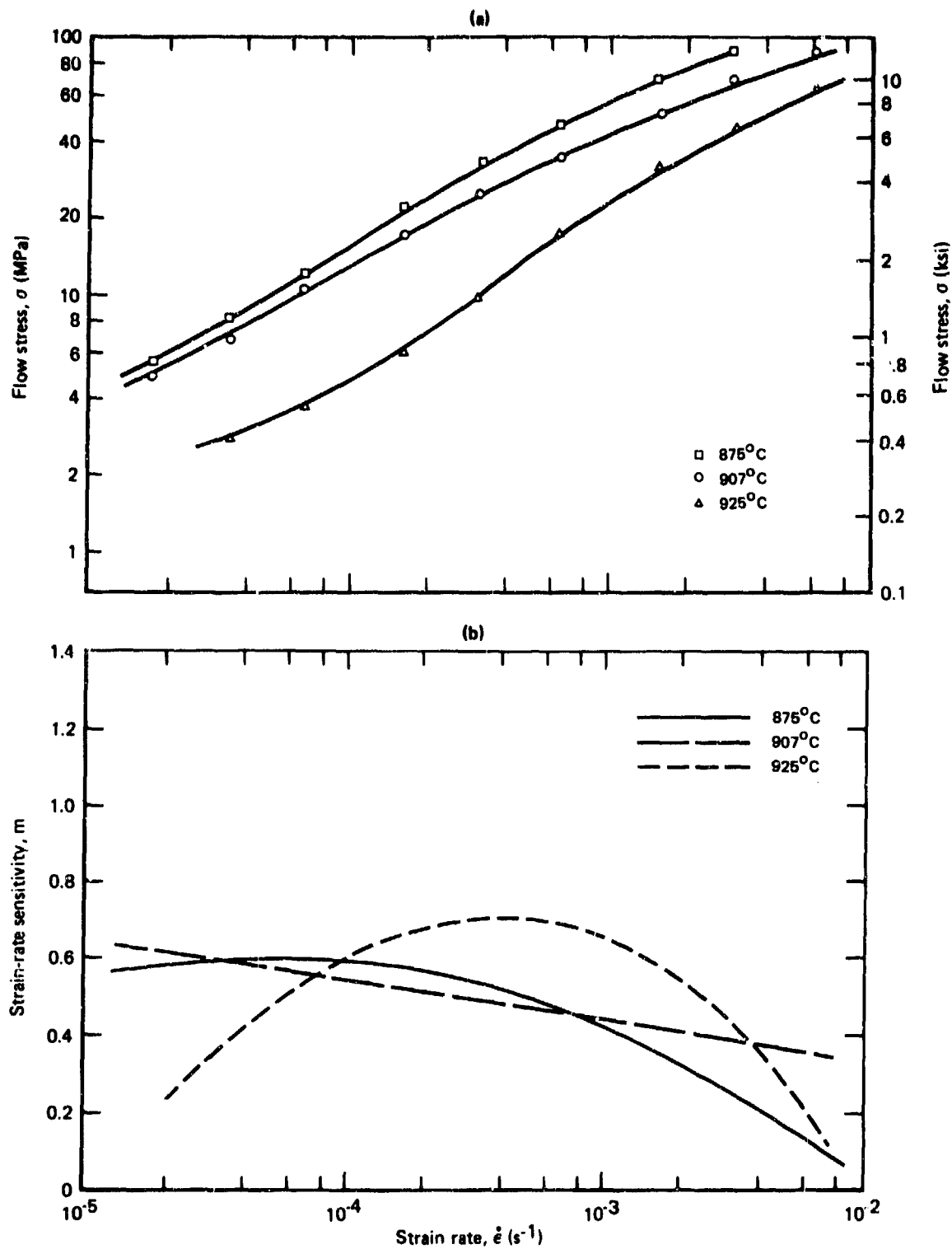


Figure 98. Strain-rate dependence of (a) flow stress and (b) strain-rate sensitivity for Ti-6Al-2Sn-4Zr-2Mo sample Q2 (volume % primary alpha = 65, grain size = 3.4 μm).

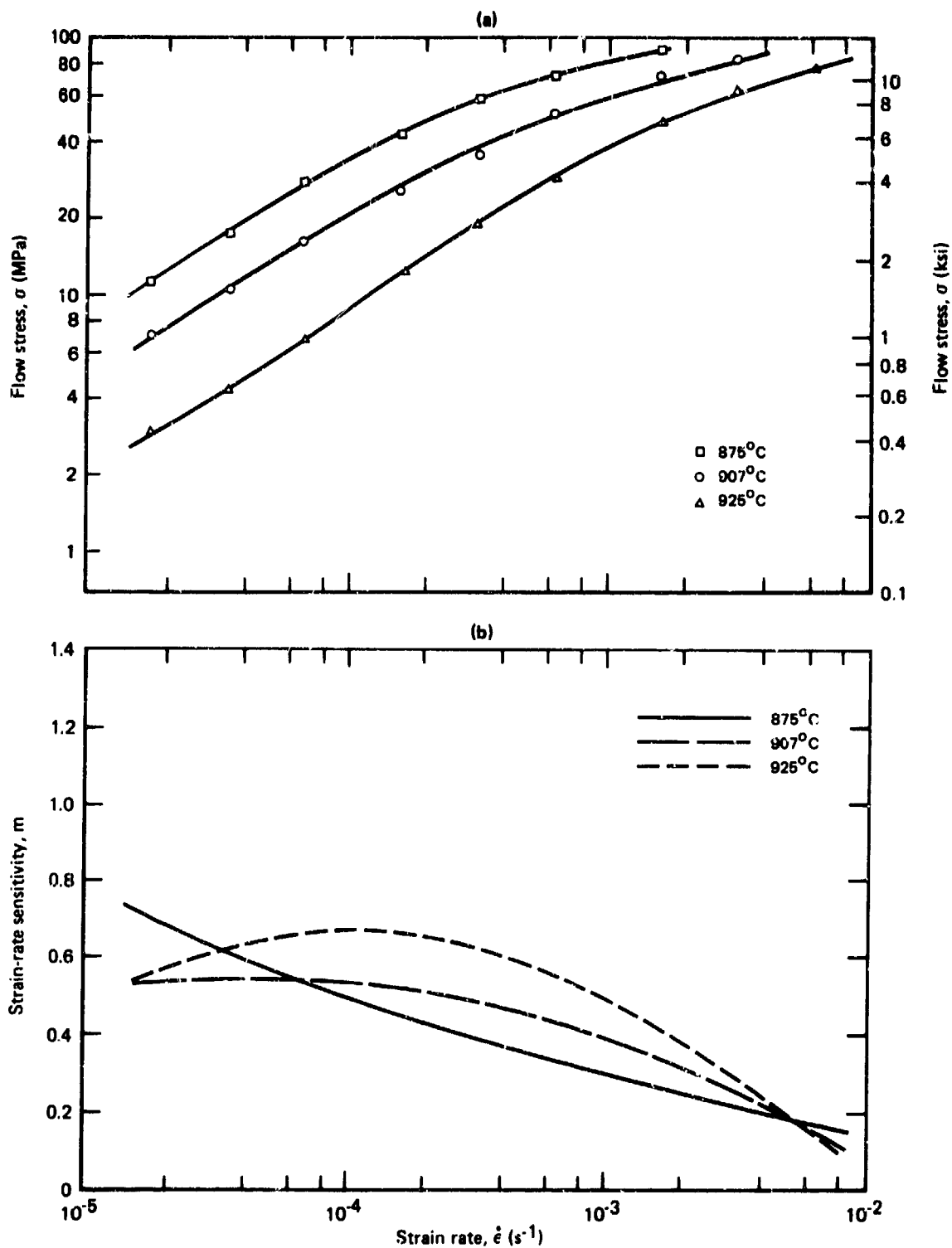


Figure 99. Strain-rate dependence of (a) flow stress and (b) strain-rate sensitivity for Ti-6Al-2Sn-4Zr-2Mo sample Q3 (volume % primary alpha = 86, grain size = 8.2 μm).

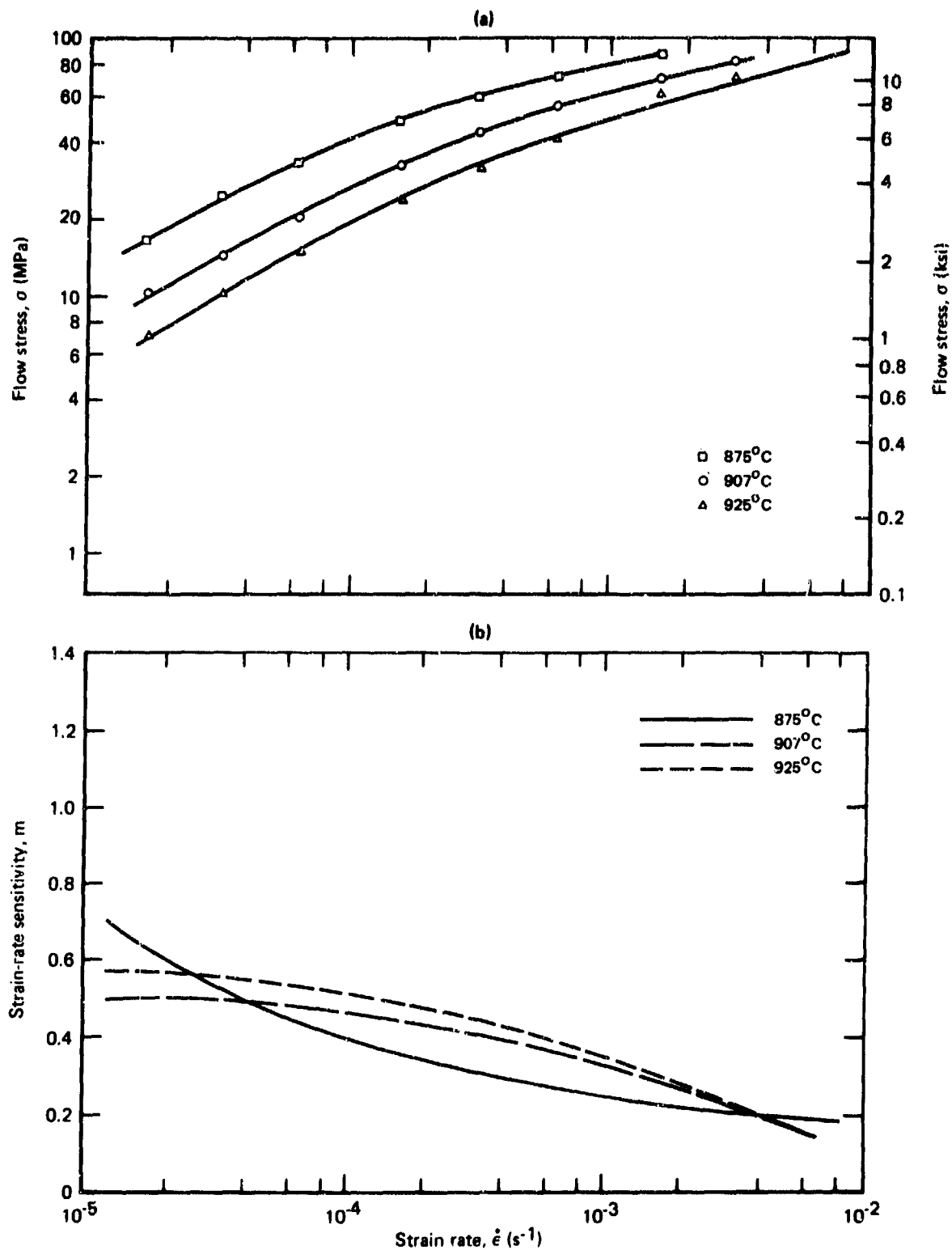
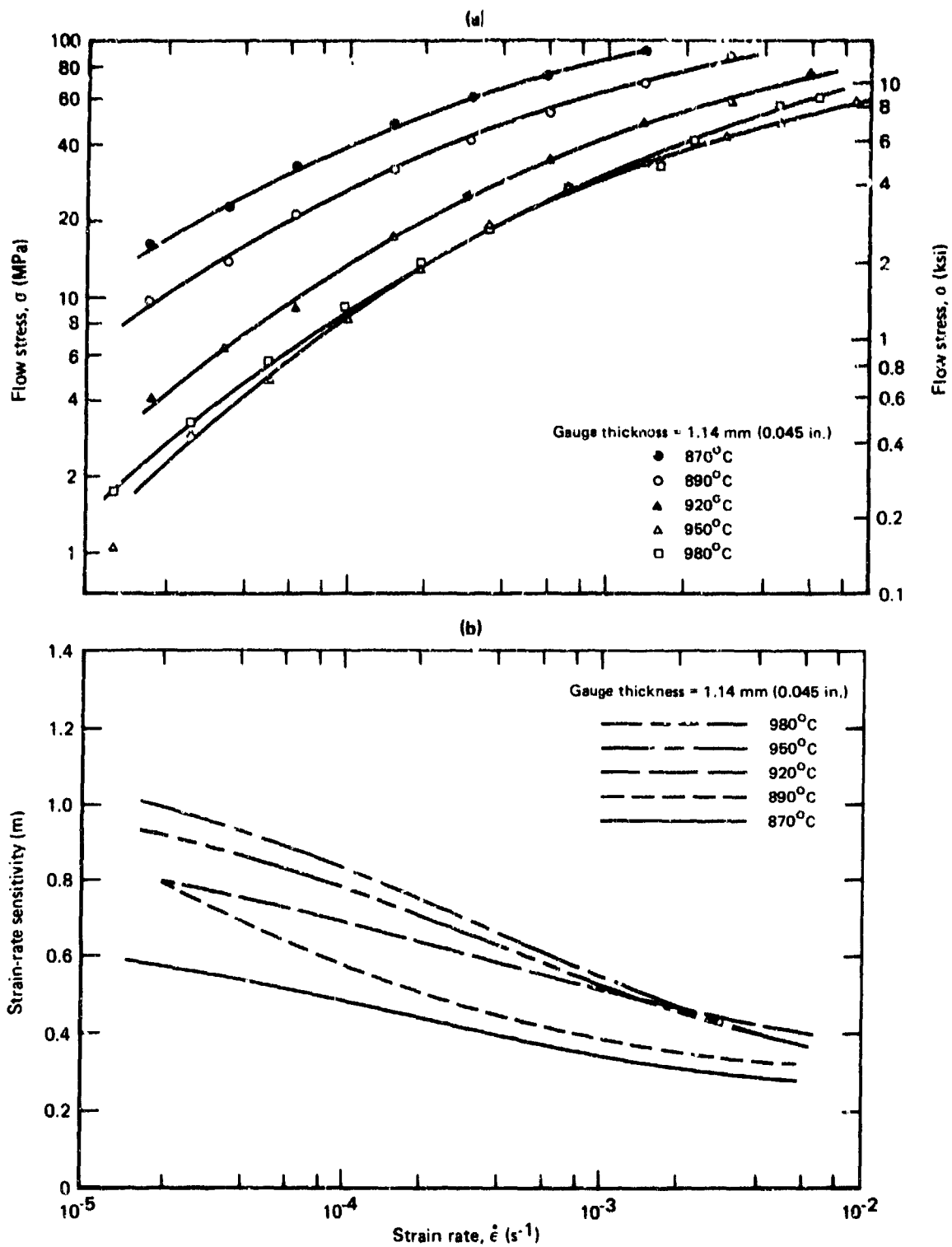


Figure 100. Strain-rate dependence of (a) flow stress and (b) strain-rate sensitivity for Ti-6Al-2Sn-4Zr-2Mo sample Q4 (volume % primary alpha = 55, grain size = 8.8 μm).



GP03-0248-78

Figure 101. Strain-rate dependence of (a) flow stress and (b) strain-rate sensitivity for Ti-8Al-1Mo-1V.

strain-rate-sensitivity of Ti-8Al-1Mo-1V is comparable to that of regular-grade Ti-6Al-4V. The variation of strain and strain-rate with time determined from constant-stress tests at 925°C (1700°F), 950°C (1740°F), and 1010°C (1850°F) are shown in Figures 102 through 104.

4.6 Ti-3Al-2.5V ($T_{\beta} = 930^{\circ}\text{C}$)

The lightly alloyed alpha-beta alloy, Ti-3Al-2.5V, has the lowest beta-transus temperature of all the alpha-beta alloys tested in this program. The alloy exists as a single alpha-phase below about 760°C (1400°F), and is all beta phase above 930°C (1706°F). Thus, the possible superplastic range for this alloy is 800-900°C (1472-1652°F). The strain-rate dependences at 800°C (1470°F), 840°C (1544°F) and 875°C (1607°F) of the flow stress and strain-rate-sensitivity for Ti-3Al-2.5V with primary volume-fractions of 0.87 and 0.57 and grain sizes of 4.3-10.2 μm are shown in Figures 105 through 108. The alloy at 840-875°C (1544-1607°F) exhibits excellent superplastic characteristics with lower flow stresses and strain-rate sensitivity values comparable with those of regular-grade Ti-6Al-4V. In agreement with the trends observed in Ti-6Al-4V, the flow stress in Ti-3Al-2.5V increases with increasing grain size and does not vary significantly with the amount of primary alpha.

4.7 Ti-15V-3Cr-3Sn-3Al ($T_{\beta} = 746^{\circ}\text{C}$)

The strain-rate dependences of flow stress and strain-rate-sensitivity of different microstructural variations of Ti-15V-3Al-3Cr-3Sn alloy are listed in Table 24 and shown in Figures 109 through 113. The results indicate that the maximum strain-rate sensitivity of this beta alloy is ≈ 0.4 . The flow stresses are high in the low-temperature region, and at high temperatures where grain growth is rapid, m_{max} occurs at very slow strain rates. The grain size of specimens tested at 700-920°C (1290-1690°F) are shown in Table 25. The extensive grain growth observed at high temperatures is the cause for the high flow stress and low strain-rate-sensitivity in the alloy.

The true-stress/true-strain curves (Figures 114 and 115) determined from constant-strain-rate tests clearly show the unstable deformation at small strains of this alloy at 810°C (1490°F) and 760°C (1400°F). The results indicate that superplastic forming of Ti-15V-3Cr-3Sn-3Al is not feasible at practical pressures.

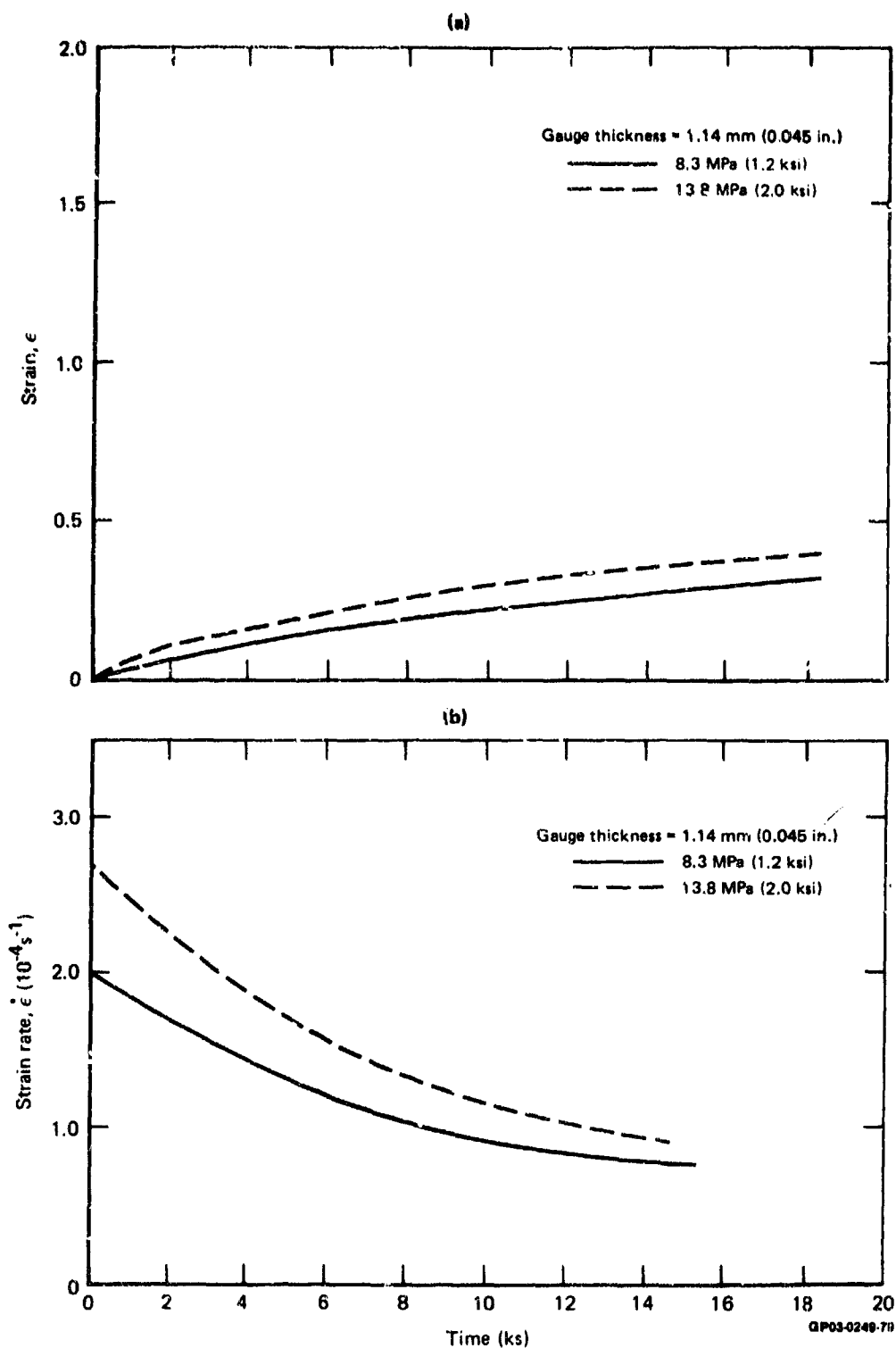


Figure 102. Variation of (a) strain and (b) strain rate with time at 925°C determined from constant stress tests for Ti-8Al-1Mo-1V.

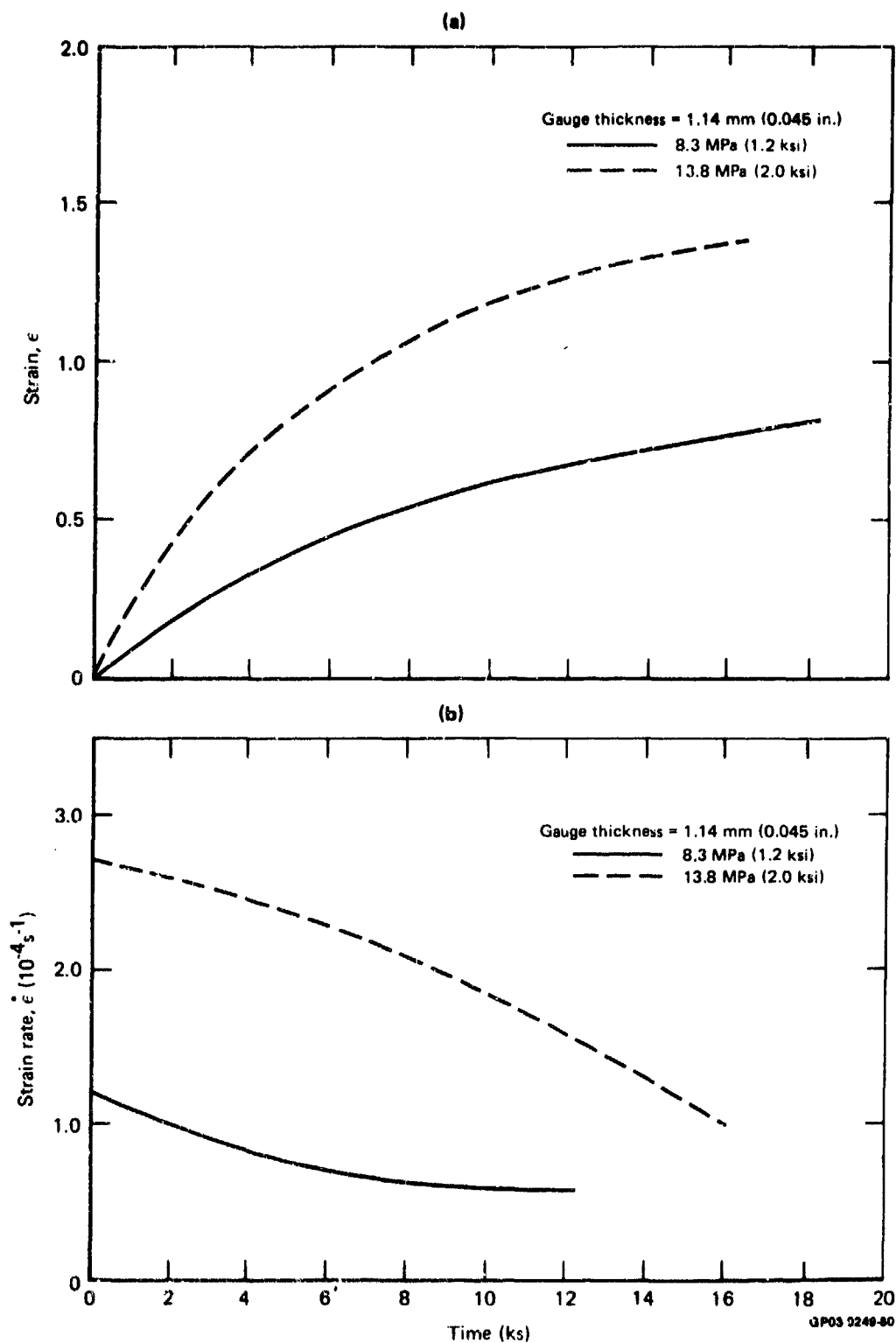


Figure 103. Variation of (a) strain and (b) strain rate with time at 950°C (1742°F) determined from constant stress tests for Ti-8Al-1Mo-1V.

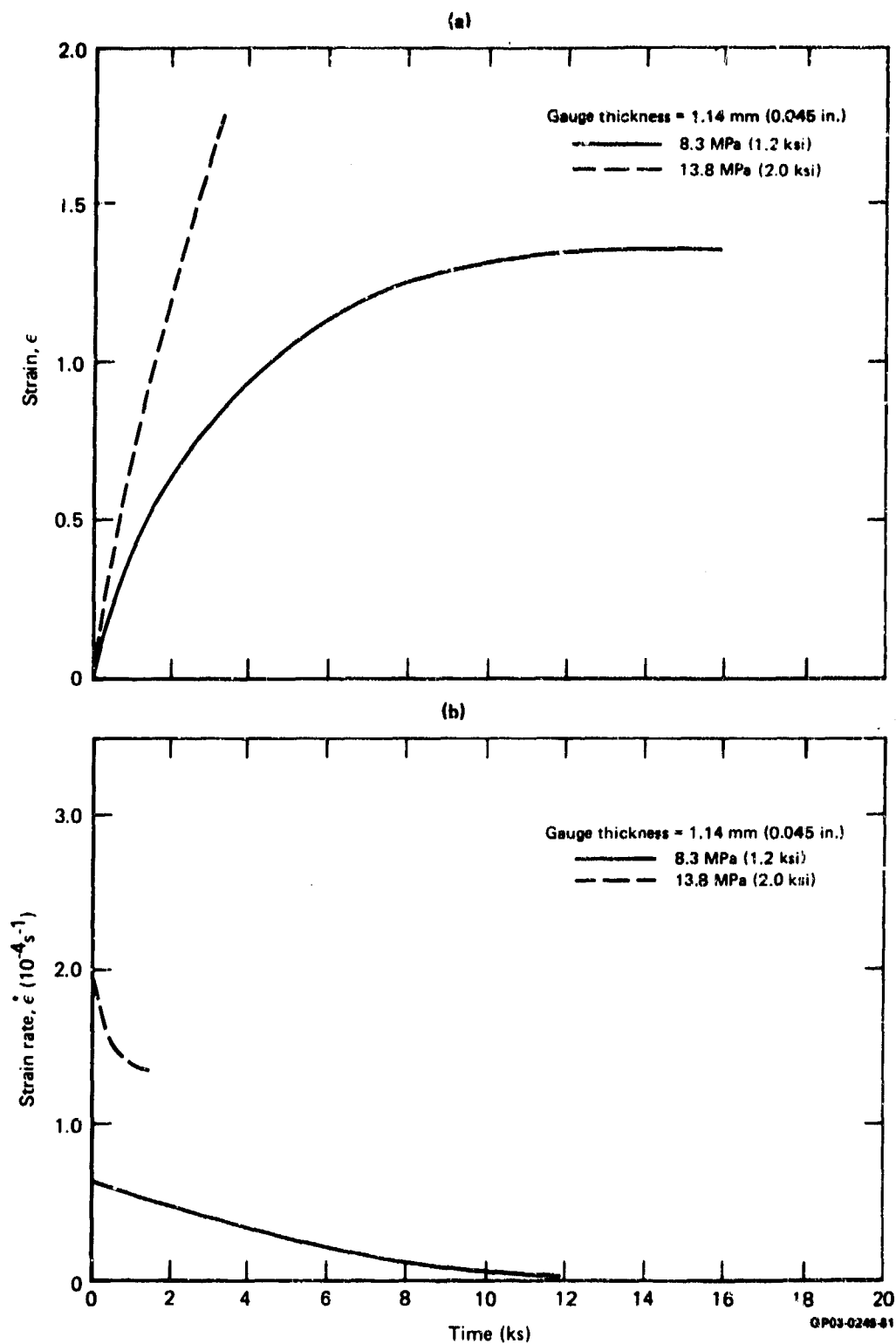


Figure 104. Variation of (a) strain and (b) strain rate with time at $1010^{\circ}C$ ($1850^{\circ}F$) determined from constant stress tests for Ti-8Al-1Mo-1V.

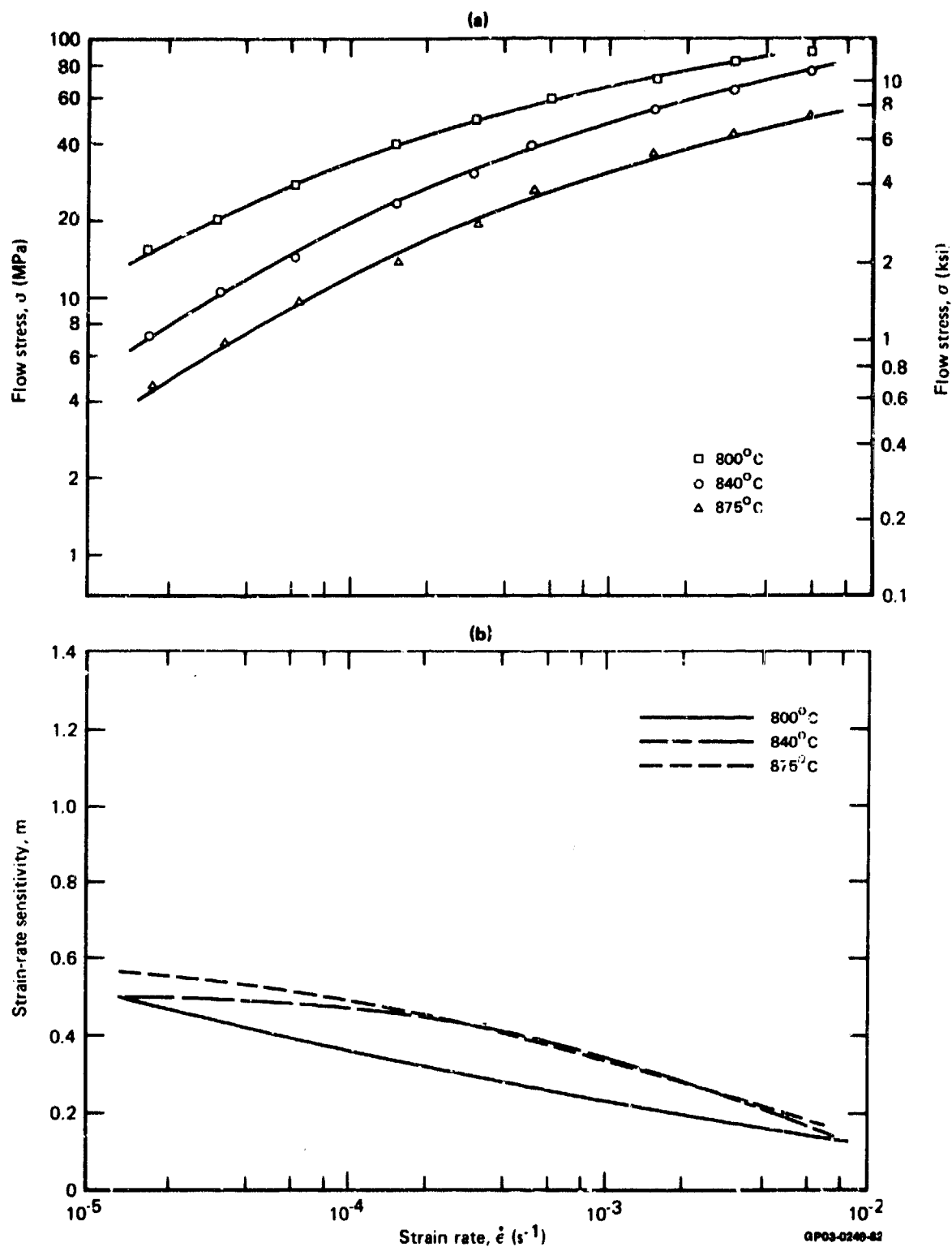


Figure 105. Strain-rate dependence of (a) flow stress and (b) strain-rate sensitivity for Ti-3Al-2.5V sample RI (volume % primary α = 87, grain size = $5.6 \mu m$).

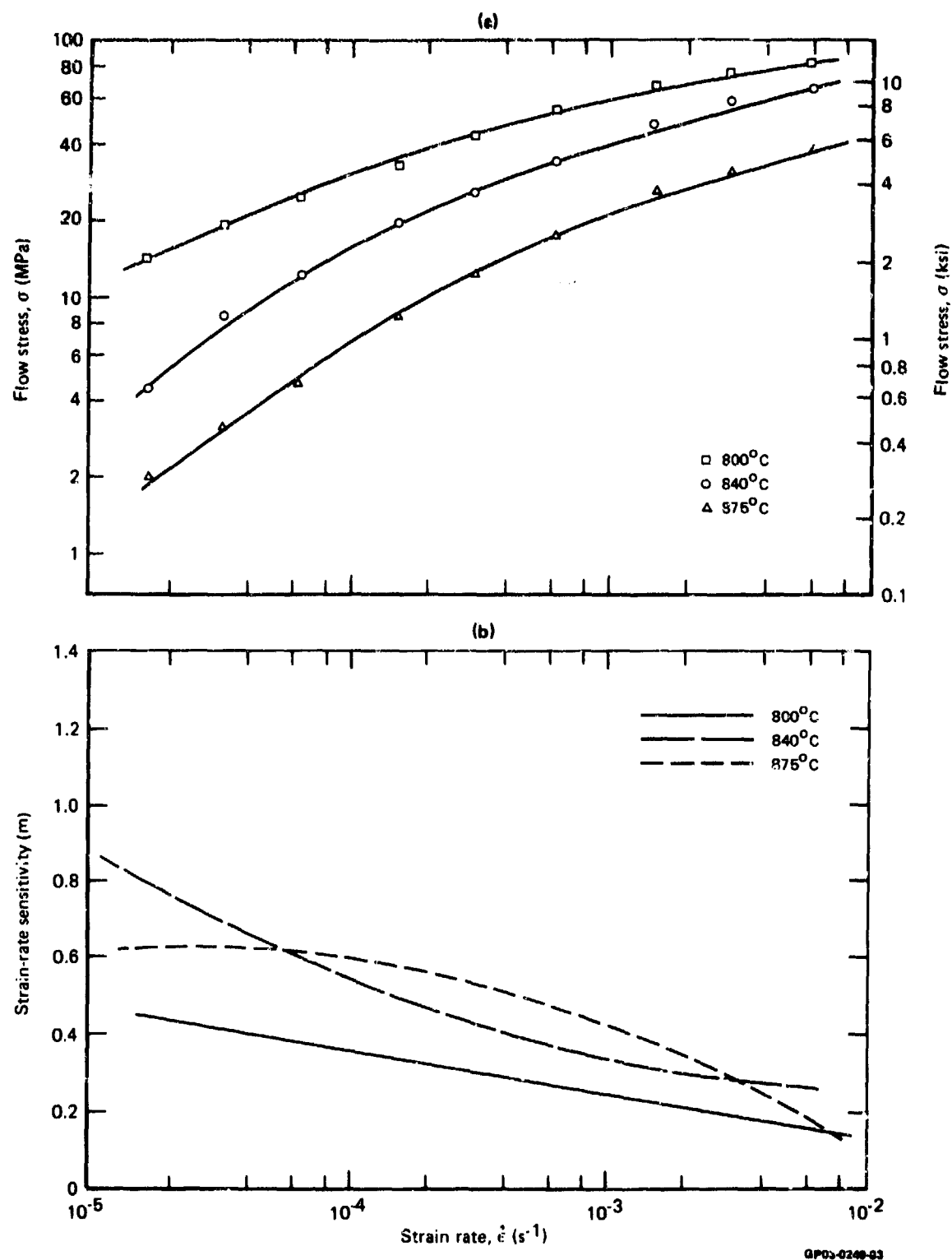


Figure 106. Strain-rate dependence of (a) flow stress and (b) strain-rate sensitivity for Ti-3Al-2.5V sample R2 (volume % primary α = 57, grain size = 4.3 μm).

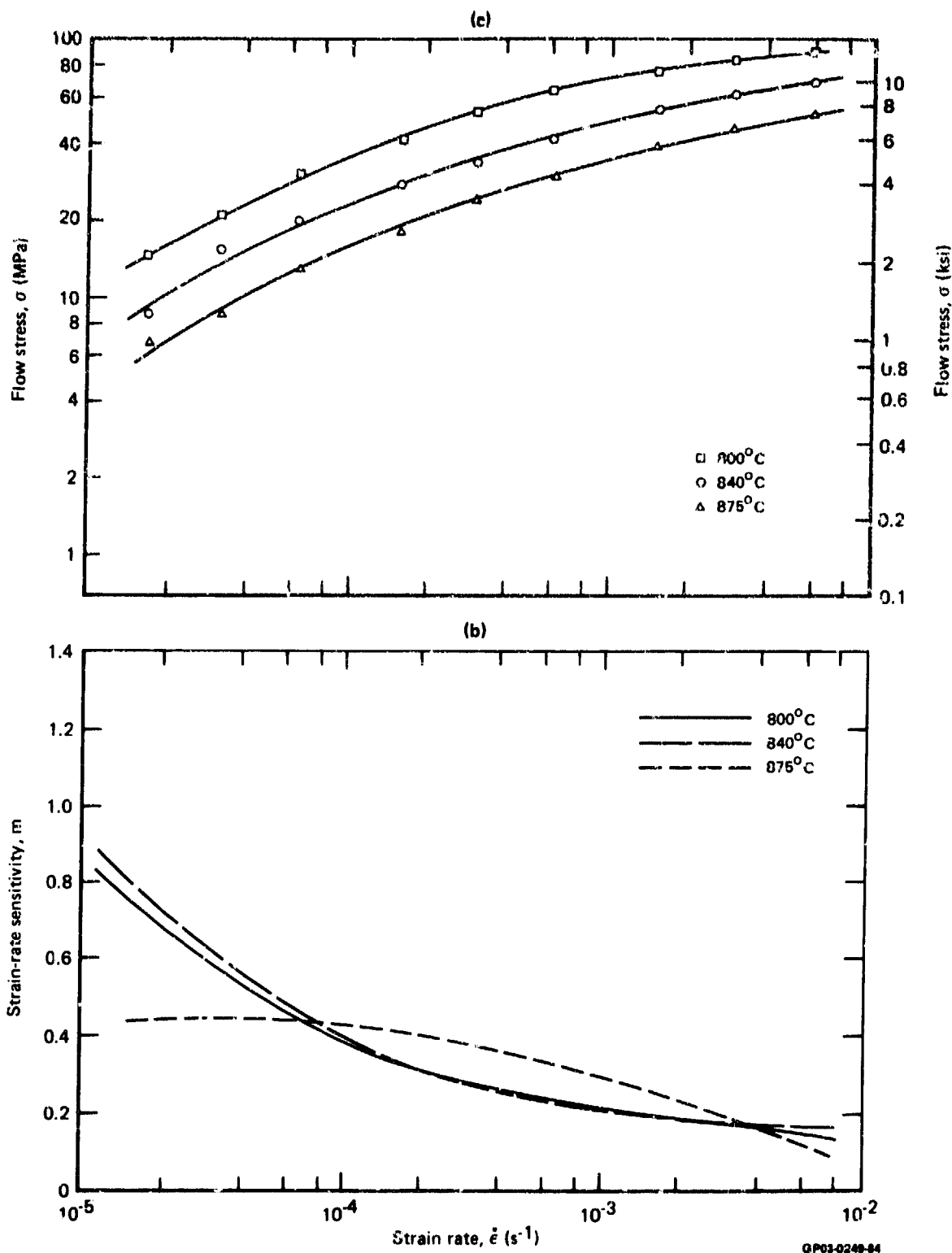


Figure 107. Strain-rate dependence of (a) flow stress and (b) strain-rate sensitivity for Ti-3Al-2.5V sample R3 (volume % primary α = 87, grain size = 10.2 μm).

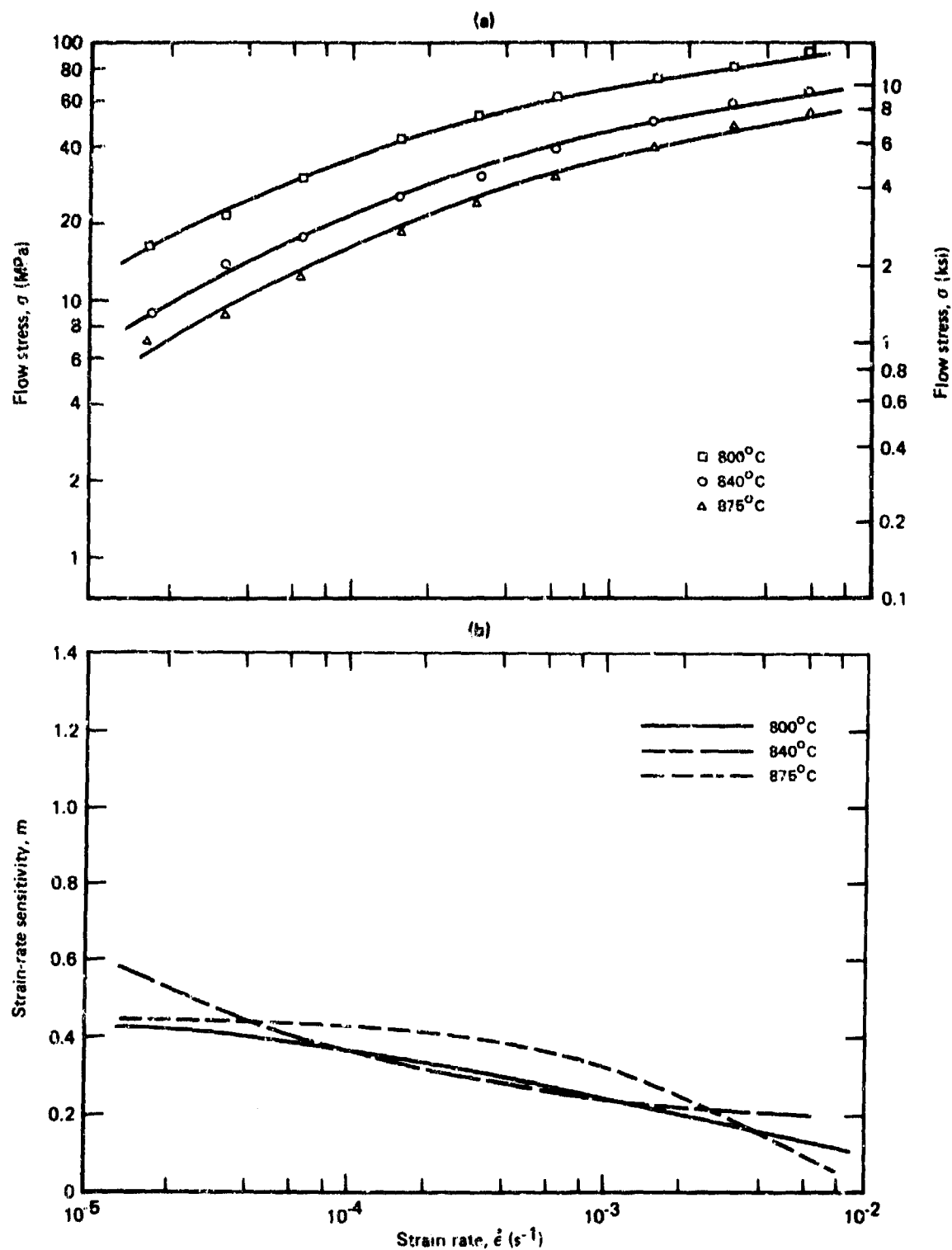


Figure 108. Strain-rate dependence of (a) flow stress and (b) strain-rate sensitivity for Ti-3Al-2.5V sample R4 (volume % primary alpha = 58, grain size = 8.6 μm).

TABLE 24. MICROSTRUCTURE VARIABLES FOR THE STUDY OF THE SUPERPLASTICITY OF Ti-15V-3Cr-3Sn-3Al.

Specimen	Microstructure	Grain size (μm)
Z1	Cold-worked	--
Z2	Partially recrystallized, fine alpha precipitates	--
Z3	Fully recrystallized, small grain size	32
Z4	Fully recrystallized, small grain size, fine alpha precipitates	32
Z5	Fully recrystallized, small grain size, coarse alpha precipitates	32
Z6	Fully recrystallized, large grain size, fine alpha precipitates	52
Z7	Fully recrystallized, large grain size, coarse alpha precipitate	52

GP03-0249-11

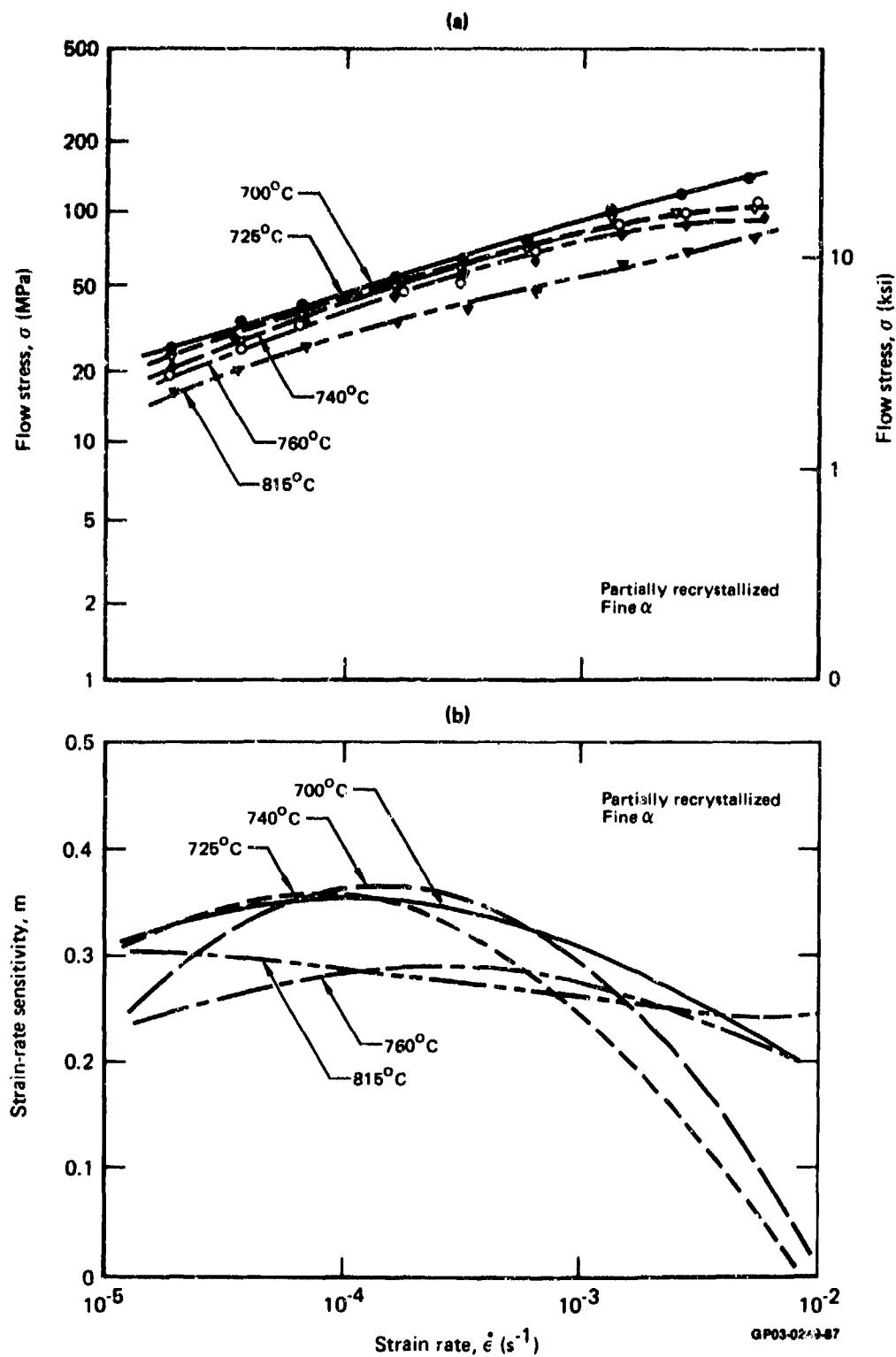


Figure 109. Strain-rate dependence of (a) flow stress and (b) strain-rate sensitivity for Ti-15V-3Al-3Sn-3Cr sample Z2.

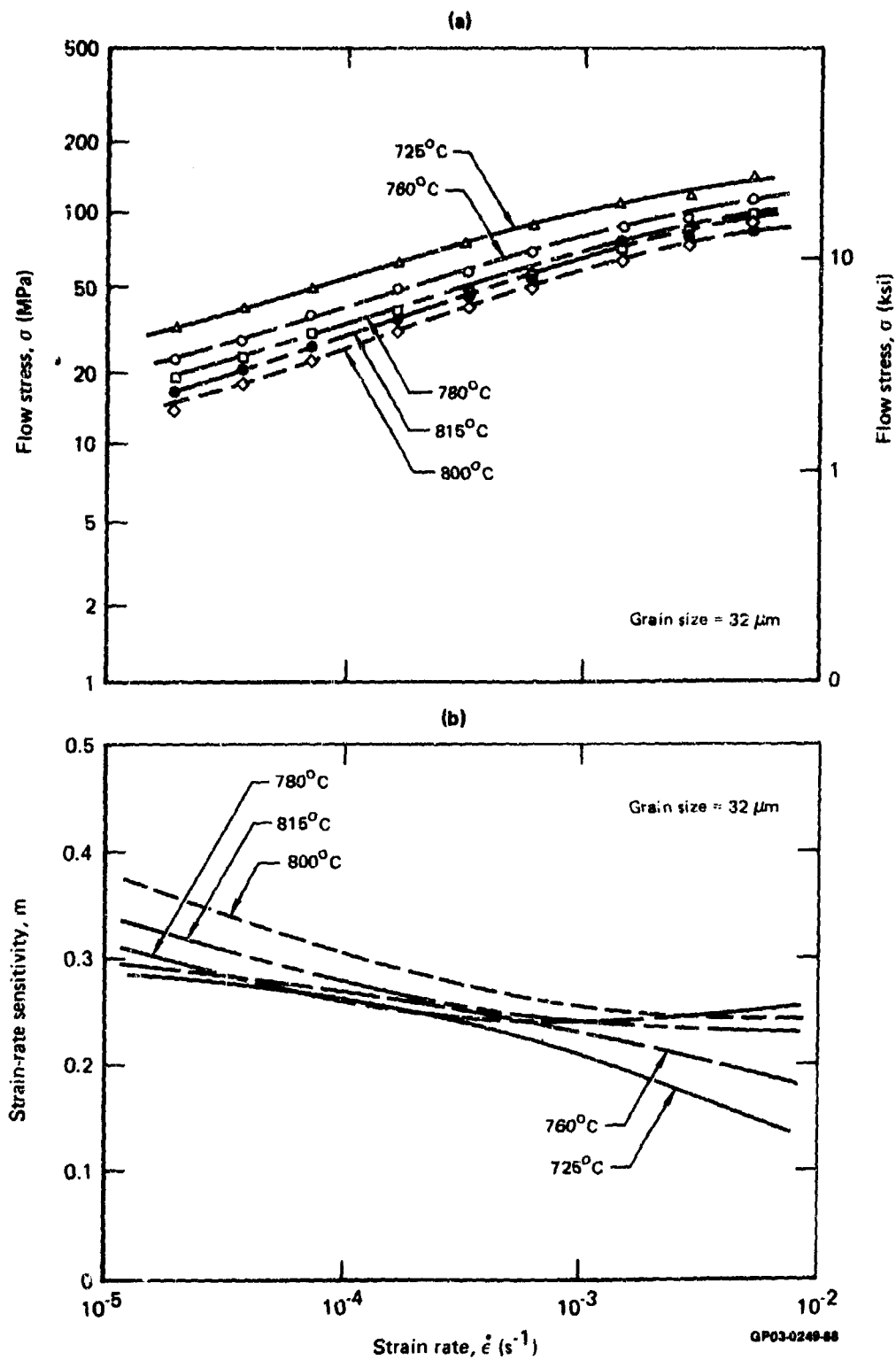


Figure 110. Strain-rate dependence of (a) flow stress and (b) strain-rate sensitivity for Ti-15V-3Al-3Sn-3Cr sample Z3.

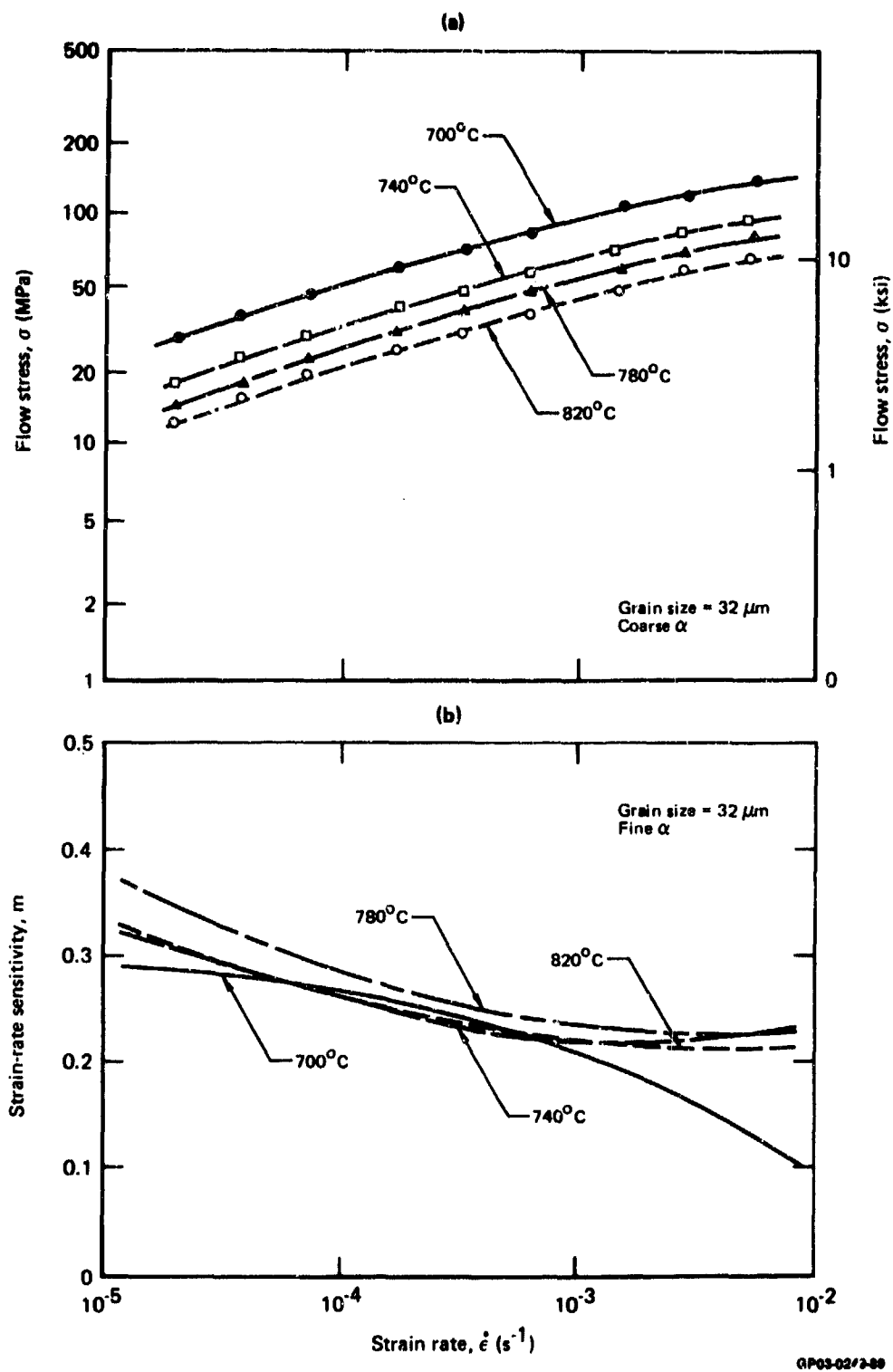


Figure 111. Strain-rate dependence of (a) flow stress and (b) strain-rate sensitivity for Ti-15V-3Al-3Sn-3Cr sample Z5.

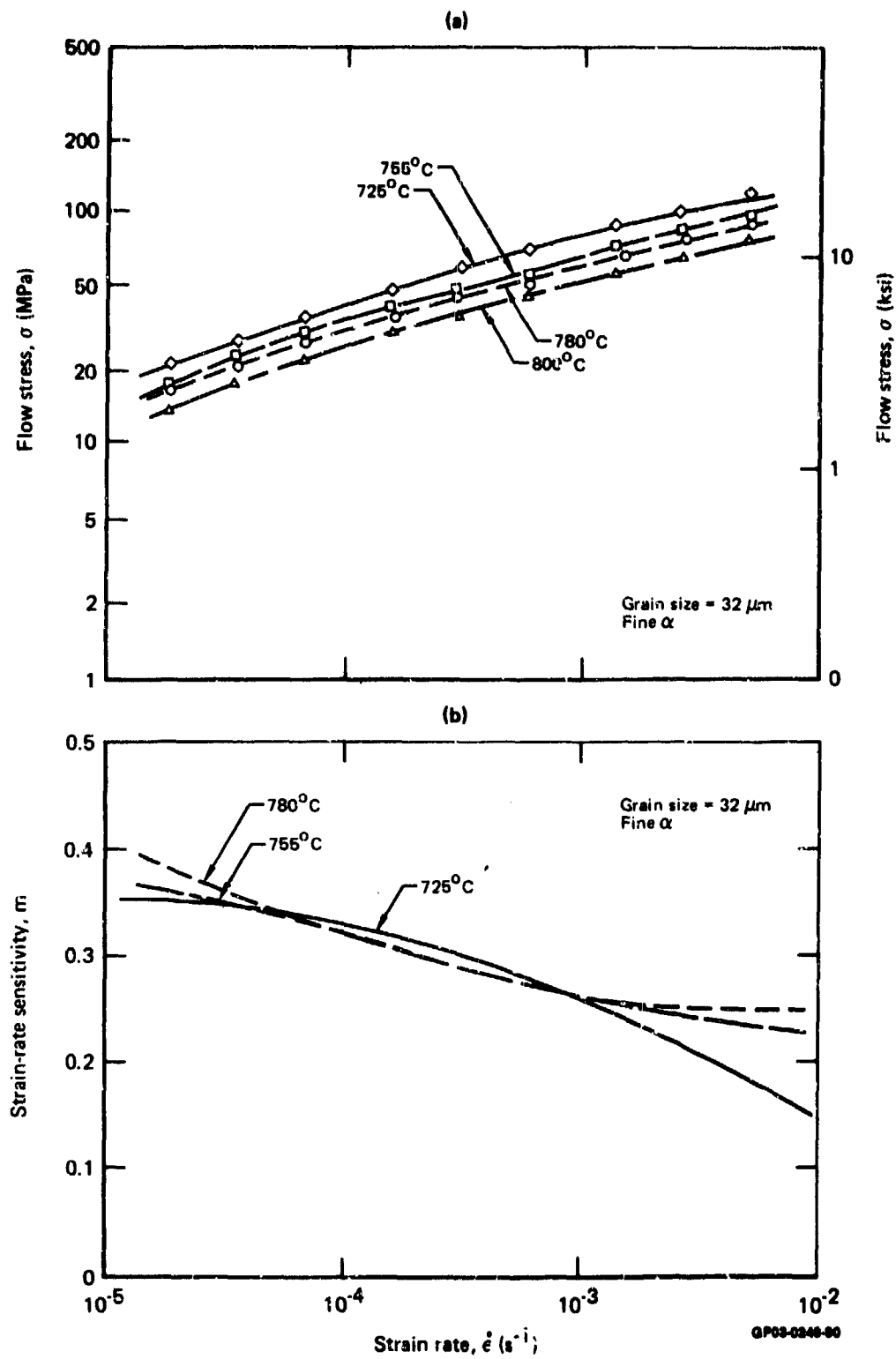


Figure 112. Strain-rate dependence of (a) flow stress and (b) strain-rate sensitivity for Ti-15V-3Al-3Sn-3Cr sample Z4.

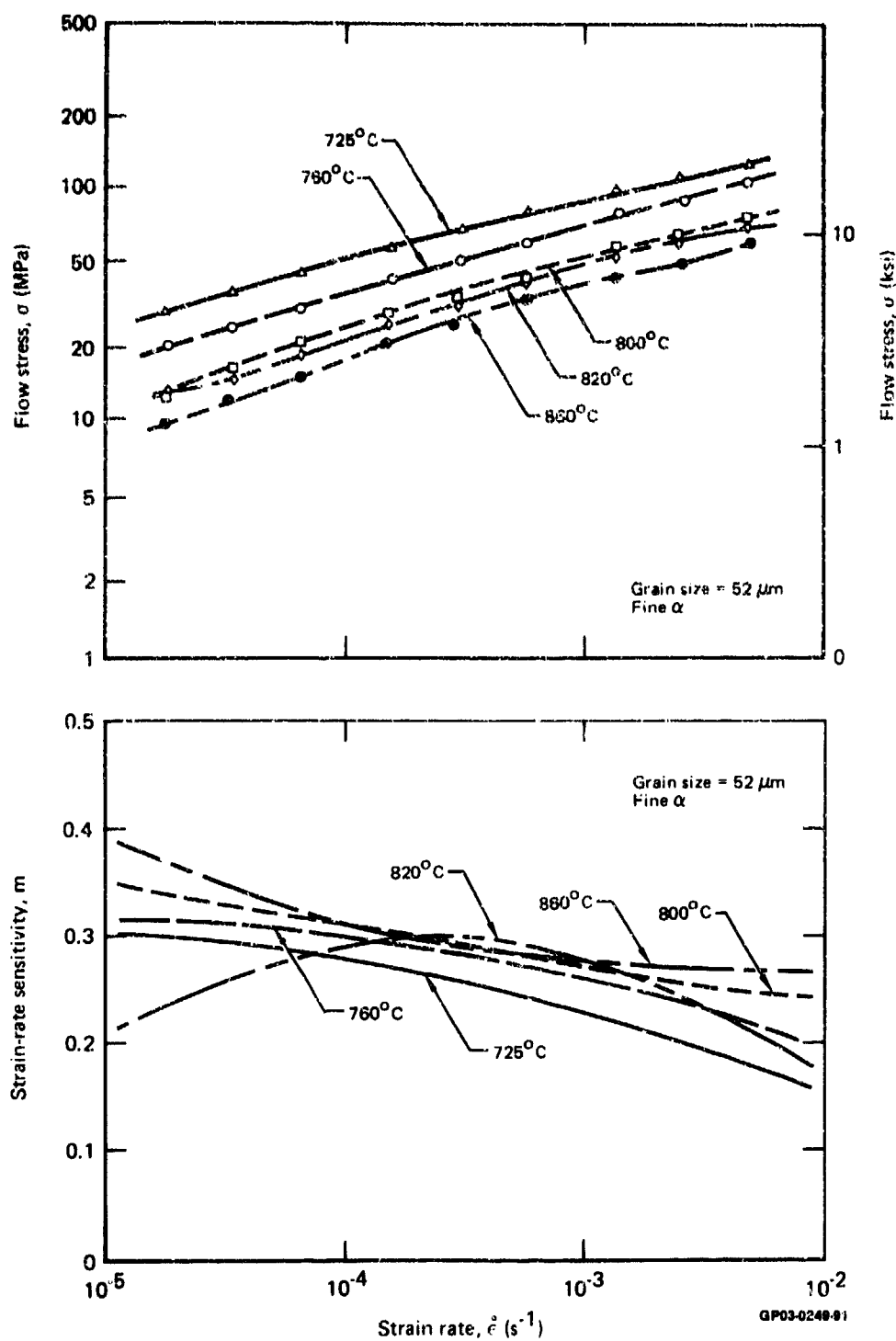


Figure 113. Strain-rate dependence of (a) flow stress and (b) strain-rate sensitivity for Ti-15V-3Al-3Sn-3Cr sample Z6.

TABLE 25. GRAIN GROWTH IN Ti-15V-3Al-3Sn-3Cr DURING INCREMENTAL STRAIN-RATE TESTS.

Test temperature (Test duration: \approx 2 hr) ($^{\circ}$ C)	Grain size before test (μ m)	Grain size after test (μ m)
700	32	35
740	32	60
780	32	90
820	32	150
920	32	250

GP03-0240-12

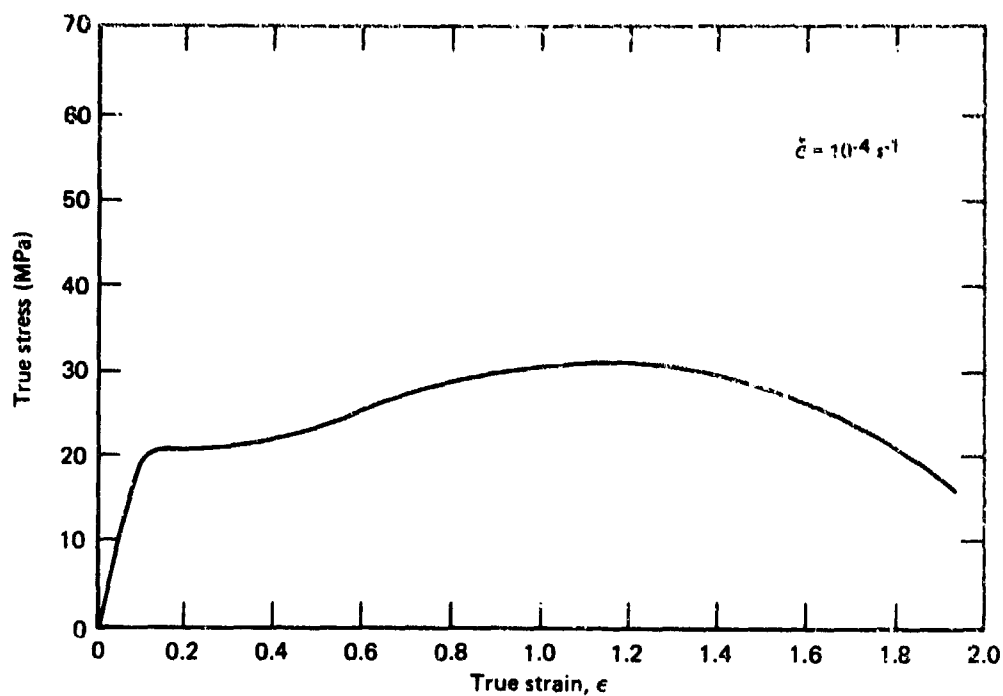


Figure 114. True-stress as a function of true-strain at 810°C (1490°F) for Ti-15V-3Al-3Sn-3Cr (sample Z1) determined from constant strain-rate tests.

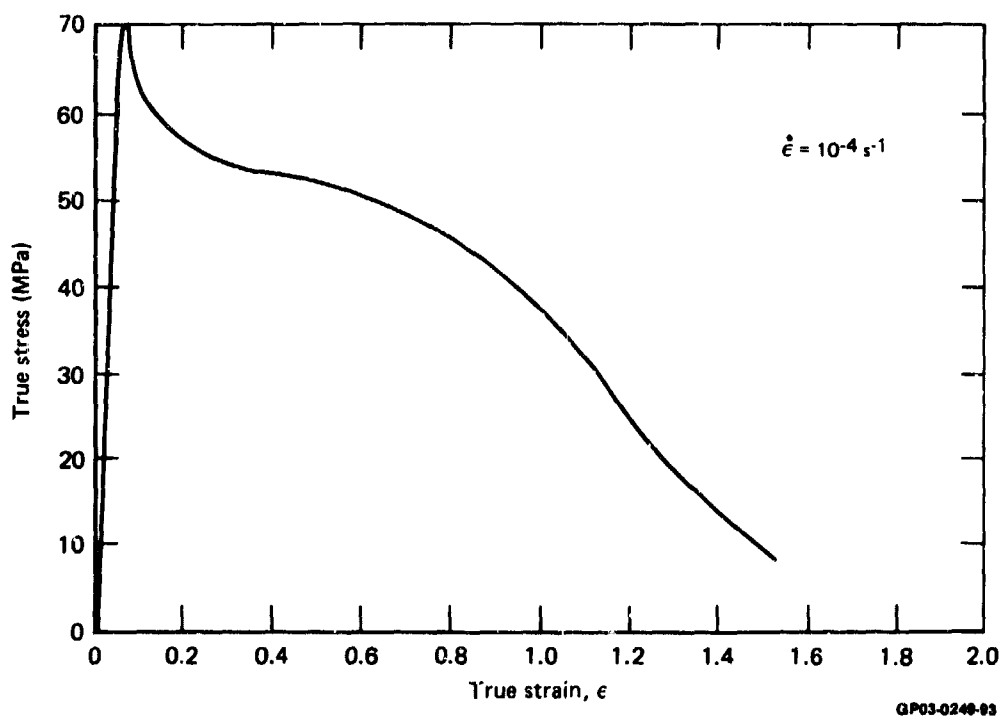


Figure 115. True-stress as a function of true-strain at 760°C (1400°F) for Ti-15V-3Al-3Sn-3Cr sample Z1 determined from constant strain-rate tests.

4.8 Comparisons of Superplastic Behavior of Different Titanium Alloys

Figures 116 through 118 show comparisons of strain-rate dependences of flow-stress and strain-rate for several alpha-beta titanium alloys with similar initial microstructures. Of all the alloys, ELI-grade Ti-6Al-4V and Ti-3Al-2.5V have the lowest flow stresses and highest strain-rate sensitivities. However, all the fine-grained alpha-beta titanium alloys have acceptable superplasticity parameters at 840-910°C (1540-1670°F). The beta alloy, Ti-15V-3Cr-3Sn-3Al has unacceptably high flow stress and low strain-rate sensitivity.

The effects of crystallographic texture on the superplastic parameters of Ti-6Al-4V at 850°C (1560°F) are shown in Figure 119. The differences in the flow stresses and strain-rate sensitivities between basal-textured and transverse-basal-textured specimens are due mainly to the microstructural differences rather than texture differences because the contribution of orientation-dependent slip processes to the overall deformation in the superplastic range is negligible. Furthermore, the difference in flow-stress between the longitudinal and transverse directions even in the basal-textured specimen, which should have nearly isotropic slip-related properties in the rolling plane, indicates that the anisotropy of the high-temperature flow-stress results not from texture but from the differences in microstructural parameters in different directions.

Figures 120a and 120b show comparisons of variations of strain and strain-rate with time for the alpha-beta alloy, Ti-6Al-4V, and the near-alpha alloy, Ti-8Al-1Mo-1V. The strain rates of the alpha-beta alloy are significantly higher than those of the near-alpha alloy because of large differences in the equilibrium volume fractions of alpha and beta phases. A significantly higher amount of equilibrium primary-alpha present in Ti-8Al-1Mo-1V at 906°C (1663°F) and 925°C (1697°F) results in decreased diffusion rates and increased grain-size, both of which adversely affect the superplastic characteristics. The strain-rate dependence of flow stress for several alpha-beta titanium alloys plotted at different T/T_β values (Figure 121) clearly indicates the unique dependence of flow stress on the equilibrium volume-fractions of the constituent phases at test temperatures.

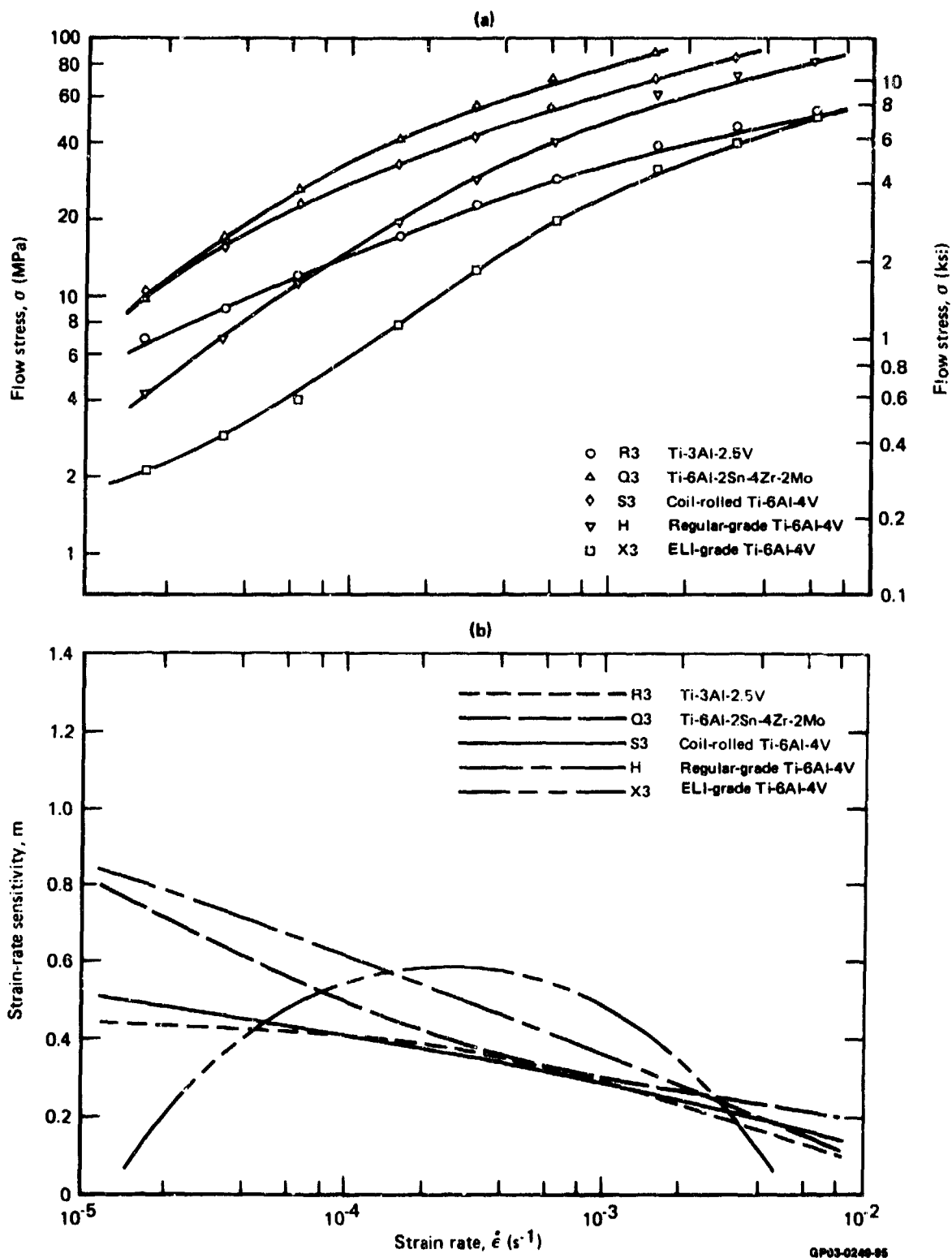


Figure 116. Effects of alloy chemistry on strain-rate dependence of (a) flow stress and (b) strain-rate sensitivity of titanium alloys.

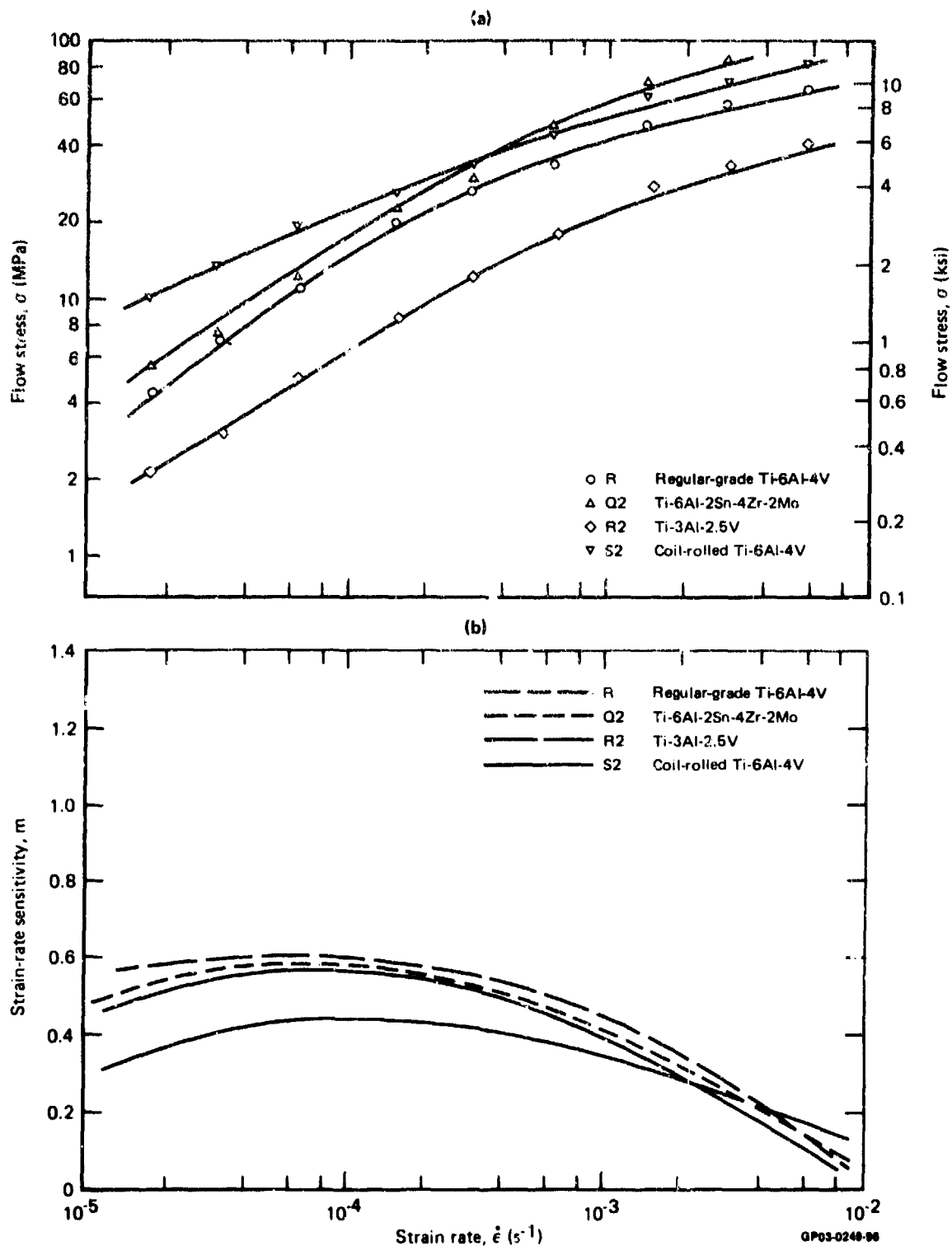


Figure 117. Effects of alloy chemistry on strain-rate dependence of (a) flow stress and (b) strain-rate sensitivity of titanium alloys at 850°C (1562°F).

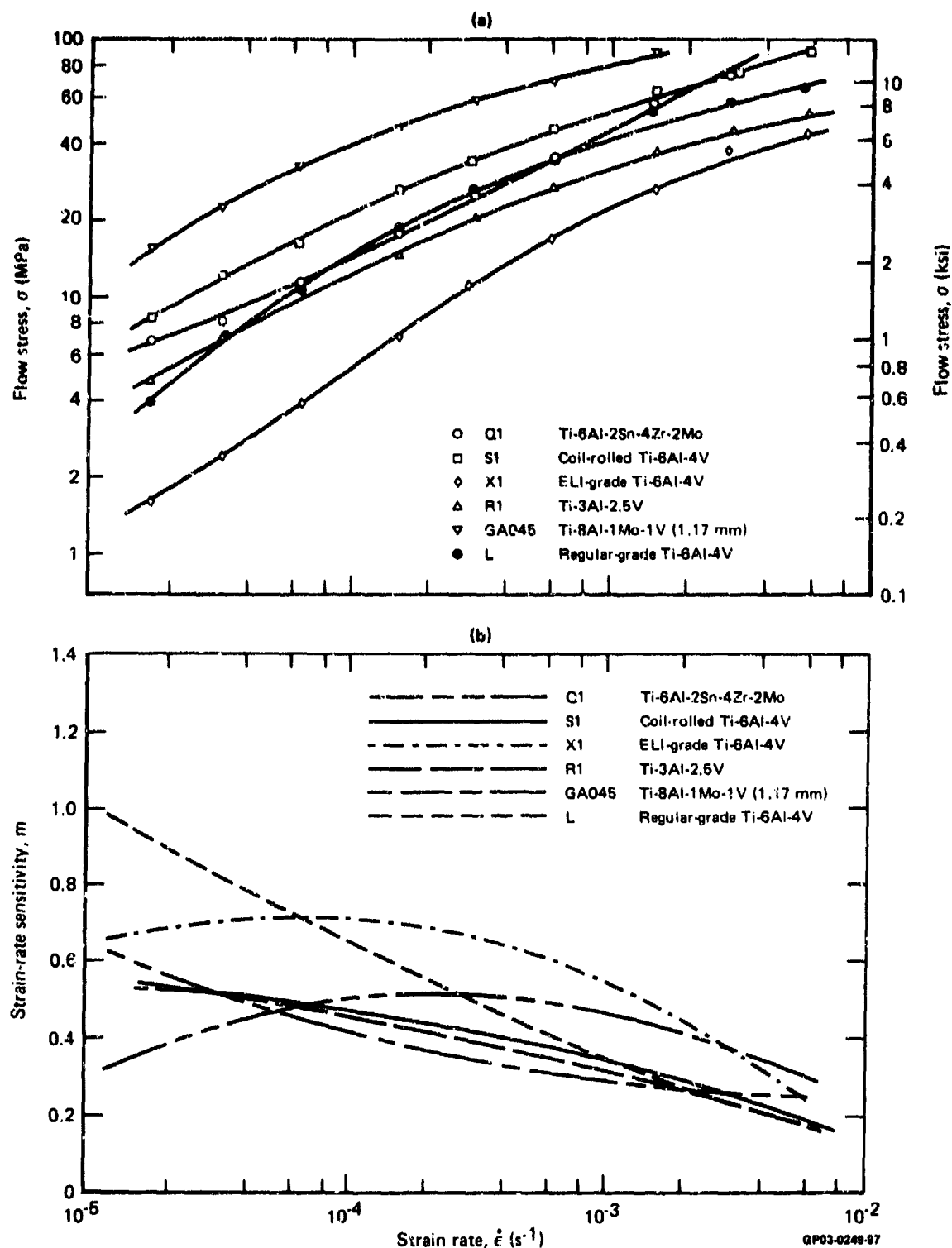
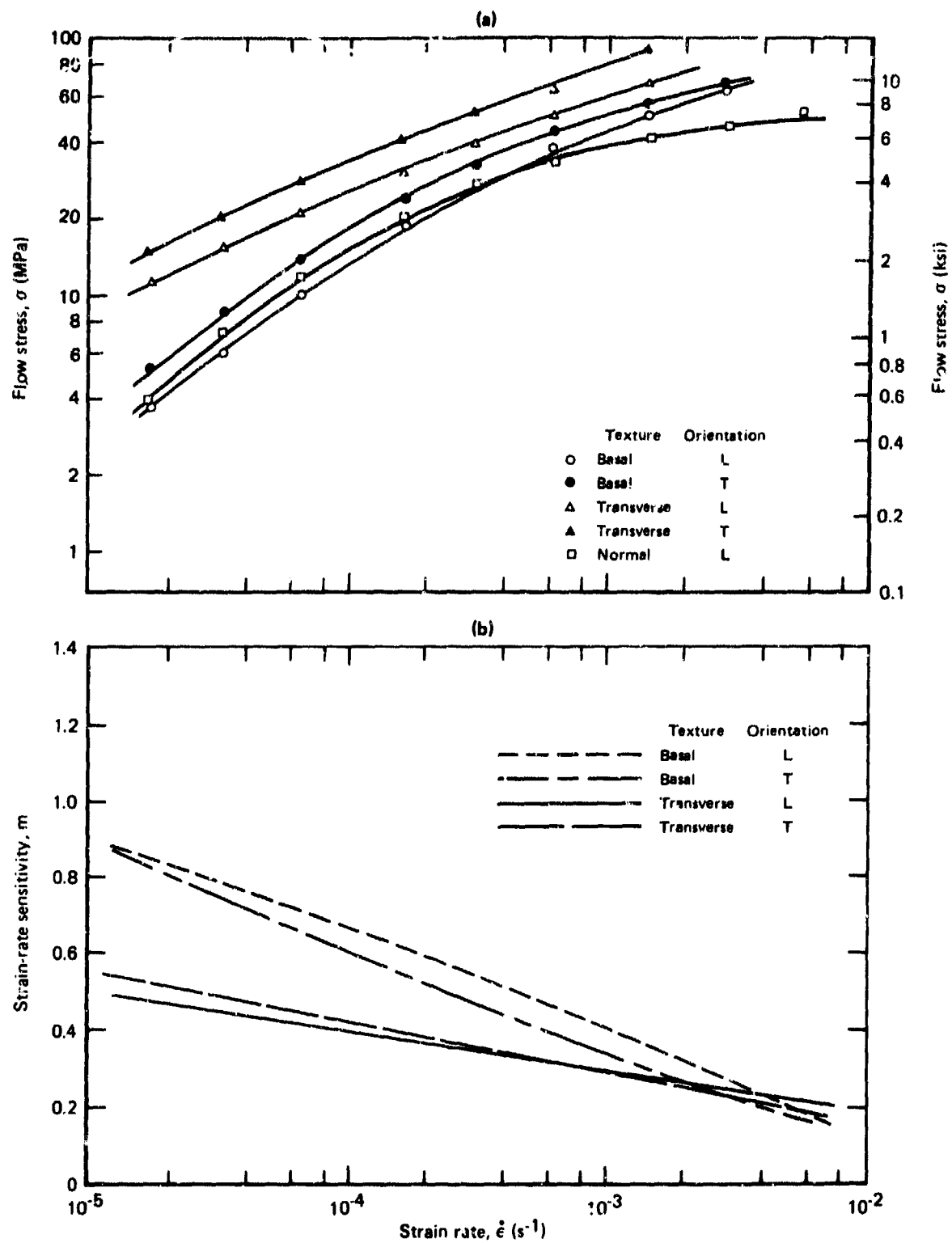


Figure 118. Effects of alloy chemistry on strain-rate dependence at 850°C (1562°F) of (a) flow stress and (b) strain-rate sensitivity of alpha-beta and near-alpha alloys determined from incremental strain-rate tests.



GP03-0240-03

Figure 119. Effects of texture on strain-rate dependence of (a) flow stress and (b) strain-rate sensitivity of Ti-6Al-4V at 850°C (1560°F).

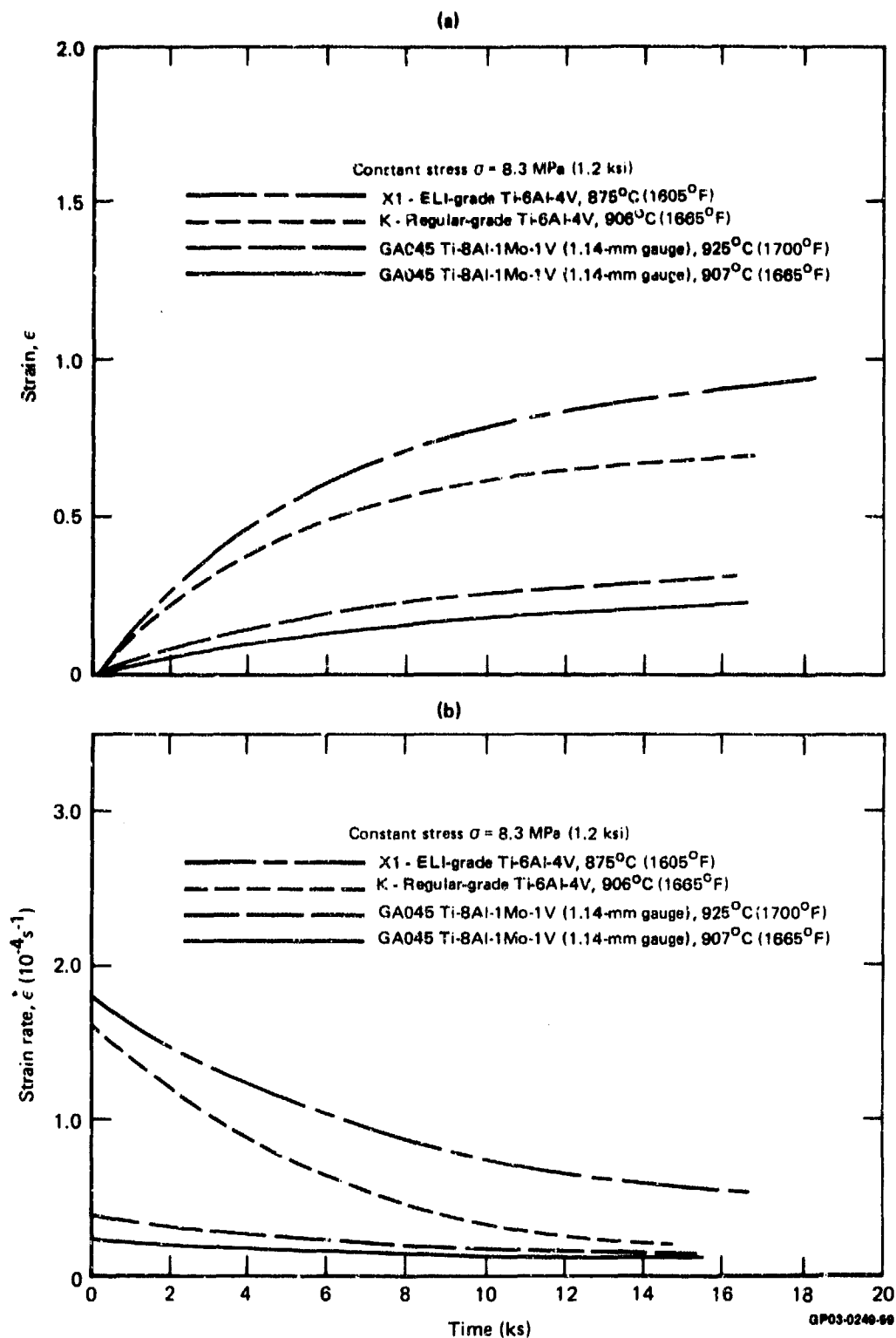


Figure 120. Comparisons of variation of (a) strain and (b) strain-rate with time determined from constant stress tests for Ti-6Al-4V and Ti-8Al-1Mo-1V.

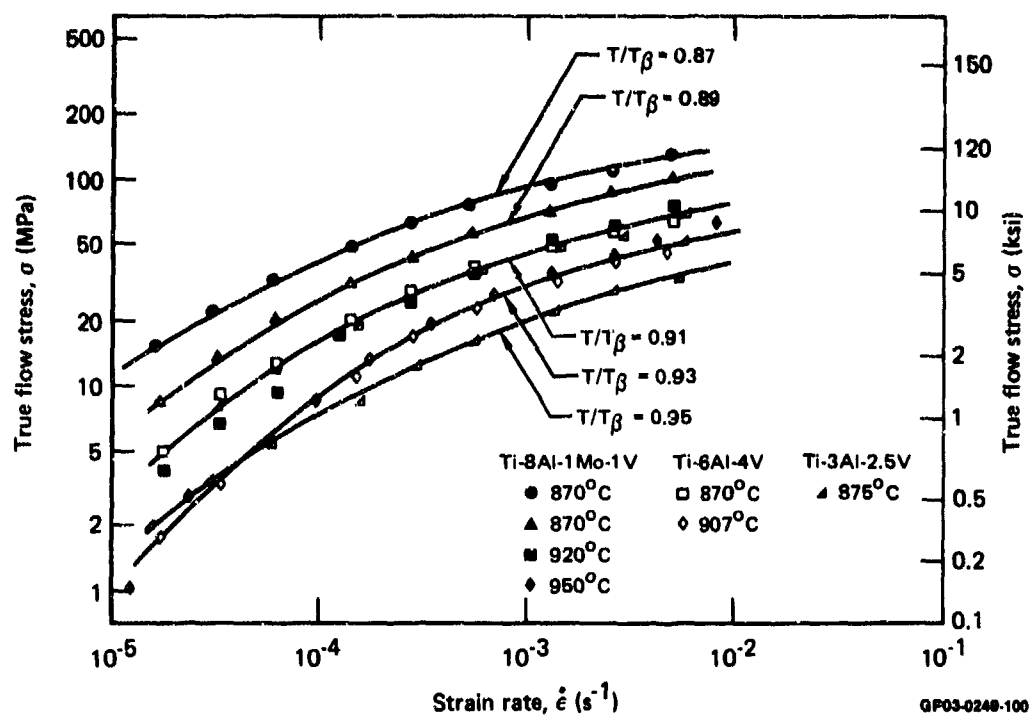


Figure 121. Strain-rate dependence of flow stress for Ti-8Al-1Mo-1V, Ti-6Al-4V, and Ti-3Al-2.5V showing the unique dependence of flow stress at constant strain rate on T/T_{β} .

SECTION V

SUPERPLASTIC FORMING EVALUATION

5.1 Verification of Biaxial Conical Die Forming

For microstructure E (0.87 α , 12.2 μm), an intermediate grain size normal textured regular-grade Ti-6Al-4V, a wide range of strains were made at 907°C (1665°F).

The largest cones of 38.1 mm (1.5 inch) diameter were sectioned and the thicknesses were measured at the bottom of the cones along with the depth in cone. The constant stress predicted for forming in the cone, Equation 1, in Section 2.3.3 was compared with the stresses calculated from thickness measurements for biaxial forming of membrane, Equation 2, in Section 2.3.3. These stresses are shown in Table 26. The variations in stress calculated from thickness with predicted constant stress (when material first touches die wall, $H = .595$) were within $\pm 6\%$, and the test thus simulates constant-stress conditions with acceptable accuracy for cones with H values (ratio of depth in cone to radius) greater than 0.5.

The validity of Equation 3 in section 2.3.3 for calculating the strain in a cone from the depth-in-cone measurements was made by comparing the total strain from thickness measurements with the total strain determined by adding the strain from equation 3 and the strain for the sheet material to reach the conical die surface, $\epsilon = 0.3$. The results are shown in Figure 122. Because of the excellent agreement between these two methods of measuring strain, depth measurements in the cone can be used with confidence to determine the strain.

TABLE 26. COMPARISON OF STRAIN DEPENDENCE OF STRESS CALCULATED FROM THICKNESS MEASUREMENTS WITH PREDICTED VALUES FOR SUPERPLASTIC CONE-FORMING AT 907°C (1665°F) OF 38-mm (1.5 IN.) DIAM REGULAR-GRADE Ti-6Al-4V (PANEL E; GRAIN SIZE = 12.2 μm , VOLUME % PRIMARY ALPHA = 87).

Final depth in cone mm (in.)	H	Final thickness in core mm (in.)	Strain from thickness	Calculated stress MPa (psi)	Predicted constant stress MPa (psi)
3.11 (0.350)	0.49	1.401 (0.055)	0.21	9.07 (1316)	— —
13.3 (0.523)	0.73	1.191 (0.047)	0.37	8.55 (1240)	8.96 (1300)
17.8 (0.700)	0.98	0.940 (0.037)	0.61	8.41 (1220)	8.96 (1300)
19.8 (0.778)	1.09	0.737 (0.029)	0.84	9.38 (1360)	8.96 (1300)
24.9 (0.979)	1.37	0.508 (0.020)	1.22	8.55 (1240)	8.96 (1300)

GP03-0240-255

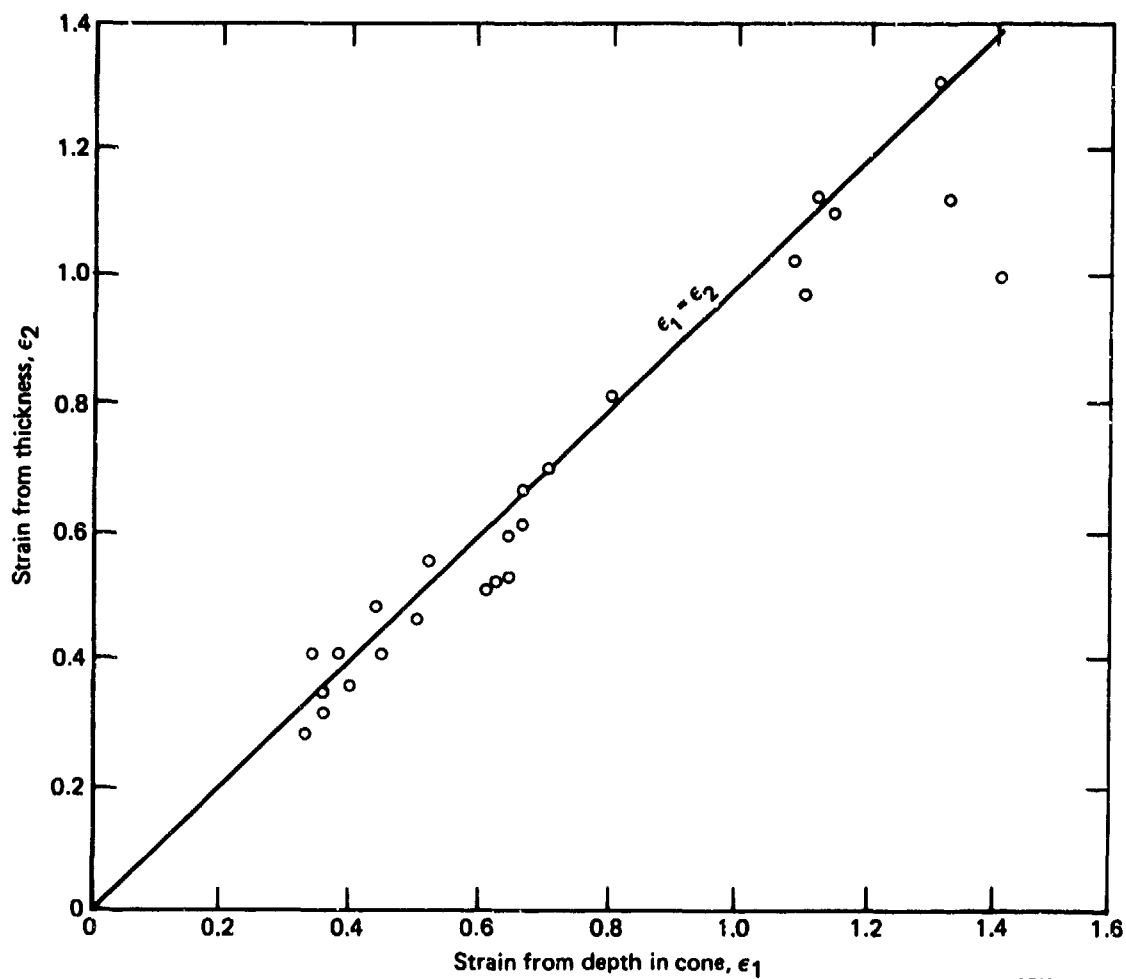


Figure 122. Correlation of strain calculated from formed-cone thickness with strain calculated from cone depth.

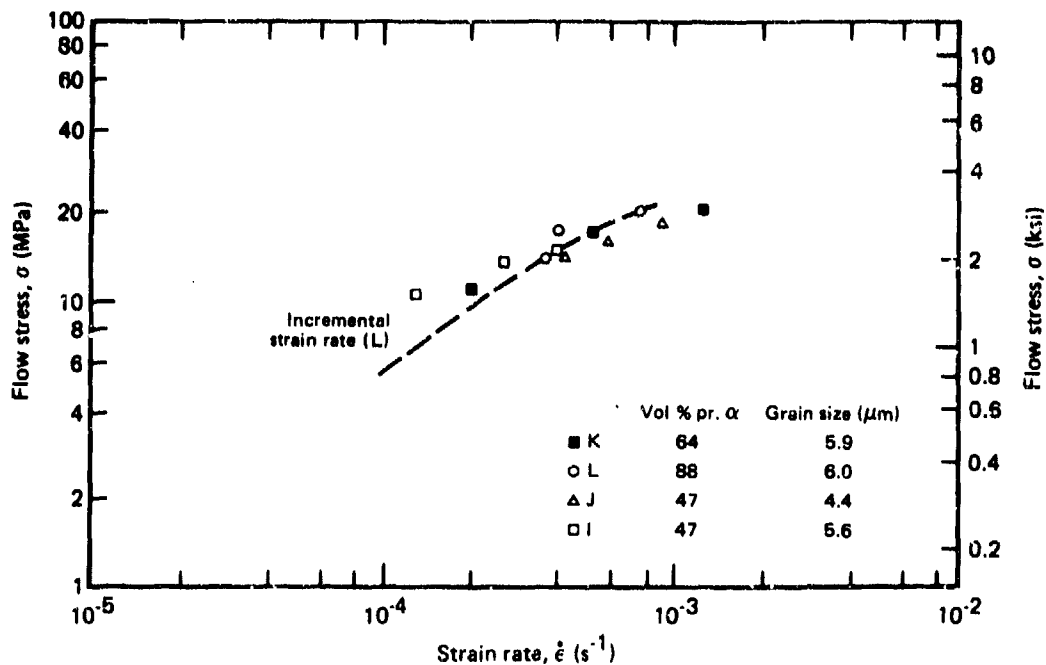
5.2 Biaxial Conical-Die Forming of Regular-Grade Ti-6Al-4V and ELI-Grade Ti-6Al-4V (Normal Texture)

Biaxial cone-forming tests were performed at 871°C (1600°F) and 907°C (1665°F) with forming times of 0.5 hour and 5.0 hour. The strain rate dependence of flow stress was correlated with laboratory tests results, and microstructural modifications produced by forming were characterized. The effects of a diffusion-bonding cycle on subsequent superplastic forming rates were determined.

The initial biaxial cone forming tests were performed on normal textured, regular-grade Ti-6Al-4V with short forming times 0.5 hours, at 907°C (1665°F), and the results are tabulated in Appendix C. The strain rates obtained from the conical-die forming are compared with incremental strain-rate test results in Figure 123 through 125 and the agreement between the two kinds of test at high strain rates is excellent. The microstructures having similar primary alpha grain sizes for all regular-grade Ti-6Al-4V have been plotted together in Figures 123 through 125 because the strain rate varies little with changes in primary-alpha level. For microstructures K (0.64 α , 5.9 μm) and J (0.47 α , 4.4 μm) of normal textured regular-grade Ti-6Al-4V, forming extended to the bottom of the bottom of the largest-diameter cone, with failure occurring at strains of 2.0 and 2.3, respectively. These strains represent the upper limit for biaxial, superplastic forming of titanium alloys in conical dies.

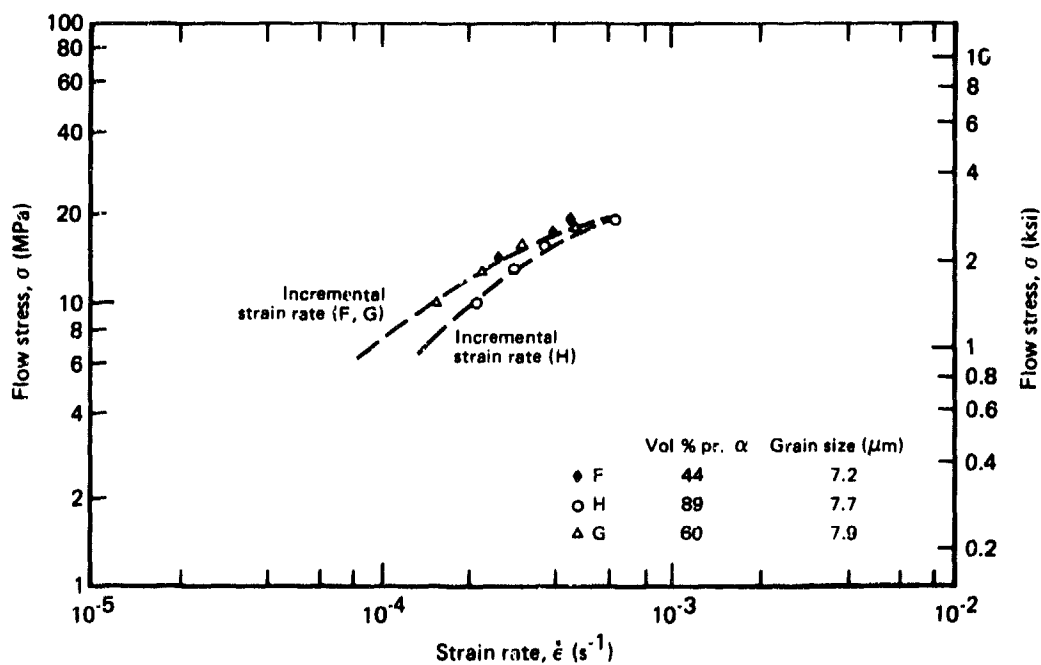
Biaxial forming in conical dies was performed also on ELI-grade Ti-6Al-4V at 871°C (1600°F) and 907°C (1665°F) at high strain rates and forming times ≤ 0.5 hour. Results shown in Figures 126 and 127 agree well with incremental-strain-rate tests.

Normal textured regular-grade Ti-6Al-4V and ELI-grade Ti-6Al-4V were biaxially, superplastically formed at slow strain rates at 871°C (1600°F) and 907°C (1665°F). A constant forming pressure was applied for 5 hours to obtain forming in all of the cones. Average strains were calculated from Equation (3) using the forming times after the alloy sheets first touched the cone surface. The low strain-rate cone-forming results are plotted in Figures 128 through 131 and compared with incremental-strain-rate test results. At the lower strain-rates, or longer forming times, the cone-forming data do not agree with the results of incremental-strain-rate tests,



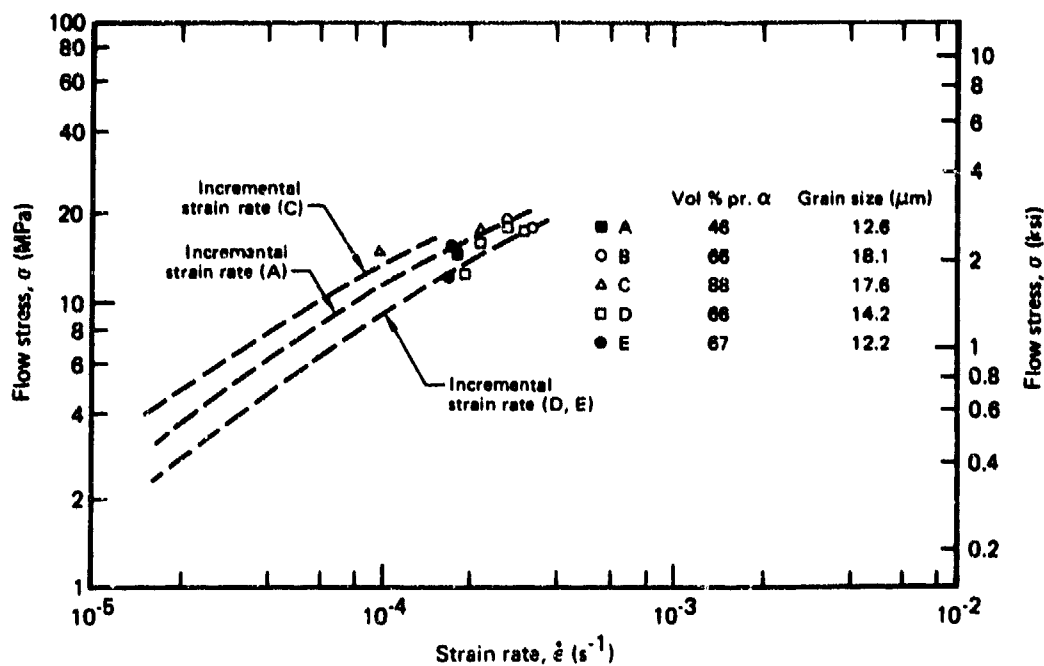
GP03-0249-158

Figure 123. Strain-rate dependence of flow stress at 907°C (1665°F) of normal-textured regular-grade Ti-6Al-4V determined from cone-forming tests (symbols) and incremental strain-rate tests (dashed curve).



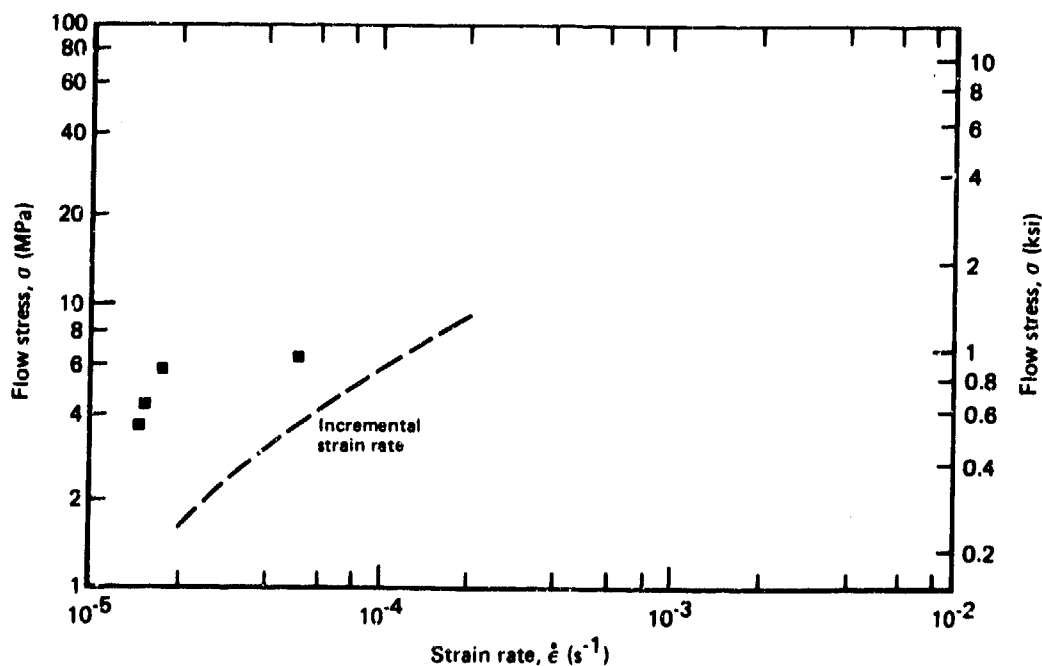
GP03-0249-160

Figure 124. Strain-rate dependence of flow stress at 907°C (1665°F) of normal-textured regular-grade Ti-6Al-4V determined from cone-forming tests (symbols) and incremental strain-rate tests (dashed curves).



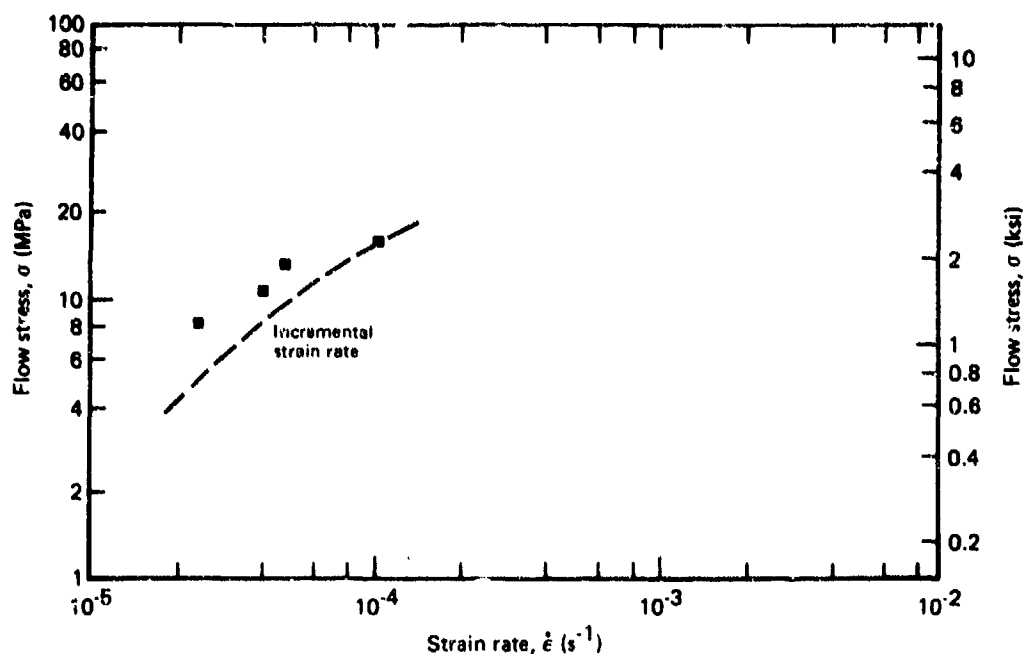
QP03-0249-181

Figure 125. Strain-rate dependence of flow stress at 907°C (1665°F) of normal-textured regular-grade Ti-6Al-4V determined from cone-forming tests (symbols) and incremental strain-rate tests (dashed curves).



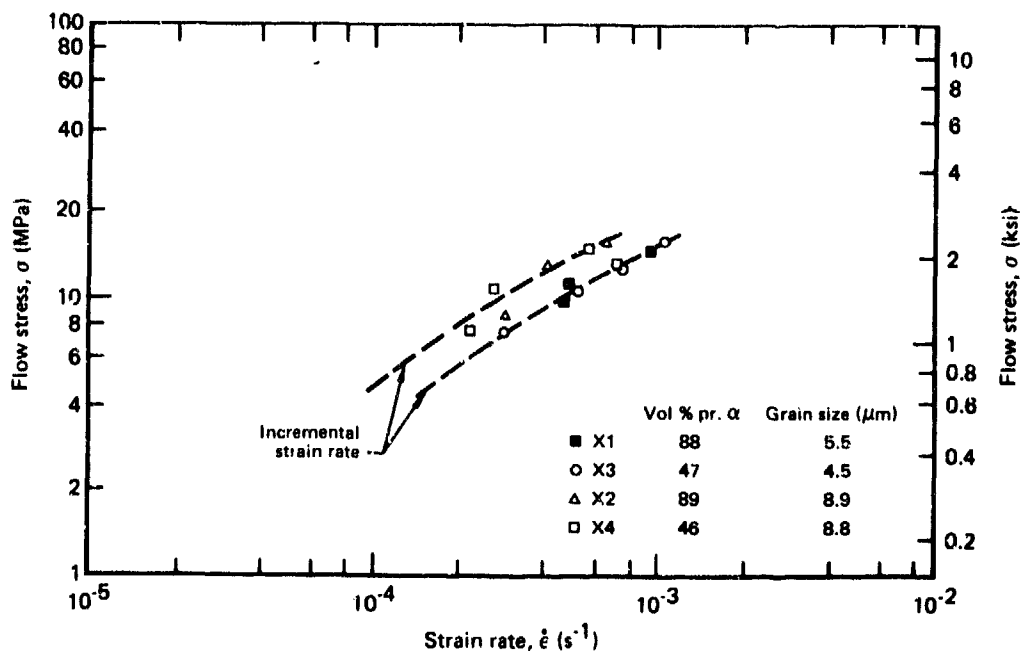
QP03-0249-184

Figure 126. Strain-rate dependence of flow stress at 907°C (1665°F) for normal-textured regular-grade Ti-6Al-4V determined from cone-forming tests (symbol) and incremental strain-rate tests (dashed curve); grain size = 6.0 μm , volume % primary alpha = 88.



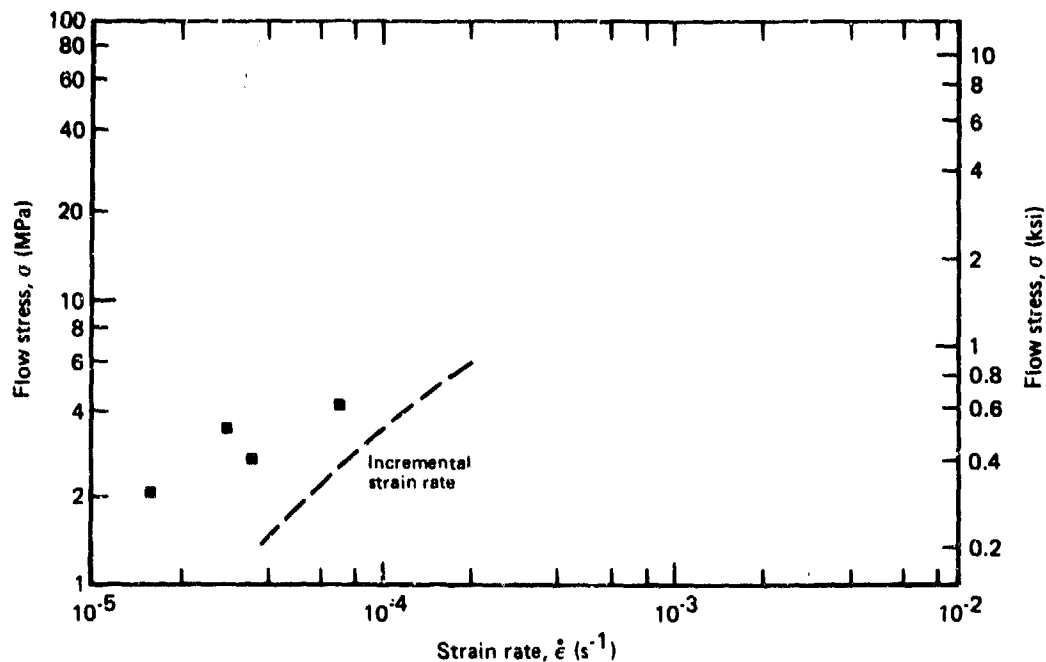
GP03-0240-166

Figure 127. Strain-rate dependence of flow stress at 871°C (1600°F) for normal-textured regular-grade Ti-6Al-4V determined from cone-forming tests (symbol) and incremental strain-rate tests (dashed curve); grain size = 6.0 μm , volume % primary α = 88.



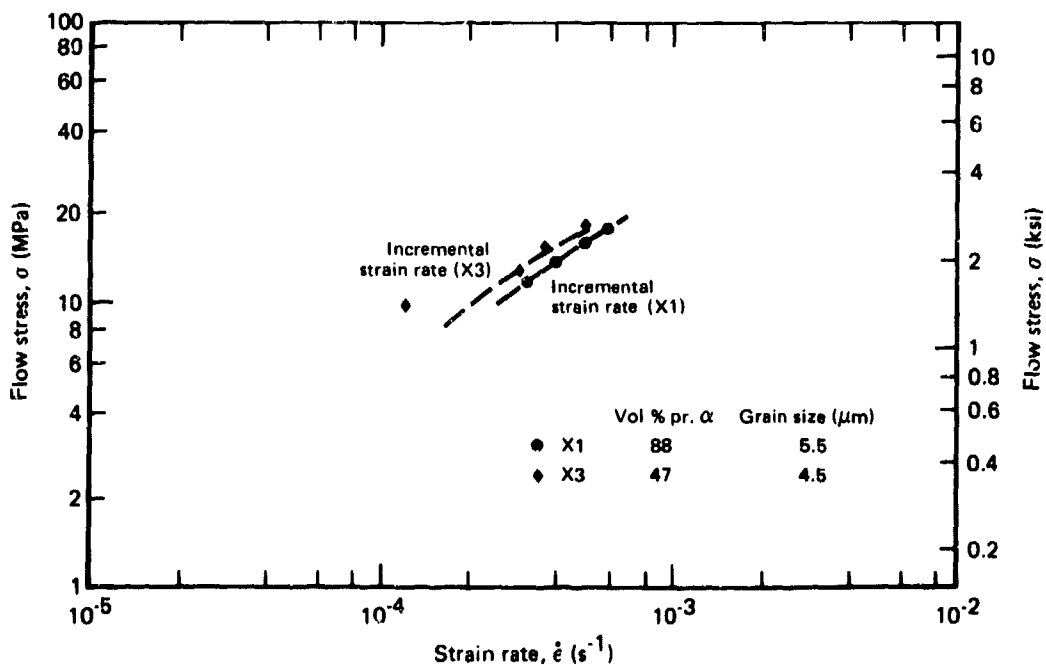
GP03-0240-166

Figure 128. Strain-rate dependence of flow stress at 907°C (1665°F) of ELI-grade Ti-6Al-4V determined from cone-forming tests (symbols) and incremental strain-rate tests (dashed curves).



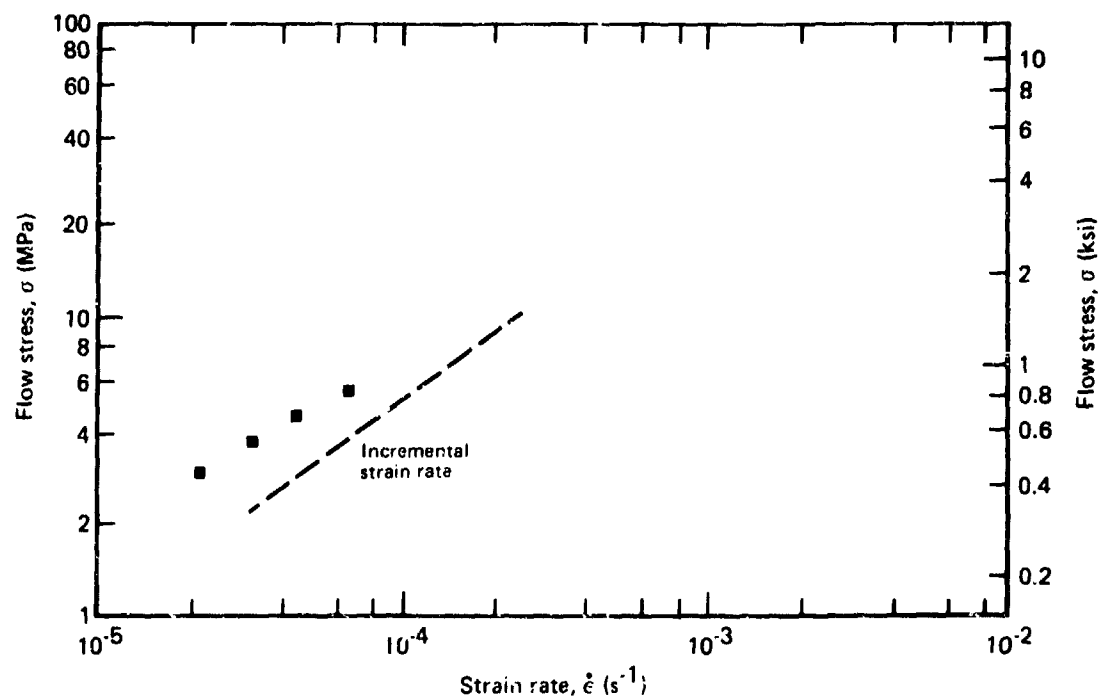
GP03-0246-163

Figure 129. Strain-rate dependence of flow stress at 907°C (1665°F) for normal-textured ELI-grade Ti-6Al-4V determined from cone-forming tests (symbol) and incremental strain-rate tests (dashed curve); grain size = 5.5 μm , volume % primary α = 88.



GP03-0246-162

Figure 130. Strain-rate dependence of flow stress at 871°C (1600°F) of ELI-grade Ti-6Al-4V determined from cone-forming tests (symbols) and incremental strain-rate tests (dashed curves).



GP03-0249-168

Figure 131. Strain-rate dependence of flow stress at 871°C (1600°F) for normal-textured ELI-grade Ti-6Al-4V determined from cone-forming tests (symbol) and incremental strain-rate tests (dashed curve); grain size = 5.5 μm , volume % primary alpha = 88.

which are low-strain, short-time tests. The incremental-strain-rate tests are not reliable for predicting superplastic forming involving large strains and long forming times, and the conical die or some other test method is thus required.

5.3 Grain-Growth During Superplastic Forming of Ti-6Al-4V

Alpha grain size measurements of regular-grade Ti-6Al-4V and ELI-grade Ti-6Al-4V were made with materials slowly cooled from a biaxial-forming temperature to evaluate effects of initial grain size, strain, time at temperature and volume fraction primary alpha at 907°C (1665°F). The linear intercept method was used to measure the alpha grain size. A minimum of six readings was used for each measurement. Alpha grain sizes were measured in two orthogonal directions to show any elongation effects of strain. The volume fraction of alpha-phase used for each alloy was the room temperature value from Tables 4 and 9.

For regular-grade Ti-6Al-4V microstructures having an initial primary alpha phase of 0.88, the alpha grain sizes for the largest cones are shown in Table 27. The equiaxed microstructure is maintained quite well in the biaxial conical die forming test for all of these microstructures. For all microstructures shown in Table 27, some recrystallization occurred at the highest strain. For microstructures $>7.6 \mu\text{m}$, this recrystallization is responsible for a small reduction in average alpha-grain size at the highest strain. For smaller grain sizes, a higher strain is required to initiate recrystallization. The most significant factor contributing to alpha-phase grain growth is time at temperature, with the highest alpha-phase grain growth occurring in the finer microstructures.

For regular-grade Ti-6Al-4V having an initial primary-alpha volume fraction of 0.45 and 0.56, the average alpha grain sizes after forming in a conical die at 907°C (1665°F) are shown in Tables 28 and 29. The grain growth of the alpha phase is similar for all of the equiaxed regular-grade microstructures of Ti-6Al-4V, and the volume fraction primary alpha had little influence on the alpha-phase grain growth.

TABLE 27. EFFECT OF SUPERPLASTIC STRAIN ON GRAIN GROWTH AT 907°C (1665°F) IN REGULAR-GRADE Ti-6Al-4V (INITIAL PRIMARY ALPHA VOLUME FRACTION = 88).

Initial primary alpha grain size (μm)	Total time at temperature (min)	Strain	Grain size (μm)
17.6	330	0	20.0
		0.23	21.0
		0.58	18.8*
12.2	330	0	13.0
		0.46	14.0
		1.03	13.5*
7.6	330	0	11.4
		0.52	13.8
		1.13	13.0*
6.0	330	0	10.0
		0.7	10.7
		0.78	10.8
		1.1	11.8
6.0	75	0	8.7
		0.5	10.0
		1.55	8.8*

*Partial recrystallization

GP03-0248-120

TABLE 28. EFFECTS OF SUPERPLASTIC STRAIN ON GRAIN GROWTH AT 907°C (1665°F) IN REGULAR-GRADE Ti-6Al-4V (INITIAL PRIMARY ALPHA VOLUME FRACTION = 66).

Initial primary alpha grain size (μm)	Total time at temperature (min)	Strain	Grain size (μm)
18.1	330	0	17.6
		0.35	17.6
		0.64	19.4
14.2	330	0	14.5
		0.43	15.9
		1.0	18.2
7.9	330	0	14.1
		0.46	12.9
		1.0	14.5
5.9	330	0	11.0
		0.57	12.6
		1.3	13.9

GP03-0248-121

TABLE 29. EFFECTS OF SUPERPLASTIC STRAIN ON GRAIN GROWTH AT 907°C (1665°F) IN REGULAR-GRADE Ti-6Al-4V (INITIAL PRIMARY ALPHA VOLUME FRACTION = 46).

Initial primary alpha grain size (μm)	Total time at temperature (min)	Strain	Grain size (μm)
12.6	330	0	14.4
		0.29	16.3
		0.53	15.9
7.2	330	0	11.3
		0.51	14.7
		0.93	16.8
4.4	330	0	10.8
		0.53	13.7
		1.25	11.3*

*Partial recrystallization

GP03-0248-122

Grain sizes after forming in a conical die at 871°C (1600°F) are given in Table 30 for regular grade Ti-6Al-4V panels that had a primary-alpha volume fraction of 0.88 and an initial grain size of 6.0 μm. The grain growth and the effects of strain are similar to results shown in Table 27 for forming at 907°C (1665°F).

Grain growth in conical die forming was measured for ELI grade Ti-6Al-4V for grain size of 5.6 μm which had a primary-alpha content of 0.88. These results are shown in Table 31. The kinetics of grain growth in ELI-grade Ti-6Al-4V in equiaxed microstructure follows closely the grain growth kinetics in regular-grade Ti-6Al-4V of similar grain size.

5.4 Effects of a Diffusion-Bonding Cycle on Superplastic Forming

The effects of a prior diffusion-bonding cycle on the superplastic, conical-die forming at 907°C (1665°F) were studied for normal-textured, regular-grade Ti-6Al-4V with the following coarse- and fine-grain microstructures: L (primary-alpha volume fraction = 0.88, grain size = 6.0 μm); E (primary-alpha volume fraction = 0.88, grain size = 12.2 μm); and J (primary-alpha volume fraction = 0.47, grain size = 4.4 μm). Microstructure X1 (primary-alpha volume fraction = 0.88, grain size = 5.6 μm) was selected for ELI-grade Ti-6Al-4V. The forming schedules were: (1) zero pressure at 907°C (1665°F) for 4.0 hour followed by 1.10 MPa (160 psi) at 907°C (1665°F) for 2.0 hour and (2) zero pressure at 907°C (1665°F) for 2.0 hours followed by 1.10 MPa (160 psi) for 2.5 hours. The times in these schedules do not include the initial 2.0 hour heating time to temperature, 0.25 hour dwell time at temperature, and pressurization time at the rate of 0.172 MPa/min (25 psi/min).

The average strain rates calculated from conical-die forming are compared with strain rates obtained from uniaxial incremental-strain-rate test data at 907°C (1665°F) in Figures 132 through 135. For all microstructures, good agreement at 907°C (1665°F) is observed between strain rates in biaxial conical-die forming with strain rates predicted from uniaxial incremental-strain-rate test data for conical-die forming times up to one hour. For forming times greater than one hour, strain rates become significantly reduced with increasing forming times. Holding at temperature to simulate the diffusion bonding cycle reduces the strain-rate compared to direct forming for all the microstructures.

TABLE 30. EFFECTS OF SUPERPLASTIC STRAIN ON GRAIN GROWTH AT 871°C (1600°F) IN REGULAR-GRADE Ti-6Al-4V (INITIAL PRIMARY ALPHA VOLUME FRACTION = 38).

Initial primary alpha grain size (μm)	Total time at temperature (min)	Strain	Grain size (μm)
6.0	330	0.0	10.0
		0.55	11.5
		1.88	11.2*

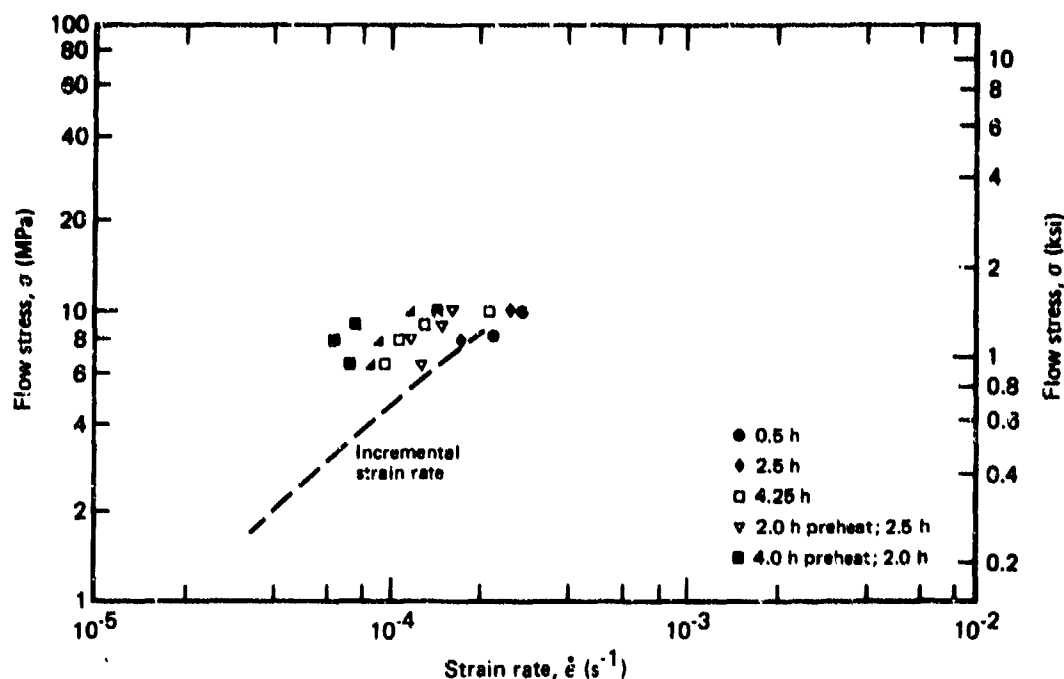
*Partial recrystallization

QP03-0249-123

TABLE 31. EFFECTS OF SUPERPLASTIC STRAIN ON GRAIN GROWTH IN ELI-GRADE Ti-6Al-4V.

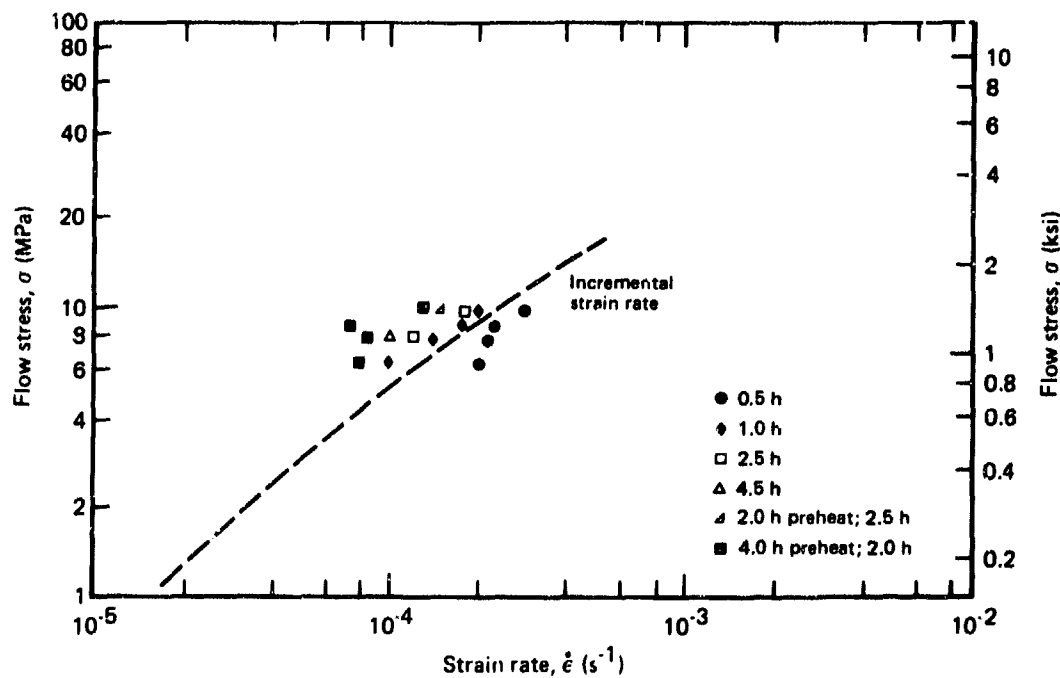
Initial primary alpha grain size (μm)	Temperature °C (°F)	Time (min)	Strain	Grain size (μm)
5-6	970 (1665)	330	0	9.5
			0.9	9.9
			1.2	10.3
5-6	970 (1665)	70	0	8.3
			0.56	9.0
			1.58	9.9
5-6	871 (1600)	330	0	9.0
			0.35	9.7
			0.77	10.4

QP03-0249-124



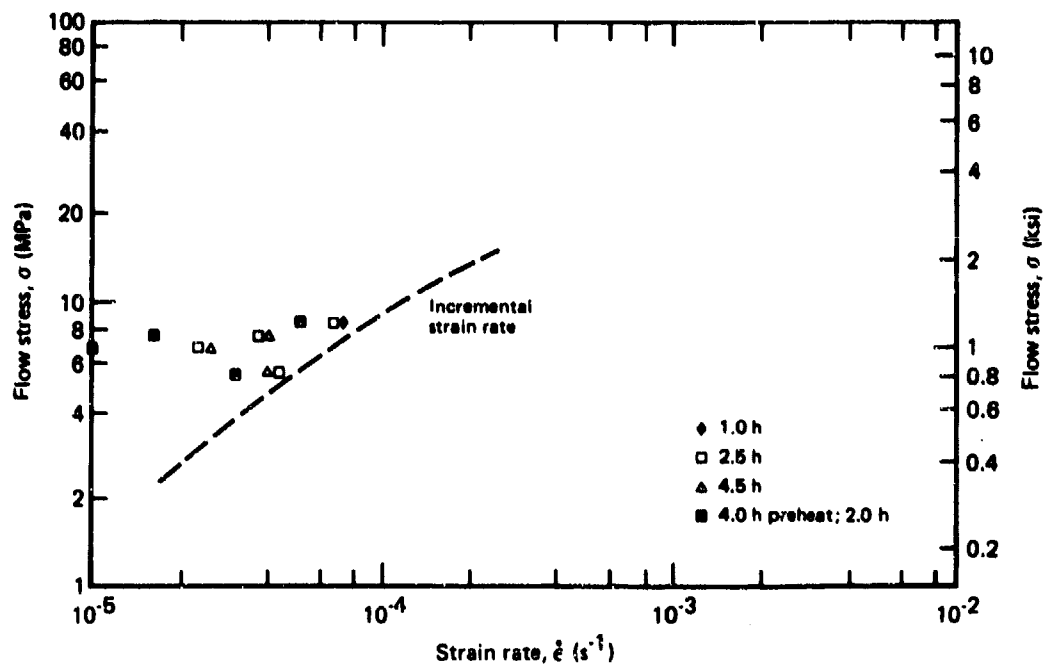
GP03-0246-167

Figure 132. Strain-rate dependence of flow stress at 907°C (1665°F) for regular-grade Ti-6Al-4V determined from cone-forming tests (symbols) and incremental strain-rate tests (dashed curve); specimen J, grain size = 4.4 μm , volume % primary alpha = 47.



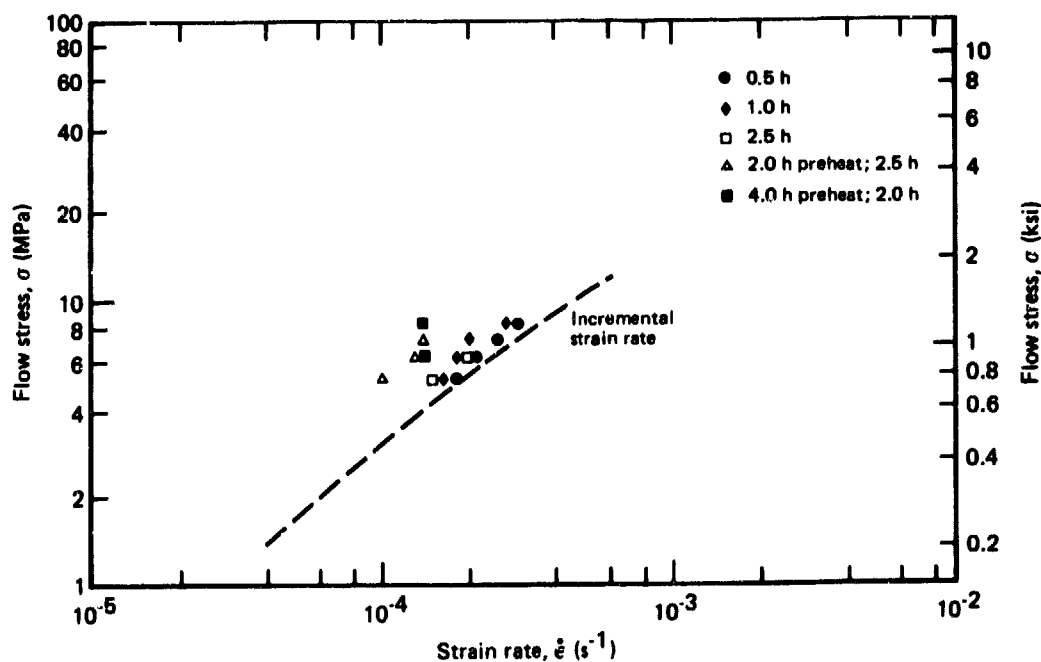
GP03-0246-168

Figure 133. Strain-rate dependence of flow stress at 907°C (1665°F) for regular-grade Ti-6Al-4V determined from cone-forming tests (symbols) and incremental strain-rate tests (dashed curve); specimen L, grain size = 6.0 μm , volume % primary alpha = 88.



GP03-0246-160

Figure 134. Strain-rate dependence of flow stress at 907°C (1665°F) for regular-grade Ti-6Al-4V determined from cone-forming tests (symbols) and incremental strain-rate tests (dashed curve); specimen E, grain size = 12.2 μ m, volume % primary alpha = 88.



GP03-0246-170

Figure 135. Strain-rate dependence of flow stress at 907°C (1665°F) for ELI-grade Ti-6Al-4V determined from cone-forming tests (symbols) and incremental strain-rate tests (dashed curve); specimen X1, grain size = 5.5 μ m, volume % primary alpha = 88.

The largest cone in each of these tests were sectioned into two equal pieces. One-half of the cone was heated to 907°C (1665°F) in a vacuum to establish the microstructure at the forming conditions, and it was subsequently quenched in water. The other half of the cone represents the microstructure obtained by slow cooling in furnace. The grain sizes at the conclusion of forming are shown for regular-grade Ti-6Al-4V and ELI-grade Ti-6Al-4V in Tables 32 through 35. Results in these tables are the average of six separate measurements per condition. The alpha grain size for slow cooling was measured by the linear-intercept method. The alpha grain size and beta grain size in water-quenched specimens were determined by measurements of sizes of individual grains along six separate lines drawn on micrographs. Figures 136 and 137 show typical water-quenched micrographs of regular-grade Ti-6Al-4V with an initial grain size of 6.0 μm and ELI-grade Ti-6Al-4V with an initial grain size of 5.5 μm .

The following conclusions can be made from these tests:

1. The grain size remains equiaxed during all of the forming cycles.
2. The most important parameter affecting grain growth is time at temperature.
3. Grain growth was basically the same in normal-textured, regular-grade Ti-6Al-4V and ELI-grade Ti-6Al-4V.
4. The volume percent of beta phase increases in highly-strained, superplastically-formed, regular-grade Ti-6Al-4V and ELI-grade Ti-6Al-4V with time at temperature. The volume fraction alpha-phase measured at the bottom of the cone of water-quenched specimens for ELI-grade microstructure X1 (Q88 α , 5.5 μm) after 0.5 hour forming cycle at 907°C (1665°F) was 0.68 and after 0 psi for two hour plus 160 psi for 2.5 hour forming cycle at 907°C (1665°F) was 0.55 (Table 35).

5.5 Biaxial Cone-Forming of Basal-Textured and Transverse-Basal-Textured Ti-6Al-4V

Biaxial conical-die forming tests were performed at the slower strain rates at 907°C (1665°F) using a five-hour, constant-pressure, forming period for basal-textured and transverse-basal-textured Ti-6Al-4V. The results are shown in Figure 138. Slow forming rates were observed for the transverse-basal-texture, which is in agreement with incremental-strain-rate test data. The strain rates observed for basal-textured and transverse-basal-textured Ti-6Al-4V are similar to strain rates of normal-textured regular-grade Ti-6Al-4V having a comparable grain size (See Figure 128).

TABLE 32. EFFECTS OF FORMING CYCLES AT 907°C (1665°F) ON GRAIN GROWTH IN NORMAL-TEXTURED REGULAR-GRADE Ti-6Al-4V, PANEL J (GRAIN SIZE = 4.4 μm , VOLUME % PRIMARY ALPHA = 47).

Forming cycle (h)	Total strain, ϵ	Alpha grain size at forming temperature (μm)	Beta grain size at forming temperature (μm)	Final alpha grain size on slow cooling (μm)
0.5	0	7.2	7.1	7.4
0.5	4.0	9.0	8.3	9.4
1.0	0	6.4	7.3	6.6
1.0	1.17	7.7	7.8	8.6
2.5	0	7.1	6.6	7.8
2.5	2.1	9.8	10.4	10.5
4.25		8.9	8.5	8.4
4.25	2.7	9.8	10.2	10.6
0 MPa, 2.0 + 1.1 MPa, 2.5	0	8.9	6.3	9.3
0 MPa, 2.0 + 1.1 MPa, 2.5	1.8	11.4	7.1	11.9

GP03-0246-183

TABLE 33. EFFECTS OF FORMING CYCLE AT 907°C (1665°F) ON GRAIN GROWTH IN NORMAL-TEXTURED REGULAR-GRADE Ti-6Al-4V, PANEL K (GRAIN SIZE = 6.0 μm , VOLUME % PRIMARY ALPHA = 88).

Forming cycle (h)	Total strain, ϵ	Alpha grain size at forming temperature (μm)	Beta grain size at forming temperature (μm)	Final alpha grain or slow forming (μm)
0.5	0	7.2	7.0	10.5
0.5	0.7	8.1	9.4	
1.0	0	7.1	7.5	8.3
1.0	0.9	8.4	7.6	9.7
2.5	0	7.1	7.0	8.9
2.5	1.9	8.3	8.2	10.3*
4.25	0	8.6	6.9	10.9
4.25	1.7	9.2	8.7	11.1*
0 MPa, 2.0 + 1.1 MPa, 2.5	0	11.7	9.8	12.1
0 MPa, 2.0 + 1.1 MPa, 2.5	1.4	11.7	7.2	10.3

*Smaller size cone, 30.5 mm (1.2 in.)

GP03-0246-188

TABLE 35. EFFECTS OF FORMING CYCLE AT 907°C (1665°F) ON GRAIN GROWTH IN ELI-GRADE Ti-6Al-4V, PANEL X1 (GRAIN SIZE = 5.5 μm , VOLUME % PRIMARY ALPHA = 88).

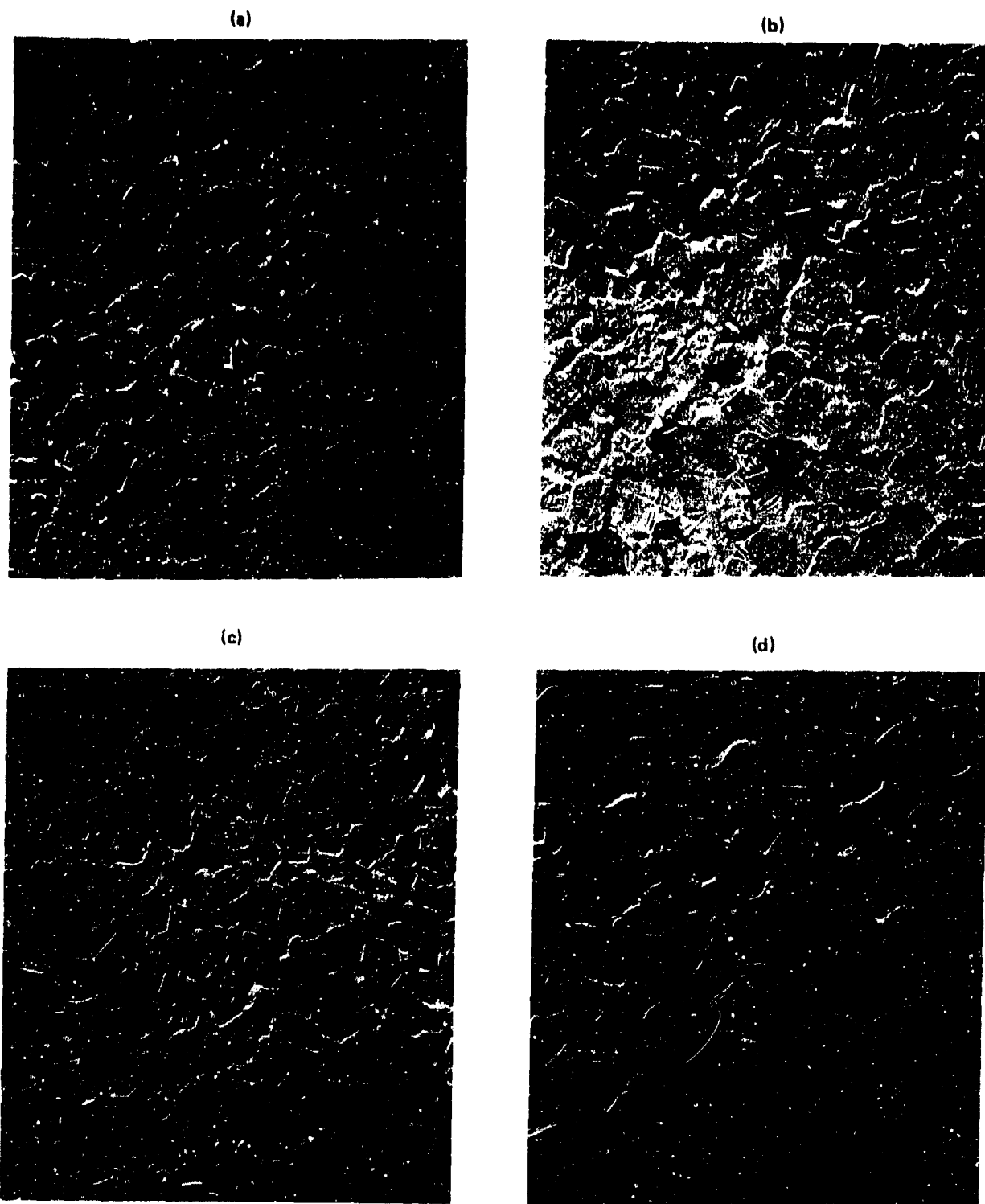
Forming cycle (h)	Total strain, ϵ	Alpha grain size at forming temperature (μm)	Beta grain size at forming temperature (μm)	Final alpha grain or slow cooling (μm)
0.5	0	6.2	7.2	7.2
0.5	0.8	7.5	6.8	8.5
1.0	0	6.2	7.8	7.1
1.0	1.3	7.3	8.1	8.6
2.5	0	6.3	7.2	7.9
2.5	2.1	8.3	8.4	10.4
0 MPa, 2.0 + 1.1 MPa, 2.5	0	7.0	7.3	8.1
0 MPa, 2.0 + 1.1 MPa, 2.5	1.5	8.9	8.9	9.8

GP03-0248-185

TABLE 34. EFFECTS OF FORMING CYCLE AT 907°C (1665°F) ON GRAIN GROWTH IN NORMAL-TEXTURED REGULAR-GRADE Ti-6Al-4V, PANEL E (GRAIN SIZE = 12.2 μm , VOLUME % PRIMARY ALPHA = 88).

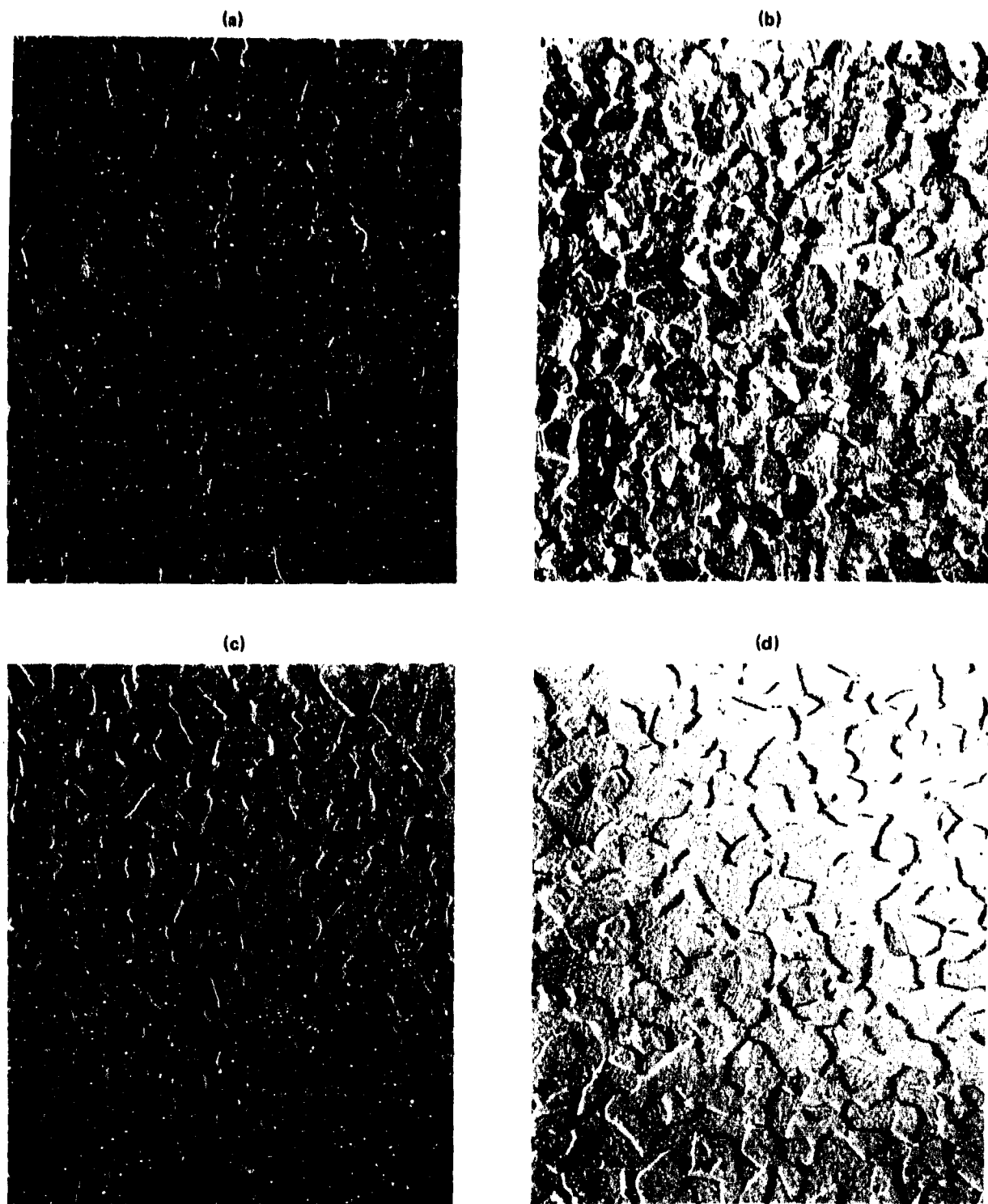
Forming cycle (h)	Total strain, ϵ	Alpha grain size at forming temperature (μm)	Beta grain size at forming temperature (μm)	Final alpha grain size or slow cooling (μm)
0.5	0	8.0	7.7	10.9
0.5	0.30	8.9	8.1	10.5
1.0	0	8.5	9.0	9.7
1.0	0.41	10.1	9.4	10.1
2.5	0	7.6	8.8	10.8
2.5	0.80	10.5	8.9	11.8
4.25	0	10.5	12.0	11.5
4.25	1.3	11.2	11.9	12.8
0 MPa, 2.0 + 1.1 MPa, 2.5	0	10.2	9.8	10.3
0 MPa, 2.0 + 1.1 MPa, 2.5	0.67	11.4	10.9	12.3

GP03-0243-184



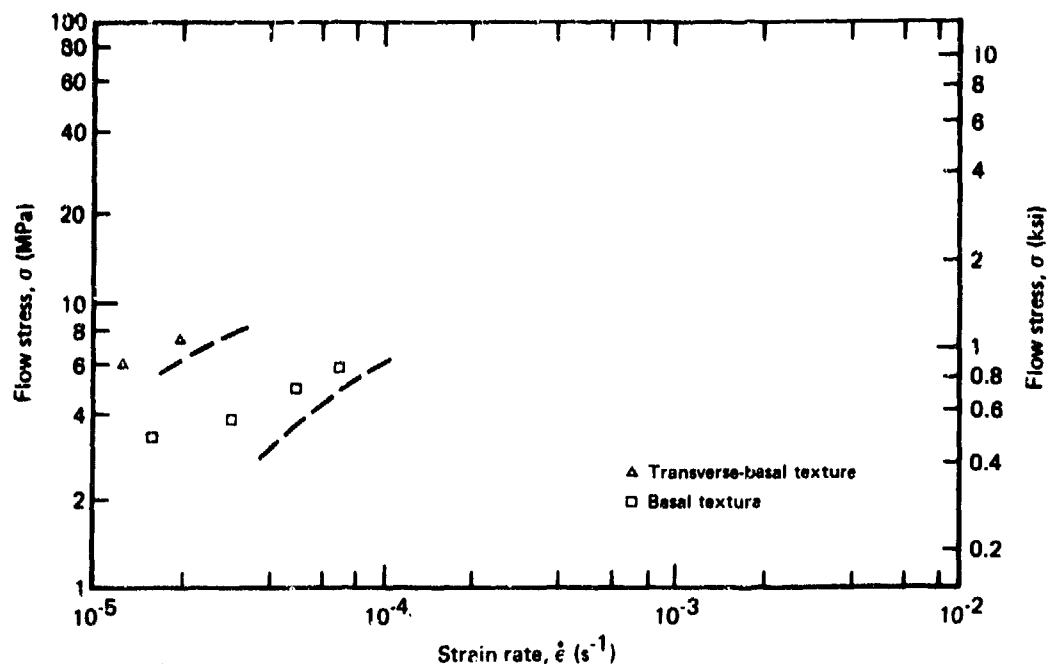
GP03-0249.217

Figure 136. Photomicrographs of water-quenched specimens of superplastically-formed normal-textured regular-grade Ti-6Al-4V (initial grain size = $6.0\ \mu\text{m}$, volume % primary $\alpha = 88$) with a forming temperature of 907°C (1665°F) for (a) 1.0 h, strain = 0, (b) 1.0 h, strain = 0.9, (c) 4.25 h, strain = 0, and (d) 4.25 h, strain = 1.7.



GP03-0249-216

Figure 137. Photomicrographs of water-quenched specimens of superplastically-formed normal-textured ELI-grade Ti-6Al-4V (initial grain size = $5.5 \mu\text{m}$, volume % primary alpha = 88) with a forming temperature of 870°C (1600°F) for (a) 0.5 h, strain = 0, (b) 0.5 h, strain = 0.8, (c) 2.5 h, strain = 0, and (d) 2.5 h, strain = 2.1.



GP03-0246-171

Figure 138. Strain-rate dependence of flow stress at 907°C (1665°F) for basal and transverse-basal texture Ti-6Al-4V determined from cone-forming tests (symbols) and incremental strain-rate tests (dashed curves).

Biaxial conical-die forming tests were also made at 870°C (1600°F) for basal-textured and transverse-basal-textured Ti-6Al-4V at slow strain rates, and the results are shown in Table 36. From these biaxial forming tests and incremental-strain-rate test data, it was concluded that texturing (basal-texture and transverse-basal-texture) had very little adverse effect on the superplastic forming properties of Ti-6Al-4V.

TABLE 36. COMPARISONS OF SUPERPLASTIC STRAIN RATES AT 871°C (1600°F) DETERMINED FROM CONE-FORMING TESTS AND LABORATORY INCREMENTAL STRAIN-RATE TESTS.

Alloy microstructure	Diam of cone mm (in.)	Stress in cone MPa (psi)	Forming pressure MPa (psi)	Final depth in cone mm (in.)	Strain in cone, ϵ	Strain rate in cone (s ⁻¹)	Strain rate from laboratory tests (s ⁻¹)	Strain from laboratory tests, ϵ
Transverse-basal texture	37.7 (1.485)	16.8 (2440)	1.72 (250)	14.1 (0.555)	0.16	2.2×10^{-4}	4.3×10^{-5}	0.38
Basal texture	37.3 (1.468)	13.85 (1980)	1.72 (250)	17.2 (0.677)	0.35	3.3×10^{-5}	3.0×10^{-5}	0.32
	31.1 (1.225)	11.3 (1640)	1.72 (250)	10.7 (0.421)	0.11	1.6×10^{-5}	2.5×10^{-5}	0.19

GP03-0246-126

5.6 Biaxial Conical-Die Forming of Ti-6Al-4V with Anomalous Microstructure

Conical biaxial forming tests were performed at 870°C (1600°F) and at 907°C (1665°F) with banded Ti-6Al-4V, blocky alpha Ti-6Al-4V, and elongated alpha Ti-6Al-4V. The Ti-6Al-4V banded microstructures O (Level I) and OI (Level II) had high forming rates at 870°C (1600°F), and 907°C (1665°F). The biaxial cone forming rates are shown for Ti-6Al-4V banded microstructure O (Level I) in Figure 139 along with data from incremental strain-rate tests. These biaxial forming tests confirm the conclusion from incremental strain-rate tests that superplasticity in Ti-6Al-4V with banded microstructures were controlled by the fine primary alpha phase and were not adversely affected by the low level of worked Widmanstätten alpha phase.

The biaxial conical die forming rates at 907°C (1665°F) are shown in Figure 140 for Ti-6Al-4V with blocky microstructures N (Level I), and NI (Level II) (described in Section III). The biaxial forming rates appear to be controlled by the matrix alpha phase grains, and the larger "blocky" alpha grains for both microstructures had little influence on superplastic flow properties. The Ti-6Al-4V with "blocky" alpha microstructures had biaxial forming rates at 907°C (1665°F) similar to regular-grade Ti-6Al-4V microstructure E (0.88 α , 12.2 μ m) (See Figure 125).

Slow biaxial forming rates were observed for elongated alpha microstructures. Forming in the conical die occurred only in the largest cones. The results of forming at 870°C (1600°F) and 907°C (1665°F) are shown in Table 37 and Table 38. The two levels of elongated alpha demonstrated essentially equivalent forming stresses in biaxial conical die forming. These rates compare favorably with incremental strain-rate data for elongated alpha Ti-6Al-4V microstructures. Both levels of elongated alpha Ti-6Al-4V showed the adverse affects of elongated alpha grains compared to equiaxed regular grade Ti-6Al-4V.

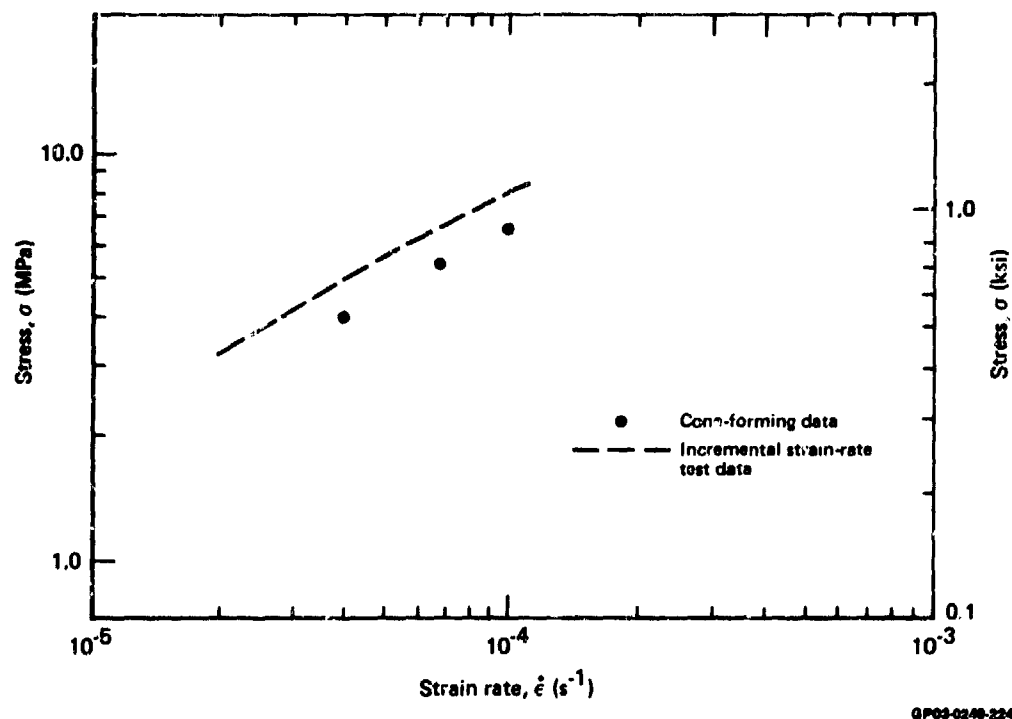


Figure 139. Strain-rate dependence of flow stress at 907°C (1665°F) of banded Ti-6Al-4V (panel O) determined from cone-forming and laboratory incremental strain-rate tests.

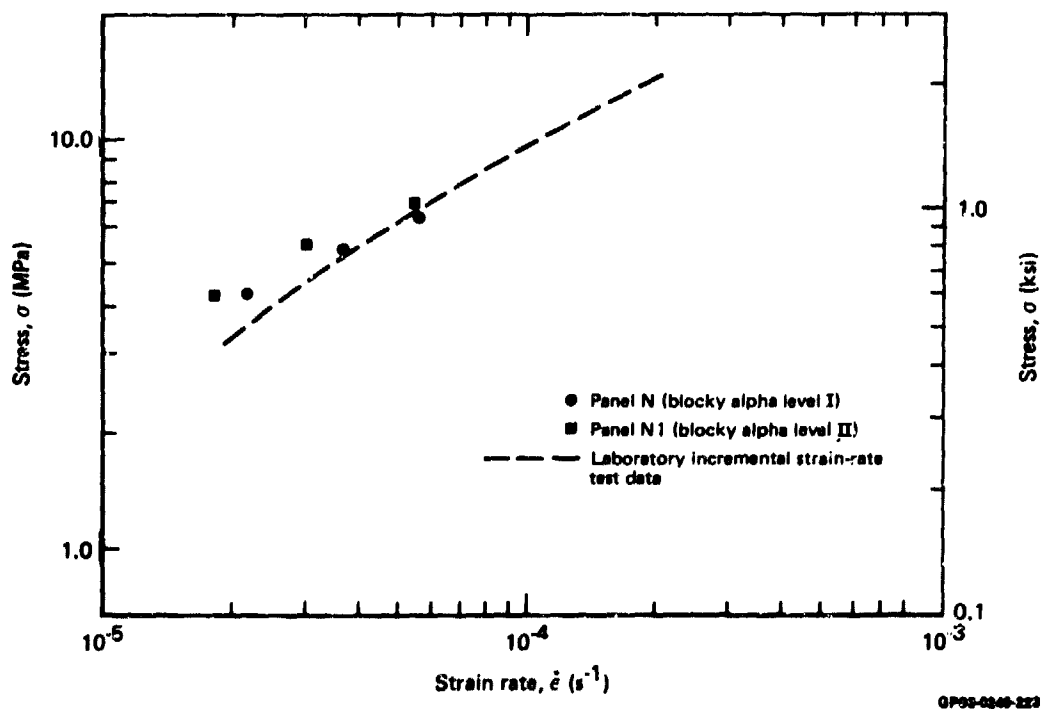


Figure 140. Strain-rate dependence of flow stress at 907°C (1665°F) of blocky alpha Ti-6Al-4V (panels N and N1) determined from cone-forming and laboratory incremental strain-rate tests.

TABLE 37. COMPARISONS OF SUPERPLASTIC STRAIN RATES AT 871°C (1600°F)
DETERMINED FROM CONE-FORMING TESTS AND LABORATORY
INCREMENTAL STRAIN-RATE TESTS.

Alloy microstructure	Diam of cone mm (in.)	Stress in cone MPa (psi)	Final depth in cone mm (in.)	Strain in cone, ε	Strain rate in cone (s ⁻¹)	Strain rate from laboratory tests (s ⁻¹)	Strain from laboratory tests, ε
Elongated alpha, Level I	37.4 (1.474)	17.6 (2550)	25.8 (1.018)	1.1	8.5×10^{-5}	6.6×10^{-5}	0.85
	31.2 (1.227)	14.7 (2135)	11.9 (0.467)	0.17	2.4×10^{-5}	4.6×10^{-5}	0.33
Elongated alpha, Level II	37.7 (1.485)	15.5 (2250)	27.6 (1.083)	1.36	9.7×10^{-5}	2.0×10^{-5}	0.28
	34.0 (1.34)	13.9 (2020)	14.9 (0.587)	0.50	5.3×10^{-5}	1.62×10^{-5}	0.15
	30.0 (1.18)	12.2 (1770)	10.6 (0.416)	0.11	2.2×10^{-5}	1.22×10^{-5}	0.06
Blocky alpha, Level I	37.3 (1.468)	15.9 (2280)	23.1 (0.910)	0.82	6.3×10^{-5}	8.1×10^{-5}	1.05
	31.1 (1.225)	11.8 (1710)	10.8 (0.425)	0.12	2.4×10^{-5}	5.2×10^{-5}	0.41
Block alpha, Level II	37.3 (1.468)	15.6 (2260)	23.1 (0.910)	0.82	6.3×10^{-5}	9.8×10^{-5}	1.28
	31.5 (1.241)	13.1 (1900)	12.8 (0.505)	0.235	3.0×10^{-5}	7.4×10^{-5}	0.58
	25.4 (1.0)	10.4 (1510)	8.89 (0.350)	0.127	2.5×10^{-5}	5.2×10^{-5}	0.41
Banding, Level I	37.4 (1.474)	15.9 (2310)	28.3 (1.116)	1.55	9.2×10^{-5}	1.8×10^{-4}	3.03
	31.2 (1.227)	13.2 (1910)	16.9 (0.667)	0.58	4.5×10^{-5}	1.27×10^{-4}	1.64
	25.4 (1.0)	10.4 (1510)	10.9 (0.430)	0.29	3.0×10^{-5}	8.6×10^{-5}	1.1
Banding, Level II	31.5 (1.241)	13.5 (1965)	17.7 (0.698)	0.635	4.9×10^{-5}	7.8×10^{-5}	1.01
	25.4 (1.0)	10.8 (1560)	10.3 (0.405)	0.24	3.0×10^{-5}	5.0×10^{-5}	0.40

* Failed in cone

GP03-0248-127

TABLE 38. COMPARISONS OF SUPERPLASTIC STRAIN RATES AT 907°C (1665°F)
DETERMINED FROM CONE-FORMING TESTS AND LABORATORY
INCREMENTAL STRAIN-RATE TESTS.

Alloy microstructure	Diam of cone mm (in.)	Stress in cone MPa (psi)	Final depth in cone mm (in.)	Strain in cone, ε	Strain rate in cone (s ⁻¹)	Strain rate from laboratory tests (s ⁻¹)	Strain from laboratory tests, ε
Elongated, Level I	37.7 (1.485)	6.83 (990)	19.2 (0.757)	0.47	3.0×10^{-5}	3.3×10^{-5}	0.51
	34.0 (1.34)	6.13 (890)	12.75 (0.502)	0.17	1.4×10^{-5}	2.65×10^{-5}	0.30
Elongated, Level II	37.3 (1.468)	7.58 (1100)	18.9 (0.743)	0.46	3.0×10^{-5}	4×10^{-5}	0.61
Blocky alpha, Level I	37.3 (1.468)	6.31 (915)	24.0 (0.944)	0.93	5.5×10^{-5}	5.3×10^{-5}	0.9
	31.5 (1.241)	5.31 (770)	16.9 (0.664)	0.56	3.6×10^{-5}	4.1×10^{-5}	0.63
	25.4 (1.0)	4.21 (610)	11.2 (0.442)	0.33	2.2×10^{-5}	2.9×10^{-5}	0.43
Block alpha, Level II	37.4 (1.474)	6.90 (1000)	24.05 (0.947)	0.91	5.4×10^{-5}	5.0×10^{-5}	0.85
	31.2 (1.227)	5.68 (824)	15.7 (0.617)	0.46	3.0×10^{-5}	3.7×10^{-5}	0.56
	25.4 (1.0)	4.58 (664)	10.4 (0.410)	0.25	1.8×10^{-5}	2.75×10^{-5}	0.35
Banding, Level I	37.3 (1.468)	—	33.3 (1.31)*	—	—	—	—
	31.1 (1.225)	6.14 (890)	24.1 (0.950)	1.786	1.0×10^{-4}	7.0×10^{-5}	1.26
	25.4 (1.0)	4.96 (720)	18.3 (0.722)	1.4	7.8×10^{-5}	4.6×10^{-5}	0.83
	19.7 (0.777)	3.79 (550)	10.6 (0.416)	0.6	4×10^{-5}	2.8×10^{-5}	0.42

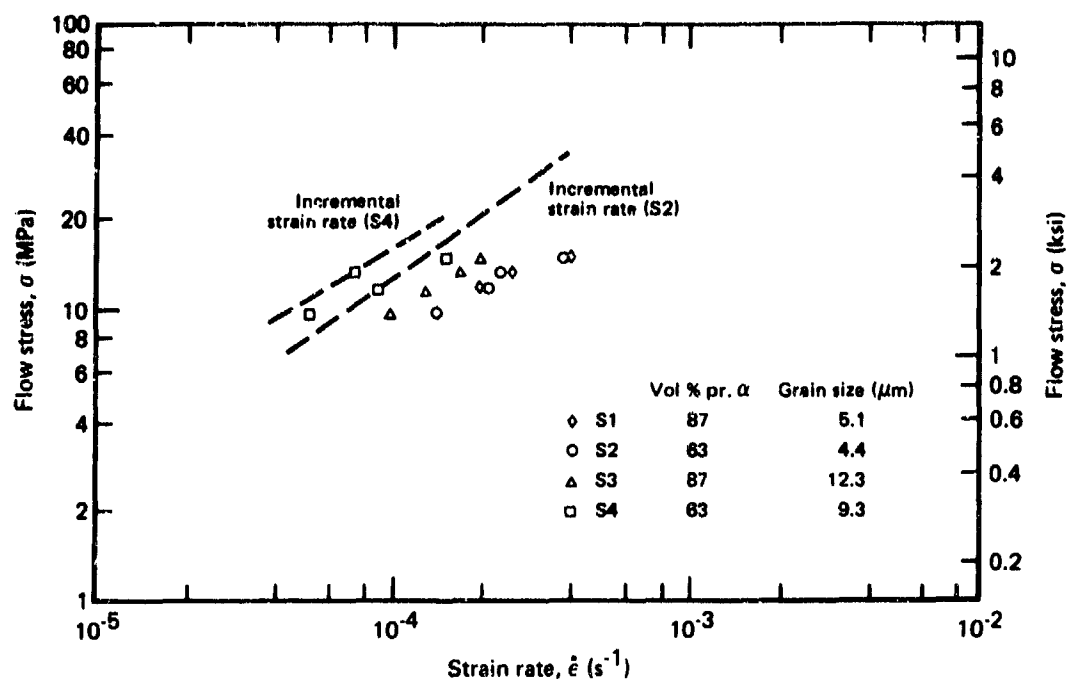
* Failed in cone

GP03-0248-128

5.7 Biaxial Conical-Die Forming of Simulated-Coil Ti-6Al-4V

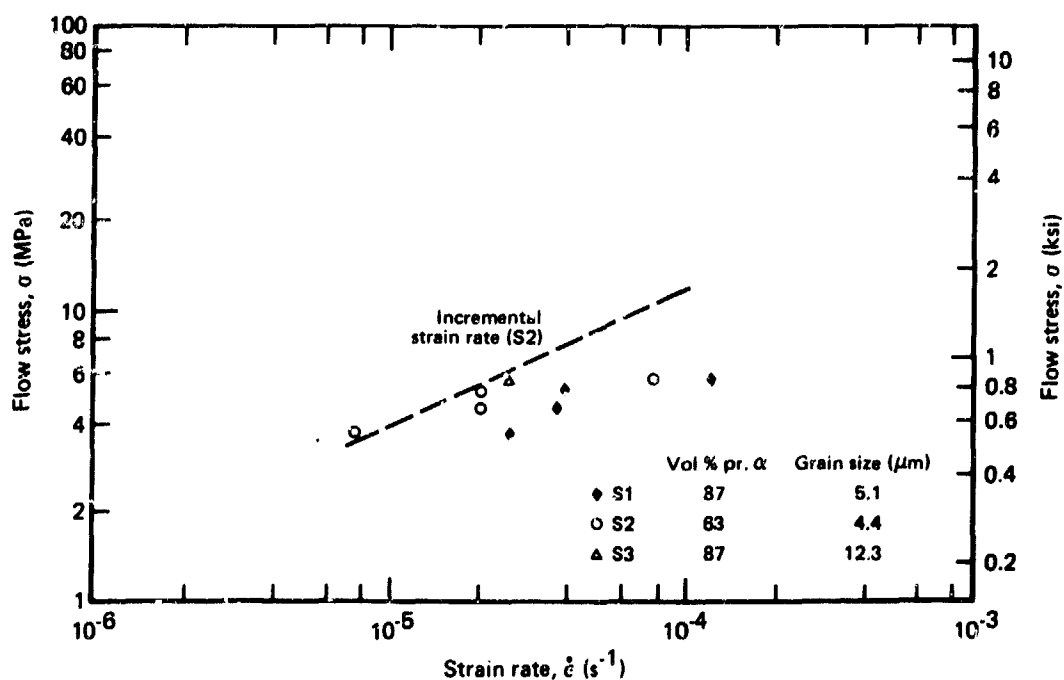
Biaxial conical-die forming tests were performed at 907°C (1665°F) for simulated-coil Ti-6Al-4V. Results at high forming rates and short forming times are shown in Figure 141. The flow stresses in simulated-coil Ti-6Al-4V in biaxial conical-die forming are comparable with those obtained for regular-grade, Ti-6Al-4V (see Figures 123 through 125). The flow stresses from incremental-strain-rate tests on simulated-coil Ti-6Al-4V were higher than those obtained from regular-grade, Ti-6Al-4V. The specimens for uniaxial incremental-strain-rate tests were taken from the longitudinal or rolling direction of the sheet material. These results indicate that the higher flow stresses observed in incremental-strain-rate tests arise from the processing procedures used in making simulated-coil-Ti-6Al-4V sheet material. Biaxial conical-die forming tests at slower strain rates and longer forming times were made on simulated-coil Ti-6Al-4V at 907°C (1665°F) and 870°C (1600°F). These results are shown in Figures 142 and 143, respectively. The flow stresses for simulated coil-rolled Ti-6Al-4V obtained by conical-die forming approached the flow stresses measured by incremental-strain-rate tests as the strain rate decreased. In contrast, at the longer forming times (5 hour) at 870°C (1600°F) and 907°C (1665°F) for regular-grade, Ti-6Al-4V, grain growth reduced the conical-die strain rates below the incremental-strain-rate test values. It should be pointed out that the conical die strain rates were reduced for the same flow stress at the slower strain rates and longer forming times in simulated coil-rolled Ti-6Al-4V.

The alpha grain size in the largest cone formed at 907°C (1665°F) with forming time of 5.0 hours of microstructure S1 (primary-alpha volume fraction = 0.87, grain size = 5.1 μm) was 10 μm . The grain growth in this microstructure of simulated-coil Ti-6Al-4V was similar to the grain growth for microstructure L (primary - alpha volume fracture = 0.88, grain size = 6.0 μm) (See Table 27). The increase in the flow stresses caused by grain growth during conical-die forming at the longer forming times in simulated-coil Ti-6Al-4V appears to diminish the differences in the flow stresses between incremental-strain-rate tests and conical-die forming observed at the higher strain rates and short forming times.



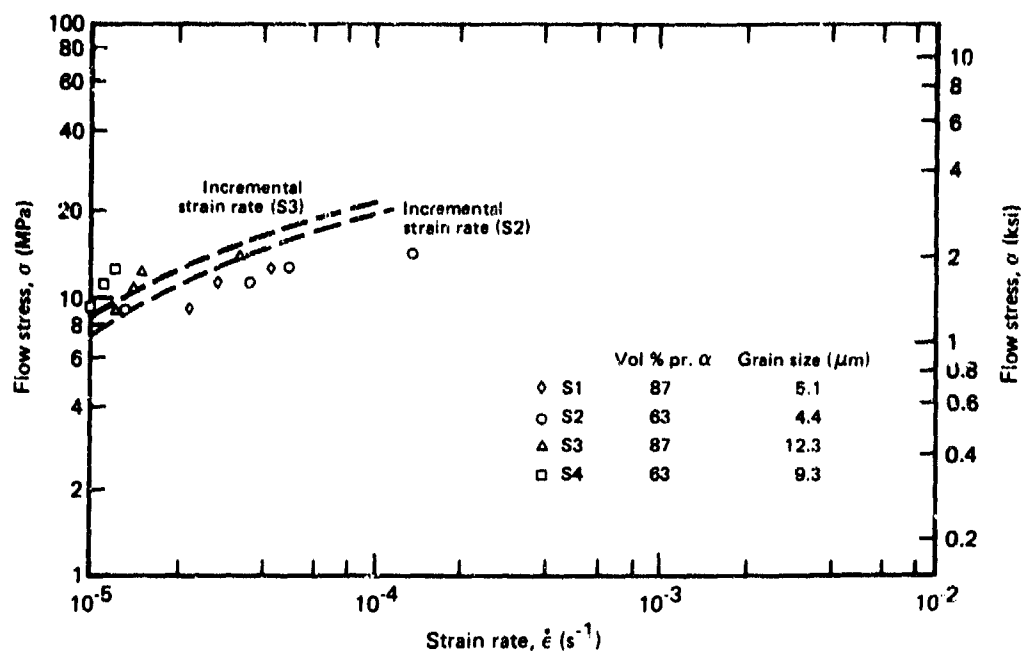
GP03-0248-172

Figure 141. Strain-rate dependence of flow stress at 907°C (1665°F) of simulated-coil Ti-6Al-4V determined from cone-forming tests (symbols) and incremental strain-rate tests (dashed curves).



GP03-0248-173

Figure 142. Strain-rate dependence of flow stress at 907°C (1665°F) for simulated-coil Ti-6Al-4V determined from cone-forming tests (symbols) and incremental strain-rate tests (dashed curve).



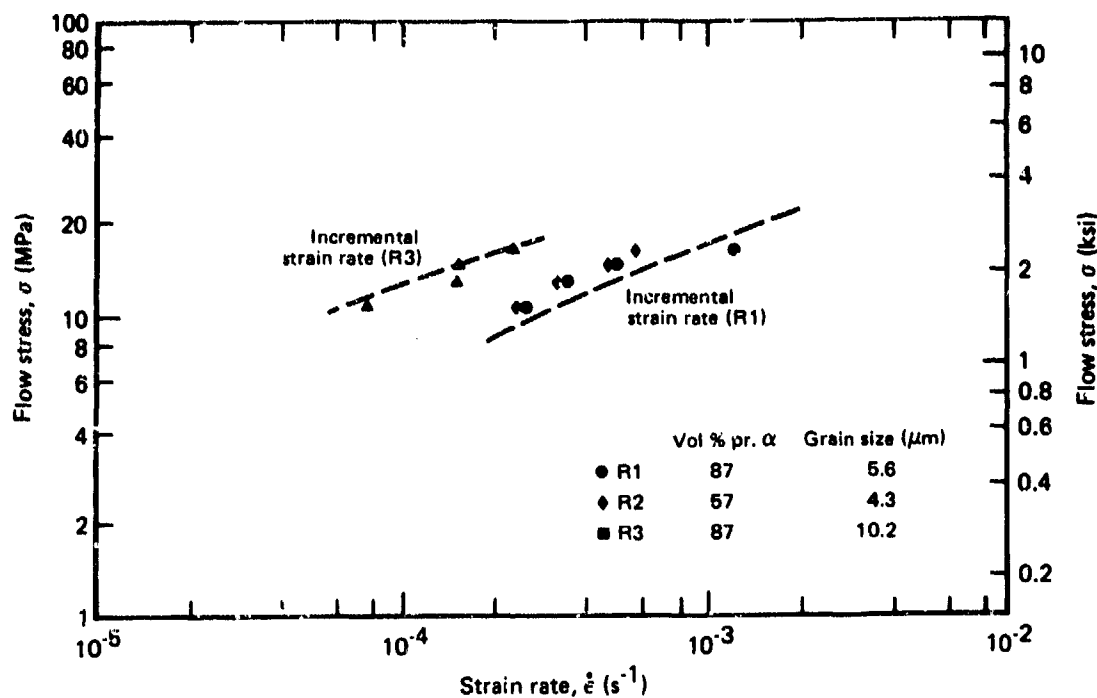
GP03-0240-174

Figure 143. Strain-rate dependence of flow stress at 870°C (1600°F) for simulated-coil Ti-6Al-4V determined from cone-forming tests (symbols) and incremental strain-rate tests (dashed curves).

The superplastic-forming testing of simulated-coil Ti-6Al-4V was quite limited, but the following conclusions can be made: (1) the forming stress in incremental-strain-rate tests for simulated-coil Ti-6Al-4V is higher than for regular-grade, Ti-6Al-4V of equivalent grain size, but there is no increase in flow stress in conical-die forming tests for simulated-coil Ti-6Al-4V; and (2) the increase in flow stress in the longitudinal direction observed in incremental-strain-rate tests compared to flow stresses in conical die forming shown in Figure 141 through 143 for simulated-coil Ti-6Al-4V is attributed to the processing of this material which creates anisotropy of flow stresses and adversely affects its biaxial superplastic behavior.

5.8 Biaxial Conical-Die Forming of Ti-3Al-2.5V

The beta-transus temperature of Ti-3Al-2.5V, 932°C (1710°F) is considerably lower than the beta transus for Ti-6Al-4V, 999°C (1830°F). The incremental-strain-rate tests of regular-grade Ti-6Al-4V indicated that the ratio of forming temperature to beta-transus temperature is critical for determining the superplastic temperature range, with the ratio of approximately 0.95 being optimum. Using this ratio as a guide-line a forming temperature of 877°C (1610°F) was selected for superplastic-forming evaluation of Ti-3Al-2.5V. The results of biaxial conical-die forming at high strain rates and short forming times are shown in Figure 144. Good agreement exists between incremental-strain-rate test data and biaxial forming in a conical die.



GP03-0246-175

Figure 144. Strain-rate dependence of flow stress at 877°C (1610°F) for Ti-3Al-2.5V determined from cone-forming tests (symbols) and incremental strain-rate tests (dashed curves).

The effect of longer forming times and slower strain rates at 935°C (1610°F) is shown in Figure 145. The agreement is not as good because of microstructural changes, as previously demonstrated for regular-grade Ti-6Al-4V.

One biaxial forming test was made at 841°C (1545°F). Failure occurred in the largest cone for the fine grain-size material after three hours forming time. The results of this test are shown in Figure 146. Excellent agreement is shown between incremental-strain-rate tests and conical-die forming. Since grain growth is strongly temperature dependent, good agreement can be anticipated between incremental-strain-rate tests and biaxial forming even at slow strain rates and long forming times at the lower forming temperatures.

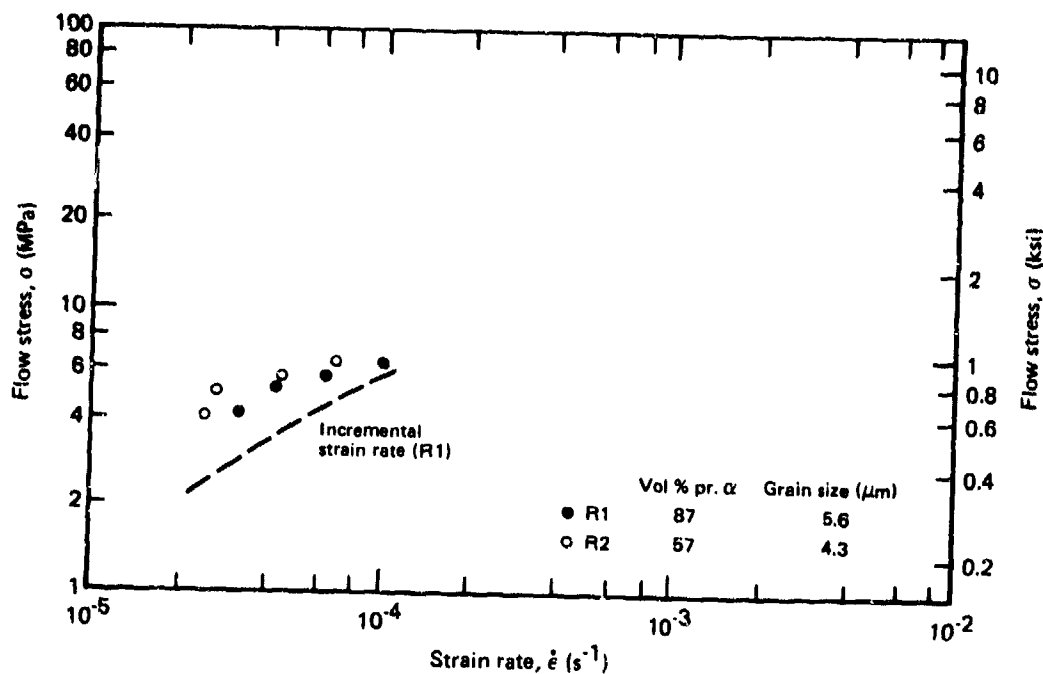


Figure 145. Strain-rate dependence of flow stress at 877°C (1610°F) for Ti-3Al-2.5V determined from cone-forming tests (symbols) and incremental strain-rate tests (dashed curve).

GP03-0249-176

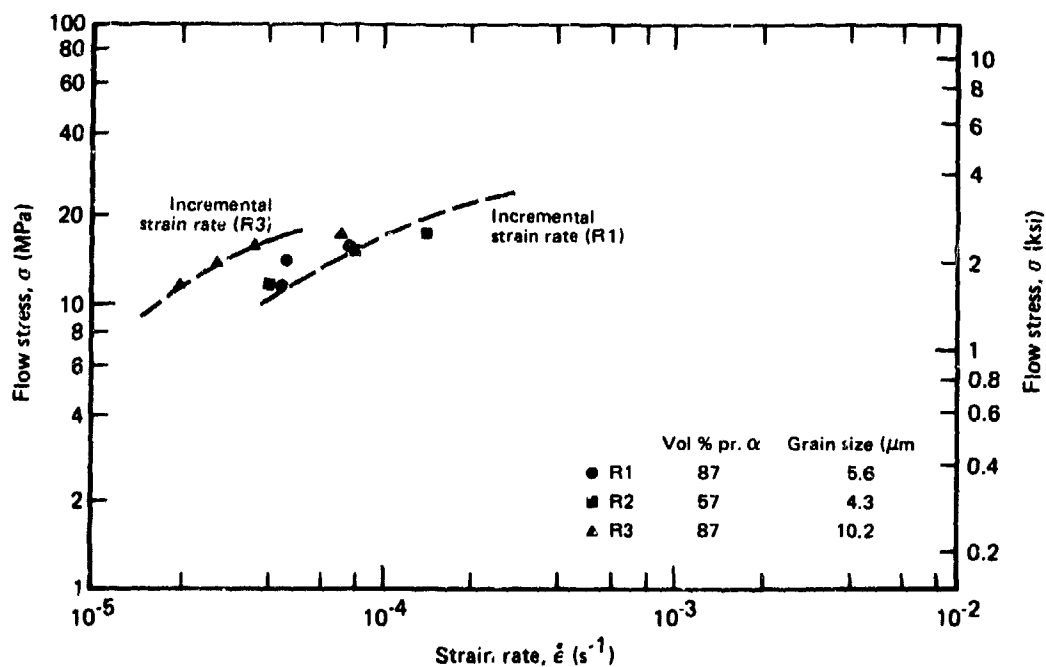


Figure 146. Strain-rate dependence of flow stress at 841°C (1546°F) for Ti-3Al-2.5V determined from cone-forming tests (symbols) and incremental strain-rate tests (dashed curves).

GP03-0249-177

The results obtained from these biaxial forming tests confirm the importance of the ratio of the forming temperature to the beta-transus temperature for alpha-beta titanium alloys. The range of the ratio of forming temperature to beta-transus temperature used in these tests was 0.90 to 0.95, and excellent biaxial superplasticity was observed in the titanium alloy Ti-3Al-2.5V. This is in good agreement with the results obtained in regular-grade, Ti-6Al-4V.

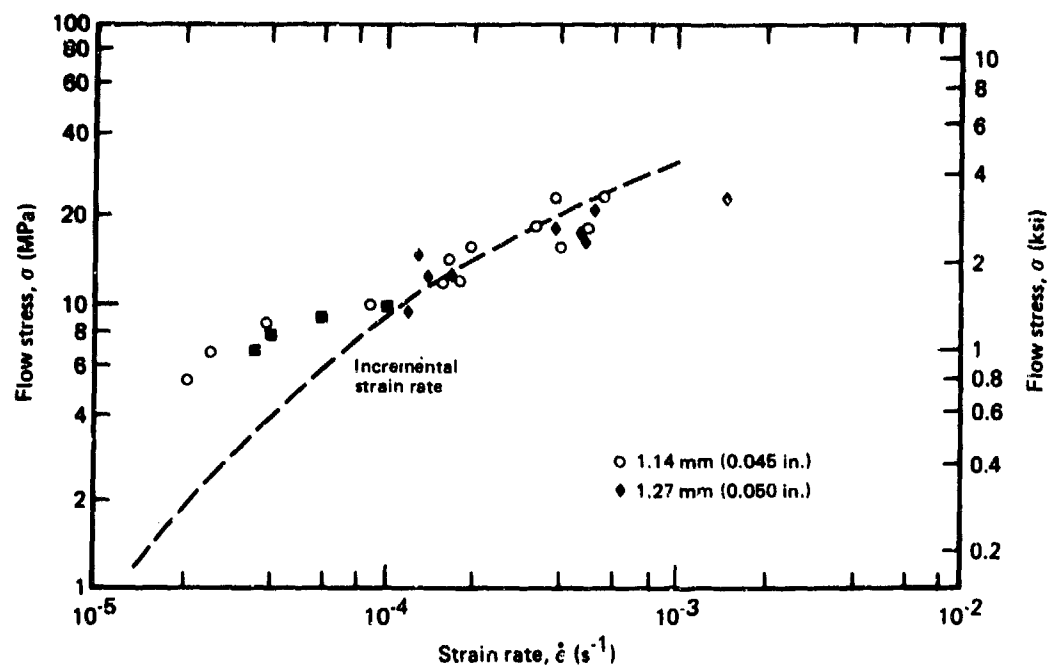
5.9 Biaxial Conical-Die Forming of Ti-8Al-1Mo-1V

The beta-transus temperature of Ti-8Al-1Mo-1V commercial sheet material used in this program was 1032°C (1890°F), which is considerably higher than the beta transus of regular-grade, Ti-6Al-4V, 999°C (1830°F). Using the ratio of forming temperature to beta-transus temperature for Ti-6Al-4V as a guideline, a temperature of 949°C (1740°F) was selected for conical-die forming. Biaxial conical-die forming tests at high, intermediate, and slow strain rates at this temperature were made for two sheet thicknesses of commercial Ti-8Al-1Mo-1V, 1.14 mm (0.045 in.) and 1.27 mm (0.050). The results are shown in Figure 147. The strain rates for both sheet gauges were similar; apparently, the small amount of elongated alpha shown in Figure 39 did not interfere with the superplastic behavior of the fine-grain bulk material.

The high and intermediate strain rates with relatively short forming times (≥ 1 hour) compare favorably with incremental-strain-rate test data. At the slower strain rates and longer forming times, poor agreement was observed between forming in a conical die and incremental-strain-rate test data. The ratio of forming temperature to beta-transus temperature for these tests was 0.94, and the strain rates are similar to strain rates of regular-grade, Ti-6Al-4V at 907°C (1665°F), which has a ratio of 0.95 (see Figure 123).

Alpha grain sizes of slow cooled Ti-8Al-1Mo-1V were measured in the largest cones. Table 39 shows results made with an average of six measurements. The initial grain size of the commercial sheet was not determined, but from Figure 39 this material had extremely fine grain size. The grain growth at 949°C (1740°F) in this superplastically-formed, fine-grained, Ti-8Al-1Mo-1V sheet was comparable with the grain

growth in fine-grained, regular-grade, Ti-6Al-4V superplastically formed at 907°C (1665°F), as shown in Table 33. This grain growth accounts for the increased forming stresses at the lower strain rates and longer forming times.



GP03-0240-178

Figure 147. Strain-rate dependence of flow stress at 949°C (1740°F) for regular-grade Ti-8Al-1Mo-1V determined from cone-forming tests (symbols) and incremental strain-rate tests (dashed curve).

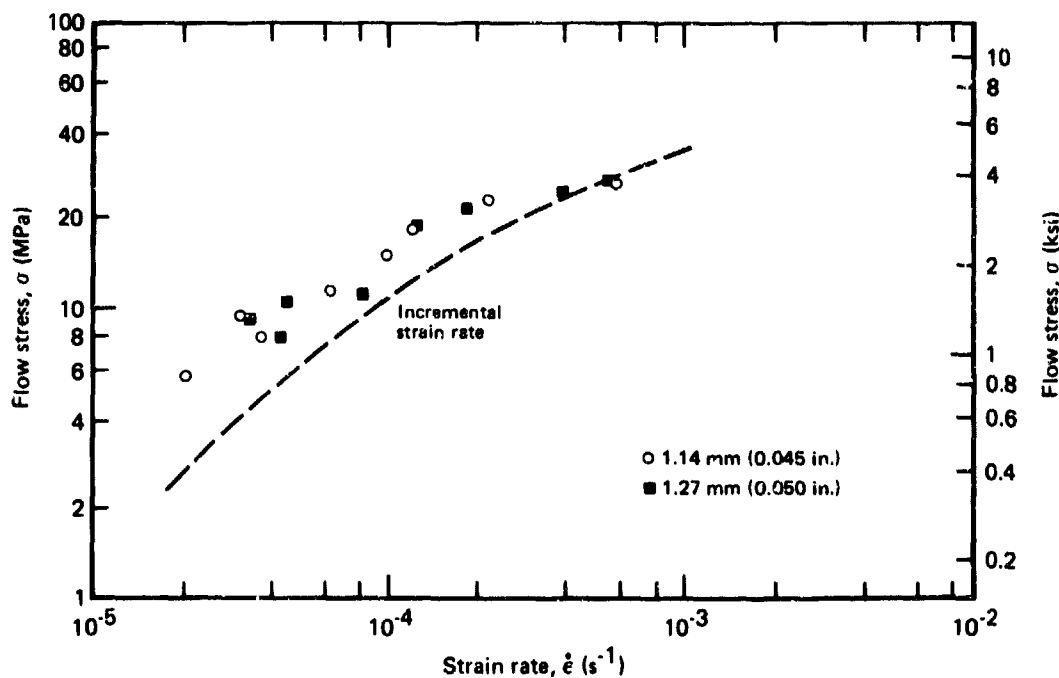
TABLE 39. EFFECT OF SUPERPLASTIC STRAIN ON GRAIN GROWTH OF COMMERCIAL-GRADE Ti-8Al-1Mo-1V FORMED AT 949°C (1740°F).

Forming time (h)	Strain, ϵ	Alpha grain size (μm)
1	0	6.5
1	1.8	7.4
5	0	7.8
5	1.7	13.0

GP03-0240-125

Conical-die forming tests were made at 932°C (1710°F) similar to 949°C (1740°F). The results are shown in Figure 148. Good superplastic properties were observed at this temperature similar to results obtained at 949°C (1740°F).

These biaxial forming tests with Ti-8Al-1Mo-1V further confirmed that the ratio of forming temperature to beta-transus temperature is the primary factor for superplastic behavior in alpha-beta titanium alloys. Since the superplastic forming temperatures for Ti-8Al-1Mo-1V are higher than for Ti-6Al-4V, the increased flow stresses caused by grain growth at the longer forming times in Ti-8Al-1Mo-1V must be considered in the forming cycle for this material.



GP03-0248-178

Figure 148 Strain-rate dependence of flow stress at 932°C (1710°F) for regular-grade Ti-8Al-1Mo-1V determined from cone-forming tests (symbols) and incremental strain-rate tests (dashed curve).

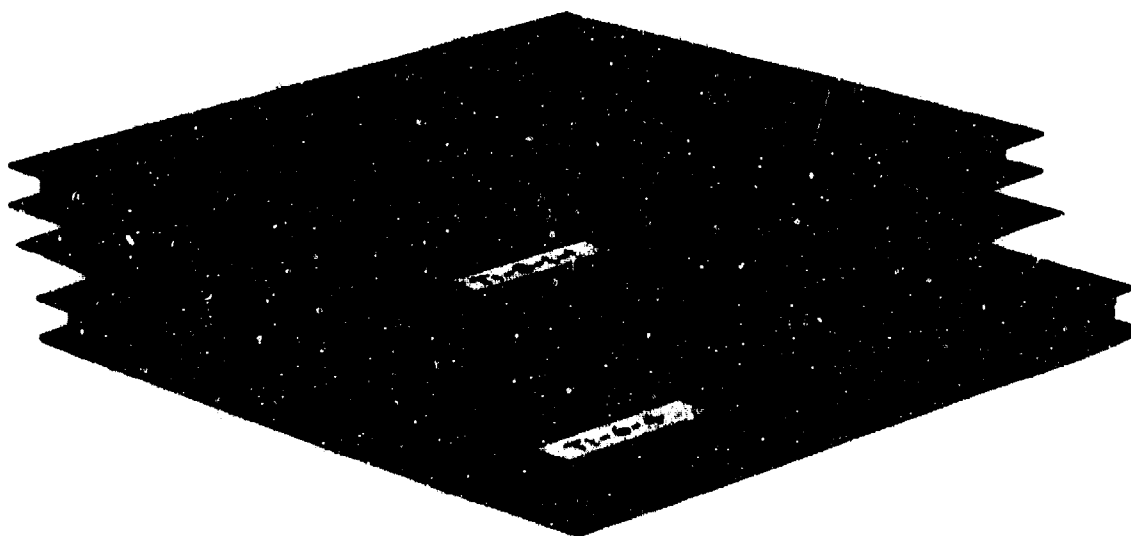
To demonstrate the superplastic forming and diffusion bonding capabilities of Ti-8Al-1Mo-1V, sandwich panels were fabricated. These panels were fabricated by a Douglas proprietary SPF/DB resistance-welding process. Figure 149 shows sandwich panels delivered to AFML. The Ti-8Al-1Mo-1V was fabricated at 1016°C (1760°F), and the Ti-6Al-4V was fabricated at 927°C (1700°F). The rectangular cell arrangement in these panels is shown in the x-ray photograph shown in Figure 150. Good panels were produced for both materials.

5.10 Biaxial Conical-Die Forming of Ti-6Al-2Sn-4Zr-2Mo

Because the beta-transus temperature of Ti-6Al-2Sn-4Zr-2Mo sheet, 993°C (1820°F), is close to the beta-transus temperature of regular-grade, normal-textured Ti-6Al-4V, 999°C (1830°F), the same forming parameters developed for regular-grade, Ti-6Al-4V were used for the forming evaluation of Ti-6Al-2Sn-4Zr-2Mo sheet. Biaxial conical-die forming was performed at 907°C (1665°F) and 870°C (1600°F). The results for high forming rates and short forming times are shown in Figure 151. The biaxial forming stresses measured in this test were similar to those measured for regular-grade, Ti-6Al-4V of similar grain size (size Figures 123 and 124). Incremental-strain-rate tests showed higher flow stresses for Ti-6Al-2Sn-4Zr-2Mo than were observed in biaxial conical-die forming. Biaxial conical-die forming stresses at slower strain rates and longer forming times are shown in Figure 152. The biaxial forming stresses are less than the flow stresses obtained by incremental-strain-rate tests. The increases in the forming stresses were similar to those observed for regular-grade, normal-textured Ti-6Al-4V (Figures 142 and 143), as was anticipated from the effects of grain growth on forming stress for regular-grade, normal-textured Ti-6Al-4V.

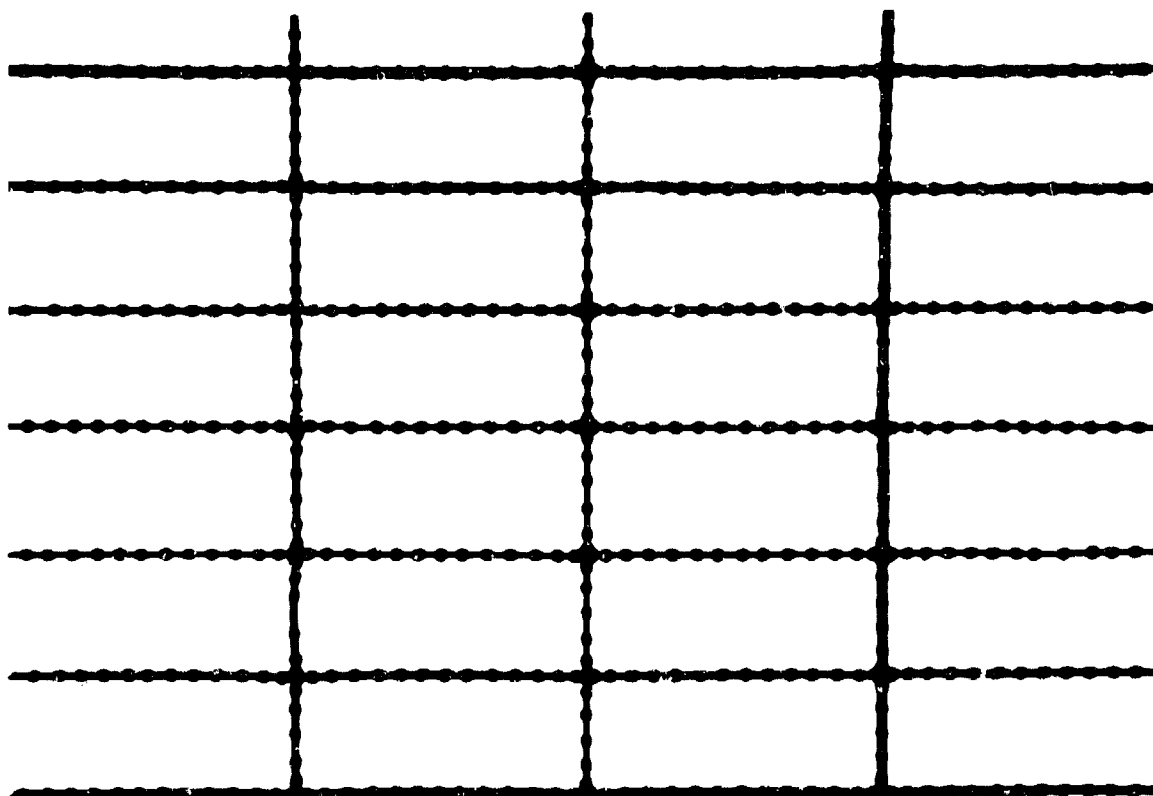
One biaxial conical-die forming test was made at 870°C (1600°F), and failure in the largest cone occurred after 3.5 hours. These results are shown in Figure 153. The flow stresses obtained by conical-die forming were only slightly less than those obtained by incremental-strain-rate tests.

The increase in flow stress found in incremental-strain-rate cycling tests for Ti-6Al-2Sn-4Zr-2Mo compared to Ti-6Al-4V were not confirmed in the biaxial conical-die forming tests. The reason for this discrepancy was not fully explored; however, the time to reach the forming temperature was approximately 30 minutes longer in the conical die experiments which would permit a higher volume fraction of beta phase to form in the conical die tests. This would promote a more favorable superplastic forming condition. Since Ti-6Al-2Sn-4Zr-2Mo has approximately the same beta transus temperature as regular grade Ti-6Al-4V, the stresses were similar in the conical die tests for the same strain rate in similar grain size microstructure.



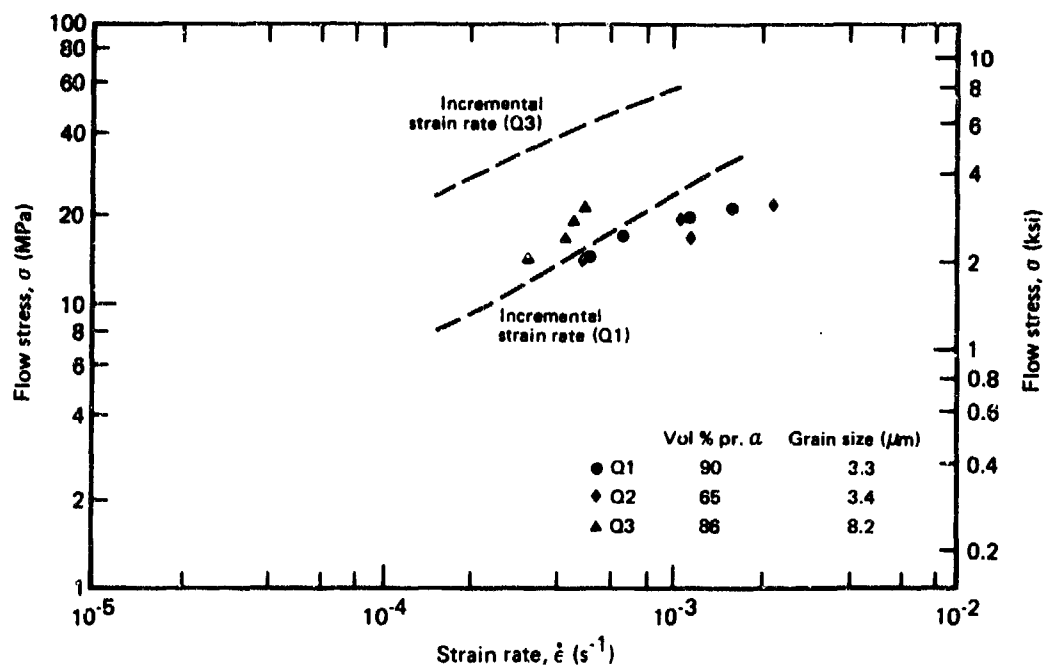
GP03-0240-218

Figure 149. Sandwich panels of Ti-8Al-1Mo-1V and Ti-6Al-4V fabricated by superplastic forming/diffusion bonding.



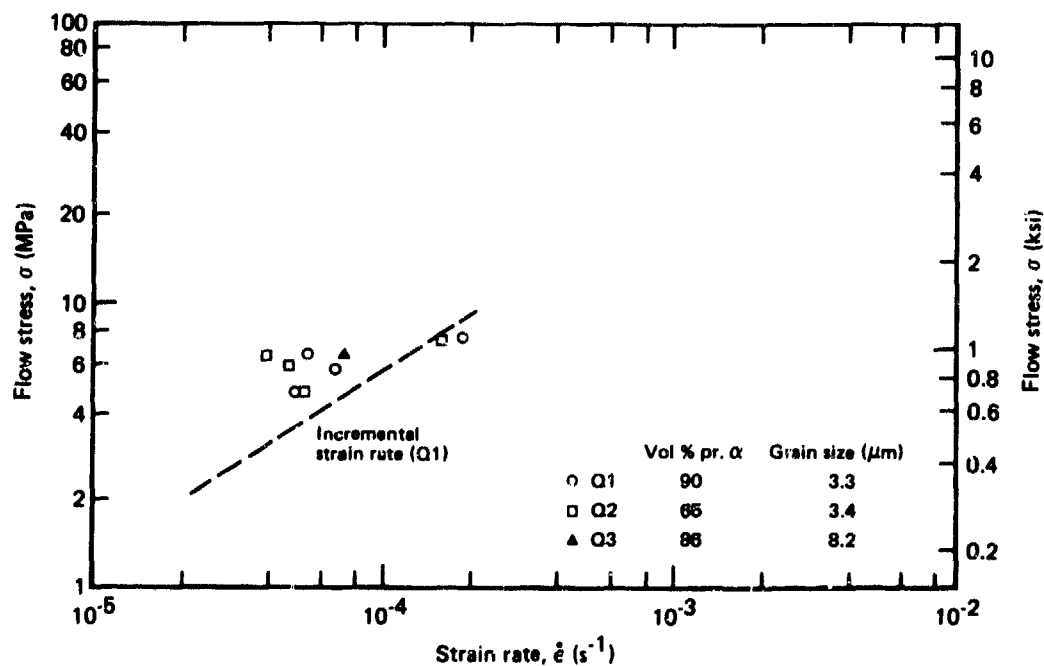
GP03-0240-219

Figure 150. X-ray photograph of cell arrangement of Ti-8Al-1Mo-1V alloy sandwich panel.



GP03-0249-180

Figure 151. Strain-rate dependence of flow stress at 907°C (1665°F) for Ti-6Al-2Sn-4Zr-2Mo determined from cone-forming tests (symbols) and incremental strain-rate tests (dashed curves).



GP03-0249-181

Figure 152. Strain-rate dependence of flow stress at 907°C (1665°F) for Ti-6Al-2Sn-4Zr-2Mo determined from cone-forming tests (symbols) and incremental strain-rate tests (dashed curve).

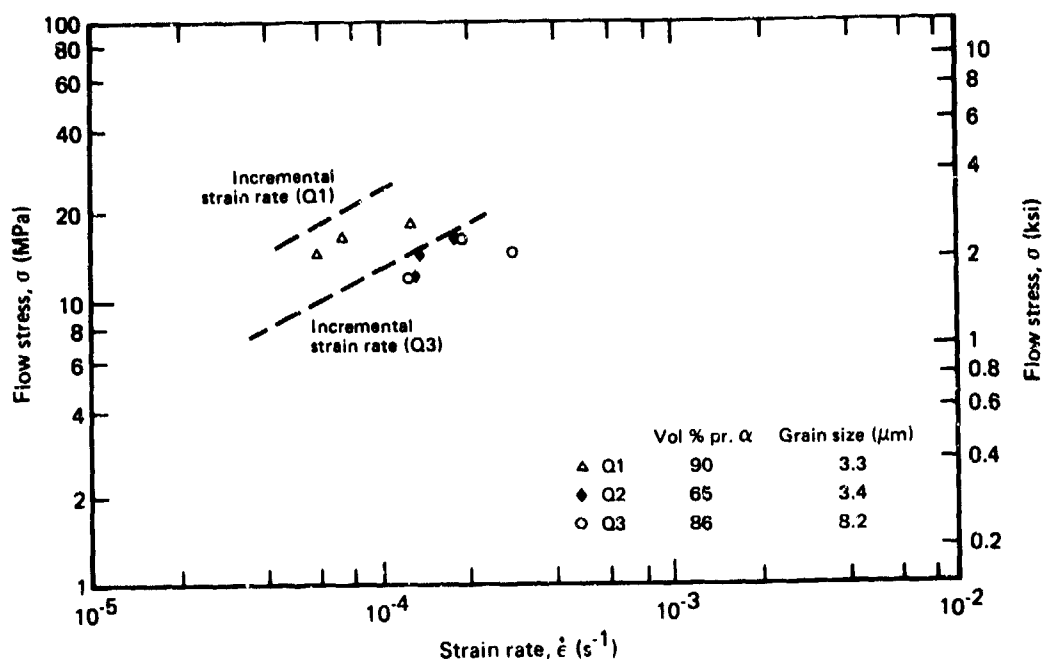


Figure 153. Strain-rate dependence of flow stress at 871°C (1600°F) for Ti-6Al-2Sn-4Zr-2Mo determined from cone-forming tests (symbols) and incremental strain-rate tests (dashed curves).

5.11 Biaxial Conical-Die Forming of Ti-15V-3Cr-3Sn-3Al

Forming in conical die with Ti-15V-3Cr-3Sn-3Al sheet was initiated at 760°C (1400°F) which is close to the beta transus. A forming time of five hours was used in these tests. The results are shown in Table 40. Forming down into the cone was limited to the larger cones because of the high stresses required to form this beta alloy. Although only small strains were accomplished, the strain rates obtained by conical die forming agreed with incremental strain-rate tests at equivalent flow stresses for all microstructures.

Additional tests were made with Ti-15V-3Cr-3Sn-3Al at 802°C (1475°F), which is above beta transus for this alloy. These results are shown in Table 41. Again, only limited forming similar to biaxial forming at 760°C (1400°F) was achieved with this material. Failure occurred at low strains (less than 1.0).

A finer initial grain size material would undoubtedly lower the flow stresses at the forming temperatures used for this study. However, because of the rapid grain growth in beta alloys at elevated temperatures, and high flow stresses, superplastic forming of beta alloy Ti-15V-3Cr-3Sn-3Al does not appear to be a practical process.

TABLE 40. COMPARISONS OF SUPERPLASTIC STRAIN RATES AT 760°C (1400°F) OF
Ti-15V-3Cr-3Sn-3Al DETERMINED FROM CONE-FORMING TESTS AND
LABORATORY INCREMENTAL STRAIN-RATE TESTS.

Panel code	Processing schedule	Grain size (μm)	Diameter of cone mm (in.)	Forming pressure MPa (psi)	Stress in cone MPa (psi)	Time at pressure (min)	Final depth in cone mm (in.)	Strain in cone, ϵ	Strain rate in cone (s^{-1})	Strain rate from laboratory tests (s^{-1})
Z1	As-cold-rolled	—	37.4 (1.474)	2.41 (350)	16.4 (2380)	300	14.1 (0.557)	0.18	1.7×10^{-5}	1.7×10^{-5}
Z2	Cold-rolled + 482°C (900°F) for 8 h	—	37.7 (1.485) 34.0 (1.34)	2.41 (350) 2.41 (350)	17.9 (2600) 15.9 (2300)	300 300	16.4 (0.647) 11.6 (0.459)	0.33 0.10	3.0×10^{-5} 1.0×10^{-5}	8.6×10^{-6} 6.6×10^{-6}
Z3	Cold-rolled + 774°C (1425°F) for 5 min	32	37.3 (1.468)	2.41 (350)	17.3 (2500)	300	15.4 (0.608)	0.25	2.4×10^{-5}	1.1×10^{-5}
Z4	Cold-rolled + 774°C (1425°F) for 5 min + 482°C (900°F) for 3 h	32	37.3 (1.468)	2.41 (350)	16.4 (2372)	300	13.9 (0.545)	0.17	1.6×10^{-5}	1.35×10^{-5}
Z5	Cold-rolled + 774°C (1425°F) for 5 min + 566°C (1050°F) for 8 h	32	37.4 (1.474)	2.41 (350)	15.9 (2447)	300	15.4 (0.608)	0.25	2.5×10^{-5}	1.6×10^{-5}
Z6	Cold-rolled + 774°C (1425°F) for 2.25 h	52	37.7 (1.485) 34.0 (1.34)	2.41 (350)	19.2 (2768) 17.1 (2484)	300	20.0 (0.788) 12.5 (0.493)	0.55 0.16	4.2×10^{-5} 1.4×10^{-5}	1.1×10^{-5} 8.6×10^{-6}
Z7	Cold-rolled + 774°C (1425°F) for 2.25 h + 482°C (900°F) for 8 h	52	37.3 (1.468)	2.41 (350)	17.5 (2540)	300	16.6 (0.652)	0.32	3.3×10^{-5}	1.34×10^{-5}

GP03-0749-256

TABLE 41. COMPARISONS OF SUPERPLASTIC STRAIN RATES AT 802°C (1475°F) OF
Ti-15V-3Cr-3Sn-3Al DETERMINED FROM CONE-FORMING TESTS AND
LABORATORY INCREMENTAL STRAIN-RATE TESTS.

Panel code	Processing/ heat treatment schedule	Grain size (μm)	Diameter of cone mm (in.)	Forming pressure MPa (psi)	Stress in cone MPa (psi)	Forming time (min)	Final depth in cone mm (in.)	Strain in cone, ϵ	Strain rate in cone (s^{-1})	Strain rate from laboratory tests (s^{-1})
Z1	Cold-rolled 57%	—	37.3 (1.468)	2.41 (350)	16.5 (2400)	150	17.3 (0.682)	0.37	4×10^{-5}	2.7×10^{-5}
Z2	Cold-rolled + 482°C (900°F) for 8 h	—	37.5 (1.485)	2.41 (350)	17.9 (2600)	250	29.6 (0.94)*	0.89	6×10^{-5}	3.2×10^{-4}
			34.0 (1.34)	2.41 (350)	16.1 (2341)	250	15.0 (0.592)	0.319	2.5×10^{-5}	2.5×10^{-5}
Z3	Cold-rolled + 774°C (1425°F) for 5 min	32	37.5 (1.485)	2.41 (350)	17.5 (2535)	150	22.0 (0.866)	0.71	8.0×10^{-5}	3.0×10^{-5}
Z4	As in Z3 + 482°C (900°F) for 8 h	32	37.3 (1.468)	2.41 (350)	16.4 (2375)	250	20.6 (0.810)	0.61	4.7×10^{-5}	2.25×10^{-5}
Z5	As in Z3 + 566°C (1050°F) for 8 h	32	37.3 (1.468)	2.41 (350)	16.4 (2375)	250	26.8 (1.880)*	0.75	5.0×10^{-5}	2.6×10^{-5}
			31.5 (1.241)	2.41 (350)	13.9 (2013)	250	12.1 (0.477)	0.19	1.3×10^{-5}	1.5×10^{-5}
Z6	Cold-rolled + 774°C (1425°F) for 2.25 h	52	37.4 (1.474)	2.41 (350)	17.6 (2550)	150	29.1 (0.900)*	0.78	5.0×10^{-5}	2.6×10^{-5}
		52	31.5 (1.241)	2.41 (350)	15.9 (2290)	150	12.6 (0.495)	0.23	3.6×10^{-5}	2.1×10^{-5}
Z7	As in Z6 + 482°C (900°F) for 8 h	52	37.4 (1.474)	2.41 (350)	17.6 (2550)	250	29.1 (0.901)*	0.78	5.0×10^{-5}	2.5×10^{-5}

*Failed

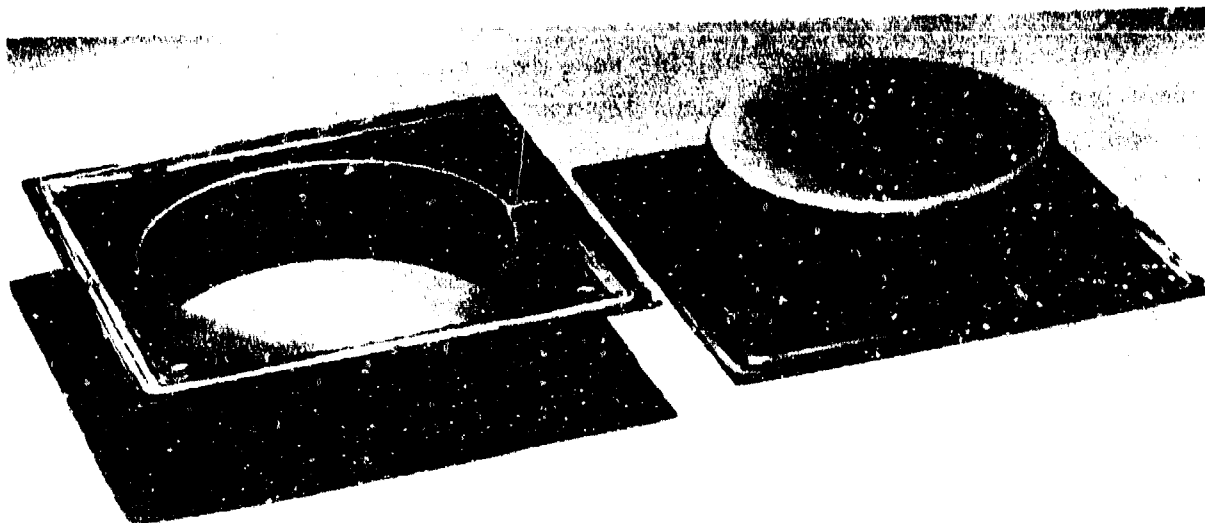
G700-0248-257

5.12 Mechanical Properties of Superplastically Formed Panels

Superplastically biaxially formed pans for the alpha-beta titanium alloys were made for properties evaluation. Pans with a 89-mm (3.5 in.) depth and 254-mm (10 in.) diam were formed from selected microstructures for all alpha-beta titanium alloys studied in this program. A typical pan is shown in Figure 154. Forming strain rates of 10^{-3} s^{-1} and 10^{-4} s^{-1} were used for each microstructures. The walls of pans were made flat by annealing at a temperature of 760°C (1500°F), as shown in Figure 155. Thickness measurements were made on pan bottoms at the center, midradius, and edge and on walls of pans at the top, midheight, and bottom. These measurements for each microstructure are shown in Appendix D.

Tensile specimens were cut from the walls and the bottoms of superplastic formed pans. The mechanical properties of normal-textured, regular-grade Ti-6Al-4V and ELI-grade Ti-6Al-4V formed at 907°C (1665°F) and 870°C (1600°F) are shown in Tables 42 and 43 for as-fabricated and superplastically formed conditions. The ductility measured from the walls of the pans were generally lower than the ductility measured from the bottoms of the pans. Since there was more taper in the walls of the pan than in the bottom of the pan as shown by thickness measurements, the mechanical properties measured from the bottom of the pan were considered to be more reliable; therefore, these values are more representative of the mechanical properties in the superplastic formed condition.

Superplastically formed microstructures having a high volume fraction of primary alpha phase compared to initial properties before forming exhibited only small drops in the tensile strength and ductility for both regular-grade Ti-6Al-4V microstructures ELI grade Ti-6Al-4V microstructures. For regular-grade Ti-6Al-4V microstructures A (0.45 α , 4.4 μm) and J (0.46 α , 4.4 μm) which have a low primary alpha phase, a considerable larger drop in the tensile properties compared to initial properties was observed. Since the superplastic formed pans were slow cooled, the larger drop in tensile properties can be attributed mostly to increasing the volume fraction of primary alpha-phase in these initially low primary alpha-phase microstructures of regular-grade Ti-6Al-4V and ELI grade Ti-6Al-4V. The mechanical properties in a superplastically formed material of an initially low primary alpha-phase approach the mechanical properties of a superplastic alloy formed high primary alpha-phase microstructure of similar grain size. A comparison of mechanical properties of microstructure E (0.88 α , 12.6 μm) and microstructure A (0.44 α , 12.6 μm) in Table 42 best illustrates this fact.



GP03-0249-221

Figure 154. Superplastically-formed 254-mm (10 in.) diam Ti-6Al-4V pan.



GP03-0249-220

Figure 155. Superplastically-formed 254-mm (10 in.) diam Ti-6Al-4V pans sectioned for mechanical property evaluation.

**TABLE 42. COMPARISON OF MECHANICAL PROPERTIES OF NORMAL-TEXTURED
REGULAR-GRADE TI-6Al-4V AND ELI-GRADE TI-6Al-4V IN
AS-FABRICATED AND SUPERPLASTICALLY-FORMED CONDITIONS
WITH A SUPERPLASTIC FORMING TEMPERATURE OF 907°C (1665°F).**

Microstructure		Location	Strain rate (s ⁻¹)	0.2% offset yield stress MPa (ksi)	Ultimate tensile strength MPa (ksi)	Total elongation (%)
Grain size (μm)	α (%)					
Regular grade 17.6	0.88	L	As-fabricated	0.851 (123.4)	0.909 (131.9)	16.0
		L	As-fabricated	0.834 (120.9)	0.906 (131.4)	12.0
		T	As-fabricated	0.794 (115.1)	0.875 (126.9)	5.0
		T	As-fabricated	0.843 (122.3)	0.867 (128.7)	13.5
		Wall	10 ⁻³	0.800 (116.0)	0.859 (124.6)	8.0
		Wall	10 ⁻³	0.778 (112.9)	0.850 (123.3)	12.2
		Bottom	10 ⁻³	0.815 (118.2)	0.848 (123.0)	6.5
		Bottom	10 ⁻³	0.837 (121.4)	0.866 (125.6)	10.0
		Bottom	10 ⁻⁴	0.859 (124.6)	0.910 (132.0)	14.8
		Bottom	10 ⁻⁴	0.833 (120.8)	0.964 (139.7)	15.7
12.2	0.88	L	As-fabricated			
		T	As-fabricated			
		Wall	10 ⁻⁴	0.797 (115.6)	0.848 (123.0)	8.3
		Wall	10 ⁻⁴	0.813 (117.9)	0.857 (124.3)	8.9
		Bottom	10 ⁻⁴	0.898 (128.8)	0.928 (134.6)	10.8
12.6	0.46	Bottom	10 ⁻⁴	0.833 (120.8)	0.909 (131.8)	15.2
		L	As-fabricated	0.976 (141.6)	1.05 (152.2)	16.1
		L	As-fabricated	0.923 (133.7)	1.06 (153.5)	17.4
		Wall	10 ⁻³	0.845 (122.6)	0.879 (127.4)	10.3
		Wall	10 ⁻³	0.807 (117.0)	0.860 (124.8)	9.6
		Bottom	10 ⁻³	0.738 (107.1)	0.803 (116.4)	7.0
		Bottom	10 ⁻³	0.811 (117.6)	0.850 (123.2)	10.0
		Bottom	10 ⁻⁴	0.834 (121.0)	0.947 (137.3)	14.0
7.7	0.89	Bottom	10 ⁻⁴	0.863 (125.2)	0.922 (133.7)	11.9
		L	As-fabricated			
		T	As-fabricated			
		Wall	10 ⁻³	0.805 (116.8)	0.778 (122.9)	7.0
		Wall	10 ⁻³	0.820 (118.9)	0.874 (126.7)	6.6
		Wall	10 ⁻⁴	0.786 (114.0)	0.869 (126.0)	8.5
		Wall	10 ⁻⁴	0.803 (116.5)	0.880 (127.6)	8.0
		Bottom	10 ⁻³	0.845 (122.5)	0.915 (132.7)	9.9
		Bottom	10 ⁻³	0.855 (124.0)	0.919 (133.3)	11.5
		Bottom	10 ⁻⁴	0.856 (124.2)	0.912 (132.2)	14.3
		Bottom	10 ⁻⁴	0.866 (125.6)	0.917 (132.0)	14.1

GP03-0249-262

TABLE 42. (Continued) COMPARISON OF MECHANICAL PROPERTIES OF NORMAL-TEXTURED REGULAR-GRADE Ti-6Al-4V AND ELI-GRADE Ti-6Al-4V IN AS-FABRICATED AND SUPERPLASTICALLY-FORMED CONDITIONS WITH A SUPERPLASTIC FORMING TEMPERATURE OF 907°C (1665°F).

Microstructure		Location	Strain rate (s ⁻¹)	0.2% offset yield stress MPa (ksi)	Ultimate tensile strength MPa (ksi)	Total elongation (%)
Grain size (μm)	α (%)					
Regular grade 6.0	0.88	L	As-fabricated	—	—	16.4
		L	As-fabricated	—	—	17.2
		Wall	10 ⁻³	0.776 (112.5)	0.838 (121.5)	9.0
		Wall	10 ⁻³	0.803 (116.5)	0.871 (126.3)	9.5
		Wall	10 ⁻⁴	0.797 (115.6)	0.855 (124.0)	8.0
		Wall	10 ⁻⁴	0.803 (116.5)	0.851 (123.4)	11.2
		Bottom	10 ⁻³	0.796 (115.4)	0.855 (124.0)	8.3
		Bottom	10 ⁻³	0.821 (119.1)	0.855 (124.0)	6.4
		Bottom	10 ⁻⁴	0.840 (121.8)	0.888 (128.8)	15.7
		Bottom	10 ⁻⁴	0.843 (122.2)	0.883 (128.0)	14.4
		Bottom	10 ⁻⁴	0.843 (122.2)	0.883 (128.0)	14.4
4.4	0.47	L	As-fabricated	0.923 (133.9)	1.026 (148.8)	17.4
		L	As-fabricated	0.925 (134.1)	1.011 (146.7)	17.8
		Wall	10 ⁻⁴	0.823 (119.4)	0.887 (128.6)	10.9
		Wall	10 ⁻⁴	0.792 (114.8)	0.858 (124.5)	10.0
		Bottom	10 ⁻⁴	0.843 (122.3)	0.903 (130.9)	15.6
		Bottom	10 ⁻⁴	0.865 (125.4)	0.907 (131.5)	14.4
ELI-grade 5.6	0.88	L				
		Wall	10 ⁻³	0.682 (98.9)	0.706 (105.3)	7.6
		Wall	10 ⁻³	0.666 (96.6)	0.744 (107.9)	10.1
		Wall	10 ⁻⁴	0.660 (95.7)	0.734 (106.5)	12.9
		Wall	10 ⁻⁴	0.674 (97.7)	0.752 (109.1)	12.5
		Bottom	10 ⁻³	0.747 (108.0)	0.790 (114.6)	14.5
		Bottom	10 ⁻³	0.765 (111.0)	0.814 (118.0)	15.5
		Bottom	10 ⁻⁴	0.739 (107.2)	0.786 (114.0)	13.9
		Bottom	10 ⁻⁴	0.739 (107.2)	0.787 (114.1)	16.8
		Bottom	10 ⁻⁴	0.739 (107.2)	0.787 (114.1)	16.8
8.9	0.89	L	As-fabricated	0.731 (106.1)	0.779 (113.0)	20.3
		L	As-fabricated	0.731 (106.0)	0.775 (112.4)	21.4
		Wall	10 ⁻³	0.740 (107.3)	0.783 (113.6)	9.0
		Wall	10 ⁻³	0.713 (103.4)	0.763 (110.6)	12.9
		Bottom	10 ⁻³	0.752 (109.0)	0.834 (120.9)	15.6
		Bottom	10 ⁻³	0.772 (112.1)	0.819 (118.8)	16.8
		Bottom	10 ⁻⁴	0.747 (108.0)	0.808 (117.2)	16.9
		Bottom	10 ⁻⁴	0.741 (107.4)	0.798 (115.7)	18.2
8.8	0.46	Bottom	10 ⁻³	0.719 (104.3)	0.764 (110.8)	9.8
		Bottom	10 ⁻³	0.745 (108.1)	0.772 (111.9)	7.7
		Bottom	10 ⁻⁴	0.743 (107.7)	0.800 (116.0)	14.3
		Bottom	10 ⁻⁴	0.743 (107.8)	0.806 (117.0)	19.5

GP03-1248-113

TABLE 43. PROPERTIES OF NORMAL-TEXTURED REGULAR-GRADE Ti-6Al-4V AND ELI-GRADE Ti-6Al-4V SUPERPLASTICALLY-FORMED AT 870°C (1600°F).

	Grain size (μm)	Volume fraction primary alpha	Location	Strain rate (s ⁻¹)	0.2% offset yield stress MPa (ksi)	Ultimate tensile strength MPa (ksi)	Total elongation (%)
Regular-grade Ti-6Al-4V	12.2	0.87	Bottom	10 ⁻⁴	858 (121.5)	927 (134.5)	13.0
	12.2	0.87	Bottom	10 ⁻⁴	867 (125.8)	912 (132.2)	17.1
	6.0	0.88	Bottom	10 ⁻⁴	827 (120.0)	882 (127.9)	16.0
	6.0	0.88	Bottom	10 ⁻⁴	844 (122.4)	893 (129.5)	15.2
	4.4	0.47	Bottom	10 ⁻⁴	859 (124.6)	923 (133.8)	15.2
	4.4	0.47	Bottom	10 ⁻⁴	872 (126.4)	912 (132.3)	12.5
ELI-grade Ti-6Al-4V	5.6	0.88	Bottom	10 ⁻⁴	753 (109.2)	796 (115.4)	16.0
			Bottom	10 ⁻⁴	753 (109.2)	814 (118.1)	16.1

GP03-0248-129

The grain size in regular-grade normal textured Ti-6Al-4V microstructure L (0.88α, 6.0μm), after forming at a strain rate of 10⁻⁴ s⁻¹, was measured at the three locations shown for thickness measurements of the bottom of the pan. An average grain size of 10.5μm was measured at each of the three locations. This grain growth in a superplastic formed pan agrees with the grain growth in superplastic conical die forming (See Table 27).

One superplastic formed pan was made with a basal-texture Ti-6Al-4V panel at 907°C (1665°F). The mechanical properties measured from the bottom of the pan are shown in Table 44. A comparison of the mechanical properties in basal texture Ti-6Al-4V (0.90 α , 7.4 μ m) with regular grade normal texture Ti-6Al-4V microstructure L (0.88 α , 6.0 μ m) in Table 42 showed a similar small drop compared to initial properties before forming in the tensile properties and the ductility of superplastic formed material. The grain size was measured at the three locations indicated for thickness measurements of the bottom of the pan. The average grain size was 11.1 μ m at each of three locations. Pole figures of material taken from superplastic formed bottom of the pan showed a weak texture similar to regular-grade normal texture Ti-6Al-4V. The superplastic flow stresses, grain growth and mechanical properties in superplastic formed basal-texture Ti-6Al-4V followed closely the results established for normal texture Ti-6Al-4V of similar grain size.

TABLE 44. COMPARISON OF TENSILE PROPERTIES OF BASAL-TEXTURED TI-6Al-4V IN AS-RECEIVED AND SUPERPLASTICALLY-FORMED CONDITIONS; SUPERPLASTIC FORMING TEMPERATURE = 907°C (1665°F).

Initial microstructure		Location	Strain rate (s ⁻¹)	Yield stress MPa (ksi)	Ultimate tensile strength MPa (ksi)	Elongation (%)
Grain size (μ m)	Volume fraction primary alpha					
7.4	0.9	L	As-fabricated	854 (123.8)	922 (133.7)	21.3
7.4	0.9	L	As-fabricated	842 (122.1)	910 (132.0)	20.0
7.4	0.9	Bottom	10 ⁻⁴	858 (124.4)	896 (129.9)	17.7
7.4	0.9	Bottom	10 ⁻⁴	854 (123.8)	887 (128.7)	17.3

GP03-0249-258

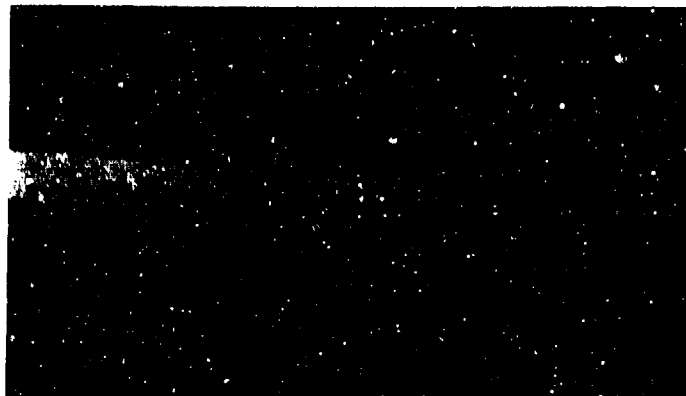
One pan was superplastically formed at a strain rate of 10^{-4} s^{-1} at 907°C (1665°F) with a fine grain microstructure of simulated coil Ti-6Al-4V (0.98α , $5.6\mu\text{m}$). When the bottom of the pan was sectioned for the fabrication of tensile specimens, wide local variations were observed in the thickness of the sheet. These thickness variations are illustrated in Figure 156. These thickness variations existed over the entire area of the pan. Due to these thickness variations, tensile properties could not be accurately measured.

The lack of agreement between biaxial conical forming and incremental strain-rate tests and the thickness variation shown in superplastically formed pans are both indicate that the superplastic flow stresses in longitudinal and transverse directions are significantly different in simulated-coil Ti-6Al-4V. These anisotropic properties are probably related to the processing procedures used in the fabrication of the simulated coil Ti-6Al-4V.

Superplastic formed pans were made at 877°C (1610°F) at a strain rate of 10^{-4} s^{-1} with Ti-3Al-2.5V with the finest microstructures R1 (0.87α , $5.6\mu\text{m}$) and R2 ($0.57\mu\text{m}$, $4.3\mu\text{m}$) and a coarser microstructure R3 (0.87α , $10.2\mu\text{m}$) of Ti-63Al-2.5V. Tensile properties measured from as-received and from the bottom of superplastic formed pans are shown in Table 45. For the fine grain microstructures a small drop compared to initial properties in tensile properties in superplastic formed material was observed similar to results for regular grade Ti-6Al-4V and ELI grade Ti-6Al-4V shown in Table 42. In the larger grain microstructure R3 (0.87α , $10.2\mu\text{m}$), a larger drop in tensile drop was observed. These results are not consistent with the results obtained with a regular grade normal texture Ti-6Al-4V microstructure E (0.87α , $12.2\mu\text{m}$) of similar grain size (see Table 42)

Superplastic formed pans from selected microstructures of Ti-6Al-2Sn-4Zr-2Mo were made at 907°C (1665°F) at a strain rate of 10^{-4} s^{-1} . Tensile properties from as-received and from the bottom of superplastic formed pans are shown in Table 46. Only a small drop in the tensile properties and the ductility was observed in superplastic formed material.

The small decreases in the tensile strength and ductility compared to initial properties before forming of superplastically formed equiaxed microstructures of Ti-6Al-4V, Ti-3Al-2.5V and Ti-6Al-2Sn-4Zr-2Mo with large volume fractions of primary alpha can be attributed to the grain growth observed in these microstructures.



8 X

GP03-0240-222

Figure 156. Photograph showing thickness variation of a cross section of the bottom of superplastically-formed simulated-coil Ti-6Al-4V.

TABLE 45. COMPARISON OF TENSILE PROPERTIES OF Ti-3Al-2.5V SHEET IN AS-FABRICATED AND SUPERPLASTICALLY FORMED CONDITIONS; SUPERPLASTIC FORMING TEMPERATURE = 877°C (1610°F).

Panel code	Microstructure		Direction or location	Strain rate (s^{-1})	Yield stress MPa (ksi)	Ultimate tensile strength MPa (ksi)	Elongation (%)
	Grain size (μm)	Volume fraction primary alpha					
R1	5.6	0.87	L	As-fabricated	496 (72.0)	641 (93.0)	23.3
R1	5.6	0.87	L	As-fabricated	519 (75.3)	648 (94.0)	23.6
R1	5.6	0.87	Bottom	10^{-4}	510 (74.1)	628 (91.1)	19.2
R1	5.6	0.87	Bottom	10^{-4}	500 (72.5)	620 (90.0)	20.8
R2	4.3	0.57	Bottom	10^{-4}	511 (74.1)	628 (91.1)	14.9
R2	4.3	0.57	Bottom	10^{-4}	500 (72.5)	621 (90.0)	19.2
R3	10.2	0.87	L	As-fabricated	514 (74.6)	664 (96.3)	20.6
R3	10.2	0.87	L	As-fabricated	502 (72.8)	652 (94.6)	21.0
R3	10.2	0.87	Bottom	10^{-4}	447 (64.8)	561 (81.4)	10.0
R3	10.2	0.87	Bottom	10^{-4}	456 (66.2)	578 (83.9)	12.0

GP03-0240-200

TABLE 46. COMPARISON OF TENSILE PROPERTIES OF Ti-6Al-2Sn-4Zr-2Mo SHEET IN AS-RECEIVED AND SUPERPLASTICALLY-FORMED CONDITIONS; SUPERPLASTIC FORMING TEMPERATURE = 907°C (1665°F).

Panel code	Microstructure		Direction or location	Strain rate (s ⁻¹)	Yield stress MPa (ksi)	Ultimate tensile strength MPa (ksi)	Elongation (%)
	Grain size (μm)	Volume fraction primary alpha					
Q1	3.5	0.9	L	As-fabricated	936 (135.8)	982 (142.4)	14.9
Q1	3.5	0.9	L	As-fabricated	944 (136.9)	989 (143.5)	14.4
Q1	3.5	0.9	Bottom	10 ⁻⁴	925 (134.2)	925 (143.1)	12.5
Q1	3.5	0.9	Bottom	10 ⁻⁴	935 (135.6)	997 (144.6)	11.8
Q3	8.2	0.86	L	As-fabricated	900 (130.5)	903 (130.9)	4.0
Q3	8.2	0.86	L	As-fabricated	909 (131.8)	912 (132.3)	3.9
Q3	8.2	0.86	Bottom	10 ⁻⁴	765 (120.9)	870 (126.2)	7.0
Q3	8.2	0.86	Bottom	10 ⁻⁴	803 (126.5)	822 (129.3)	8.5

QP03-0246-260

Superplastic formed pans with Ti-8Al-1Mo-1V were formed at 949°C (1740°F) at a forming rate of 10⁻³ s⁻¹ and 10⁻⁴ s⁻¹. A comparison of mechanical properties Ti-8Al-1Mo-1V in as-received and superplastic formed pans are shown in Table 47. The material for tensile specimens for superplastically formed Ti-8Al-1Mo-1V was taken from the bottoms of pans.

TABLE 47. COMPARISON OF MECHANICAL PROPERTIES OF 1.27-mm (0.06 in.) Ti-8Al-1Mo-1V SHEET IN MILL-ANNEALED AND SUPERPLASTICALLY-FORMED CONDITIONS; FORMING TEMPERATURE = 949°C (1740°F).

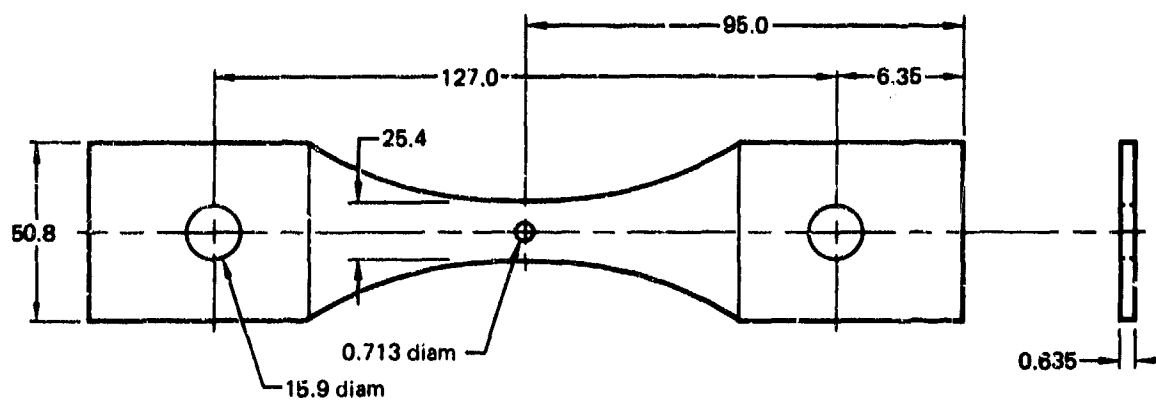
Direction or location	Strain rate (s ⁻¹)	Yield stress MPa (ksi)	Ultimate tensile strength MPa (ksi)	Elongation %
L	As-received	1060 (152.6)	1130 (163.8)	14.1
L	As-received	1070 (155.1)	1120 (162.5)	13.5
Bottom	10 ⁻³	760 (120.2)	820 (126.0)	8.5
Bottom	10 ⁻³	818 (118.6)	874 (126.8)	7.5
L	Unstrained flange	885 (128.4)	954 (138.3)	18.4
L		909 (133.3)	1000 (145.0)	13.2
Bottom	10 ⁻⁴	807 (117.0)	882 (127.9)	10.6
Bottom	10 ⁻⁴	774 (112.2)	650 (123.3)	12.5
L	Unstrained flange	865 (125.5)	939 (136.2)	19.4
L		852 (123.5)	921 (133.6)	18.6

The results from Table 47 show a large decrease in mechanical properties of superplastically formed compared with mill-annealed material. The grain growth at 949°C (1740°F) in Ti-8Al-1Mo-1V (see Table 39) was similar to Ti-6Al-4V at 907°C (1665°F) and would, therefore, not account for such large decreases. Since mill-annealed Ti-6Al-1Mo-1V has some retained work in its microstructure, additional tensile specimens were taken from the rim of the panel which had been subjected to the thermal cycle but had not been strained. These results are also shown in Table 47. A comparison of tensile properties of superplastic formed pans with as-received material and material subjected to the thermal cycle showed that the large drop in tensile properties compared to initial properties in Ti-8Al-1Mo-1V was due to removal of the retained work in commercial mill-annealed sheet.

5.13 Effect of Superplastic Forming on Damage Tolerant Properties of Ti-6Al-4V

Notched fatigue properties were measured in selected microstructures of superplastic formed pans of Ti-6Al-4V. Figure 157 shows a schematic of the notch fatigue specimen with a K_t of 2.6 used in this program. Notch fatigue specimens were taken from material from the walls of the pan. The fatigue properties of regular-grade Ti-6Al-4V and ELI-grade Ti-6Al-4V from superplastic formed pans are listed in Table 48. The stress ratio for all of these tests was +0.1. These tests did not show any appreciable differences in notched fatigue properties in superplastic formed regular-grade Ti-6Al-4V or ELI-grade Ti-6Al-4V as a function of grain size and forming rate.

101.6 mm (4.0 inches) wide fatigue crack growth panels were fabricated from a strip taken from the center portion of the bottoms of superplastic formed pans. Doublers were resistance spot welded to the ends of superplastic formed panels for gripping in the fatigue machine. Fatigue crack growth measurements were made with selected microstructures of normal-textured, regular-grade Ti-6Al-4V and ELI-grade Ti-6Al-4V pans. These tests were made in laboratory air at ambient temperature with a relative humidity of 45%. Fatigue crack growth measurements were made in the range of 10^{-6} to 4×10^{-4} mm/cycle (4×10^{-8} to 1.6×10^{-5} inches/cycle) at a stress ratio of +0.1.



Dimensions in mm

GP03-0249-148

Figure 157. Notch fatigue specimen.

TABLE 48. FATIGUE PROPERTIES OF SUPERPLASTICALLY-FORMED NORMAL-TEXTURED REGULAR-GRADE Ti-6Al-4V AND ELI-GRADE Ti-6Al-4V.

	Grain size (μm)	Volume fraction primary alpha (%)	Forming rate (s^{-1})	Max stress MPa (ksi)	No. of kilocycles for failure
Normal-textured regular-grade Ti-6Al-4V	17.6	0.88	10^{-3}	448 (65)	28
	17.6	0.88	10^{-3}	379 (55)	36
	12.2	0.88	10^{-4}	379 (55)	61
	12.2	0.88	10^{-4}	379 (55)	52
	12.6	0.46	10^{-3}	448 (65)	40
	12.6	0.46	10^{-3}	379 (55)	47
	7.7	0.88	10^{-3}	379 (55)	39
	7.7	0.88	10^{-3}	379 (55)	41
	7.7	0.88	10^{-4}	379 (55)	45
	7.7	0.88	10^{-4}	379 (55)	52
	6.0	0.88	10^{-3}	379 (55)	36
	6.0	0.88	10^{-3}	379 (55)	48
	6.0	0.88	10^{-4}	379 (55)	33
	6.0	0.88	10^{-4}	379 (55)	38
ELI-grade Ti-6Al-4V	4.4	0.47	10^{-4}	379 (55)	44
	4.4	0.47	10^{-4}	379 (55)	45
	5.5	0.88	10^{-3}	379 (55)	50
	5.5	0.88	10^{-3}	379 (55)	31
	5.5	0.88	10^{-4}	379 (55)	49
	5.5	0.88	10^{-4}	379 (55)	44
	8.9	0.88	10^{-3}	379 (55)	51
	8.9	0.88	10^{-3}	379 (55)	50
	8.9	0.88	10^{-4}	379 (55)	48
	8.9	0.88	10^{-4}	379 (55)	45

GP03-0249-150

Fatigue crack growth measurements were made from superplastic formed pans of regular-grade Ti-6Al-4V microstructures L(0.88 α , 6.0 μ m) and J(0.47 α , 4.4 μ m) and ELI-grade microstructures X1(0.88 α , 5.5 μ m). There were insufficient panels in regular grade Ti-6Al-4V microstructures L (0.88 α , 6.0 μ m) and J (0.47 α , 4.4 μ m), and ELI grade Ti-6Al-4V microstructure X1 (0.88 α , 5.5 μ m) to make fatigue crack-propagation measurements in the superplastically formed condition as well as in the as-received condition therefore, panels were selected in normal-textured, regular-grade Ti-6Al-4V and ELI-grade Ti-6Al-4V with similar initial microstructures in as-received material as those used for making superplastic formed pans. These tests were made in laboratory air at ambient temperature with a relative humidity of 45%. Fatigue crack-growth measurements were made in the range of 10^{-6} to 3×10^{-4} mm/cycle (4×10^{-8} to 1.6×10^{-5} inches/cycle) at a stress ratio of +0.1. The results are shown in Figures 158 and 159. These results show that the fatigue crack propagation rates in superplastically formed, normal-textured, Ti-6Al-4V are not degraded by superplastic forming, and that excellent damage-tolerant properties are retained.

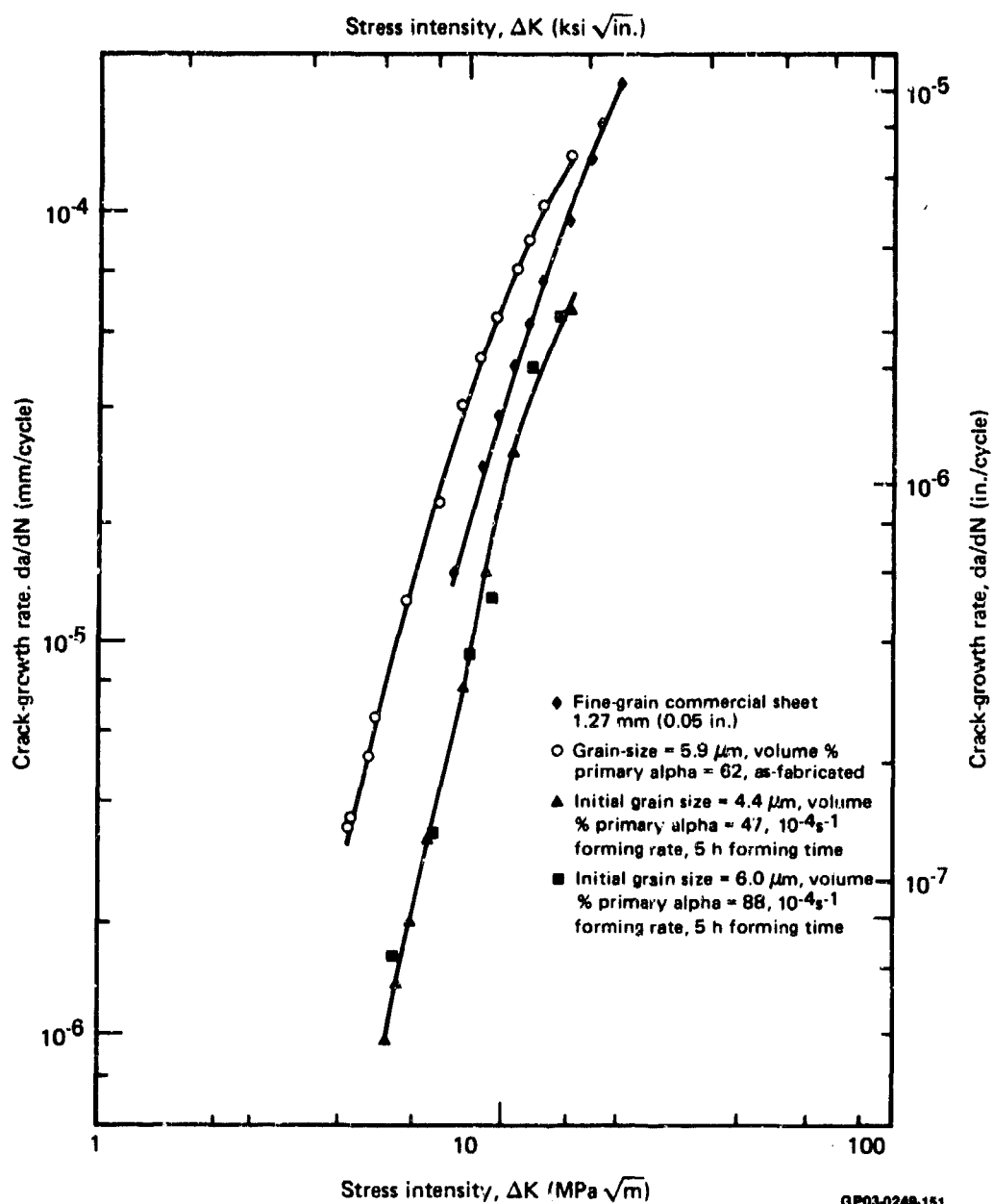


Figure 158. Fatigue-crack propagation for normal-textured regular-grade Ti-6Al-4V sheet in as-fabricated and superplastically-formed condition.

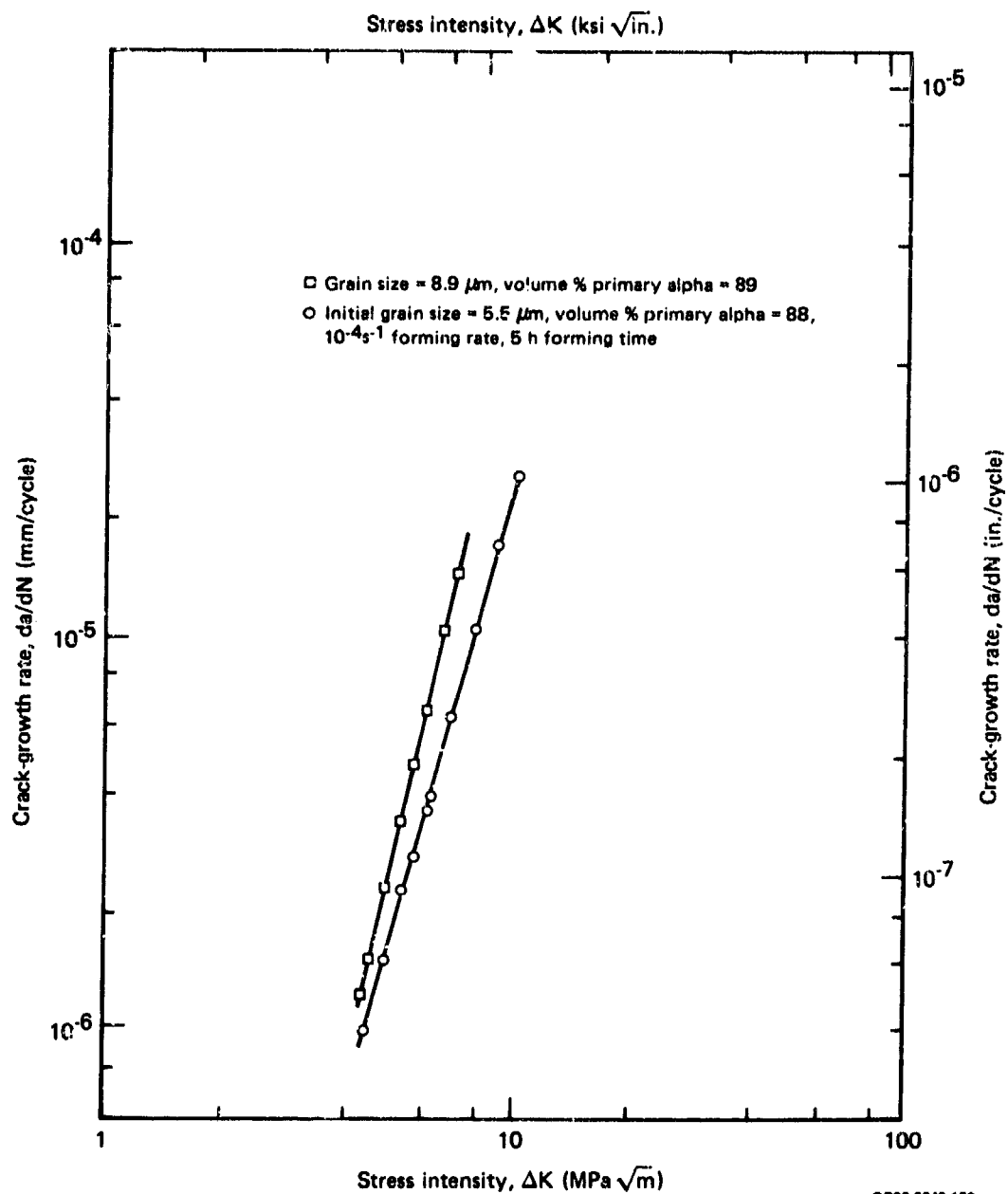


Figure 159. Fatigue-crack propagation for normal-textured ELI-grade Ti-6Al-4V in as-fabricated and superplastically-formed condition.

SECTION VI

CONSTITUTIVE EQUATION FOR SUPERPLASTIC FORMING

6.1 Time and Strain Dependence of Flow Stress-Strain Rate Relationship

Comparisons of the strain-rate dependence of flow stress determined from incremental-strain-rate tests, constant-stress tests, and cone-forming tests are shown in Figures 160a through 160d. There is excellent agreement between the data for the three tests at high stresses. At stresses < 10MPa, however, the strain rates obtained from short-time incremental-strain-rate tests are higher than those obtained from cone-forming and constant-stress tests, which can be corrected for grain growth using a constitutive equation of the form

$$\ln \left\{ (d_0 + K_1 t^{n_1}) \right\} \propto \frac{1}{m(t)} \quad (9)$$

where d_0 is the initial grain size, t is the time, K_1 and n_1 are grain-growth rate constants, and $m(t)$ is the strain-rate sensitivity as a function of time. Flow-stress/strain-rate characteristics for any condition simulating superplastic forming can be determined from flow-stress/strain-rate data obtained in incremental-strain-rate tests if the time (or equivalently, strain) dependence of grain-size and strain-rate-sensitivity are known.

6.2 Temperature Dependence of Strain Rates of Titanium Alloys

The temperature dependence of the strain rates of alpha-beta and near-alpha alloys were determined from incremental-strain-rate tests at 800-950°C (1470-1740°F) and stresses of 5-50 MPa (0.72-7.2 ksi), and the results are shown in Figures 161 through 164. The apparent activation energies for the different alloys are listed in Table 49. The activation energies determined from Figures 161 through 164 should not be used as indicators of the rate-controlling deformation processes because the strain rates shown in Figures 161 through 164 are not obtained under steady-state conditions. The steady-state strain rate of regular-grade Ti-6Al-4V as determined from constant-stress tests at a stress of 8.4 MPa is plotted in Figure 165. The activation energies at higher stresses agree with the

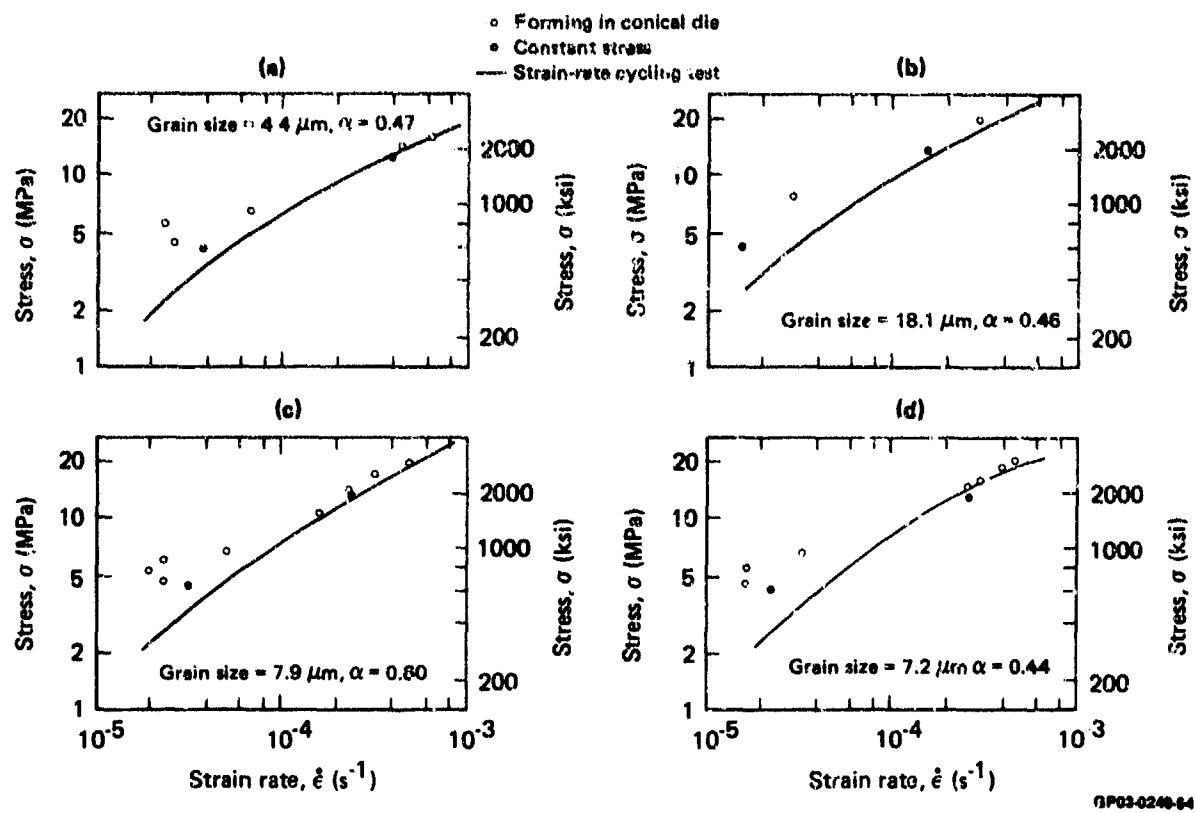
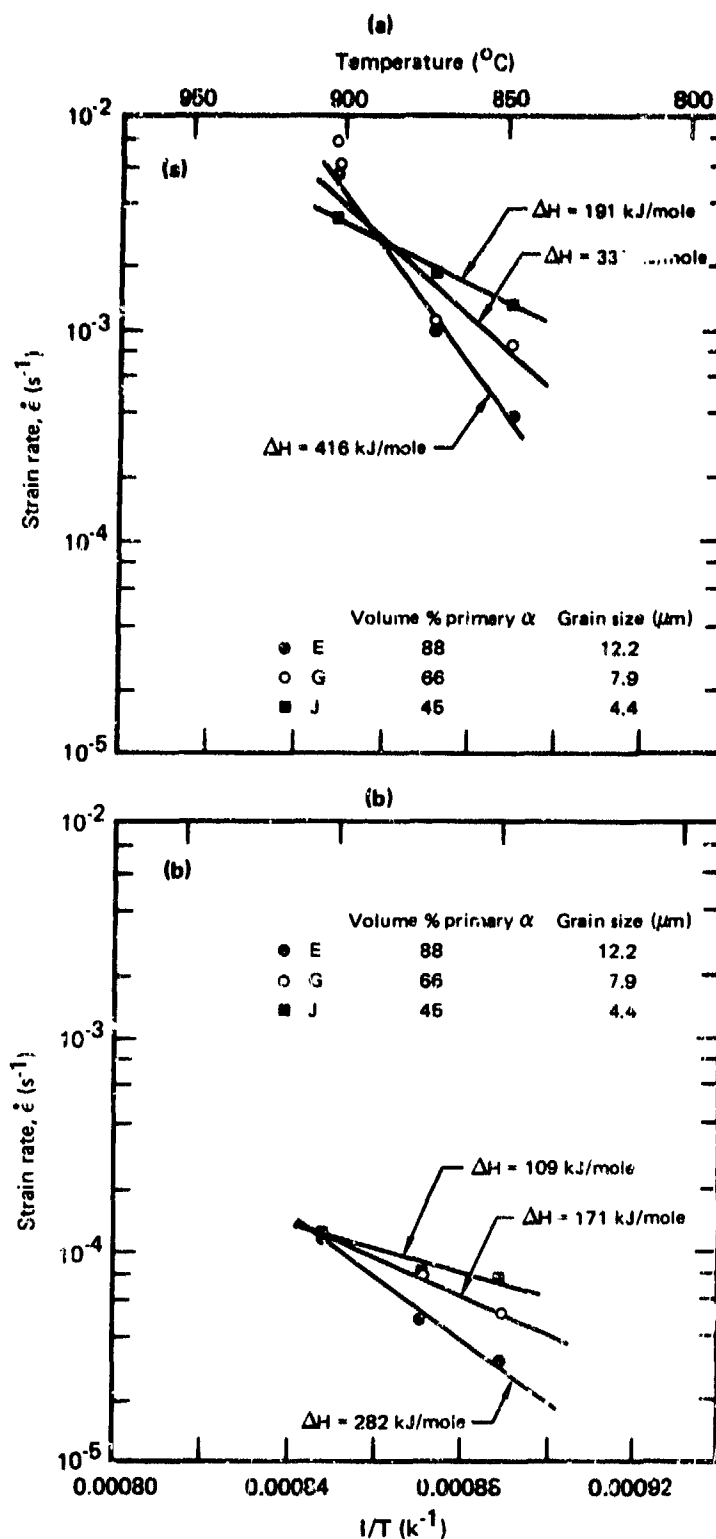


Figure 160. Comparison of strain-rate dependence of flow stress of Ti-6Al-4V determined from cone-forming test, constant stress test, and strain-rate cycling tests; (a) specimen J, (b) specimen B, (c) specimen G, and (d) specimen F.



GP03-0240-101

Figure 161. Temperature dependence of strain rate in regular-grade Ti-6Al-4V;
(a) $\sigma = 44.8 \text{ MPa}$ (6.5 ksi) and (b) $\sigma = 10.3 \text{ MPa}$ (1.5 ksi).

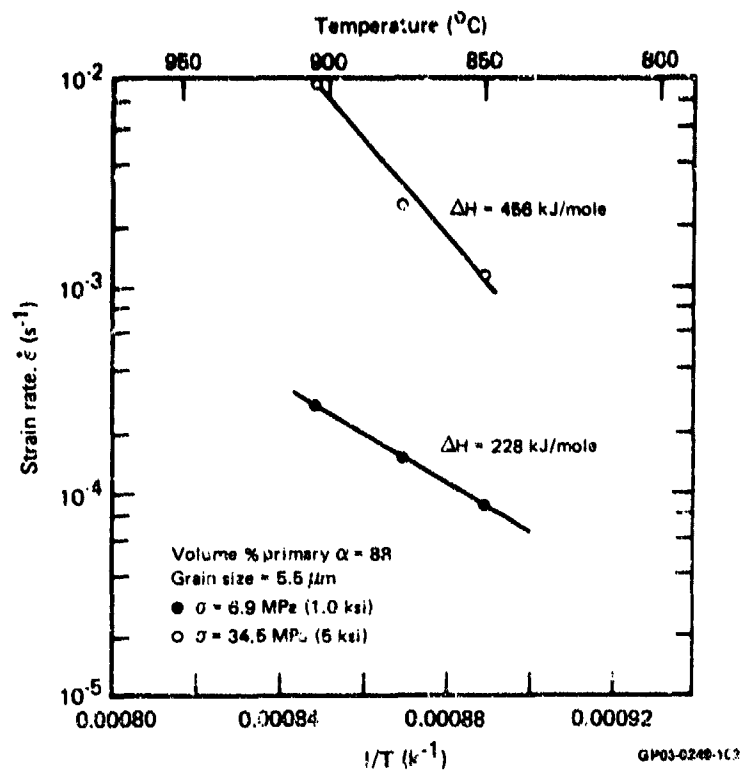


Figure 162. Temperature dependence of strain rate in ELI-grade Ti-6Al-4V sample X1.

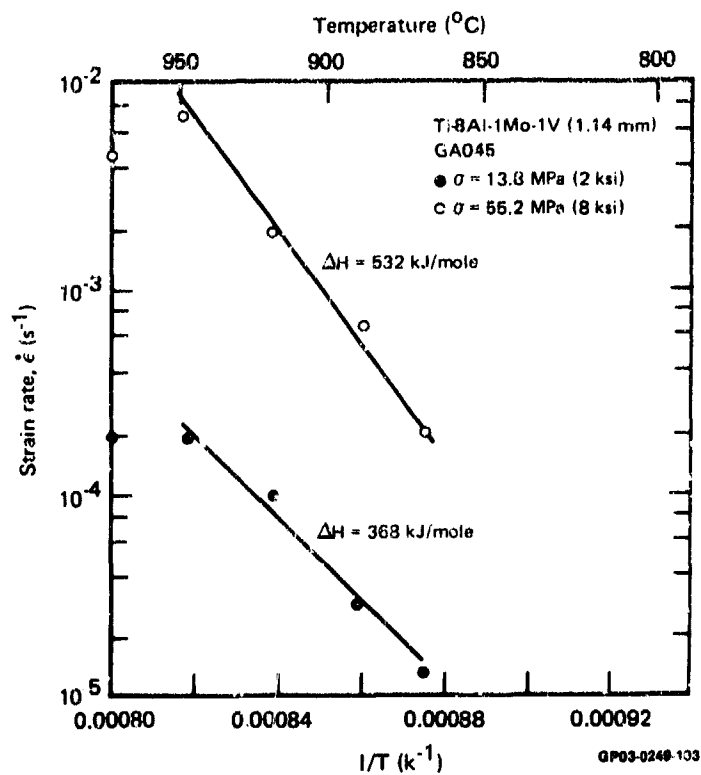
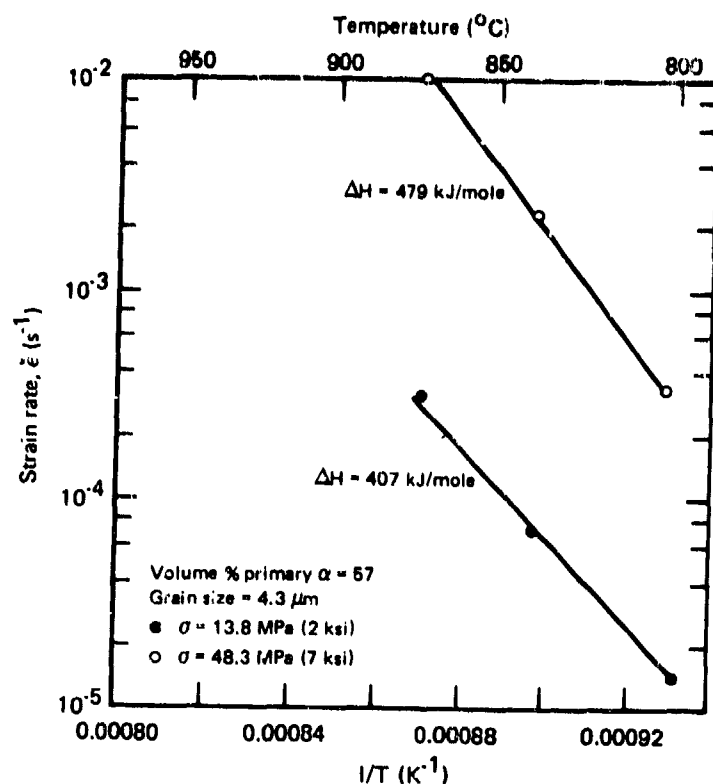


Figure 163. Temperature dependence of strain rate in Ti-8Al-1Mo-1V.



GP03-0248-104

Figure 164. Temperature dependence of strain rate in Ti-3Al-2.5V sample R2.

TABLE 49. APPARENT ACTIVATION ENERGIES FOR HIGH-TEMPERATURE FLOW OF TITANIUM ALLOYS.

Alloy	Stress [MPa (ksi)]	Temperature ($^{\circ}C$)	Apparent activation energy (kJ/mol $^{-1}$)
Regular-grade Ti-6Al-4V	45.0 (6.5)	850-910	191-416
ELI-grade Ti-6Al-4V	34.5 (5.0)	880-910	456
Regular-grade Ti-6Al-4V	10.3 (1.5)	850-910	109-282
ELI-grade Ti-6Al-4V	6.9 (1.0)	850-910	228
Ti-3Al-2.5V	48.3 (7.0)	800-875	479
Ti-3Al-2.5V	13.8 (2.0)	800-875	407
Ti-8Al-1Mo-1V	55.2 (8.0)	875-950	532
Ti-8Al-1Mo-1V	13.8 (2.0)	875-950	368

GP03-0248-13

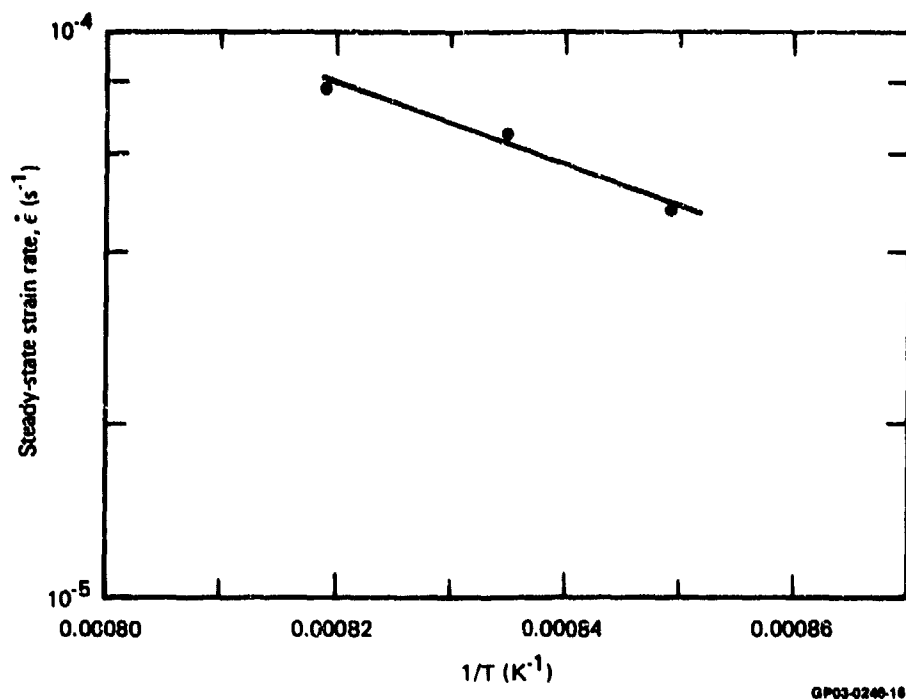


Figure 165. Temperature dependence of steady-state strain rate of regular-grade Ti-6Al-4V at a stress of 8.4 MPa.

activation energy for self diffusion in alpha and beta titanium (Reference 25), and the lower activation energy observed at a stress of 8.4 MPa (1.2 ksi) indicates the dominance of grain-boundary diffusion at lower stresses. The trends in activation energy values are consistent with the different strain-rate sensitivities observed at low and high stresses.

6.3 Constitutive Equations and Superplasticity Diagrams for Alpha-Beta Titanium Alloys

From the effects on the superplasticity of different metallurgical and testing variables discussed in previous sections, some important correlations can be made which are useful in developing constitutive equations for high-temperature, slow-strain-rate deformation of titanium alloys. The correlations also are useful as guidelines for selecting superplastic-forming parameters for alloys with known properties.

The most important correlation required for designing a superplastic forming operation is the temperature, strain-rate, and strain (or equivalently, time) dependence of flow stress, and the most important microstructural variables that affect these parameters in titanium alloys are grain size and shape, volume fractions of the phases at the forming temperature, contiguity of alpha, and the microstructural anomalies. From a practical standpoint, a single constitutive relation incorporating all microstructural and testing variables is most useful,

but because of the complexity of the alloy systems and the large number of variables involved, some approximations are necessary to construct a tractable constitutive equation.

A phenomenological expression relating the strain-rate, $\dot{\epsilon}$, to flow stress, σ , under steady-state conditions at high temperature can be written in the form (Reference 24),

$$\frac{\dot{\epsilon} k T}{D G b} = A \left(\frac{b}{d}\right)^p \left(\frac{\sigma}{G}\right)^n, \quad (10)$$

where

$\dot{\epsilon}$ = steady-state strain rate,

k = Boltzman constant,

T = temperature,

D = diffusion coefficient,

G = shear modulus,

b = Burgers vector,

d = grain size,

n = stress exponent = $\frac{1}{m}$ (m being the strain-rate sensitivity),
and A and p are constants.

The grain-size exponent, p , can be approximated by unity in the superplastic region. Since the microstructure continuously changes with time and strain during superplastic deformation of titanium alloys, the time dependences of grain size, stress, and strain-rate should be incorporated into Equation (10). If the property changes are assumed to be mainly due to grain growth, the time dependence of the flow-stress/strain-rate relationship can be written as

$$\frac{\dot{\epsilon} k T (K_1 t^{n_1})}{D G b^2} = \left(\frac{\sigma}{G}\right)^{1/(m_0 + K_2 d)}, \quad (11)$$

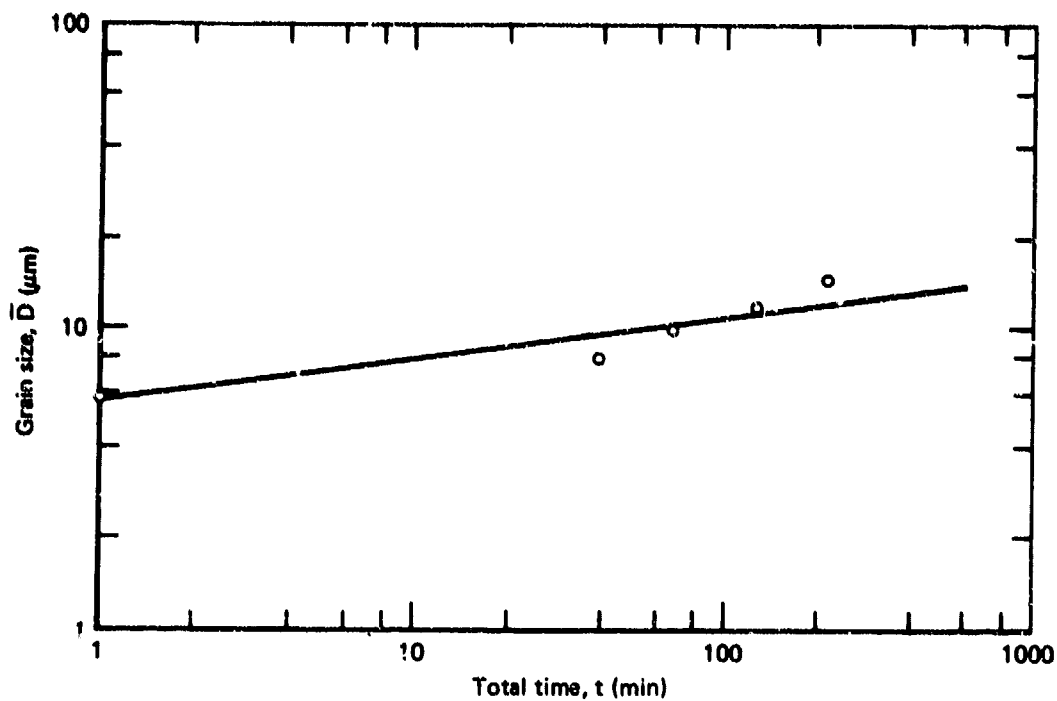
where d_0 is the initial grain size, m_0 is the initial strain-rate-sensitivity, and t is the time. K_1 , n_1 and K_2 are experimentally determined constants. The grain-size dependence of m can be converted to a time dependence by writing

$K_1 t^{n_1}$ for d , and Equation (10) then becomes

$$\frac{\dot{\epsilon} k T (K_1 t^{n_1})}{D G b^2} = \left(\frac{\sigma}{G} \right)^{1/(m_0 + K_2 K_1 t^{n_1})} \quad (12)$$

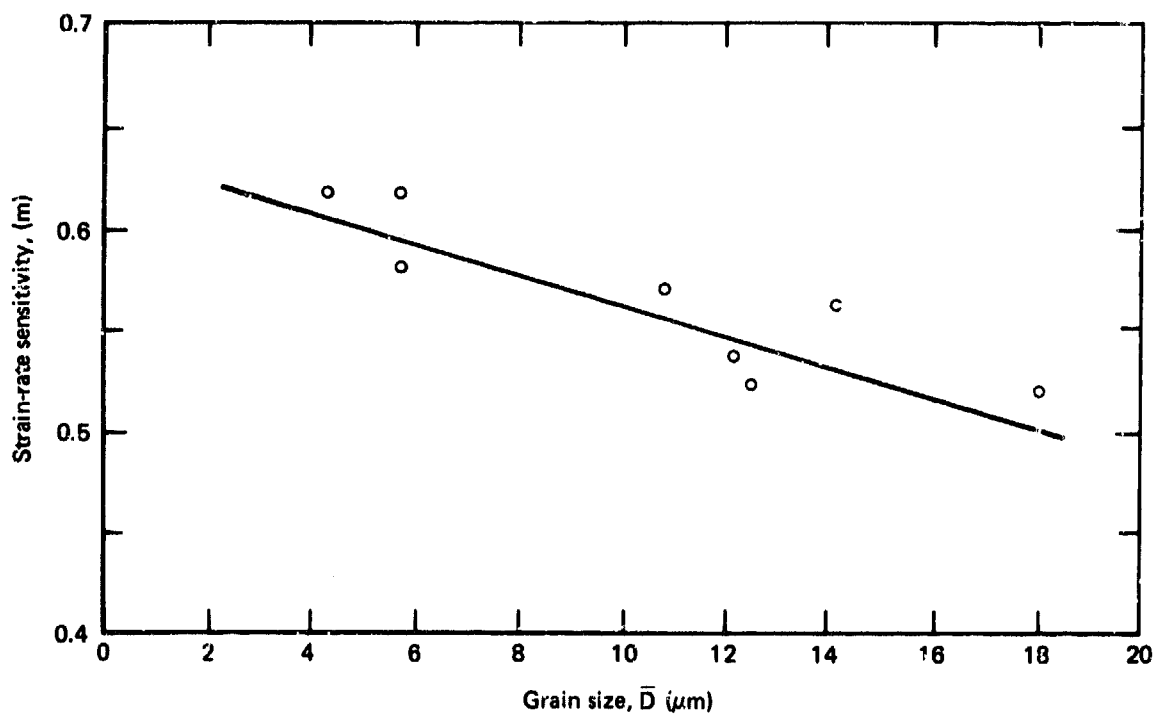
From the results of this study, the best values for the constants in Equation (12) for Ti-6Al-4V (Specimen I: volume fraction of primary alpha = 0.45 and grain size = 5-6 μm) were determined to be $A = 18$, $K_1 \approx$ initial grain size, and $K_2 = -0.038$ (Figures 166 and 167). Since all constants in Equation (12) are experimentally determined, the variation of superplastic strain-rate with time at any applied stress can be predicted with accuracy. As an example, the interrelationship between flow stress, strain-rate, and time as calculated from Equation (11) is plotted in Figure 168.

The interrelationships between strain-rate, grain-size, strain-rate-sensitivity of flow stress, and test temperature to beta-transus ratio are shown in Figures 169 and 170. In this type of graphical representation, the effects of grain-size and volume-fractions of constituent phases at temperature are incorporated in the ratio, T/T_β , and such diagrams thus are universal for all alpha-beta titanium alloys having similar two-phase fields at the superplastic temperatures. The diagrams shown in Figures 169 and 170 were constructed from data for three different alpha-beta titanium alloys, Ti-6Al-4V, Ti-3Al-2.5V, and Ti-8Al-1Mo-1V, with widely varying beta-transus temperatures. Figures 169 and 170 can be used for obtaining superplasticity screening parameters and determining the suitability for a particular superplastic forming operation of a material of known grain size and beta-transus temperature, and the time dependence of superplastic strain rates of the alloy can be predicted from the constitutive relation, Equation (11).



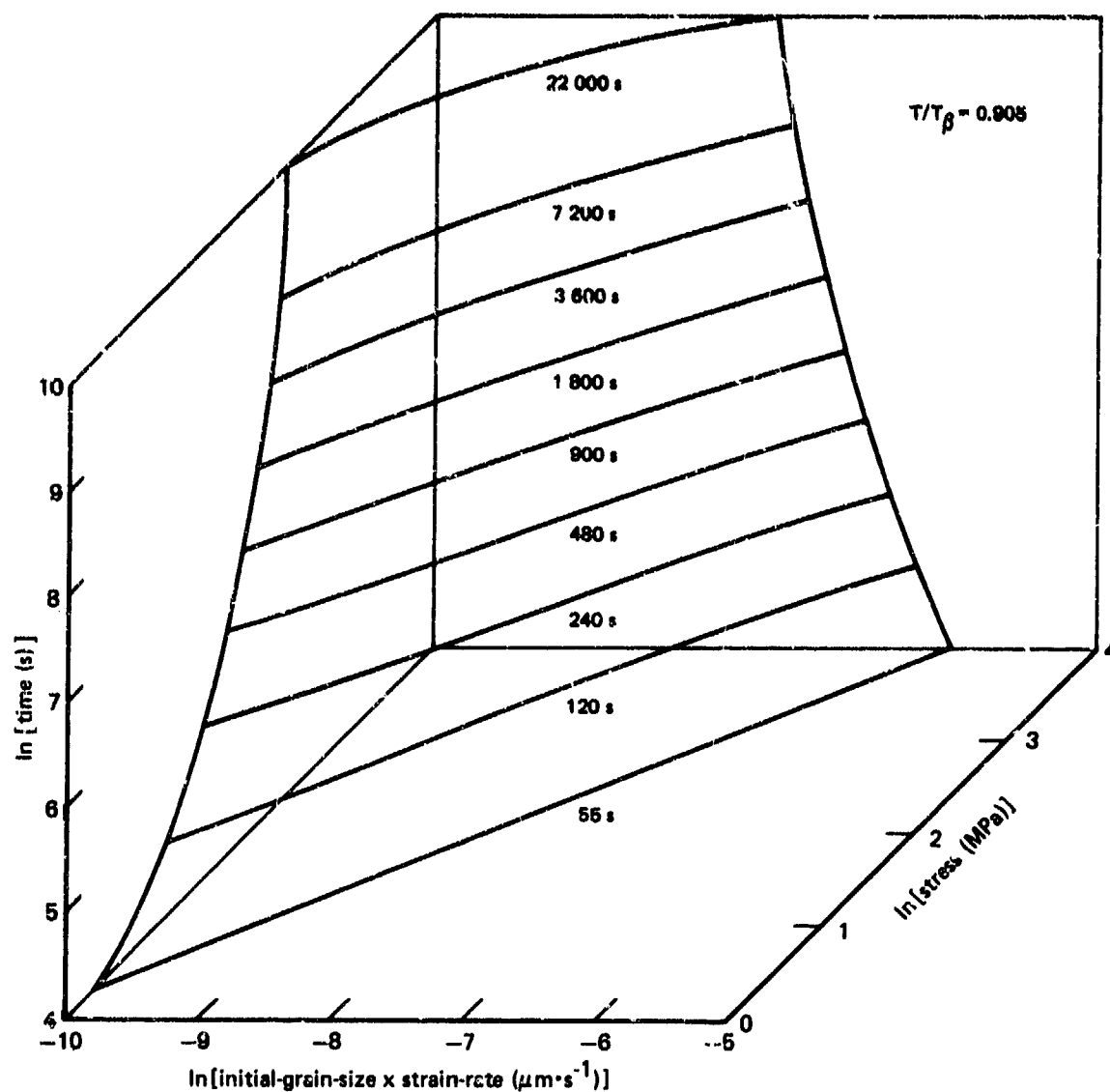
GP03-0248-17

Figure 166. Variation of grain size with time of regular-grade Ti-6Al-4V annealed at 907°C (1665°F)



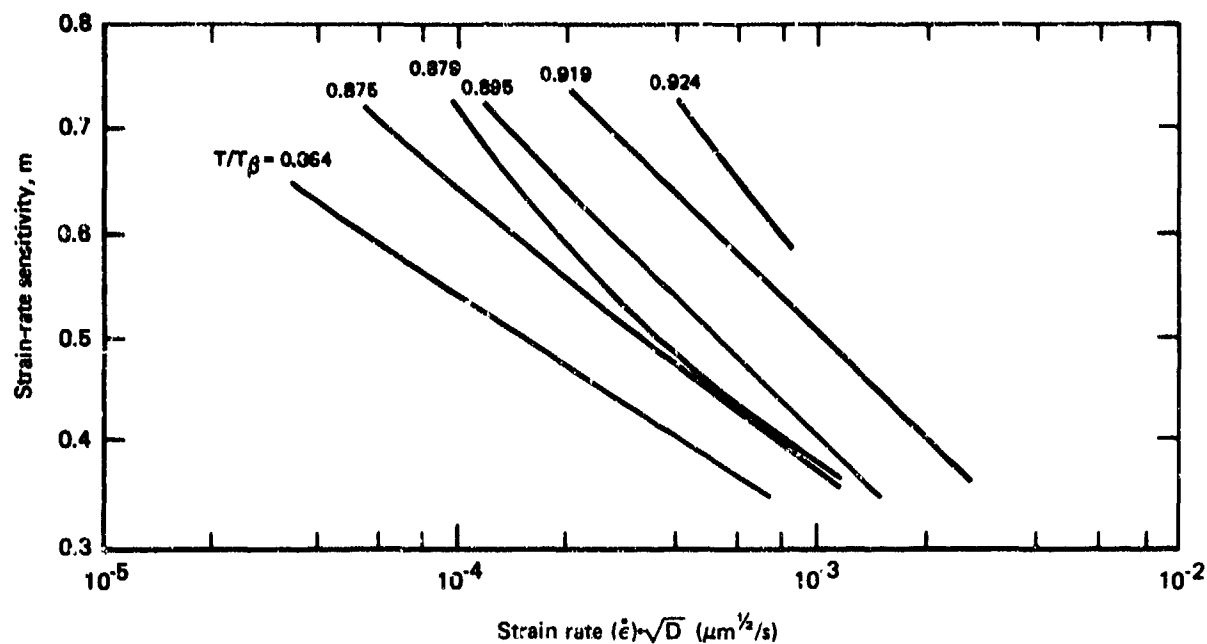
GP03-0249-18

Figure 167. Grain-size dependence of strain-rate sensitivity of regular-grade Ti-6Al-4V at 875°C (1604°C) at a strain rate of 10^{-4} s^{-1} .



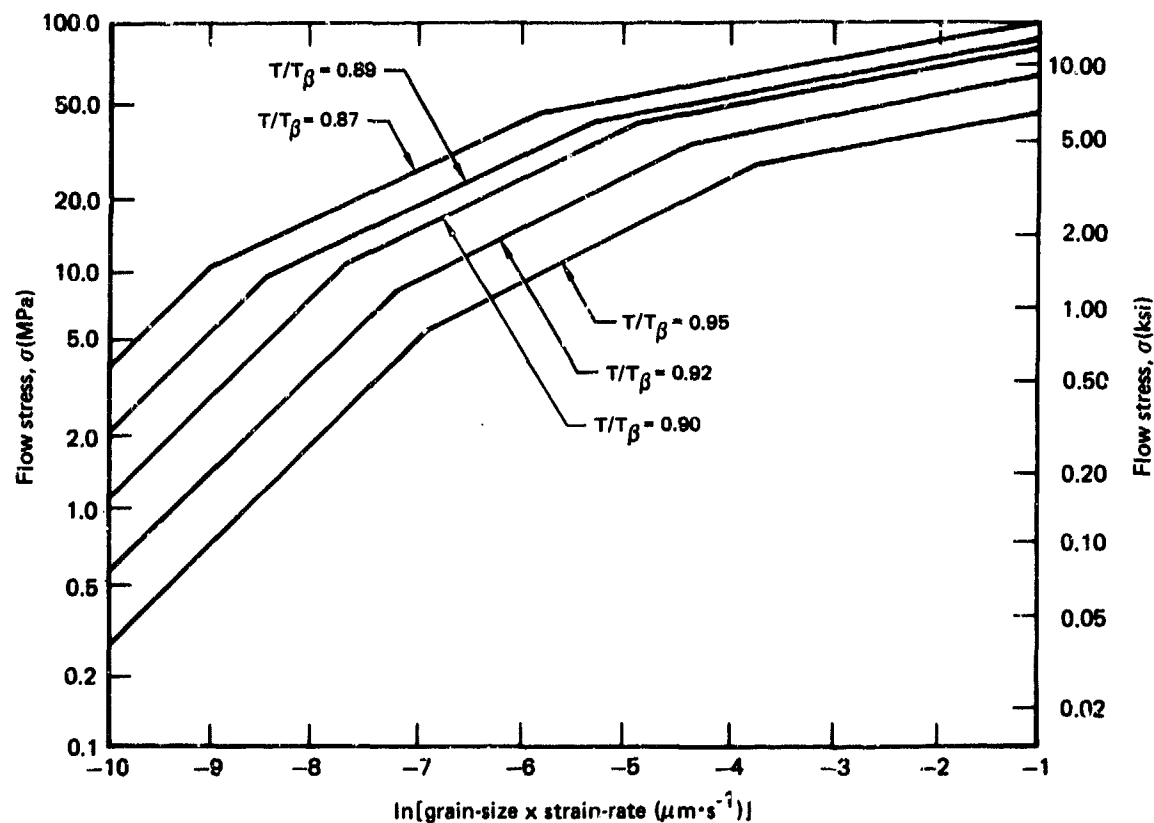
GP03-0248-136

Figure 168. Three-dimensional representation of the constitutive equation for superplastic forming of alpha-beta titanium alloys. The surface shown is for $T/T_\beta = 0.905$; other forming temperatures generate different surfaces.



GP03-0249-20

Figure 169. Temperature and strain-rate dependence of strain-rate sensitivity for alpha-beta titanium alloys.



GP03-0249-134

Figure 170. Flow stress as a function of strain rate and grain size at different forming-temperature/beta-transus ratios for alpha-beta titanium alloys.

The results of different laboratory tests discussed in previous sections clearly indicate that because of the extensive microstructural changes and strain hardening that occur during superplastic forming of titanium alloys, the complete characterization of superplastic formability of these alloys requires the strain and time dependences of flow stress and strain-rate-sensitivity to be determined. This information can be obtained either by constant-stress tests or constant strain-rate tests. Techniques for determining the generalized three-dimensional plots of the interrelationship between flow stress, strain rate, and strain described in previous sections should thus be valuable for evaluating the relative superplasticities of different titanium alloys.

SECTION VII

SUMMARY AND CONCLUSIONS

The effects of alloy chemistry, grain size, volume fractions of constituent phases, and anomalous microstructures on the superplasticity parameters at 800-980°C (1472-1796°F) of alpha-beta, near-alpha, and beta titanium alloys were determined.

Ti-6Al-4V was the base material studied in this program. Equiaxed alpha grain sizes ranging from 4.5 μm to 18 μm were produced in weakly textured sheet for regular-grade, ELI-grade and simulated-coil Ti-6Al-4V. The microstructural variables which were investigated in Ti-6Al-4V included the volume fraction of primary alpha phase, basal and transverse-basal texture, and anomalous microstructures (elongated alpha, banding and blocky alpha).

Equiaxed microstructures were produced in sheet material for the following alpha-beta titanium alloys: Ti-3Al-2.5V, Ti-6Al-2Sn-4Zr-2Mo and Ti-8Al-1Mo-1V.

A very fine recrystallized beta grain size could not be produced in the beta alloy Ti-15V-3Cr-3Sn-3Al. The finest equiaxed beta grain size achieved was 32 μm .

The processing procedures for making the desired microstructures for each of the titanium alloys outlined in Section II were initially developed with laboratory tests, and subsequently, panels 381 x 381 x 1.52 mm (14 x 14 x .060 inches) were produced in a production facility using the procedures developed in the laboratory.

Uniaxial incremental-strain-rate tests were used to obtain flow-stress as a function of strain rate for each microstructure of all titanium alloy sheet materials produced in this program. To show the effects of microstructural changes as a function of time at temperature on flow stresses, constant stress and constant strain-rate tests for selected microstructures were conducted. A few flat-ring compression tests were performed with regular-grade normal-texture Ti-6Al-4V to compare with incremental strain-rate tests.

A simplified biaxial conical-die forming test was developed for superplastic gas forming evaluation of sheet material at elevated temperatures. Biaxial forming tests were performed for each microstructure of all the titanium alloys studied in this program. A correlation of the results obtained by biaxial conical-die forming were made with the results from laboratory uniaxial tests.

The effects of superplastic forming on the mechanical and fatigue properties of selected alpha-beta titanium alloys microstructures were determined by comparison with properties in the as-received material.

The conclusions from all of the superplastic forming tests performed in this program are:

1. The strain-rate dependence of flow stress and strain-rate sensitivity, m , determined from short-time strain-rate cycling tests does not completely describe the superplastic characteristics of alpha-beta titanium alloys because of microstructural changes with strain and time.
2. The strain and time dependences of flow stress and strain rate required to simulate production superplastic-forming operations can be obtained by laboratory constant-stress and constant-strain-rate tests. The superplastic strain rates determined from laboratory constant-stress tests are equal to the strain rates obtained from biaxial cone-forming tests.
3. The most important microstructural variables affecting superplasticity of titanium alloys are grain-size, grain shape and volume-fractions of constituent phases at temperature. With increasing grain-size, and elongated grain shape, the flow stress increases and the strain-rate-sensitivity and necking-resistance decrease.
4. The flow stress, σ , at constant temperature, T , and constant strain rate, $\dot{\epsilon}$, of different alpha-beta titanium alloys is uniquely related to grain size, L , and beta-transus, T_B , by a relation of the form

$$\ln (\dot{\epsilon} \cdot L) \propto \sigma^m (T/T_B) . \quad (13)$$

5. All of the alpha-beta titanium alloys studied in this program which had a fine equiaxed grain microstructures showed good SPF properties at $T/T_B = .9$. A high forming stress was required for superplastic forming of the beta alloy Ti-15V-3Cr-3Sn-3Al. The high forming stresses and rapid grain growth in beta alloy Ti-15V-3Cr-3Sn-3Al appear to make superplastic forming in this material impractical.

6. Strain rates obtained in biaxial conical die agreed with incremental strain-rate data for short forming times and high strain rates in all alpha-beta titanium alloys.
7. For slow strain rates and long forming times, grain growth was a major factor for decreasing strain rate in conical die at a fixed constant stress. The grain growth resulted in slower strain rates than predicted by incremental strain-rate data.
8. A small drop in tensile properties due grain growth is observed in superplastically formed alpha-beta titanium alloys compared to initial properties before forming with high primary alpha microstructures. No degradation was observed in fatigue properties of superplastically formed Ti-6Al-4V sheet.
9. A constitutive equation for the stress, time, temperature, and grain-size dependence of superplastic strain-rate obtained from experimentally determined constants correctly predicts the magnitude and time dependence of strain rate.
10. Three-dimensional plots of the interrelationship between flow stress, strain, strain rate, strain-rate sensitivity, grain size, and temperature are required for obtaining superplasticity parameters for alpha-beta titanium alloys.

REFERENCES

1. E. D. Weisert and G. W. Stacher, "Fabricating Titanium Parts with SPF/DB Process", *Metal Progress*, 111 No. 3, 1977 p. 32.
2. A. Arieli and A. Rosen, "Measurements of the Strain Rate Sensitivity Coefficient in Superplastic Ti-6Al-4V Alloy," *Scripta Metallurgica*, 10, 1976 p. 471.
3. F. Povolo, "On the Measurement of the Strain-Rate Sensitivity Parameter," *Journal of Nuclear Materials*, 78, 1978, p. 309.
4. R. H. Geiss, W. F. Marley, Jr., "Survey of Research on Superplasticity-Worldwide," NTIS Document FSTC-CW-01-106-74 (1973).
5. M. F. Ashby and R. A. Verrall, "Diffusion Accommodated Flow and Superplasticity," *Acta Met.* 21, 1973, p. 149.
6. A. K. Mukherjee, "High Temperature Creep," in *Treatise on Materials Science and Technology*, Vol. 6, ed. by R. J. Arsenault, (Academic Press, New York 1975), p. 163.
7. G. Rai and N. J. Grant, "On the Measurements of Superplasticity in an Al-Cu Alloy," *Met. Trans.* 6A, 385 (1975).
8. A. K. Mukherjee, "Deformation Mechanisms in Superplasticity," *Annual Review of Materials Science*, Vol. 9, 1979, p. 191.
9. J. E. Lytle, G. Fischer, and A. R. Marder, "Superplasticity in an Alpha-Beta Titanium Alloy," *Journal of Metals*, 17, 1965, p. 1055.
10. D. Lee and W. A. Backofen, "Superplasticity in Some Titanium and Zirconium Alloys," *Trans. AIME* 239, 1967, p. 1034.
11. C. H. Hamilton, G. W. Stacher, J. A. Mills and H. W. Li, "Superplastic Forming of Titanium Structures," AFML-TR-75-62, April 1975.

12. A. Arieli and A. Rosen, "Superplastic Deformation of Ti-6Al-4V Alloy," Met. Trans. 8A, 1977, p. 1591.
13. S. M. L. Sastry, R. J. Lederich, P. S. Pao, and J. E. O'Neal, "Influence of Rare-Earth Additions on Properties of Titanium Alloys: Plane-Strain Fracture Toughness, Creep, and High Temperature Deformation of Ti-6Al-4V with Erbium and Yttrium Additions," McDonnell Douglas Report Q0684 (31 May 1979), Technical Report, ONR Contract No. N00014-76-C-0626.
14. S. M. L. Sastry, P. S. Pao, and K. K. Sankaran, "Influence of Yttrium and Erbium Additions on High Temperature-Creep and Superplasticity of Titanium," to be published.
15. L. J. Pionke, J. S. Bonini and S. M. L. Sastry, "Effects of Yttrium Additions on Microstructure and Properties of Ti-6Al-2Sn-4Zr-2Mo-0.1Si," 12th National SAMPE Technical Conference, Seattle, Washington, 7-9 October, 1980.
16. J. W. Edington, "Physical Metallurgy of Superplasticity, Metals Technology, 3, 1976, p. 138.
17. J. J. Jonas and M. J. Luton, "Flow Softening at Elevated Temperatures" in Advances in Deformation Processing ed. by J. J. Burke and V. Weiss, Plenum Publishing Corporation, New York, 1978, p. 215.
18. J. W. Edington, K. N. Melton and C. P. Cutler, "Superplasticity," Prog. Materials Sci., 21 1976, p. 63.
19. V. DePierre and F. Gurney, "A Method for Determination of Constant and Varying Friction Factors During Ring Compression Tests," AFML-TR-72-135, 1972.
20. F. Jovane, "Superplasticity in Titanium", Science, Technology and Application of Titanium, Proceedings of International Conference on Titanium, London, May 1968, ed. by R. I. Jaffee, and N. E. Promise, (Pergamon Press, New York, 1970), p. 615.

21. A. W. Sommer and M. Craeger, Research Towards Developing and Understanding of Crystallographic Texture of Mechanical Properties of Titanium Alloys, AFML-TR-76-222, January 1977.
22. E. E. Underwood, Quantitative Stereology, Addison-Wesley 1970.
23. S. M. L. Sastry and J. E. O'Neal, "Substructural Changes During High Temperature Deformation of Ti-6Al-4V" to be published.
24. S. M. L. Sastry "Texture Modifications During High Temperature Deformation of Ti-6Al-4V" to be published.
25. R. J. Wasilewski and G. L. Kehl, "Diffusion of Hydrogen in Titanium", Metallurgia, 50, 1954, p. 225.

APPENDIX A

CONICAL DIE FOR SUPERPLASTIC FORMING

1.0 Analysis of Conical Die

The design of a conical die that would give a constant strain rate at a fixed constant pressure has been made with the following assumptions:

1. No plastic forming occurs after material contacts the surface walls of the die.
2. Constant stress does not exist until the spherical shape in conical cavity is tangent to the walls of the die.

A schematic of conical die is shown in Figure 1-A. From Figure 1-A the following relationships are applicable:

$$\left. \begin{aligned} X &= \frac{R}{\cos \frac{\alpha}{2}} \\ x &= \frac{r}{\cos \frac{\alpha}{2}} \\ h &= R \tan \frac{\alpha}{2} \end{aligned} \right\} \quad (14)$$

$$\text{Area of Hemisphere} = \frac{\pi(2X)^2}{2} = \frac{2\pi R^2}{(\cos \frac{\alpha}{2})^2} \quad (15)$$

$$\text{Area of Spherical Zone (h)} = 2\pi x h = \frac{2\pi R^2 \tan \frac{\alpha}{2}}{\cos \frac{\alpha}{2}} \quad (16)$$

$$\text{Area of Spherical Section in Cone} = \left[\frac{2\pi R^2}{(\cos \frac{\alpha}{2})^2} - \frac{2\pi R^2 \tan \frac{\alpha}{2}}{\cos \frac{\alpha}{2}} \right] \quad (17)$$

$$\text{Initial Area of Material Used for Forming} = \pi R^2 \quad (18)$$

From Volume Equivalents*:

$$\begin{aligned} \pi R^2 t_1 &= \left[\frac{2\pi R^2}{(\cos \frac{\alpha}{2})^2} - \frac{2\pi R^2 \tan \frac{\alpha}{2}}{\cos \frac{\alpha}{2}} \right] t_2 \\ t_1 &= \left[\frac{2 - 2 \sin \frac{\alpha}{2}}{(\cos \frac{\alpha}{2})^2} \right] t_2 \\ \frac{t_1}{t_2} &= \frac{2}{1 + \sin \frac{\alpha}{2}} \end{aligned} \quad (19)$$

*Does not account for metal consumed in corners.

$$S = \frac{R}{\sin \frac{\alpha}{2}} \quad , \quad \Delta = \frac{r}{\sin \frac{\alpha}{2}} \quad (20)$$

$$\left. \begin{aligned} \text{Total Conical Surface} &= \frac{1}{2} (2\pi R) S \\ &= \frac{\pi R^2}{\sin \frac{\alpha}{2}} \\ \text{Area of Small Cone} &= \frac{\pi r^2}{\sin \frac{\alpha}{2}} \end{aligned} \right\} \quad (21)$$

$$\text{Area of Truncated Cone} = \frac{\pi (R^2 - r^2)}{\sin \frac{\alpha}{2}} \quad (22)$$

$$\text{Area of Spherical Section} = \frac{2\pi r^2}{(\cos \frac{\alpha}{2})^2} - \frac{2\pi r^2 \tan \frac{\alpha}{2}}{\cos \frac{\alpha}{2}} \quad (\text{From Eq. 17})$$

Volume Equivalents:

$$\pi R^2 t_1 = \frac{\pi (R^2 - r^2)(t_2 + t)}{2 \sin \frac{\alpha}{2}} + t \left[\frac{2\pi r^2}{(\cos \frac{\alpha}{2})^2} - \frac{2\pi r^2 \tan \frac{\alpha}{2}}{\cos \frac{\alpha}{2}} \right]$$

$$R^2 t_1 = \frac{(R^2 - r^2)(t_2 + t)}{2 \sin \frac{\alpha}{2}} + \left[\frac{2r^2 - 2r^2 \sin \frac{\alpha}{2}}{(\cos \frac{\alpha}{2})^2} \right] t$$

$$R^2 t_1 = \frac{(R^2 - r^2)t_2 + t}{2 \sin \frac{\alpha}{2}} + \frac{2r^2 t}{1 + \sin \frac{\alpha}{2}} \quad (23)$$

Substitute the expression for t_1 from Eq. 19 into Eq. 23.

$$R^2 \left(\frac{2t_2}{1 + \sin \frac{\alpha}{2}} \right) = \frac{R^2 - r^2}{2 \sin \frac{\alpha}{2}} (t_2 + t) + \frac{2r^2 t}{1 + \sin \frac{\alpha}{2}} \quad (24)$$

Multiply by $2 (1 + \sin \frac{\alpha}{2}) \sin \frac{\alpha}{2}$:

$$4R^2(t_2)^2 \sin \frac{\alpha}{2} = (R^2 - r^2)(t_2 + t)(1 + \sin \frac{\alpha}{2}) + 4r^2 t \sin \frac{\alpha}{2} \quad (25)$$

Thus we have, dividing by t , the result

$$4R^2 \frac{t_2}{t} \sin \frac{\alpha}{2} - (R^2 - r^2) \left(\frac{t_2}{t} + 1 \right) \left(1 + \sin \frac{\alpha}{2} \right) - 4r^2 \sin \frac{\alpha}{2} = 0 \quad (26)$$

Simplifying

$$4R^2 t_2 \sin \frac{\alpha}{2} - (R^2 - r^2)(t_2 + t) - (R^2 - r^2)(t_2 + t) \sin \frac{\alpha}{2} - 4r^2 t \sin \frac{\alpha}{2} = 0$$

$$\sin \frac{\alpha}{2} \left[4R^2 t_2 - (R^2 - r^2)(t_2 + t) - 4r^2 t \right] - (R^2 - r^2)(t_2 + t) = 0$$

$$\sin \frac{\alpha}{2} \left[4R^2 t_2 - (R^2 - r^2)t_2 - (R^2 - r^2)t - 4r^2 t \right] - (R^2 - r^2)(t_2 + t) = 0$$

$$\sin \frac{\alpha}{2} \left[3R^2 t_2 + r^2 t_2 - tR^2 - 3r^2 t \right] - (R^2 - r^2)(t_2 + t) = 0$$

$$\sin \frac{\alpha}{2} = \frac{(R^2 - r^2)(t_2 + t)}{t_2 (r^2 + 3R^2) - t (R^2 + 3r^2)}$$

$$\frac{\alpha}{2} = \sin^{-1} \left[\frac{(R^2 - r^2)(t_2 + t)}{t_2 (r^2 + 3R^2) - t (R^2 + 3r^2)} \right] \quad (27)$$

Equation 26 can be rewritten as follows:

$$\frac{\alpha}{2} = \sin^{-1} \left[\frac{\left(\frac{R^2}{r^2} - 1 \right) \left(\frac{t_2}{t} + 1 \right)}{\frac{t_2}{t} \left(1 + 3 \frac{R^2}{r^2} \right) - \left(\frac{R^2}{r^2} + 3 \right)} \right] \quad (28)$$

For constant pressure the following relation applies when a constant stress is maintained:

$$\frac{t_2}{t} = \frac{R}{r}$$

(29)

Equation becomes

$$\frac{\alpha}{2} = \sin^{-1} \left[\frac{\left(\left(\frac{t_2}{t} \right)^2 - 1 \right) \left(\frac{t_2}{t} + 1 \right)}{\frac{t_2}{t} \left(1 + 3 \frac{t_2^2}{t^2} \right) - \left(\frac{t_2^2}{t^2} + 3 \right)} \right]$$

$$= \sin^{-1} \frac{(\chi^2 - 1)(\chi + 1)}{\chi(1 + 3\chi^2) - (\chi^2 + 3)}$$

Where $\chi = \frac{t_2}{t}$

This expression can be simplified; consider the denominator

$$\begin{aligned} \chi(1 + 3\chi^2) - (\chi^2 + 3) &= \chi + 3\chi^3 - \chi^2 - 3 \\ &= 3(\chi^3 - 1) - \chi(\chi - 1) \end{aligned}$$

$$\text{BUT } \chi^3 - 1 = (\chi - 1)(\chi^2 + \chi + 1)$$

So

$$\therefore 3\chi^3 + \chi - \chi^2 - 3 = (\chi - 1)(3\chi^2 + 2\chi + 3)$$

$$\frac{\alpha}{2} = \sin^{-1} \left[\frac{(\chi^2 - 1)(\chi + 1)}{(\chi - 1)(3\chi^2 + 2\chi + 3)} \right]$$

$$= \sin^{-1} \left[\frac{(\chi - 1)(\chi + 1)^2}{(\chi - 1)(3\chi^2 + 2\chi + 3)} \right]$$

Thus

$$\frac{\alpha}{2} = \sin^{-1} \left[\frac{(\chi + 1)^2}{3\chi^2 + 2\chi + 3} \right]$$

(30)

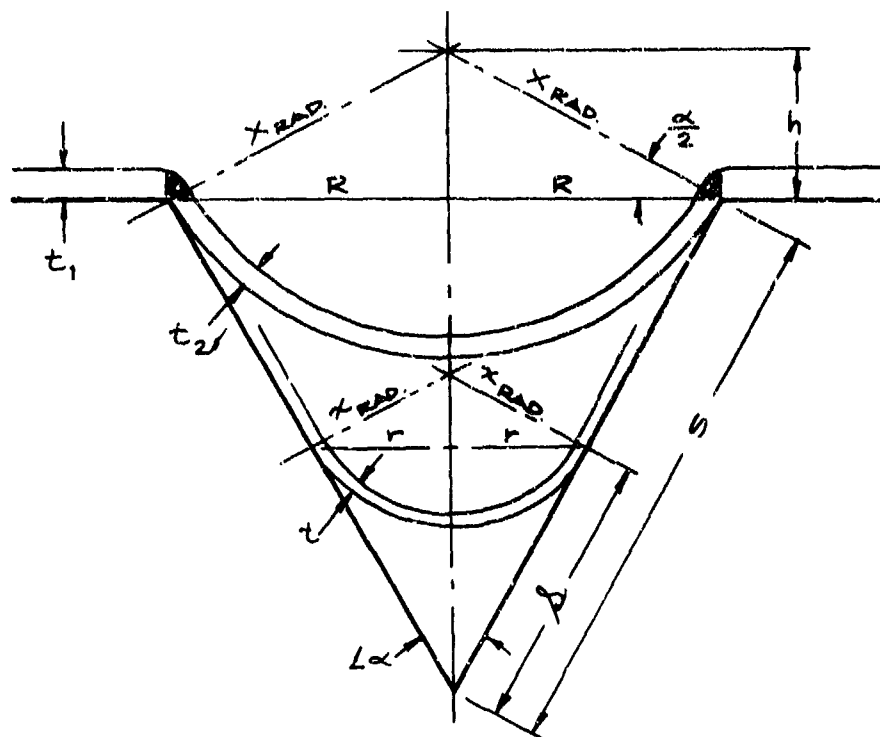


FIGURE 1-A. SCHEMATIC OF CONICAL DIE

Using equation (29) a plot of $\frac{OC}{2}$ versus R/r is shown in Figure 2A. As seen from Figure 2A a small divergence from linear cone would be required to achieve this condition; however the assumptions used to make these calculations probably introduce errors equal to greater than those that would be introduced by using a linear cone. A mean cone angle of 28.5° was selected as being representative for most engineering applications.

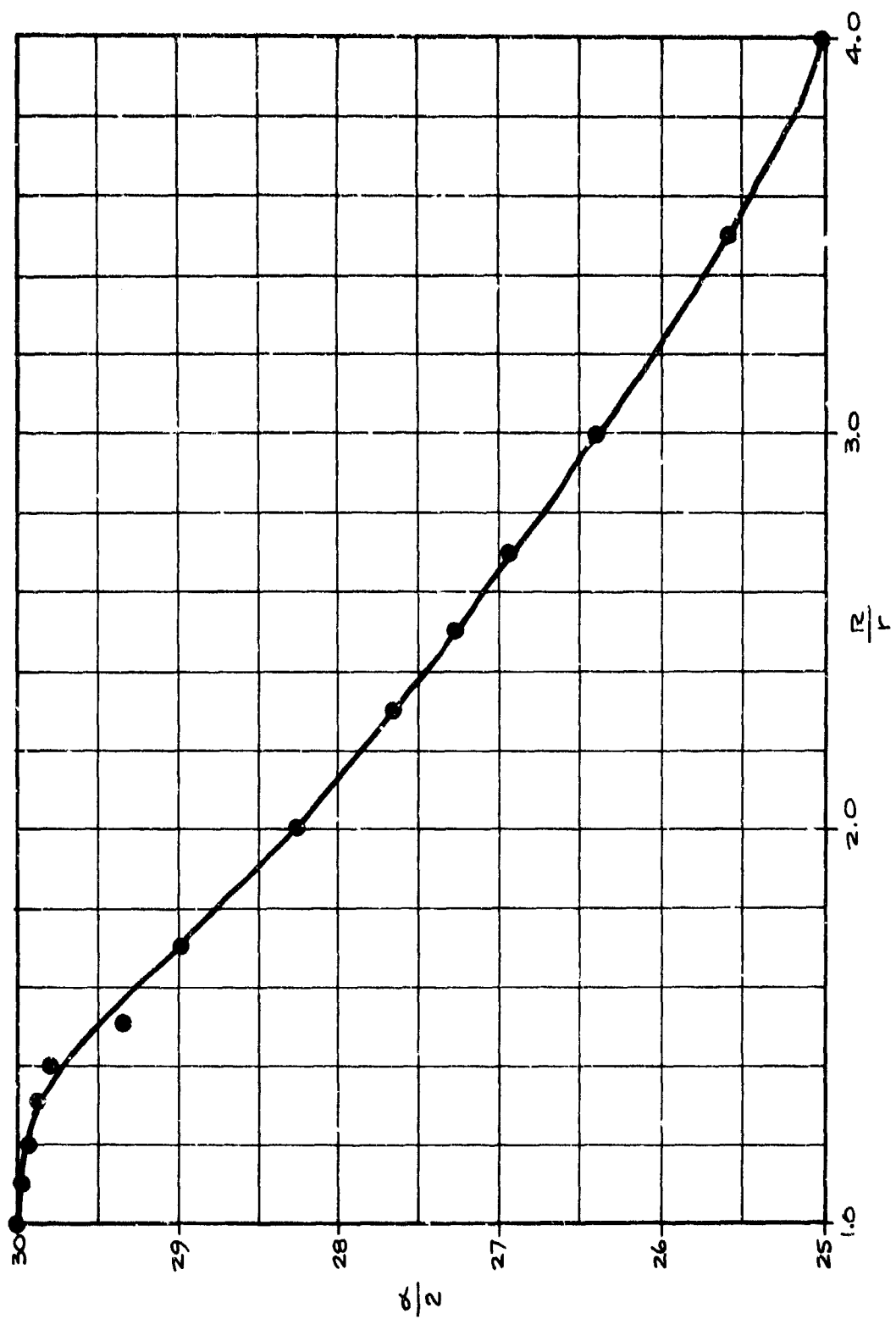


FIGURE 2-A. PLOT OF $\frac{\delta}{2}$ VERSUS $\frac{R}{r}$

2.0 RELATIONSHIP BETWEEN DEPTH IN CONE AND STRAIN

Figure 3-A shows a schematic of forming in a conical die.

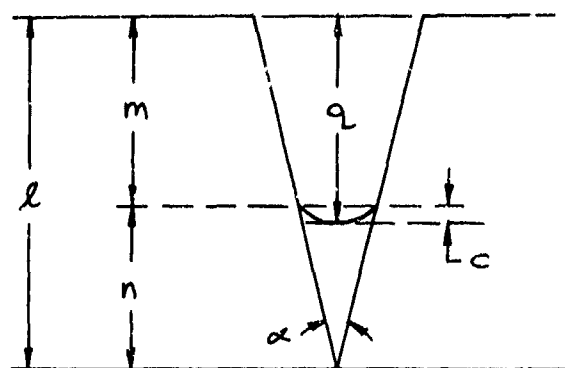


FIGURE 3-A. FORMING IN CONICAL DIE

The following relationships apply from Figure 3-A:

$$q = m + c \quad (31)$$

$$\tan \frac{\alpha}{2} = \frac{r}{n} \quad (32)$$

and

$$m = l - n$$

$$m = l - \frac{r}{\tan \frac{\alpha}{2}}$$

From Eq. 31, one can get an expression q

$$q = l + c - \frac{r}{\tan \frac{\alpha}{2}} \quad (33)$$

The area of hemispherical cone is:

$$A = 2\pi r c = \pi (r^2 + c^2) \quad (34)$$

In Equation 32

$$x = \frac{r^2 + c^2}{2c} = \frac{c}{1 - \sin \frac{\alpha}{2}}$$

So that solving for r^2 we obtain:

$$r^2 = \frac{2c^2}{1 - \sin \frac{\alpha}{2}} - c^2 = \frac{c^2(1 + \sin \frac{\alpha}{2})}{(1 - \sin \frac{\alpha}{2})} \quad (35)$$

Equation 34 can be used to eliminate r in the above equation

$$q = l + c - c \frac{\left[\frac{1 + \sin \frac{\alpha}{2}}{1 - \sin \frac{\alpha}{2}} \right]^{\frac{1}{2}}}{\tan \frac{\alpha}{2}} = l - c \csc \frac{\alpha}{2}$$

$$q - l = -c \csc \frac{\alpha}{2} \quad (36)$$

Taking the derivative

$$dq = -dc \csc \frac{\alpha}{2}$$

$$d\varepsilon = -\frac{dt}{t} \quad (37)$$

Substituting from Equation 28 and Equation 34

$$d\varepsilon = \frac{dt}{t} = \frac{dr}{r} = \frac{dc}{c} \quad (38)$$

Substituting from Equation 35 in Equation 37 we obtain the relationship

$$d\varepsilon = \frac{dq}{l - q} = \frac{dt}{t}$$

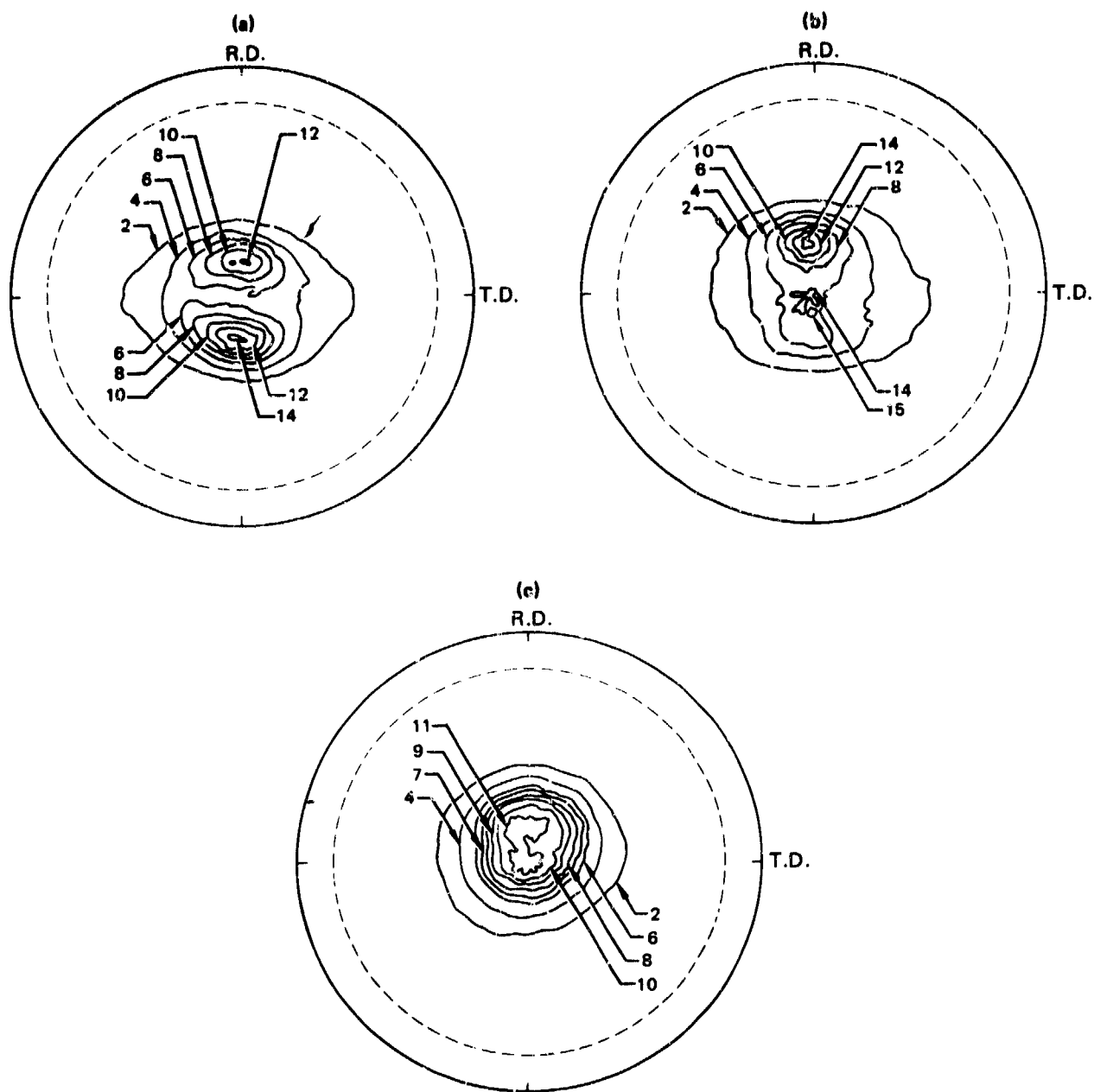
$$\varepsilon = \int_{q_1}^{q_2} \frac{dq}{l - q} = \int_{t_1}^{t_2} \frac{dt}{t}$$

$$\varepsilon = \ln \left(\frac{l - q_2}{l - q_1} \right) = \ln \frac{t_2}{t_1} \quad (39)$$

APPENDIX B

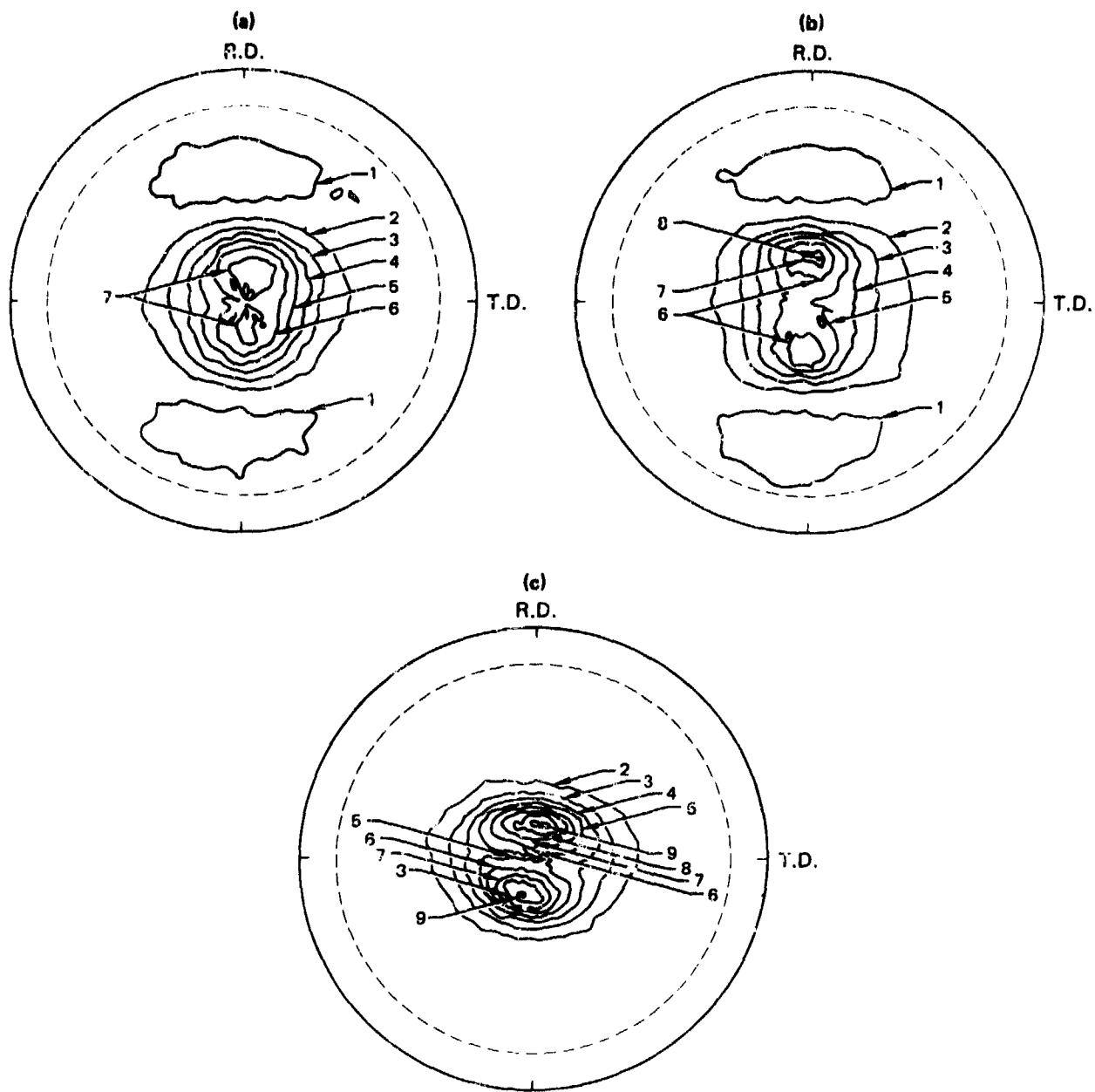
POLE FIGURES FOR

Ti-6Al-4V



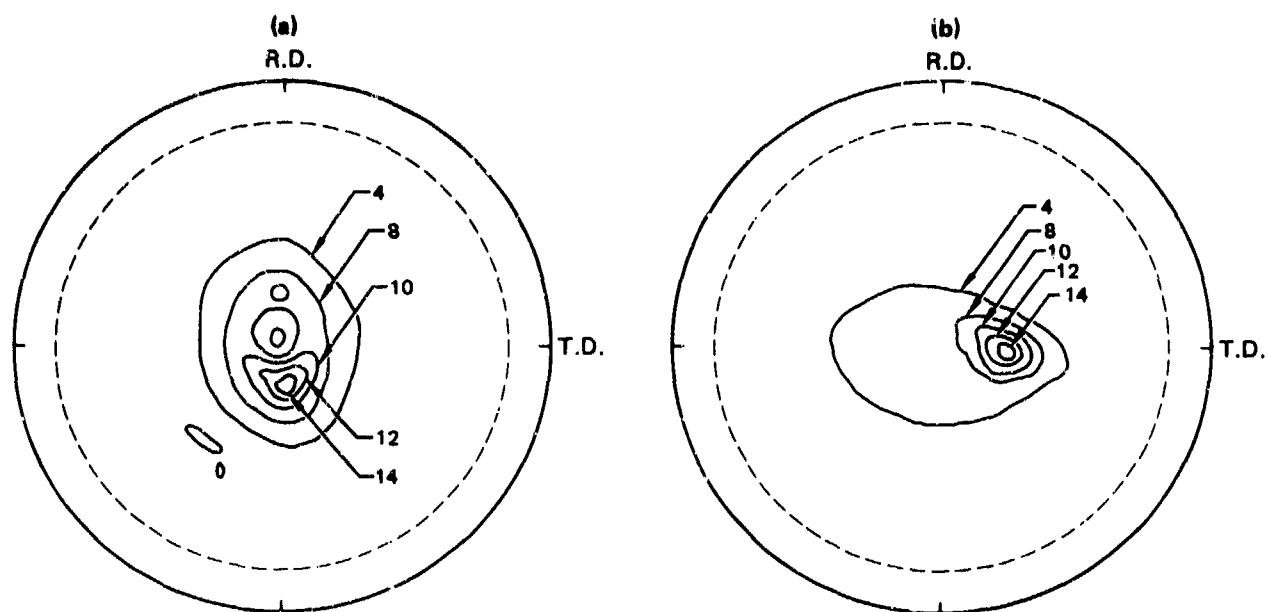
GP03-0240-156

Figure B1. (002) pole figures for normal-textured Ti-6Al-4V (volume % primary α = 88); (a) grain size = 12.2 μm , (b) grain size = 7.7 μm , and (c) grain size = 5.8 μm .



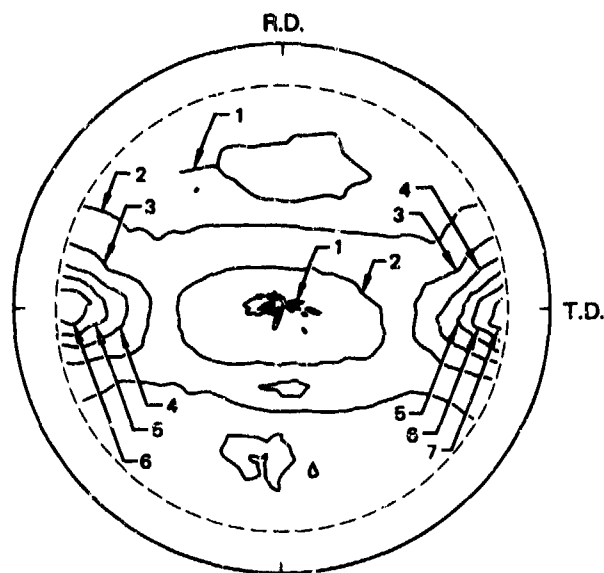
GP03-0249-155

Figure B2. (0002) pole figures for normal-textured Ti-6Al-4V; (a) volume % primary alpha = 65 and grain size = 5.8 μm , (b) volume % primary alpha = 47 and grain size = 5.6 μm , and (c) volume % primary alpha = 47 and grain size = 4.4 μm .



GP03-0249-154

Figure B3. (002) pole figures of regular-grade Ti-6Al-4V "clock-rolled" at 704°C (1300°F); (a) rotated 90° each pass, and (b) rotated 45° each pass.



GP03-0248-23

Figure B4. (0002) pole figure of transverse-basal-textured Ti6Al-4V (panel T1).

APPENDIX C

SUPERPLASTIC CONICAL DIE FORMING OF TITANIUM ALLOYS

TABLE C1. SUPERPLASTIC STRAIN RATES AT 907°C (1665°F) OF NORMAL-TEXTURED
REGULAR-GRADE Ti-6Al-4V DETERMINED FROM CONE-FORMING TESTS.

Alloy microstructure		Diameter of cone mm (in.)	Forming pressure MPa (psi)	Stress in cone MPa (psi)	Time at pressure (min)	Final depth in cone mm (in.)	Strain in cone, ε	Average strain rate in cone (s ⁻¹)
Grain size (μm)	Volume fraction primary alpha							
5.9	0.64	37.44 (1.474)	2.41 (350)	22.31 (3235)	24	29.97 (1.18)*	1.96	1.3 × 10 ⁻³
		31.17 (1.227)		18.41 (2670)		18.92 (0.745)	0.80	5.3 × 10 ⁻⁴
		25.40 (1.0)		14.82 (2150)		13.11 (0.516)	0.53	4.0 × 10 ⁻⁴
		20.32 (0.8)		11.72 (1700)		7.47 (0.294)	0.17	2.2 × 10 ⁻⁴
6.0	0.88	27.29 (1.468)	2.41 (350)	22.20 (3220)	24	27.33 (1.076)	1.14	7.6 × 10 ⁻⁴
		31.52 (1.241)		18.62 (2700)		18.54 (0.730)	0.73	5.1 × 10 ⁻⁴
		25.40 (1.0)		14.82 (2150)		12.73 (0.501)	0.47	3.6 × 10 ⁻⁴
		20.32 (0.8)		11.69 (1695)		8.31 (0.327)	0.26	2.8 × 10 ⁻⁴
7.2	0.44	37.72 (1.485)	2.41 (350)	20.99 (3044)	24	20.45 (0.805)	0.66	4.6 × 10 ⁻⁴
		34.04 (1.34)		18.86 (2735)		17.78 (0.700)	0.52	3.8 × 10 ⁻⁴
		29.97 (1.18)		16.48 (2390)		14.48 (0.570)	0.4	3.4 × 10 ⁻⁴
		26.42 (1.040)		14.48 (2100)		1.19 (0.047)	0.2	2.3 × 10 ⁻⁴
7.7	0.89	37.29 (1.468)	2.41 (350)	20.40 (2958)	24	25.48 (1.003)	1.1	7.6 × 10 ⁻⁴
		31.12 (1.225)		16.89 (2450)		15.60 (0.614)	0.47	3.6 × 10 ⁻⁴
		25.40 (1.0)		13.58 (1970)		11.56 (0.455)	0.36	2.8 × 10 ⁻⁴
		19.74 (0.777)		10.34 (1500)		7.26 (0.286)	0.18	2.2 × 10 ⁻⁴
7.9	0.60	37.29 (1.468)	2.41 (350)	20.69 (3000)	25	21.82 (0.859)	0.70	4.7 × 10 ⁻⁴
		31.12 (1.225)		16.96 (2460)		15.60 (0.614)	0.40	3.0 × 10 ⁻⁴
		25.40 (1.0)		13.79 (2000)		9.86 (0.388)	0.20	2.3 × 10 ⁻⁴
		19.56 (0.77)		10.34 (1500)		6.27 (0.247)	0.08	1.5 × 10 ⁻⁴
4.4	0.47	37.72 (1.485)	2.41 (350)	23.03 (3340)	25	31.24 (1.230)*	2.30	1.5 × 10 ⁻³
		34.04 (1.340)		20.20 (2930)		24.84 (0.978)	1.38	9.2 × 10 ⁻⁴
		29.97 (1.18)		17.65 (2560)		19.18 (0.755)	0.89	5.9 × 10 ⁻⁴
		26.42 (1.04)		15.51 (2250)		15.11 (0.595)	0.67	4.6 × 10 ⁻⁴
5.6	0.47	37.44 (1.474)	2.41 (350)	21.93 (3180)	25	26.37 (1.038)	1.2	8.0 × 10 ⁻⁴
		31.17 (1.227)		18.89 (2740)		16.69 (0.657)	0.55	4.1 × 10 ⁻⁴
		25.40 (1.0)		14.89 (2160)		11.38 (0.448)	0.34	3.0 × 10 ⁻⁴
		19.74 (0.777)		11.58 (1680)		6.10 (0.240)	0.06	1.3 × 10 ⁻⁴
12.6	0.88	37.29 (1.468)	2.41 (350)	19.17 (2780)	25	16.43 (0.647)	0.3	2.8 × 10 ⁻⁴
		31.52 (1.241)		16.07 (2330)		10.06 (0.396)	0.11	1.85 × 10 ⁻⁴
		25.40 (1.0)				7.04 (0.277)	None	
		20.32 (0.8)				5.08 (0.20)	None	
14.2	0.66	37.72 (1.485)	2.41 (350)	19.31 (2800)	25	17.88 (0.704)	0.38	3.2 × 10 ⁻⁴
		34.04 (1.34)		17.38 (2520)		12.73 (0.501)	0.18	2.2 × 10 ⁻⁴
		26.42 (1.04)		13.31 (1930)		9.32 (0.367)	0.14	2.0 × 10 ⁻⁴
18.1	0.63	37.29 (1.468)	2.41 (350)	19.76 (2870)	25	16.36 (0.644)	0.30	2.8 × 10 ⁻⁴
		31.52 (1.241)		16.55 (2400)		10.67 (0.420)	0.10	1.8 × 10 ⁻⁴
12.2	0.87	37.29 (1.468)	2.41 (350)	19.17 (2780)	25	18.44 (0.726)	0.45	3.5 × 10 ⁻⁴
		31.12 (1.225)		15.86 (2300)		11.43 (0.450)	0.16	2.1 × 10 ⁻⁴
		25.40 (1.0)		12.74 (1848)		8.64 (0.340)	0.10	1.7 × 10 ⁻⁴
17.6	0.88	37.44 (1.474)	2.41 (350)	19.24 (2790)	25	14.94 (0.588)	0.21	2.3 × 10 ⁻⁴
		31.17 (1.227)		16.34 (2370)		9.02 (0.355)	0.014	1.0 × 10 ⁻⁴

*Failure in cone

GP03-0246-225

TABLE C2. SUPERPLASTIC STRAIN RATES AT 907°C (1665°F) OF NORMAL-TEXTURED
REGULAR-GRADE Ti-6Al-4V DETERMINED FROM CONE-FORMING TESTS.

Alloy microstructure		Diameter of cone mm (in.)	Forming pressure MPa (psi)	Stress in cone MPa (psi)	Time at pressure (h)	Final depth in cone mm (in.)	Strain in cone, ϵ	Average strain rate in cone (s ⁻¹)
Grain size (μ m)	Volume fraction primary alpha							
5.9	0.64	37.36 (1.471)	0.76 (110)	6.90 (1000)	5	25.40 (1.0)	1.014	6.0×10^{-5}
		31.17 (1.227)		5.79 (840)		14.12 (0.556)	0.33	2.2×10^{-5}
		25.40 (1.0)		4.62 (670)		12.19 (0.48)	0.40	2.5×10^{-5}
		20.32 (0.8)		3.45 (500)		7.37 (0.29)	0.18	1.5×10^{-5}
6.0	0.88	37.29 (1.468)	0.76 (110)	6.96 (1010)	5	23.83 (0.938)	0.84	5.1×10^{-5}
		31.52 (1.241)		5.52 (800)		12.75 (0.502)	0.22	1.7×10^{-5}
		25.40 (1.0)		4.62 (670)		9.86 (0.388)	0.19	1.5×10^{-5}
		20.32 (0.8)		3.79 (550)		7.49 (0.295)	0.17	1.4×10^{-5}
7.7	0.89	37.72 (1.485)	0.76 (110)	6.45 (935)	5	23.32 (0.912)	0.79	4.7×10^{-5}
		34.04 (1.34)		5.58 (810)		17.27 (0.680)	0.53	3.3×10^{-5}
		29.97 (1.19)		5.07 (735)		13.67 (0.538)	0.34	2.2×10^{-5}
		26.42 (1.04)		4.45 (645)		13.11 (0.516)	0.45	3.0×10^{-5}
7.2	0.44	37.29 (1.468)	0.76 (110)	6.31 (915)	5	19.69 (0.775)	0.50	3.2×10^{-5}
		31.12 (1.225)		5.24 (760)		12.32 (0.485)	0.20	1.6×10^{-5}
		25.40 (1.0)		4.21 (611)		9.88 (0.389)	0.20	1.6×10^{-5}
		19.74 (0.777)		3.21 (466)		5.89 (0.232)	0.06	1.0×10^{-5}
5.6	0.47	37.29 (1.468)	0.76 (110)	6.62 (957)	5	24.64 (0.970)	1.03	7.3×10^{-5}
		31.52 (1.241)		5.55 (800)		14.50 (0.571)	0.34	2.2×10^{-5}
		25.40 (1.0)		4.41 (633)		11.46 (0.451)	0.33	2.2×10^{-5}
		20.32 (0.8)		None		5.38 (0.212)	None	None
4.4	0.47	37.44 (1.474)	0.76 (110)	6.90 (1000)	5	25.98 (1.023)	1.09	6.5×10^{-5}
		31.17 (1.227)		5.69 (825)		14.12 (0.556)	0.32	2.1×10^{-5}
		25.40 (1.0)		4.55 (660)		12.22 (0.481)	0.4	2.5×10^{-5}
		19.56 (0.77)		3.45 (500)		7.04 (0.277)	0.15	1.3×10^{-5}
14.2	0.66	37.72 (1.485)	0.76 (110)	7.65 (1110)	5	23.04 (0.907)	0.76	4.7×10^{-5}
		34.04 (1.34)		6.90 (1000)		16.00 (0.630)	0.36	2.3×10^{-5}
		29.97 (1.18)		6.21 (900)		12.40 (0.488)	0.21	1.6×10^{-5}
		26.42 (1.040)		5.31 (770)		12.40 (0.488)	0.37	2.4×10^{-5}
12.2	0.87	37.29 (1.468)	0.97 (140)	7.93 (1150)	5	23.50 (0.925)	0.82	5.5×10^{-5}
		31.12 (1.225)		6.55 (950)		14.22 (0.560)	0.34	2.1×10^{-5}
		25.40 (1.0)		5.31 (770)		12.04 (0.474)	0.36	3.0×10^{-5}
		19.74 (0.777)		4.00 (580)		6.50 (0.256)	0.1	1.2×10^{-5}
18.1	0.66	37.29 (1.468)	0.97 (140)	8.27 (1200)	5	17.91 (0.705)	0.38	2.7×10^{-5}
		31.52 (1.241)		6.62 (960)		9.91 (0.390)	0.08	1.1×10^{-5}
		25.40 (1.0)		5.24 (760)		8.33 (0.328)	0.03	10^{-5}
17.6	0.88	37.44 (1.474)	0.97 (140)	7.79 (1130)	5	16.26 (0.640)	0.28	2.0×10^{-5}
		31.17 (1.227)		6.45 (935)		9.83 (0.387)	0.05	10^{-5}
		25.40 (1.0)		5.24 (760)		7.95 (0.313)	0.06	1.0×10^{-5}
12.6	0.88	37.29 (1.468)	0.76 (110)	6.96 (1010)	5	12.80 (0.504)	0.12	1.2×10^{-5}
		31.12 (1.225)		5.79 (840)		9.19 (0.362)	0.016	10^{-5}
		25.40 (1.0)		3.79 (576)		7.54 (0.297)	0.04	10^{-5}
		19.74 (0.777)		—		4.29 (0.169)	None	
7.9	0.60	37.54 (1.478)	0.76 (110)	6.27 (910)	5	22.23 (0.875)	0.76	4.7×10^{-5}
		33.53 (1.32)		5.52 (800)		15.09 (0.594)	0.33	2.2×10^{-5}
		29.97 (1.18)		4.93 (715)		12.22 (0.481)	0.23	1.7×10^{-5}
		26.42 (1.04)		4.31 (625)		12.01 (0.473)	0.34	2.2×10^{-5}

QP03-0249-228

**TABLE C3. SUPERPLASTIC STRAIN RATES AT 870°C (1598°F) OF NORMAL-TEXTURED
REGULAR-GRADE Ti-6Al-4V DETERMINED FROM CONE-FORMING TESTS.**

Alloy microstructure		Diameter of cone mm (in.)	Forming pressure MPa (psi)	Stress in cone MPa (psi)	Time at pressure (h)	Final depth in cone mm (in.)	Strain in cone, ϵ	Average strain rate in cone (s ⁻¹)
Grain size (μ m)	Volume fraction primary alpha							
5.9	0.64	37.44 (1.474)	1.72 (250)	15.93 (2310)	5	30.99 (1.22*)	2.36	1.3×10^{-4}
		31.17 (1.227)		13.10 (1900)		21.54 (0.848)	1.6	1.94×10^{-5}
		25.40 (1.0)		10.55 (1530)		14.94 (0.588)	0.73	6.1×10^{-5}
		19.56 (0.77)		8.00 (1160)		8.92 (0.351)	0.3	2.1×10^{-5}
7.7	0.89	37.29 (1.468)	1.72 (250)	14.55 (2110)	5	29.67 (1.168)	1.94	1.1×10^{-4}
		31.12 (1.225)		12.07 (1750)		21.26 (0.837)	1.1	7.0×10^{-5}
		25.40 (1.0)		9.72 (1410)		14.68 (0.578)	0.69	5.1×10^{-5}
		20.32 (0.8)		7.65 (1110)		8.03 (0.316)	0.23	2.6×10^{-5}
7.2	0.44	37.72 (1.485)	1.72 (250)	17.24 (2500)	5	28.55 (1.124)	1.56	9.2×10^{-5}
		34.04 (1.34)		13.17 (1910)		21.16 (0.833)	0.89	5.5×10^{-5}
		29.97 (1.18)		11.79 (1710)		16.41 (0.646)	0.59	4.5×10^{-5}
		25.78 (1.015)		10.07 (1460)		14.27 (0.562)	0.108	1.9×10^{-5}
6.0	0.88	37.29 (1.468)	1.72 (250)	15.86 (2300)	5	29.34 (1.155)	1.8	1.05×10^{-4}
		31.52 (1.241)		13.31 (1930)		17.91 (0.705)	0.65	4.8×10^{-5}
		25.40 (1.0)		10.62 (1540)		12.57 (0.495)	0.48	3.9×10^{-5}
		20.32 (0.8)		8.34 (1210)		9.27 (0.365)	0.37	3.4×10^{-5}
18.1	0.66	37.44 (1.474)	2.24 (325)	18.42 (2671)	5	29.18 (1.149)*	1.8	1.05×10^{-4}
		31.17 (1.227)		15.17 (2200)		14.94 (0.588)	0.41	3.6×10^{-5}
		25.40 (1.0)		12.20 (1770)		10.82 (0.426)	0.29	3.0×10^{-5}
		19.56 (0.77)		9.24 (1340)		6.22 (0.245)	0.03	
17.6	0.88	37.72 (1.485)	2.24 (325)	18.41 (2670)	5	25.07 (0.987)	1.01	6.5×10^{-5}
		34.04 (1.340)		16.69 (2420)		16.64 (0.655)	0.42	3.6×10^{-5}
		29.97 (1.18)		14.58 (2115)		13.23 (0.521)	0.32	3.1×10^{-5}
		26.42 (1.04)		12.82 (1860)		11.28 (0.444)	0.26	2.8×10^{-5}
14.1	0.66	37.29 (1.468)	2.24 (325)	17.79 (2580)	5	24.71 (0.973)	1.01	6.5×10^{-5}
		31.12 (1.225)		14.69 (2130)		13.87 (0.546)	0.32	3.1×10^{-5}
		25.40 (1.0)		11.86 (1720)		10.36 (0.408)	0.21	2.6×10^{-5}
		19.74 (0.777)		9.00 (1305)		6.60 (0.260)	0.11	1.9×10^{-5}
12.2	0.87	37.29 (1.468)	2.24 (325)	17.99 (2580)	5	29.92 (1.178)	2.0	1.15×10^{-4}
		31.52 (1.241)		14.89 (2160)		17.86 (0.703)	0.68	4.8×10^{-5}
		25.40 (1.0)		11.86 (1720)		12.19 (0.480)	0.42	3.6×10^{-5}
		20.32 (0.8)		9.31 (1350)		9.02 (0.355)	0.11	1.9×10^{-5}
4.4	0.47	37.72 (1.485)	1.72 (250)	16.07 (2330)	5	31.24 (1.23)	2.3	1.3×10^{-4}
		34.04 (1.34)		14.41 (2090)		25.78 (1.015)	1.6	9.4×10^{-5}
		29.97 (1.18)		12.62 (1830)		21.54 (0.848)	1.3	7.9×10^{-5}
		26.42 (1.040)		10.89 (1580)		10.95 (0.746)	0.43	3.7×10^{-5}
5.6	0.47	37.29 (1.468)	1.72 (250)	15.31 (2220)	5	31.24 (1.123)	1.5	8.9×10^{-5}
		31.52 (1.241)		12.62 (1830)		20.50 (0.807)	0.97	6.3×10^{-5}
		25.40 (1.0)		10.07 (1460)		15.18 (0.597)	0.64	4.7×10^{-5}
		20.32 (0.8)		7.93 (1150)		9.98 (0.393)	0.47	3.9×10^{-5}
7.9	0.60	37.29 (1.468)	1.72 (250)	14.13 (2050)	5	28.37 (1.117)	1.6	9.4×10^{-4}
		31.12 (1.225)		11.24 (1630)		17.20 (0.677)	0.84	4.7×10^{-4}
		25.40 (1.0)		9.45 (1370)		13.34 (0.525)	0.54	4.3×10^{-4}
12.6	0.88	37.44 (1.474)	1.72 (250)	13.72 (1990)	5	21.06 (0.829)	0.63	4.7×10^{-4}
		31.17 (1.227)		11.31 (1640)		12.65 (0.498)	0.24	2.8×10^{-4}
		25.40 (1.0)		9.10 (1320)		9.09 (0.358)	0.15	2.2×10^{-4}

* Failure in cone

GP03-0246-227

TABLE C4. SUPERPLASTIC STRAIN RATES AT 907°C (1665°F) OF ELI-GRADE
TI-6Al-4V DETERMINED FROM CONE-FORMING TESTS.

Alloy microstructure		Diameter of cone mm (in.)	Forming pressure MPa (psi)	Stress in cone MPa (psi)	Time at pressure (h)	Final depth in cone mm (in.)	Strain in cone, ϵ	Average strain rate in cone (s ⁻¹)
Grain size (μ m)	Volume fraction primary alpha							
5.5	0.88	37.47 (1.475)	0.55 (80)	4.14 (600)	5	25.04 (0.986)	1.05	6.3×10^{-5}
		31.17 (1.227)		3.41 (495)		15.80 (0.614)	0.48	3.0×10^{-5}
		25.40 (1.0)		2.74 (397)		12.70 (0.500)	0.48	3.6×10^{-5}
		19.56 (0.770)		2.08 (301)		7.57 (0.298)	0.22	1.6×10^{-5}
4.5	0.47	37.72 (1.485)	0.55 (80)	4.39 (636)	5	26.52 (1.044)	1.26	7.5×10^{-5}
		34.04 (1.34)		3.88 (563)		19.94 (0.785)	0.76	4.6×10^{-5}
		26.91 (1.020)		2.98 (432)		13.26 (0.522)	0.69	4.4×10^{-5}
8.9	0.89	37.29 (1.468)	0.55 (80)	4.52 (655)	5	25.20 (0.992)	1.25	7.7×10^{-5}
		31.12 (1.225)		3.73 (541)		15.65 (0.616)	0.47	3.0×10^{-5}
		25.40 (1.0)		3.01 (436)		13.23 (0.521)	0.54	4.1×10^{-5}
		19.74 (0.777)		2.29 (332)		7.11 (0.280)	0.16	1.2×10^{-5}
8.8	0.46	37.29 (1.468)	0.55 (80)	4.51 (654)	5	20.57 (0.810)	0.6	4.5×10^{-5}
		31.52 (1.241)		3.77 (547)		10.92 (0.430)	0.11	1.0×10^{-5}
		25.40 (1.0)		3.00 (435)		8.43 (0.332)	0.095	1.0×10^{-5}
		20.32 (0.8)		2.35 (341)		6.60 (0.260)	0.093	0.96×10^{-5}

QP03-0246-224

TABLE C5. SUPERPLASTIC STRAIN RATE AT 907°C (1665°F) OF ELI-GRADE
Ti-6Al-4V DETERMINED FROM CONE-FORMING TESTS.

Alloy microstructure		Diameter of cone mm (in.)	Forming pressure MPa (psi)	Stress in cone MPa (psi)	Time at pressure (min)	Final depth in cone mm (in.)	Strain in cone, ϵ	Average strain rate in cone (s ⁻¹)
Grain size (μ m)	Volume fraction primary alpha							
5.5	0.88	37.29 (1.468)	2.07 (300)	15.47 (2244)	25	29.39 (1.157)	1.46	9.7×10^{-4}
		34.04 (1.34)		13.76 (1996)		23.67 (0.932)	1.12	7.5×10^{-4}
		29.97 (1.18)		12.11 (1757)		18.72 (0.737)	0.76	5.06×10^{-4}
		25.91 (1.020)		10.51 (1524)		17.09 (0.673)	0.7	4.7×10^{-4}
4.5	0.47	37.44 (1.474)	2.07 (300)	16.48 (2390)	25	30.05 (1.183)	1.59	1.05×10^{-3}
		31.17 (1.227)		13.58 (1970)		22.02 (0.867)	1.18	7.7×10^{-4}
		25.40 (1.0)		10.92 (1584)		15.14 (0.596)	0.82	5.5×10^{-4}
		19.56 (0.77)		8.00 (1160)		9.27 (0.365)	0.43	2.9×10^{-4}
8.9	0.89	37.29 (1.468)	2.07 (300)	15.93 (2456)	25	25.65 (1.010)	0.99	6.7×10^{-4}
		25.40 (1.0)		14.19 (2058)		14.22 (0.560)	0.63	4.2×10^{-4}
		20.32 (0.8)		9.86 (1285)		8.36 (0.329)	0.43	2.9×10^{-4}
2.2	0.48	37.29 (1.468)	2.07 (300)	16.16 (2344)	25	24.13 (0.950)	0.86	5.7×10^{-4}
		31.12 (1.225)		13.35 (1936)		16.64 (0.655)	0.54	3.6×10^{-4}
		25.40 (1.0)		10.76 (1560)		12.42 (0.489)	0.41	2.7×10^{-4}
		19.74 (0.777)		8.18 (1186)		7.70 (0.303)	0.33	2.2×10^{-4}

GP03-0240-229

TABLE C6. SUPERPLASTIC STRAIN RATES AT 870°C (1600°F) OF ELI-GRADE
Ti-6Al-4V DETERMINED FROM CONE-FORMING TESTS.

Alloy microstructure		Diameter of cone mm (in.)	Forming pressure MPa (psi)	Stress in cone MPa (psi)	Time at pressure (min)	Final depth in cone mm (in.)	Strain in cone, ε	Average strain rate in cone (s ⁻¹)
Grain size (μm)	Volume fraction primary alpha							
5.5	0.88	37.72 (1.485)	2.41 (350)	18.20 (2640)	30	24.66 (0.971)	0.98	5.0 x 10 ⁻⁴
		34.04 (1.34)		16.41 (2380)		21.39 (0.842)	0.85	5.2 x 10 ⁻⁴
		29.97 (1.18)		14.31 (2075)		16.97 (0.668)	0.65	4.0 x 10 ⁻⁴
		25.91 (1.020)		12.24 (1775)		13.21 (0.520)	0.52	3.2 x 10 ⁻⁴
4.5	0.4	37.44 (1.474)	2.41 (350)	19.24 (2790)	30	23.37 (0.920)	0.83	5.1 x 10 ⁻⁴
		31.17 (1.227)		15.86 (2300)		16.94 (0.667)	0.60	3.7 x 10 ⁻⁴
		25.40 (1.0)		12.74 (1848)		12.57 (0.495)	0.48	3.0 x 10 ⁻⁴
		19.56 (0.77)		9.58 (1390)		6.63 (0.261)	0.18	1.2 x 10 ⁻⁴
8.9	0.89	37.29 (1.468)	2.41 (350)	19.93 (2890)	30	22.07 (0.869)	0.73	4.5 x 10 ⁻⁴
		31.52 (1.241)		16.75 (2430)		16.03 (0.631)	0.48	3.0 x 10 ⁻⁴
		25.40 (1.0)		13.31 (1930)		9.04 (0.356)	0.14	1.0 x 10 ⁻⁴
		20.32 (0.8)		10.48 (1520)		7.14 (0.281)	0.15	1.0 x 10 ⁻⁴
3.8	0.46	37.29 (1.468)	2.41 (350)	19.17 (2780)	30	18.95 (0.746)	0.48	3.0 x 10 ⁻⁴
		31.12 (1.225)		15.79 (2290)		13.79 (0.543)	0.32	2.0 x 10 ⁻⁴
		25.40 (1.0)		12.76 (1850)		9.04 (0.356)	0.15	1.0 x 10 ⁻⁴

GP03-0346-230

**TABLE C7. SUPERPLASTIC STRAIN RATES AT 870°C (1600°F) OF ELI-GRADE
Ti-6Al-4V DETERMINED FROM CONE-FORMING TESTS.**

Alloy microstructure		Diameter of cone mm (in.)	Forming pressure MPa (psi)	Stress in cone MPa (psi)	Time at pressure (h)	Final depth in cone mm (in.)	Strain in cone, ε	Average strain rate in cone (s ⁻¹)
Grain size (μm)	Volume fraction primary alpha							
8.8	0.46	37.29 (1.468)	0.76 (110)	6.00 (870)	5	18.24 (0.718)	0.41	3.1 × 10 ⁻⁵
		31.12 (1.225)		4.98 (720)		11.51 (0.447)	0.18	2.1 × 10 ⁻⁵
		25.40 (1.0)		4.00 (580)		8.74 (0.344)	0.12	1.8 × 10 ⁻⁵
				3.04 (441)				
5.5	0.88	37.44 (1.474)	0.76 (110)	5.69 (825)	5	23.90 (0.941)	0.91	5.5 × 10 ⁻⁵
		31.17 (1.227)		4.69 (680)		17.53 (0.690)	0.65	4.3 × 10 ⁻⁵
		25.40 (1.0)		3.79 (550)		12.04 (0.474)	0.42	3.2 × 10 ⁻⁵
		20.32 (0.8)		2.96 (430)		7.49 (0.295)	0.18	2.1 × 10 ⁻⁵
4.5	0.47	37.29 (1.468)	0.76 (110)	6.00 (870)	5	22.81 (0.898)	0.77	4.9 × 10 ⁻⁵
		31.52 (1.241)		5.03 (730)		16.18 (0.637)	0.50	3.6 × 10 ⁻⁵
		25.40 (1.0)		4.00 (580)		10.77 (0.424)	0.31	2.7 × 10 ⁻⁵
		20.32 (0.8)		3.14 (455)		7.62 (0.300)	0.19	2.2 × 10 ⁻⁵
8.9	0.89	37.72 (1.485)	0.76 (910)	6.27 (910)	5	23.11 (0.91)	0.80	5.0 × 10 ⁻⁵
		34.04 (1.34)		5.65 (820)		17.75 (0.700)	0.52	3.7 × 10 ⁻⁵
		29.97 (1.18)		4.93 (715)		13.72 (0.540)	0.39	3.0 × 10 ⁻⁵

GP03-0248-231

TABLE C8. SUPERPLASTIC STRAIN RATES AT 907°C (1665°F) OF NORMAL-TEXTURED ELI-GRADE Ti-6Al-4V (GRAIN SIZE = 5.5 μ m, VOLUME % PRIMARY ALPHA = 0.88) DETERMINED FROM CONE-FORMING TESTS.

Diameter of cone mm (in.)	Forming pressure MPa (psi)	Stress in cone MPa (psi)	Soak time (h)	Forming time (h)	Final depth in cone mm (in.)	Strain in cone, ϵ	Strain rate in cone (s^{-1})
38.10 (1.5)	1.10 (160)	8.48 (1230)	0.0	0.5	20.32 (0.800)	0.53	2.9×10^{-4}
34.29 (1.35)		7.58 (1100)			16.66 (0.656)	0.425	2.5×10^{-4}
30.48 (1.2)		6.69 (970)			13.00 (0.512)	0.289	2.1×10^{-4}
25.40 (1.0)		5.52 (800)			10.21 (0.402)	0.263	1.8×10^{-4}
38.10 (1.5)	1.10 (160)	8.48 (1230)	0.0	1.0	25.02 (0.985)	0.967	2.7×10^{-4}
34.29 (1.345)		7.58 (1100)			19.89 (0.783)	0.712	2.0×10^{-4}
30.48 (1.2)		6.69 (970)			16.33 (0.643)	0.575	1.8×10^{-4}
25.40 (1.0)		5.48 (795)			12.98 (0.511)	0.538	1.6×10^{-4}
38.10 (1.5)	1.10 (160)	8.48 (1230)	0.0	2.5	Failed	—	—
34.29 (1.350)		7.58 (1100)			26.54 (1.045)	1.8	2.0×10^{-4}
30.48 (1.2)		6.69 (970)			23.55 (0.927)	1.8	2.0×10^{-4}
25.40 (1.0)		5.48 (795)			17.63 (0.694)	1.3	1.5×10^{-4}
38.10 (1.5)	1.10 (160)	8.48 (1230)	2.0	2.5	Failed	—	—
34.29 (1.35)		7.58 (1100)			23.37 (0.920)	1.2	1.4×10^{-4}
30.48 (1.2)		6.69 (970)			20.57 (0.810)	1.1	1.3×10^{-4}
25.40 (1.0)		5.48 (795)			15.42 (0.607)	0.866	1.0×10^{-4}
38.10 (1.5)	1.10 (160)	8.48 (1230)	4.0	2.0	25.48 (1.003)	1.0	1.4×10^{-4}
30.48 (1.2)		6.69 (970)			19.69 (0.775)	0.98	1.4×10^{-4}

QP03-0248-241

**TABLE C9. SUPERPLASTIC STRAIN RATES AT 907°C (1665°F) OF NORMAL-TEXTURED
REGULAR-GRADE Ti-6Al-4V (GRAIN SIZE = 6.0 μm, VOLUME % PRIMARY
ALPHA = 68) DETERMINED FROM CONE-FORMING TESTS.**

Diameter of cone mm (in.)	Forming pressure MPa (psi)	Stress in cone MPa (psi)	Soak time (h)	Forming time (h)	Final depth in cone mm (in.)	Strain in cone, ε	Strain rate in cone (s ⁻¹)
36.10 (1.5)	1.10 (160)	10.55 (1530)	0.0	0.5	17.91 (0.706)	0.39	2.9 × 10 ⁻⁴
34.29 (1.35)		9.31 (1350)			14.22 (0.560)	0.25	2.3 × 10 ⁻⁴
30.48 (1.2)		8.27 (1200)			12.52 (0.493)	0.24	2.2 × 10 ⁻⁴
25.40 (1.0)		6.76 (980)			9.65 (0.380)	0.18	2.0 × 10 ⁻⁴
38.10 (1.5)	1.10 (160)	10.55 (1530)	0.0	1.0	21.64 (0.852)	0.613	2.0 × 10 ⁻⁴
34.29 (1.35)		9.31 (1350)			18.03 (0.710)	0.52	1.8 × 10 ⁻⁴
30.48 (1.2)		8.27 (1200)			14.61 (0.575)	0.40	1.4 × 10 ⁻⁴
25.40 (1.0)		6.76 (980)			10.08 (0.397)	0.22	1.0 × 10 ⁻⁴
38.10 (1.5)	1.10 (160)	10.55 (1530)	0.0	2.5	29.62 (1.166)	1.6	1.9 × 10 ⁻⁴
30.48 (1.2)		8.27 (1200)			20.32 (0.800)	1.045	1.25 × 10 ⁻⁴
30.48 (1.2)	1.10 (160)	8.27 (1200)	0.0	4.25	22.23 (0.875)	1.4	1.0 × 10 ⁻⁴
38.10 (1.5)	1.10 (160)	10.55 (1530)	2.0	2.5	26.16 (1.03)	1.06	1.5 × 10 ⁻⁴
30.48 (1.2)		8.27 (1200)			18.42 (0.725)	0.78	1.0 × 10 ⁻⁴
38.10 (1.5)	1.10 (160)	10.55 (1530)	4.0	2.0	24.77 (0.975)	0.90	1.3 × 10 ⁻⁴
34.29 (1.35)		9.31 (1350)			17.45 (0.687)	0.47	7.4 × 10 ⁻⁵
30.48 (1.2)		8.27 (1200)			15.93 (0.627)	0.52	8.4 × 10 ⁻⁵
25.40 (1.0)		6.76 (980)			11.38 (0.448)	0.34	5.8 × 10 ⁻⁵

GP03-02-8-242

**TABLE C10. SUPERPLASTIC STRAIN RATES AT 907°C (1665°F) OF NORMAL-TEXTURED
REGULAR-GRADE Ti-6Al-4V (GRAIN SIZE = 12.2 μm, VOLUME % PRIMARY
ALPHA = 87) DETERMINED FROM CONE-FORMING TESTS.**

Diameter of cone mm (in.)	Forming pressure MPa (psi)	Stress in cone MPa (psi)	Soak time (h)	Forming time (h)	Final depth in cone mm (in.)	Strain in cone, ε	Strain rate in cone (s ⁻¹)
38.10 (1.5)	1.10 (160)	8.96 (1300)	0.0	1	13.28 (0.523)	0.115	7.1 × 10 ⁻⁵
38.10 (1.5)	1.10 (160)	8.96 (1300)	0.0	2.5	19.76 (0.778)	0.50	7.2 × 10 ⁻⁵
34.29 (1.35)		8.07 (1170)			14.15 (0.557)	0.24	3.8 × 10 ⁻⁵
30.48 (1.2)		7.07 (1025)			11.38 (0.448)	0.17	2.3 × 10 ⁻⁵
25.40 (1.0)		5.83 (845)			10.03 (0.395)	0.23	4.4 × 10 ⁻⁵
38.10 (1.5)	1.10 (160)	8.96 (1300)	0.0	4.25	24.87 (0.979)	0.97	7.3 × 10 ⁻⁵
34.29 (1.35)		8.07 (1170)			17.81 (0.701)	0.50	4.0 × 10 ⁻⁵
30.48 (1.2)		7.07 (1025)			13.69 (0.539)	0.34	2.45 × 10 ⁻⁵
25.40 (1.0)		5.83 (845)			12.32 (0.485)	0.44	4.0 × 10 ⁻⁵
38.10 (1.5)	1.10 (160)	8.96 (1300)	2.0	2.5	17.78 (0.700)	0.37	7.1 × 10 ⁻⁵
38.10 (1.5)	1.10 (160)	8.96 (1300)	4.0	2.0	17.58 (0.692)	0.35	5.1 × 10 ⁻⁵
34.29 (1.35)		8.07 (1170)			11.79 (0.464)	0.10	1.6 × 10 ⁻⁵
30.48 (1.2)		7.07 (1025)			9.53 (0.375)	0.056	9.6 × 10 ⁻⁵
25.40 (1.0)		5.83 (845)			8.86 (0.349)	0.13	3.1 × 10 ⁻⁵

GP03-0240-243

TABLE C11. SUPERPLASTIC STRAIN RATES AT 907°C (1665°F) OF NORMAL TEXTURED REGULAR-GRADE Ti-6Al-4V (GRAIN SIZE = 44 μm, VOLUME % PRIMARY ALPHA = 47) DETERMINED FROM CONE-FORMING TESTS.

Diameter of cone mm (in.)	Forming pressure MPa (psi)	Stress in cone MPa (psi)	Soak time (h)	Forming time (h)	Final depth in cone mm (in.)	Strain in cone, ε	Strain rate in cone (s ⁻¹)
38.10 (1.5)	1.10 (160)	10.34 (1500)	0.0	0.5	17.96 (0.707)	0.393	2.8×10^{-4}
30.48 (1.2)		8.27 (1200)			12.75 (0.502)	0.26	2.3×10^{-4}
38.10 (1.5)	1.10 (160)	10.34 (1500)	0.0	1.0	23.88 (0.940)	0.867	2.7×10^{-4}
30.48 (1.2)		8.27 (1200)			16.13 (0.635)	0.537	1.8×10^{-4}
38.10 (1.5)	1.10 (160)	10.34 (1500)	0.0	2.5	30.20 (1.189)	1.896	2.2×10^{-4}
34.29 (1.35)		9.31 (1350)			23.62 (0.930)	1.135	1.35×10^{-4}
30.48 (1.20)		8.27 (1200)			19.48 (0.767)	0.9194	1.1×10^{-4}
24.50 (1.0)		6.76 (980)			15.49 (0.610)	0.827	1.1×10^{-4}
38.10 (1.5)		10.34 (1500)			31.67 (1.247)	2.44	1.7×10^{-4}
34.29 (1.35)	1.10 (160)	9.31 (1350)	0.0	4.25	28.02 (1.103)	2.24	1.55×10^{-4}
30.48 (1.2)		8.27 (1200)			23.65 (0.931)	1.78	1.2×10^{-4}
25.40 (1.0)		6.76 (980)			19.71 (0.776)	1.85	1.3×10^{-4}
38.10 (1.5)		10.34 (1500)			28.25 (1.125)	1.51	1.76×10^{-4}
34.29 (1.35)		9.31 (1350)			22.99 (0.905)	1.04	1.2×10^{-4}
30.48 (1.2)	1.10 (160)	8.27 (1200)	2.0	2.5	18.62 (0.733)	0.808	9.6×10^{-5}
25.40 (1.0)		6.76 (980)			14.73 (0.580)	0.716	8.9×10^{-5}
38.10 (1.5)		10.34 (1500)			25.91 (1.02)	1.096	1.5×10^{-4}
34.29 (1.35)	1.10 (160)	9.31 (1350)	4.0	2.0	17.91 (0.705)	0.51	7.8×10^{-5}
30.48 (1.2)		8.27 (1200)			14.99 (0.590)	0.43	6.6×10^{-5}
25.40 (1.0)		6.76 (980)			12.62 (0.497)	0.46	7.4×10^{-5}

QP03-0246-244

TABLE C12. SUPERPLASTIC STRAIN-RATES AT 949°C (1740°F) OF Ti-8Al-1Mo-1V
DETERMINED FROM CONE-FORMING TESTS.

Panel thickness mm (in.)	Diameter of cone mm (in.)	Forming pressure MPa (psi)	Stress in cone MPa (psi)	Time at pressure (min)	Final depth in cone mm (in.)	Strain in cone, ε	Strain rate in cone (s ⁻¹)
1.27 (0.050)	37.29 (1.468)	2.07 (300)	24.65 (3575)	18	30.07 (1.184)	1.79	1.67 x 10 ⁻³
	37.72 (1.485)	2.07 (300)	24.96 (3620)		29.95 (1.179)	1.61	1.5 x 10 ⁻³
	34.04 (1.340)	2.07 (300)	22.41 (3250)		18.64 (0.734)	0.57	5.3 x 10 ⁻⁴
	31.12 (1.225)	2.07 (300)	19.31 (2800)		14.60 (0.575)	0.41	3.9 x 10 ⁻⁴
	25.91 (1.020)	2.07 (300)	16.89 (2450)		12.95 (0.510)	0.55	5.0 x 10 ⁻⁴
	25.4 (1.000)	2.07 (300)	16.55 (2400)		12.75 (0.502)	0.46	4.2 x 10 ⁻⁴
	19.74 (0.777)	2.07 (300)	12.69 (1840)		6.3 (0.248)	0.1	1.4 x 10 ⁻⁴
1.14 (0.045)	37.44 (1.474)	2.07 (300)	24.75 (3590)	18	21.21 (0.835)	0.41	3.9 x 10 ⁻⁴
	37.29 (1.468)	2.07 (300)	24.65 (3575)		23.06 (0.908)	0.63	5.8 x 10 ⁻⁴
	31.16 (1.227)	2.07 (300)	19.31 (2800)		14.6 (0.575)	0.36	3.4 x 10 ⁻⁴
	25.4 (1.000)	2.07 (300)	16.55 (2400)		12.75 (0.502)	0.46	4.2 x 10 ⁻⁴
	19.56 (0.770)	2.07 (300)	12.55 (1820)		6.77 (0.265)	0.117	1.6 x 10 ⁻⁴

GP03-0249-245

TABLE C13. SUPERPLASTIC STRAIN RATES AT 949°C (1740°F) OF Ti-8Al-1Mo-1V
DETERMINED FROM CONE-FORMING TESTS.

Panel thickness mm (in.)	Diameter of cone mm (in.)	Forming pressure MPa (psi)	Stress in cone MPa (psi)	Time at pressure (h)	Final depth in cone mm (in.)	Strain in cone, ε	Strain rate in cone (s ⁻¹)
1.14 (0.045)	37.72 (1.485)*	1.55 (225)	18.68 (2710)	1	30.28 (1.192)*	1.8	5 × 10 ⁻⁴
	34.04 (1.34)	1.55 (225)	16.82 (2440)		19.05 (0.750)	0.61	2 × 10 ⁻⁴
	29.97 (1.18)	1.55 (225)	14.75 (2140)		14.40 (0.567)	0.43	1.7 × 10 ⁻⁴
	25.91 (1.02)	1.55 (225)	12.62 (1830)		14.07 (0.554)	0.54	1.8 × 10 ⁻⁴
1.27 (0.050)	37.29 (1.468)	1.55 (225)	18.48 (2680)	1	29.82 (1.174)*	1.77	4.9 × 10 ⁻⁴
	31.12 (1.225)	1.55 (225)	15.31 (2220)		14.02 (0.552)	0.32	1.3 × 10 ⁻⁴
	25.4 (1.0)	1.55 (225)	12.82 (1860)		12.60 (0.496)	0.43	1.7 × 10 ⁻⁴
	20.32 (0.8)	1.55 (225)	9.79 (1420)		8.763 (0.345)	0.29	1.2 × 10 ⁻⁴

*Cone failure.

GP33-0249-246

TABLE C14. SUPERPLASTIC STRAIN RATES AT 949°C (1740°F) OF Ti-8Al-1Mo-1V
DETERMINED FROM CONE-FORMING TESTS.

Panel thickness mm (in.)	Diameter of cone mm (in.)	Forming pressure MPa (psi)	Stress in cone MPa (psi)	Time at pressure (min)	Final depth in cone mm (in.)	Strain in cone, ϵ	Strain rate in cone (s ⁻¹)
1.14 (0.045)	37.29 (1.468)	0.86 (125)	10.27 (1490)	5	29.39 (1.157)	1.52	8.9×10^{-5}
	31.52 (1.241)	0.86 (125)	8.62 (1250)		18.29 (0.720)	0.65	4.1×10^{-5}
	25.4 (1.0)	0.86 (125)	6.9 (1000)		11.94 (0.470)	0.37	2.4×10^{-5}
	20.32 (0.8)				8.79 (0.346)	0.3	2.0×10^{-5}
1.27 (0.050)	37.72 (1.485)	0.86 (125)	10.41 (1510)	5	29.64 (1.167)	1.71	1.0×10^{-4}
	34.04 (1.34)	0.86 (125)	9.34 (1355)		22.50 (0.886)	0.97	6.0×10^{-5}
	29.97 (1.18)	0.86 (125)	8.20 (1190)		16.76 (0.660)	0.63	4.1×10^{-5}
	25.91 (1.020)	0.86 (125)	7.24 (1050)		14.48 (0.570)	0.56	3.5×10^{-5}

GP03-0249-247

TABLE C15. SUPERPLASTIC STRAIN RATES AT 932°C (1710°F) OF Ti-8Al-1Mo-1V
DETERMINED FROM CONE-FORMING TESTS.

Panel thickness mm (in.)	Diameter of cone mm (in.)	Forming pressure MPa (psi)	Stress in cone MPa (psi)	Time at pressure (min)	Final depth in cone mm (in.)	Strain in cone, ε	Strain rate in cone (s ⁻¹)
1.14 (0.045)	37.29 (1.468)	2.41 (350)	28.75 (4170)	50	30.17 (1.188)	1.84*	6.1 × 10 ⁻⁴
	31.52 (1.241)	2.41 (350)	24.13 (3500)		16.76 (0.660)	0.525	2.2 × 10 ⁻⁴
	25.4 (1.0)	2.41 (350)	19.30 (2800)		10.74 (0.423)	0.285	1.2 × 10 ⁻⁴
	20.32 (0.8)	2.41 (350)	15.24 (2210)		8.636 (0.340)	0.26	1.0 × 10 ⁻⁴
1.27 (0.050)	37.72 (1.485)	2.41 (350)	29.1 (4220)	50	30.28 (1.192)	1.75*	5.8 × 10 ⁻⁴
	34.04 (1.340)	2.41 (350)	26.13 (3790)		24.13 (0.950)	1.2	4 × 10 ⁻⁴
	29.97 (1.18)	2.41 (350)	22.89 (3320)		15.04 (0.592)	0.445	1.85 × 10 ⁻⁴
	25.91 (1.020)	2.41 (350)	19.72 (2860)		11.18 (0.440)	0.3	1.25 × 10 ⁻⁴

* Failure in cone

GP03-0249-248

TABLE C16. SUPERPLASTIC STRAIN RATES AT 932°C (1710°F) OF Ti-8Al-1Mo-1V DETERMINED FROM CONE-FORMING TESTS.

Panel thickness mm (in.)	Diameter of cone mm (in.)	Forming pressure MPa (psi)	Stress in cone MPa (psi)	Time at pressure (h)	Final depth in cone mm (in.)	Strain in cone, ε	Strain rate in cone (s ⁻¹)
1.14 (0.045)	37.29 (1.468)	0.96 (140)	11.51 (1670)	5	24.48 (0.964)	0.936	5.9 × 10 ⁻⁵
	31.12 (1.225)	0.96 (140)	9.51 (1380)		13.84 (0.545)	0.31	3 × 10 ⁻⁵
	25.4 (1.0)	0.96 (140)	8.07 (1170)		12.72 (0.501)	0.47	3.5 × 10 ⁻⁵
	19.57 (0.77)	0.96 (140)	5.86 (850)		6.86 (0.270)	0.12	1.9 × 10 ⁻⁵
1.27 (0.050)	37.72 (1.485)	0.96 (140)	11.65 (1690)	5	6.86 (1.037)	1.135	7.6 × 10 ⁻⁵
	34.04 (1.34)	0.96 (140)	10.51 (1525)		18.64 (0.734)	0.565	4.3 × 10 ⁻⁵
	29.97 (1.18)	0.96 (140)	9.17 (1330)		14.88 (0.586)	0.43	3.3 × 10 ⁻⁵
	25.91 (1.020)	0.96 (140)	7.86 (1140)		13.59 (0.535)	0.53	4.2 × 10 ⁻⁵

QP03-0249-249

TABLE C17. SUPERPLASTIC STRAIN RATES AT 907°C (1665°F) OF Ti-6Al-2Sn-4Zr-2Mo
DETERMINED FROM CONE-FORMING TESTS.

Alloy microstructure		Diameter of cone mm (in.)	Forming pressure MPa (psi)	Stress in cone MPa (psi)	Time at pressure (h)	Final depth in cone mm (in.)	Strain in cone, ε	Average strain rate in cone (s ⁻¹)
Grain size (μm)	Volume fraction primary alpha							
3.5	0.90	38.10 (1.50)	0.69 (100)	7.58 (1100)	5	33.02 (1.300)	3.27	1.8 × 10 ⁻⁴
		34.29 (1.35)		6.83 (990)		22.17 (0.873)	0.930	5.16 × 10 ⁻⁵
		30.48 (1.20)		6.37 (890)		20.90 (0.826)	1.114	6.6 × 10 ⁻⁵
		25.40 (1.00)		5.00 (725)		15.95 (0.628)	0.846	4.7 × 10 ⁻⁵
3.4	0.85	38.10 (1.50)	0.69 (100)	7.58 (1100)	5	32.36 (1.274)	2.7	1.5 × 10 ⁻⁴
		34.29 (1.35)		6.83 (990)		19.76 (0.778)	0.674	3.7 × 10 ⁻⁵
		30.48 (1.20)		6.07 (880)		18.80 (0.740)	0.740	4.44 × 10 ⁻⁵
		25.40 (1.00)		5.00 (725)		16.18 (0.637)	0.884	4.9 × 10 ⁻⁵
8.2	0.86	38.10 (1.50)	0.69 (100)	7.58 (1100)	5	32.66 (1.286)	2.88	1.6 × 10 ⁻⁴
		34.29 (1.35)		6.83 (990)		24.89 (0.980)	1.33	7.4 × 10 ⁻⁵
		30.48 (1.20)		6.07 (880)		22.05 (0.868)	1.71	8.1 × 10 ⁻⁵
		25.40 (1.00)		5.00 (725)		19.61 (0.772)	1.72	9.6 × 10 ⁻⁵
8.8	0.55	38.10 (1.50)	0.69 (100)	7.58 (1100)	5	29.59 (1.165)	1.684	9.36 × 10 ⁻⁵
		34.29 (1.35)		6.83 (990)		25.48 (1.003)	1.44	8 × 10 ⁻⁵
		30.48 (1.20)		6.07 (880)		21.34 (0.840)	1.21	6.7 × 10 ⁻⁵
		25.40 (1.00)		5.00 (725)		13.08 (0.515)	0.47	2.6 × 10 ⁻⁵

GP03-0246-232

TABLE C18. SUPERPLASTIC STRAIN RATES AT 907°C (1665°F) OF Ti-3Al-2Sn-4Zr-2Mo DETERMINED FROM CONE-FORMING TESTS.

Alloy microstructure		Diameter of cone mm (in.)	Forming pressure MPa (psi)	Stress in cone MPa (psi)	Time at pressure (min)	Final depth in cone mm (in.)	Strain in cone, ϵ	Average strain rate in cone (s ⁻¹)
Grain size (μ m)	Volume fraction primary alpha							
3.5	0.90	38.10 (1.50)	2.07 (300)	22.95 (3320)	19	31.47 (1.239)	1.695	1.48×10^{-3}
		34.29 (1.35)		20.55 (2980)		24.18 (0.952)	1.200	1.05×10^{-3}
		30.48 (1.20)		18.13 (2630)		21.84 (0.860)	0.394	6.27×10^{-5}
		25.40 (1.00)		15.00 (2175)		13.77 (0.542)	0.548	4.8×10^{-4}
3.4	0.85	38.10 (1.50)	2.07 (300)	22.95 (3320)	19	33.10 (1.303)	2.428	2.1×10^{-3}
		34.29 (1.35)		20.55 (2980)		23.88 (0.940)	1.193	1.05×10^{-3}
		30.48 (1.20)		18.13 (2630)		21.34 (0.840)	1.220	1.07×10^{-3}
		25.40 (1.00)		15.00 (2175)		13.84 (0.545)	0.532	4.67×10^{-4}
8.2	0.86	38.10 (1.50)	2.07 (300)	22.95 (3320)	19	19.35 (0.762)	0.5379	4.718×10^{-4}
		34.29 (1.35)		20.55 (2980)		17.22 (0.678)	0.538	4.3×10^{-4}
		30.48 (1.20)		18.13 (2630)		13.92 (0.548)	0.456	4×10^{-4}
		25.40 (1.00)		15.00 (2175)		10.46 (0.412)	0.340	3×10^{-4}
8.8	0.55	38.10 (1.50)	2.07 (300)	22.95 (3320)	19	13.21 (0.520)	0.232	2.0×10^{-4}
		34.29 (1.35)		20.55 (2980)		12.52 (0.493)	0.25	2.2×10^{-4}
		30.48 (1.20)		18.13 (2630)		9.65 (0.380)	0.100	8.8×10^{-5}
		25.40 (1.00)		15.00 (2175)		8.53 (0.336)	0.226	1.9×10^{-4}

QP03-0246-223

**TABLE C19. SUPERPLASTIC STRAIN RATES AT 870°C (1600°F) OF Ti-6Al-2Sn-4Zr-2Mo
DETERMINED FROM CONE-FORMING TESTS.**

Alloy microstructure		Diameter of cone mm (in.)	Forming pressure MPa (psi)	Stress in cone MPa (psi)	Time at pressure (h)	Final depth in cone mm (in.)	Strain in cone, ϵ	Average strain rate in cone (s ⁻¹)
Grain size (μ m)	Volume fraction primary alpha							
3.5	0.90	38.10 (1.50)	1.72 (250)	17.10 (2480) 15.17 (2200)	Failed			
		34.29 (1.35)			3.5	28.30 (1.114)	2.28	1.81×10^{-4}
		30.48 (1.20)				25.96 (1.022)	2.99	2.37×10^{-4}
		25.40 (1.00)				18.96 (0.746)	1.50	1.19×10^{-4}
3.4	0.65	38.10 (1.50)	1.72 (250)	17.10 (2480) 15.17 (2200) 12.48 (1810)	Failed			
		34.29 (1.35)			3.5	27.61 (1.087)	2.19	1.74×10^{-4}
		30.48 (1.20)				23.39 (0.921)	1.66	1.32×10^{-4}
		25.40 (1.00)				19.23 (0.757)	1.59	1.26×10^{-4}
8.2	0.88	38.10 (1.50)	1.72 (250)	19.10 (2770) 17.10 (2480) 15.12 (2193) 12.49 (1811)	3.5	27.79 (1.094)	1.516	1.20×10^{-4}
		34.29 (1.35)				21.77 (0.857)	0.882	7.00×10^{-5}
		30.48 (1.20)				15.37 (0.606)	0.480	3.80×10^{-5}
		25.40 (1.00)				9.14 (0.360)	0.11	8.8×10^{-6}
8.8	0.55	38.10 (1.50)	1.72 (250)	19.10 (2770) 17.10 (2480) 15.12 (2193) 12.40 (1811)	3.5	23.11 (0.910)	0.77	6.1×10^{-5}
		34.29 (1.35)				15.14 (0.596)	0.31	2.5×10^{-5}
		30.48 (1.20)				10.34 (0.407)	0.119	9.6×10^{-6}
		25.40 (1.00)				9.70 (0.382)	0.154	1.2×10^{-5}

GP03-0246-221

TABLE C20. SUPERPLASTIC STRAIN RATES AT 877°C (1610°F) OF Ti-3Al-2.5V
DETERMINED FROM CONE-FORMING TESTS.

Alloy microstructure		Diameter of cone mm (in.)	Forming pressure MPa (psi)	Stress in cone MPa (psi)	Time at pressure (h)	Final depth in cone mm (in.)	Strain in cone, ε	Average strain rate in cone (s ⁻¹)
Grain size (μm)	Volume fraction primary alpha							
5.6	0.87	38.10 (1.5)	0.62 (90)	6.90 (1000)	5	29.44 (1.159)	1.7	9.5 × 10 ⁻⁵
		34.29 (1.35)		6.21 (900)		22.86 (0.900)	1.08	6.0 × 10 ⁻⁵
		30.48 (1.20)		5.52 (800)		17.48 (0.688)	0.722	4.0 × 10 ⁻⁵
		25.40 (1.0)		4.55 (660)		12.57 (0.495)	0.52	2.9 × 10 ⁻⁵
4.3	0.57	38.10 (1.5)	0.62 (90)	6.90 (1000)	5	24.38 (0.960)	0.95	5.3 × 10 ⁻⁵
		34.29 (1.35)		6.21 (900)		17.91 (0.706)	0.82	4.1 × 10 ⁻⁵
		30.48 (1.2)		5.52 (800)		14.15 (0.557)	0.43	2.4 × 10 ⁻⁵
		25.40 (1.0)		4.55 (660)		11.63 (0.458)	0.40	2.2 × 10 ⁻⁵
10.2	0.87	38.10 (1.5)	0.62 (90)	6.90 (1000)	5	22.00 (0.866)	0.735	4.0 × 10 ⁻⁵
		34.29 (1.35)		6.21 (900)		15.75 (0.620)	0.41	2.3 × 10 ⁻⁵
		30.48 (1.2)		5.52 (800)		14.15 (0.557)	0.42	2.4 × 10 ⁻⁵
		25.40 (1.0)		4.55 (660)		8.51 (0.335)	0.095	5 × 10 ⁻⁶
8.6	0.58	38.10 (1.5)	0.62 (90)	6.90 (1000)	5	24.18 (0.952)	0.97	5.4 × 10 ⁻⁵
		34.29 (1.35)		6.21 (900)		15.32 (0.603)	0.43	2.4 × 10 ⁻⁵
		30.48 (1.2)		5.52 (800)		12.27 (0.483)	0.29	1.6 × 10 ⁻⁵
		25.40 (1.0)		4.55 (660)		9.35 (0.368)	0.245	1.4 × 10 ⁻⁵

GP03-0240-235

TABLE C21. SUPERPLASTIC STRAIN RATES AT 841°C OF Ti-3Al-2.5V
DETERMINED FROM CONE-FORMING TESTS.

Alloy microstructure		Diameter of cone mm (in.)	Forming pressure MPa (psi)	Stress in cone MPa (psi)	Time at pressure (h)	Final depth in cone mm (in.)	Strain in cone, ε	Average strain rate in cone (s ⁻¹)
Grain size (μm)	Volume fraction primary alpha							
5.6	0.87	38.10 (1.5)	1.52 (220)	15.17 (2200) 13.45 (1950) 11.10 (1610)	3	Failed	0.82 0.50 0.49	7.6 x 10 ⁻⁵ 4.6 x 10 ⁻⁵ 4.5 x 10 ⁻⁵
		34.29 (1.35)				20.27 (0.798)		
		30.48 (1.2)				14.71 (0.579)		
		25.40 (1.0)				12.12 (0.477)		
4.3	0.57	38.10 (1.5)	1.52 (220)	16.96 (2460) 15.17 (2200) 13.45 (1950) 11.10 (1610)	3	28.65 (1.128)	1.56	1.4 x 10 ⁻⁴
		34.29 (1.35)				20.70 (0.815)	0.86	8.0 x 10 ⁻⁵
		30.48 (1.20)				14.86 (0.585)	0.51	4.7 x 10 ⁻⁵
		25.40 (1.0)				11.53 (0.454)	0.44	4.1 x 10 ⁻⁵
10.2	0.87	38.10 (1.5)	1.52 (220)	16.96 (2460) 15.17 (2200) 13.45 (1950) 11.10 (1610)	3	22.00 (0.866)	0.76?	7.1 x 10 ⁻⁵
		34.29 (1.35)				14.48 (0.570)	0.39	3.6 x 10 ⁻⁵
		30.48 (1.2)				11.05 (0.435)	0.29	2.7 x 10 ⁻⁵
		25.40 (1.0)				8.48 (0.334)	0.22	2.0 x 10 ⁻⁵
8.6	0.58	38.10 (1.5)	1.52 (220)	16.96 (2460) 15.17 (2200) 13.45 (1950) 11.10 (1610)	3	24.36 (0.959)	0.99	9.2 x 10 ⁻⁵
		34.29 (1.35)				13.72 (0.540)	0.35	3.2 x 10 ⁻⁵
		30.48 (1.2)				12.07 (0.475)	0.34	3.2 x 10 ⁻⁵
		25.40 (1.0)				8.97 (0.353)	0.25	2.3 x 10 ⁻⁵

GP03-0248-238

**TABLE C22. SUPERPLASTIC STRAIN RATES AT 877°C (1610°F) OF Ti-3Al-2.5V
DETERMINED FROM CONE-FORMING TESTS.**

Alloy microstructure		Diameter of cone mm (in.)	Forming pressure MPa (psi)	Stress in cone MPa (psi)	Time at pressure (min)	Final depth in cone mm (in.)	Strain in cone, ϵ	Average strain rate in cone (s ⁻¹)
Grain size (μ m)	Volume fraction primary alpha							
5.6	0.87	38.10 (1.5)	1.72 (250)	19.31 (2800)	30	31.45 (1.238)	2.3	1.3×10^{-3}
		34.29 (1.35)		17.24 (2500)		21.34 (0.840)	0.93	5.2×10^{-4}
		30.48 (1.2)		15.31 (2220)		16.51 (0.650)	0.66	3.7×10^{-4}
		25.40 (1.0)		12.62 (1830)		11.94 (0.47)	0.48	2.7×10^{-4}
4.3	0.57	38.10 (1.5)	1.72 (250)	19.31 (2800)	30	26.04 (1.025)	1.12	6.2×10^{-4}
		34.29 (1.35)		17.24 (2500)		21.06 (0.829)	0.90	5.0×10^{-4}
		30.48 (1.2)		15.31 (2220)		16.03 (0.631)	0.61	3.4×10^{-4}
		25.40 (1.0)		12.62 (1830)		11.71 (0.461)	0.45	2.5×10^{-4}
10.2	0.87	38.10 (1.5)	1.72 (250)	19.31 (2800)	30	17.40 (0.685)	0.44	2.4×10^{-4}
		34.29 (1.35)		17.24 (2500)		12.90 (0.508)	0.29	1.6×10^{-4}
		30.48 (1.2)		15.31 (2220)		10.92 (0.430)	0.29	1.6×10^{-4}
		25.40 (1.0)		12.62 (1830)		7.39 (0.291)	0.145	8.0×10^{-5}
8.6	0.58	38.10 (1.5)	1.72 (250)	19.31 (2800)	30	20.50 (0.807)	0.55	3.1×10^{-4}
		34.29 (1.35)		17.24 (2500)		13.92 (0.548)	0.36	2×10^{-4}
		30.48 (1.2)		15.31 (2220)		11.43 (0.450)	0.322	1.8×10^{-4}
		25.40 (1.0)		12.62 (1830)		9.58 (0.377)	0.3	1.7×10^{-4}

GP03-0246-237

TABLE C23. SUPERPLASTIC STRAIN RATES AT 870°C (1600°F) OF SIMULATED-COIL Ti-6Al-4V DETERMINED FROM CONE-FORMING TESTS.

Alloy microstructure		Diameter of cone mm (in.)	Forming pressure MPa (psi)	Stress in cone MPa (psi)	Time at pressure (h)	Final depth in cone mm (in.)	Strain in cone, ε	Average strain rate in cone (s ⁻¹)
Grain size (μm)	Volume fraction primary alpha							
3.6	0.90	38.10 (1.5)	1.72 (250)	14.48 (2100)	5	31.12 (1.225)	2.36	1.3 × 10 ⁻⁴
		34.29 (1.35)		12.96 (1880)		18.85 (0.742)	0.76	4.2 × 10 ⁻⁵
		30.48 (1.2)		11.38 (1650)		13.72 (0.540)	0.49	2.7 × 10 ⁻⁵
		25.40 (1.0)		9.38 (1360)		10.41 (0.410)	0.4	2.2 × 10 ⁻⁵
3.4	0.85	38.10 (1.5)	1.72 (250)	14.48 (2100)	5	31.06 (1.223)	2.36	1.3 × 10 ⁻⁴
		34.29 (1.35)		12.96 (1880)		17.78 (0.700)	0.85	4.75 × 10 ⁻⁵
		30.48 (1.2)		11.38 (1650)		15.34 (0.604)	0.64	3.5 × 10 ⁻⁵
		25.40 (1.0)		9.38 (1360)		8.51 (0.335)	0.24	1.3 × 10 ⁻⁵
8.2	0.86	38.10 (1.5)	1.72 (250)	14.48 (2100)	5	18.42 (0.725)	0.60	3.3 × 10 ⁻⁵
		34.29 (1.35)		12.96 (1880)		10.92 (0.430)	0.27	1.5 × 10 ⁻⁵
		30.48 (1.2)		11.38 (1650)		9.40 (0.370)	0.26	1.4 × 10 ⁻⁵
		25.40 (1.0)		9.38 (1360)		7.62 (0.300)	0.23	1.25 × 10 ⁻⁵
8.8	0.55	38.10 (1.5)	1.72 (250)	14.48 (2100)	5	18.29 (0.720)	0.6	3.3 × 10 ⁻⁵
		34.29 (1.35)		12.96 (1880)		9.91 (0.390)	0.22	1.2 × 10 ⁻⁵
		30.48 (1.2)		11.38 (1650)		8.26 (0.325)	0.2	1.1 × 10 ⁻⁵
		25.40 (1.0)		9.38 (1360)		7.01 (0.276)	0.18	1.0 × 10 ⁻⁵

GP03-0248-238

TABLE C24. SUPERPLASTIC STRAIN RATES AT 907°C (1665°F) OF SIMULATED-COIL Ti-6Al-4V DETERMINED FROM CONE-FORMING TESTS.

Alloy microstructure		Diameter of cone mm (in.)	Forming pressure MPa (psi)	Stress in cone MPa (psi)	Time at pressure (h)	Final depth in cone mm (in.)	Strain in cone, ϵ	Average strain rate in cone (s ⁻¹)
Grain size (μ m)	Volume fraction primary alpha							
3.5	0.90	38.10 (1.5)	0.69 (100)	5.93 (860)	5	30.45 (1.199)	2.0	1.2×10^{-4}
		34.29 (1.35)		5.34 (775)		18.85 (0.742)	0.64	3.8×10^{-5}
		30.48 (1.2)		4.69 (680)		16.05 (0.632)	0.58	3.6×10^{-5}
		25.40 (1.0)		3.86 (560)		11.48 (0.452)	0.40	2.5×10^{-5}
3.4	0.85	38.10 (1.5)	0.69 (100)	5.93 (860)	5	26.80 (1.055)	1.25	7.4×10^{-5}
		34.29 (1.35)		5.34 (775)		14.91 (0.587)	0.34	2.0×10^{-5}
		30.48 (1.2)		4.69 (680)		13.26 (0.522)	0.34	2.0×10^{-5}
		25.40 (1.0)		3.86 (560)		8.13 (0.32)	0.12	7.6×10^{-6}
8.2	0.86	38.10 (1.5)	0.69 (100)	5.93 (860)	5	17.78 (0.700)	0.40	2.5×10^{-5}
8.8	0.55	38.10 (1.5)	0.69 (100)	5.93 (860)	5	16.38 (0.645)	0.32	1.9×10^{-5}

QP03-0246-239

TABLE C25. SUPERPLASTIC STRAIN RATES AT 907°C (1665°F) OF SIMULATED COIL Ti-6Al-4V DETERMINED FROM CONE-FORMING TESTS.

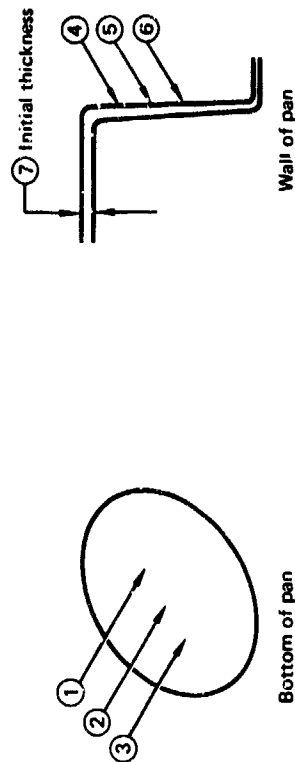
Alloy microstructure		Diameter of cone mm (in.)	Forming pressure MPa (psi)	Stress in cone MPa (psi)	Time at pressure (min)	Final depth in cone mm (in.)	Strain in cone, ϵ	Average strain rate in cone (s ⁻¹)
Grain size (μ m)	Volume fraction primary alpha							
3.5	0.90	38.10 (1.5)	1.72 (250)	14.48 (2100)	30	21.13 (0.832)	0.69	3.8×10^{-4}
		34.29 (1.35)		12.96 (1880)		14.40 (0.567)	0.45	2.5×10^{-4}
		30.48 (1.2)		11.38 (1650)		11.81 (0.465)	0.35	2.0×10^{-4}
		25.40 (1.0)		9.38 (1360)		8.69 (0.342)	0.26	1.4×10^{-4}
3.4	0.65	38.10 (1.5)	1.72 (250)	14.48 (2100)	30	20.32 (0.800)	0.67	3.7×10^{-4}
		34.29 (1.35)		12.96 (1880)		14.10 (0.555)	0.40	2.25×10^{-4}
		30.48 (1.2)		11.38 (1650)		11.76 (0.463)	0.38	2.1×10^{-4}
		25.40 (1.0)		9.38 (1360)		8.69 (0.342)	0.25	1.4×10^{-4}
8.2	0.86	38.10 (1.5)	1.72 (250)	14.48 (2100)	30	14.68 (0.578)	0.375	2.0×10^{-4}
		34.29 (1.35)		12.96 (1880)		11.53 (0.455)	0.3	1.7×10^{-4}
		30.48 (1.2)		11.38 (1650)		8.97 (0.353)	0.23	1.3×10^{-4}
		25.40 (1.0)		9.38 (1360)		6.93 (0.273)	0.18	1.0×10^{-4}
8.8	0.55	38.10 (1.5)	1.72 (250)	14.48 (2100)	30	12.70 (0.50)	0.26	1.5×10^{-4}
		34.29 (1.35)		12.96 (1880)		8.51 (0.335)	0.135	7.5×10^{-5}
		30.48 (1.2)		11.38 (1650)		7.52 (0.296)	0.16	8.9×10^{-5}
		25.40 (1.0)		9.38 (1360)		5.56 (0.219)	0.09	5.2×10^{-5}

GP03-0248-240

APPENDIX D

THICKNESS MEASUREMENTS OF
SUPERPLASTICALLY FORMED PANS

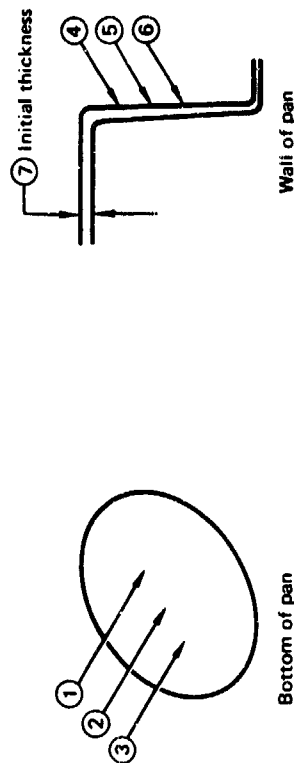
TABLE D1. THICKNESSES AT DIFFERENT LOCATIONS OF SUPERPLASTICALLY FORMED 254-mm (10.0 IN.) DIAM Ti-6Al-4V, PAN-FORMING TEMPERATURE AT 907°C (1665°F).



	Grain size (μm)	Volume fraction primary alpha (%)	Forming rate (s^{-1})	Location						
				1	2	3	4	5	6	7
Normal-textured regular-grade Ti-6Al-4V	17.6	0.88	10^{-3}	0.559 (0.022)	0.406 (0.016)	0.508 (0.020)	1.33 (0.053)	0.940 (0.037)	0.635 (0.025)	1.73 (0.068)
	17.6	0.88	10^{-4}	0.635 (0.025)	0.584 (0.023)	0.635 (0.025)	1.29 (0.051)	0.965 (0.038)	0.660 (0.026)	1.73 (0.068)
	12.2	0.88	10^{-3}	0.635 (0.025)	0.533 (0.021)	0.559 (0.022)	1.29 (0.051)	1.02 (0.040)	0.737 (0.029)	1.73 (0.068)
	12.2	0.88	10^{-4}	0.660 (0.026)	0.813 (0.032)	0.584 (0.023)	1.32 (0.052)	0.991 (0.039)	0.686 (0.027)	1.73 (0.068)
	7.7	0.89	10^{-3}	0.635 (0.025)	0.457 (0.018)	0.508 (0.020)	1.27 (0.050)	0.813 (0.032)	0.508 (0.020)	1.63 (0.064)
	7.7	0.89	10^{-4}	0.711 (0.028)	0.635 (0.025)	0.559 (0.022)	1.07 (0.042)	0.787 (0.031)	0.508 (0.020)	1.63 (0.064)
	6.0	0.88	10^{-3}	0.559 (0.022)	0.457 (0.018)	0.584 (0.023)	1.14 (0.045)	0.889 (0.035)	0.584 (0.023)	1.50 (0.059)
	6.0	0.88	10^{-4}	0.584 (0.023)	0.533 (0.021)	0.508 (0.020)	1.14 (0.045)	0.838 (0.033)	0.610 (0.024)	1.50 (0.059)
	4.4	0.47	10^{-3}	0.610 (0.024)	0.508 (0.020)	0.483 (0.019)	1.12 (0.044)	0.813 (0.032)	0.584 (0.023)	1.50 (0.059)
	4.4	0.47	10^{-4}	0.635 (0.025)	0.533 (0.021)	0.508 (0.020)	1.17 (0.046)	0.838 (0.033)	0.610 (0.024)	1.50 (0.059)
Base-textured ELI-grade Ti-6Al-4V	5.5	0.88	10^{-3}	0.686 (0.027)	0.584 (0.023)	0.635 (0.025)	1.38 (0.055)	1.07 (0.042)	0.737 (0.029)	1.83 (0.072)
	5.5	0.88	10^{-4}	0.762 (0.030)	0.660 (0.026)	0.686 (0.027)	1.42 (0.044)	1.12 (0.056)	0.787 (0.031)	1.83 (0.072)
	8.9	0.88	10^{-3}	0.635 (0.025)	0.508 (0.020)	0.660 (0.026)	1.24 (0.049)	1.02 (0.040)	0.787 (0.031)	1.68 (0.066)
	8.9	0.88	10^{-4}	0.762 (0.030)	0.686 (0.027)	0.660 (0.026)	1.40 (0.055)	0.965 (0.038)	0.584 (0.023)	1.68 (0.066)
	8.9	0.47	10^{-3}	0.660 (0.026)	0.432 (0.017)	0.660 (0.022)	1.37 (0.054)	0.965 (0.038)	0.584 (0.023)	1.68 (0.066)
	8.9	0.47	10^{-4}	0.737 (0.029)	0.318 (0.0125)	0.584 (0.023)	1.19 (0.047)	0.914 (0.036)	0.711 (0.028)	1.68 (0.066)

GP03-0248-131

TABLE D2. THICKNESSES AT DIFFERENT LOCATIONS OF SUPERPLASTICALLY FORMED 254-mm (10.0 IN.) DIAM TI-6Al-4V PAN WITH A FORMING TEMPERATURE OF 870°C (1600°F).



Grain size (μm)	Volume fraction primary alpha (%)	Forming rate (s^{-1})	Location						
			1	2	3	4	5	6	7
12.2	0.88	10^{-4}	mm (in.)	mm (in.)	mm (in.)	mm (in.)	mm (in.)	mm (in.)	mm (in.)
			0.660 (0.026)	0.584 (0.023)	0.559 (0.022)	1.295 (0.051)	0.965 (0.038)	0.762 (0.030)	1.73 (0.068)
6.0	0.88	10^{-4}	0.584 (0.023)	0.533 (0.021)	0.533 (0.021)	1.14 (0.045)	0.864 (0.034)	0.635 (0.025)	1.50 (0.059)
4.4	0.47	10^{-4}	0.686 (0.027)	0.559 (0.022)	0.533 (0.021)	1.17 (0.046)	0.940 (0.037)	0.686 (0.027)	1.50 (0.059)
5.5	0.88	10^{-4}	0.711 (0.28)	0.660 (0.026)	0.635 (0.025)	1.295 (0.051)	0.991 (0.039)	0.737 (0.029)	1.83 (0.072)

GP00-0208-122

TABLE D3. THICKNESSES AT DIFFERENT LOCATIONS OF SUPERPLASTICALLY-FORMED BASAL-TEXTURED Ti-6Al-4V AT A FORMING TEMPERATURE OF 907°C (1665°F).

Forming rate (s ⁻¹)	1 mm (in.)	2 mm (in.)	3 mm (in.)	4 mm (in.)	5 mm (in.)	6 mm (in.)	7 mm (in.)
10 ⁻⁴	0.736 (0.029)	0.660 (0.026)	0.635 (0.025)	1.295 (0.051)	0.991 (0.039)	0.666 (0.027)	1.57 (0.062)

GP03-0248-250

TABLE D4. THICKNESSES AT DIFFERENT LOCATIONS OF SUPERPLASTICALLY-FORMED SIMULATED-COIL Ti-6Al-4V (PANEL S1, GRAIN SIZE = 4.7 μm , VOLUME % PRIMARY ALPHA = 87) FORMED AT 907°C (1665°F)

Forming rate (s ⁻¹)	1 (mm in.)	2 (mm in.)	3 (mm in.)	4 (mm in.)	5 (mm in.)	6 (mm in.)	7 (mm in.)
10 ⁻⁴	0.711 (0.028)	0.559 (0.022)	0.553 (0.021)	1.47 (0.058)	1.09 (0.043)	0.886 (0.027)	1.79 (0.068)

GP03-0248-251

TABLE D6. THICKNESSES AT DIFFERENT LOCATIONS OF SUPERPLASTICALLY-FORMED COMMERCIAL-GRADE 1.14-mm (0.045 IN.) Ti-8Al-1Mo-1V FORMED AT 949°C (1740°F).

Forming rate (s ⁻¹)	1 (mm in.)	2 (mm in.)	3 (mm in.)	4 (mm in.)	5 (mm in.)	6 (mm in.)	7 (mm in.)
10 ⁻³	0.457 (0.018)	0.381 (0.015)	0.258 (0.014)	1.02 (0.040)	0.737 (0.029)	0.483 (0.019)	1.12 (0.044)
10 ⁻⁴	0.483 (0.019)	0.381 (0.015)	0.305 (0.012)	0.406 (0.016)	0.686 (0.027)	0.483 (0.019)	1.12 (0.044)

GP03-0246-252

TABLE D8. THICKNESSES AT DIFFERENT LOCATIONS OF SUPERPLASTICALLY-FORMED Ti-3Al-2.5V FORMED AT 877°C (1610°F).

Panel code	Grain size (μm)	Volume fraction primary alpha	Forming rate (s^{-1})	1 mm (in.)	2 mm (in.)	3 mm (in.)	4 mm (in.)	5 mm (in.)	6 mm (in.)	7 mm (in.)
R1	4.5	0.87	10^{-4}	0.584 (0.023)	0.508 (0.020)	0.508 (0.020)	0.940 (0.037)	0.737 (0.029)	0.483 (0.019)	1.27 (0.050)
R2	4.3	0.47	10^{-4}	0.559 (0.022)	0.453 (0.019)	0.408 (0.016)	0.940 (0.037)	0.585 (0.023)	0.457 (0.018)	1.27 (0.050)
R3	10.2	0.87	10^{-4}	0.483 (0.019)	0.381 (0.015)	0.356 (0.014)	0.965 (0.038)	0.686 (0.027)	0.432 (0.017)	1.14 (0.045)

GP03-0240-253

**TABLE D7. THICKNESSES AT DIFFERENT LOCATION OF
SUPERPLASTICALLY-FORMED Ti-6Al-2Sn-4Zr-2Mo
FORMED AT 907°C (1665°F).**

Panel code	Grain size (μm)	Volume fraction primary alpha	Forming rate (s^{-1})	1 mm (in.)	2 mm (in.)	3 mm (in.)	4 mm (in.)	5 mm (in.)	6 mm (in.)	7 mm (in.)
Q1	3.5	0.90	10^{-4}	0.559 (0.022)	0.483 (0.019)	0.483 (0.019)	0.965 (0.038)	0.787 (0.031)	0.533 (0.021)	1.27 (0.050)
Q2	8.2	0.86	10^{-4}	0.533 (0.021)	0.457 (0.018)	0.406 (0.016)	1.09 (0.043)	0.864 (0.034)	0.584 (0.023)	1.27 (0.050)

GP05-0248-324